Graduate School of Science
Shimane University
Doctor Thesis No …….

Mass transfer processes and impact on the geochemistry of terrestrial, estuarine and marine environments in Sri Lanka and SW Japan

September 2013

Department of Geoscience, Graduate School Science
Shimane University
S109707

Sansfica Marlyn Young

ABSTRACT

Study 1 - Mahaweli River and Trincomalee Bay system

The Mahaweli River is of a continental river and is the longest with a length of 335km and an altitude of 2500m. The Kuma River is of Japanese Island arc and is the longest river in Kyushu, south west of Japan with a length of 115km and an altitude of 1500m. Both rivers are dammed and thus were selected to be studied and to find out the mass transfer processes and the geochemical impacts of Mahaweli River and Trincomalee Bay System and the Kuma River and Yatsushiro Bay System.

Geochemical variations in stream sediments (n=54) from the Mahaweli River of Sri Lanka have been evaluated from the viewpoints of lithological control, sorting, heavy mineral concentration, influence of climatic zonation (wet, intermediate, and dry zones), weathering, and downstream transport. Compositions of soils (n=22) and basement rocks (n=38) of the catchment and those of <180 μm and 180 – 2000 μm fractions of the stream sediments were also examined. The sediments, fractions, soils and basement rocks were analyzed by X-ray fluorescence. Abundances of HFS and ferromagnesian elements in the sediments indicate concentration of durable heavy minerals including zircon, tourmaline, rutile, monazite, garnet, pyriboles, and titanite, especially in <180 μm fractions. The basement rocks range from mafic through to felsic compositions, as do the soils. $Al_2O_3/(K_2O+Na_2O)$ and K_2O/Na_2O ratios of the sediments and LOI values of the soils correlate well with the climatic zones, suggesting intense weathering in the wet zone, lesser weathering in the intermediate zone, and least weathering in the dry zone. Low Sr and CaO contents and Cr/V ratios in stream sediments in the wet zone also suggest climatic influence. Fe-normalized enrichment factors (EF) for As, Pb, Zn, Cu, Ni and Cr in stream sediments in the main channel are nearly all <1.5, indicating there is no significant environmental contamination. The chemistry of the sediments, rocks and the soils in the Mahaweli River are thus mainly controlled by source lithotype, weathering, sorting, and heavy mineral accumulation. Enrichment Factor (EF) and composition of heavy minerals were used to examine the effects of climatic and weathering conditions, variation of river gradient, and hydraulic fractionation. The EFs of stream sediments in the Mahaweli River and its tributaries show that fining, accumulation due to transport, influence of tributaries, climate and weathering are major geochemical and physical factors contributing to downstream variation.

Compositions of sediments from three sectors in Trincomalee Bay (Koddiyar Bay, Thambalagam Bay and the Inner Harbour) in Sri Lanka were examined to determine fluvial and marine contributions, and the effects of sorting and heavy mineral concentration. Sediments in the three sectors differ significantly in chemical composition, according to position relative to the Mahaweli River delta source, depositional environment, heavy mineral concentration, and marine influence. Sediments in Koddiyar Bay, closest to the Mahaweli River delta, have geochemical compositions similar those supplied by the river. Sediments in the semi-enclosed and more distal Thambalagam Bay are also mainly derived from the Mahaweli River, but are modified by additions of Ca, Mg, and Sr from marine biogenic carbonate sources. This marine component is even greater in the Inner Harbour.

Compositions of four core sediments from the Trincomalee Bay were examined to determine possible depositional environment and provenance of the sediments. Heavy mineral content and variation in C1 differed from the other cores. C3 contained clay and organic matter in the middle part of the core. The results show that the bottom most C1 for the sediments were subjected to major wave and current activities. Sand bar formation near the Mahaweli River mouth acted as a barrier, causing weaker currents entering the area of C1. Finer sediments then accumulated. The study indicates that the sediment texture is the major controlling factor in the distribution of elements here. The deposition of sediments within Trincomalee Bay is dominantly controlled by wave and current activity. The CMI index and SiO_2 of >80% content suggest that the sediments are highly matured.

In the Trincomalee Bay 89 ostracode taxa were identified from surface sediments in the study area. Many of these taxa were typical tropical water species that have been reported from inner bay and shallow marine areas around the coasts of the Indo-Pacific region. Comparison with the trace element distributions showed that ostracod biofacies were not associated with heavy metal pollutions.

Study 2 - Kuma River and Yatsushiro Bay system

Surface and bottom sediments from 10 cm long cores (representing before and after dam removal), and two grain size fractions (fine 0.075 – 0.25 mm and medium 0.25 – 0.85mm) of the Kuma River and Yatsushiro Bay were compared. As the next step the chemical composition of

sediments from the Yatsushiro tidal flat, Kuma River, and Arase dam (southwest Kyushu, Japan) have been determined to examine changes between 2002 and 2012. In 2002 sediment delivered to the bay by the Kuma River was restricted by the Arase dam; however in 2010 two gates were opened, allowing resumption of natural sediment transport.

Abundances of 24 elements in Yatsushiro tidal flat sediments, suspended solids in the bay, Kuma River stream sediments and suspended solids were determined by XRF. Water physical-chemical parameters, temperature, pH, EC, DO and ORP were determined in the field using a Horiba D-24 pH/Conductivity meter. Grain size was measured for all sediments. Diatoms were classified using SEM.

Surface and bottom sediments do not show major chemical changes due to the removal of Arase dam. However, the grain size analysis shows that there is a significant difference before and after dam removal. Lower Br and Zn than 2000 indicate that biogenic processes and redox conditions have changed in the Kuma River. The removal of the Arase dam caused a decrease in most elemental concentrations. The elements for which changes are observed (As, Pb, Zn, Cu, Ni, Cr, V, Fe and total sulfur) can be very environmentally important, affecting the chemical behavior in the river and bay sediments. Abundance of these elements has decreased after dam removal. Ripple marks in the Yatsushiro tidal flat indicate inflow of coarser material from the reinvigorated river. Bulk chemical composition of the tidal flat sediments has changed since 2002, with marked decreases in As, Zn, and total sulfur, and lesser and more variable decrease in Pb. Manganese values are higher (>0.16ppm) in the northern tidal flats, suggesting anoxic conditions in the sediments at those sites. Suspended solids in both the Kuma River and Yatsushiro Bay have very low values of heavy metals, indicating low absorption, flocculation and dilution by organic matter due to strong water circulation. Kuma River sediments are characteristically coarser than those in Yatsushiro Bay, except at three locations. Average values in both suites are similar to UCC.

Thus as the synthesizing conclusions, the Mahaweli River falls to the Trincomalee Bay a deep natural canyon and sand is deposited, fine fraction is flushed to the open sea while the Kuma River forms a large tidal flat at Yatsushiro Bay with mud at distal end and sand at the proximal end. In the Mahaweli River the sediments are fractionated, influenced by tributaries, dams, heavy minerals, weathering. The wet and intermediate zone sediments are mixing in the dry zone due to length and heavy minerals are deposited in the Koddiyar Bay by winnowing and

wave actions. No such mixing due to short distance of the Kuma River. Flooding occurs in the Mahaweli River but is weakened since river is long, and the sediments are transported to the bay. In the Kuma River flooding causes mud drapes and sand deposits in the Yatsuahiro Bay and flooding causes mud drapes and sand deposits in the Yatsuahiro Bay.

DECLARATION

I do hereby declare that the work reported in this project thesis was exclusively carried out by me under the supervision of Prof. Hiroaki Ishiga and local advisor Dr. H. M. T. G. A. Pitawala. It describes the results of my own independent research except where due reference has been made in the text. No part of this project thesis has been submitted earlier or concurrently for the same or any other degree.

Date …….. ……..

Signature of the Candidate

Certified by:

1. Supervisor (Name) :…….. Date:…….

   (Signature):…….

2. Supervisor (Name) :…….. Date:…….

   (Signature):…….

Shimane University Stamp:

Dedicated to my Loving

Parents and Sisters

ACKNOWLEDGMENTS

It is with great pleasure and a sense of gratitude that I thank my supervisor Prof Hiroaki Ishiga and local advisor Dr. H.M.T.G.A Pitawala for encouraging me to initiate, and see me through the completion of this study. If not for their gentle but persuasive suggestions at various points I would not have been able to come thus far. It was a pleasure to work under them; I benefited in particular from their wide knowledge of the subject, their quick comprehension and patient explanations. My thinking was stretched by these comments and suggestions. They also took time to transform lengthy confusing sentences into short, methodical explanations. I owe an unending debt of gratitude to them for guidance, kindness and tolerance shown throughout this study.

I am also very grateful and a special thank you to Dr. Barry Roser for the unending advice, encouragement and guidance given during the course of this study. Not forgetting all the editing he does and improved all my manuscripts, and for the templates and spread sheets provided.

My thanks are extended to each and every member of the Department of Geoscience, for helping me in one way or the other. I am grateful for Prof. Toshiaki Irizuki, Prof. Yoshikazu Sampei, Prof. Tetsuya Sakai and Prof. Hiroto Ohira for their support and providing the facilities to carry out Ostracode analysis, CHN analysis, grain size analysis and heavy mineral analysis respectively.

I very specially thank the Sri Lankan Naval Force and Mr. Amila Rathnayake who helped during the field work undertaken for this study. I thank the staff of the Geological Survey and Mines Bureau of Sri Lanka for the support given for transporting samples from Sri Lanka to Japan. I thank all of the willing hands that helped me in field and laboratory work, especially the technical assistance. Throughout my research, I benefited from the stimulating atmosphere provided by my fellow graduate students. For this and for their help and concern an overall atmosphere of friendship, I am thankful to each one of them.

The samples were imported via plant protection of the Ministry of Agriculture, Forestry and Fisheries, Japan and thus thank the Ministry for the support given. I am very much grateful for financial assistance provided from the Japanese MEXT scholarship for my study here in Japan without which this research would have not been a reality.

The tremendous contributions made by my parents and sisters are too numerous to record individually. Learning was a natural part of the home they provided, exemplified by their very lives. I thank them sincerely for always being there for me in times of need specially since I was so far away from home; their never-failing love, prayers and encouragement are acknowledged with deep gratitude.

Finally this thesis would not have been completed without the love and support of all my friends and associates mentioned and unmentioned. I thank them for their patience.

None of this would have been possible if not for the sustenance, strength and guidance I received from my Heavenly Father, who is the giver of all wisdom and knowledge and every good thing in life. I humbly thank him for all the blessings He has granted to me.

CONTENTS

CHAPTER		PAGE
	Abstract	i
	Declaration	iv
	Acknowledgments	v
	Contents	viii
	List of Figures	xvi
	List of Tables	xxiii
1	**INTRODUCTION: MASS TRANSFER PROCESS AND THEIR POTENTIAL IMPACTS ON TERRESTRIAL AND MARINE ENVIRONMENTS**	
	1.1 GEOCHEMISTRY OF STREAM SEDIMENTS AND BAY ENVIRONMENT	1
	1.2 PROVENANCE	1
	1.3 IMPORTANCE OF PROVENANCE STUDIES	2
	1.4 SEDIMENTARY PROVENANCE	2
	1.4.1 Stream sediments	2
	1.4.2 Sandstone provenance	3
	1.4.3 Mudrock provenance	4
	1.5 MATURITY OF SEDIMENTS	5
	1.6 WEATHERING	7
	1.6.1 Chemical weathering of minerals	8
	1.6.2 Biological weathering	10
	1.6.3 Weathering and soil formation	11
	1.6.4 Waters, pH, Eh and Complex ions	11
	1.7 CLIMATIC IMPLICATIONS	14
	1.8 SEDIMENTARY PROCESSES	15
	1.9 HEAVY MINERAL CONCENTRATION	15
	1.10 SORTING AND MIXING EFFECT	16

1.11 GRAIN SIZE 17
1.12 TRANSPORT AND DOWNSTREAM ACCUMULATION 18
1.13 EFFECT OF TRIBUTARIES 19
1.14 SEDIMENT RECYCLING 19
1.15 DIAGENESIS AND METAMORPHISM 19
1.16 MICROPALENTOLOGY OF OSTRACODE 21

2 MAHAWELI RIVER AND TRINCOMALEE BAY SYSTEM 22
2.1 BACKGROUND 22
2.1.1 Mahaweli River 22
2.1.2 Sediment fractions of Mahaweli River - Heavy minerals and chemical composition 25
2.1.3 Trincomalee Bay 27
2.1.4 Trincomalee Bay core sediments 29
2.1.4.1 Sedimentary environments and deposition 29
2.1.4.2 Heavy Minerals and sorting 30
2.2 SCOPE OF THE RESEARCH 31
2.2.1 Mahaweli River 31
2.2.2 Trincomalee Bay 31
2.3 OBJECTIVE OF THE STUDY 31
2.3.1 Mahaweli River 31
2.3.2 Trincomalee Bay 32
2.3.2.1 Trincomalee Bay surface sediments 32
2.3.2.1. Trincomalee Bay core sediments 33
2.4 EXPECTED OUTCOME 33
2.4.1 Mahaweli River 33
2.4.2 Trincomalee Bay surface and core sediments 33
2.5 GEOLOGY OF SRI LANKA 34
2.6 STUDY AREA 35
2.6.1 Location and Accessibility 35
2.6.1.1 The Mahaweli River 35

2.6.1.2 The Trincomalee Bay 37
2.6.2 Historical Perspective of Water Resource Management of Mahawli area 37
2.6.3 Historical activities in Trincomalee Bay 37
2.6.4 Physiography and Geology 38
2.6.4.1 Physiography and Geology of Mahaweli River 38
2.6.4.2 Physiography and Geology of Trincomalee Bay 41
2.6.5 Drainage and Land use of Mahaweli River and Trincomalee Bay area 42
2.7 CLIMATIC ZONES OF SRI LANKA 42
2.7.1 The Wet zone 43
2.7.1.1 The Low-country Wet zone 43
2.7.1.2 The Up-country Wet zone or Montane zone 44
2.7.2 Intermediate Zone 45
2.7.3 The Dry zone 45
2.8 PREVIOUS WORK AND BACKGROUND 47
2.8 1 Mahaweli River 47
2.8.2 Trincomalee Bay 49

3 METHOD OF STUDY 50
3.1 INCEPTION AND BASE DATA COLLECTION 50
3.2 FIELD SAMPLING 50
3.2.1 Mahaweli Stream sediment samples 50
3.2.2 Mahaweli area Rock Samples 50
3.2.3 Mahaweli area Soil samples 52
3.2.4 Polgolla Dam surface and core sediments 53
3.2.5 Trincomalee Bay surface sediments 53
3.2.5.1 Statistics of Trincomalee Bay surface sediments 53
3.2.6 Trincomalee Bay core sediments 54
3.3 SAMPLE PREPARATION 55
3.3.1 Sediment samples 55
3.3.2 Rock samples 56
3.3.3 Soil samples 56

3.4 X-RAY FLUORESCENCE (XRF) ACCURACY AND PRECISION 56
3.5 GRAIN SIZE ANALYSIS 59
3.6 HEAVY MINERAL SEPERATION 60
3.7 OSTRACODE ANALYSIS 60
3.8 DATA ANALYSIS, INTERPRETATIONS AND PRESENTATION 62
3.8.1 GIS maps of element distributions 62

4 RESULTS 63
4.1 MAHAWELI RIVER 63
4.1.1 Textural and mineralogical characteristics 63
4.1.2 Data description 64
4.1.3 Major element discriminates for sediment (bulk and fraction) rock and soil 70
4.1.4 Heavy Minerals 78
4.2 POLGOLLA DAM 86
4.2.1 Surface and Core Sediments 86
4.3 TRINCOMALEE BAY 87
4.3.1 Surface Sediments 87
4.3.1.1 Texture 88
4.3.1.2 Major elements 90
4.3.1.3 Trace elements 95
4.3.1.4 Principal Component Analysis 98
4.3.2 Core sediments 102
4.3.2.1 Texture 105
4.3.2.2 Major elements 108
4.3.2.2.1 Core One (1C) 108
4.3.2.2.2 Core Two Three and Four (2C, 3C, 4C) 108
4. 3.2.3 Trace elements 109
4.3.2.3.1 Core One (1C) 109
4.3.2.3.2 Core Two, Three and Four (2C, 3C, 4C) 110

4. 3.2.4 Heavy Minerals 110
4.3.3 Ostracode 111
4.3.3.1 Grain size 111
4.3.3.2 TN and TOC contents 112

5 DISCUSSION 115
5.1 MAHAWELI RIVER 115
5.1.1 Provenance indicators 115
5.1.2 Sorting 121
5.1.3 Heavy mineral indicators 124
5.1.4 Climatic zone variation and weathering 126
5.1.5 Tributary effect 131
5.1.6 Environmental effects 132
5.1.7 Heavy Minerals 134
5.1.7.1 Fractional variations of heavy minerals 134
5.1.7.2 Downstream chemical variation 137
5.1.7.1.1 Variation of Zr, Th, Nb 137
5.1.7.1.2 Variation of Ferromagnesian elements - TiO_2, Fe_2O_3, Sc, V, Ni and Cr ,Y 139
5.1.7.1.3 Large ion lithophile elements - CaO, P_2O_5, Sr 143
5.1.7.1.4 Chalcophile elements - As, Pb, Zn, Cu 144
5.1.7.3 Proportionate tributary contributions 145
5.1.8 Major Elements and its geochemical assessment for sediments rock and soil 147
5.2 POLGOLLA DAM 158
5.2.1 Surface processes 158
5.2.2 The upper catchments of Mahaweli River 159
5.2.3 The Polgolla reservoir core sediments 160
5.3 TRINCOMALEE BAY 161
5.3.1 Surface Sediments 161
5.3.1.1 UCC-normalized geochemical characteristics 161
5. 3.1.2 Source rock signatures 163

5. 3.1.3 Hydraulic sorting and heavy minerals 165
5. 3.1.4 Spatial geochemical variations 167
5. 3.1.5 Present environmental status 171
5.3.2 Core sediments 175
5. 3.2.1 Variation of elements in four cores and its environments 175
5. 3.2.2 Heavy mineral concentration in core one 177
5. 3.2.3 Provenance indicators and maturity 177
5.3.4 Ostracode assemblages in Trincomalee Bay 180

6 CONCLUSIONS OF MAHAWELI RIVER AND TRINCOMALEE BAY SYSTEM 187
6.1 Mahaweli River 187
6.2 Mahaweli river fractions and heavy minerals 188
6.2.1 Climate, weathering, downstream accumulation, sorting and Transport 188
6.2.2 Heavy minerals and chemical fractionation 188
6.3 Polgolla Dam 189
6.4 Trincomalee Bay surface sediments 189
6.5 Trincomalee Bay core sediments 190
6.6 Ostracode of Trincomalee Bay 191

KUMA RIVER AND YATSUSHIRO BAY SYSTEM-JAPAN

7 INTRODUCTION TO THE KUMA RIVER AND YATSUSHIRO BAY SYSTEM 192
7.1.1 Introduction to Kuma River 192
7.1.2 Introduction to Yatsushiro Bay 194
7.2 BACKGROUND 195
7.3 SCOPE OF THE RESEARCH 195
7.4 OBJECTIVE OF THE STUDY 195
7.4.1 Kuma River and Arase Dam 195
7.4.2 Yatsushiro Bay 196
7.5 EXPECTED OUTCOME 196
7.6 GEOLOGY OF KYUSHU 196

7.7 GENERAL INFORMATION OF THE PROJECT AND PROJECT AREA 197
7.7.1 Location and Accessibility 197
7.7.2 Historical Perspective of Water Resource Management in the Kuma River 197
7.7.3 Historical activities in the Yatsushiro Bay 197
7.7.4 Physiography and Geology 197
7.7.4.1 Kuma River area 197
7.7.4.2 Yatsushiro Bay area 200
7.8 DAM CONSTRUCTION AND DESTRUCTION 203
7.9 SUSPENDED SOLIDS AND SEM OBSERVATION 203
7.10 WATER QUALITY 204
7.11 PREVIOUS WORK AND BACKGROUND 206

8 METHOD OF STUDY 207
8.1 INCEPTION AND BASE DATA COLLECTION 207
8.2 FIELD SAMPLING 207
8.2.1 Kuma River sediment samples 207
8.2.2 Kuma River Core sediments 208
8.2.3 Yatsushiro Bay sediments 208
8.2.4 Suspended solids and SEM 208
8.2.5 Water quality analysis 209
8.3 SAMPLE PREPARATION 209
8.3.1 Sediment samples 209
8.4 GRAIN SIZE ANALYSIS 209

9 RESULTS 210
9.1 Kuma River and Arase dam 210
9.2 Yatsushiro Bay Tidal flat 216
9.3 Suspended solids and SEM in the Kuma River and Yatsushiro Bay 216
9.4 Water Quality of Kuma River and Yatsushiro Bay 217

10 DISCUSSION 221

10.1 Kuma River and Arase dam 221

10.1.1 Surface and bottom sediment chemical variation and grain size 221

10.1.2 Composition change since 2002 223

10.1.3 Fine (0.075-0.25mm) and medium (0.25-0.85mm) fraction 226

10.2 Yatsushiro Bay and Tidal flat 231

10.2.1 Environmental change between 2002 and the present 231

10.2.2 Grain size 236

10.2.3 Water environment 237

10.2.4 Scanning electron microscope analysis 238

11 CONCLUSIONS OF KUMA RIVER AND YATSUSHIRO BAY SYSTEM 240

11.1 Kuma River 240

11.2 Yatsushiro Bay 240

12 SYNTHESIS 242

13 REFERENCES 244

Appendix 280

List of Figures

Fig 1.6.1:	Alteration cover (alterite + soil) in relation to atmosphere and continental biosphere (Pedro, 1985)	8
Fig 1.6.2:	Lateritic profile of a tropical soil (Melfi et al., 1999)	8
Fig 1.6.3:	Mineral weatherability (decreasing from top to bottom)	10
Fig 1.6.4:	$\sum CO_2$ (Carbonate species) versus pH - $\sum CO_2$ = 10-3 mol/l	13
Fig 2.1.1:	Simplified geological and climatic map of Sri Lanka (after Cooray, 1994), showing location of the Mahaweli River and the Walawe Basin	23
Fig 2.1.2:	Location of sediment, rock, and soil sample sites along the Mahaweli River and distribution of the wet, intermediate and dry climatic zones in the study area	24
Fig 2.1.3:	Location map of the upper catchment of Mahaweli River and the Polgolla Reservoir	27
Fig 2.1.4:	Location of Trincomalee Bay, and sample sites within the Inner Harbour (IH), Thambalagam Bay (TB) and Koddiyar Bay (KB)	29
Fig 2.6.1:	Mahaweli River of Sri Lanka also showing the other rivers of the country	36
Fig 2.6.2:	Map showing the Mahawelli River and the elevation of the basin area	39
Fig 2.6.3:	Map showing the geology of the Mahawelli River- upper reaches	40
Fig 2.6.4:	Simplified geological map of the area surrounding Trincomalee Bay (after Wijayananda 1985)	42
Fig 2.7.1:	Map showing the climatic zones of Sri Lanka	47
Fig 3.1.1 :	Rock sampling locations along the Mahaweli River	51
Fig 3.1.2 :	Soil sampling locations along the Mahaweli River	52
Fig 3.2.1:	Trincomalee core sediment locations and the simplified geological map of the area surrounding Trincomalee Bay (after Wijayananda 1985)	54
Fig 3.2.2:	Photographs of the four cores in Trincomalee bay and variation in grain size and TS (Total Sulphur)	55
Fig 3.3.1:	Map showing the locations selected for Ostracode analysis in Trincomalee bay	61

Fig 4.1.1:	Variation in stream sediment size fractions along the Mahaweli River	64
Fig 4.1.2a:	PAAS-normalized averages for the sediments, soils and basement rocks of the Mahaweli River	70
Fig 4.1.2b:	Fine/Sand-normalized averages for the sediments of the Mahaweli River	71
Fig 4.1.2c:	Selected major oxide–Al_2O_3 variation diagrams for the <180µm and 180-2000µm feactions, rock and soils of the Mahaweli River sediments	72
Fig 4.1.3:	Total heavy mineral weight percent of eighteen selected samples along the main stream and selected tributaries	82
Fig 4.1.4a:	The magnetite content along the Mahaweli River	84
Fig 4.1.4b:	Frantzed heavy mineral count plot of selected eighteen locations along the Mahaweli River after taking out the magnetite	85
Fig 4.3.5:	Contour maps showing the spatial variation of (a) mean grain size and (b) sorting in Trincomalee Bay	89
Fig 4.3.6:	Selected major oxide–Al_2O_3 variation diagrams for Inner Harbour (IH), Thambalagam Bay (TB) and Koddiyar Bay (KB) surface sediments, compared to UCC	95
Fig 4.3.7:	Selected trace element–Al_2O_3 variation diagrams for Inner Harbour (IH), Thambalagam Bay (TB) and Koddiyar Bay (KB) surface sediments, compared to UCC	97
Fig 4.3.8:	Selected elemental variation of core one from Trincomalee Bay	103
Fig 4.3.9:	Selected elemental variation of core two, three and four from Trincomalee Bay	104
Fig 4.3.10:	Distribution of (a) water depth (b) median grain size, (c) total nitrogen content and (d) total organic carbon content of surface sediments in Trincomalee Bay	112
Fig 5.1.1:	Plots of (a) Y, (b) Nb, (c) Zr and (d) Sc versus Th for the bulk stream sediments, rocks and soils	116
Fig 5.1.2:	Zr/Sc–Th/Sc ratio plots (McLennan et al., 1993) for (a) stream sediments, basement rocks and soils from the Mahaweli River, showing zircon concentration (arrow) and typical source rock compositions; (b) <180 µm	

and 180 – 2000 μm fractions 118

Fig 5.1.3: (a) Cr-Ni plot for the Mahaweli stream sediments, rocks and soils, showing the Post-Archean field (Taylor and McLennan, 1985) and fractionation from source rocks to the sediments. (b) and (c): Cr/V-Y/Ni plots (McLennan et al., 1993) for the stream sediments, rocks and soils (b); and <180 μm and 180 - 2000 μm fractions (c), showing the lack of ultrabasic sources 120

Fig 5.1.4: Fe_2O_3–TiO_2 plots for (a) bulk stream sediments, rocks and soils, and (b) the <180 μm and 180 - 2000 μm fractions, illustrating hydraulic fractionation and heavy mineral concentration. MC – main channel; TB – tributaries; LM – lower main channel 123

Fig 5.1.5: Plots of (a) Y, (b) Nb, and (c) Zr versus Th for the <180 μm and 180 – 2000 μm fractions 125

Fig 5.1.6: (a) Al_2O_3/K_2O+Na_2O (b) K_2O/Na_2O ratios in bulk sediments down the Mahaweli River showing the weathering trend with the climatic zones. (c) Loss On Ignition of soils down the Mahaweli River 128

Fig 5.1.7: Variation in CaO and Sr abundances in bulk stream sediments down the Mahaweli River, also showing tributary entries and the climatic zones 129

Fig 5.1.8: (a) Variation in Cr/V ratios in <180μm and Cr 180 - 2000 μm fractions in sediments down the Mahaweli River, also showing tributary entries and the climatic zones. (b) Cr/V Enrichment Factor (Cr/V_{EF}) downstream, derived by normalizing Cr/V in the 180 - 2000 μm fraction against Cr/V in the <180μm fraction 130

Fig 5.1.9: Fe-normalized enrichment factors for (a) As, Pb, and Zn, and (b) Cu, Ni, and Cr down the Mahaweli River, also showing tributary entries and the climatic zones 134

Fig 5.1.10: Variation of magnetite content and Frantzed amp separates (wt%) along the Mahaweli River (a, b): 63-180 μm fraction, (c, d): 180-300μm fraction 136

Fig 5.1.11: EF of the <180 μm (E_F – For fine fraction) and 180 – 2000 μm (E_C - For coarse fraction) sediment fractions for Zr, Th and Nb 139

Fig 5.1.12: EF of the <180 µm (E_F – For fine fraction) and 180 - 2000 µm (E_F – For coarse fraction) sediment fractions for ferromagnesian elements (Ti, Fe, Sc, Ni) and Y 141

Fig 5.1.13: EF of the <180 µm (E_F – For fine fraction) and 180 - 2000 µm (E_F – For coarse fraction) sediment fractions for ferromagnesian elements (V , Ni) and Cr 143

Fig 5.1.14: EF of the <180 µm (E_F – For fine fraction) and 180 - 2000 µm (E_F – For coarse fraction) sediment fractions for large ion lithophile elements (Ca, P, Sr) 144

Fig 5.1.15 : EF of the <180 µm (E_F – For fine fraction) and 180 - 2000 µm (E_F – For coarse fraction) sediment fractions for Chalcophile elements (As, Pb, Zn, Cu) 145

Fig 5.1.16 : Al_2O_3/SiO_2 – Basicity index SiO_2/Al_2O_3 – Basisity index plots for the <180µm, 180- 2000µm sediment fractions, rocks and soils of the Mahaweli river basin 147

Fig 5.1.17a : A–CN–K plot (Nesbitt & Young 1984) for the Rock Soils and sediment fractions of the Mahaweli River 149

Fig 5.1.17b : A–CN–K plot (Nesbitt & Young 1984) for the (a) sediment fractions (b) soils and rocks of the Mahaweli River 149

Fig 5.1.17c: A–CN–K plot (Nesbitt & Young 1984) for the Rock Soils and sediment fractions of the Mahaweli River for the three climatic zones 150

Fig 5.1.18a: (A–K)–C–N plot (Fedo et al. 1997) for the Rock Soils and sediment fractions of the Mahaweli River for the three climatic zones 151

Fig 5.1.18b: (A–K)–C–N plot (Fedo et al. 1997) for the (a) sediment fractions (b) soils and (c) rocks of the Mahaweli River 152

Fig 5.1.18c: (A–K)–C–N plot (Fedo et al. 1997) for the Rock Soils and sediment fractions of the Mahaweli River for the three climatic zones 152

Fig 5.1.19a: Mafics ternary plot of A-CN-K (Nesbitt and Young 1984) and A-CNK-FM (Nesbitt and Young 1989) for the sediment factions, soils and rocks of Mahaweli River and its catchment 153

Fig 5.1.19b: Mafics A-CNK-FM ternary plot of Nesbitt and Young (1984) 154

Fig 5.1.20a : SAM-plot (after Kroonenburg, 1994) for the sediment factions, soils and rocks of the Mahaweli River and its catchment 155
Fig 5.1.20b : SAM-plot (after Kroonenburg, 1994) for the sediment factions, soils and rocks of the Mahaweli River and its catchment based on climatic zones 155
Fig 5.1.21a : MFW ternary plot (Ohta and Arai, 2007) for the sediment factions, soils and rocks of the Mahaweli River and its catchment 156
Fig 5.1.21b : MFW ternary plot (Ohta and Arai, 2007) for the sediment factions, soils and rocks of the Mahaweli River and its catchment 157
Fig 5.1.21c : MFW ternary plot (Ohta and Arai, 2007) for the sediment factions, soils and rocks of Mahaweli River and its catchment based on climatic zones 157
Fig 5.2.1: Graphs of Fe_2O_3 and As, Pb, Zn and Cu for the upper catchment of Mahaweli River and Polgolla reservoir 160
Fig 5.2.2: Vertical distribution of As, Fe_2O_3, Zn, Total sulfur (TS), Pb, Cu, Sr CaO and P_2O_5 of the Polgolla reservoir 161
Fig 5.3.1: UCC-normalized averages for the Trincomalee Bay sediments, compared to average lower Mahaweli River sediment (data from Young et al. 2012) 163
Fig 5.3.2: (a) Zr/Sc–Th/Sc (McLennan et al. 1993) and (b) Zr/Ti-Th/Ti (Roser et al. 2000) plots for the Trincomalee Bay sediments 164
Fig 5.3.3: (a) Fe_2O_3–TiO_2 and (b) TiO_2–Zr plots for the Trincomalee Bay data, illustrating hydraulic fractionation and heavy mineral concentration 166
Fig 5.3.4: GIS contour maps for (a) Al_2O_3, (b) K_2O, (c) Th, (d) Nb, (e) Y and (f) Sc showing spatial elemental distribution within Trincomalee Bay 169
Fig 5.3.5: GIS contour maps for (a) Cr, (b) V, (c) Ni, (d) Ce, (e) Zr and (f) TiO_2 showing spatial elemental distribution within Trincomalee Bay 170
Fig 5.3.6: GIS contour maps for Enrichment Factor (EF) for (a) As, (b) Zn, (c) Pb, (d) Cu, (e) Ni, and (f) Cr showing spatial distribution within Trincomalee Bay 174
Fig 5.3.7: Zr/Sc–Th/Sc ratio plots (McLennan et al., 1993) for the four cores From Trincomalee Bay, showing zircon concentration (arrow) and typical source rock compositions 178
Fig 5.3.8: Cr/V-Y/Ni plots (McLennan et al., 1993) for the four cores from

Trincomalee Bay, showing the lack of ultrabasic sources 179
Fig 5.3.9: MFW ternary plot for igneous rocks and weathering profiles 180
Fig 5.3.10: Dendrogram showing the result of Q-mode cluster analysis 182
Fig 5.3.11: Scanning electron micrographs of ostracodes from Trincomalee Bay used for the Q-mode cluster analysis 184
Fig 5.3.12: Distribution of ostracode density (a), diversity (b), equitability (c), and biofacies (d) in Trincomalee Bay 185
Fig 7.1.1: Geology of the Kuma River and sampling locations in Kumamoto prefecture, Kyushu Island, Japan 193
Fig 7.1.2: Schematic diagram showing Arase dam removal starting from April 2010 to 2017 199
Fig 7.1.3: Simplified geological map and sediment sampling locations of the Kuma River and the Yatsushiro tidal flat 200
Fig 8.1.1: Grain size variation of the (a) fine (0.25-0.005mm) and (b) medium (0.25-2mm) fractions of surface and bottom sediments 208
Fig 9.1.1: (a) Zn-Fe_2O_3 (b) TiO_2-Fe_2O_3 (c) P_2O_5-As (d) Zr-Th plots showing provenance and environmental status for bottom and surface sediments 211
Fig 9.1.2: (a) Cumulative grain size of surface sediments (b) Locations that do not follow the normal cumulative grain size curve of surface sediments (c) Cumulative grain size of bottom sediments (d) Locations that do not follow the normal cumulative grain size curve of bottom sediments 215
Fig 9.1.3: Grain size variation of the (a) fine (0.25-0.005mm) and (b) medium (0.25-2mm) fractions of surface and bottom sediments 216
Fig 10.1.1: (a) Cu-mean grain size (b) Ni- mean grain size (c) Zr- mean grain size (d) TiO_2- mean grain size for the Kuma River and Yatsushiro Bay surface and bottom sediments 223
Fig 10.1.2: (a) Non - Provenance elements cluster analysis plot (b) Provenance elements cluster analysis plot of the Kuma River sediments 226
Fig 10.1.3: (a)-(l) Elemental difference of the fine and medium fraction along the Kuma River and Yatsushiro Bay 229
Fig 10.1.4: Plots of (a) As, (b) Pb, (c) Zn versus Fe_2O_3 and (d) P_2O_5 versus TS for Kuma

River and Yatsushiro Bay sediments 232
Fig 10.1.5: (a) Cr-Ni plot and (b) Fe_2O_3–TiO_2 plot showing the mafic contribution and the sorting effect 234
Fig 10.1.6: MnO and Fe_2O_3 plots showing redox conditions of the Yatsushiro tidal flat, compared with 2006 data for the Ariake and Sirunai area 235
Fig 10.1.7: Cumulative grain size variation of Kuma River and Yatsushiro Bay sediments 235
Fig 10.1.8: SEM images of diatoms (a, b, c) in suspended solids of the Kuma River and Yatsushiro Bay. (d) Salt crystals and diatoms 237
Fig 12.1.1 : Mass transfer processes in the (a) Mahaweli River and Trincomalee Bay system (b) Kuma River and Yatsushiro Bay system 245

List of Tables

Table 1.1 : Trace elements in oxic and anoxic sediments from the Oslo Fjord (in ppm except where noted) 20

Table 4.1.1a: XRF analyses of Mahaweli River bulk stream sediments. Major elements as oxide wt%, trace elements ppm 66

Table 4.1.1b: XRF analyses of soils from the Mahaweli River basin. Major elements as oxide wt%, trace elements ppm 67

Table 4.1.1c: XRF analyses of basement rocks from the Mahaweli River basin. Major elements as oxide wt%, trace elements ppm 68

Table 4.1.2: Average, minimum and maximum values for bulk stream sediments, basement rocks, soils and tributaries of the Mahaweli River basin compared to the PAAS values of Taylor and McLennan (1985) 69

Table 4.1.3a : Major element composition for bulk sediment of the Mahaweli River Sediments 74

Table 4.1.3b: Major element composition for <180 µm fraction of the Mahaweli River sediments 75

Table 4.1.3c : Major element composition for 180- 2000 µm fraction of the Mahaweli River sediments 76

Table 4.1.3d : Major element composition for basement rocks of the Mahaweli River sediments 77

Table 4.1.3e : Major element composition for soils of the Mahaweli River sediments 77

Table 4.1.4a: Analyses of Mahaweli River <180 µm fraction stream sediments. Major elements as oxide wt%, trace elements are in ppm 80

Table 4.1.4b: Analyses of Mahaweli River 180 - 2000 µm fraction stream sediments 81

Table 4.1.5a: Frantzed magnetic separate heavy mineral weight percent 63-180 µm fraction 83

Table 4.1.5b: Frantzed magnetic separate heavy mineral weight percent 180 - 2000 µm fraction 84

Table 4.1.5c: Individual XRF analyses of the core sediments of Polgolla reservoir 86

Table 4.1.6: Individual XRF analyses of the surface sediments of Polgolla

	reservoir	87
Table 4.3.1	Average, minimum and maximum elemental concentrations in the three sectors of Trincomalee Bay, compared to sediments from the lower Mahaweli River	88
Table 4.3.2:	Individual XRF analyses and texture of sediments from Trincomalee Bay, Sri Lanka	92
Table 4.3.3:	Average metal contents in the Trincomalee Bay sediments compared to Established pollution guidelines and UCC	93
Table 4.3.4:	Statistical Analyses. (A) Correlation matrices for the Inner Harbour, Thambalagam Bay and Koddiyar Bay datasets	94
Table 4.3.5:	Principal Component Analysis. PCA plots for all data analyzed and factor 1 and 2 loadings for (a) Inner Harbour (b) Thambalagam Bay (c) Koddiyar Bay	100
Table 4.3.6:	Individual XRF analyses and texture of core one (C1) sediments from Trincomalee Bay, Sri Lanka	106
Table 4.3.7:	Individual XRF analyses and texture of core two (C2), three (C3) and four (C4) sediments from Trincomalee Bay, Sri Lanka	107
Table 4.3.8 :	Sample information and results of grain size and CN analyses	111
Table 4.3.9:	List of ostracodes from the Trincomalee Bay. Solid stars show species and samples used for quantitative analyses	113
Table 5.1.1:	Analyses of basement rocks from the Mahaweli River basin	121
Table 5.1.2:	Average, minimum and maximum values for the bulk stream sediments, basement rocks, soils and tributaries of the Mahaweli River basin	126
Table 5.1.3:	Calculated EF values for fine and coarse fraction of the Mahaweli River and its tributaries	138
Table 5.2.1:	Geoaccumulation index for the upper catchment of Mahaweli River and Polgolla reservoir	159
Table 5.2.2:	Geoaccumulation index (Muller, 1979) of heavy metal concentration in sediments	159
Table 7.1.1:	Elemental concentrations, Loss on Ignition (LOI), Md50 (median grain size) and sorting of surface and bottom sediments, Kuma River and	

	Yatsushiro Bay	202
Table 9.1.1:	Elemental concentrations of fine (0.075 – 0.25mm) and medium (0.25-0.85mm) grained sediments of the Kuma River and Yatsushiro Bay	213
Table 9.1.2:	Grain size analysis data from the Kuma River and Yatsushiro Bay	214
Table 9.2.1:	XRF analyses of Kuma River and Yatsushiro Bay bulk sediments	218
Table 9.2.2:	Analyses of Kuma River and Yatsushiro Bay suspended solids	219
Table 9.2.3:	Physical and chemical properties of sediments and water from the Kuma River and Yatsushiro Bay	220
Table 12.1.1:	The synthesis of the Mahaweli River and Trincomalee Bay System and the Kuma River and Yatsushiro Bay System	244

CHAPTER 1

INTRODUCTION: MASS TRANSFER PROCESS AND THEIR POTENTIAL IMPACTS ON TERRESTRIAL AND MARINE ENVIRONMENTS

1.1 GEOCHEMISTRY OF STREAM SEDIMENTS AND BAY ENVIRONMENT

The composition of clastic sediments and rocks is controlled by a complex suite of parameters operating during pedogenesis, erosion, transport, deposition and burial (Johnsson, 1993). The principal first-order parameters include source rock composition, modification by chemical weathering, mechanical disaggregation and abrasion, authigenic inputs, hydrodynamic sorting, and diagenesis (Johnsson, 1993). Each of these first-order parameters is influenced to varying degrees by such factors as transportational system and depositional environment, climate, vegetation, relief, slope, and the nature and energy of transportational and depositional systems. These factors are not independent, rather they are a complicated web of interrelationships and feedback mechanisms cause many factors to be modulated by others. Deferential weathering, hydraulic sorting and dissimilar dissolution during diagenesis, skew the distribution of heavy minerals in sands and sandstones relative to their distribution in parent rocks (Basu and Molinaroli, 1991).

The main processes involved in the Mahaweli River and Trincomalee Bay sediment environments are; transport, sorting, erosion, weathering, deposition, heavy minerals, tributary input and climate. The Kuma River and Yatsushiro Bay involves erosion, deposition, sorting and transport.

1.2 PROVENANCE

It is well known that part of the tectonic and climatic and magmatic history of continents is retained in detrital sediments. Detrital sediments may be the only record available of crust that has been removed by erosion, covered with younger deposits or ice, or buried deep in the crust.

1.3 IMPORTANCE OF PROVENANCE STUDIES

The abundance of chemical elements has been used in defining sediment sources, elucidating mechanisms of formation of the sediments, estimating abundance of different components, quantifying authigenic deposition rates and fluxes of various elements, and in understanding depositional environments (Goldberg and Arrhenius, 1958; Krishnaswami, 1976; Graybeal and Heath, 1984; Thomson et al., 1984; Toyoda and Masuda 1990; and references therein). Riverine transport of minerals provides important information on the cycling of elements on Earth, and on the contribution of continental crust to the oceanic sedimentation. In most cases fluvial input is the major source of minerals to the ocean. Suspended mineral phases in rivers are sensitive to environmental changes caused by natural processes and human activities and therefore may be useful indicators of events which last long enough to exhibit their effects to the environment.

Trace elements such as Y, Sc, Cr, Th, Zr, Nb, and particularly TiO_2 among other major elements are best suited for provenance and tectonic setting determination studies, because of their relatively low mobility during sedimentary processes (McLennan et al., 1983). In addition, the relative distribution of the immobile elements that differ in concentration in felsic and basic rocks such as Th (enriched in felsic rocks) and Sc, and Cr (enriched in basic rocks relative to felsic rocks) has been used to infer the relative contribution of felsic and basic sources in shales from different tectonic environments (Wronkiewicz and Condie, 1990).

1.4 SEDIMENTARY PROVENANCE

1.4.1 Stream sediments

Stream sediments are composites of the lithologies present in their drainage basins, and thus provide a mechanism for mapping regional geochemical characteristics of their source terranes (Ottesen & Theobald 1994). However, the compositions of clastic sediments differ from those of their source rocks because of the combined effects of a number of interacting factors that operate between source and sediment. These factors include weathering, hydrodynamic sorting, heavy mineral concentration, alluvial storage and many others. Johnsson (1993) gives a succinct review of the influence exerted by those factors.

1.4.2 Sandstone provenance

Many of the more recent developments concern sandstone provenance. The high level of interest in this area is mirrored by the predominance of papers dealing with sandstones in 1991. Since sandstones almost invariably comprise mixtures of source materials, sandstone provenance is often best tackled using a range of techniques rather than relying on any one method, an approach emphasized by Humphreys et al. (1991).

Conventional heavy mineral analysis has been revitalized by studies of compositional variation within a single mineral species, thus circumventing the detrimental effect of intrastratal solution, often the dominant control on subsurface heavy mineral distribution. Amphibole, pyroxene, epidote, staurolite, monazite, zircon, garnet, spinel, chloritoid, mica and tourmaline are all amenable to this sort of analysis and the development of the approach is discussed by Morton (1991), Basu and Molinaroli (1991) explore the use of the opaque heavy mineral phases often disregarded in provenance work. They show that detrital Fe-Ti minerals can retain a provenance record, although no individual character is diagnostic and diagenetic alteration can occur in some instances.

In addition to looking at sediment distribution, specific mineral compositions can have important petrogenetic implications for source areas. Detrital pyroxene and amphibole compositions can be used as petrogenetic tracers in volcaniclastic sequences (Cawood 1983 and 1991; Morris 1988; Styles et al. 1989), whilst certain white mica compositions and the presence of glaucophane can identify erosion of high pressure metamorphic rocks (Sanders and Morris 1978). Geochemical analysis of sandstones has largely concentrated on tectonic discrimination, following a suggestion by Crook (1974) that active and trailing margin sandstones might be distinguished on the basis of their SiO_2 content sand K_2O/Na_2O ratios. The advantage here is that geochemistry might allow the tectonic setting of metasediments to be identified despite the loss of original petrographic detail (assuming isochemical metamorphism). More complex multivariate techniques were accordingly developed using both major (Bhatia 1983, Roser and Korsch 1988) and trace element concentrations (Bhatia 1985; Bhatia and Crook 1986). As with all discriminant techniques, the methods are only as good as the data base used to erect them, and problems have been encountered distinguishing sediments from different plate settings e.g. Van der Kamp and Leake (1985). Reworking of older arcs can produce spurious arc chemistry.

McCann (1991) illustrates the problem of recycling by demonstrating how the provenance of Ordovician-Silurian sediments of the Welsh basin fails to reflect accurately the palaeotectonic setting of the area. An alternative way of utilizing sediment chemistry is the use of specific provenance tracers e.g. the high Cr and MgO contents of sediments with a significant ultramafic source. This approach has been used to trace the original distribution of Caledonian ophiolites with some success (Hiscott 1984; Wraeter and Graham 1989). The geochemistry of modern sands and soils (Cullers et al. 1988) can be used to evaluate provenance signatures in different tectonic and climatic settings. The text is taken from Haughton et al. 1991.

1.4.3 Mudrock provenance

In spite of being the most abundant sedimentary rock, logistical problems mean that mudrocks have been relatively poorly studied in terms of provenance. In principle, it is possible to study the constituent clay minerals by X-ray diffraction analysis and make some inference of provenance. However, the approach is in practice fraught with difficulties, not least the rapid diagenetic alteration of primary clay mineral species on burial (Humphreys et al. 1991). Although the primary mineralogy of mudrocks is easily modified, a useful axiom is to assume that the primary rock chemistry remains unaltered, allowing major, trace and isotopic analyses of mudrocks to discriminate provenance (Humphreys et al. 1991; McCann 1991). Blatt (1985) also recommends that greater attention be paid to the non-clay mineralogy of mudrocks.

Developments in REE and trace element geochemistry, and isotopic techniques, have been particularly important in fine-grained rocks, and have also been widely used in sandstone provenance work. The uniformity of REE patterns in post-Archaean shales has been used to estimate the composition of the upper crust, and to contrast this with an Archaean upper crustal composition revealed by distinct REE patterns for sediments in that era (Taylor and McClennan 1985). Various ratios of the REE, Th and Sc in pelites exhibit secular changes across the Archaean-Proterozoic boundary and these have been related to a worldwide change in upper crustal composition at this time (Condie and Wronkiewicz 1990).

From a provenance perspective, several aspects of the procedure are pertinent. First, the residence age returned by sediment is a weighted average of the different source contributions. Petrographic or other constraints on the mixture of various components present may aid

interpretation (Nelson and DePaolo 1988; Evans et al. 1991; Floyd et al. 1991). Secondly, fractionation of REEs, by hydraulic segregation and concentration of heavy minerals or pumaceous lithic fragments may occur in some sandstones (Frost and Winston 1987; McLennan et al. 1989) and may bias residence ages. No significant fractionation according to grain-size occurs in other sequences (Mearns et al. 1989). Thirdly, the behaviour of the REEs during diagenesis needs to be further investigated. Milodowski and Zalasiewicz (1991) identify REE mobilization and fractionation during diagenesis of a mud-dominated turbidite-hemipelagic sequence. The third factor is not related to the current study, and thus is not further described. The text is taken from Haughton et al. 1991.

1.5 MATURITY OF SEDIMENTS

Sediment Maturity refers to the length of time that the sediment has been in the sedimentary cycle. Texturally mature sediment is sediment that is well rounded, (as rounding increases with transport distance and time) and well sorted (as sorting gets better as larger clasts are left behind and smaller clasts are carried away. Because the weathering processes continues during sediment transport, mineral grains that are unstable near the surface become less common as the distance of transport or time in the cycle increases. Thus compositionally mature sediment is composed of only the most stable minerals.

Four stages of textural maturity in sediments are defined by the occurrence of three sequential events (1) removal of clays, (2) sorting of the sand fraction, and (3) attainment of high roundness (Folk, 1951).

This concept proposes that, as sediments suffer a greater input of mechanical energy thorugh the abrasive and sorting action of waves or currents, they pass sequentially through the following four stages (Folk, 1974):

I. Immature stage. Sediment contains over 5 percent terrigenous clay matrix; sand grains usually poorly sorted and angular.

II. Submature stage. Sediment contains under 5 percent clay, but sand grains are still poorly sorted (σ over 0.5~Φ) and are not well rounded.

Ill. Mature stage. Sediment contains little or no clay, and sand grains are well sorted (σ under 0.5~Φ), but still not rounded.

IV. Supermature stage. Sediment contains no clay, sand grains are well sorted and well rounded (Waddell roundness over .35; ρ over 3.0). This determination should be made, if possible, on quartz grains of medium and fine sand size.

Textural maturity is thus one of the most important keys to the physical nature of the environment of deposition, since it provides a descriptive scale that indicates the effectiveness of the environment in winnowing, sorting, and abrading the detritus furnished to it. Thus immature sediments accumulate in loci such as flood plains, alluvial fans, or neritic or lagoonal environments where current action is either weak or deposition is very rapid so that sediments do not have a chance to be subjected to input of any mechanical energy after deposition. Supermature sediments, on the other hand, indicate deposition in loci of intense abrasion and sorting, such as beaches or desert dunes, where energy is constantly being expended on the grains.

It is established that the bulk chemical composition of sandstone and siltstone facies are indication of paleo climate in terms of its chemical maturity. Chemically maturity can be expressed in terms of the SiO_2 contents and the chemical maturity index (CMI). CIM is expressed as a ratio of SiO_2/Al_2O_3, by Peters (1978). High SiO_2/Al_2O_3 ratio and high silica content (> 80%) of sediments indicate that they are derived from a deeply weathered source, and now have silica contents comparable to quartz arenites (Suttner and Dutta, 1986, Fakolade and Obasi, 2012).

Major oxide analyses provide an indirect but quantitative estimate of mineralogy, where key oxides serve as proxies for common minerals found in sand. Examples include SiO_2 (quartz), K_2O (K-feldspar), Na_2O (plagioclase), Al_2O_3 (all feldspars) and CaO and MgO (carbonates). Thus, SiO_2 is reflective of quartz content and the $Al_2O_3 + Na_2O + K_2O$ is reflective of feldspar content.

1.6 WEATHERING

Weathering is a process characterized mainly by physical disaggregation and chemical decomposition of rocks transforming structures of more complex minerals in others with simpler structures. The transformation of tectosilicates (feldspars) in 1:1 phylosilicates represents well this process. At the same time the neoformation of minerals such as kaolinites, iron oxides (goethite, hematite), aluminum oxides-hydroxides (gibbsite, boehmite) which are stable at low temperature and pressure (25^0C, 1 atm) replacing higher temperature and pressure minerals is also representative of supergene alteration.

The supergene alteration is dependent upon climate (rainfall and temperature), topography, nature of rock (fissural system, texture and composition), influence of biosphere and controlled by drainage conditions of the profile.

The hydrolysis of silicates is the most important process during the weathering. For example:

$$2KAlSi_3O_{8s,c,K\text{-feldspar}} + 11H_2O_l = 4H_4SiO4_{aq} + Al_2Si_2O_5(OH)_{4s,c,kaolinite} + 2K^+_{aq} + 2OH^-_{aq}$$

s = solid; c = crystalline; aq = aqueous; l = liquid

Hydrolysis of silicates is characterized by increasing of pH (OH^-), leaching of alkaline and earth alkaline cations and the partial or total leaching of H_4SiO_4. The formation of kaolinite means a partial leaching of H_4SiO_4.

The supergene alteration of rocks produces “alterites” (Fig. 1.6.1 and 1.6.2). Alterites are constituted by neoformed supergenic minerals plus some primary minerals from preexisting rocks. (Fig. 1.6.1; Pedro 1985 in Melfi et al., 1999).

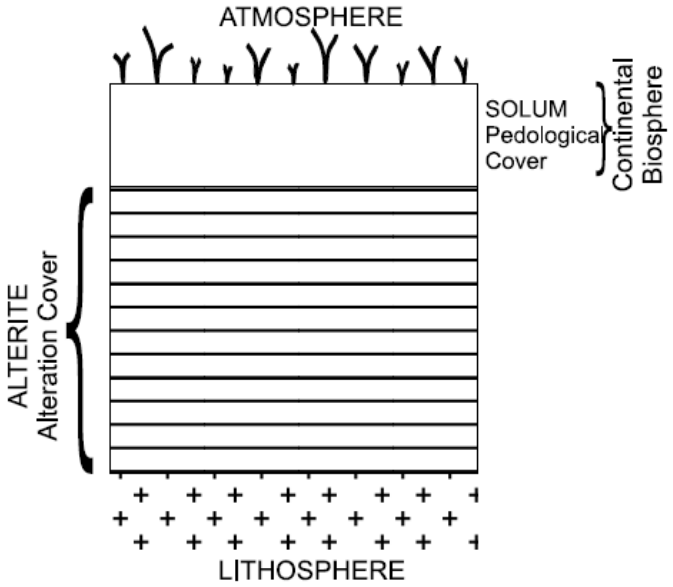

Fig. 1.6.1: Alteration cover (alterite + soil) in relation to atmosphere and continental biosphere (Pedro, 1985).

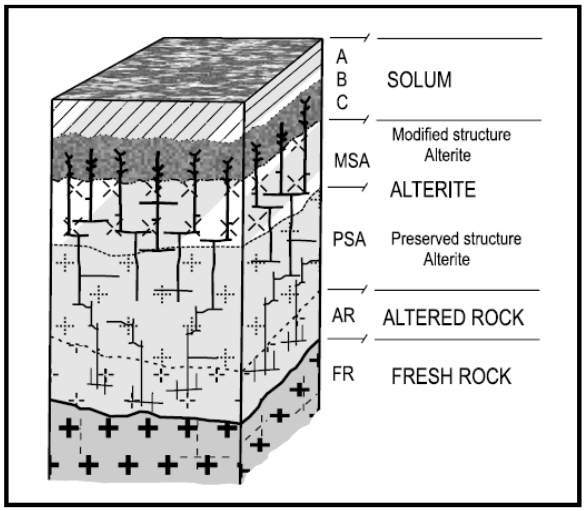

Fig: 1.6.2 Lateritic profile of a tropical soil (Melfi et al., 1999)

1.6.1 Chemical weathering of minerals

In principle, all minerals can undergo destruction by weathering but normally the primary minerals are less resistant than the secondary ones. Minerals can be listed according to their

degree of resistance to weathering. Fig. 1.6.3 displays a list of minerals in order of increasing resistance to weathering.

Note: The exact position of minerals depends upon grain size, environmental conditions. Secondary minerals are at the bottom of the list as it could be expected. (Loughnan, 1969; Carrol, 1970; Berner and Berner, 1996).

The weathering of silicates especially their dissolution is not clearly explained. Muir and Nesbitt (1992), concluded that silicate dissolution occurs by means of a protective layer of altered composition which inhibits the migration of dissolved species to and from the surface of the mineral (Berner and Berner 1996). However, detailed studies showed that the existence of the protective layer could not be proved. It seems more reasonable that most silicate react with soil solutions not as a homogeneous process but more as a selective etching controlled by crystallographical directions (dislocations) on the mineral surface (Nahon, 1991). In general different chemical compositions and the formation of etch pits (feldspars, pyroxenes and amphiboles) control the dissolution of minerals. Holdsen and Berner (1979) and Meunier (2003) present a discussion on the dissolution of primary phases during the supergene alteration. Meunier (2003) emphasizes that the dissolution starts by the more energetic sites: surface, edges and vertices. The supergene alteration advances under corrosion zones formed by the coalescence of dissolution of materials at the sites of dissolution.

Pyrite
Calcite
Dolomite
Olivine
Ca – plagioclase
Pyroxenes
Ca – Na plagioclase
Amphiboles
Biotite
K – feldspar
Muscovite
Smectite
Quartz
Kaolinite
Gibbsite, hematite

Fig: 1.6.3 Mineral weatherability (decreasing from top to bottom)

1.6.2 Biological weathering

Although the weathering of rocks is both a mechanical and mainly a chemical process the biological influence is very important in the changes suffered by the rocks close to the surface. Acids produced around the roots of living plants and by the bacterial decomposition of plants interact with rock minerals increasing the chemical alteration of those minerals.

The upper part of the soil is a zone of intense biochemical activity. The bacterial population near the surface is large but decreases downward with a steep gradient. The organic acids mainly those with low molecular weight attack silicate minerals which commonly dissolve incongruently.

For instance, an organic acid, as oxalic acid, dissociates to form H^+ ions:

$$H_2C_2O_{4aq} = 2H^+_{aq} + C_2O^{2-}_{4aq}$$

The H^+ ions attack the silicate liberating its constituent chemical species:

$$H^+_{aq} + 4H_2O_l + \text{silicate} = Al^{3+}_{aq} + Mn^+_{aq} + mH_4SiO_{4aq}$$

The $C_2O_2^{-4}$ reacts with Al^{3+} to form a chelate:

$$Al^{3+}_{aq} + C_2O^{2-}_{4aq} = Al(C_2O_4)^+_{aq}$$

This latter reaction is a dissolution reaction very common at the uppermost acid portion of most temperate soils.

Bacterial activity is responsible by the decomposition of the $Al(C_2O_4)^+$ and $H_2C_2O_4$. The oxalic acid and the oxalate are oxidized to CO_2 and HCO^{-3} and the Al^{3+} is liberated and precipitates as $Al(OH)_3$ or clay minerals. Thus the organic acids are responsible mainly by the low pH and formation of organic complexes. The process does not preserve the organic acid.

1.6.3 Weathering and soil formation

When alterite material comes into contact with air (atmosphere), water (hydrosphere) and biosphere (decomposing organic matter, living plants and animals; Fig. 1.6.1 and 1.6.2), becomes organized into structural patterns (soils) under the influence of the environmental conditions. Perhaps, climate is the principal control of soil formation. High rainfall and low temperature both favor the accumulation of organic debris in soils (Loughnan, 1969, Retallack, 1990). Retallack (1990) displays a soil classification with ten types of soils according to climate and evolution. For example, oxysol is considered a deeply weathered, reddish, kaolinite, clay-rich and iron-rich soil of tropical humid climates with almost no remaining primary minerals (formerly called laterites, lateritic soils, latosols). In tropical soils there is little burial of organic matter and there is still intense leaching of cations and silica due to heavier rainfall (> 2000 mm per year).

1.6.4 Waters, pH, Eh and Complex ions

Rain waters coming into contact with rocks (and derived soils) react with primary and secondary minerals or amorphous phases modifying the compositions of those waters. Rain waters increase their content of ions released from the rocks and organic matter from the biosphere constituting the soil waters. The composition of surface waters (in tropical and temperate areas) is represented by common cations Ca^{2+}, Na^+, Mg^{2+}, K^+ and normally the principal anion is HCO^-_3 . Activity of ions, pH, Eh, complex ions can control the composition of soil, surface and ground waters. In dilute solutions activities and concentrations are almost equal

because the activity coefficients are close to one ($a = \gamma m$; a = activity; m = concentration and γ = activity coefficient).

pH ($= -\log aH^+$) is controlled by the activity of various anions and cations. The

$$CO_2 = aH_2CO_3 + aHCO_3^- + aCO_3^{2-}$$

(or in dilute solutions the concentrations of those anions) is very important in controlling the pH. The presence of organic acids is also of great importance. There is a competition between the hydrolysis of silicates and the decomposition (bacterial or chemical decomposition) of organic material. Rain water is a dilute solution of carbonic acid and its pH is around 5.65 (without pollution). Rain water and surface waters coming into contact with rocks react with them which release cations, H_4SiO_4 and OH^- from the hydrolysis of silicates. Normally without the presence of organic matter and vegetation, the hydrolysis of silicates predominates and the pH is higher than 7. The OH^- predominates in comparison with organic acids and the pH is basic as happens in semiarid climates. In ground waters, the confined interaction between meteoric waters and rocks is still the most important factor and the influence of organic matter and products of its decomposition is much less important. The pH of ground waters is generally higher than 7. In surface waters (and in soil waters), the hydrolysis of silicates and the OH^- produced are neutralized by the CO_{2aq} and by the organic acids formed in soils from the decomposition of organic debris. The resultant pH is lower than 7, in general, between 5.5 and 7 without anthropic pollution. In organic layers of the podsols, the pH may reach 3.5. The industrial contamination increases the content of sulfuric and nitric acids of the rain water constituting the acid rain. Normally the acid rain waters destroy the buffering ability of HCO^-_3 leading to the decrease of pH of waters.

In sea water, there is also a competition between the acid volcanic gases and the hydrolysis of silicates (Sillén, 1961); the acid volcanic gases are CO_2, HCl, HF, SO_2, H_2S and the hydrolysis of silicates is from sea floor and from erosion products of continents. The resultant pH is around 8.2– 8.4. The sea water is buffered by the system CO_2 especially the HCO^-_3 ion.

TheHCO^-_3 presents buffering ability in seawater and also in lakes and even in some rivers. The equation $HCO^-_{3aq} + H^+_{aq} = H_2CO_{3aq}$ shows that the H^+ reacts with HCO^-_3 forming H_2CO_3 which ionizes very little. The concentration of HCO^-_3 is almost equal at pH = 6.4 and 10.3 explaining

the buffering behavior of HCO^{-}_{3} at a $CO_2 = 10^{-3}$ (Fig. 1.6.4). In the presence of carbonate rocks the buffering ability of HCO^{-}_{3} increases because of higher HCO^{-}_{3} concentration:

$$H^{+}_{aq} + CaCO_{3s} = Ca^{2+}_{aq} + HCO^{-}_{3aq}.$$

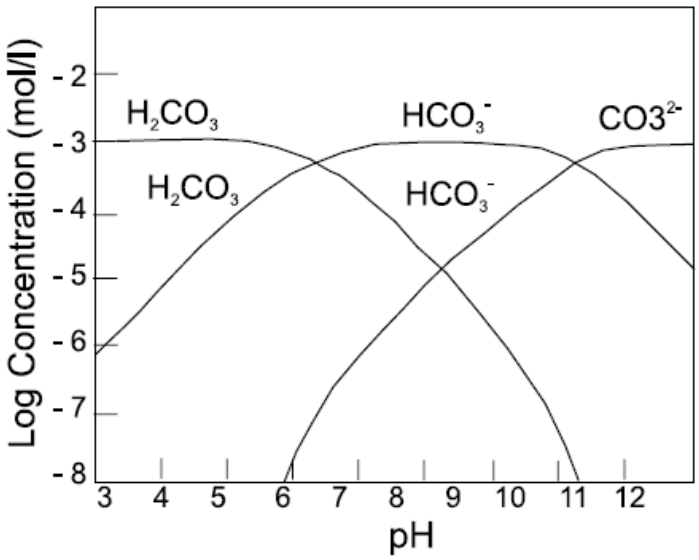

Fig: 1.6.4 $\sum CO_2$ (Carbonate species) versus pH - $\sum CO_2$ = 10-3 mol/l

The oxidation potential is another important parameter for the definition of geochemical characteristics of water. Chemical species of Fe, S, Mn and C present several oxidation numbers and have their behaviors dependent of Eh. The ratio $Fe^{3+/}Fe^{2+}$ is very important and the tendency is the oxidation of Fe^{2+}_{aq} and the precipitation of $Fe(OH)_3$ (or goethite and hematite). In latosols, the oxidation-reduction of the Fe species is responsible ($Fe^{2+}_{aq} = Fe^{3++} e^{-}$) by the dissolution – precipitation of the Fe in this type of soil associated certainly to the oscillation of water table in wet and dry seasons.

Sulfur species especially S^{2-} and SO^{2-}_{4} are important in terms of Eh/pH and the occurrence of sulfides (FeS_2) and SO^{2-}_{4} are quite characteristic. In acid mine drainage (Kim and Chon, 2001, Roisenberg et al., 2004), the oxidation of pyrite forms Fe^{2+}_{aq}, SO^{2-}_{4aq}+ $2H^{+}_{aq}$ and the later oxidation of Fe^{2+} to Fe^{3+} (or $Fe(OH)_3$). The pH reaches values close to 2 and Fe^{3+}_{aq} is in solution. When the pH increases, the Fe^{3+} precipitates. Manganese species are present in five oxidation numbers (2^{+}, 3^{+},4^{+}, 6^{+} and 7^{+}). The Mn^{2+}, Mn^{3+} and Mn^{4+} are very common and Mn^{6+}

and Mn^{7+} are normally present in laboratory conditions (MnO_2^{-4} and MnO^{-4}). The most common oxidation reaction in terms of manganese is

$$Mn^{2}+ aq + 2H_2O_l = MnO_2 s,c+ 4H+aq+ 2e-.$$

Mn^{2+} is more stable than Fe^{2+}; in other words, the oxidation of Fe^{2+} is faster than $Mn^{2+.}$

The oxidation of carbon compounds to CO_2 is one of the most common oxidation processes in nature. The oxidation of carbon chemical species to CO_2, H_2CO_3 or HCO^{-3} is very common in soils, sediments and waters.

The use of Eh-pH diagrams became very frequent in geochemical literature in the last fifty years. (Garrels and Christ, 1965).

Complex ions (inorganic or organic), ionic pairs (sea water) are association between ions or with other chemical species which are responsible by the transport of chemical species in solution. The stability of complex ions depends on their constants of stability. Carbonates form more stable complexes with HREE than LREE (it depends on ionic radius).

1.7 CLIMATIC IMPLICATIONS

Climate can play an important role in determining the composition of sedimentary rocks and it may be possible to make palaeoclimatic inferences on the basis of provenance data (Velbel and Saad 1991). Climate is particularly important in considering the origin of first-cycle quartz-arenites (Johnsson et al. 1988). These are produced where there is intense chemical weathering (generally under tropical weathering conditions) and in environments where such weathering can operate on sediments over an extended period of time. Evidence from coeval palaeosols can be important in assessing the connection between contemporary weathering and resulting sediment composition (Russell and Allison 1985). In fine-grained marine sequences, mineralogical (kaolinite/smectite ratios) and chemical (Th/K ratios) parameters have been used to monitor climate change (Wignall and Ruffell 1990).

1.8 SEDIMENTARY PROCESSES

The study of sedimentary provenance interfaces several of the mainstream geological disciplines (mineralogy, geochemistry, geochronology, sedimentology, igneous and metamorphic petrology).

Its remit includes the location and nature of sediment source areas, the pathways by which sediment is transferred from source to basin of deposition, and the factors that influence the composition of sedimentary rocks (e.g. relief, climate, tectonic setting). Materials subject to study are as diverse as recent muds in the Mississipi River basin (Potter et al. 1975), Archaean shales (McLennan et al. 1983), and soils on the Moon (Basu et al. 1988).

A range of increasingly sophisticated techniquesis now available to workers concerned with sediment provenance. Provenance data can play a critical role in assessing palaeogeographic reconstructions, in constraining lateral displacements in orogens, in characterizing crust which is no longer exposed, in testing tectonic models for uplift at fault block or orogen scale, in mapping depositional systems, in sub-surface correlation and in predicting reservoir quality. On a global scale, the provenance of fine-grained sediments has been used to monitor crustal evolution.

1.9 HEAVY MINERAL CONCENTRATION

Heavy minerals have been traditionally used in sedimentological studies in order to determine source areas and conditions of erosional grain. They provide useful information about sediment transport trends and longshore drift processes (Li & Komar, 1992; Heikoop, 1993; Anfuso et al., 1999; Hoffman et al., 1999). Heavy minerals are resistant to mechanical and chemical alteration processes; consequently, they are useful as natural tracers, so much for their hydrodynamic behavior and their potential of preservation (Pettijohn, 1975; Morton, 1985).

The concentration and distribution of heavy minerals in detritic sediments is mainly controlled by the rate and the source type of sediment supply, the hydraulic processes, as well as by the grain size and the specific weight (Berquist et al., 1990; Haughton et al., 1991; Poppe, & Commeau, 1996; Dill, 1998; Ergin et al., 2007). Another factor controlling the distribution of the heavy minerals content is their mode of erosion, transport and sedimentation, due to their

selective resistance to weathering and hydrodynamic processes (Flores & Shideler, 1978; Mezzadri & Saccani, 1988; Frihy & Dewidar, 2003).

1.10 SORTING AND MIXING EFFECT

When different grain sizes differ markedly in composition, hydrodynamic sorting may be of paramount importance in determining local sediment composition (Garzanti, 1986). Hydrodynamic sorting is responsible for drastic differences in composition between the suspended load and bed load of most rivers (cf. Koehnken, 1990; Johnsson et al., 1991); the former typically is dominated by clay minerals and monomineralic silt grains whereas the latter usually consists of more varied primary minerals and lithic fragments. Within the bead load, compositional sorting resulting from density differences is most pronounced when rapid changes in current velocity occur, such as on point bars, transverse bars, and behind obstructions. Local concentrations dense minerals may drastically affect local sediment composition but the overall composition of the material within the system not quantitatively changed (Garzanti, 1986).

Overall sediment composition does, of course, vary as a result of addition of new sources, such as incoming tributaries in fluvial system. Secondary sources may carry sediment of different provenance and history than that of the principle source, then complicating interpretation of compositional information. Columbia River sands, for example, show a downstream reduction in the quartz/feldspar ratio, coupled with an increase in grain size; this clearly suggests that the effects of downstream dilution or sorting overwhelm any abrasion or chemical weathering effects operating in that river (Kelley and Whetten, 1969; Whetten et al., 1969).

Subsequent to deposition, sediment may be subjected to significant modification in the depositional environment. Mechanical and chemical weathering continues to be of great importance prior to final burial. Davies and Ethridge (1975) suggest that composition reflects characteristics of the depositional environment; they found that recent and ancient fluvial deltaic, and beach sands could be distinguished on the basis of composition alone.

1.11 GRAIN SIZE

Sediments are integral and inseparable parts of the river ecosystem, so any environmental program concerning river water quality would be incomplete without the proper study of its sediments. The sediments existing at the bottom of the water column (bed sediment) play an important role in the pollution scheme of the river system as they are less susceptible to flow conditions than the water column. When the effluent-loaded water meets the river, various physico-chemical reactions take place and a large part of the effluent in one form or other either settles down, adheres to, or is adsorbed by the river sediments depending upon the physico-chemical conditions and on the species of the pollutants, nutrients, or trace metals under consideration. Heavy metals are not permanently fixed on sediments and can be released back to the water column by changes in environmental conditions, such as pH, redox potential, and the presence of organic chelators (Förstner 1987).

The elemental concentration of sediments not only depends on anthropogenic and lithogenic sources, but also upon the textural characteristic, organic matter content, mineralogical composition and depositional environment of sediments (Presley et al., 1980). It is generally believed that metals are associated with smaller grain-size particles (Whitney 1975; Gibbs 1977; Filipek and Owen 1979; Ackermann 1980; Salomons and Förstner 1984; Martincic et al., 1990; Biksham et al., 1991). This trend is predominantly attributed to sorption, coprecipitation and complexing of metals on particle surfaces and coatings. Smaller particles have a larger surface area: volume ratio and therefore contain higher concentration of metals. The specific surface area of sediments is dependent on granulometric parameters and mineral composition (Juracic et al., 1980, 1982). Increased concentration of metals in coarse fractions is also observed and it is believed that the coarser particles may better document anthropogenic inputs because of their limited transport and longer residence time at any particular site (Tessier et al., 1982; Salomons and Förstner 1984; Moore et al., 1989). In addition, the grain size distribution of sediments may show spatial heterogeneity, so that a wide range in heavy metal concentration may be found. Several studies have indicated that in environments, where grain size distributions vary considerably, valid intersite comparisons of metal concentrations cannot be made without a correction for grain size effect (Helmke et al., 1977; Groot et al., 1982; Förstner and Wittmann 1983). It is, therefore, often necessary to correct metal concentrations for the effects of grain size

in order to correctly document lateral or vertical variations and identify trends away from a particular source.

Knowledge of total metal concentration in the sediments does not help in understanding their bioavailability and mobilisation in aquatic environment. So as to appreciate the potential effects of heavy metals and their complexity in mobilisation, one must understand the various forms of the elements present in the sediments (Presley et al., 1972). This has led to a shift of attention in recent years from the determination of total heavy metals in sediments to other techniques which include the quantitative distribution of metals among various chemical phases such as adsorptive or exchangeable, carbonate, reducible – i.e. Fe-Mn oxide – organic and residual phase. Several researchers have undertaken studies on quantitative distribution of metals among various chemical phases of sediments under natural conditions to assess the ecotoxic potential (Gibbs 1977; Rapin et al., 1986; Rosental et al., 1986; Ridgway and Price 1987; Pardo et al., 1990; Vaithiyanathan et al., 1993; Panda et al., 1995).

1.12 TRANSPORT AND DOWNSTREAM ACCUMULATION

Entrainment of sediment particles are governed by fluid, flow and particle characteristics (James, 1993). The hydraulic conditions under which sediment particles are just able to move depend on the size, shape and density of the particles and the micro-topography of the bed. Under given hydraulic conditions, therefore, particles with different characteristics will be entrained with different relative ease. As entrainment is a continually repeated process during sediment transport it is therefore an important agent in the sorting of sediments by flowing water.

It has been also widely recognized that the physical characteristics of fluvial bed sediments in river channels alter systematically in a downstream direction. Sternberg (1875) was the first to quantify such a trend, fitting an exponential curve to the downstream decrease in size of Rhine bed sediments. Subsequent studies have established other trends for particles roundness (Wentworth, 1922; Krumbein, 1942; Goede, 1975), shape (Krumbein, 1941; Bradley, 1970), volume and various other derived indices (Sneed and Folk, 1958; McPherson, 1971).

Once a clast is entrained, it may be selectively transported according to its size, density and shape (Russel, 1939). These clast characteristics and the channel hydraulic conditions combine to dictate whether particles are transported in suspension or as bed load, with sediment

sorting possible within either transport mode (Rana et al., 1973). Selective deposition as and where the competence of the flow reduces (Knighton, 1984). Larger clasts will generally be deposited first and thus create flow disturbances around them; deposition of finer sediment may then occur upstream or downstream of such clasts. Other studies of mixed grain sediments and of pebble clustering have revealed how complex selective hydraulic factors are in natural environments (Laronne and Carson, 1976; Brayshow, 1985).

1.13 EFFECT OF TRIBUTARIES

In general, sediments from tributaries may have very different elemental compositions (Caitcheon 1998), concentrations of heavy metals and heavy minerals tend to increase as grain size decreases (Zdenek 1996; Singh et al. 1999; Yang et al. 2009). As a result of abrasion and sorting, rivers with gravel beds show strong downstream fining (Ferguson et al. 1996). This process takes place by grain size decreasing exponentially with distance, provided there are no lateral inputs of coarse sediment from tributaries and valley sides (Surian 2002; Radoane et al. 2008).

1.14 SEDIMENT RECYCLING

The extent of Phanerozoic recycling means that the distribution of characteristic detrital grains (for instance, grains of zircon of known age) must be sought first in the oldest sediments in which they might be expected to occur, and then in successively younger formations into which the grains may have been recycled (Haughton et al. 1991). Only then can the provenance of grains in the younger sediments be interpreted. Although single grain studies are still in their infancy, this approach promises to tell us much about the complex prehistory of sediment grains (Haughton et al. 1991).

1.15 DIAGENESIS AND METAMORPHISM

Erosion and transport of sediment generally occurs under fairly oxidizing conditions, at more or less constant pH, pressure and temperature. Upon deposition these parameters can

change drastically and thus influence the composition of sediment (Price, 1976; Curtis, 1977). As in the case of weathering, the more soluble the alkali and alkaline earth elements are liable to movement and/or redistribution (Hower, 1976). The anoxic conditions under which many types of sediment are deposited can have severe consequences; for example Fe and Mn which are generally insoluble at surface conditions, may change oxidation state and become readily soluble and mobilized. Table 2.6 compares trace element data for oxic and anoxic sediments from the same basin (Oslo Fiord). As well as Mn the elements Cu, Mo, Pb, Zn, S and C are clearly enriched in the anoxic sediments. The reasons for enrichment are not entirely clear but incorporation in sulfide phases or adsorption on organic compounds is obvious possibilities (Calvert, 1976).

Shaw 1954, found little change in the major elements beyond loss of water and carbon dioxide during regional metamorphism (up to about sillimanite grade). Trace elements also showed little evidence of mobility except that Li and Pb increased. Possible decreases in Ni and Cu were considerably less well defined. Ronow, et al., 1977 also noted only minor geochemical effects during progressive regional metamorphism of sedimentary rocks. Under very high grades of metamorphism, such as in the granulite facies, many elements, including K, Rb, Cs, Th, U are mobile, probably in fluid phases (Heier, 1973).

	Anoxic	Oxic	Probable significant Difference†
Sr	241	230	
Pb	148	94	*
Y	37	38	
Zr	197	235	
Cr	125	113	
V	181	186	
Ni	55	54	
Cu	133	54	*
Mn	5743	3990	*
Zn	571	342	*
P	1322	1305	
S %	1.55	0.22	*

Table 1.1 : Trace elements in oxic and anoxic sediments from the Oslo Fjord (in ppm except where noted)

1.16 MICROPALENTOLOGY OF OSTRACODE

Ostracods represent an important group of meiobenthic organisms inhabiting a great range of aquatic environments from freshwater pools to marine deep-sea basins. Ostracods possess a calcareous carapace which is usually well-preserved in sediments after burial. Their wide distribution, high abundance in sediments and occurrence in certain environments make ostracods a valuable tool for paleoreconstructions in seas subjected to strong riverine influence (Stepanova, 2007).

A delta is a discrete geomorphologic feature that forms where a river enters an ocean, a semi-enclosed sea, a lake, or a lagoon (Elliott, 1986). Along Asian coasts, the sediments of large-river deltas (megadeltas) formed during the Holocene record delta evolution and human impacts on coastal landforms (Rao et al., 1990; Saito et al., 2001; Tanabe et al., 2003).

CHAPTER 2

MAHAWELI RIVER AND TRINCOMALEE BAY SYSTEM

2.1BACKGROUND

2.1.1 Mahaweli River

Geochemical investigations based on the chemical analysis of active stream sediments are effective tools with multiple applications (Grunsky et al., 2009). Such geochemical surveys were initially used as an exploration tool, but their application has now evolved into a more extensive technique, particularly for environmental purposes (Ranasinghe et al., 2008; Grunsky et al., 2009). The geochemical compositions of stream sediments reflect the average composition of an entire drainage basin (Reimann and Melezhik, 2001; Halamic, 2001). Although the combined effects of chemical, biological and physical weathering processes transform bedrocks into soils and ultimately into sediments, original geochemical signatures of the source may be retained (Formoso, 2006). Trace elements such as Sc, Th, Zr, Cr, Ni and Co are generally immobile during surficial processes (Taylor and McLennan, 1985), and their abundances in sediments are thus useful indicators of source composition. However, consideration of whole-rock and soil chemistry gives a more comprehensive overview of the processes that have operated during the production of sediments. Consequently, considering data for soils and source rocks in combination with data for stream sediments is advantageous.

Few geochemical studies of stream sediments have been carried out in Sri Lanka, and most of those conducted to date have focused on mineral exploration (Dept. of Mineralogy 1959; Dissanayake and Rupasinghe, 1992; Gamage et al., 1992; Fernando, 1995; Ruapasinghe, 2000; Dissanayake and Chandrajith, 2003; Ranasinghe et al., 2009). Dissanayake and Chandrajith (2003) examined stream sediments in the Walawe basin, which covers part of the Highland and Vijayan complexes (Fig 2.1.1). The Walawe basin is not subject to variable climatic influence, as it lies entirely within the wet zone of Sri Lanka. In contrast, the Mahaweli River, the focus of the present study, transects the three climatic zones (wet, intermediate and dry) of Sri Lanka.

The Mahaweli River is about 335 km in length, and enters the Indian Ocean in Trincomalee Bay. The Mahaweli River receives sediment from many tributaries that flow across metamorphic basement, resulting in mixing of detrital components. A feature of this river is that it has relatively few tributaries in its lower reaches, whereas many tributaries are found in its upper reaches (Fig 2.1.2).

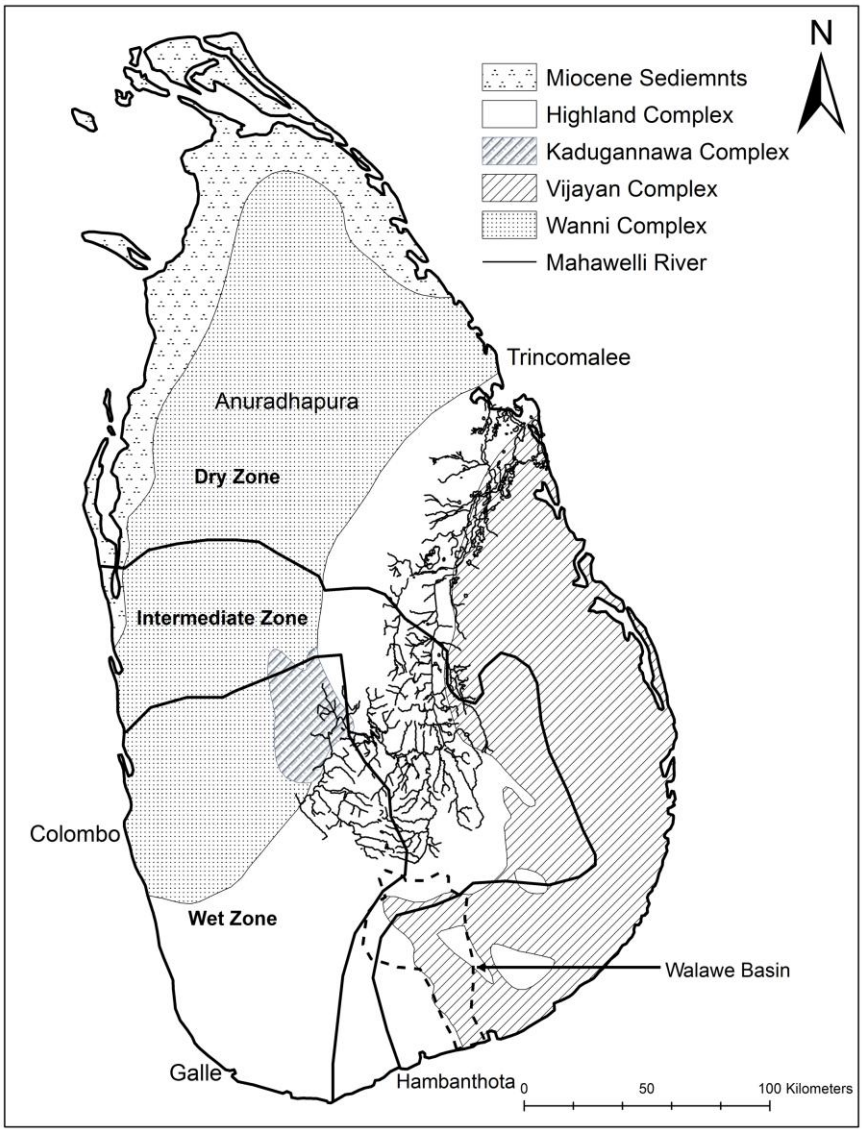

Fig. 2.1.1Simplified geological and climatic map of Sri Lanka (after Cooray, 1994), showing location of the Mahaweli River and the Walawe Basin

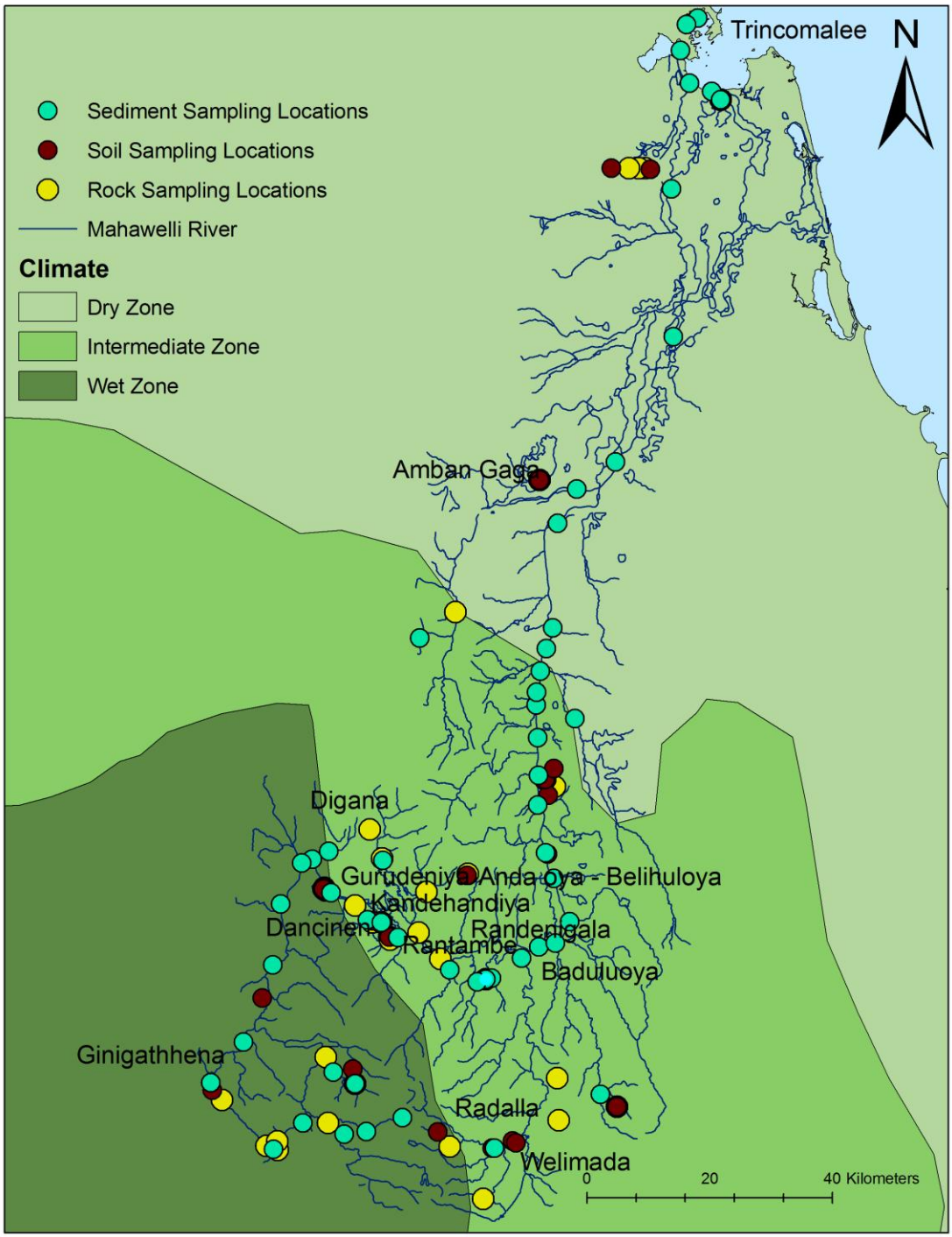

Fig. 2.1.2: Location of sediment, rock, and soil sample sites along the Mahaweli River and distribution of the wet, intermediate and dry climatic zones in the study area

2.1.2 Sediment fractions of Mahaweli River - Heavy minerals and chemical composition

Downstream fining, climatic and weathering conditions, and differing contributions from tributaries are major factors that control the geochemical and mineralogical compositions of river sediments (Fordyce et al. 1993; Rice 1998; Naseem et al. 2002; Yang et al. 2009). Provenance studies are aimed at reconstructing the parent-rock assemblages of sediments, and interpreting the climatic conditions under which they formed (Joshua 2010). The geochemical and mineralogical compositions of stream sediments can thus be used for (i) identifying the prevailing environmental conditions in an area (Alexakis 2008; Ranasinghe et al. 2008), (ii) interpreting weathering processes affecting the source materials (Singh et al. 2005), (iii) determining provenance (Vital et al. 1999; Ortiz and Roser 2006a,b; Singh, 2010) and (iv) interpreting processes taking place during sediment transport and downstream fining (Dai et al. 1995; Surian 2002). The geochemical compositions of differing size fractions of river sediments have also been used extensively for mineral exploration (Ma et al., 2011) and for evaluating pollution (Rice 1998; Surian 2002; Purushothaman and Chakrapani 2007; Singh 2010).

Heavy minerals have a long history of application in sand provenance studies, and to identify the influence of tributaries, heavy mineral durability, and transport, among other processes (Yang et al. 2009; Silva and Vital 2000). Mineral sorting during fluvial transportation is one of the most important factors controlling the geochemistry of fluvial sediments, and hence strongly influences major and trace element distributions in individual sediment samples (Singh et al. 2005). Heavy mineral assemblage and sizing, climatic conditions, and the geochemical processes operating during transport therefore strongly influence the bulk composition of river sediments. Identifying the geochemical processes operating within this system is thus important.

Environmental enrichment factors (EF) are powerful tools to identify the pollution conditions of river catchments (Ghrefat and Yusuf 2006; Aprile and Bouvy 2008; Naji and Ismail 2011). The method has also been applied in diverse studies such as studying air pollutants using the chemical characteristics of lichens (Bergamaschi et al. 2002; Klos et al. 2011) or street and household dusts (Hassan and Ismail 1993), the contamination of water (Hagan et al. 2011), and heavy metal contaminations from solid waste (Agunbiade and Fawale 2009; Fagbote and Olanipekum 2010). Sutherland (2000) proposed an equation for Enrichment Ratio (ER) using

immobile Al as the reference element. However, in previous studies, equivalent Enrichment Factors (EF) have also been derived using the formula EF= $(C_{sample}/C_{Fe})/(C_{Background}/C_{Background\ Fe})$. Iron has been used as the reference because it is the fourth most abundant major element in the earth's crust, although it may also be a potential contaminant (Naji and Ismail 2011). Many authors have adopted the Upper Continental Crustal (UCC) values of Taylor and McLennan (1985) as background values. In this study Fe has been used as the reference element in EF calculations.

This present study focuses on the mineralogical and chemical compositions of sediments from the Mahaweli River, the longest river in Sri Lanka. The potential role of the influence of downstream variation in the composition of bedload sediments in the Mahaweli River, based on the chemical characteristics of two size fractions, and evaluation of heavy mineral assemblages were examined. The <180 µm and 180-2000 µm fractions were used (Koval et al. 1995; Licht and Tarvainen 1996; Ferreira et al. 2001; Amorosi et al. 2002; Ortiz and Roser 2006a,b) to examine geochemical fractionation between size grades from the upper to the lower reaches of the river. EF is used in this work, but based on fractionation between the two sediment fractions (<180µm (E_f) and 180-2000µm (E_c)), derived as ($EF=E_f/E_c$), to illustrate relative changes in their compositions. The results show that there is a high input of heavy minerals from the tributaries, and suggest heavy minerals are accumulating in the downstream reaches.

Heavy metal pollution of the natural environment is a wide-reaching problem because these metals are permanent and most of the metals cause adverse health effects on living organisms, when they exceed a certain concentration (Forstner, 1990). Due to self purification heavy metals are not removed from water while they accumulate in reservoirs and enter the food chain (Loska and Wiechula, 2003) The bottom sediments of a reservoir show the accumulation and enrichment of heavy metals while the occurrence in the environment results primarily from anthropogenic activities and natural processes such as weathering of rocks (Nriagu, 1989). In addition, sediments are the ultimate sinks for heavy metals discharged into the environment (Gibbs, 1977). Many indexes are used to assess the environmental pollution levels of sediment deposited in various environments. On the other hand, analysis of pollutants in sediments is vital since they are absorbed by material in suspension and by fine-grained particles (Shriadah, 1999). Thus, the upper catchment area of the Mahaweli River sediments (30), sediments (6) of the

dammed reservoir at Polgolla of the river were used in order to assess the environmental pollution due to heavy metals. Also, one representative core (depth of 28 cm) is used to study the temporal changes in terms of geochemistry of sediments. In this study the geoaccumulation index of Muller, 1979 has been used.

The basement is mainly comprised of Precambrian metamorphic rocks of granulate faces metamorphism. Polgolla is subjected to high urban settlements, developments with roads and intensive agriculture. Heavy rains in the upper catchments of the river cause high flushing of fine grains and suspended matter along the river. Therefore, heavy metals from the runoff of the urban areas and agricultural lands can be accumulated in the river sediments, especially in the reservoir at Polgolla (Fig 2.1.3).

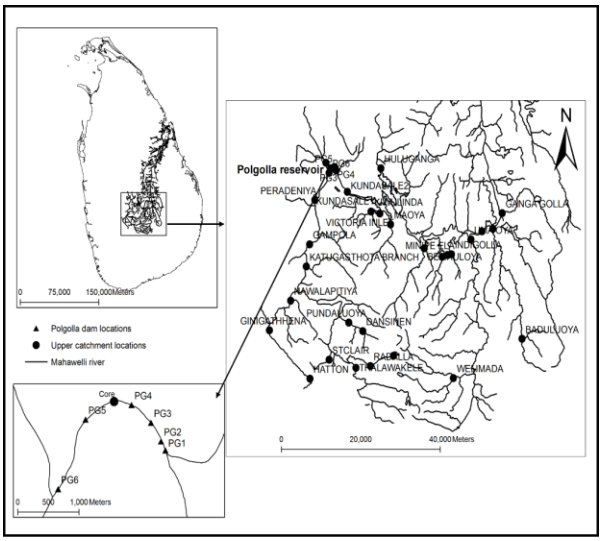

Fig 2.1.3: Location map of the upper catchment of Mahaweli River and the Polgolla reservoir

2.1.3 Trincomalee Bay

Estuaries are sites where the energy available to transport sediments decreases abruptly, and tidal influences can produce ebb and flow of sediments. The environment of such estuarine and coastal zones is thus both dynamic and complex (Morris et al. 1995). Interactions between freshwater and saltwater bodies in this land/sea interface, and resultant changes in physical, chemical, and biogenic inputs can strongly affect the transport and deposition of trace elements

(Lapido et al. 2011). Transport of trace elements from rivers, through estuaries, and into the open ocean is influenced by partitioning between dissolved and particulate phases (Ip et al. 2007). Modern or historic anthropogenic inputs of trace metals can be identified in river and bay sediments (Lin et al. 2007; Li et al. 2012), and contamination of these sensitive aquatic ecosystems is unfortunately not uncommon. Major and trace element compositions of sediments are often used to study the geochemical impacts of provenance, environmental issues, transport of weathering products, and climatic events (e.g. Hirst 1962; Pattan et al. 1995; Dellwing et al. 2000; Borrego et al. 2002; Ip et al. 2007).

Trincomalee Bay is located in northeast Sri Lanka (Fig. 2.1.4). The sheltered deep-water port of Trincomalee has been used for centuries, and has a European history dating back to the days of Marco Polo. Trincomalee Bay comprises an estuarine system open to the Indian Ocean. Physiographically the bay can be divided into three distinct sectors; Koddiyar Bay in the south; Thambalagam Bay in the west; and the Inner Harbour in the north (Fig. 2.1.4). Four major channels of the Mahaweli River, the longest in Sri Lanka, enter Koddiyar Bay in a delta system in its south. Koddiyar Bay thus receives voluminous clastic detritus from these river systems. In contrast, Thambalagam Bay is almost fully enclosed, and is not fed by any major rivers. The Inner Harbour also lacks major river inflow and is more open to the sea. Sediment supply and estuarine dynamics should thus differ in these three parts of Trincomalee Bay.

Utilization of the three parts of the bay also differs. The Inner Harbour is the main site of port and shipbuilding facilities, and the area surrounding it is urbanized and industrialized. The shallow waters of Thambalagam Bay restrict activity mainly to small-scale fishing, and Koddiyar Bay is the main estuary zone of the Mahaweli River delta. These contrasting uses may also have caused varying anthropogenic impacts.

With the exception of studies of stratigraphy and groundwater availability in the delta sediments of the Mahaweli River (Jayawardena 2005) and the basement geology around Trincomalee Bay (Fig. 2.1.4, Wijayananda 1985), no other major studies have been carried out in the area. Hydrogeological investigations by Jayawardena (2005) found that the sediments in the Mahaweli delta were mainly deposits of the river itself, and not a mixture of sea sediments. This present study sets out to test that hypothesis, utilizing the first compositional data from this major fluvial-estuarine system, which is the most important in Sri Lanka.

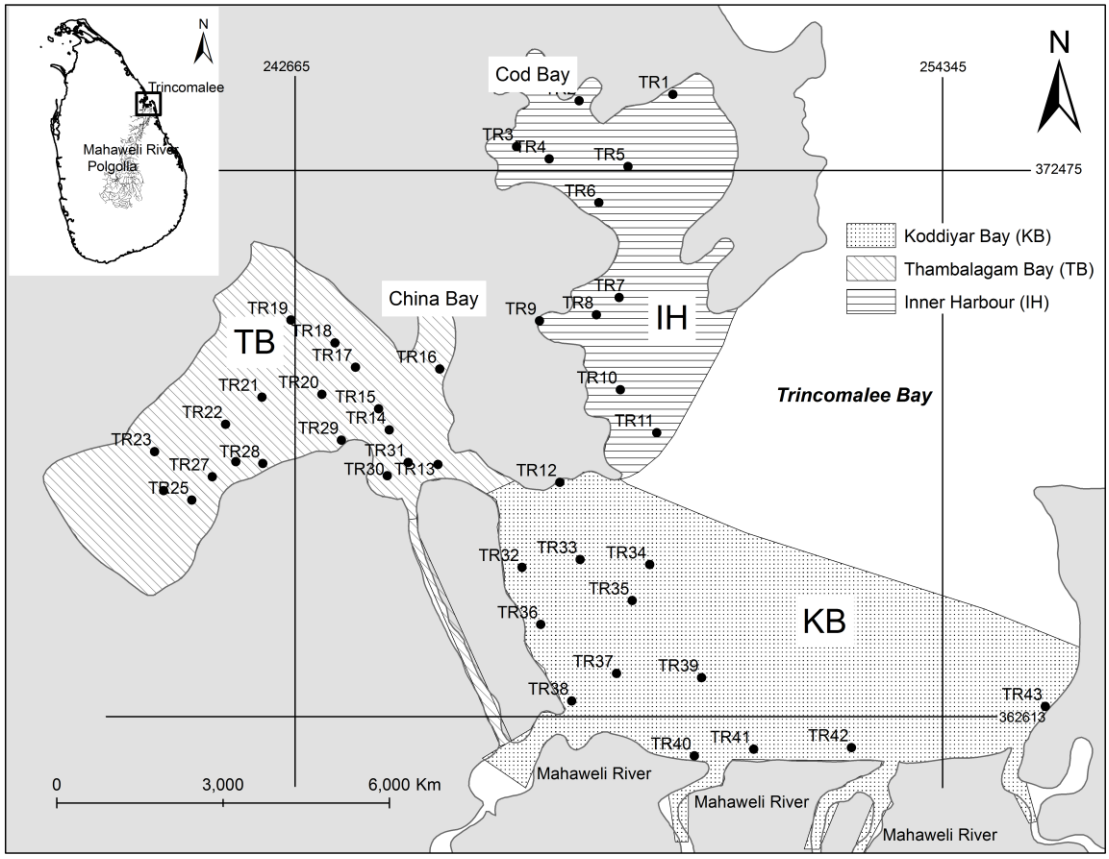

Fig 2.1.4 Location of Trincomalee Bay, and sample sites within the Inner Harbour (IH),

2.1.4 Trincomalee Bay core sediments

2.1.4.1 Sedimentary environments and deposition

The sediments that are brought carried the river are deposited at the river mouth in bays or estuaries. As for the morphology, in some places the sediments form deltas or tidal flats. The long, short or pocket beaches are form as for the geomophological features of the area. The geochemical variation, texture and composition of littoral sediments are controlled by diverse factors including wind, waves, longshore currents, climate, relief and source composition (Folk, 1974; Komar, 1976; Carranza-Edwards et al., 1998; Kasper-Zubillaga and Carranza-Edwards, 2005). Beaches are exposed to different marine, fluvial, and eolian processes such as wave and tidal regimes, fluvial discharges and wind transport among other factors. Furthermore, these

factors control the grain-size and sand composition of the beaches in terms of mineralogy and geochemistry.

In addition the grain size, composition and geochemistry of beaches may be controlled by geomorphological features in the coast (Le Pera and Critelli, 1997). Thus, the beaches within protected embayments may have coarser grain sizes as a result of little energy and removal of finer sizes offshore (Komar, 1976).

Nwajide and Reijers, 1996 described that each unit in a vertical stratigraphic succession is the product of a particular sedimentary environment and when these units are compiled vertically, they represent a sequence of environment formed by a detailed and general sedimentary process, such as regression and transgression. When several vertical units of one bay and river mouth are compared a clear understanding of the deposition can be found. Thus, detailed investigation of chemical and textural features can give a sound understanding of the processes that involve in the beach sand formations and deposition events.

2.1.4.2 Heavy Minerals and sorting

In order to determine source areas and conditions of erosional grain, heavy minerals have been traditionally used in sedimentological studies (Biswas and Roy, 1976; Guedes et al., 2011). Sorting is one major feature used in heavy mineral studies. Sorting of sediment according to one or more grain properties is present in depositional environments (Hughes et al., 2000). The sediment sorting or a mechanical agent can result in concentrations of economically important residual or detrital minerals within a depositional unit forming small or large placer deposits (Slingerland and Smith, 1986; Hughes et al., 2000). The four hydraulic sorting mechanisms as for Slingerland and Smith, (1986) are; suspension sorting, entrainment sorting, transport sorting and shear sorting. High silica content (>80%) relates to maturity of sediments and can be used as an indicator to determine if the sediment is matured or immature.

2.2 SCOPE OF THE RESEARCH

2.2.1 Mahaweli River

The major and trace element composition of the bulk sediments, two fractions of sediments (<180µm – 180-2000µm), rock and soils collected from the Mahaweli river banks and its catchment was determined. The heavy minerals was used as provenance indicators.

- Study the major and trace element distribution patterns of sediments derived from three different climatic conditions
- Human influence on the chemical nature of sediments can be understood.
- The upper catchment area of the Mahaweli River sediments (30), sediments (6) of the dammed reservoir at Polgolla of the river were used to assess any environmental pollution due to heavy metals.
- One representative core (depth of 28 cm) is used to study the temporal changes in terms of geochemistry of sediments. In this study the geoaccumulation index of Muller, 1979 has been used.

2.2.2 Trincomalee Bay

The major and trace element composition of Trincomalee Bay surface sediments and core sediments will be determined.

- Study the major and trace element distribution patterns of surface and core sediments derived from the Mahaweli River and/or marine sediment conditions.
- Human influence on the chemistry of the sediments can be understood.

2.3 OBJECTIVES OF THE STUDY

2.3.1 Mahaweli River

This study examines the effects of provenance, climate, heavy mineral accumulation, grain size, and hydraulic sorting in Mahaweli River sediments, using selected major and trace elements. Data for bulk composition (<2000 µm) and two size fractions (<180 µm and 180 –

2000 μm) are employed for the stream sediments, along with whole rock data for source rocks and soils. In addition, the EF (enrichment factor) for Pb, Zn, Cu, Ni, Cr and As contents have been calculated using Fe as the reference element, to identity any potential environmental effects.

The objective of the research project is to study the geochemical characteristics of sediments in the Mahaweli River, in order to

- Understand the intensity of weathering and erosion;
- Identify the provenance signature of the sediments; and
- Assess the effects of anthropogenic activity on the chemistry of the sediments.
- Asses the environmental pollution due to heavy metals in the Polgolla Reservoir.
- Identify the temporal changes in terms of geochemistry of sediments.

2.3.2 Trincomalee Bay

2.3.2.1 Trincomalee Bay surface sediments

The geochemical characteristics of surface sediments in the three sectors of Trincomalee Bay; was used to:

i. Determine their provenance, by comparison with data for main river channel sediments in the lower Mahaweli River;
ii. Evaluate the possible roles of circulation and oceanic influence within the bay in modifying sediment compositions;
iii. Assess present environmental conditions by comparison with established sediment quality guidelines, and
iv. Evaluate the results from those guidelines compared to those using local background values derived from sediment data from the Mahaweli River.

The results show that sediments in Trincomalee Bay mainly reflect detrital influx from the Mahaweli River, but that significant compositional contrasts occur between the three sectors, due to a variety of factors including spatial relationships, heavy mineral concentration, and bioclastic carbonate content. Apparent enrichment for several elements according to established

environmental guidelines are shown to be spurious, and related to elevated local backgrounds from the original source rocks. This illustrates the importance of considering local background data in conjunction with established environmental guidelines.

2.3.2.1 Trincomalee Bay core sediments

The aim of this study is to determine their provenance and to identify the mechanisms, processes responsible for variation within them, compositions of sediments of four cores collected around Trincomalee Bay.

2.4 EXPECTED OUTCOME

2.4.1 Mahaweli River

- Investigation of possible geochemical and environmental changes along the Mahaweli river.
- Mobilization of major and trace elements in the two main litho-tectonic units of the Mahaweli River, Sri Lanka.
- Effect of tributaries on the main stream using heavy minerals as traces.
- Investigation of causative factors affecting human health.
- Investigate the Polgolla dam and its effect on the river sediments.

2.4.2 Trincomalee Bay surface and core sediments

- Investigation of possible geochemical and environment of three sectors of Trincomalee Bay.
- GIS approach to effectively utilize geochemical mapping environmental special variation in the Trincomalee Bay.
- Investigation of causative factors affecting human health.

2.5 GEOLOGY OF SRI LANKA

Nine tenth of Sri Lankan basement consists of crystalline, non fossiliferous rocks of Precambrian age. The rest of the island, mainly the northwestern portion is formed of Mesozoic (Jurassic), Tertiary (Miocene) and Quaternary sedimentary formations, some of which are fossiliferous. As for the distribution, origin, age and interrelationships, the crystalline rocks are subdivided into four main sub-divisions, (Fig 2.1.1). These groups are (a) Highland Complex (b) Wanni Complex and (c) Vijayan Complex and (d) Kadugannawa Complex (Cooray, 1994). The basement metamorphic rocks consist of a variety of orthogneisses and metasediments which were metamorphosed under amphibolite to granulite facies conditions at about 610 – 550 Ma.

The Highland Complex (HC) is the largest lithotectonic unit of the island and covers the entire hilly country of central Sri Lanka. It consists of a supracrustal suite (comprising various types of metasediments), orthogneisses of largely granitoid composition and charnockitic rocks. Supracrustal rocks are fairly widespread in the HC and are represented by garnet-sillimanite gneisses, metaquartzites, marbles and calc-silicates. The abundance of marbles and calc silicate rocks is higher in the central and northcentral parts than in the southeastern part of the HC. The mode of occurrence and chemical composition of quartzites and marbles suggest their derivation from sediments deposited in shallow marine stable continental shelves (Katz, 1978).

Some granulite-facies outliers comprising rock types similar to those of the HC are exposed in the southern part of the VC, not far from the southern coast near the villages of Buttala and Kataragama (Fig. 2.1.1). Kröner et al. (1991) have interpreted these outliers as appendices of the southeastern HC. The Kataragama outlier had been originally buried to a depth >30 km under an approximate geotherm of 30 - 40 ^{o}C/km and had suffered a significant thermal loss before its exhumation.

The Wanni Complex occupies the western and northwestern part of Sri Lanka and is made up of granitoid gneisses, migmatites, granites and scattered metasediments (garnet-cordierite gneisses, meta-quartzites) as well as charnockitic rocks. Inspite of geological and geochemical investigations, the boundary between the Highland Complex and Wanni Complex still appears to be rather blurred. Marbles are not that abundant in the Wanni Complex as in the Highland Complex.

The Vijayan Complex is exposed in eastern and south-eastern Sri Lanka. It is dominated by granitoids, migmatites, granitic gneisses and hornblende-biotite gneisses with scattered occurrences of metasediments (mainly calc-silicates and quartzites). The regional metamorphism in the Vijayan gneisses is that of the upper amphibolite facies. Hölzl et al. (1991) have shown that the age of the orthogneisses is about 1100 Ma, and that the granitoid intrusions were emplaced during the interval 1000 - 1100 Ma.

The smaller Kadugannawa Complex is located in central Sri Lanka and is sandwiched between the Highland Complex in the east and Wanni Complex in the west. Hornblende and biotite gneisses, pelitic gneisses, slightly foliated granite, minor metaquartzites, amphibolites and quartzo-feldspathic rocks constitute the local rock assemblage.

2.6 STUDY AREA

The Mahawelli River is one of the 103 rivers in Sri Lanka and is the largest river basin. Trincomalee Bay is a deep submarine canyon and has been a very famous natural harbor for more than 300 years.

2.6.1 Location and Accessibility

Sri Lanka is a tropical island situated in the Indian Ocean with a total land area of 65,525 km^2. Its rainfall feeds a radial network of rivers that begin in the highlands in the central part. Some 103 distinct rivers cover about 59,217 Sq. km (Fig 2.6.1) of their basins. Large percentage of water resources in these basins are mainly used for irrigated agriculture and hydropower generation.

2.6.1.1 The Mahaweli River

The radial drainage that carries surface water down from the high watersheds includes 103 distinct natural river basins that cover over 90% of the Island (Fig 2.6.1, Arumugam, 1969). Mahaweli is the name of the longest river and the largest river basin that starts from the top of

the central mountains in Sri Lanka (Fig.2.6.1, Fig.2.1.2) at the Hatton platue. Its' total length is 335km and total runoff is approximately 8,878 x 103 cubic meters. This volume is more than 20% of total run off of all other rivers in the Island. The total catchment of Mahaweli River is about 10,448 square kilometers (NARESA Report, 1991). It is 16% of the total land area of the country (Jayawardena 2005). Therefore the total sediment transportation by this river may be very large (Jayawardena 2005). The Mahaweli River is flowing to the sea at the bay of Trincomalee through several distributaries in N-E of the country. The area is almost flat and close to the sea level. A very large flat floodplain occurs around the area where the river flows to the sea. Therefore deltaic type sediments as well as alluvium can be expected within this area.

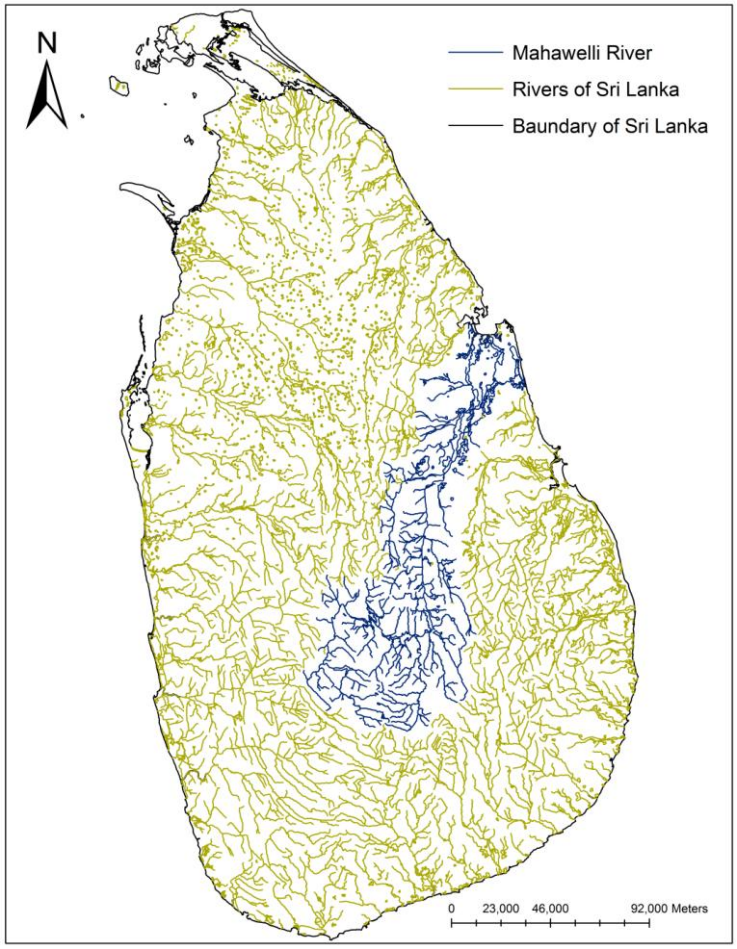

Fig : 2.6.1 Mahaweli River of Sri Lanka also showing the other rivers of the country

2.6.1.2 Trincomalee Bay

Trincomalee is a major port city in Eastern Province, Sri Lanka and lies on the east coast of the island, about 113 miles south of Jaffna. It is also the administrative capital of Eastern Province, Sri Lanka. Trincomalee Bay is the fifth largest natural harbour in the world, is overlooked by terraced highlands, its entrance is guarded by two headlands, and there is a carriage road along its northern and eastern edges.

2.6.2 Historical Perspective of Water Resource Management of the Mahaweli area

Sri Lanka is a country with a long history of hydraulic civilization, which had been developed along the main river basins of the country. Early settlers began developing their network of irrigation systems in the main river basins around the 5th Century B.C. Some of the major basins developed by them were; Malwathu, Mahaweli, Deduru, Kelani, Kalu, Walawe, Kirindi, Menik and Kumbukkan. Many of these rivers originate in the Central Highlands and flow towards plateaus in other parts of the country, providing opportunities for irrigated agriculture. This geographical situation helped the early settlers to conserve the watersheds in the highlands and to develop plateaus in agriculture by storing water in a network of reservoirs.

2.6.3 Historical activities in Trincomalee Bay

Trincomalee is located on the east coast of the island overlooking Trincomalee Harbour, 113 miles south of Jaffna and 69 miles north of Batticaloa. The city is built on a peninsula of the same name, which divides its inner and outer harbours.

The recorded history as in Wikipedia of Trincomalee spans more than two and a half thousand years beginning with civilian settlement associated with the Koneswaram temple in the pre-modern era. One of the oldest cities in Asia, it has served as a major maritime seaport in the international trading history of the island with South East Asia. Trincomalee's urbanization continued when made into a fortified port town following the Portuguese conquest of the Jaffna kingdom, changing hands between the Danish in 1620, the Dutch, the French following a battle

of the American Revolutionary War and the British in 1795, being absorbed into the British Ceylon state in 1815. Attacked by the Japanese as part of the Indian Ocean raid during World War II in 1942, the city and district were affected after Sri Lanka gained independence in 1948. The city also has the largest Dutch fort on the island. The Trincomalee Bay Harbour, bridged by the Mahavilli Ganga River to the south is referred to as "Gokarna" in Sanskrit.

2.6.4 Physiography and Geology

2.6.4.1 Physiography and Geology of Mahaweli River

More than 25% of the Central Highlands of Sri Lanka lies in the upper catchment of river Mahaweli (3118 km^2), the longest river (335 km) of Sri Lanka (Fig. 2.6.1). Elevation of the area ranges from 300– 2500 m and it comprises of a highly dissected terrain consisting of a unique arrangement of plateaus, ridges, escarpments, intermontane basins, and valleys (Fig. 2.6.2). The southern and western parts of the Central Highlands receive an annual rainfall of 2500 –5000 mm from the southwestern monsoon and inter monsoon while the northern and eastern parts receive an annual rainfall of 750 - 2000mm from the northeastern monsoon and inter monsoon (Survey Department, 1988). Geologically, the Upper Mahaweli catchment area lying in the Highland Complex of Sri Lanka mainly consists of granulite grade metasedimentary and meta-igneous rocks, belonging to the early Proterozoic (Cooray, 1994). Quartzite, quartzofeldspathic gneisses, marble, calc silicate gneisses, pelitic and semi-pelitic gneisses, charnockite and chranockitic gneisses are the major lithologies of the Upper Mahaweli catchment area (Geological Survey & Mines Bureau, 1996, 1997, Fig. 2.6.3). Natural erosion rates, calculated from the low cosmogenic nuclides, of the Upper Mahaweli catchment are 10– 30 mm/ky (Hewawasam et al., 2003). However, the average erosion rate of the area has been calculated presently as 100–500 mm/ky. Improper soil management practices in this area and the presence of easily weathered feldspar-rich rocks and high annual rainfall are responsible for these high rates of erosion (Hewawasam et al., 2003).

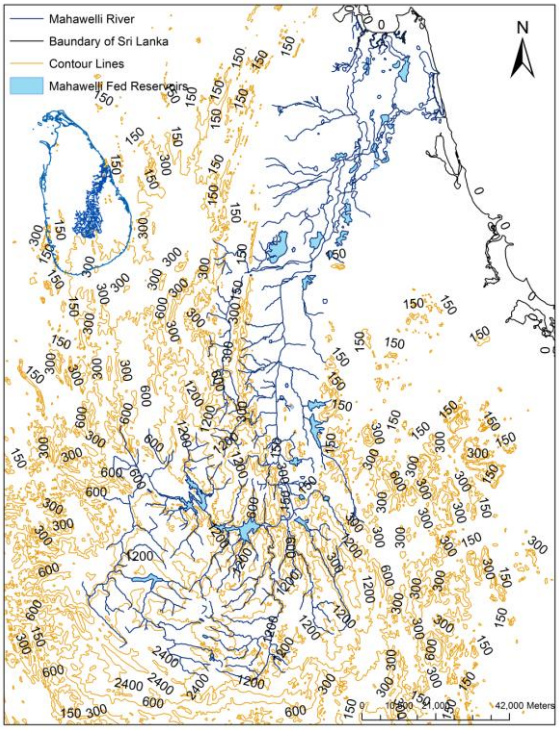

Fig 2.6.2: Map showing the Mahawelli River and the elevation of the basin area (Digitized using the 1:50,000 topo sheets of the survey department, Sri Lanka with ArcGIS 9.2)

The southern and western parts of the Central Highlands receive an annual rainfall of 2500mm – 5000 mm from the southwestern monsoon and inter monsoon while the northern and eastern parts receive an annual rainfall of 750mm – 2000mm from the northeastern monsoon and inter monsoon (Survey Department, 1988).

The Mahaweli River also flows through three climatic zones (wet, intermediate and dry, Fig 2.1.2), which are categorized simply on their annual precipitation. In the upper reaches of the river the wet zone receives some 2032 mm to 5080 mm precipitation annually, spread more or less throughout the year (Survey Department 1988). In the lower reaches the dry zone experiences drought during the SW monsoon (March to September), and receives rain only during the NE monsoon (October to March). Average annual rainfall in the dry zone ranges from 1270 to 1905 mm (Survey Department 1988). Rainfall in the intervening intermediate zone lies between the extremes in the dry and wet zones.

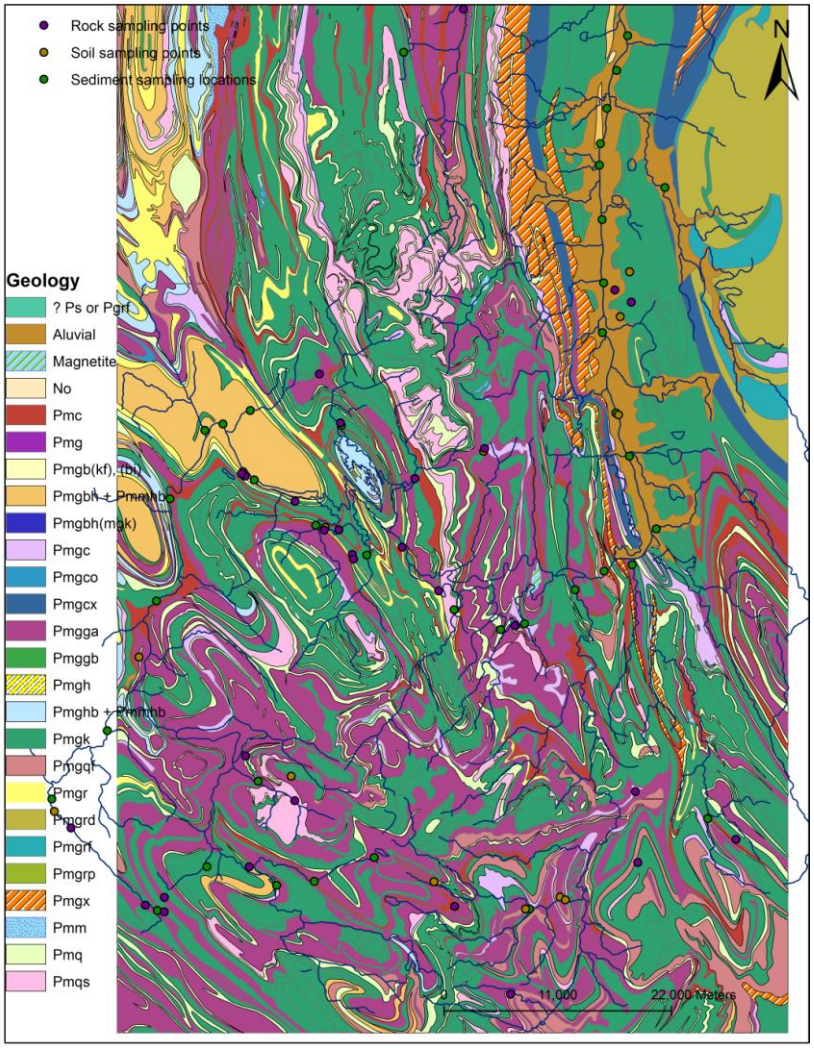

Fig. 2.6.3: Map showing the geology of the Mahawelli River- upper reaches- Abbreviations of the legend is in the Annex (prepared using digitized data of the Survey Department, Sri Lanka using ArcGIS 9.2)

The central plain is bordered by highlands featuring a trellised drainage network (Cooray 1984). The largest tributaries in the upstream reaches are the Uma oya and Baduluoya Rivers, but in the lower reaches very few tributaries are present. The headwaters of the Mahaweli River lie mainly within the Highland Complex, a major lithotectonic unit in the Sri Lankan basement (Fig 2.1.1).

2.6.4.2 Physiography and Geology of Trincomalee Bay

Trincomalee Harbour is a natural bay trending NE-SW, with a gentle average slope of about 3° (Wijayananda 1985; Bush and Bush 1969, Shepard 1963; Stewart et al. 1964; Shepard and Dill 1966). The three sectors of the bay developed due to the configuration of the local basement rocks and operation of coastal and fluvial processes. The dimensions of the Inner Harbour are mainly controlled by the basement geology, whereas those of Thambalagam Bay are influenced by beach deposits, and the more open Koddiyar Bay is dominated by deposits of the Mahaweli River delta.

The inland area is slightly undulating, with small hills forming 'turtle back' topography. The topographic highs are mantled by soils, whereas the lows are characterized by alluvial deposits, peaty clays developed due to marshy conditions, and thick soils derived from gneissic basement rocks. Mean annual rainfall is more than 900 mm, and most precipitation falls during the NE monsoons from October to January. Lowest rainfall occurs from March to June. Mean monthly temperatures vary from 25.6°C to 30.0°C.

Basement in the study area consists of Precambrian Highland Complex rocks (Fig. 2.6.4). The Highland Complex consists of upper amphibolite to granulite facies metamorphic rocks and minor igneous rocks (Cooray 1994). Garnet-cordierite gneisses, meta-quartzites, marbles, orthogneisses and charnockitic gneisses are common lithotypes. The general trend of the basement rocks is NW-SE, and the area is characterized by megascale deformational features such as synforms and an antiform (Wijayananda 1985). Quartzites are the most common rocks in the Trincomalee Bay area (Fig. 2.6.4). These are highly resistant to weathering, and form ridges along the coast. Interbedded charnockite, the next most prominent lithology, is less resistant and underlies areas of lower elevation. Marbles occur as limited bands or patches in the southeastern part of the bay. Pink feldspar granulitic gneiss occurs north of the Inner Harbour and east of Koddiyar Bay.

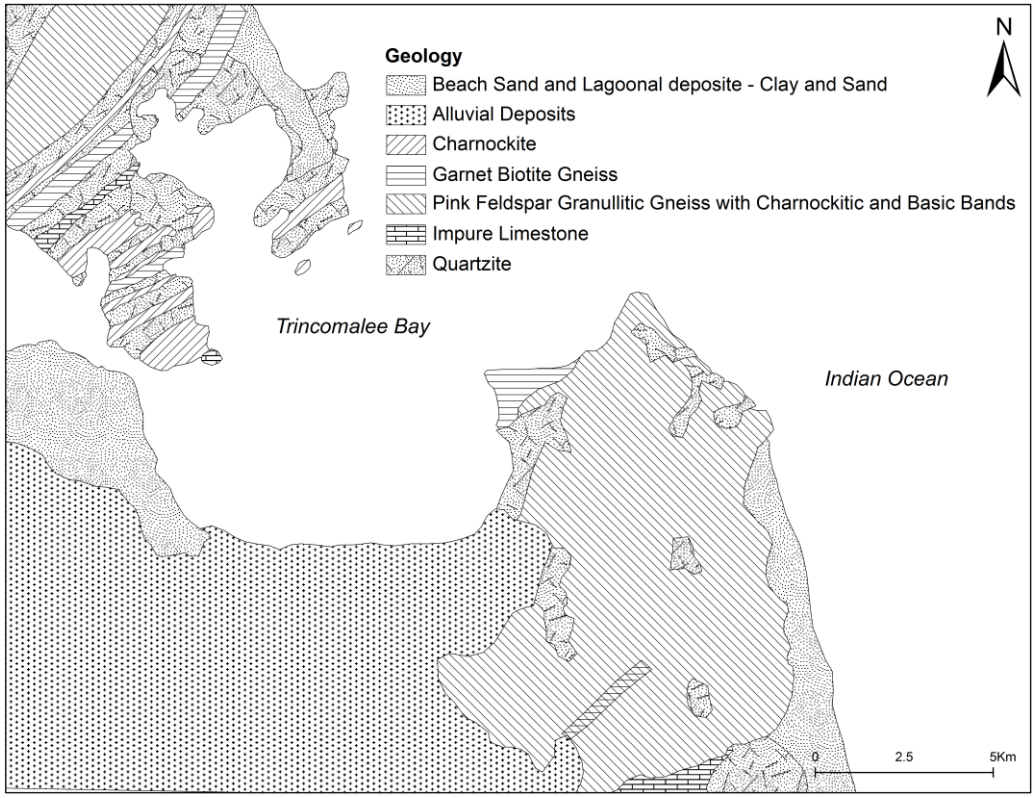

Fig 2.6.4 Simplified geological map of the area surrounding Trincomalee Bay (after Wijayananda 1985)

2.6.5 Drainage and Land use of Mahaweli River and Trincomalee Bay area

The area extending from the western edge of the Horton Plains, where Agra Oya begins, to Minipe is considered as the upper regime of the Mahaweli River. Kotmala Oya, Puna Oya, Hulu Ganga, Maha Oya, Badulu Oya, Uma Oya, Kurundu Oya, Belihul Oya are some of the main tributaries of the Mahaweli River that join the main river along this upper regime (Fig. 2.6.1). The upper catchments of the tributaries are covered with tropical montane forests, tea cultivation and vegetable plots with paddy fields and human settlements found in between.

2.7 CLIMATIC ZONES OF SRI LANKA

Based on the precipitation received, the country can be divided into three main climatic zones:-

(1) Wet zone
(2) Intermediate zone
(3) Dry zone

2.7.1 The Wet zone

The wet zone receives rain from both, the south-west and north-east Monsoons, as well as the inter-Monsoon period. The annual precipitation in this region varies from 80 to 200 ins (2,032 - 5,080 mm) and is evenly distributed throughout the year. The wet zone can be divided into;

(a) The low-country wet zone and
(b) The montane or up-country wet zone.

2.7.1.1 The Low-country Wet zone

The low-country wet zone extends over three provinces-the Western Province, the Southern Province' and the Sabaragamuwa Province-consisting of the following districts:- Gampaha, Colombo, Kalutara, Galle, Matara, Ratnapura and Kegalle. The average annual rainfall varies between 80 to 125 ins.(2,032 - 3,175 mm),and rises to 130 to 200 ins (3,302 to 5,080 mm) in the Ratnapura and Kalutara districts, parts of Kegalle and Galle districts and the lower valley of the Kelani Ganga. In this region floods are a recurrent problem. The vegetation is luxuriant and dense, and farmers in this area have to struggle continuously to control the growth of weeds that can invade cleared and cultivated land. The rivers are perennial, broad and deep. the need to store water for irrigation does not arise, as there is no lack of water at any time. Sometimes droughts do occur, but they are not prolonged and do not cause any serious problems. The land is flat only near the sea coast, but rises gradually inwards, often interrupted by high outcrops, to the foothills of the central mountains.

In modern Sri Lanka the main population centres are all situated in the low-country wet zone, but in ancient times (before 10th century A.D.,) there is no evidence of any settled population in the south-western region from Kalu Ganga in Kalutara to Nilwala Ganga in Matara,

and in the Ratnapura district, which lies immediately inland of it. The earliest inscriptions from this region belong to the 10th century A.D. It is recorded that in the 12th century A.D. Parakramabahu I drained the swamps and marshes of Pasdun Korale in Kalutara district, into the rivers and made the land habitable. However inscriptions recovered from Colombo, Gampaha, and Kegalle districts and Chilaw, show that these areas were populated in pre-Christian times.

2.7.1.2 The Up-country Wet zone or Montane zone

The up-country wet zone extends over the entire south-central highlands, that include the Central and Uva Provinces, consisting of the following districts:-Kandy district, Matale district, Nuwara-Eliya district and Badulla district. The average rainfall is 80 ins.to 125 ins (2,032 mm - 3,175 mm), rising to 140 to 200 ins.(3,556 - 5080 mm) in the upper valley of the Mahaweli Ganga around Ramboda and the Knuckles, and falling away to 65 to 100 ins (1,651 to 2,540 mm) in the mountains of Uva and the easterly hills, which form a drier sub-zone. The wettest town in Sri Lanka, Watawala, having the highest annual rainfall of over 200 ins.(5080 mm) is situated in this region.

The montane zone above 2,500 ft.(762 meters) was largely unpopulated till the 10th century A.D, but large scale movement of people into the hills did not take place until the fall of the Polonnaru kingdom and the virtual abandonment of the northern plains in the 13th Century A.D. However by the end of the 1st Century B.C. the lower montane zone between 1,000 to 2,000 ft.(305 to 610 meters) in elevation, was populated as indicated by rock inscriptions left in the Buddhist monasteries, mainly in the regions such as the Mahaweli Ganga valley, around Teldeniya, Kandy, and Gampola, and the lesser hills to the north-west of Badulla and the northern and western slopes of the Matale hills. The Kandyan Kingdom, the last stronghold of the Sinhalese Monarchy, was essentially a mountain kingdom, a refuge of independence from the European enemies below. Currently the low-country wet zone and the up-country wet zone or montane zone are together the intermediate zone (Fig. 2.7.1).

2.7.2 Intermediate zone

The intermediate zone is the area within the wet and the dry zone that has intermediate rain fall of 1750 – 2500 mm.

2.7.3 The Dry zone

The low-country dry zone is historically the most important region in Sri Lanka, because it was the cradle of the Sinhalese Civilization. The main population centers in ancient times were situated in this region, including the kingdoms of the Sinhalese Monarchies from the 6th century B.C. up to the 13th Century A.D. The highly sophisticated irrigation systems consisting of vast irrigation tanks and an intricate system of irrigation channels, that has marveled and earned the respect and admiration of modern day scientists and engineers, was developed in this region, and was responsible for converting the dry zone into the main food producing area of the country.

The dry zone embraces the north-western, northern, north-eastern, north-central, eastern, and south-eastern parts of Sri Lanka, which constitutes about 70% of the total land area. The provinces that fall under this area are the North-Western, North-Central, Eastern, Northern and parts of Uva and Southern Provinces. The districts that come under this area are Puttalam, Anuradhapura, Polonnaruwa, Batticaloa, Trincomalee, Digamadulla, Jaffna,Vanni, Moneragala and Hambantota.

The dry zone receives rain only during the north-east Monsoon between the months of December and March, while during the south-west Monsoon it undergoes a period of drought. The average annual rainfall is between 50 to 75 ins.(1,270 to 1,905 mm) and decreases to 30ins. to 45ins. (762 to 1,143 mm) in the two arid sub-zones, Hambantota in the south-east and Mannnar-Puttlam in the north-west.

During the annual drought the temperature rises and a strong dry south-west wind blows throughout the day. The grass dries up and turns to stubble and can be easily set on fire. The vegetation droops and the under-growth die out. The smaller irrigation tanks dry up or shrink to muddy pools. The streams and water courses run dry. The larger rivers except the Mahaweli Ganga and Walawe Ganga, are reduced to mere trickle of flowing water or break up into

disconnected pools. Thus the main problem in the dry zone is the lack of an adequate supply of water during the annual drought, for agricultural and domestic purposes.

Fully realizing this drawback in the dry zone areas the ancient Sinhalese, built a sophisticated irrigation system, consisting of large and small reservoirs, some rain fed and others receiving water along artificial canals from rivers that were dammed at higher levels. The creation of this vast irrigation network was a great boon to the population of the dry zone, in overcoming water shortages during the annual drought period, as well as at times when the north-east Monsoon rains failed.

After the fall of the Polonnaru Kingdom early in the 13th Century, the North-Central Province was abandoned, and the vast irrigation systems were neglected and fell into total ruin. Malaria became a serious scourge and large scale population movements took place from the dry zone, towards the low-country and up-country wet zone regions, which subsequently became the main population center of the country. The re-occupation and re-development of the dry zone was possible only in the recent past after the Second World War, following the extensive use of the insectide DDT to eradicate the malarial vector, the Anopheles mosquito.

After the eradication of malaria in the early 1940s, the Government embarked upon a massive re-construction and re-habilitation project, the primary aim of which was to reconstruct and restore the major ancient irrigation tanks and channels in the dry zone, and encourage farmers in re-occupying the land which they abandoned during the Malarial scourge. Independent Sri Lanka's first Prime Minister Honorable Don Stephen Senanayake was deeply involved in these projects, and was also instrumental in the construction of a massive irrigation project in the Eastern Province, under the Gal oya development scheme, which resulted in the creation of a vast irrigation tank, known as the Senanayake Samudra, that supplied much needed water to thousands of acres of old and new paddy lands, and led to the establishment of new settlements and townships. Currently the climatic zones are represented by the map shown in Fig. 2.7.1.

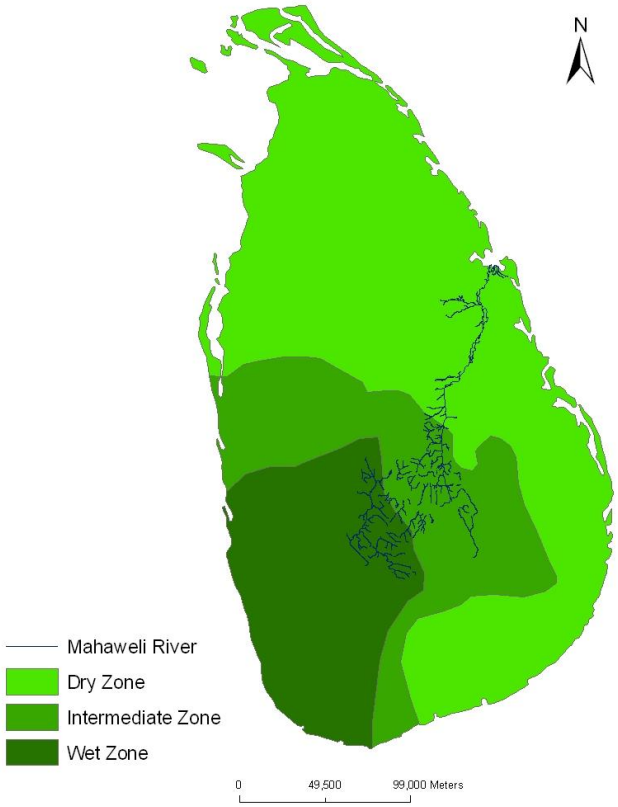

Fig . 2.7.1: Map showing the climatic zones of Sri Lanka (Digitized and prepared using ArcGIS 9.2)

2.8 PREVIOUS WORK AND BACKGROUND

2.8 1 Mahaweli River

As for Dissanayake and Weerasooriya (1986), the water pollution levels of Mahaweli River basin of which covers one sixth of the Island, have been monitored to probe the impacts of the urban environment in Sri Lanka. It has been observed that the chemical quality is largely controlled by natural factors. From among the metals however, vanadium, zinc and copper have shown higher concentrations. Pb and Cd have shown a correlation co-efficient of r = 0.58 with each other, and Co has a highly significant correlation of r = 0.98 with Cu. The lack of correlation of Pb and Cd with the total dissolved solids (TDS) has indicated an anthropogenic

input of Pb and Cd into the aquatic environment. In general, the chemical quality of the water in the Mahaweli River is satisfactory for most purposes, as none of the major dissolved constituents and nutrients exceed the limit suggested by the WHO for potable water.

Ranasingha et al., (2008) carried out a study based on stream sediment geochemistry of the Upper Mahaweli River Basin of Sri Lanka—Geological and environmental significance. However, that study covers only the Upper Mahaweli River Basin, which is less than half of the entire Mahawelli River basin. The Mahawelli is a classic river basin with a vast central plain bordered by highlands and a terrestrial drainage network within which the main channel and its extensive floodplain receive input from a series of variously sized tributaries (Ranasinghe et al., 2008).

Ranasingha et al., (2008) concluded that the distribution pattern of different elements in stream sediments of the study area is greatly influenced by geological as well as anthropological factors. The distribution of K, Rb, Ba and Sr which have a similar geochemical behaviour and occupy the feldspar structure is almost identical in most of the basins. Such a similarity has been shown by Ca and Mg as well. Fe–Cu and Ni–Cr distributions in Belihul Oya and Badulu Oya basins have to be investigated in detail to identify the possible presence of mineralization in the areas. Al and Pb that are reported in excess concentrations close to agricultural and urban areas respectively may be influenced by anthropogenic activities such as poor land use planning and unleaded gasoline used in vehicles. Na, Mn, Ti, Nb, Y, Zn and Zr distributions in stream sediment seems to have a relationship with the underlying lithologies of the area.

Except these there is no other significant work that has been carried out for the geochemistry of the Mahawelli River basin. The present study was thus, carried out to investigate the provenance, weathering process, sorting effect, diagenesis, tectonic setting and heavy minerals in the Mahawelli River using the river sediments, rock and soils of the basin.

Fig 2.6.2 shows the elevation of the Mahawelli River. Geologically, the Mahaweli catchment area (10,448 km^2) lying in the Highland Complex of Sri Lanka Pohl and Emmermann, (1991) is predominantly made up of granulite-facies assemblages with quartzofeld-spathic gneisses, quartzites, metapelites, calc-silicate rocks and marbles interlayered with mafic granulites and charnokite, granulite grade metasedimentary and meta-igneous rocks, belonging to the early Proterozoic (Cooray, 1994). The Highland Complex is composed of inter-banded

metamorphosed sediments and charnockitic gneisses, and it occupies broad belt running across the center of the Island from southwest to north-east (Cooray, 1984). Concentrations of several elements are strongly influenced by detritus from these units.

The Mahawelli River flows through the dry, wet and intermediate zones (Fig. 2.7.1) of Sri Lanka thus, based on the precipitation received the Country is divided into two main climatic zones. The wet zone receives rain from both, the south-west and north-east Monsoons, as well as the inter-Monsoon period. The annual precipitation in this region varies from 2,032 to 5,080 mm and is evenly distributed throughout the year. The dry zone receives rain only during the north-east Monsoon between the months of December and March, while during the south-west Monsoon it undergoes a period of drought. The average annual rainfall is between 1,270 mm to 1,905 mm and decreases 762 to 1,143 mm in the two arid sub-zones, Hambantota in the south-east and Mannar-Puttlam in the north-west.

The drainage basin the Mahawelli River is the largest in Sri Lanka, and covers almost one-fifth of the total area of the island supplying water for a major area of the island for drinking, irrigation, domestic purposes and hydropower generation. The river is heavily dammed in order to produce hydroelectricity and water for irrigation. This has brought almost 1,000 km² of land under irrigation. Number of tributaries carries water to the large river which also carries many gem bearing minerals. The river reaches the Bay of Bengal at Trincomalee in the north-east of Sri Lanka. It continues as a major submarine canyon, making Trincomalee one of the finest deep sea harbors in the world.

2.8.2 Trincomalee Bay

Trincomalee Bay and its sediments have not been studied previously. This is the first geochemical study of the sediments of Tricomalee Bay. The bay is divided into three areas: Koddiyar Bay, Thambalagam Bay and the Inner Harbor. Since the harbor is over 300 years old, it is worthwhile to look into the environmental factors, processes and the provenance of the Trincomalee Bay sediments.

CHAPTER 3

METHOD OF STUDY

3.1 INCEPTION AND BASE DATA COLLECTION

Investigation of aerial photographs and topographic maps was carried out in this phase of the study. Existing aerial photographs available at the Department of Geology, University of Peradeniya, were used to study the hydrological and morphological conditions of the area before the field investigations.

The Mahaweli River basin was selected to carry out this study since this is the largest river basin in Sri Lanka and it flows through the Highland Complex. The area mainly falls within the wet zone, intermediate zone and the dry zone. Trincomalee Bay was selected since the Mahaweli River falls into Trincomalee Bay at Koddiyar Bay.

3.2 FIELD SAMPLING

3.2.1 Mahaweli Stream sediment samples

Stream sediment samples were collected along the Mahaweli River, taking into account sediment deposition, flow rate, river gradient, erosion and human impact on natural sedimentation. Samples were taken at varying distances based on accessibility (Fig. 2.1.2), considering locations of tributaries, geological factors, and the distribution of the three climatic zones. Four to five kg bulk samples were taken at each location.

3.2.2 Mahaweli Basement Rock Samples

Rock samples (n = 38) were collected along the Mahaweli main stream. Samples were taken from the fresh bedrock. Thirty eight rock samples were collected (Fig 3.1.1) from the Mahaweli catchment area.

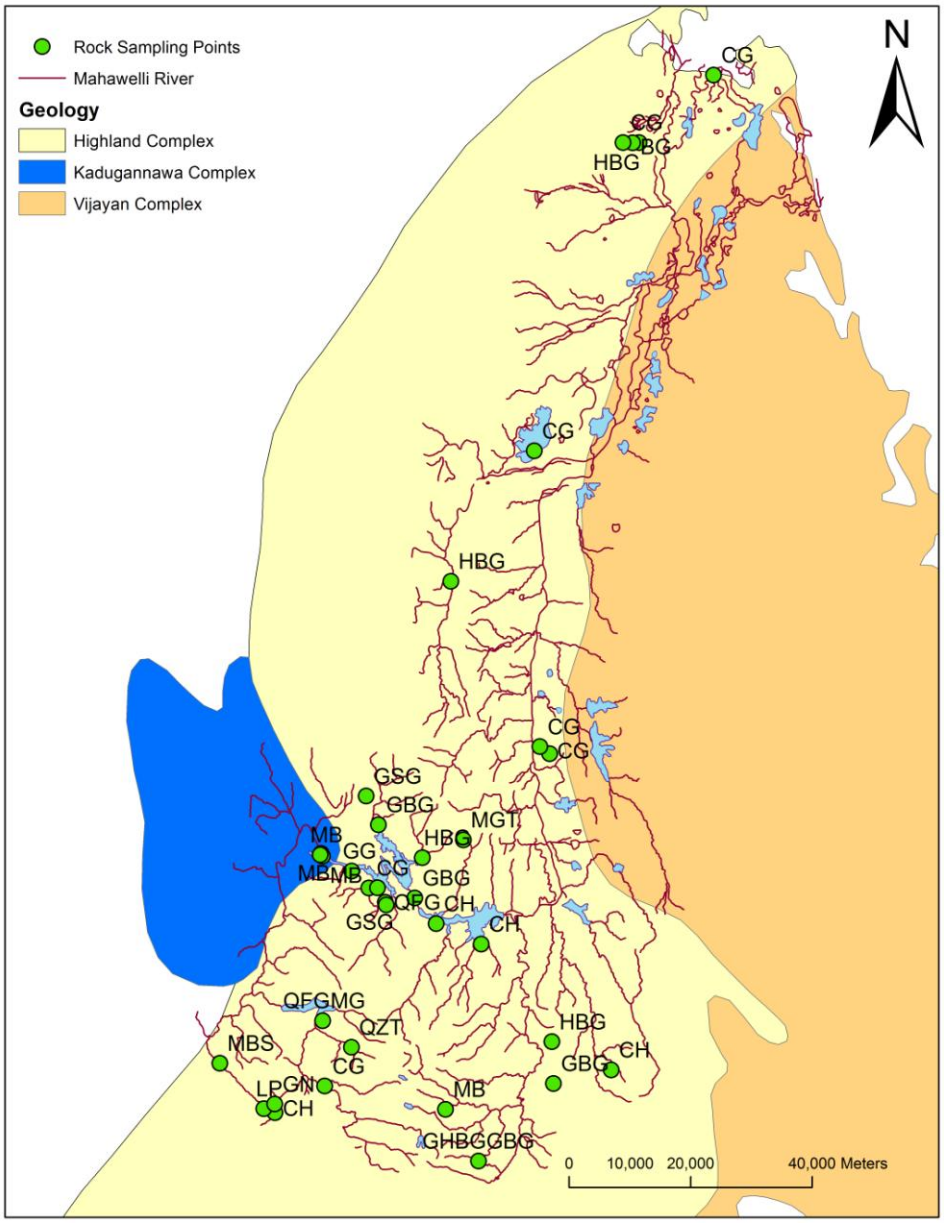

Fig. 3.1.1 : Rock sampling locations along the Mahawelli River (MB-Metabasite, HBG-Hornblende biotite gneiss, GG-Granitic gneiss, QFG-Quartzo-feldspathic gneiss, QTZ-Quartzite, MG-Migmatitic gneiss, MGT-Migmatite, LP-Leptynite, GSG-Garnet sillimanite gneiss, CH-Charnockite, CG-Charnockitic gneiss, GBG-Garnet biotite gneiss, MB-Marble, BG-Biotite gneiss, GHBG-Garnetiferrous hornblende biotite gneiss)

3.2.3 Mahaweli area Soil samples

Soil samples (n = 22) of weathered rocks and agricultural soil were taken along the main Mahawelli stream. Twenty two sampling points were selected (Fig 3.1.2) in the Mahaweli catchment.

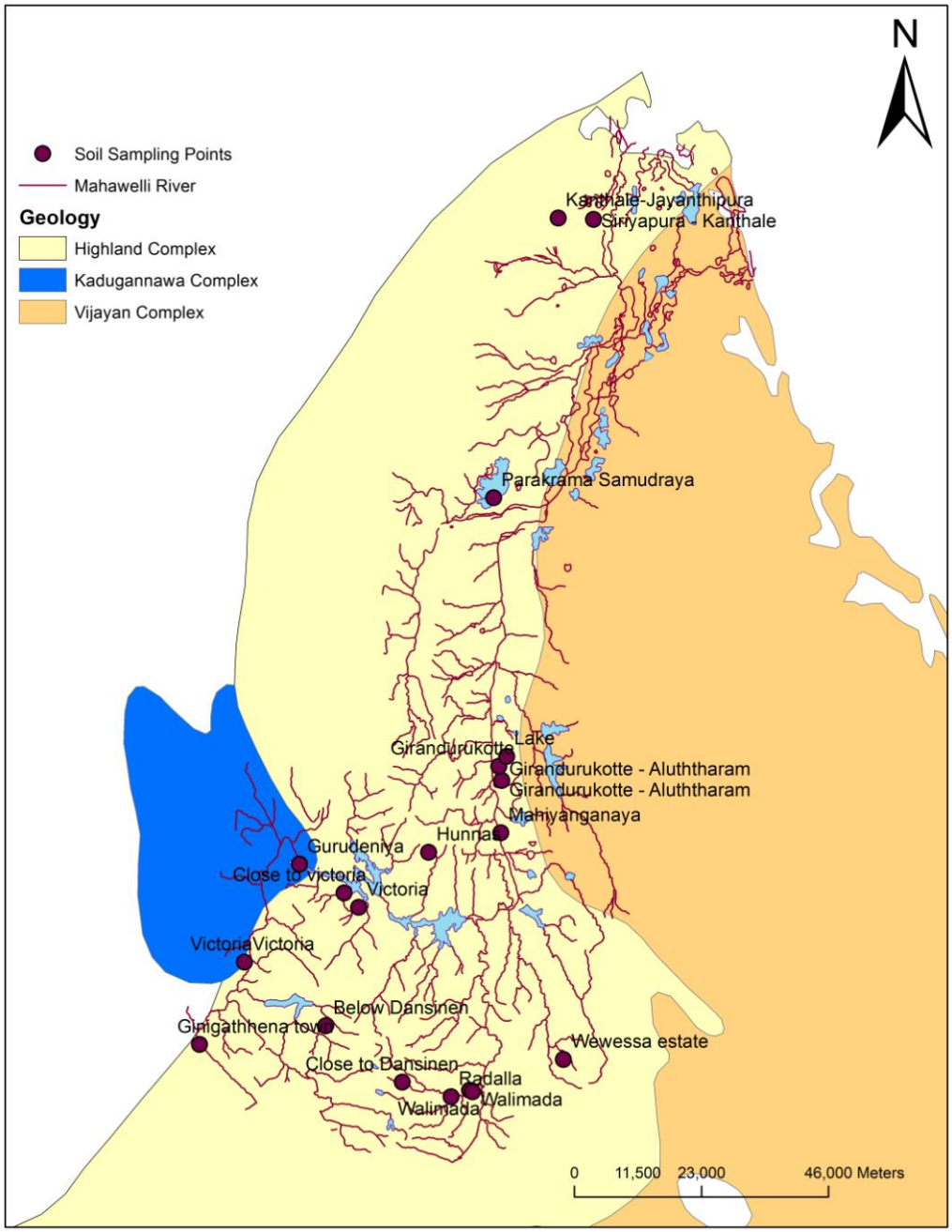

Fig. 3.1.2 : Soil sampling locations along the Mahawelli River

3.2.4 Polgolla Dam surface and core sediments

Sediment samples were collected from the upper catchment of the Mahaweli River and the Polgolla reservoir (Fig 2.1.3), using grab sampler method. The core was taken from the middle of the reservoir, so that it is most representative of the sediment deposition.

3.2.5 Trincomalee Bay surface sediments

Surface sediments in Trincomalee Bay were collected taking the proximity of the Mahaweli River mouth into account, and location in Koddiyar Bay, Thambalagam Bay and the Inner Harbour (Fig. 2.1.4). Samples from the Inner Harbour (n=12) and Thambalagam Bay (n=19) were collected using an Ekman-Birge bottom sampler. Water depths at sampling points ranged up to 11.5 m. Sample positions were recorded using GPS. The grab samples (1-2 kg) were sub-sampled (about 500 g) at a depth of 3 – 6 cm below surface. Some samples from Koddiyar Bay (n=17) were taken by free diving, as strong current activity at the time of sampling precluded use of the Ekman-Birge sampler.

The samples were air dried, and then halved by coning and quartering. One split was archived, and the other used for textural and geochemical analysis. This split was oven-dried at 120°C for one week at the University of Peradeniya.

3.2.5.1 Statistics of Trincomalee Bay surface sediments

Statistical analyses (p-values, t-values) were calculated using Minitab 14 software to determine if differences were present between the three sectors. Principal component analysis (PCA) was carried out using the Pearson method in XLSTAT 12. GIS contour maps of element distributions were generated using ARC-GIS 9.2. The maps were generated using the nearest neighbor method with inverse distance weighted (IDW) interpolation, with contours in five classes.

3.2.6 Trincomalee Bay core sediments

Cores of beach sediments in Trincomalee Bay were collected taking into account proximity to the Mahaweli River mouth (C2) and locations in west (C1) and east (C3) of Koddiyar Bay and the Thambalagam Bay (C4). The four cores were taken as shown in Fig 3.2.1. C1 is to the west of Koddiyar Bay beach, and is covered with black sand. The location of C2 is at the Mahaweli River mouth. Location C3 is in the east of Koddiyar Bay and was selected because it also is the site where the other branch of the Mahaweli River enters Trincomalee Bay. Location C4 is within Thambalagam Bay. The Inner Harbor was not considered for core sampling because the water depth was too great. The core samples were collected using a PVC pipe of 1m length by pushing it down in the sampling site. The four cores were 62cm, 20cm, 36cm and 34cm of length for C1, C2, C3 and C4 respectively (Fig 3.2.2).

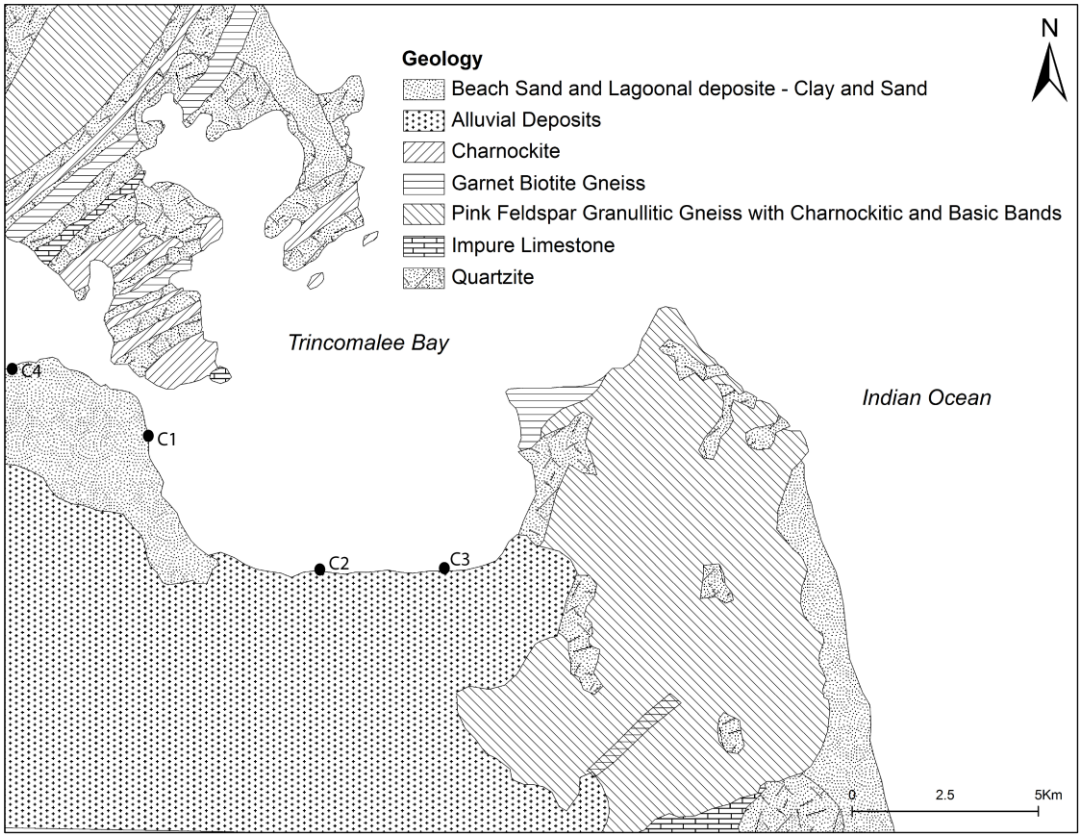

Fig. 3.2.1: Trincomalee core sediment locations and the simplified geological map of the area surrounding Trincomalee Bay (after Wijayananda 1985)

The cores were collected and cut into 2cm thick slices and stored in a 4°C cooling box. The sliced core sediment samples were air dried, and then halved. One split was archived, and the other reserved for textural and geochemical analysis. This split was then oven dried at 120°C for one week at the University of Peradeniya. All analyses were carried out at Shimane University.

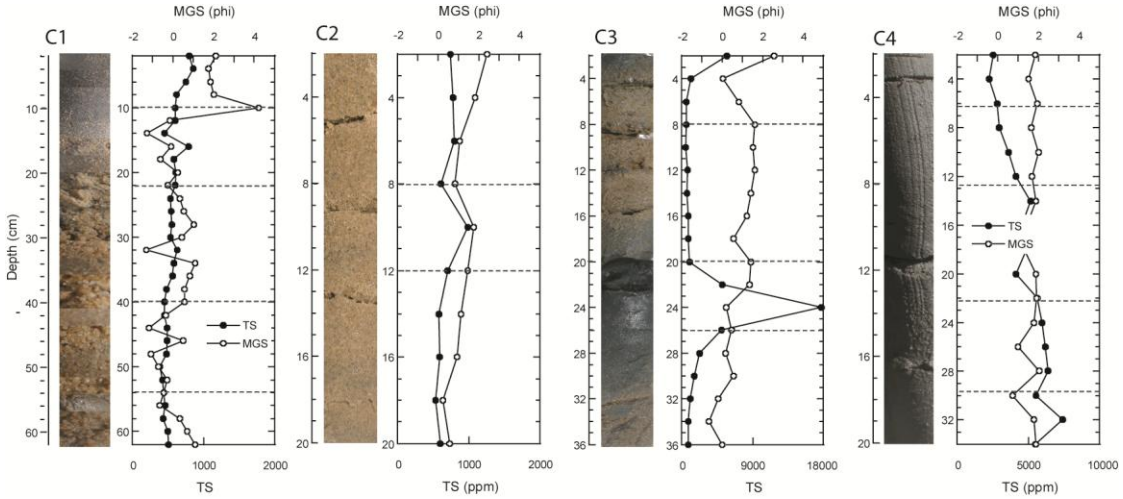

Fig. 3.2.2: Photographs of the four cores in Trincomalee bay and variation in grain size and TS (Total Sulphur)

3.3 SAMPLE PREPARATION

3.3.1 Sediment samples

The stream sediment samples were oven dried at 120°C prior to geochemical analysis at Shimane University. Samples were first hand-sieved to remove the small amount of material >2000 µm. The <2000 µm fraction was then split to provide a sample for bulk sediment analysis (<2000µm). A second split was then sieved to separate <180 µm and 180 – 2000 µm fractions for fractional analysis. The <180µm and 180 – 2000µm fractions are often used as the most appropriate and convenient fractions for the examination of stream sediment geochemistry (Amorosi et al., 2002; Ferreira et al., 2001; Koval et al., 1995; Licht and Tarvainen, 1996; Ortiz and Roser, 2006a,b). Consequently, the <180 µm and 180 – 2000 µm fractions were also used for this study.

3.3.2 Rock samples

Whole-rock samples were cut into small chips and washed with distilled water, ultrasonically cleaned for ten minutes to remove clay particles, again rinsed with distilled water, and then oven dried at 110°C for 48 hours.

3.3.3 Soil samples

Approximately 50g of each fraction, bulk sediment and soil samples were oven-dried at 160°C for 48 hrs before crushing. All samples were crushed using a ROCKLABS tungsten carbide ring mill, with mill times of <60 seconds.

3.4 X-RAY FLUORESCENCE (XRF) ACCURACY AND PRECISION

Glass fusion beads for X-ray fluorescence (XRF) analysis (anhydrous basis) were prepared with an alkali flux, following the method described in detail in Kimura and Yamada (1996). The flux used comprised 80% lithium tetraborate (Merck Spectromelt®A10) and 20% lithium metaborate (Merck Spectromelt®A20). Both components were dried for at least 24 h at 110 ^{0}C before mixing. The beads contained 1.8 g of the anhydrous sample from the LOI determinations and 3.6 g of flux, giving a sample to flux ratio of 1:2. Abundances of the major elements and 14 trace elements were determined from these fusion beads using a Rigaku RIX-2000 XRF spectrometer equipped with an Rh-anode tube. The instrument conditions, interference corrections, and calibration used were those described by Kimura and Yamada (1996). Primary calibration was made using the same beads from that study, including both international rock standards, synthetic mixes, and standards with elemental ranges extended by standard addition. These standards thus had elemental ranges spanning that expected in most geological situations. Major element matrix corrections were made as described by Kimura and Yamada (1996). Overlap corrections were applied for significant spectral interferences among the trace elements, as specified by Kimura and Yamada (1996).

During routine analysis, the primary calibration was verified by analysis and cross-calibration of nine Geological Survey of Japan rock standards spanning the compositional range from gabbro to granite. Average results, standard deviations, and two-sigma coefficients of variation for repeat analyses (n=6) of these standards during normal operation are listed in the Table 3.4.1. These data show that average precision of the major elements ranges from ±0.29 wt% of the amount present (SiO_2) to ±4.72 wt% (Na_2O). Among the 14 trace elements analyzed by this method the two-sigma values range from a low of 0.6% relative (Zr) to 26.5% (Th). The trace element two-sigma CVs are, however, influenced by higher values when abundances are <10 ppm, even though the disparity between the observed and recommended values may only be a few ppm. When values where abundances are <10 ppm are excluded, the range of two-sigma values for the trace elements falls to a maximum of 12.7% relative (Ce), and for half of the analyzed elements (Nb. Ni, Pb, Rb, Sr, Y, Zr) the precision is better than 5%.

Abundances of three additional trace elements (As, Cu, Zn) were determined from pressed powder briquettes (sample weight 3.0-3.5 g), prepared using a force of 200KN for 60 s. The pressed powder analysis followed Ogasawara (1987), using conventional peak over background (Ip/Ib) method, with calibration against recommended or preferred values for seven GSJ rock standards (Table 3.4.2). Arsenic values were also corrected for Pb peak overlap. Precision was estimated as for the glass bead data, but based on 5 analyses of the seven calibration standards during normal operation. Average 2-sigma coefficients of variation for the three elements range from 3.5-6.7% relative at concentrations of > 5 ppm. This was confirmed by repeat analysis (n=5) of seven samples from this study, yielding similar results.

Table 3.4.1: Mean concentrations from repeat analyses (n=6) of GSJ rock standards using the glass bead method. Analyst: Barry Paul Roser.

Std	SiO2	TiO2	Al2O3	Fe2O3	MnO	MgO	CaO	Na2O	K2O	P2O5	Sum	Ba	Ce	Cr	Ga	Nb	Ni	Pb	Rb	Sc	Sr	Th	V	Y	Zr
Standards run (n=6 each																									
JG-1a (granite)																									
RV	**72.65**	**0.25**	**14.31**	**2.06**	**0.06**	**0.69**	**2.14**	**3.43**	**4.04**	**0.08**	**99.72**	**460.9**	**47.4**	**18.7**	**17.1**	**12.1**	**6.4**	**27.2**	**181.1**	**6.2**	**186.2**	**12.2**	**23.1**	**32.2**	**115.7**
Mean	**72.47**	**0.24**	**14.47**	**2.03**	**0.06**	**0.76**	**2.17**	**3.51**	**3.98**	**0.08**	**99.77**	**471.5**	**41.9**	**9.6**	**17.9**	**11.5**	**6.2**	**26.5**	**183.1**	**8.5**	**187.6**	**12.7**	**20.7**	**27.8**	**124.9**
SDp	0.12	0.01	0.05	0.03	0.00	0.01	0.01	0.03	0.02	0.00	0.09	15.9	2.8	2.9	0.9	0.2	0.5	0.2	0.8	0.9	0.9	0.4	2.7	0.3	0.4
CV%	0.33	4.96	0.69	2.68	2.39	2.17	1.07	1.79	0.85	11.89	0.19	6.7	13.6	60.3	10.2	3.6	15.4	1.9	0.9	22.1	1.0	5.8	25.9	2.0	0.6
JG-2 (granite)																									
RV	**77.09**	**0.04**	**12.51**	**0.97**	**0.02**	**0.04**	**0.70**	**3.55**	**4.73**	**0.00**	**99.65**	**81.3**	**48.5**	**6.4**	**18.7**	**14.7**	**4.4**	**31.6**	**302.0**	**2.4**	**18.0**	**31.7**	**3.8**	**86.8**	**97.9**
Mean	**76.87**	**0.03**	**12.89**	**1.00**	**0.01**	**0.16**	**0.69**	**3.67**	**4.60**	**0.00**	**99.92**	**87.4**	**50.5**	**1.8**	**19.7**	**16.5**	**6.6**	**30.2**	**300.9**	**3.7**	**16.4**	**31.1**	**n.d.**	**79.0**	**109.0**
SDp	0.10	0.00	0.04	0.00	0.00	0.00	0.00	0.06	0.02	0.00	0.08	6.3	2.6	4.4	0.9	0.2	0.4	0.7	1.2	0.8	0.3	0.3	2.4	0.6	0.2
CV%	0.25	9.93	0.57	0.22	0.24	2.56	0.24	3.25	0.66	-	0.16	14.4	10.1	483.8	9.3	2.0	10.9	4.5	0.8	41.1	3.3	2.0	-	1.6	0.5
JA-2 (andesite)																									
RV	**57.40**	**0.68**	**15.65**	**6.27**	**0.11**	**7.85**	**6.62**	**3.15**	**1.84**	**0.15**	**99.73**	**323.9**	**33.7**	**475.1**	**16.8**	**14.3**	**142.0**	**19.3**	**68.0**	**20.0**	**257.5**	**4.8**	**132.8**	**15.6**	**121.6**
Mean	**57.50**	**0.68**	**15.79**	**6.40**	**0.11**	**7.19**	**6.45**	**3.10**	**1.90**	**0.16**	**99.29**	**324.9**	**30.7**	**447.7**	**17.3**	**9.7**	**139.1**	**20.4**	**73.7**	**21.0**	**256.8**	**4.8**	**128.0**	**16.7**	**117.1**
SDp	0.06	0.01	0.07	0.05	0.00	0.05	0.01	0.03	0.02	0.00	0.07	8.2	1.4	7.4	1.1	0.2	2.0	0.6	0.4	0.7	1.7	0.3	8.8	0.6	0.3
CV%	0.19	1.87	0.83	1.64	0.80	1.50	0.42	1.87	2.55	1.86	0.13	5.0	9.4	3.3	12.6	3.9	2.8	5.6	1.2	6.7	1.3	13.7	13.8	6.8	0.6
JA-3 (andesite)																									
RV	**62.39**	**0.70**	**15.59**	**6.61**	**0.10**	**3.73**	**6.25**	**3.20**	**1.41**	**0.12**	**100.11**	**324.0**	**23.0**	**66.3**	**16.3**	**3.4**	**32.3**	**7.7**	**36.8**	**22.0**	**287.6**	**3.3**	**169.3**	**21.2**	**118.2**
Mean	**61.98**	**0.68**	**15.67**	**6.63**	**0.11**	**3.66**	**6.33**	**3.18**	**1.34**	**0.11**	**99.70**	**324.8**	**25.3**	**68.6**	**17.7**	**4.5**	**32.3**	**7.4**	**35.7**	**22.8**	**289.5**	**1.6**	**171.1**	**18.9**	**113.8**
SDp	0.10	0.01	0.05	0.06	0.00	0.04	0.01	0.02	0.03	0.00	0.13	18.1	1.5	3.5	1.0	0.2	1.2	0.4	0.3	1.3	1.8	0.4	11.0	0.4	0.3
CV%	0.33	1.55	0.58	1.91	1.20	2.43	0.24	1.56	3.94	3.54	0.26	11.2	11.7	10.1	10.8	9.4	7.6	10.9	1.6	11.3	1.2	51.4	12.8	4.2	0.5
JB-1b (basalt)																									
RV	**51.91**	**1.28**	**14.60**	**9.16**	**0.15**	**8.27**	**9.75**	**2.67**	**1.34**	**0.26**	**99.40**	**N/A**	**N/A**	**445.9**	**N/A**	**N/A**	**150.3**	**6.9**	**39.7**	**29.0**	**445.9**	**N/A**	**217.3**	**N/A**	**N/A**
Mean	**51.87**	**1.27**	**14.07**	**9.24**	**0.15**	**8.53**	**9.87**	**2.60**	**1.30**	**0.26**	**99.17**	**515.5**	**55.4**	**479.6**	**17.9**	**23.4**	**155.3**	**6.0**	**34.9**	**30.9**	**450.7**	**9.0**	**227.1**	**20.7**	**128.4**
SDp	0.05	0.00	0.03	0.08	0.00	0.08	0.03	0.07	0.03	0.00	0.15	15.8	2.9	10.4	1.1	0.9	1.3	0.4	0.6	1.6	2.6	0.5	8.5	0.4	0.2
CV%	0.20	0.60	0.49	1.77	0.63	1.79	0.56	5.21	4.31	1.29	0.31	6.1	10.6	4.3	12.3	7.9	1.7	12.6	3.7	10.6	1.2	10.6	7.5	4.2	0.3
JB-3 (basalt)																									
RV	**51.05**	**1.44**	**17.23**	**11.84**	**0.18**	**5.20**	**9.81**	**2.73**	**0.78**	**0.29**	**100.56**	**245.5**	**21.5**	**58.2**	**19.8**	**2.5**	**36.3**	**5.6**	**15.1**	**33.9**	**403.7**	**1.3**	**372.7**	**26.9**	**98.0**
Mean	**50.76**	**1.43**	**16.86**	**11.85**	**0.18**	**5.26**	**9.78**	**2.70**	**0.67**	**0.29**	**99.85**	**232.0**	**20.2**	**67.5**	**20.1**	**3.3**	**35.6**	**5.0**	**13.9**	**33.0**	**405.4**	**0.8**	**396.4**	**24.0**	**93.9**
SDp	0.05	0.00	0.03	0.01	0.00	0.02	0.01	0.04	0.03	0.00	0.20	6.7	2.9	2.7	1.0	0.2	0.7	0.5	0.5	0.6	2.4	0.4	15.5	0.4	0.3
CV%	0.21	0.36	0.34	0.21	0.51	0.69	0.29	3.30	9.37	1.26	0.40	5.8	28.5	7.9	9.5	9.9	3.7	20.5	7.1	3.7	1.2	84.6	7.8	3.6	0.6
JGb-1 (gabbro)																									
RV	**44.22**	**1.62**	**17.72**	**15.25**	**0.19**	**7.95**	**12.05**	**1.22**	**0.24**	**0.06**	**100.53**	**65.1**	**8.3**	**58.5**	**18.1**	**3.4**	**25.7**	**1.9**	**7.0**	**36.3**	**331.2**	**0.5**	**643.2**	**10.5**	**33.2**
Mean	**44.22**	**1.61**	**17.24**	**15.25**	**0.19**	**8.26**	**12.01**	**1.14**	**0.28**	**0.05**	**100.24**	**56.5**	**7.5**	**73.5**	**18.8**	**3.2**	**22.1**	**2.2**	**7.8**	**35.9**	**325.9**	**1.5**	**648.1**	**9.3**	**31.0**
SDp	0.09	0.01	0.03	0.01	0.00	0.03	0.01	0.08	0.01	0.00	0.11	8.9	1.7	7.3	0.9	0.3	0.7	0.6	0.3	1.8	1.4	0.4	13.3	0.3	0.2
CV%	0.40	0.72	0.35	0.19	0.66	0.74	0.22	13.65	4.85	1.76	0.22	31.4	44.2	20.0	9.8	18.4	6.5	55.8	7.1	10.0	0.9	52.1	4.1	7.5	1.1
JSL-1 (shale)																									
RV	**62.86**	**0.77**	**18.60**	**7.29**	**0.06**	**2.55**	**1.56**	**2.31**	**3.01**	**0.21**	**99.22**	**322.4**	**64.0**	**64.4**	**21.9**	**10.0**	**39.7**	**18.4**	**123.7**	**17.7**	**204.0**	**10.5**	**138.5**	**31.7**	**183.9**
Mean	**63.42**	**0.76**	**18.85**	**7.10**	**0.06**	**2.51**	**1.59**	**2.49**	**3.20**	**0.21**	**100.19**	**342.7**	**61.2**	**62.6**	**23.2**	**10.9**	**41.8**	**20.5**	**125.5**	**14.3**	**207.8**	**9.8**	**154.5**	**28.7**	**179.7**
SDp	0.12	0.00	0.03	0.01	0.00	0.01	0.00	0.06	0.00	0.00	0.17	9.2	3.7	2.1	0.8	0.2	0.9	0.6	0.8	0.6	1.4	0.4	8.0	0.7	0.7
CV%	0.38	0.49	0.33	0.22	1.86	0.75	0.26	5.00	0.09	0.70	0.33	5.3	12.1	6.6	6.8	3.5	4.3	5.9	1.2	9.1	1.3	8.0	10.4	4.9	0.8
JSL-2 (shale)																									
RV	**62.87**	**0.68**	**19.22**	**7.03**	**0.08**	**2.52**	**1.99**	**1.42**	**3.18**	**0.17**	**99.18**	**319.9**	**73.7**	**68.5**	**24.2**	**13.0**	**43.0**	**20.9**	**125.0**	**17.8**	**243.7**	**12.2**	**129.2**	**33.2**	**202.3**
Mean	**63.51**	**0.79**	**19.44**	**6.93**	**0.09**	**2.48**	**1.98**	**1.64**	**3.27**	**0.18**	**100.31**	**339.5**	**71.9**	**64.7**	**24.5**	**13.1**	**46.5**	**23.0**	**126.6**	**15.3**	**250.2**	**12.5**	**144.9**	**30.8**	**202.8**
SDp	0.10	0.00	0.04	0.01	0.00	0.01	0.00	0.06	0.00	0.00	0.14	8.4	2.0	4.0	0.9	0.3	1.2	0.5	0.6	0.6	1.4	0.7	7.0	0.5	0.8
CV%	0.33	1.14	0.37	0.38	1.30	0.69	0.50	6.83	0.27	1.90	0.27	5.0	5.7	12.2	7.3	5.0	5.2	4.0	0.9	8.3	1.1	10.7	9.7	3.5	0.8
Average CV%	**0.29**	**2.40**	**0.51**	**1.02**	**1.06**	**1.48**	**0.42**	**4.72**	**2.99**	**3.03**	**0.25**	**10.1**	**16.2**	**67.6**	**9.8**	**7.1**	**6.4**	**13.5**	**2.7**	**13.7**	**1.4**	**26.5**	**10.2**	**4.3**	**0.6**
Standards >10 ppm												**10.1**	**12.7**	**9.2**	**9.8**	**4.3**	**4.5**	**4.4**	**2.2**	**8.5**	**1.4**	**7.4**	**11.5**	**3.8**	**0.6**

RV - recommended or preferred values, recalculated on an anhydrous basis, from Geological Survey of Japan data, available at https://gbank.gsj.jp/geostandards/welcome.html

SDp - Standard deviation; CV% - 2-sigma coefficient of variation. N/A - not available. Dash (-) not detected.

Table 3.4.2: Pressed powder standard analyses (n=5). RV- Recommended or preferred values, source as in Table 4.3.2. SD- Standard deviation, CV% - 2 sigma coefficient of variation. n.d. - not detected. Analyst: Barry Paul Roser.

Standard	As	Zn	Cu
JA-2 RV	**0.9**	**64.7**	**29.7**
Mean	**1.0**	**70.9**	**28.4**
SD	0.4	1.0	1.0
CV%	38.5	1.4	3.5
JA-3 RV	**4.7**	**67.7**	**43.4**
Mean	**3.9**	**71.2**	**47.4**
SD	0.3	1.3	2.4
CV%	14.9	3.6	10.1
JB-3 RV	**1.8**	**100.0**	**194.0**
Mean	**1.1**	**91.0**	**182.1**
SD	0.3	3.4	4.2
CV%	47.7	7.5	4.6
JG-2 RV	**0.7**	**13.6**	**0.5**
Mean	**1.6**	**10.0**	**n.d.**
SD	0.2	1.4	-
CV%	28.9	28.5	-
JLk-1 RV	**26.8**	**152.0**	**62.9**
Mean	**28.2**	**161.8**	**72.6**
SD	0.3	1.9	1.7
CV%	2.4	2.4	4.7
JR-3 RV	**1.1**	**209.0**	**2.9**
Mean	**2.7**	**200.7**	**n.d.**
SD	0.2	2.0	-
CV%	12.1	2.0	-
JSL-1 RV	**14.9**	**108.0**	**40.8**
Mean	**12.9**	**118.3**	**41.3**
SD	0.3	1.4	0.7
CV%	2.3	1.2	1.7
Average CV%	21.0	6.7	4.1
Average >5 ppm	3.5	6.7	4.1

3.5 GRAIN SIZE ANALYSIS

The grain size analysis was made using a laser diffraction particle size analyzer SALD-3000 and a settling tube grain size analyzer at Shimane University, after treating the oven dried sediments with 30% H_2O_2 for at least twenty four hours to digest the organic matter.

In core1 the samples 1C25 – 1C31 were sieved using a -1.0 ϕ (2 mm) sieve. The remainder for each sample in the sieve was the weighed.

3.6 HEAVY MINERAL SEPARATION

Heavy mineral separates were prepared from the 18 samples which exhibited the highest elemental concentrations. The heavy minerals were separated from the 63-180μm and 180-300 μm fractions using a combination of conventional heavy liquid (bromoform, specific gravity 2.85) and magnetic separation (Frantz Isodynamic L-1). These fractions were selected after experimentation, due to difficulties in heavy liquid separation from finer or coarser fractions. Magnetite was first removed from the heavy liquid concentrate using a hand magnet. Frantz separation of the remaining concentrate was then made in runs at 0.2-0.3, 0.3-0.4, 0.4-0.5, 0.5-1.0, and >1.0 amps. The weights of each Frantz separate were recorded at each step. Heavy mineral counts were made of 0.3-0.5 amp portions of 180-300 μm fractions, using a binocular microscope at magnifications of 20~40x. Two hundred and fifty grains were counted for each of 18 samples spread over a main channel length of 310 km; of these, seven samples were from tributaries entering at 67, 107, 109, 119, 131, 170, 184, and 229 km from the uppermost point. The 63-180 μm fraction was only observed under a binocular microscope at magnifications of 20~40x. The heavy mineral count of the single Trincomalee Bay sample (MC 310) analyzed was made on the 180-300μm fraction, because the 63-180 μm fraction was too small for analysis.

3.7 OSTRACODE ANALYSIS

In August 2010, a total of 43 surface sediment samples were collected from Trincomalee Bay using an Ekman-Berge grab sampler. In this study, we selected 15 surface sediment samples, which seem to reflect a spatial distribution of ostracode assemblages in the study area (Fig. 3.3.1).

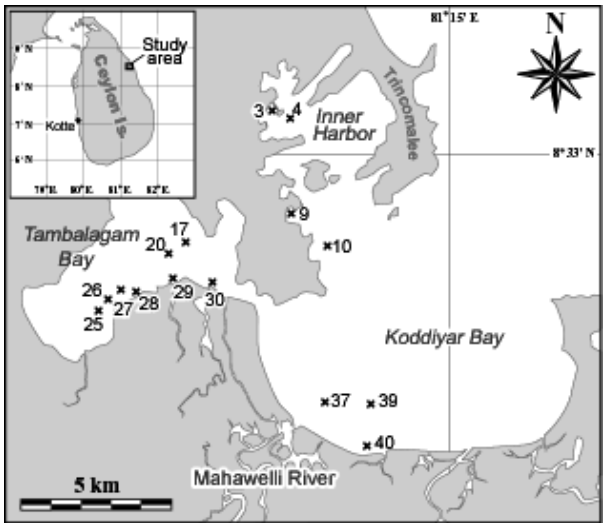

Fig. 3.3.1 Map showing the locations selected for Ostracode analysis in Trincomalee bay

Grain size analysis: Fifteen samples, from which organic matters were decomposed by 30% hydrogen peroxide water solution, were used for the grain size analysis. The integrated value of grain size was then measured using a laser diffraction particle size analyzer (SALD-3000S Shimadzu Co., Ltd.) at the Department of Geoscience, Interdisciplinary Faculty of Science and Engineering, Shimane University.

CN analysis: For CN analysis, part of each dried sample was powdered in an agate vessel. total organic carbon (TOC) and total nitrogen (TN) contents of powdered sediment samples (approximately 10 mg) were determined using a Carlo Erba 1108 elemental analyzer and YANACO CHNS-corder MT-3, after treatment with 1M HCl added to the sediment weighed in the cup and dried to remove the carbonate fraction. The errors (coefficient of variation) inherent in this analysis are within ±3%.

Ostracode analysis: For ostracode analyses, approximately 20 g of dried sediment samples were weighed and washed through a 0.063 mm sieve. The residues were divided using a sample splitter, each with approximately 200 specimens to be picked from residues coarser than 0.125 mm. The number of specimens refers to both valves and carapaces. One carapace was counted as two valves.

3.8 DATA ANALYSIS, INTERPRETATIONS AND PRESENTATION

The software used for statistical data analysis was Minitab 14, Kaleidagraph 4.0 and Microsoft Office Excel. ArcGIS 9.2 was used to prepare all maps used for the study. Discrimination diagrams and ratio plots were used to interpret the data.

3.8.1 GIS maps of element distributions

The maps were generated using the nearest neighbor method with inverse distance weighted (IDW) interpolation, with contours in five classes. IDW interpolation explicitly implements the assumption that sites that are close to one another are more alike than those that are farther apart. To predict a value for any unmeasured location, IDW will use the measured values surrounding the prediction location. Those measured values closest to the prediction location will have more influence on the predicted value than those farther away. IDW thus assumes that each measured point has a local influence that diminishes with distance. Points closer to the prediction location are given greater weighting than those farther away. The optimal power (p) value is determined by minimizing the root mean square prediction error (RMSPE). The RMSPE is the statistic that is calculated from cross-validation, in which each measured point is removed and compared to the predicted value for that location. The RMSPE is a summary statistic quantifying the error of the prediction surface. Geostatistical Analyst tries several different powers for IDW to identify the power that produces the minimum RMSPE. The error for generating the maps is less than ±7% (Text based on the ArcGIS 9.2 software manual).

CHAPTER 4

RESULTS

4.1 MAHAWELI RIVER

4.1.1 Textural and mineralogical characteristics

The main channel sediments were coarse to medium sand with lesser clay fractions, except for eleven samples in the middle reaches that contained more than 20 percent clay (Fig. 4.1.1). The gravel content of most samples was low (< 20 percent), except for one sample in the middle reaches and two in the lower reaches.

In general, sediment grain size in rivers decreases downstream (Parker, 1991; Surian, 2002) but this is not the case for the Mahaweli. There is little improvement in sorting along most of the main channel, and median grain size is also highly variable. This is probably due to the number of tributaries entering the main channel, even in the middle reaches. The sediments only become well sorted in the lowermost reaches of the river, where tributaries are fewer.

The main minerals present in the stream sediments include quartz, plagioclase, K-feldspar, muscovite, hornblende and biotite. Based on visual estimates, the stream sediments in the upper reaches are richer in feldspar, whereas quartz content increases in the lower reaches. Common minor or accessory minerals include garnet, sillimanite, monazite, zircon and apatite. The river and its tributaries run along or across basement rocks including charnockitic gneiss, marble, hornblende-biotite gneiss, quartzite, garnet-sillimanite gneiss and metabasite. Microscope examination of the heavy mineral separates showed that zircon, magnetite, ilmenite, garnet, tourmaline, hornblende and allanite were the most abundant heavy minerals, whereas biotite and apatite were less abundant.

The soil samples collected were mostly pale loamy to clayey residual soils. A few samples that were rich in organic matter were darker in hue, and others were pink to red. The basement rocks sampled represent a variety of lithotypes. These included medium- to coarse-grained charnockites, granitic gneisses, marbles, meta-pelites, quartzites, and metabasites.

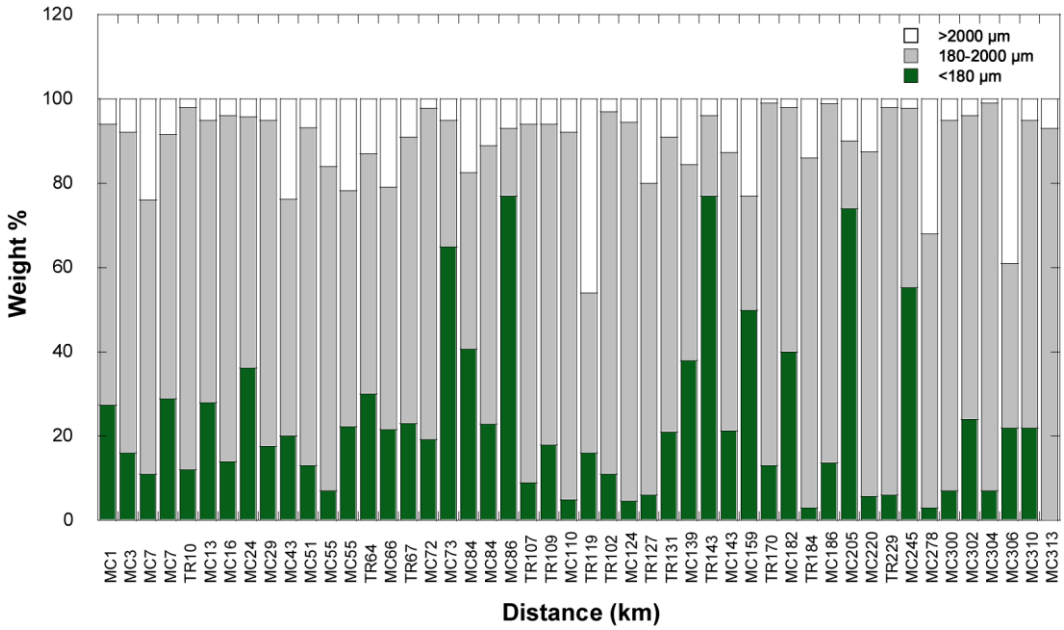

Fig. 4.1.1: Variation in stream sediment size fractions along the Mahaweli River

4.1.2 Data description

Individual analyses and averages of the bulk stream sediments, rocks and soils are given in Tables 4.1.1a, 4.1.1b and 4.1.1c, respectively, as supplementary data. Averages and minimum and maximum values are summarized in Table 4.1.2. Average values of Fe_2O_3, TiO_2, MnO and P_2O_5 are highest in the river sediments and lowest in the source rocks, whereas average CaO is highest in the source rocks and lowest in the soils (Table 4.1.2). Many of the trace elements (Zn, Cr, V, Sr, Y, Nb, Zr, Th, TS) have highest average values in the river sediments, which also tend to record the highest maximum values.

In order to highlight the differences between the sample types and to compare with typical upper crustal values, average values in the sediments, rocks and soils were normalized against average post-Archean Australian shale (PAAS; Table 4.1.2, Taylor and McLennan, 1985). The river sediments are highly enriched in CaO, V and Zr, and moderately enriched in TiO_2, Cu, Cr, Sr, Nb, Th and Sc relative to PAAS (Fig. 4.1.2). Several elements in the sediments (Pb, MnO and Y) exhibit PAAS-like values, and Cu and Ni are depleted. The sediments are slightly enriched in P_2O_5 relative to the soils and rocks, possibly due to concentration of accessory phases such as apatite and monazite (Nagarajan et al., 2007).

Most elements in the soils are depleted (e.g. Zn, Cu, Ni, Y and Nb), whereas CaO is moderately to highly enriched relative to PAAS. The rocks are also mostly depleted relative to PAAS, especially for TiO_2, Cu, Ni, Nb, Zr and Th. In contrast, CaO and Sr are enriched.

Table 4.1.1a: XRF analyses of Mahaweli River bulk stream sediments. Major elements as oxide wt%, trace elements ppm. Distance: distance downstream (km) from the uppermost sample point. The highlighted rows are the tributary values

S-No	Distance	As	Pb	Zn	Cu	Ni	Cr	V	Sr	Y	Nb	Zr	Th	Sc	TS	TiO_2	Fe_2O_3	MnO	CaO	P_2O_5
Wet Zone																				
2	1	10	26	165	49	58	153	355	65	20	21	338	18	26	1224	1.52	12.44	0.11	1.02	0.32
6	3	7	19	105	22	19	169	514	31	12	36	753	44	23	584	2.46	11.43	0.07	1.01	0.19
3	7	10	36	231	52	70	346	963	163	35	105	1405	95	44	954	4.44	25.80	0.20	2.10	0.47
5	7	7	17	138	42	33	165	295	48	8	18	436	13	15	755	1.70	9.34	0.03	0.84	0.25
10	**10**	**4**	**31**	**148**	**59**	**68**	**304**	**389**	**522**	**33**	**17**	**366**	**17**	**41**	**826**	**1.60**	**16.25**	**0.22**	**5.65**	**0.42**
1	13	4	28	73	26	37	124	180	208	22	14	248	12	16	620	0.91	6.87	0.09	1.58	0.19
7	16	5	23	87	27	31	156	270	86	19	27	354	32	18	406	1.70	8.35	0.06	0.94	0.14
4	24	5	18	98	18	26	129	554	101	14	65	1092	36	19	514	2.96	9.10	0.06	1.26	0.21
11	29	5	23	96	40	32	166	286	59	13	17	290	17	27	587	1.49	10.40	0.07	1.02	0.20
13	43	4	17	81	27	26	154	381	77	21	28	545	28	19	407	1.98	11.02	0.09	1.15	0.16
9	51	4	17	91	28	30	127	241	90	19	14	212	12	20	559	1.26	9.08	0.07	1.37	0.22
14	55	6	34	151	52	43	140	280	134	21	19	391	21	21	1045	1.41	10.44	0.12	1.65	0.30
13	55	8	32	147	72	72	315	690	81	29	47	1140	67	18	1249	2.87	20.52	0.13	1.77	0.44
12	**64**	**6**	**35**	**179**	**45**	**61**	**283**	**588**	**601**	**40**	**49**	**1042**	**76**	**41**	**725**	**3.00**	**15.08**	**0.24**	**6.67**	**0.32**
16	66	2	11	88	76	80	163	302	227	16	7	111	2	30	375	1.01	15.10	0.22	2.79	0.10
Wet Zone Avarage		5.8	24.5	125.2	42.3	45.7	192.9	419.2	166.2	21.5	32.3	581.5	32.7	25.2	722.0	2.02	12.75	0.12	2.05	0.26
Intermediate Zone																				
15	**67**	**6**	**27**	**55**	**26**	**24**	**113**	**84**	**2713**	**20**	**6**	**175**	**5**	**31**	**4178**	**0.42**	**4.29**	**0.09**	**49.44**	**0.26**
17	72	3	18	74	33	33	112	189	371	17	8	136	7	20	480	0.96	7.56	0.11	2.84	0.17
18	73	5	27	164	94	60	149	333	182	30	12	145	10	33	969	1.12	15.61	0.25	1.58	0.26
20	84	3	23	61	19	18	94	169	331	23	16	226	8	16	720	1.09	5.70	0.06	3.86	0.18
19	**84**	**7**	**33**	**150**	**56**	**56**	**147**	**281**	**91**	**31**	**11**	**186**	**11**	**26**	**1322**	**0.84**	**15.08**	**0.25**	**1.23**	**0.22**
21	86	4	39	151	87	110	224	303	477	51	17	320	12	41	1777	1.40	13.83	0.17	11.04	0.41
22	**91**	**3**	**15**	**69**	**13**	**17**	**121**	**287**	**102**	**20**	**25**	**462**	**37**	**14**	**318**	**1.85**	**8.26**	**0.09**	**1.71**	**0.12**
23	**102**	**3**	**19**	**59**	**18**	**23**	**112**	**208**	**207**	**23**	**14**	**301**	**14**	**13**	**323**	**1.20**	**6.90**	**0.08**	**2.64**	**0.17**
45	**107**	**6**	**34**	**183**	**35**	**32**	**193**	**698**	**323**	**69**	**105**	**1244**	**66**	**39**	**806**	**3.92**	**20.88**	**0.28**	**4.84**	**0.43**
25	**109**	**6**	**39**	**121**	**25**	**39**	**260**	**559**	**444**	**47**	**69**	**916**	**49**	**28**	**578**	**2.97**	**14.26**	**0.15**	**4.25**	**0.38**
26	110	2	17	50	16	18	97	178	175	22	23	191	11	15	363	1.02	8.10	0.11	2.08	0.18
27	**119**	**5**	**43**	**167**	**46**	**62**	**189**	**376**	**595**	**54**	**48**	**538**	**24**	**33**	**929**	**1.70**	**16.33**	**0.22**	**4.87**	**0.50**
28	124	3	13	77	17	17	139	339	119	25	39	412	25	20	273	2.01	10.55	0.12	2.00	0.16
29	**127**	**4**	**27**	**101**	**52**	**59**	**192**	**196**	**273**	**25**	**9**	**170**	**8**	**20**	**714**	**0.69**	**9.56**	**0.10**	**1.80**	**0.19**
30	**131**	**6**	**37**	**87**	**29**	**65**	**217**	**287**	**600**	**36**	**28**	**618**	**54**	**29**	**631**	**1.89**	**10.34**	**0.14**	**5.88**	**0.20**
31	139	4	22	95	43	46	150	232	186	26	18	331	19	20	671	1.06	9.89	0.13	1.64	0.22
32	143	3	17	58	16	22	126	148	167	20	13	270	9	14	330	0.87	6.36	0.07	1.85	0.13
33	151	2	11	34	7	14	102	113	76	14	9	154	6	12	266	0.65	5.46	0.07	1.39	0.09
34	159	1	12	44	8	10	100	105	78	15	9	159	7	11	248	0.68	5.54	0.07	1.42	0.09
35	167	2	10	49	6	17	119	147	70	17	11	170	5	16	241	0.97	6.67	0.09	1.61	0.10
36	**170**	**7**	**32**	**73**	**16**	**17**	**120**	**313**	**828**	**40**	**42**	**1090**	**37**	**16**	**682**	**2.64**	**8.22**	**0.17**	**5.16**	**0.24**
37	173	2	16	34	8	15	79	63	141	13	5	109	3	8	240	0.33	3.75	0.05	1.48	0.08
38	174	1	13	22	4	16	74	45	78	9	3	124	1	5	238	0.24	3.26	0.04	1.14	0.07
39	178	1	10	30	6	10	78	66	54	11	6	127	4	8	236	0.50	4.02	0.05	1.12	0.07
Intermediate Zone A		3.7	23.1	83.7	28.3	33.3	137.8	238.3	361.7	27.4	22.8	357.3	18.0	20.3	730.5	1.29	9.18	0.12	4.87	0.21
Dry Zone																				
41	182	3	23	93	49	56	133	185	132	23	7	134	7	23	757	0.64	10.15	0.19	1.39	0.21
40	**184**	**8**	**32**	**156**	**29**	**41**	**209**	**762**	**216**	**44**	**80**	**1426**	**141**	**26**	**1065**	**3.54**	**17.41**	**0.18**	**3.07**	**0.25**
42	186	2	10	18	6	11	62	35	83	9	3	112	2	6	258	0.17	2.89	0.05	1.04	0.07
43	205	4	24	91	41	54	142	230	219	27	16	336	16	25	990	1.01	10.53	0.20	1.60	0.19
45	220	2	13	50	6	12	92	214	141	17	25	356	24	12	243	1.8	5.82	0.07	1.65	0.09
44	**229**	**6**	**30**	**166**	**11**	**17**	**263**	**1158**	**379**	**46**	**125**	**1299**	**95**	**31**	**667**	**4.32**	**15.82**	**0.21**	**4.23**	**0.22**
46	245	4	23	51	17	25	96	135	333	22	11	231	8	16	319	0.84	5.31	0.07	2.34	0.17
47	278	4	29	85	13	37	139	353	371	33	42	670	33	14	526	2.07	8.81	0.14	3.51	0.19
50	300	7	35	61	13	26	128	221	577	35	32	531	24	20	16404	1.69	6.01	0.08	4.12	0.12
49	302	5	39	61	8	31	141	241	526	34	29	535	19	16	2756	1.67	6.17	0.09	4.20	0.15
48	304	6	35	80	28	42	137	213	455	35	24	480	23	18	3635	1.39	8.84	0.13	3.23	0.24
51	306	10	36	63	12	26	169	185	620	30	27	589	31	24	2981	1.61	5.90	0.07	11.34	0.20
52	310	3	25	1114	98	48	270	25	152	14	3	174	4	4	1844	0.27	1.56	0.02	2.42	0.09
53	313	8	29	61	20	25	78	129	2695	31	13	522	18	41	7973	1.06	4.04	0.05	53.72	0.34
Dry Zone Avarage		5.1	27.4	153.6	25.1	32.2	147.1	291.9	492.8	28.6	31.2	528.2	31.8	19.7	2887.0	1.58	7.80	0.11	6.99	0.18
Overall Average		4.7	24.6	113.5	31.6	36.7	156.2	304.6	338.2	26.0	27.7	466.0	25.8	21.6	1277.0	1.58	9.87	0.12	4.59	0.22

Table 4.1.1b: XRF analyses of soils from the Mahaweli River basin. Major elements as oxide wt%, trace elements ppm. Distance: distance downstream (km) from the uppermost sample point

S_ No	Distance (km)	As	Pb	Zn	Cu	Ni	Cr	V	Sr	Y	Nb	Zr	Th	Sc	TS	TiO_2	Fe_2O_3	MnO	CaO	P_2O_5
Wet Zone																				
1	3	2	22	22	12	16	29	58	22	6	3	163	1	11	298	0.62	4.02	0.01	0.53	0.07
2	6	8	46	53	24	15	68	168	204	25	8	163	11	13	272	0.46	6.38	0.07	1.73	0.11
3	13	1	12	78	45	22	68	310	143	20	5	168	2	46	511	0.83	12.98	0.25	2.36	0.11
4	17	10	75	57	10	21	25	8	41	41	6	82	3	1	295	0.20	2.36	0.02	0.57	0.14
5	18	4	25	52	96	100	168	311	2	22	13	153	13	30	339	1.08	13.54	0.16	0.54	0.08
6	18	4	24	94	44	79	154	183	224	24	10	198	12	20	675	0.66	11	0.12	1.08	0.40
7	37	5	8	30	49	35	62	64	44	11	4	59	6	21	2472	0.41	3.45	0.04	18.27	0.14
8	37	1	8	71	56	66	528	284	92	19	6	149	3	42	463	0.72	12.43	0.21	3.83	0.14
9	54	6	12	33	26	23	112	156	4	5	4	159	9	24	616	0.54	7.42	0.04	0.58	0.15
10	72	5	30	89	37	63	103	158	170	30	11	147	31	16	770	0.50	9.28	0.11	1.16	0.24
Wet Zone Avarage		4.5	26.3	57.6	39.9	43.9	131.8	169.8	94.6	20.3	6.9	144.0	9.1	22.4	671.1	0.60	8.26	0.10	3.07	0.16
Intermediate Zone																				
11	84	4	30	118	60	43	107	178	156	35	11	154	19	23	1118	0.69	9.92	0.07	1.31	0.11
12	89	3	13	65	97	83	720	353	22	18	7	138	8	50	460	0.95	16.85	0.11	1.00	0.10
13	96	5	43	46	26	24	32	83	187	40	4	90	6	1	244	0.27	2.06	0.01	0.60	0.05
14	143	5	21	84	30	39	140	288	262	28	28	643	33	20	873	1.47	9.80	0.21	1.96	0.18
15	154	2	16	33	14	19	87	162	211	13	8	321	12	12	442	1.06	4.56	0.10	1.77	0.07
16	154	2	14	46	8	28	100	277	139	16	16	496	66	11	307	1.98	6.48	0.16	1.52	0.10
17	157	2	13	28	11	20	59	129	191	13	8	249	8	9	366	0.92	4.41	0.09	1.70	0.08
Intermediate Zone Avarage		3.3	21.3	60.0	35.1	36.6	177.6	209.8	166.7	23.3	11.8	298.5	21.7	18.1	544.3	1.05	7.73	0.11	1.41	0.10
Dry Zone																				
18	161	2	13	47	12	15	65	173	346	15	6	200	5	18	416	0.88	5.71	0.07	2.31	0.09
19	223	1	11	64	13	9	62	215	447	13	6	142	3	20	365	1.06	6.65	0.08	3.42	0.18
20	283	4	23	83	49	61	129	267	212	25	13	297	13	25	609	1.19	9.85	0.13	1.94	0.20
21	289	1	15	27	6	11	78	142	215	13	10	345	3	9	439	1.18	4.33	0.04	2.16	0.08
Dry Zone Avarage		2.1	15.4	55.2	20.0	24.0	83.3	199.0	305.0	16.3	8.6	245.9	5.9	18.2	457.3	1.08	6.64	0.08	2.46	0.14
Overall Average		3.7	22.6	58.0	34.8	37.9	139.3	188.8	156.3	20.6	8.9	215.5	12.9	20.1	589.8	0.84	7.79	0.10	2.38	0.13

Table 4.1.1c: XRF analyses of basement rocks from the Mahaweli River basin. Major elements as oxide wt%, trace elements ppm. Distance: distance downstream (km) from the uppermost sample point

S-No	Distance (Km)	Rock type	As	Pb	Zn	Cu	Ni	Cr	V	Sr	Y	Nb	Zr	Th	Sc	TS	TiO_2	Fe_2O_3	MnO	CaO	P_2O_5
Wet Zone																					
1	3	Charnokite	5	38	24	5	3	17	5	175	22	5	132	39	3	306	0.11	1.55	0.01	1.80	0.06
2	4	Leptynite	1	10	3	8	18	54	5	10	4	3	108	3	2	248	0.02	0.05	0.02	0.54	0.03
3	5	Granitic Gneiss	4	30	86	11	3	14	28	203	50	19	263	16	6	748	0.44	5.67	0.06	2.10	0.17
4a	6	Garnetiferrous HBG	3	20	63	4	16	55	44	186	27	10	222	30	4	349	0.57	4.60	0.04	2.82	0.25
4b	6	Garnet Biotite Gneiss	3	34	13	1	4	6	5	135	25	3	78	9	2	248	0.09	1.12	0.01	1.32	0.07
5	6	Marble	0	7	2	0	5	5	5	22	2	2	10	1	22	235	0.02	0.05	0.01	43.37	0.02
6	6	Charnokite	2	11	107	3	5	4	18	24	35	18	657	0	2	367	0.38	6.13	0.14	1.84	0.05
7	14	Charnokitic Gneiss	1	6	108	336	42	57	668	107	20	7	87	1	44	4874	2.06	15.79	0.17	8.21	0.26
8	15	Metabasite	1	11	141	7	78	635	284	73	31	8	48	1	50	404	0.68	11.50	0.15	7.71	0.07
9	17	Hornblende Biotite Gneiss	2	12	95	44	58	108	106	259	18	8	98	5	18	9619	0.56	7.01	0.08	8.70	0.14
10	27	Garnet Biotite Gneiss	1	10	38	8	85	240	119	422	13	6	97	14	8	283	0.62	4.34	0.03	3.20	0.06
11a	46	Quartzofeldspathc Gneiss	4	36	17	1	5	9	5	119	13	5	320	1	2	251	0.14	0.96	0.02	1.09	0.02
11b	46	Migmatitic Gneiss	1	15	39	13	31	39	40	381	11	3	166	1	5	303	0.37	3.36	0.04	3.38	0.07
12	55	Quartzite	0	7	2	3	5	30	5	2	2	1	124	3	2	236	0.06	0.05	0.02	0.55	0.02
13	71	Marble - Calk-gneiss	3	9	2	2	0	30	5	60	10	3	52	3	21	745	0.19	0.69	0.02	27.42	0.09
14	71	Marble -Blue apatite	2	6	0	2	5	4	5	36	2	2	17	1	19	273	0.02	0.05	0.04	37.23	0.99
15	72	Marble -Blue apatite	0	5	2	2	5	5	5	19	2	2	10	0	21	498	0.02	0.05	0.00	40.53	0.03
Wet Zone Avarage			2.0	15.7	43.6	26.2	21.6	77.2	79.6	131.3	16.8	6.1	146.4	7.4	13.6	1175.7	0.37	3.70	0.05	11.28	0.14
Intermediate Zone																					
16a	80	Hornblende Biotite Gneiss	3	28	35	1	5	15	5	44	53	14	117	14	2	228	0.12	0.67	0.01	0.84	0.03
16b	80	Granitic Gneiss	0	9	78	23	82	87	196	408	17	5	74	1	26	1096	0.97	10.92	0.15	8.47	0.34
17	83	Garnet Sillimanite Gneiss	7	36	77	3	1	11	6	179	49	19	337	8	1	353	0.40	4.18	0.04	1.77	0.10
18	84	Garnet Biotite Gneiss	1	8	47	1	60	98	154	59	21	8	127	6	7	245	0.75	6.12	0.08	1.58	0.14
19	85	Charnokitic Gneiss	0	6	65	38	5	33	201	201	8	2	58	0	38	1420	0.53	9.95	0.14	9.73	0.09
20	86	Garnet Biotite Gneiss	0	7	32	1	44	116	134	49	27	7	141	6	9	260	0.75	6.05	0.07	1.45	0.08
21	89	Garnet Sillimanite Gneiss	1	11	63	2	37	121	140	101	25	8	169	5	14	247	0.75	7.38	0.14	1.20	0.06
22	89	Quartzofeldspathc Gneiss	2	25	29	19	1	25	96	778	32	8	33	14	9	244	0.34	3.93	0.04	2.28	0.47
23	90	Hornblende Biotite Gneiss	1	11	149	3	59	233	285	81	14	2	56	1	48	318	1.06	11.79	0.16	9.16	0.15
24	94	Garnet Biotite Gneiss	3	24	54	4	16	60	87	488	16	5	97	3	8	477	0.45	4.06	0.05	3.17	0.22
25	97	Migmatite	2	18	118	75	35	107	175	85	53	17	215	12	21	16002	1.01	10.90	0.14	2.23	0.04
26	100	Charnockite	1	7	81	29	8	442	241	151	13	4	73	0	42	568	0.67	9.90	0.14	9.50	0.13
27	109	Charnockite	2	19	44	11	5	24	41	336	28	14	209	1	5	386	0.32	4.13	0.06	2.42	0.20
28	155	Charnokitic Gneiss	2	12	98	28	14	111	108	1093	17	6	102	2	23	3240	0.52	7.62	0.10	6.24	0.38
Intermediate Zone Avarage			1.7	15.6	69.3	17.1	26.5	105.9	133.4	289.5	26.7	8.6	129.1	5.3	18.0	1792	0.62	6.97	0.09	4.29	0.17
Dey Zone																					
29	157	Charnokitic Gneiss	2	24	15	3	2	14	5	293	13	2	91	1	2	280	0.04	0.58	0.20	1.54	0.05
30	193	Hornblende Biotite Gneiss	2	9	82	129	137	155	654	212	22	4	120	4	15	14421	0.53	3.40	0.02	3.30	0.26
31	223	Charnokitic Gneiss	1	11	91	8	10	38	125	369	28	10	136	1	23	449	0.78	6.54	0.09	5.04	0.22
32	283	Hornblende Biotite Gneiss	1	10	56	21	5	14	14	1878	21	6	102	2	18	254	0.25	3.14	0.05	13.66	0.12
33	284	Biotite Gneiss	3	21	51	9	7	13	62	1754	18	11	88	21	3	291	0.48	3.28	0.03	3.00	0.36
34	286	Charnokitic Gneiss	1	9	66	17	11	37	107	440	26	9	98	3	21	507	0.60	6.97	0.17	5.36	0.24
35	304	Charnokitic Gneiss	2	14	85	3	2	6	10	112	22	9	375	1	4	310	0.28	3.77	0.09	1.76	0.09
Dey Zone Avarage			1.6	13.9	63.8	27.1	24.7	39.5	139.4	722.6	21.6	7.4	144.3	4.8	12.3	2359	0.42	3.95	0.09	4.81	0.19
Overall Average			1.8	15.3	56.7	22.9	24.0	81.3	110.2	294.1	21.4	7.3	139.5	6.1	15.0	1614	0.47	4.97	0.07	7.53	0.16

Table 4.1.2: Average, minimum and maximum values for bulk stream sediments, basement rocks, soils and tributaries of the Mahaweli River basin compared to the PAAS values of Taylor and McLennan (1985). Major elements as oxide wt%, trace elements ppm

	Sediment			Rock			Soil			Tributaries			PAAS
	Avg	Min	Max	Avg	Min	Max	Avg	Min	Max	Avg	Min	Max	
Fe_2O_3	9.83	1.56	25.80	4.95	0.05	15.79	7.77	2.06	16.85	**20.88**	4.29	12.76	7.18
TiO_2	1.57	0.17	4.44	0.47	0.02	2.06	0.84	0.20	1.98	**4.32**	0.42	2.18	0.99
MnO	0.12	0.02	0.28	0.07	0.00	0.20	0.10	0.01	0.25	0.28	0.08	0.17	0.11
CaO	4.63	0.84	53.72	7.51	0.54	43.37	2.40	0.53	18.27	**49.44**	1.23	7.25	1.29
P_2O_5	0.21	0.07	0.50	0.16	0.02	0.99	0.13	0.05	0.40	0.50	0.12	0.28	0.16
As	5	1	10	2	0	7	4	1	10	8	3	6	5
Pb	25	10	43	15	5	38	23	8	75	43	15	31	20
Zn	114	18	1114	57	0	149	58	22	118	183	55	122	85
Cu	31	4	98	23	0	336	34	6	97	59	11	33	50
Ni	37	10	110	24	0	137	38	9	100	68	17	41	55
Cr	156	62	346	81	4	635	138	25	720	**304**	112	194	110
V	304	25	1158	110	5	668	189	8	353	**1158**	84	442	150
Sr	341	31	2713	299	2	1878	159	2	447	**2713**	91	564	200
Y	26	8	69	21	2	53	21	5	41	**69**	20	38	27
Nb	28	3	125	7	1	19	9	3	28	**125**	6	45	19
Zr	466	109	1426	140	10	657	215	59	643	**1426**	170	702	210
Th	26	1	141	6	0	39	13	1	66	**141**	5	45	15
Sc	22	4	44	15	1	50	20	1	50	41	13	28	16
TS	1298	236	16404	1621	228	16002	588	244	2472	**4178**	318	983	621

Titanium is relatively immobile compared to other elements during sedimentary processes, and hence is a good indicator of source rock composition (McLennan et al., 1993); it is also mainly concentrated in phyllosilicates (Condie, 1992). Average TiO_2 content in the basement rocks is depleted relative to PAAS, suggesting they are more evolved (felsic) than typical upper continental crust (Nagarajan et al., 2007). Enrichment of CaO in the rock average (5.82 wt%) is due to inclusion of five marbles in the dataset. If these samples are removed, average CaO falls to 3.10 wt%, only double that of PAAS (1.29 wt.%). High Sr values (>1000 ppm) in three gneisses also contribute to the enrichment in Sr in the basement rocks relative to PAAS. Overall, the rocks and the soils are mainly depleted relative to PAAS, whereas the sediments are mainly enriched. This indicates that geochemical changes have occurred in the steps from source to sediment.

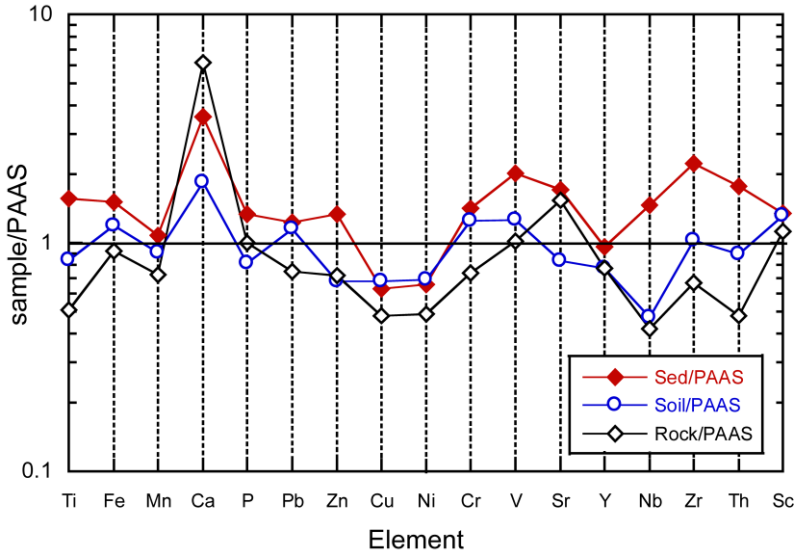

Fig. 4.1.2a: PAAS-normalized averages for the sediments, soils and basement rocks of the Mahaweli River. PAAS values from Taylor and McLennan (1985). Major elements are normalized as oxides

4.1.3 Major element discriminates for sediment (bulk and fraction) rock and soil

The PAAS normalization of major oxides and trace elements of the Mahaweli River for the three climatic zones are shown in Fig 4.1.2b. The major oxides are comparatively enriched in the fine fraction in the dry zone. The wet zone is in between the values of the dry and intermediate zones. The lowest enrichment is seen in the intermediate zone. The trace elements are also enriched in the fine fraction in the dry zones except for Sr. The Ti, Ca and Na content is enriched in the Dry zone samples and the Ca may relate to the harbor samples that has high Ca due to biogenic components. The trace elements are not discussed in this section.

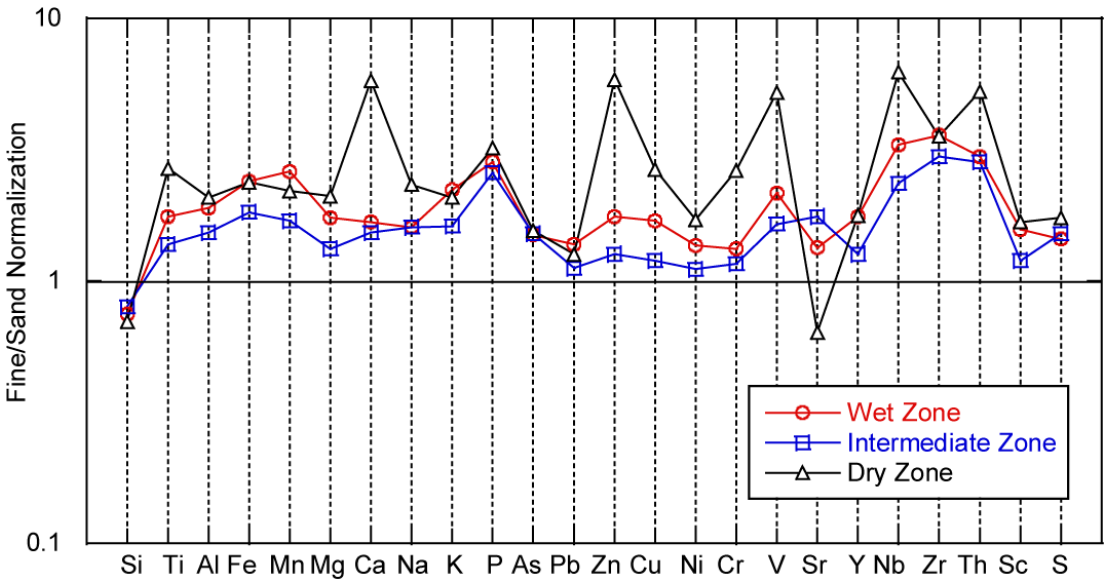

Fig. 4.1.2b: Fine/Sand-normalized averages for the sediments of the Mahaweli River. PAAS values from Taylor and McLennan (1985). Major elements are normalized as oxides

Representative trace element–Al_2O_3 variation diagrams show that the elements Ti, Fe, Mg, Ca and K show relatively strong positive correlations with Al_2O_3 (Fig. 4.1.2c). The elements Fe, Ti, Mg show as much or greater scatter than the other major elements but no clear differences in trend between sediment fractions, soils and rocks can be seen. Ti and Fe is very high in the <180µm fraction of the sediments and they relate to the heavy minerals of the <180µm fraction. The two fractions separate well in two clusters indicating that they are sorted. The content of Mg, Ca and K is also slightly high in the <180µm fraction. The enrichment of Mg, Ca and P may be due to bioclastic carbonate or apatite while the high very high Ca in the rocks is due to marbles. The high K_2O may relate to the charnokites and the K-feldspars in the rocks.

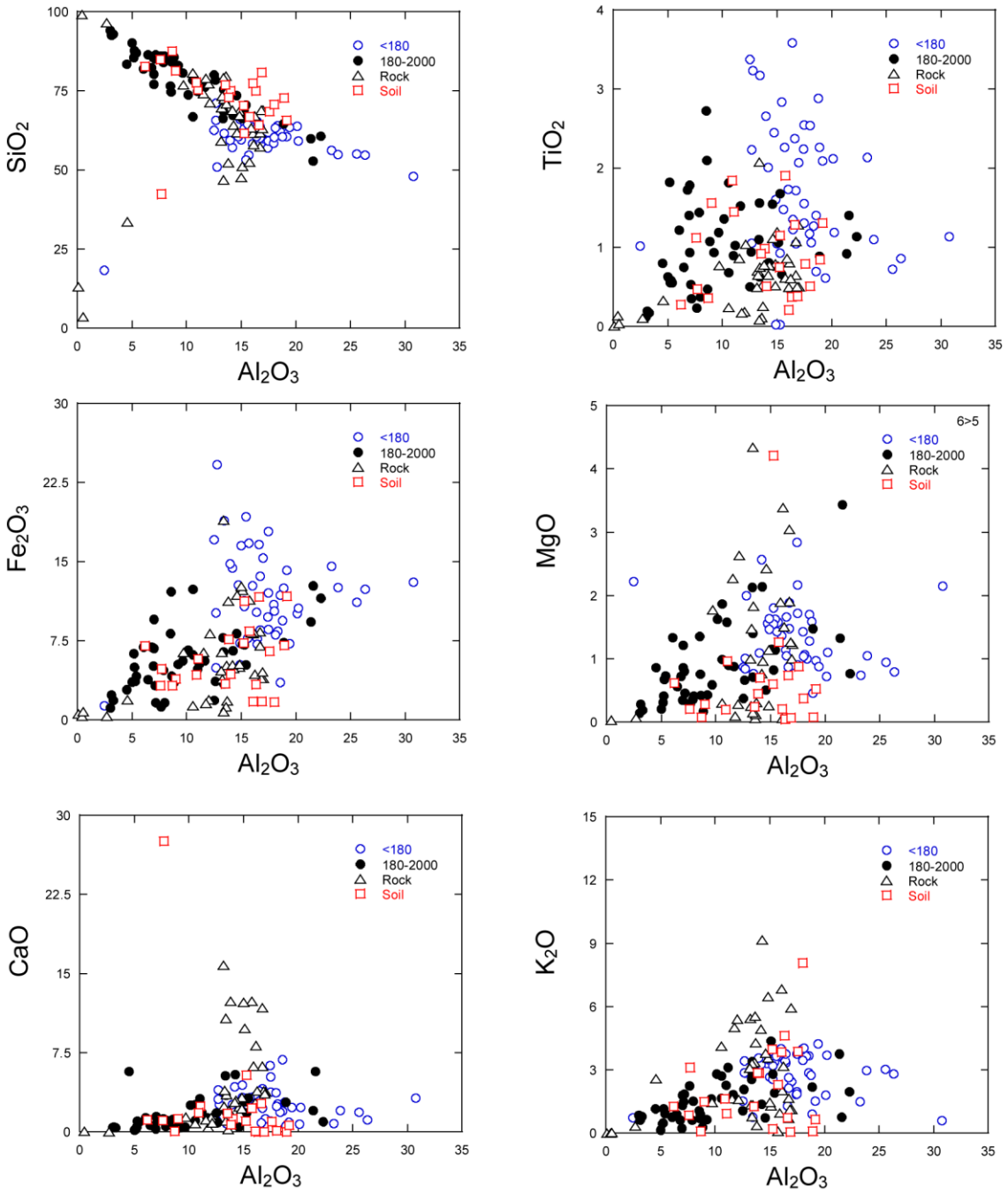

Fig. 4.1.2c: Selected major oxide–Al_2O_3 variation diagrams for the <180µm and 180-2000µm factions, rock and soils of the Mahaweli River sediments

Tables 4.1.3a – 4.1.3e conntain of the major element composition for bulk sediment, <180µm , 180 – 2000 µm sediments, rock and soils of the Mahaweli River and its catchments.

The average SiO_2 content of the bulk, <180µm and 180-2000µm sediment fractions are 73.95, 57.77, 78.24 respectively (Table 4.1.3a – 3c). The <180µm fraction consists of comparatively low SiO_2 content lower than UCC 66.0 (Taylor and McLennan 1985). Thus, the clay content is higher in the <180µm fraction and the quartz content is higher in the <180-2000µm fraction. The Al_2O_3 average content of the <180µm fraction is high 16.73 and the average of 180-2000µm fraction is comparatively less (10.00, Table 4.1.3b – 3c) but is less than UCC content of 15.00 (Taylor and McLennan 1985). The average Fe_2O_3 content of the <180µm fraction (11.20) is much higher than the average 180-2000µm fraction (5.64) and are higher than UCC 4.5. However, the average Fe_2O_3 content in the rocks and soils are much lower than the sediment fractions which are 5.62 and 5.71 respectively, and is very slightly higher than UCC. The P_2O_5 contents in the bulk, <180µm and 180-2000µm sediment fractions are very less (avg; 0.11, 0.21, 0.08 respectively; Table 4.1.3a – 3c).

Although the Fe_2O_3 content is high in the sediments the average MnO is low in the bulk, <180µm and 180-2000µm sediment fractions (0.09, 0.14, 0.07) whereas UCC is 0.1wt% indicating presence in different phases. The soils and the rocks also consist of low values similar to the sediments (0.08, 0.09 respectively).

The average Na_2O and K_2O content in the rocks (2.01, 2.77) are higher than soils and the sediment fractions but lower than UCC (3.9, 3.4). In the soils average Na_2O and K_2O content are 0.75 and 2.12. The average Na_2O and K_2O content of <180µm fraction are 1.31, 2.71 and 180-2000µm sediment fractions are 0.75, 1.54 respectively.

Table 4.1.3a : Major element composition of Mahaweli River bulk sediments

Sample	Distance (Km)	Weigh A	Weight B	Total	SiO_2	Al_2O_3	Na_2O	K_2O	MgO	TiO_2	Fe_2O_3*	CaO	MnO	P_2O_5	K_2O/Na_2O	Al_2O_3/K_2O+Na_2O
SLML 2A	1	137.08	332.52	469.6	67.92	16.88	0.21	0.94	0.56	2.72	9.89	0.54	0.05	0.29	4.51	18.15
SLML 6A	3	81.36	382.28	463.64	80.52	7.93	0.14	0.31	0.41	2.91	7.26	0.38	0.06	0.08	2.26	25.41
SLM 7A	7	55	324	379	70.10	9.56	0.27	0.85	0.75	4.94	12.59	0.70	0.11	0.15	3.15	11.55
SLML 5A	7	144.36	313.63	457.99	78.09	11.83	0.20	0.47	0.26	2.43	6.24	0.32	0.03	0.12	2.34	25.45
SLM 24A	10	59.17	428	487.17	82.59	7.36	0.44	1.10	0.66	1.75	5.19	0.78	0.06	0.06	2.50	7.15
SLML 1A	13	141.74	336.01	477.75	73.74	14.24	0.82	2.52	0.76	1.56	5.00	1.19	0.07	0.10	3.06	6.48
SLML 7A	16	69.59	411.25	480.84	77.83	11.10	0.23	1.64	0.60	1.74	6.23	0.50	0.05	0.08	7.06	6.98
SLML 3A	24	181.34	279.33	460.67	73.04	9.26	0.46	0.91	0.53	5.94	8.98	0.71	0.08	0.09	1.99	10.62
SLML 8A	29	88.23	387.78	476.01	78.52	10.96	0.28	0.80	0.52	1.76	6.85	0.50	0.06	0.10	2.82	14.04
SLM 27A	38	151.64	284.61	436.25	63.75	15.42	2.14	1.55	2.39	1.01	7.71	5.74	0.12	0.18	0.72	12.11
SLML 9A	43	99.89	281.01	380.9	78.29	8.12	0.33	0.94	0.46	2.68	8.52	0.51	0.07	0.07	2.85	8.93
SLML 4A	51	65.23	400.56	465.79	79.19	8.41	0.32	0.93	0.80	1.90	7.55	0.74	0.07	0.09	2.89	9.39
SLM 9A	55	387	37.24	424.24	60.68	14.85	0.20	1.14	0.78	6.48	14.75	0.76	0.11	0.24	5.66	13.18
SLM 28A	67	116.4	339.5	455.9	79.03	8.99	0.64	1.73	1.03	1.89	5.14	1.38	0.09	0.09	2.68	5.85
SLML 10A	72	108.15	286.79	394.94	51.45	24.08	1.16	0.72	3.08	1.41	12.78	5.02	0.19	0.11	0.62	34.67
SLML 11A	73	110.95	280.37	391.32	79.34	8.37	0.43	1.06	0.70	1.65	7.32	0.94	0.07	0.12	2.50	8.29
SLML 13A	84	324.07	152.15	476.22	63.66	17.39	1.66	2.15	1.75	1.30	8.10	3.69	0.12	0.18	1.30	9.75
SLML 12A	84	96.02	392.75	488.77	68.23	15.79	1.63	1.88	1.33	1.10	6.53	3.28	0.09	0.13	1.16	10.01
SLM 35A	86	260	79.5	339.5	62.92	17.24	2.14	3.39	1.79	1.19	4.54	6.46	0.09	0.23	1.58	7.23
SLML 14A	91	209.99	203.68	413.67	57.50	24.31	0.43	2.38	0.78	1.15	11.94	1.05	0.21	0.25	5.52	10.64
SLML 15A	102	144.27	330.29	474.56	65.22	14.51	2.02	3.47	1.49	2.07	7.02	3.98	0.09	0.14	1.72	6.21
SLM 45A	107	43.48	427.26	470.74	64.15	10.75	1.06	2.73	1.80	4.16	12.46	2.57	0.18	0.14	2.58	4.99
SLM 47A	109	90.8	381.86	472.66	72.10	11.73	1.15	3.12	1.01	2.04	6.64	2.02	0.08	0.11	2.71	4.92
SLML 16A	110	24.61	434.14	458.75	74.41	7.14	0.45	1.38	1.23	3.69	10.07	1.45	0.12	0.07	3.03	5.64
SLM 48A	119	81.72	189.96	271.68	63.55	15.89	1.83	4.24	1.23	1.60	8.22	3.11	0.11	0.22	2.31	5.58
SLML 17A	124	57.02	429.03	486.05	71.45	10.57	1.19	2.84	1.72	1.85	7.44	2.72	0.11	0.10	2.38	4.91
SLML 18A	127	28.96	372.41	401.37	78.59	7.62	0.78	1.93	0.90	1.23	7.16	1.61	0.09	0.11	2.49	4.72
SLM 49A	131	102.68	350.44	453.12	71.99	12.18	1.45	2.51	1.59	1.39	5.46	3.29	0.08	0.07	1.74	6.30
SLML 19A	139	23.02	449.55	472.57	75.08	8.81	0.44	1.16	1.36	3.11	8.61	1.25	0.12	0.06	2.63	8.03
SLML 20A	143	385.37	94.27	479.64	62.60	19.77	1.48	4.12	0.96	0.98	7.61	2.23	0.08	0.16	2.79	6.27
SLML 21A	151	190.1	232.34	422.44	68.07	15.37	1.03	2.64	0.97	2.14	7.77	1.76	0.10	0.15	2.55	6.86
SLML 22A	159	106.76	330.1	436.86	80.99	8.44	0.62	1.68	0.81	0.91	5.07	1.34	0.07	0.08	2.72	5.65
SLML 23A	167	0.5	452.33	452.83	89.57	5.26	0.63	1.30	0.31	0.32	1.81	0.73	0.04	0.03	2.06	4.67
SLM 55A	170	64.42	428.18	492.6	78.03	12.52	1.88	1.30	0.43	0.87	2.91	1.95	0.06	0.05	0.69	11.53
SLML 24A	173	249.68	135.29	384.97	72.25	10.56	1.22	2.28	1.01	3.27	7.10	2.12	0.10	0.09	1.87	5.85
SLML 29A	182	199.9	287.86	487.76	72.21	15.54	0.67	1.78	0.63	0.69	7.01	1.16	0.15	0.16	2.64	9.42
SLML 73A	184	16.25	415.22	431.47	86.50	4.65	0.31	1.06	0.49	1.33	4.91	0.65	0.06	0.05	3.37	4.72
SLML 30A	186	68	426.34	494.34	87.60	6.04	0.42	1.07	0.31	0.53	3.29	0.64	0.06	0.06	2.56	6.06
SLML 31A	205	371.49	81.35	452.84	61.28	17.38	1.46	3.29	0.99	3.31	9.65	2.29	0.18	0.17	2.25	6.75
SLML 32A	220	29.08	408.45	437.53	85.03	5.79	0.56	1.28	0.70	1.13	4.31	1.09	0.07	0.04	2.29	5.07
SLM 50A	229	2.39	333.5	335.89	92.42	3.21	0.23	0.64	0.29	0.22	2.44	0.49	0.04	0.03	2.77	5.28
SLM 59A	229	31.48	459.55	491.03	78.10	8.64	0.87	2.24	0.95	2.18	5.27	1.60	0.08	0.06	2.58	4.72
SLML 33A	245	276.44	212.88	489.32	69.22	15.01	1.77	3.30	0.89	1.67	5.49	2.46	0.07	0.11	1.86	6.32
SLM 69A	300	32.62	441.34	473.96	84.47	8.45	1.01	1.64	0.48	0.63	2.03	1.24	0.04	0.02	1.62	6.15
SLM 68A	302	118.05	360.91	478.96	80.81	9.39	1.22	2.53	0.57	0.98	2.70	1.72	0.04	0.04	2.07	4.93
SLM 70A	306	110.7	194.21	304.91	78.59	7.40	0.96	1.97	0.91	1.40	3.57	5.09	0.05	0.07	2.06	4.72
SLM 71A	310	111.25	367.41	478.66	81.57	8.89	1.37	2.24	0.72	0.70	2.44	1.97	0.04	0.06	1.63	5.35
SLML 72A	313	35.13	464.87	500.00	77.49	5.81	0.33	0.76	1.41	1.15	6.51	6.61	0.11	0.06	2.31	8.01
Avarage					73.95	11.45	0.89	1.83	0.96	1.94	6.84	1.96	0.09	0.11	2.53	8.86
Min					51.45	3.21	0.14	0.31	0.26	0.22	1.81	0.32	0.03	0.02	0.62	4.67
Max					92.42	24.31	2.14	4.24	3.08	6.48	14.75	6.61	0.21	0.29	7.06	34.67

Table 4.1.3b : Major element composition for <180 µm fraction of the Mahaweli River sediments

Sample	Distance (km)	SiO_2	TiO_2	Al_2O_3	Fe_2O_3*	MnO	MgO	CaO	Na_2O	K_2O	P_2O_5	K_2O/Na_2O	Al_2O_3/K_2O+Na_2O
SLML 2A	1	54.13	5.58	22.46	14.04	0.16	0.71	0.77	0.30	1.43	0.40	4.72	15.97
SLML 6A	3	57.28	9.97	12.48	17.53	0.13	0.72	0.74	0.25	0.72	0.19	2.87	17.69
SLM 7A	7	53.75	8.52	16.44	16.75	0.14	0.85	0.97	0.49	1.83	0.27	3.78	9.45
SLML 5A	7	61.79	5.38	18.30	12.09	0.06	0.45	0.53	0.27	0.87	0.26	3.21	21.20
SLM 24A	10	54.78	9.01	13.80	15.18	0.15	1.42	1.99	1.08	2.45	0.15	2.26	6.72
SLML 7A	16	62.01	4.96	19.57	9.78	0.09	0.70	0.69	0.29	1.75	0.14	5.98	11.45
SLML 3A	24	57.35	11.43	11.49	15.65	0.13	0.80	1.03	0.59	1.39	0.15	2.37	8.84
SLML 8A	29	58.33	5.42	18.52	13.67	0.13	0.94	0.90	0.42	1.45	0.21	3.43	13.17
SLM 27A	38	57.49	1.39	17.59	9.84	0.15	2.86	6.35	2.14	1.85	0.34	0.86	11.67
SLML 9A	43	58.07	5.10	16.49	14.88	0.13	0.87	1.20	0.71	2.36	0.20	3.30	7.71
SLML 4A	51	59.78	2.98	18.25	11.62	0.10	1.25	1.95	0.96	2.80	0.29	2.91	7.47
SLM 9A	55	57.84	7.05	15.80	15.83	0.12	0.83	0.81	0.22	1.24	0.25	5.67	12.95
SLM 28A	67	61.32	5.85	14.40	10.67	0.17	1.70	2.40	0.90	2.41	0.20	2.68	6.88
SLML 10A	72	47.86	1.44	30.66	13.02	0.22	2.14	3.16	0.76	0.58	0.16	0.76	53.48
SLML 11A	73	58.39	4.43	16.29	13.26	0.12	1.44	2.19	1.08	2.56	0.25	2.37	7.44
SLML 13A	84	63.26	1.50	16.68	8.46	0.13	1.87	4.09	1.68	2.13	0.21	1.26	9.53
SLML 12A	84	58.60	2.92	17.23	11.89	0.18	2.13	3.67	1.27	1.83	0.28	1.45	10.68
SLM 35A	86	61.90	1.22	18.44	3.54	0.09	1.69	6.81	2.42	3.64	0.26	1.50	7.49
SLML 14A	91	54.52	1.18	26.26	12.35	0.22	0.79	1.13	0.51	2.78	0.26	5.46	9.94
SLML 15A	102	57.94	3.24	17.15	8.39	0.10	1.68	5.12	2.48	3.67	0.23	1.48	7.16
SLM 45A	107	51.60	7.60	14.85	15.80	0.19	1.49	3.09	1.67	3.38	0.33	2.02	6.06
SLM 47A	109	58.14	6.32	14.15	12.24	0.14	1.50	2.74	1.39	3.16	0.23	2.28	5.86
SLML 16A	110	46.07	12.46	11.56	21.88	0.20	1.81	2.35	0.93	2.55	0.19	2.74	5.46
SLM 48A	119	57.34	2.85	17.68	10.72	0.15	1.41	3.62	1.95	3.91	0.37	2.01	6.46
SLML 17A	124	55.09	5.50	13.67	13.87	0.18	2.47	4.10	1.71	3.15	0.26	1.84	6.05
SLML 18A	127	56.30	5.04	15.50	12.31	0.19	1.32	3.27	1.93	3.87	0.28	2.00	5.94
SLML 1A	131	62.94	3.03	18.03	8.24	0.11	0.98	1.81	1.09	3.58	0.18	3.28	6.13
SLM 49A	131	62.38	3.08	16.19	7.55	0.10	1.63	3.78	1.86	3.29	0.14	1.76	6.79
SLML 19A	139	48.94	10.68	14.17	17.70	0.17	1.49	2.28	1.24	3.10	0.24	2.50	5.81
SLML 20A	143	63.26	1.00	19.37	7.20	0.08	0.87	2.28	1.57	4.22	0.15	2.69	6.16
SLML 21A	151	58.15	2.90	19.90	10.42	0.13	1.09	2.25	1.28	3.65	0.23	2.84	6.74
SLML 22A	159	62.57	2.03	17.93	7.97	0.11	1.05	2.61	1.57	3.99	0.17	2.54	6.06
SLM 55A	170	64.90	3.28	12.54	10.02	0.22	0.83	3.04	2.17	2.84	0.16	1.30	6.59
SLML 24A	173	60.50	4.97	14.65	10.32	0.14	1.49	3.04	1.70	3.06	0.12	1.81	6.48
SLML 29A	182	54.97	1.02	25.51	11.11	0.25	0.94	1.86	1.04	3.03	0.29	2.92	9.46
SLM 73A	184	60.89	2.30	18.90	9.49	0.14	1.59	2.83	0.90	2.76	0.20	3.07	7.75
SLML 30A	186	54.00	2.73	23.48	12.35	0.23	1.03	2.00	0.99	2.91	0.28	2.94	9.06
SLML 31A	205	59.60	3.67	17.84	10.21	0.19	1.02	2.39	1.52	3.39	0.18	2.24	6.77
SLML 32A	220	55.56	8.89	13.06	13.82	0.15	1.03	2.42	1.64	3.34	0.11	2.04	5.55
SLM 50A	229	60.87	2.91	16.50	10.27	0.17	1.15	2.80	1.73	3.45	0.16	2.00	6.50
SLML 33A	245	64.43	2.48	16.26	7.07	0.09	1.04	2.88	1.88	3.71	0.15	1.97	6.26
SLM 69A	300	62.80	4.01	15.20	7.55	0.11	1.39	3.17	2.15	3.56	0.06	1.65	6.43
SLM 68A	302	64.96	3.28	14.61	7.16	0.11	1.44	3.20	1.74	3.41	0.10	1.96	6.03
SLM 70A	306	70.00	2.45	12.47	4.86	0.06	1.00	3.94	1.74	3.37	0.10	1.94	5.44
SLM 71A	310	65.59	1.86	14.61	5.11	0.07	1.60	4.34	3.19	3.47	0.16	1.09	7.39
SLM 72A	313	19.05	0.17	2.57	1.42	0.03	2.32	76.14	0.67	0.75	0.14	1.13	4.08
Avarage		57.77	4.46	16.73	11.20	0.14	1.32	4.23	1.31	2.71	0.21	2.50	9.22
Min		19.05	0.17	2.57	1.42	0.03	0.45	0.53	0.22	0.58	0.06	0.76	4.08
Max		70.00	12.46	30.66	21.88	0.25	2.86	76.14	3.19	4.22	0.40	5.98	53.48

Table 4.1.3c : Major element composition for 180- 2000 µm fraction of the Mahaweli River sediments

Sample	Distance (km)	SiO_2	TiO_2	Al_2O_3	Fe_2O_3*	MnO	MgO	CaO	Na_2O	K_2O	P_2O_5	K_2O/Na_2O	Al_2O_3/K_2O+Na_2O
SLML 2B	1	73.60	1.55	14.58	8.17	0.01	0.50	0.45	0.17	0.74	0.24	4.35	19.93
SLML 6B	3	85.47	1.40	6.96	5.07	0.05	0.35	0.31	0.12	0.23	0.05	1.98	30.60
SLM 7B	7	72.87	4.33	8.39	11.88	0.10	0.74	0.65	0.23	0.68	0.13	2.92	12.57
SLML 5B	7	85.60	1.07	8.85	3.54	0.02	0.17	0.23	0.17	0.28	0.06	1.69	31.59
SLM 24B	10	86.44	0.75	6.47	3.81	0.05	0.56	0.61	0.35	0.91	0.04	2.60	7.45
SLML 7B	16	80.51	1.19	9.66	5.62	0.05	0.59	0.47	0.22	1.63	0.07	7.30	6.17
SLML 3B	24	83.23	2.37	7.81	4.66	0.04	0.36	0.50	0.37	0.60	0.05	1.61	13.41
SLML 8B	29	83.11	0.93	9.24	5.29	0.04	0.43	0.41	0.25	0.65	0.07	2.58	14.52
SLM 27B	38	67.08	0.81	14.26	6.58	0.10	2.14	5.41	2.14	1.39	0.10	0.65	12.43
SLML 9B	43	85.48	1.82	5.15	6.26	0.05	0.31	0.26	0.20	0.44	0.03	2.27	11.82
SLML 4B	51	82.35	1.73	6.81	6.89	0.07	0.72	0.54	0.22	0.62	0.06	2.88	11.17
SLM 9B	55	90.20	0.63	4.98	3.56	0.03	0.20	0.16	0.03	0.13	0.06	5.07	37.04
SLM 28B	67	85.10	0.53	7.13	3.24	0.07	0.80	1.03	0.56	1.49	0.05	2.68	5.34
SLML 10B	72	52.80	1.40	21.59	12.69	0.18	3.44	5.72	1.31	0.77	0.09	0.59	29.34
SLML 11B	73	87.62	0.55	5.23	4.97	0.05	0.41	0.45	0.17	0.47	0.07	2.84	11.28
SLML 13B	84	64.52	0.89	18.90	7.35	0.10	1.48	2.82	1.61	2.20	0.13	1.37	10.21
SLML 12B	84	70.58	0.66	15.44	5.22	0.07	1.14	3.19	1.72	1.90	0.09	1.11	9.85
SLM 35B	86	66.28	1.10	13.32	7.81	0.11	2.13	5.32	1.23	2.56	0.14	2.08	6.43
SLML 14B	91	60.57	1.13	22.30	11.53	0.20	0.77	0.96	0.35	1.97	0.24	5.61	11.69
SLML 15B	102	68.40	1.56	13.37	6.43	0.08	1.40	3.48	1.82	3.38	0.09	1.86	5.77
SLM 45B	107	65.42	3.81	10.34	12.12	0.18	1.83	2.51	1.00	2.67	0.12	2.68	4.87
SLM 47B	109	75.42	1.03	11.16	5.30	0.06	0.89	1.85	1.10	3.10	0.08	2.83	4.69
SLML 16B	110	76.01	3.19	6.89	9.40	0.11	1.20	1.40	0.43	1.31	0.06	3.07	5.68
SLM 48B	119	66.22	1.06	15.12	7.15	0.09	1.15	2.89	1.78	4.38	0.15	2.46	5.24
SLML 17B	124	73.63	1.36	10.16	6.59	0.10	1.62	2.54	1.12	2.80	0.07	2.49	4.75
SLML 18B	127	80.32	0.93	7.00	6.76	0.09	0.86	1.48	0.69	1.78	0.10	2.59	4.62
SLML 1B	131	78.30	0.94	12.64	3.63	0.05	0.66	0.93	0.71	2.07	0.07	2.92	6.81
SLM 49B	131	74.80	0.89	11.00	4.85	0.08	1.58	3.14	1.32	2.28	0.05	1.72	6.15
SLML 19B	139	76.42	2.72	8.53	8.15	0.12	1.35	1.20	0.40	1.06	0.05	2.66	8.44
SLML 20B	143	59.92	0.92	21.38	9.28	0.11	1.32	2.02	1.11	3.75	0.19	3.38	6.81
SLML 21B	151	76.18	1.52	11.66	5.60	0.08	0.88	1.36	0.83	1.82	0.08	2.19	7.25
SLML 22B	159	86.95	0.55	5.37	4.13	0.06	0.73	0.92	0.31	0.93	0.05	3.01	6.09
SLM 55B	170	80.01	0.50	12.52	1.84	0.04	0.37	1.79	1.83	1.07	0.03	0.58	13.59
SLML 24B	173	93.94	0.12	3.00	1.14	0.03	0.14	0.41	0.35	0.84	0.02	2.40	3.93
SLML 29B	182	84.19	0.47	8.62	4.16	0.08	0.42	0.67	0.42	0.91	0.07	2.16	9.92
SLM 73B	184	78.30	0.68	10.55	6.13	0.09	0.99	1.06	0.43	1.64	0.13	3.79	6.85
SLML 30B	186	92.96	0.18	3.25	1.85	0.03	0.19	0.42	0.33	0.78	0.02	2.38	4.52
SLML 31B	205	68.98	1.68	15.29	7.12	0.15	0.82	1.83	1.22	2.80	0.12	2.30	6.69
SLML 32B	220	87.13	0.58	5.27	3.63	0.06	0.67	1.00	0.48	1.14	0.03	2.35	5.11
SLM 50B	229	92.65	0.20	3.12	2.39	0.04	0.28	0.47	0.22	0.62	0.03	2.81	5.28
SLML 33B	245	75.43	0.62	13.38	3.43	0.05	0.71	1.92	1.63	2.76	0.06	1.70	6.47
SLM 69B	300	86.07	0.38	7.95	1.62	0.03	0.42	1.10	0.93	1.50	0.01	1.62	6.22
SLM 68B	302	86.00	0.23	7.68	1.24	0.02	0.29	1.24	1.06	2.24	0.01	2.13	4.48
SLM 70B	306	83.49	0.80	4.51	2.84	0.04	0.86	5.75	0.51	1.17	0.04	2.29	4.37
SLM 71B	310	86.41	0.35	7.16	1.63	0.03	0.45	1.26	0.83	1.86	0.03	2.26	4.67
SLM 72B	313	81.90	1.22	6.06	6.89	0.12	1.34	1.36	0.30	0.76	0.05	2.51	8.30
Avarage		78.24	1.16	10.00	5.64	0.07	0.88	1.64	0.75	1.54	0.08	2.55	10.01
Min		52.80	0.12	3.00	1.14	0.01	0.14	0.16	0.03	0.13	0.01	0.58	3.93
Max		93.94	4.33	22.30	12.69	0.20	3.44	5.75	2.14	4.38	0.24	7.30	37.04

Table 4.1.3d : Major element composition for basement rocks of the Mahaweli River sediments

Sample -No	Distance(km)	Rock type	LOI	SiO_2	TiO_2	Al_2O_3	Fe_2O_3*	MnO	MgO	CaO	Na_2O	K_2O	P_2O_5	K_2O/Na_2O	Al_2O_3/K_2O+Na_2O
SLM1	3	Charnokite	0.56	75.04	0.25	13.68	1.77	0.02	0.31	1.88	2.70	4.29	0.06	1.59	5.89
SLM2	4	Leptynite	1.19	96.43	0.10	2.68	0.33	0.01	0.06	0.03	0.02	0.33	0.01	14.27	8.24
SLM3	5	Granitic Gneiss	0.06	69.52	0.70	13.20	6.41	0.08	0.26	2.42	1.82	5.45	0.15	2.99	4.24
SLM13B	6	Garnetiferrous HBG	0.11	77.16	0.19	12.01	1.91	0.03	0.28	1.37	1.61	5.40	0.04	3.34	3.84
SLM13A	6	Garnet Biotite Gneiss	0.33	68.70	0.79	14.82	4.97	0.05	1.14	3.27	2.48	3.55	0.23	1.43	6.65
SLM15	6	Marble	35.92	13.13	0.01	0.07	0.56	0.04	29.31	56.88	0.00	0.00	0.01	0.00	
SLM22	6	Charnokite	0.03	61.57	0.49	16.06	8.21	0.19	0.06	2.73	3.83	6.83	0.03	1.78	6.18
SLM8	14	Charnokitic Gneiss	0.09	46.41	2.82	13.29	18.78	0.21	4.31	10.65	2.55	0.78	0.20	0.30	19.70
SLM4	15	Metabasite	0.30	51.12	0.76	15.09	12.25	0.17	7.32	9.80	2.16	1.29	0.05	0.59	13.90
SLM21	17	Honblane Biotite Gneiss	1.39	57.32	0.65	16.71	8.34	0.12	3.04	11.75	1.26	0.70	0.11	0.55	25.30
SLM20	27	Garnet Biotite Gneiss	0.10	72.37	0.75	13.42	4.62	0.05	1.83	3.54	2.03	1.34	0.04	0.66	12.03
SLM12A	46	Quartzofeldspathc Gneiss	0.82	80.54	0.24	10.56	1.35	0.03	0.30	0.77	2.09	4.11	0.00	1.96	4.66
SLM12B	46	Migmatitic Gneiss	0.77	68.89	0.50	16.97	3.95	0.06	1.23	3.80	3.42	1.11	0.06	0.32	18.70
SLM9	55	Quartzite	0.19	99.03	0.13	0.44	0.32	0.01	0.03	0.04	0.00	0.00	0.00	0.00	
SLM30	71	Marble - Calk-gneiss	18.92	33.65	0.33	4.57	1.92	0.05	20.00	36.74	0.09	2.57	0.07	29.88	1.87
SLM31	71	Marble -Blue apatite	43.59	3.60	0.04	0.50	0.77	0.09	31.57	61.15	0.00	0.05	2.23	0.00	11.00
SLM29	72	Marble -Blue apatite	33.93	68.92	0.50	16.85	3.95	0.06	1.26	3.86	3.41	1.13	0.06	0.33	18.27
SLM32A	80	Honblane Biotite Gneiss	0.11	79.77	0.12	13.61	1.22	0.01	0.06	0.23	1.60	3.37	0.01	2.12	5.63
SLM32B	80	Granitic Gneiss	0.13	79.01	0.18	11.76	1.56	0.02	0.10	0.39	1.97	5.01	0.02	2.55	4.31
SLM38	83	Garnet Siluminite Gneiss	0.02	70.95	0.52	13.64	5.16	0.07	0.13	2.05	1.87	5.54	0.08	2.96	4.34
SLM39	84	Garnet Biotite Gneiss	0.11	76.94	0.77	9.68	6.38	0.11	1.78	1.39	1.37	1.47	0.11	1.07	7.95
SLM33	85	Charnokitic Gneiss	0.01	52.47	0.61	15.77	11.36	0.18	5.66	12.37	1.44	0.08	0.06	0.06	199.03
SLM35	86	Garnet Biotite Gneiss	0.05	73.98	0.86	11.55	6.37	0.09	2.27	1.15	2.01	1.64	0.08	0.82	9.04
SLM36	89	Garnet siluminite Gneiss	0.01	71.32	1.04	12.14	8.16	0.16	2.63	0.83	2.07	1.60	0.06	0.78	9.64
SLM37	89	Quartzofeldspathc Gneiss	0.38	64.24	0.77	14.32	4.90	0.05	0.97	2.95	2.22	9.16	0.42	4.13	3.78
SLM40	90	Honblane Biotite Gneiss	0.21	47.58	1.19	15.01	12.66	0.18	7.40	12.24	2.15	1.47	0.12	0.68	12.37
SLM41	94	Garnet Biotite Gneiss	0.29	67.07	0.60	16.27	4.32	0.06	1.50	3.85	2.94	3.17	0.23	1.08	8.07
SLM43	97	Migmatite	1.31	61.69	1.11	14.60	11.81	0.19	2.42	2.34	2.02	3.78	0.04	1.87	5.88
SLM42	100	Charnockite	0.08	52.30	0.78	13.81	11.28	0.17	7.21	12.39	1.61	0.36	0.09	0.23	39.51
SLM46	109	Charnockite	0.10	68.92	0.65	14.21	5.19	0.08	0.77	2.79	2.26	4.94	0.18	2.19	5.14
SLM52	155	Charnokitic Gneiss	2.99	58.11	0.81	16.14	8.31	0.11	3.39	8.18	2.56	2.02	0.38	0.79	10.55
SLM53	157	Charnokitic Gneiss	0.19	79.06	0.08	13.39	0.78	0.02	0.15	0.99	2.22	3.29	0.02	1.49	6.28
SLM57	193	Honblane Biotite Gneiss	8.09	73.29	0.65	13.27	3.85	0.02	1.48	3.91	1.96	1.35	0.22	0.69	11.80
SLM58	223	Charnokitic Gneiss	0.76	61.71	1.08	16.73	6.99	0.10	1.91	6.22	3.41	1.64	0.22	0.48	13.59
SLM63	283	Honblane Biotite Gneiss	7.52	59.23	0.50	13.14	4.65	0.07	1.00	15.79	2.46	3.07	0.10	1.25	6.73
SLM62	284	Biotite Gneiss	0.62	63.00	1.29	16.96	4.53	0.04	1.00	3.58	3.30	5.94	0.36	1.80	6.15
SLM61	286	Charnokitic Gneiss	0.12	63.22	0.86	15.93	8.25	0.20	1.90	6.20	2.29	0.97	0.20	0.42	18.78
SLM67	304	Charnokitic Gneiss	0.28	67.15	0.52	14.85	5.25	0.12	0.27	2.21	3.10	6.47	0.07	2.09	5.40
Avarage			4.25	64.06	0.64	12.57	5.62	0.09	3.85	8.23	2.01	2.77	0.17	2.36	15.40
Min			0.01	3.60	0.01	0.07	0.32	0.01	0.03	0.03	0.00	0.00	0.00	0.00	1.87
Max			43.59	99.03	2.82	16.97	18.78	0.21	31.57	61.15	3.83	9.16	2.23	29.88	199.03

Table 4.1.3e : Major element composition for soils of the Mahaweli River sediments

Sample	LOI	Distance (km)	SiO_2	TiO_2	Al_2O_3	Fe_2O_3*	MnO	MgO	CaO	Na_2O	K_2O	P_2O_5	K_2O/Na_2O	Al_2O_3/K_2O+Na_2O
SLMS14	12.86	3	72.71	0.85	18.96	7.07	0.11	0.08	0.03	0.01	0.10	0.08	14.86	194.37
SLMS 3	5.30	6	42.33	0.47	7.72	4.81	0.06	13.58	27.56	0.24	3.12	0.12	13.24	2.71
SLMS 32	6.40	13	74.95	0.37	16.34	3.39	0.01	0.05	0.02	0.21	4.61	0.06	22.29	3.75
SLMS 35	4.22	17	75.04	0.51	14.05	4.34	0.05	0.70	1.22	1.21	2.82	0.07	2.33	6.20
SLMS 6	6.10	18	72.87	0.99	13.86	7.59	0.09	0.45	0.66	0.32	2.84	0.31	8.79	5.20
SLMS 5	3.32	18	70.33	0.74	15.21	7.30	0.09	0.60	1.00	0.56	3.97	0.20	7.09	4.39
SLMS7	7.41	37	61.66	1.15	15.29	11.24	0.19	4.21	5.40	0.52	0.21	0.13	0.39	74.55
SLMS 25	5.98	37	68.42	0.79	17.60	6.50	0.06	0.88	0.95	0.84	3.88	0.07	4.60	5.38
SLMS 10	4.72	54	77.46	0.21	16.05	1.76	0.02	0.21	0.07	0.30	3.83	0.08	12.64	4.49
SLMS 14	7.42	72	76.87	0.92	13.55	3.41	0.05	0.24	1.74	1.94	1.25	0.03	0.65	12.75
SLMS 26	4.24	84	75.31	1.45	11.08	5.78	0.07	0.96	2.42	1.95	0.92	0.06	0.47	13.95
SLMS 36	7.98	89	81.43	1.56	8.98	3.90	0.08	0.28	1.25	1.01	1.48	0.03	1.47	7.08
SLMS 44	3.04	96	80.22	3.20	6.01	6.79	0.15	0.60	1.10	0.64	1.22	0.07	1.91	5.56
SLMS 50	4.64	143	84.86	1.12	7.62	3.24	0.07	0.21	1.05	0.98	0.83	0.03	0.85	10.14
SLMS 51A	1.96	154	64.19	1.29	16.62	11.65	0.19	0.73	2.72	1.79	0.74	0.08	0.41	24.32
SLMS 51B	0.61	154	77.65	1.84	10.91	4.29	0.05	0.20	1.81	1.61	1.62	0.03	1.01	8.36
SLMS 53A	1.65	157	80.78	0.38	16.88	1.76	0.01	0.07	0.02	0.00	0.05	0.03	13.75	341.88
SLMS 38	2.24	161	87.44	0.36	8.67	3.22	0.02	0.07	0.06	0.01	0.08	0.06	7.08	110.71
SLMS 40	1.08	223	65.72	1.30	19.16	11.70	0.09	0.53	0.64	0.12	0.64	0.09	5.23	30.01
SLMS 64	1.76	283	70.69	0.51	18.04	1.69	0.01	0.38	0.10	0.50	8.05	0.03	16.18	2.74
SLMS 60	4.41	289	66.79	1.91	15.74	8.38	0.11	1.26	2.27	1.09	2.31	0.14	2.12	7.92
Avarage			72.75	1.04	13.73	5.71	0.08	1.25	2.48	0.75	2.12	0.09	6.54	41.74
Min			42.33	0.21	6.01	1.69	0.01	0.05	0.02	0.00	0.05	0.03	0.39	2.71
Max			87.44	3.20	19.16	11.70	0.19	13.58	27.56	1.95	8.05	0.31	22.29	341.88

4.1.4 Heavy Minerals

Weight percentages of the three size fractions (>2000 µm, 180-2000 µm and <180 µm). Average values in the <180 µm, 180-2000 µm and >2000 µm fractions are 23, 66 and 11 wt% respectively, indicating that most of samples are dominated by the sand fraction (Fig 4.1.1). Five samples in the intermediate zone at 151 – 178 km contained only the 180 – 2000 µm fraction. Consequently, these five samples were not included in the fraction interpretations.

Concentrations of all measured elements are greater in the <180µm fraction than in the 180 – 2000 µm fraction (Table 4.1.4a and 4.1.4b). Average concentrations of TiO_2 and Fe_2O_3 in the <180µm fraction are 1.67 and 9.59 wt% respectively, compared to 0.79 and 6.47 wt% in the 180 – 2000 µm fraction. The overall range for Fe_2O_3 is similar in both fractions (<180µm, 0.05 – 15.99 wt%; 180 – 2000 µm, 0.16 – 14.76 wt%). However, in the <180µm fraction Fe_2O_3 contents of almost all samples exceed 3.25 wt%, and 22 samples contain more than 10 wt% (Table 4.1.4b). In the 180 – 2000 µm fraction only 10 samples exceed 10 wt% Fe_2O_3 (Table 4.1.4a). Both fractions have similar average CaO contents (<180µm, 3.18 wt%, 180 – 2000 µm, 2.85 wt%). Very high CaO values occur in one <180µm fraction (48.02 wt%) and in one 180 – 2000 µm fraction (50.26 wt%).

Among the trace elements concentrations of Zr, Th, and Nb average 544, 35, and 38 ppm in the <180µm fraction respectively, compared to 165, 10, and 12 ppm in the 180 – 2000 µm fraction (Tables 4.1.4a and 4.1.4b). Average Sc, Y and Ni contents are 30-47% greater in the <180µm fractions (19, 25, and 34 ppm, respectively), than in the 180 – 2000 µm fraction (14, 17 and 26 ppm). Average Cr content in the <180µm fractions (142 ppm) is also almost 50% more than that than in the 180 – 2000 µm fraction (97 ppm). Vanadium content in the <180µm fraction is much greater on average (345 ppm) and is more than double that in the 180 – 2000 µm fraction 153 ppm). Average Sr content shows much less contrast (259 ppm, <180 µm; versus 206 ppm, 180 – 2000 µm), but very high values are seen in one <180µm fraction sample (TR67, 2584 ppm) and in one 180 – 2000 µm fraction (MC313, 2441 ppm). Both samples also contain the extreme CaO contents. Arsenic, Pb and Cu have similar average values in both fractions (5, 21, and 32 ppm respectively in the <180 µm fractions; versus 3, 17, and 21 ppm in the 180 – 2000 µm fractions. Conversely, Zn shows higher contrast, with average content in the <180µm fraction (188 ppm) double that of the 180 – 2000 µm fractions (59 ppm).

The tributaries entering at 67, 107, 109, 119, 131, 170, 184, and 229 km from the uppermost point and the main channel at downstream distances 3, 24, 51, 66, 72, 73, 86, 245, 278, and 310 km have the highest Zr, Ti, Nb and Y contents. Consequently, these 18 samples were selected for heavy mineral separation and analysis.

Table 4.1.4a: Analyses of Mahaweli River <180 µm fraction stream sediments. Major elements as oxide wt%, trace elements are in ppm. Distance: distance downstream (km) from the uppermost sample point. Type: MC – main channel; Tri – tributary

<180 µm

S-No	Distance(Km)	Type	TiO_2	Fe_2O_3	CaO	P_2O_5	Zr	Th	Nb	Sc	V	Ni	Cr	Y	Sr	As	Pb	Zn	Cu
MC1	1	MC	2.06	14.46	1.08	0.37	545	36	45	26	459	58	158	25	69	10	28	169	46
MC3	3	MC	2.95	13.71	1.09	0.02	1258	86	78	23	703	19	187	17	42	8	26	144	33
MC7	7	MC	2.39	14.14	1.09	0.28	952	52	68	25	550	45	176	21	112	7	22	140	35
MC7	7	MC	2.19	12.72	0.89	0.31	636	27	47	19	437	44	195	13	58	9	23	205	60
TR10	10	Tri	0.96	9.82	4.43	0.30	219	6	9	30	247	36	137	21	419	2	16	102	41
MC16	16	MC	2.06	9.78	0.99	0.02	702	67	52	21	392	38	187	23	71	7	26	118	31
MC24	24	MC	3.09	10.03	1.24	0.22	917	47	114	21	628	31	145	17	101	6	19	110	24
MC29	29	MC	2.02	14.25	1.08	0.23	534	43	52	23	437	43	171	24	69	8	32	137	56
TR38	38	Tri	2.26	8.02	2.26	0.18	957	74	44	18	405	30	168	25	183	5	21	110	18
MC43	43	MC	2.00	13.29	1.27	0.20	595	41	42	24	412	37	159	34	111	5	21	97	39
MC51	51	MC	1.38	11.34	1.72	0.30	375	28	23	23	312	44	127	30	149	6	24	135	46
MC55	55	MC	2.26	14.20	1.09	0.29	992	59	42	1	557	46	198	23	71	6	21	116	51
TR67	67	Tri	0.02	0.05	48.02	0.17	35	1	1	24	5	5	13	7	2584	4	8	1	9
MC72	72	MC	1.13	15.99	1.93	0.11	143	6	9	31	338	75	130	21	123	3	12	86	93
MC73	73	MC	1.67	12.34	1.75	0.32	506	32	34	22	358	45	143	28	137	7	33	159	52
MC84	84	MC	1.04	9.00	3.04	0.02	232	8	12	26	226	35	123	20	331	3	20	89	37
MC84	84	MC	1.53	12.22	2.58	0.26	318	16	25	27	342	40	141	27	222	4	19	113	48
MC86	86	MC	0.69	6.15	5.94	0.24	194	7	8	20	140	46	114	26	293	3	21	72	38
TR91	91	Tri	0.86	15.27	1.22	0.21	187	12	11	26	280	56	146	35	96	8	32	144	52
MC102	102	MC	1.28	6.27	4.36	0.22	284	12	26	19	187	23	89	26	318	4	23	73	20
TR107	107	Tri	2.14	10.64	2.53	0.27	851	40	60	20	395	20	101	35	193	4	19	98	21
TR109	109	Tri	2.35	8.87	2.44	0.26	792	46	57	17	441	17	171	27	228	4	19	79	12
TR110	110	Tri	2.92	13.73	2.31	0.02	1355	90	85	22	722	19	176	33	153	6	20	134	24
TR119	119	Tri	1.15	9.41	2.61	0.31	424	17	34	18	239	35	107	30	298	3	22	82	25
MC124	124	MC	1.94	9.57	3.31	0.02	611	29	34	22	370	20	153	30	248	3	20	83	20
TR127	127	Tri	1.67	9.53	2.62	0.02	564	27	51	18	292	19	83	30	261	4	20	72	17
MC131	131	MC	1.25	8.15	1.63	0.02	413	22	25	22	249	44	150	26	238	4	29	92	37
TR131	131	Tri	1.33	5.85	3.07	0.12	448	33	21	16	192	34	118	20	333	4	21	53	17
MC139	139	MC	2.61	10.87	2.06	0.21	827	95	97	17	501	25	158	32	190	4	19	94	21
TR143	143	Tri	0.61	8.12	1.88	0.02	178	8	9	18	173	52	172	23	306	4	26	84	40
MC151	151	MC	1.17	10.36	1.77	0.22	400	29	25	19	249	52	148	30	211	5	25	93	37
MC159	159	MC	1.05	7.99	2.07	0.19	318	20	21	17	196	38	116	29	251	4	25	77	28
TR170	170	Tri	2.21	5.59	2.75	0.16	986	35	38	11	267	8	76	27	365	5	16	50	9
MC173	173	MC	0.89	9.54	1.95	0.18	244	14	14	19	218	45	126	31	245	4	23	84	40
MC182	182	MC	0.72	13.63	1.57	0.02	162	12	10	26	254	70	173	31	189	5	28	124	61
TR184	184	Tri	2.90	13.16	2.10	0.19	1205	126	70	18	682	29	153	31	160	6	19	129	21
MC186	186	MC	1.08	13.28	1.64	0.24	325	20	23	25	267	64	160	34	176	5	26	118	57
MC205	205	MC	2.51	10.23	1.90	0.17	762	67	61	20	522	36	321	21	217	4	19	99	27
MC220	220	MC	2.49	7.58	2.37	0.13	514	51	70	12	425	14	110	26	261	4	20	67	11
TR229	229	Tri	3.61	12.40	2.57	0.15	1137	88	113	24	1064	5	202	30	197	4	13	129	5
MC245	245	MC	1.21	6.11	2.41	0.18	343	17	23	15	189	24	100	26	290	3	23	56	16
MC278	278	MC	2.04	7.93	2.67	0.15	566	32	41	14	353	27	118	26	284	3	19	79	10
MC300	300	MC	1.44	4.74	2.53	0.08	420	22	28	15	197	15	85	23	354	5	19	48	9
MC302	302	MC	1.58	5.30	2.75	0.11	438	19	28	14	238	14	117	23	304	3	20	53	5
MC304	304	MC	1.17	7.14	2.12	0.18	345	20	21	17	193	29	104	24	317	5	22	66	23
MC306	306	MC	1.04	3.25	3.83	0.11	378	14	19	11	116	19	92	18	361	5	22	37	6
MC310	310	MC	0.02	0.28	0.53	0.02	11	1	2	1	5	38	242	1	2	1	7	1097	93
MC313	313	MC	1.06	3.88	3.46	0.18	500	18	13	16	129	16	69	25	254	5	21	59	12
Average			1.67	9.59	3.18	0.17	544	35	38	19	345	34	142	25	259	5	21	118	32
Min			0.02	0.05	0.53	0.02	11	1	1	1	5	5	13	1	2	1	7	1	5
Max			3.61	15.99	48.02	0.37	1355	126	114	31	1064	75	321	35	2584	10	33	1097	93
Metabasites			1.41	2.86	7.74	0.67	239	6	20	NA	NA	54	80	27	1220	NA	15	109	20
Monzonitic gneisses			1.4	3.14	4.88	0.56	543	7	17	NA	NA	11	16	21	1540	NA	23	98	10
Syenitic gneisses			2.01	2	5.1	1.62	616	13	21	NA	NA	75	95	19	2360	NA	38	88	21
Monzonitic gneisses opx-bearing			0.86	1.02	4.18	0.28	651	5	10	NA	NA	10	11	23	404	NA	21	78	18
Granitic gneiss			0.25	0.66	1.44	0.07	153	32	9	NA	NA	6	10	9	443	NA	44	27	10

NA - Not Analyzed

Table 4.1.4b: Analyses of Mahaweli River 180 - 2000 µm fraction stream sediments. Major elements as oxide wt%, trace elements are in ppm. Distance: distance downstream (km) from the uppermost sample point. Type: MC – main channel; Tri – tributary

180 - 2000 µm

S-No	Distance(Km)	Type	TiO_2	Fe_2O_3	CaO	P_2O_5	Zr	Th	Nb	Sc	V	Ni	Cr	Y	Sr	As	Pb	Zn	Cu
MC1	1	MC	1.19	10.87	0.92	0.31	131	9	16	19	278	43	136	16	40	8	20	114	30
MC3	3	MC	1.05	7.34	0.85	0.13	267	24	13	12	194	13	103	8	23	7	21	75	20
MC7	7	MC	2.05	11.66	1.01	0.19	454	43	37	19	413	24	170	14	50	4	14	91	18
MC7	7	MC	1.01	6.70	0.80	0.17	177	7	12	10	172	28	126	7	38	5	15	111	28
TR10	10	Tri	0.64	6.43	1.22	0.12	147	11	8	12	142	32	167	12	103	2	15	46	18
MC16	16	MC	0.83	6.57	0.84	0.10	163	19	14	12	144	32	107	17	88	4	21	61	21
MC24	24	MC	1.43	6.19	1.10	0.16	291	17	24	11	214	27	101	10	76	4	16	62	16
MC29	29	MC	0.84	8.39	0.91	0.15	139	12	13	16	181	30	130	12	48	5	22	78	32
TR38	38	Tri	0.74	7.06	4.41	0.14	86	2	5	23	183	32	116	14	418	2	14	69	27
MC43	43	MC	1.54	7.96	0.91	0.10	170	16	24	11	237	18	107	14	37	3	12	46	15
MC51	51	MC	1.20	8.68	1.14	0.17	132	12	14	18	219	20	113	18	48	3	14	70	21
MC55	55	MC	0.61	6.32	0.68	0.15	148	8	5	18	132	26	117	6	11	2	10	31	21
TR67	67	Tri	0.42	4.29	1.42	0.09	140	5	5	7	84	24	100	13	129	3	19	54	17
MC72	72	MC	1.14	14.76	3.21	0.10	108	2	8	33	332	56	147	19	191	2	10	83	63
MC73	73	MC	1.24	9.71	1.59	0.27	227	17	16	17	245	38	130	21	116	7	37	127	40
MC84	84	MC	1.09	11.34	1.94	0.19	95	4	8	22	265	55	135	22	329	3	21	124	72
MC84	84	MC	0.65	6.54	2.56	0.14	92	2	5	16	131	32	95	17	336	3	19	69	33
MC86	86	MC	0.71	7.68	5.10	0.17	126	5	8	21	164	64	109	26	184	2	18	80	49
TR91	91	Tri	0.86	14.40	1.19	0.21	142	11	11	25	265	54	138	33	71	7	32	139	49
MC102	102	MC	0.80	5.85	3.44	0.15	145	4	13	16	137	22	80	24	268	4	22	54	17
TR107	107	Tri	1.78	10.24	2.31	0.16	393	26	45	19	304	12	92	34	131	2	15	86	14
TR109	109	Tri	0.62	5.39	1.81	0.12	124	3	12	12	118	22	89	20	216	3	20	43	13
TR110	110	Tri	1.76	8.36	1.65	0.11	406	29	26	13	283	15	120	20	92	2	14	66	14
TR119	119	Tri	0.55	6.92	2.26	0.19	114	7	14	14	137	28	82	24	297	2	22	84	20
MC124	124	MC	0.79	5.75	2.30	0.11	147	9	11	11	142	15	95	22	191	2	18	50	13
TR127	127	Tri	0.61	7.13	1.61	0.14	158	9	12	14	133	16	78	18	114	1	14	42	13
MC131	131	MC	0.65	6.52	1.51	0.17	138	8	10	15	156	38	120	21	203	3	27	69	28
TR131	131	Tri	0.56	4.49	2.81	0.08	170	20	6	13	96	30	99	15	267	2	16	34	12
MC139	139	MC	2.01	9.98	1.91	0.14	216	23	50	17	317	14	121	27	92	2	12	64	8
TR143	143	Tri	0.69	11.59	1.75	0.20	128	7	9	23	238	73	215	29	219	5	27	127	62
MC151	151	MC	1.01	7.74	1.79	0.16	184	13	19	18	192	32	124	23	173	3	20	67	24
MC159	159	MC	0.44	5.06	1.32	0.10	112	6	5	8	89	16	84	14	72	1	13	36	11
TR170	170	Tri	0.43	2.63	2.41	0.08	104	3	4	6	46	9	44	13	463	2	16	24	7
MC173	173	MC	0.74	8.34	1.85	0.16	161	9	11	18	178	46	114	29	236	4	22	83	37
MC182	182	MC	0.49	6.66	1.25	0.16	129	8	6	15	120	36	104	16	104	3	17	58	28
TR184	184	Tri	0.64	4.25	0.97	0.06	222	15	10	8	81	12	55	13	56	2	13	27	8
MC186	186	MC	0.09	1.71	0.82	0.04	100	2	2	1	4	12	24	7	65	1	11	11	7
MC205	205	MC	0.90	8.75	1.72	0.17	281	14	13	21	211	38	143	23	226	4	22	72	29
MC220	220	MC	0.40	3.44	1.25	0.06	130	6	6	7	49	13	49	14	93	2	12	29	4
TR229	229	Tri	0.71	3.42	1.66	0.02	161	8	12	7	95	12	61	15	182	2	17	38	6
MC245	245	MC	0.50	4.48	2.17	0.13	103	8	8	11	93	25	78	21	288	3	23	44	14
MC278	278	MC	0.03	0.88	0.84	0.04	105	2	1	1	5	10	21	7	87	1	10	6	3
MC300	300	MC	0.25	1.27	1.59	0.04	111	2	4	5	24	11	43	12	223	3	16	13	4
MC302	302	MC	0.09	0.87	1.45	0.04	97	1	2	2	3	17	24	11	223	2	18	8	3
MC304	304	MC	0.22	1.70	1.11	0.06	134	3	3	1	20	13	34	10	138	2	13	14	5
MC306	306	MC	0.57	2.65	7.51	0.09	210	17	7	13	68	7	77	11	259	5	13	25	6
MC310	310	MC	0.27	1.28	1.89	0.07	164	4	3	4	25	10	28	13	152	2	18	17	5
MC313	313	MC	0.02	0.16	50.26	0.16	22	1	2	25	5	8	8	6	2441	3	8	2	8
Average			0.79	6.47	2.85	0.13	165	10	12	14	153	26	97	17	206	3	17	59	21
Min			0.02	0.16	0.68	0.02	22	1	1	1	3	7	8	6	11	1	8	2	3
Max			2.05	14.76	50.26	0.31	454	43	50	33	413	73	215	34	2441	8	37	139	72
Metabasites			1.41	2.86	7.74	0.67	239	6	20	NA	NA	54	80	27	1220	NA	15	109	20
Monzonitic gneisses			1.4	3.14	4.88	0.56	543	7	17	NA	NA	11	16	21	1540	NA	23	98	10
Syenitic gneisses			2.01	2	5.1	1.62	616	13	21	NA	NA	75	95	19	2360	NA	38	88	21
Monzonitic gneisses opx-bearing			0.86	1.02	4.18	0.28	651	5	10	NA	NA	10	11	23	404	NA	21	78	18
Granitic gneiss			0.25	0.66	1.44	0.07	153	32	9	NA	NA	6	10	9	443	NA	44	27	10

NA - Not Analyzed

Proportions of the 63-180 and 180-300 µm fractions in each sample are illustrated in Figs 4.1.4a and 4.1.4b, respectively. The 63-180 µm fractions in the upper reaches of the main channel and the tributaries in the middle reaches have significant heavy mineral contents (>30 wt%). Contents in the main channel samples tend to decrease downstream. Unfortunately, the tributary at 229 km, and the main channel samples at 278 km and 310 km did not contain significant 63-180 µm fractions. The 180-300 µm fractions in the tributaries at 107, 131 and 229 km have very high heavy mineral contents (76, 37 and 54 wt% respectively). In the main channel proportions are lower and more uniform, although 180-300 µm fractions at 51 and 66 km contain more than 20 wt% heavy minerals. The greatest heavy mineral content (>90 wt%) is found in sample MC310, within Trincomalee Bay.

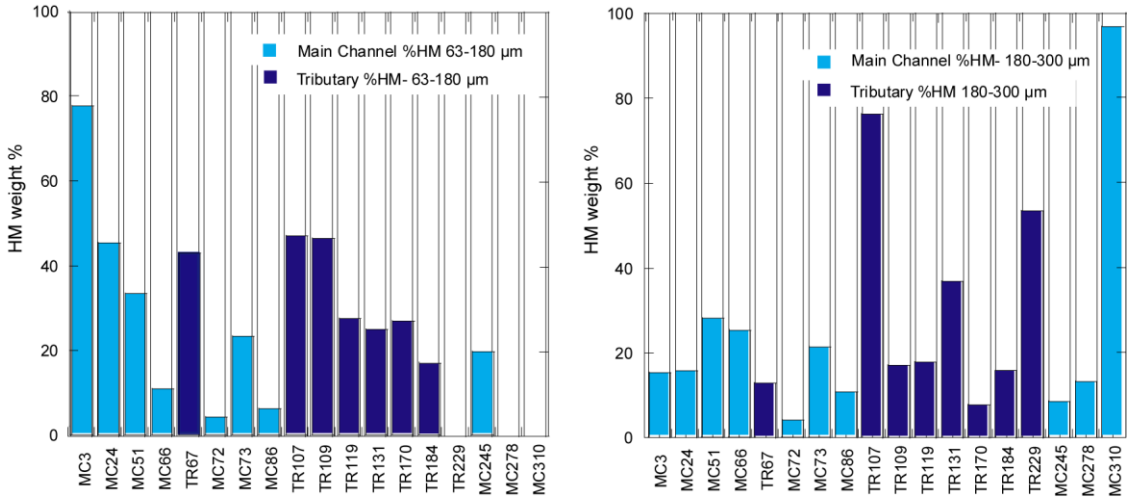

Fig 4.1.3: Total heavy mineral weight percent of eighteen selected samples along the main stream and selected tributaries. MC – mainstream, TR – Tributary and the distance is given

In the Frantz separation fraction, the highest heavy mineral contents occurred in the 0.3 – 0.5 amp portions. Although heavy mineral contents of the 63-180 µm fractions were greater than in the 180-300 µm fractions (Table 4.1.5a, 4.1.5b), the same minerals occurred in both fractions, based on the microscope observations. Mineral abundances of the 180-300µm fraction were magnetite > garnet > ilmenite> tourmaline > allanite, except for two samples which had high ilmenite contents (Fig 4). Surprisingly, zircon was not observed from any analyzed fractions. As

for Stow, 1929 sometimes such common detrital minerals as tourmaline and zircon are not found in a small amount of material under observation. The 0.2-0.3 amp portions consisted mainly of magnetite, with lesser hornblende, ilmenite, hematite and sillimanite. The 0.3-0.4 and 0.4-0.5 amp portions consisted mainly of garnet and ilmenite, with lesser quantities of tourmaline, biotite and rutile. The 0.5-1.0 amp portion had much lower heavy mineral content and consisted mainly of non-magnetic minerals, and the >1.0 amp portion contained only non-magnetic minerals (quartz, feldspar).

Table 4.1.5a: Frantzed magnetic separate heavy mineral weight percent 63-180 µm fraction

63-180 µm

S_No	Name	Distance (Km)	Initial weigh (g)	Quartz (wt%)	Weight of HM (g)	Magnetite wt%	<0.2wt%	0.2-0.3wt%	0.3-0.4wt%	0.4-0.5wt%	0.5-1.0wt%	>1.0wt%
Hatton	MC3	3	7.52	47.61	3.94	24.37	18.53	21.07	13.45	4.82	1.78	15.99
SLML3 Thalawakele	MC24	24	8.55	54.27	3.91	48.85	15.09	10.23	10.49	3.07	1.53	10.74
L33 PUNDALUOYA	MC51	51	4.16	66.35	1.40	39.29	2.86	5.00	27.86	10.71	4.29	10.00
SLML27 Polgolla	MC66	66	7.83	88.89	0.87	6.90	2.30	1.15	36.78	43.68	5.75	3.45
SLML12 Kundasale	MC72	72	3.47	95.68	0.15	6.67	6.67	6.67	13.33	13.33	6.67	46.67
SLML13 Kundasale	MC73	73	5.96	76.51	1.40	12.86	7.14	15.71	32.14	10.00	8.57	13.57
Victoria inlet	MC86	86	11.43	94.14	0.67	5.97	11.94	8.96	37.31	11.94	10.45	13.43
SLML33 Somawathiya	MC245	245	9.95	80.20	1.97	7.61	10.66	10.66	31.47	12.18	5.58	21.83
65 Somapura	MC278	278										
Min				47.61	0.15	5.97	2.30	1.15	10.49	3.07	1.53	3.45
Max				95.68	3.94	48.85	18.53	21.07	37.31	43.68	10.45	46.67
28 Suduganga	TR67	67	4.81	56.76	2.08	8.17	8.65	9.62	24.52	8.17	6.25	34.62
45 Tributary of Randenigala	TR107	107	7.26	68.04	2.32	31.90	6.90	15.52	26.72	6.90	3.02	9.05
47 Minipe-ela	TR109	109	9.35	53.05	4.39	9.11	10.48	18.45	29.38	9.11	4.10	19.36
48 Uma oya	TR119	119	6.48	72.07	1.81	16.57	6.63	16.57	39.23	7.73	3.31	9.94
49 Gangagolla	TR131	131	13.06	80.09	2.60	3.46	13.85	8.85	20.77	18.85	16.54	17.69
55 Ulhitiyaoya	TR170	170	5.00	71.60	1.42	19.72	19.72	21.83	28.87	6.34	3.52	0.00
Naulaoya-Nalanda	TR184	184	12.15	85.43	1.77	4.52	7.91	7.34	17.51	4.52	4.52	53.67
59 Ambanganga	TR229	229										
Min				53.05	1.42	3.46	6.63	7.34	17.51	4.52	3.02	0.00
Max				85.43	4.39	31.90	19.72	21.83	39.23	18.85	16.54	53.67

Table 4.1.5b: Frantzed magnetic separate heavy mineral weight percent 180 - 2000 µm fraction

180-300 µm

S_No	Name	Distance Km	Initial weight	Quartz (wt%)	Weight of HM (g)	Magnetite wt%	<0.2wt%	0.2-0.3wt%	0.3-0.4wt%	0.4-0.5wt%	0.5-1.0wt%	>1.0wt%
Hatton	MC3	3	6.65	5.24	1.41	29.08	12.77	21.99	15.60	6.38	2.13	12.06
SLML3 Thalawakele	MC24	24	5.35	4.51	0.84	36.90	3.57	9.52	27.38	7.14	2.38	13.10
L33 PUNDALUOYA	MC51	51	1.14	0.82	0.32	12.50	25.00	6.25	37.50	12.50	3.13	3.13
SLML27 Polgolla	MC66	66	3.27	2.43	0.84	3.57	1.19	3.57	22.62	61.90	5.95	1.19
SLML12 Kundasale	MC72	72	1.80	1.73	0.07	14.29	14.29	14.29	14.29	14.29	14.29	14.29
SLML13	MC73	73	5.62	4.42	1.20	7.50	10.00	17.50	29.17	13.33	10.83	11.67
Victoria inlet	MC86	86	6.91	6.25	0.66	7.58	4.55	6.06	42.42	15.15	12.12	12.12
SLML33 Somawathiya	MC245	245	11.13	10.19	0.94	3.19	2.13	4.26	42.55	19.15	9.57	19.15
65 Somapura	MC278	278	2.82	2.45	0.37	2.70	5.41	2.70	48.65	13.51	8.11	18.92
TR32	MC310	310	4.71		4.71	15.29	3.40	20.81	29.72	4.88	2.55	23.35
Min				0.82	0.07	2.70	1.19	2.70	14.29	4.88	2.13	1.19
Max				10.19	4.71	36.90	25.00	21.99	48.65	61.90	14.29	23.35
28 Suduganga	TR67	67	5.47	4.76	0.71	4.23	5.63	4.23	26.76	14.08	11.27	33.80
45 Tributary of Randenigala	TR107	107	3.86	2.19	1.67	19.16	11.38	20.96	34.73	5.39	2.99	5.39
47 Minipe-ela	TR109	109	7.74	6.41	1.33	6.02	5.26	14.29	37.59	12.78	7.52	16.54
48 Uma oya	TR119	119	6.16	5.04	1.12	11.61	4.46	10.71	51.79	12.50	4.46	4.46
49 Gangagolla	TR131	131	8.81	6.44	2.37	27.85	2.53	4.22	21.94	18.99	16.46	8.02
55 Ulhitiyaoya	TR170	170	8.03	7.41	0.62	4.84	6.45	9.68	46.77	16.13	6.45	9.68
Naulaoya-Nalanda	TR184	184	5.98	5.16	0.82	4.88	1.22	1.22	18.29	19.51	2.44	52.44
59 Ambanganga	TR229	229	2.99	1.32	1.67	7.19	8.98	8.98	43.11	8.98	5.39	17.37
Min				1.32	0.62	4.23	1.22	1.22	18.29	5.39	2.44	4.46
Max				7.41	2.37	27.85	11.38	20.96	51.79	19.51	16.46	52.44

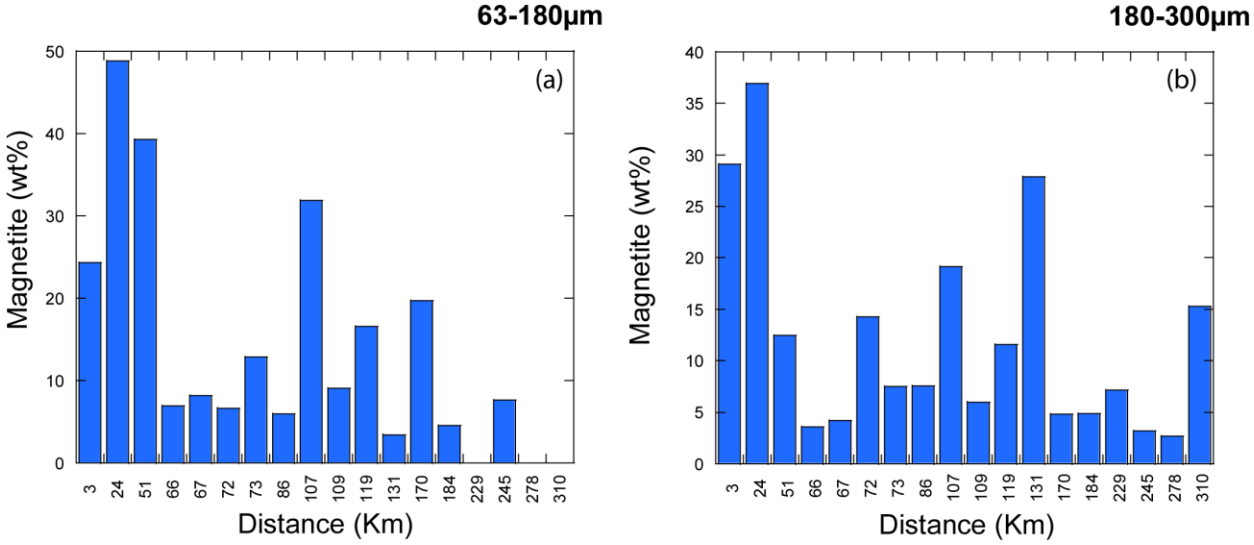

Fig 4.1.4a: The magnetite content along the Mahaweli River

The magnetite content was very high in the upper reaches and decreased downstream (Fig 4.1.4a). This was observed in both 63-180µm fractions as well as in the 180-300 µm fractions.

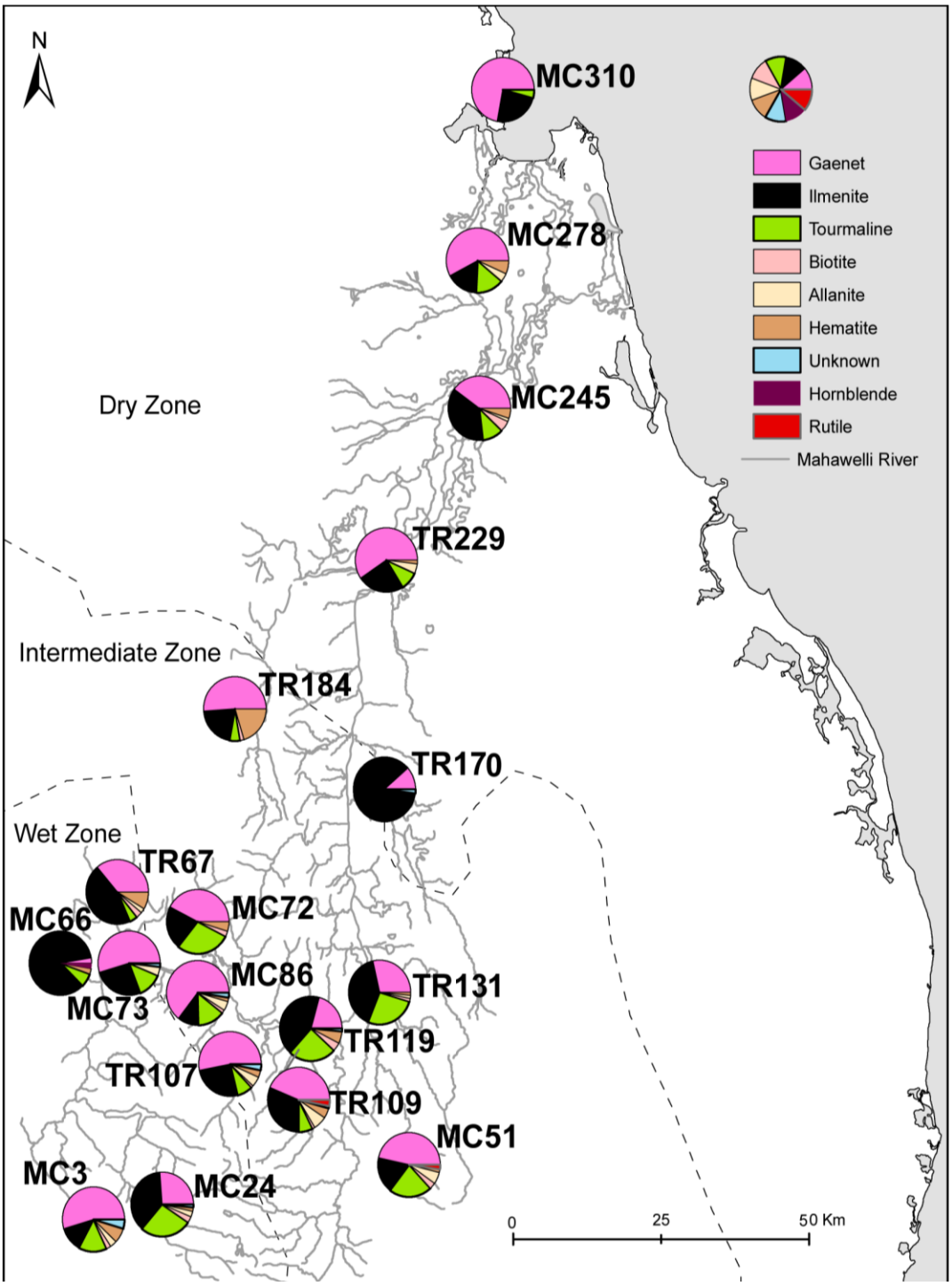

Fig 4.1.4b: Frantzed heavy mineral count pie plots of eighteen selected locations along the Mahaweli River, after removal of magnetite. MC – mainstream, TR – Tributary and the distance is given

4.2 POLGOLLA DAM

4.2.1 Surface and Core Sediments

Metal concentrations in core sediments ranged from 4.6 to 7.4 for As 26.9 to 35.2 for Pb, 168.9 to 193.9 (ppm) for Zn, 101.7 to 117 5 (ppm) for Cu, 18.71 and 10.03 (wt%) for Fe (Table 4.1.5c). The surface sediments ranged from and 3.2 to 6.1 (ppm) for As and 19.5 to 31.8 (ppm) for Pb, and 104.2 to 207.1 (ppm) for Zn, and 52.3 to 269.5 (ppm) for Cu 17.02 to 15.99 (wt%) for Fe (Table 4.1.6). The surface sediments are characterized by relatively higher concentrations of Zn and Cu. In contrast, core sediments are high in As, Pb and Fe compared to the surface sediments. The very high Fe indicates that the reservoir sediments are under highly reducing condition.

Table 4.1.5c: Individual XRF analyses of the core sediments of Polgolla reservoir

Sample no	PC1	PC2	PC3	PC4	PC5	PC6	PC7	PC8	PC9	PC10	PC11	PC12	PC13	PC14
Major Elements (wt%)														
TiO_2	1.16	1.16	1.18	1.2	1.24	1.2	1.22	1.25	1.21	1.18	1.21	1.17	1.16	1.2
Fe_2O_3	17.52	18.33	18.71	18.41	17.57	17.88	17.95	17.92	17.72	17.02	18.01	17.67	17.47	17.26
MnO	0.26	0.242	0.267	0.273	0.228	0.236	0.249	0.243	0.245	0.241	0.266	0.257	0.256	0.256
CaO	1.32	1.13	1.16	1.3	1.36	1.3	1.34	1.36	1.35	1.42	1.31	1.35	1.4	1.44
P_2O_5	0.258	0.26	0.258	0.269	0.262	0.257	0.243	0.241	0.243	0.249	0.258	0.259	0.26	0.257
Trace Elements (ppm)														
As	6.7	7.4	7.3	6.1	4.6	5.8	5.2	5.4	5.7	5.9	6.6	6.6	5.9	6.2
Pb	29.1	35.2	34	30.3	27.6	26.9	27	27.8	29.9	28.2	30.9	30.3	30.2	29
Zn	181.9	193.9	192.2	183.5	178.3	178.5	169.9	173.3	178	168.9	186.3	180.5	178.9	173.3
Cu	105.1	108.1	105.9	109.9	117	113.4	111.7	113.9	105.6	101.7	108.2	105	105.4	107.9
Ni	67.5	64.7	69.3	66.5	70.5	72.3	68.8	69.1	66	65.1	69.5	79.2	66.6	69.9
Cr	145.1	155.1	154.8	154.8	145.6	148.9	148.7	145.8	147.1	146.6	147.8	148.8	149	147.8
V	360.2	348.7	371.1	372.7	365.2	371	372.8	372.8	359.1	350.1	361.9	351.9	352.2	343.6
Sr	112	74.8	70.9	89.9	100.9	87.7	85.6	89.2	94.2	126.6	95.9	102.7	114.6	125.7
Y	36.95	40.5	38.12	35.91	36.75	37.67	37.02	36.83	37.65	37.05	37.41	37.2	36.85	36.47
Nb	12.4	14	13.7	12.5	12.3	12.7	13.3	13.9	13.4	12.6	13.1	13.3	13.1	12.7
Zr	124.2	146.9	122.8	98.6	88.8	85.7	86.8	102.2	120.1	135.1	113.7	124.1	140.2	117.5
Th	11.9	13.8	13.9	11.4	9.5	9.8	10	10.2	11.1	11.4	11.6	10.4	12.1	10.7
Sc	35.5	33.2	34.1	35.2	34.3	37.8	37.4	37.9	37.3	34.9	36.1	36.3	34.7	35.2
TS	963	1018	1001	1018	974	928	878	873	889	918	954	929	947	932
F	12	76	42	51	65	140	151	127		51		41	25	89
Br	5	4.7	5.1	5.3	4.7	4.8	4.6	4.6	4.7	4.7	5.1	4.8	4.9	4.9

Table 4.1.6: Individual XRF analyses of the surface sediments of Polgolla reservoir

Sample no	PG1	PG2	PG3	PG4	PG5	PG6	Min	Max	Avg
Major Oxides (wt%)									
TiO_2	1.05	0.96	1.07	1.13	0.90	0.94	0.90	1.13	1.01
$Fe_2O_3^*$	13.56	11.89	11.66	15.99	10.03	10.70	10.03	15.99	12.31
MnO	0.19	0.19	0.16	0.19	0.17	0.16	0.16	0.19	0.18
CaO	2.61	2.07	1.79	1.54	2.56	2.47	1.54	2.61	2.17
P_2O_5	0.27	0.24	0.23	0.27	0.22	0.33	0.22	0.33	0.26
Trace Elements (ppm)									
As	3	5	5	6	5	5	3.20	6.10	4.72
Pb	20	30	22	32	20	24	19.50	31.80	24.47
Zn	147	207	110	207	104	129	104.20	207.10	150.80
Cu	103	64	54	91	52	270	52.30	269.50	105.70
Ni	63	40	43	63	38	46	38.30	62.70	48.62
Cr	132	97	116	132	122	102	96.80	132.00	116.70
V	298	252	264	327	224	229	223.80	326.80	265.53
Sr	284	316	172	131	188	305	130.70	315.70	232.52
Y	29	26	23	33	21	27	21.47	32.72	26.45
Nb	9	10	11	13	11	10	9.10	12.90	10.57
Zr	146	119	182	104	160	135	103.60	182.30	140.93
Th	7	5	8	11	7	9	5.20	11.10	7.92
Sc	35	35	30	33	26	25	25.40	34.70	30.43
TS	760	1084	828	1359	743	1220	743.00	1359.00	999.00
F	185		48	208		198	48.00	208.00	159.75
Br	4	5	4	6	3	3	3.30	6.00	4.32
I		4	7		8	1	0.80	7.50	4.85

4.3 TRINCOMALEE BAY

4.3.1 Surface Sediments

Averages and ranges of grain size and geochemical compositions in the Inner Harbour, Thambalagam Bay, and Koddiyar Bay are listed in Table 4.3.1, compared to average Upper Continental Crust (UCC; Taylor and McLennan 1985) and stream sediments from the lower Mahaweli River (Young et al. 2012). Individual Trincomalee analyses are contained in 4.3.2. Loss on ignition values (LOI) are variable, but are higher on average in the Inner Harbour (12.9 wt%) than in Thambalagam and Koddiyar bays (3.18 and 2.69 wt% respectively; Table 4.3.2).

Total organic carbon (TOC) contents of selected samples analyzed for a separate Ostracode study are low (<0.49 wt%; Young, unpubl. data), indicating that TOC contents are not responsible for the higher LOI values.

Table 4.3.1 Average, minimum and maximum elemental concentrations in the three sectors of Trincomalee Bay, compared to sediments from the lower Mahaweli River (LMR; data from Young et al. 2012), and UCC (Taylor and McLennan 1985)

	Inner Harbour			**Thambalagam Bay**			**Koddiyar Bay**			**LMR**	**UCC**
	Mean	Min	Max	**Mean**	Min	Max	**Mean**	Min	Max	(*n*=18)	
SiO_2	**62.69**	39.04	85.65	**74.38**	59.25	86.30	**69.76**	37.06	83.37	**78.95**	**66.00**
TiO_2	**1.09**	0.32	2.15	**0.73**	0.14	2.14	**1.43**	0.13	5.18	**0.87**	**0.50**
Al_2O_3	**8.18**	2.67	11.70	**11.43**	7.68	19.00	**11.68**	5.32	15.89	**9.90**	**15.20**
Fe_2O_3*	**4.79**	1.52	8.49	**4.19**	0.82	12.97	**6.71**	0.80	32.91	**4.97**	**4.50**
MnO	**0.06**	0.02	0.13	**0.06**	0.01	0.12	**0.10**	0.01	0.48	**0.08**	**0.08**
MgO	**2.31**	0.67	4.55	**1.05**	0.33	3.12	**1.57**	0.31	5.57	**0.73**	**2.20**
CaO	**17.52**	3.02	40.60	**3.61**	1.31	13.90	**4.58**	1.38	22.33	**1.61**	**4.20**
Na_2O	**1.50**	0.61	2.12	**2.12**	1.36	2.94	**1.84**	0.93	2.56	**0.87**	**3.90**
K_2O	**1.72**	0.43	2.58	**2.34**	1.59	3.18	**2.26**	0.83	3.20	**1.95**	**3.40**
P_2O_5	**0.14**	0.04	0.55	**0.09**	0.01	0.36	**0.07**	0.01	0.14	**0.08**	**0.16**
Ba	**601**	237	1080	**840**	648	1120	**764**	370	997	**-**	**550**
Ce	**141**	28	792	**84**	11	654	**147**	11	572	**-**	**64**
Cr	**73**	26	192	**50**	11	181	**96**	7	356	**115**	**35**
Ga	**6**	0	10	**8**	1	20	**10**	0	14	**-**	**17**
Nb	**16**	2	57	**12**	3	54	**40**	4	242	**16**	**25**
Ni	**16**	3	57	**11**	4	46	**13**	0	27	**26**	**20**
Pb	**23**	3	103	**14**	8	20	**15**	9	20	**21**	**20**
Rb	**43**	15	70	**68**	44	100	**62**	11	84	**-**	**112**
Sc	**25**	10	37	**11**	3	24	**16**	4	43	**15**	**11**
Sr	**936**	319	2266	**371**	169	557	**405**	54	1658	**239**	**350**
Th	**22**	6	49	**22**	3	222	**33**	5	156	**13**	**11**
V	**105**	30	193	**84**	16	347	**194**	11	1090	**163**	**60**
Y	**29**	8	118	**17**	5	39	**26**	4	93	**22**	**22**
Zr	**1089**	164	8123	**460**	103	3914	**1064**	107	5247	**301**	**190**
As	**7**	3	19	**10**	2	43	**4**	2	9	**4**	***5**
Zn	**49**	21	152	**31**	9	79	**51**	6	181	**57**	**71**
Cu	**13**	2	41	**6**	0	23	**6**	2	14	**16**	**25**
Mean GS (p	**1.29**	-0.76	3.43	**1.71**	0.16	3.47	**1.77**	-0.95	4.60	**-**	**-**
Sorting	**2.08**	0.41	2.63	**1.64**	0.30	2.48	**1.51**	0.81	2.59	**-**	**-**
Ti/Fe	**0.26**	0.15	0.49	**0.21**	0.06	0.36	**0.23**	0.12	0.35	**-**	**-**

* Value from Rudnick and Gao (2005)

4. 3.1.1 Texture

Mean grain size of the Trincomalee Bay sediments ranged from -0.13 to 4.60 ϕ (Table 4.3.1), equivalent to very coarse sand to coarse silt. Average mean grain size of the three sectors show limited contrast, with values of 1.29 ϕ (Inner Harbour), 1.71 ϕ (Thambalagam Bay) and 1.77 ϕ (Koddiyar Bay). The sediments in Thambalagam Bay show the least variability (0.16 –

3.47 ϕ) (Fig. 4.3.5). Clay contents (< 9 Φ, 2μm) are generally low (<2% for most samples), but combined silt and clay contents can be significant, with the <4Φ fraction (clay and silt) averaging 9.05, 8.08 and 6.85 wt% in the Inner Harbour, Thambalagam Bay and Koddiyar Bay (Table 4.3.2). The sediments are also generally well sorted, with sorting greatest in the Inner Harbour (average 2.08, range 0.41–2.63), compared to 1.64 (0.30–2.48) and 1.51 (0.81–2.59) in Thambalagam and Koddiyar bays, respectively (Table 4.3.1, Fig. 4.3.5).

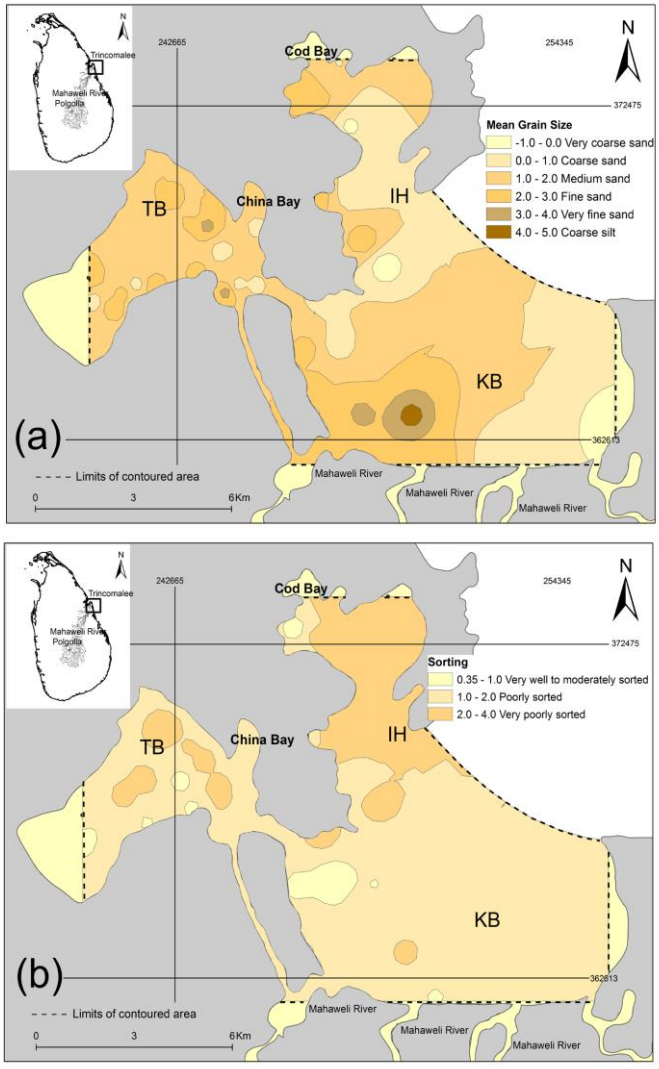

Fig 4.3.5: Contour maps showing the spatial variation of (a) mean grain size and (b) sorting in Trincomalee Bay. Grain size and sorting calculated following Folk and Ward (1957)

4. 3.1.2 Major elements

Major element concentrations show some contrast between the three sectors. Average SiO_2 contents in the Inner Harbour, Thambalagam Bay and Koddiyar Bay are 62.69, 74.38 and 69.76 wt%, respectively, intermediate between the composition of UCC 66.0 wt%) and sediments from the lower reaches of the Mahaweli River (78.95 wt% (Table 4.3.1). Average concentrations of Al_2O_3 are 8.18, 11.43 and 11.68 wt.%, respectively, less than in UCC (15.20 wt.%), but similar to lower Mahaweli River sediments (9.90 wt%; Table 4.3.1, data from Young et al. 2012).

Among the other major elements CaO contents show the greatest contrast (Table 1), with much higher levels and greater range in the Inner Harbour (average 17.52 wt%, range 3.02–40.60 wt%) than in Thambalagam (3.61; 1.31–13.90 wt%) or Koddiyar Bay (4.58; 1.38–22.33 wt%). The higher CaO contents are due to the presence of shell fragments. Average Fe_2O_3 and TiO_2 contents in Koddiyar Bay (6.71 and 1.43 wt.%, respectively) are significantly greater than in the two other sectors, UCC, and the lower Mahaweli sediments (Table 4.3.1). In contrast, average MgO, Na_2O, and K_2O contents in all three sectors are intermediate between higher levels in UCC and lower levels in the lower Mahaweli sediments. This also tends to be the case for the minor elements MnO and P_2O_5.

The statistical values of σ, p-value, and the t-value for a two sample t-test with 95% confidence and the alternative of being not equal are given in Table 4.3.1, to test (1) if there is a difference between the means of the three sectors, and (2) if there is a difference between the statistical values for the three sectors. The null hypothesis is rejected when the p-value is less than 0.05, where the three sectors differ in composition. Similarity between sectors is indicated by a variance greater than 0.05. In the t-test higher variance indicates that the two means are not equal, and hence the compositions of the three sectors differ. A lesser variance indicates that the three sectors have similar composition. Statistically, the p-values for Ti, Fe, Mn, Mg, Ca and P are much higher (> 0.05) for Inner Harbour and Thambalagam Bay, and thus the null hypothesis that the two data sets are different from each other is rejected. The t-values for major elements in Inner Harbour - Thambalagam Bay differ from those in Thambalagam Bay - Koddiyar Bay and Koddiyar Bay - Inner Harbour (Table 4.3.1). Therefore, the major element compositions of the three sectors differ.

The major elements were plotted on variation diagrams against Al_2O_3 as a proxy of grain size and clay mineral content. Correlation matrices for all elements are given in Table 4.3.4a, b, c. SiO_2 shows broad negative correlation with Al_2O_3 in the Koddiyar (R= -0.58) and Thambalagam (R= -0.53) sectors (Fig. 4.3.6a). Correlation is weakest in the Inner Harbour suite (R= -0.49), with considerable scatter towards lower values of both SiO_2 and Al_2O_3 (Fig. 4.3.6a), consistent with dilution from bioclastic CaO (Fig. 4.3.6b). Fe_2O_3, MnO, MgO, Na_2O and K_2O show good correlation (R>0.56) with Al_2O_3 in the Inner Harbour. In Koddiyar Bay Na_2O, K_2O and P_2O_5 show moderate to strong (R= 0.58-0.79) correlations with Al_2O_3. MgO shows relatively coherent trends in the Koddiyar and Thambalagam suites, but displacement to higher values in the Inner Harbour, possibly also due to carbonate content (Fig. 4.3.6c). Both Fe_2O_3 and TiO_2 show weak correlation with Al_2O_3 in all three suites, with no clear trends and scatter to high values (Fig. 4.3.6d, e). In contrast, K_2O shows relatively strong correlations with Al_2O_3 in all three sectors (R= 0.69, 0.63, and 0.58 in the Inner Harbour, Thambalagam and Koddiyar Bay, respectively; Table 4.3.4a, b), forming a broad trend coinciding with UCC and the field of the lower Mahaweli River sediments (Fig. 4.3.6f). This appears to be a product of positive correlation between Al_2O_3 and the proportion of the <4Φ (62.5μm) fraction in each sector (R=0.56, 0.75 and 0.41, respectively).

Table 4.3.2: Individual XRF analyses and texture of sediments from Trincomalee Bay, Sri Lanka

	Major elements (wt%)										Trace Elements (ppm)																		Texture	
Sample No	SiO_2	TiO_2	Al_2O_3	$Fe_2O_3^*$	MnO	MgO	CaO	Na_2O	K_2O	P_2O_5	Ba	Ce	Cr	Ga	Nb	Ni	Pb	Rb	Sc	Sr	Th	V	Y	Zr	As	Zn	Cu	Mean GS	Sorting
Inner Harbour																													
TR1	83.36	0.83	4.86	1.70	0.03	0.67	6.79	0.90	0.82	0.04	453	103	26	6	11	5	7	32	16	764	10	54	11	899	3	27	6	1.22	2.49
TR2	61.41	2.15	9.58	8.49	0.13	2.67	12.79	1.40	1.28	0.10	366	97	73	10	18	16	12	33	27	851	14	193	30	425	5	62	7	0.98	2.59
TR3	39.23	1.03	6.64	6.61	0.06	3.60	39.65	1.23	1.40	0.55	411	76	61	1	7	16	103	32	36	1790	21	89	118	315	19	152	41	2.75	0.41
TR4 Top	49.87	1.10	11.65	7.27	0.09	4.55	21.21	2.12	1.97	0.19	520	67	192	10	9	57	20	50	34	847	13	129	28	324	8	80	33	3.43	1.87
TR4 Bott	50.97	1.15	11.70	7.34	0.08	4.50	20.03	2.11	1.93	0.19	521	74	175	1	10	54	17	50	36	826	27	132	26	370	8	76	34	0.79	2.37
TR5	70.35	1.16	8.52	3.39	0.05	1.42	11.24	1.57	2.26	0.05	849	792	66	6	38	7	29	51	19	614	49	165	31	8123	10	34	5	0.79	2.37
TR6	72.13	1.06	8.03	2.97	0.07	1.55	10.60	1.54	1.99	0.07	542	115	32	7	14	6	14	54	20	579	25	70	26	532	4	22	3	-0.29	2.00
TR7	78.92	1.74	7.90	3.66	0.04	0.83	3.02	1.46	2.36	0.06	1080	88	56	7	18	5	11	70	10	319	18	120	13	645	4	23	4	0.08	2.57
TR8	70.16	1.11	10.41	4.92	0.06	1.30	7.32	2.05	2.58	0.08	1054	109	56	9	57	8	11	48	18	486	17	159	18	756	8	26	2	0.59	2.63
TR9	39.04	0.77	8.25	4.92	0.04	3.01	40.60	1.49	1.68	0.20	551	79	53	nd	2	11	23	34	37	2266	46	58	21	292	9	39	7	3.00	1.81
TR10	51.24	0.70	7.92	4.67	0.04	2.85	29.00	1.46	1.98	0.13	625	67	47	4	5	9	21	48	32	1361	13	58	21	221	9	30	5	2.86	1.62
TR11	85.65	0.32	2.67	1.52	0.02	0.78	7.94	0.61	0.43	0.05	237	28	35	0	4	3	3	15	15	531	6	30	8	164	3	21	4	-0.76	2.24
Average IH	62.69	1.09	8.18	4.79	0.06	2.31	17.52	1.50	1.72	0.14	601	141	73	6	16	16	23	43	25	936	22	105	29	1089	7	49	13	1.29	2.08
Thambalagam Bay																													
TR13	77.50	0.94	10.72	3.11	0.05	0.83	2.29	2.03	2.46	0.05	791	55	40	8	14	8	14	67	9	324	13	82	14	332	7	27	3	0.82	1.83
TR14	74.80	0.33	12.87	2.53	0.02	0.90	2.88	2.51	3.09	0.06	1011	19	41	12	5	12	19	90	7	396	4	37	10	119	6	33	9	1.11	2.20
TR15	86.30	0.24	7.68	0.90	0.02	0.33	1.31	1.48	1.72	0.02	650	16	15	3	5	4	12	64	3	264	9	20	6	160	3	14	4	0.16	2.34
TR16	71.83	2.14	9.62	9.90	0.11	1.39	1.61	1.36	1.95	0.10	729	654	181	8	54	18	8	44	14	169	222	347	39	3914	8	55	8	0.82	1.92
TR17	59.28	0.77	13.10	12.97	0.12	1.93	6.24	2.39	2.86	0.36	1005	129	79	6	13	19	13	72	16	434	20	132	38	333	34	48	7	3.47	2.24
TR18	59.25	0.95	8.96	10.01	0.12	3.12	13.90	1.62	1.79	0.28	648	100	59	6	14	15	13	45	24	488	17	130	32	370	43	34	5	1.90	2.05
TR19	69.28	0.92	8.97	7.86	0.10	1.61	7.58	1.61	1.85	0.22	679	121	82	1	13	12	12	50	15	390	29	117	27	442	26	31	5	2.09	2.24
TR20	84.78	0.14	9.06	0.82	0.01	0.33	1.43	1.69	1.72	0.02	729	15	11	8	3	4	13	68	6	311	3	16	5	105	4	9	3	1.86	0.39
TR21	79.66	0.43	11.39	1.72	0.03	0.63	1.91	2.04	2.16	0.03	832	24	38	3	8	5	16	74	8	358	14	51	10	178	6	20	2	1.31	2.41
TR22	78.80	0.66	11.40	1.86	0.04	0.63	2.19	2.16	2.23	0.03	851	42	24	11	12	7	17	71	10	375	9	62	11	282	4	25	5	1.80	2.48
TR23	64.69	0.49	14.95	4.37	0.07	1.49	7.70	2.94	3.18	0.12	1120	44	39	15	7	14	20	79	14	557	6	58	18	156	15	33	6	2.79	1.91
TR24	62.35	1.04	19.00	6.64	0.08	2.01	2.71	2.92	3.08	0.15	898	109	111	20	15	46	14	100	16	311	15	123	31	469	10	79	23	0.34	0.30
TR25	80.27	0.32	11.48	1.33	0.02	0.47	1.93	2.02	2.13	0.02	915	25	27	11	7	5	18	78	7	387	5	37	8	170	3	19	4	2.45	1.47
TR26	78.45	0.53	10.99	2.20	0.04	0.70	2.38	2.14	2.54	0.03	831	31	25	7	8	7	14	70	8	345	8	46	10	215	3	21	3	0.49	1.39
TR27	76.25	0.76	11.81	2.64	0.04	0.84	2.75	2.31	2.56	0.03	859	43	38	10	11	8	15	68	8	368	8	67	12	272	4	38	5	2.19	1.13
TR28	77.62	0.53	11.44	2.19	0.03	0.75	2.45	2.33	2.61	0.03	853	30	33	9	9	7	15	71	8	356	9	52	10	203	3	23	5	2.52	0.86
TR29	76.85	0.69	12.10	2.05	0.03	0.64	2.37	2.45	2.80	0.03	924	42	34	10	11	4	18	76	9	385	9	59	10	321	3	19	4	2.28	0.72
TR30	70.36	1.83	12.85	5.51	0.10	0.93	3.29	2.75	2.19	0.17	954	80	51	6	17	15	12	45	12	530	15	140	16	594	2	50	14	3.41	1.59
TR31	84.93	0.14	8.80	0.90	0.02	0.43	1.56	1.62	1.59	0.01	687	11	15	7	4	5	11	66	6	298	3	25	7	103	5	9	0	0.69	1.68
Average TB	74.38	0.73	11.43	4.19	0.06	1.05	3.61	2.12	2.34	0.09	840	84	50	8	12	11	14	68	11	371	22	84	17	460	10	31	6	1.71	1.64
Koddiyar Bay																													
TR12	79.14	1.19	8.98	4.21	0.04	0.81	1.96	1.65	1.96	0.06	817	106	87	9	21	9	14	52	10	251	16	109	12	702	4	29	8	0.43	2.59
TR32	37.06	5.18	13.46	32.91	0.48	5.57	3.43	0.93	0.83	0.14	370	572	356	nd	242	21	0	11	28	54	156	1090	93	5247	4	181	4	2.37	0.81
TR33	66.70	2.19	12.81	8.58	0.14	2.26	3.19	1.90	2.14	0.10	707	265	153	12	52	16	11	52	19	258	52	275	42	1876	4	63	2	2.37	0.81
TR34	60.58	2.66	13.83	12.21	0.18	2.46	3.46	2.04	2.46	0.12	799	380	170	13	81	16	10	54	17	271	77	417	48	2735	6	81	3	1.79	0.98
TR35	64.64	1.15	15.04	6.41	0.09	1.85	5.32	2.43	2.96	0.10	997	171	101	14	29	16	15	72	17	464	30	169	29	1141	6	58	5	1.79	1.51
TR36	72.94	1.05	12.27	4.76	0.08	1.37	2.74	2.12	2.60	0.07	865	121	85	0	23	10	16	70	13	313	36	132	23	799	4	41	2	2.11	1.46
TR37	57.90	1.07	15.50	7.26	0.09	1.94	10.63	2.42	3.05	0.12	988	173	95	14	29	21	15	74	22	780	31	171	30	1023	9	72	11	3.34	1.11
TR38	67.90	1.46	13.24	7.66	0.14	2.24	3.11	1.90	2.28	0.08	753	162	118	14	32	13	13	57	18	269	28	201	41	1078	4	63	4	2.15	1.27
TR39	58.30	1.75	15.89	6.69	0.08	1.79	9.62	2.56	3.20	0.12	953	153	90	7	22	27	15	82	20	646	36	145	26	896	8	65	14	4.60	2.34
TR40A	82.87	0.15	10.45	0.80	0.01	0.31	1.39	1.92	2.08	0.01	862	11	20	7	4	4	14	82	6	344	5	19	4	116	4	12	2	3.22	0.93
TR40B	77.66	1.04	11.07	2.93	0.04	0.77	1.99	1.93	2.53	0.04	832	64	50	10	15	8	18	72	9	316	13	83	14	434	3	27	4	2.56	1.12
TR41	70.96	1.63	13.46	4.75	0.07	1.19	2.64	2.25	2.98	0.07	942	101	83	13	25	15	20	84	11	334	21	136	19	720	3	41	5	2.55	0.90
TR42A	78.94	1.50	8.99	4.42	0.07	1.02	1.72	1.38	1.93	0.04	632	57	67	7	23	9	14	57	10	221	14	125	19	410	2	36	4	0.45	1.71
TR42B	83.37	0.48	8.46	2.20	0.04	0.53	1.38	1.46	2.05	0.03	688	32	37	7	9	5	15	64	4	236	6	48	9	201	2	20	5	0.31	1.90
TR42C	78.22	0.92	10.62	3.99	0.07	0.83	1.55	1.58	2.17	0.05	706	62	64	9	15	16	17	72	10	237	13	91	16	318	2	38	11	1.11	2.43
TR42D	81.25	0.74	9.21	3.17	0.05	0.68	1.40	1.46	2.00	0.04	677	51	49	7	12	11	16	65	nd	225	12	72	13	291	2	31	8	-0.13	1.96
TR43	67.58	0.13	5.32	1.05	0.03	0.99	22.33	1.28	1.24	0.04	405	17	7	nd	nd	0	9	31	43	1658	11	11	6	107	4	6	3	-0.95	1.84
Average KB	69.76	1.43	11.68	6.71	0.10	1.57	4.58	1.84	2.26	0.07	764	147	96	10	40	13	14	62	16	405	33	194	26	1064	4	51	6	1.77	1.51

nd - not detected

Table 4.3.3: Average metal contents in the Trincomalee Bay sediments compared to established pollution guidelines and UCC. COSED: Coastal Ocean Sediment Database (NYSDEC 1999) LEL –Lowest effect level, SEL – Severe effect level; ISQG – Interim Sediment Quality Guideline (SAIC 2002); PEL – Probable effect level (SAIC 2002). Enrichment factor (EF) values were calculated using the lower Mahaweli River data as the background normalizer

Element	As	Pb	Zn	Cu	Ni	Cr
IH	7	23	49	13	16	73
TB	10	14	31	6	11	50
KB	4	14	51	6	13	96
LM	4	21	57	16	26	115
EF values (Lower Mahaweli normalized)						
IH	**2.4**	1.0	1.4	1.1	0.7	0.7
TB	**2.3**	0.3	0.6	0.5	0.4	0.4
KB	0.9	0.3	0.6	0.7	0.7	0.4
Environmental guidelines						
UCC	5	20	71	25	20	35
COSED	13	45	135	42	42	125
LEL	6	31	120	16	16	26
SEL	33	110	270	110	50	110
ISQG	7	30	124	19	na	52
PEL	42	112	271	108	na	160

Table 4.3.4: Statistical Analyses. (A) Correlation matrices for the Inner Harbour, Thambalagam Bay and Koddiyar Bay datasets. Strong positive correlations are indicated in bold; negative correlations in red.

Inner Harbour

	SiO_2	TiO_2	Al_2O_3	Fe_2O_3*	MnO	MgO	CaO	Na_2O	K_2O	P_2O_5	Ba	Ce	Cr	Ga	Nb	Ni	Pb	Rb	Sc	Sr	Th	V	Y	Zr	As	Zn
TiO_2	-0.09																									
Al_2O_3	-0.49	0.45																								
Fe_2O_3*	-0.75	0.44	**0.72**																							
MnO	-0.34	0.53	**0.72**	**0.78**																						
MgO	-0.84	0.07	**0.56**	**0.81**	**0.55**																					
CaO	-0.92	-0.13	0.12	0.49	0.03	**0.69**																				
Na_2O	0.00	-0.14	**0.63**	0.07	0.32	0.11	-0.25																			
K_2O	-0.25	0.30	**0.69**	0.19	0.14	0.05	0.01	**0.61**																		
P_2O_5	-0.76	-0.04	0.11	**0.58**	0.15	**0.66**	**0.78**	-0.17	-0.12																	
Ba	0.18	0.41	0.33	-0.12	-0.16	-0.41	-0.34	0.32	**0.78**	-0.28																
Ce	0.15	0.01	0.12	-0.27	-0.06	-0.33	-0.19	0.39	0.19	-0.22	0.34															
Cr	-0.44	0.07	**0.77**	**0.64**	**0.53**	0.73	0.16	**0.52**	0.25	0.23	-0.06	-0.06														
Ga	0.28	0.55	0.45	0.15	**0.54**	-0.09	-0.53	0.35	0.38	-0.40	0.39	0.14	0.14													
Nb	0.32	0.18	0.30	-0.08	0.12	-0.48	-0.50	**0.52**	**0.56**	-0.32	**0.71**	0.48	-0.09	0.53												
Ni	-0.50	0.02	**0.72**	**0.65**	**0.53**	**0.80**	0.24	0.47	0.19	0.30	-0.19	-0.18	**0.98**	0.07	-0.21											
Pb	-0.60	-0.02	-0.01	0.39	0.05	0.44	**0.66**	-0.15	-0.12	**0.93**	-0.15	0.07	0.02	-0.33	-0.15	0.07										
Rb	0.01	**0.55**	**0.58**	0.09	0.14	-0.01	-0.25	0.46	**0.76**	-0.19	**0.78**	0.22	0.27	0.46	0.34	0.18	-0.13									
Sc	-0.95	-0.05	0.48	**0.74**	0.40	**0.90**	**0.87**	0.04	0.11	**0.69**	-0.40	-0.22	**0.54**	-0.32	-0.42	**0.62**	0.49	-0.16								
Sr	-0.82	-0.09	-0.03	0.36	-0.07	0.53	**0.96**	-0.40	-0.05	**0.67**	-0.34	-0.19	-0.03	-0.54	-0.49	0.06	**0.56**	-0.35	**0.77**							
Th	-0.35	0.06	0.26	-0.03	-0.05	-0.01	0.34	0.29	0.40	0.09	0.28	**0.65**	0.02	-0.25	0.17	-0.04	0.20	0.23	0.23	0.37						
V	-0.08	**0.60**	**0.73**	**0.54**	**0.72**	0.10	-0.26	0.44	0.41	-0.07	0.42	0.40	0.42	**0.62**	**0.65**	0.31	-0.02	0.40	0.03	-0.33	0.19					
Y	-0.57	0.04	0.04	0.47	0.20	0.47	**0.60**	-0.11	-0.16	**0.92**	-0.22	0.02	0.06	-0.24	-0.13	0.12	**0.98**	-0.15	0.48	0.48	0.12	0.07				
Zr	0.19	-0.01	0.08	-0.31	-0.10	-0.36	-0.22	0.37	0.17	-0.24	0.35	**1.00**	-0.07	0.13	0.48	-0.19	0.05	0.21	-0.25	-0.22	**0.63**	0.38	-0.01			
As	-0.75	-0.06	0.21	0.49	0.08	0.51	**0.74**	0.02	0.13	**0.88**	0.00	0.17	0.18	-0.32	0.00	0.19	**0.93**	-0.05	**0.63**	**0.62**	0.34	0.12	**0.88**	0.14		
Zn	-0.68	0.07	0.27	**0.70**	0.40	**0.73**	**0.62**	-0.04	-0.18	**0.93**	-0.35	-0.14	0.44	-0.20	-0.26	0.50	**0.85**	-0.18	**0.67**	0.47	0.00	0.18	**0.90**	-0.16	**0.80**	
Cu	-0.64	-0.07	0.39	**0.65**	0.34	**0.81**	0.53	0.17	-0.08	**0.80**	-0.33	-0.19	**0.71**	-0.23	-0.33	**0.77**	**0.65**	-0.04	**0.69**	0.33	-0.03	0.11	**0.68**	-0.20	**0.65**	**0.90**

Thambalagam Bay

	SiO_2	TiO_2	Al_2O_3	Fe_2O_3*	MnO	MgO	CaO	Na_2O	K_2O	P_2O_5	Ba	Ce	Cr	Ga	Nb	Ni	Pb	Rb	Sc	Sr	Th	V	Y	Zr	As	Zn
TiO_2	-0.43																									
Al_2O_3	-0.53	0.14																								
Fe_2O_3*	-0.86	**0.57**	0.20																							
MnO	-0.87	**0.67**	0.21	**0.95**																						
MgO	-0.87	0.47	0.30	**0.78**	**0.78**																					
CaO	-0.76	0.10	0.01	**0.62**	**0.67**	**0.78**																				
Na_2O	-0.41	-0.07	**0.74**	0.01	0.08	0.24	0.21																			
K_2O	-0.33	0.02	**0.63**	0.06	-0.04	0.22	0.01	0.42																		
P_2O_5	-0.89	0.38	0.21	**0.92**	**0.89**	**0.80**	**0.75**	0.19	0.08																	
Ba	-0.34	-0.04	**0.74**	0.03	0.02	0.03	-0.04	**0.69**	**0.65**	0.11																
Ce	-0.29	**0.59**	-0.04	**0.59**	**0.57**	0.20	0.05	-0.40	-0.17	0.25	-0.18															
Cr	-0.57	0.62	0.27	**0.76**	**0.72**	0.48	0.20	-0.13	0.01	0.48	-0.04	**0.90**														
Ga	-0.25	-0.05	**0.79**	-0.09	-0.10	0.03	-0.10	**0.56**	**0.53**	-0.14	**0.57**	-0.03	0.12													
Nb	-0.31	**0.72**	0.01	**0.58**	**0.59**	0.25	0.03	-0.35	-0.18	0.24	-0.15	**0.97**	**0.89**	-0.01												
Ni	-0.72	0.36	**0.75**	**0.61**	**0.58**	**0.57**	0.26	0.43	0.30	**0.53**	0.22	0.33	**0.66**	0.55	0.35											
Pb	0.02	-0.48	0.40	-0.43	-0.43	-0.08	0.01	**0.52**	0.46	-0.26	**0.69**	-0.57	-0.48	0.48	-0.54	-0.17										
Rb	0.06	-0.51	**0.65**	-0.36	-0.49	-0.16	-0.32	0.47	**0.60**	-0.29	**0.55**	-0.45	-0.24	**0.70**	-0.47	0.27	**0.66**									
Sc	-0.92	0.46	0.29	**0.85**	**0.89**	**0.90**	0.84	0.24	0.05	**0.84**	0.04	0.38	**0.59**	0.11	0.40	**0.63**	-0.17	-0.28								
Sr	-0.51	-0.02	0.31	0.18	0.30	0.38	**0.60**	**0.67**	0.22	0.45	**0.56**	-0.44	-0.29	0.09	-0.38	0.03	**0.51**	-0.01	0.41							
Th	-0.15	**0.53**	-0.13	0.47	0.45	0.08	-0.05	-0.47	-0.22	0.12	-0.23	**0.99**	**0.84**	-0.08	**0.96**	0.22	-0.56	-0.45	0.26	-0.51						
V	-0.51	**0.75**	0.09	**0.76**	**0.77**	0.43	0.21	-0.23	-0.15	0.47	-0.11	**0.95**	**0.94**	-0.03	**0.97**	0.48	-0.57	-0.50	**0.58**	-0.23	**0.90**					
Y	-0.85	**0.57**	0.27	**0.97**	**0.92**	**0.76**	**0.57**	-0.03	0.07	**0.83**	0.00	**0.69**	**0.86**	0.05	**0.67**	**0.70**	-0.42	-0.28	**0.85**	0.04	**0.58**	**0.82**				
Zr	-0.16	**0.58**	-0.08	0.47	0.46	0.08	-0.07	-0.42	-0.21	0.11	-0.20	**0.99**	**0.84**	-0.03	**0.97**	0.25	-0.55	-0.45	0.26	-0.49	**0.99**	**0.91**	**0.57**			
As	-0.77	0.13	-0.04	**0.79**	**0.74**	**0.80**	**0.90**	0.02	-0.02	**0.88**	-0.12	0.16	0.32	-0.21	0.10	0.32	-0.18	-0.30	**0.83**	0.39	0.05	0.31	**0.72**	0.01		
Zn	-0.75	**0.60**	**0.72**	**0.70**	**0.70**	**0.59**	0.23	0.36	0.29	**0.56**	0.31	0.50	**0.78**	0.45	**0.56**	**0.92**	-0.20	0.08	**0.63**	0.08	0.39	**0.67**	**0.76**	0.44	0.28	
Cu	-0.57	0.41	**0.79**	0.42	0.43	0.39	0.06	**0.54**	0.29	0.37	0.35	0.23	**0.53**	**0.58**	0.28	**0.90**	-0.06	0.28	0.43	0.11	0.13	0.38	0.47	0.19	0.05	**0.89**

Koddiyar Bay

	SiO_2	TiO_2	Al_2O_3	Fe_2O_3*	MnO	MgO	CaO	Na_2O	K_2O	P_2O_5	Ba	Ce	Cr	Ga	Nb	Ni	Pb	Rb	Sc	Sr	Th	V	Y	Zr	As	Zn
TiO_2	-0.81																									
Al_2O_3	-0.58	0.52																								
Fe_2O_3*	-0.86	**0.92**	0.41																							
MnO	-0.84	**0.90**	0.37	**0.99**																						
MgO	-0.90	**0.86**	0.43	**0.97**	**0.96**																					
CaO	-0.33	-0.17	-0.15	-0.10	-0.11	0.03																				
Na_2O	-0.10	0.04	**0.69**	-0.14	-0.20	-0.14	-0.02																			
K_2O	0.15	-0.19	**0.58**	-0.36	-0.40	-0.32	-0.16	**0.66**																		
P_2O_5	-0.90	**0.77**	**0.79**	0.73	**0.70**	**0.77**	0.16	0.35	0.12																	
Ba	0.19	-0.24	**0.60**	-0.40	-0.46	-0.40	-0.20	**0.76**	**0.91**	0.12																
Ce	-0.86	**0.93**	**0.54**	**0.95**	**0.94**	**0.91**	-0.10	0.01	-0.26	**0.84**	-0.25															
Cr	-0.83	**0.94**	0.49	**0.98**	0.98	0.94	-0.19	-0.06	-0.29	**0.77**	-0.31	**0.97**														
Ga	0.10	-0.07	0.51	-0.20	-0.21	-0.17	-0.26	0.45	0.47	0.20	**0.63**	-0.02	-0.08													
Nb	-0.80	**0.91**	0.32	**0.99**	**0.99**	**0.94**	-0.14	-0.23	-0.42	**0.65**	-0.46	**0.93**	**0.97**	-0.26												
Ni	-0.69	**0.66**	**0.88**	0.55	0.50	**0.59**	-0.04	0.52	0.34	**0.85**	0.32	**0.60**	**0.59**	0.32	0.45											
Pb	**0.70**	-0.62	0.03	-0.80	-0.81	-0.78	-0.22	0.39	**0.75**	-0.46	**0.71**	-0.75	-0.75	0.43	-0.82	-0.13										
Rb	0.51	-0.48	0.31	-0.65	-0.68	-0.66	-0.24	**0.60**	**0.82**	-0.27	**0.86**	-0.58	-0.61	0.48	-0.69	0.10	**0.90**									
Sc	-0.67	0.26	0.04	0.37	0.38	0.46	**0.84**	-0.05	-0.36	0.47	-0.40	0.38	0.31	-0.29	0.34	0.14	-0.60	-0.58								
Sr	-0.10	-0.38	-0.29	-0.32	-0.32	-0.19	**0.97**	-0.04	-0.12	-0.06	-0.14	-0.30	-0.40	-0.23	-0.33	-0.24	-0.06	-0.11	**0.72**							
Th	-0.87	**0.93**	0.43	**0.98**	**0.97**	**0.94**	-0.06	-0.10	-0.34	**0.76**	-0.38	**0.97**	**0.97**	-0.23	**0.97**	0.53	-0.81	-0.65	0.41	-0.27						
V	-0.83	**0.92**	0.37	**1.00**	**0.99**	**0.95**	-0.13	-0.19	-0.39	**0.69**	-0.43	**0.95**	**0.98**	-0.21	**1.00**	0.49	-0.81	-0.68	0.35	-0.33	**0.98**					
Y	-0.87	**0.90**	0.53	**0.97**	**0.97**	**0.95**	-0.11	-0.05	-0.27	**0.81**	-0.31	**0.97**	**0.98**	-0.04	**0.94**	**0.61**	-0.75	-0.60	0.38	-0.33	**0.96**	**0.96**				
Zr	-0.85	**0.93**	0.44	**0.98**	**0.97**	**0.93**	-0.11	-0.10	-0.34	**0.76**	-0.35	**0.99**	**0.98**	-0.13	**0.97**	**0.53**	-0.80	-0.65	0.37	-0.31	**0.99**	**0.98**	**0.97**			
As	-0.59	0.20	**0.68**	0.19	0.13	0.27	0.46	**0.58**	0.38	**0.70**	0.49	0.33	0.20	0.28	0.10	**0.60**	-0.12	0.15	0.45	0.36	0.24	0.14	0.26	0.23		
Zn	-0.90	**0.92**	**0.58**	**0.98**	**0.96**	**0.97**	-0.09	-0.02	-0.20	**0.83**	-0.25	**0.95**	**0.97**	-0.07	**0.94**	**0.69**	-0.71	-0.53	0.35	-0.32	**0.95**	**0.96**	**0.98**	**0.95**	0.33	
Cu	-0.10	-0.01	0.30	-0.09	-0.15	0.02	0.17	0.38	0.31	0.24	0.32	-0.13	-0.11	0.18	-0.16	**0.58**	0.29	0.34	-0.07	0.09	-0.16	-0.15	-0.13	-0.18	0.39	0.04

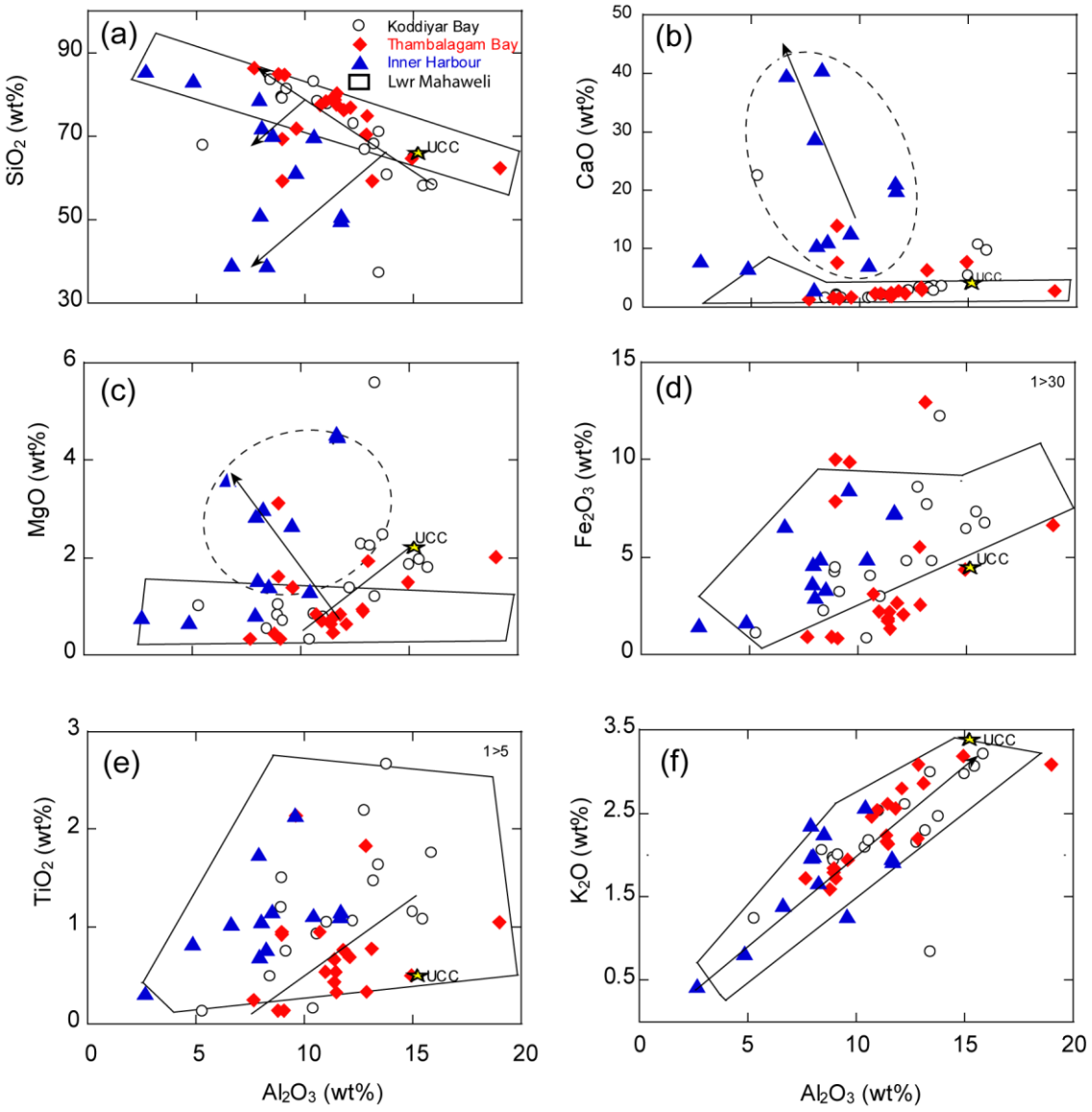

Fig 4.3.6: Selected major oxide–Al_2O_3 variation diagrams for Inner Harbour (IH), Thambalagam Bay (TB) and Koddiyar Bay (KB) surface sediments, compared to UCC (star), and fields for lower Mahaweli River sediments

4. 3.1.3 Trace elements

Of the 17 trace elements analyzed, eight (Ba, Ce, Cr, Sc, Sr, Th, V, and Zr) have higher average abundances in all three sectors of Trincomalee Bay than in UCC (Table 4.3.1). The most marked enrichment is seen for Zr, with average values of 1089, 460, and 1064 ppm in the Inner Harbour,

Koddiyar and Thambalagam, respectively, well above the 190 ppm in UCC. Maximum values of Zr are very high (8123, 3914, and 5247 ppm, respectively), as are maximums for Ce (792, 654, and 572 ppm, respectively) and Th (49, 222, and 156 ppm, respectively) (Table 1). Strontium is most enriched in the Inner Harbour (average 936 ppm; range 319–2266 ppm), where CaO is also most abundant. The remaining trace elements are present at levels similar to or less than in UCC or average lower Mahaweli River sediment (Table 4.3.1).

Representative trace element–Al_2O_3 variation diagrams show that the mobile elements Ba and Rb show moderate positive correlations with Al_2O_3 (Fig. 4.3.7a, b), as does Pb (Fig. 4.3.7c). The correlations of Ba and Rb with Al_2O_3 are 0.33 and 0.58, 0.60 and 0.31, and 0.74 and 0.65 in the Inner Harbour, Thambalagam Bay and Koddiyar Bay, respectively. Strontium shows poor correlations with Al_2O_3 (Table 4.3.4a, b, c), with relatively low values (<500 ppm) in both Koddiyar and Thambalagam bays, but scatter to higher values in the Inner Harbour (Fig. 4.3.7d), comparable to the pattern shown for CaO (Fig. 4.3.6b). These groupings suggest Sr may be associated with carbonate, Pb and Ba with plagioclase, and Rb and Ba with K-feldspar and clays. The ferromagnesian trace elements Cr (Fig. 4.3.7e), Ni, V and Sc show weak correlations with Al_2O_3, with abundances generally intermediate between UCC and the distribution of lower Mahaweli River sediments. The high field strength (HFSE) elements Th, Ce, Zr (Fig. 4.3.7f–h), Nb, and Y also show very poor correlations and scatter to very high values, especially in the Inner Harbour. The poor correlations seen in these latter two groups of elements with Al_2O_3 suggest that their abundances in individual samples are not controlled by sorting of common silicate minerals or carbonate dilution.

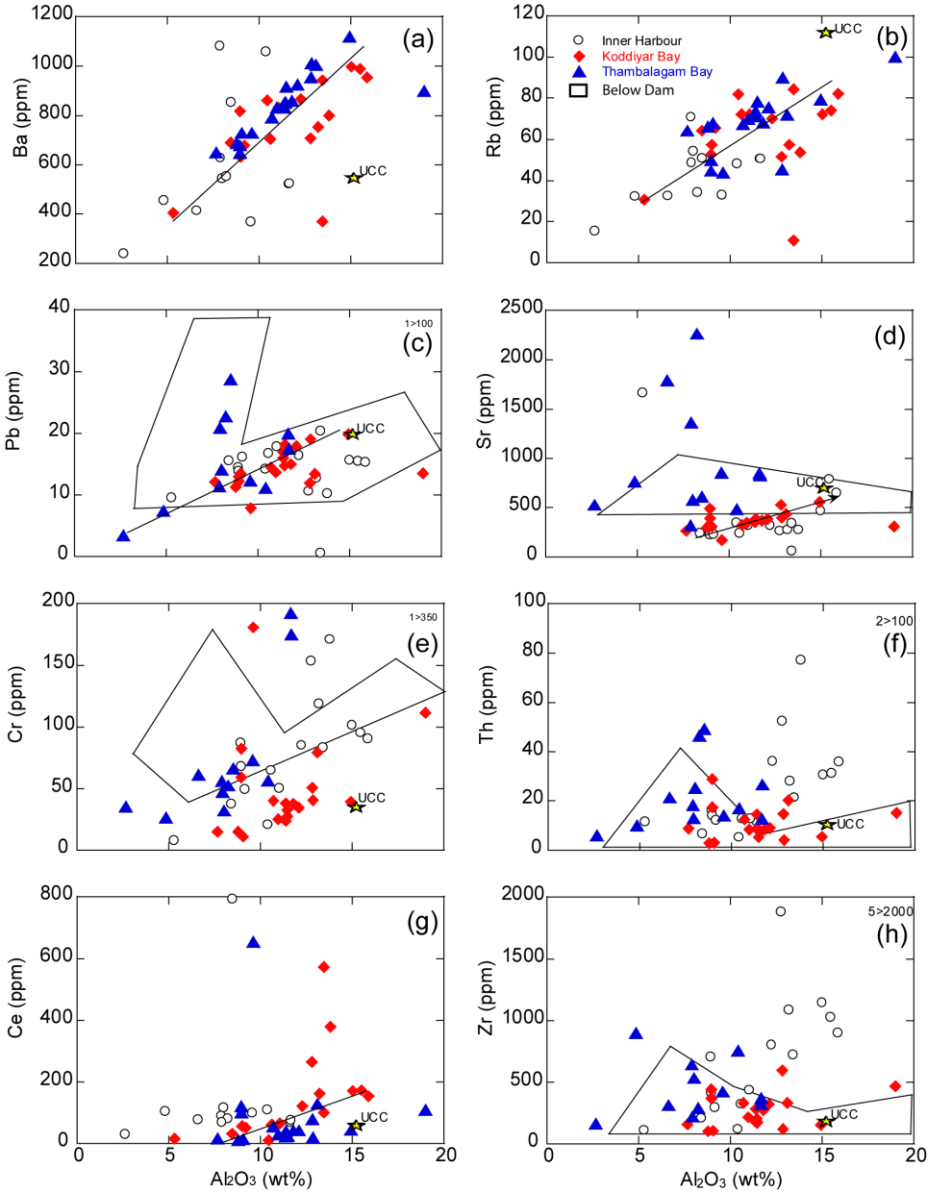

Fig 4.3.7: Selected trace element–Al_2O_3 variation diagrams for Inner Harbour (IH), Thambalagam Bay (TB) and Koddiyar Bay (KB) surface sediments, compared to UCC (star), and fields for lower Mahaweli River sediments

The p-values for Ce and Th for Inner Harbour - Thambalagam Bay are very high (0.796, 0.977, respectively, Table 4.3.1) and the null hypothesis is not rejected. The t-values of Inner Harbour - Thambalagam bay for Rb, Sc and Sr are also very high, indicating that the means for these elements in these two sectors differ significantly.

4. 3.1.4 Principal Component Analysis

The PCA analysis of the three sectors is given in Table 4.3.5 PCA has been widely used in environmental studies where the data sets are large and spatially diverse, which makes the determination of spatial characteristics difficult (Reid and Spencer 2009: Woods et al. 2012). The first two principal components account for 79%, 71% and 62% of the total variance in the Koddiyar, Thambalagam, and Inner Harbour datasets, respectively. F1 shows the greatest variability (57%, 44%, 37%, respectively), whereas F2 is relatively uniform (26%, 25%, and 22%). These loadings and differing distributions of the elements on the PCA plots, as outlined in Table 4.3.5a, b, c, suggest that significant compositional contrasts exist between the three sectors. All three statistical methods (p-value, t-values and PCA) thus show that the three sectors differ in composition.

Principal component plots and loadings of individual elements in the three sectors are given on the following pages. The plots show clear contrast between the sectors.

(a) Inner Harbour

Scattering of the elements within the three sectors is greatest in the Inner Harbour dataset, with a high positive loading on F1 for SiO_2. Most other elements are scattered, with negative F1 loadings and positive F2. A number of elements (CaO, P_2O_5, Pb, Y, Sr) cluster together with negative loadings for both F1 and F2, suggesting association with carbonates in the Inner Harbour. A broad grouping of elements with positive F2 scores (Al_2O_3, Na_2O, K_2O, TiO_2, Rb, Ga, Ba) implies association with both feldspars and clays, while a cluster of Fe_2O_3, Cr, Ni and MgO at negative F1 suggests influence of ferromagnesian and Fe-oxide minerals.

(b) Thambalagam Bay

Elements show a differing distribution to those in the Inner Harbour, with negative loading for both F1 and F2 for SiO_2 (quartz), whereas another group (Al_2O_3, Na_2O, K_2O, Ba, Ga, Rb, Pb, Sr) are characterized by positive F2 loading, suggesting association with both plagioclase and K-feldspar. The remaining elements have high F1 loadings, with both positive and negative F2. These groups suggest greater influence of clays and heavy minerals in this sector.

(c) Koddiyar Bay

Distribution are different again, with negative loading for both F1 and F2 for SiO_2 as in Thambalagam Bay, and positive F2 and negative F1 loadings for Na_2O, K_2O, Ba, Ga, Rb, Pb), again suggesting association with feldspars. Another group of elements (Fe_2O_3, TiO_2, MnO, MgO, Ce, Cr, Nb, Th, V, Y, Zr) show strong association, all with high F1 scores. This grouping of elements is consistent with stronger influence in this sector of Trincomalee Bay from ferromagnesian phases, Fe-Ti oxide minerals, and heavy minerals, including zircon.

Table 4.3.5: Principal Component Analysis. PCA plots for all data analyzed and factor 1 and 2 loadings for (a) Inner Harbour (b) Thambalagam Bay (c) Koddiyar Bay.

(a) Inner Harbour

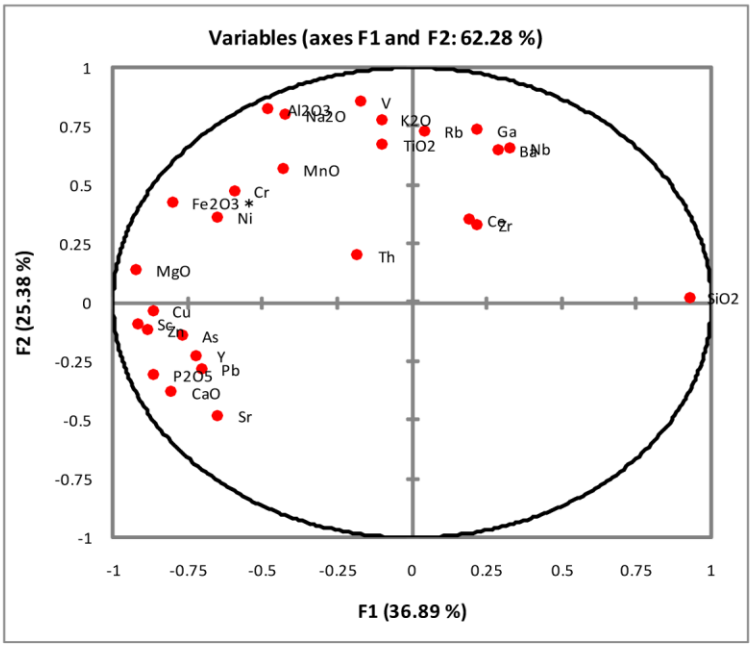

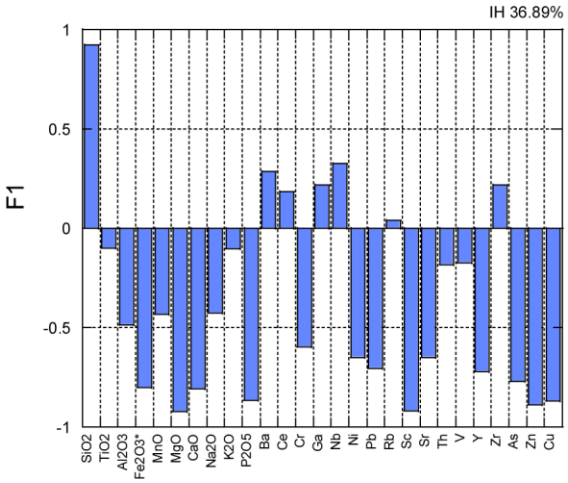

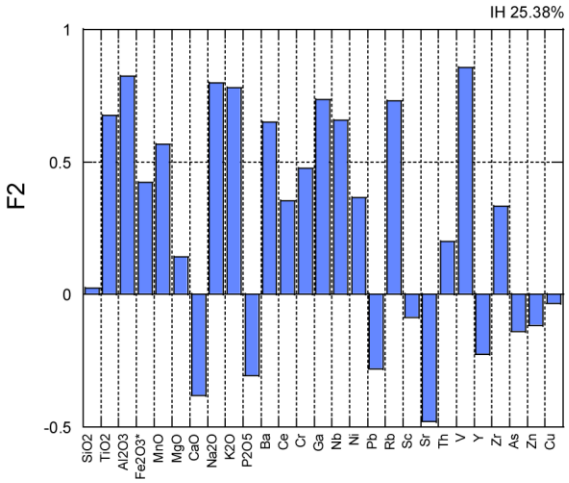

(b) Thambalagam Bay

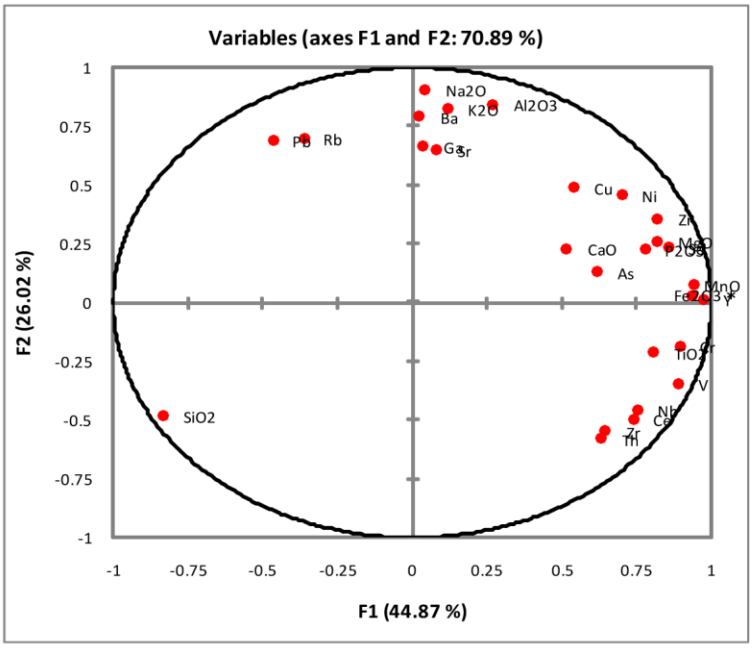

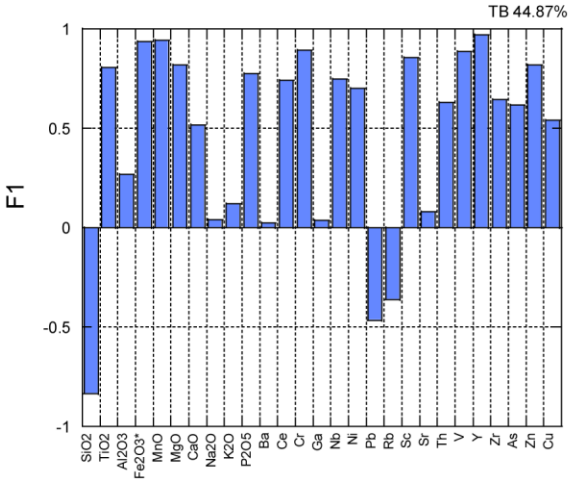

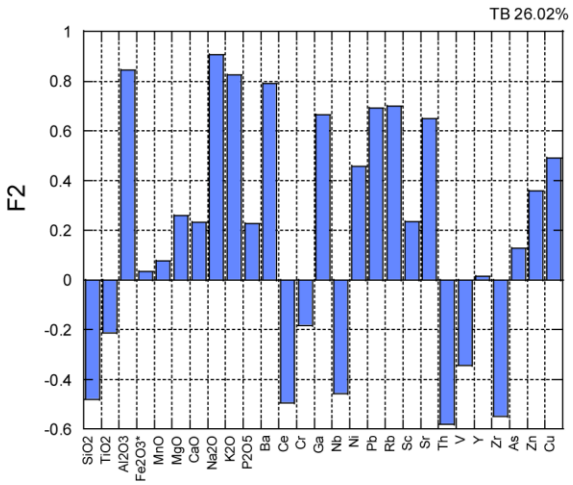

(c) Koddiyar Bay

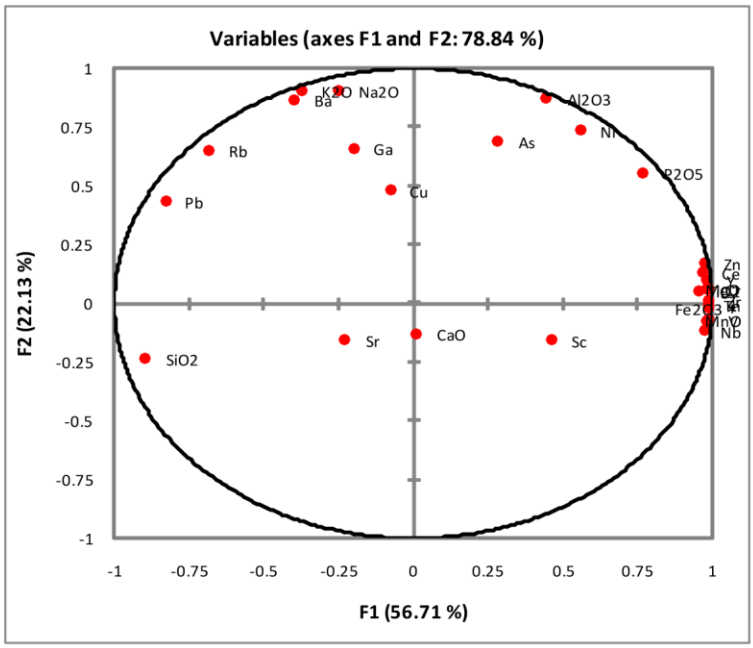

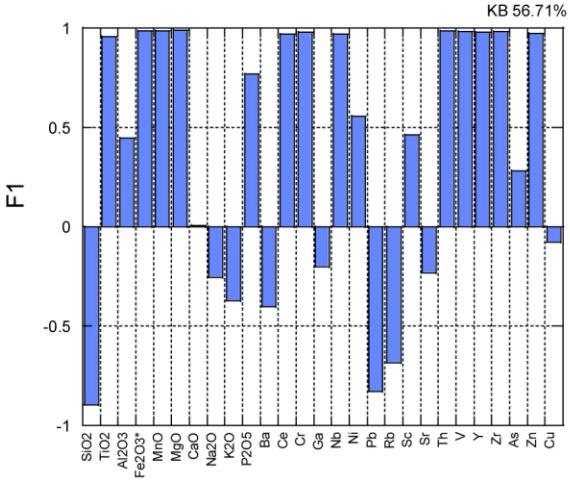

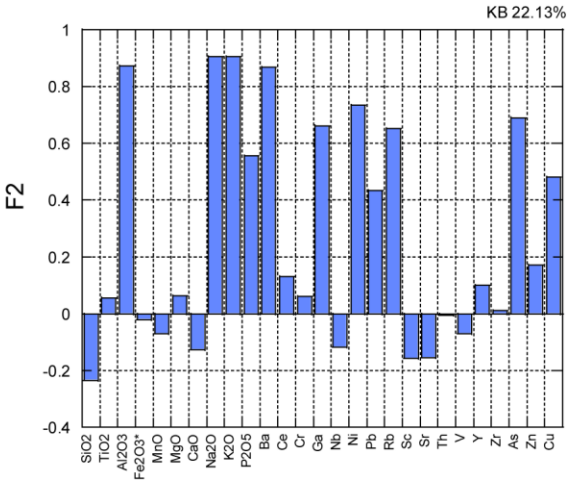

4.3.2 Core sediments

Individual analyses of grain size and geochemical compositions of core C1 are given in Table 4.3.6, data for C2, C3 and C4 are listed in Table 4.3.7. Mean grain size with TS (Total Sulfur) for all four cores is illustrated in Fig 3.2.3. The elemental variation of core 1 is given in Fig 4.3.8 and Core 2, 3 and 4 in Fig 4.3.9. The dotted lines in Fig 3.2.3, 4.3.8 and 4.3.9 of each

core indicate the change of pattern in elemental concentrations. These may indicate an event in the sediment deposition.

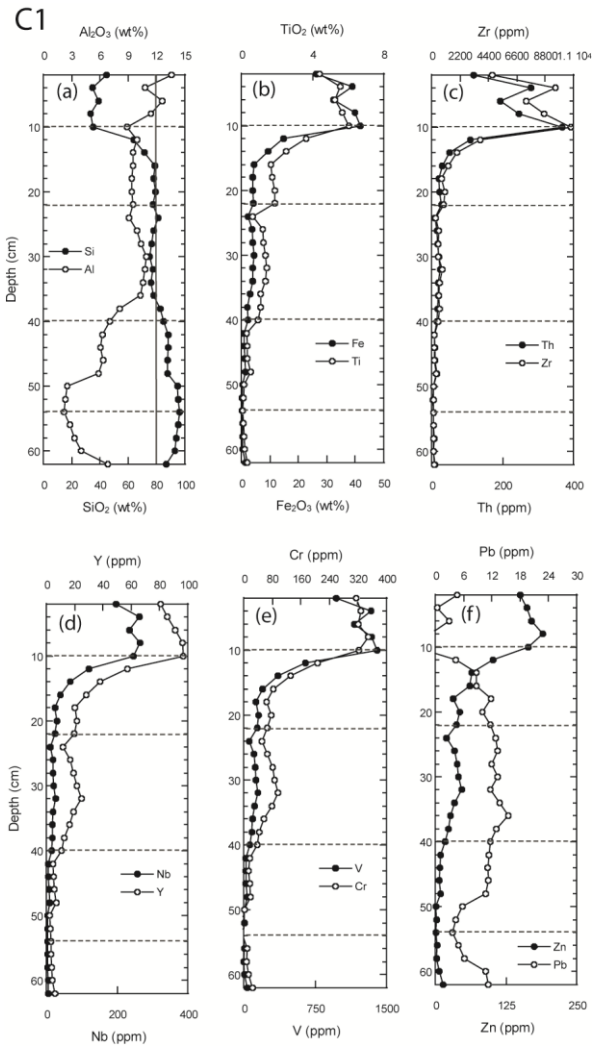

Fig. 4.3.8: Selected elemental variation of core one from Trincomalee bay

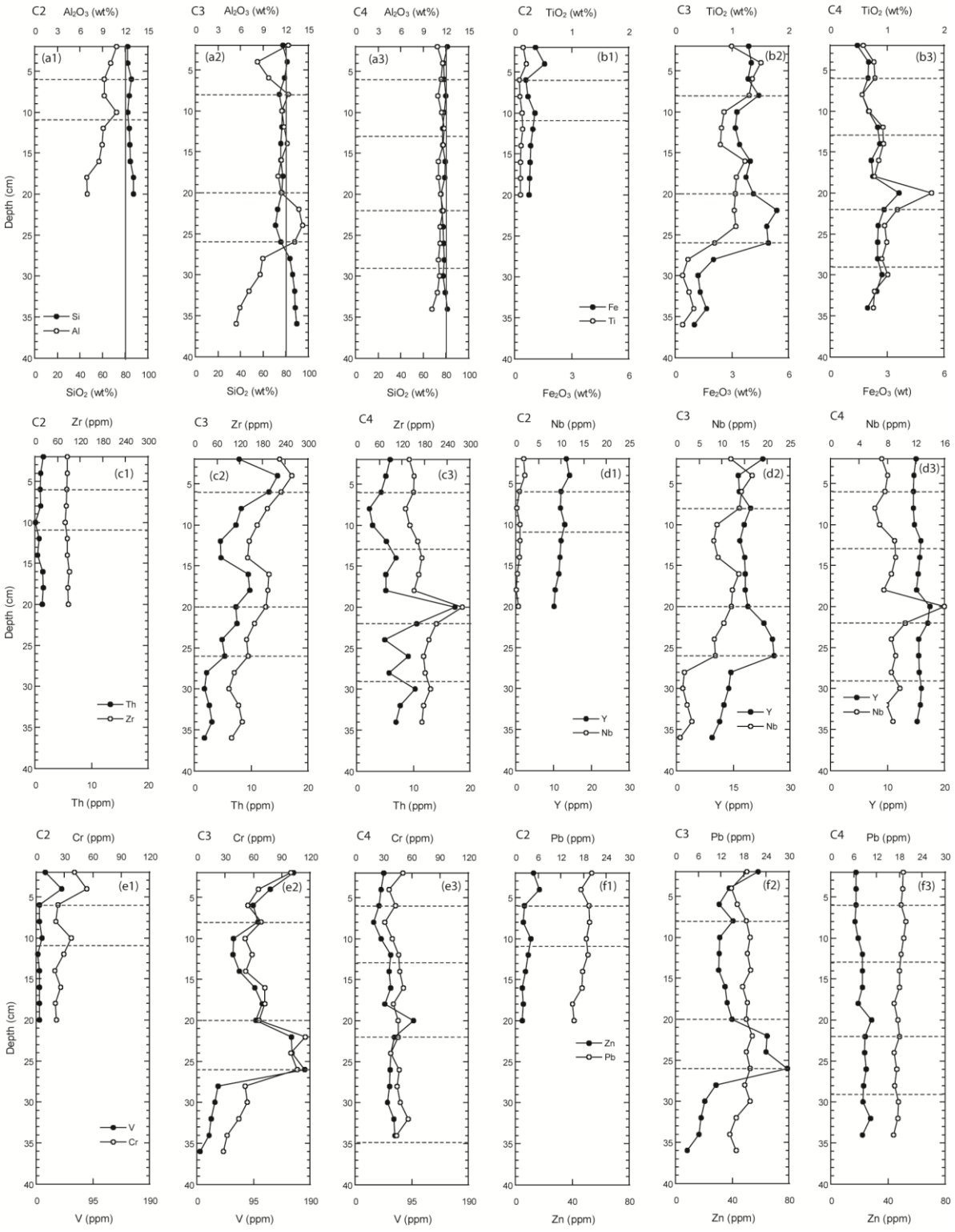

Fig. 4.3.9: Selected elemental variation of core two, three and four of the Trincomalee bay

4. 3.2.1 Texture

Mean grain size (MGS, MΦ) of C1, ranges from -1.31 and 4.20 ϕ equivalent to granule sand to coarse silt. In this core, seven samples below 50mm contained 88, 89, 69, 84, 54, 58 and 59 percent of grains larger than -1.0 ϕ (2mm) are here not included in Table 1. Mean grain size of C2 ranges from 0.24 to 2.41 ϕ, equivalent to coarse sand to fine sand. The C3 MΦ ranges between -0.65 and 2.58 ϕ, corresponding to very coarse sand to fine sand, C4 MΦ ranges between 0.75 to 2.05 ϕ and equivalent to coarse sand to fine sand. The sorting of the C1 varies greatly from top to bottom, as shown in Table 4.3.7. The top four samples (1C1 – 1C4) are moderately sorted (0.64 – 0.84). Samples 1C25 – 1C31 are extremely poorly sorted. Sorting in the rest of the core sorting ranges from 1.82 – 3.13 values indicates of very poor sort. Sorting for C2 ranges from 1.20 – 2.12 representing poorly sorted. C3 sorting ranges between 0.29 – 2.89, except for one sample that is well sorted (0.29), the rest are poorly to very poorly sorted (2.15-2.89). C4 sorting ranges from 1.92 – 2.78, and all samples are poorly to very poorly sorted.

Table. 4.3.6: Individual XRF analyses and texture of core one (C1) sediments from Trincomalee Bay, Sri Lanka

S-No	1C1	1C2	1C3	1C4	1C5	1C6	1C7	1C8	1C9	1C10	1C11	1C12	1C13	1C14	1C15	1C16	1C17	1C18	1C19	1C20	1C21	1C22	1C23	1C24	1C25	1C26	1C27	1C28	1C29	1C30	1C31	UCC
Depth (cm)	2	4	6	8	10	12	14	16	18	20	22	24	26	28	30	32	34	36	38	40	42	44	46	48	50	52	54	56	58	60	62	
Major Oxide (wt%)																																
SiO_2	44.42	34.84	39.10	33.28	35.06	64.07	71.45	79.13	78.02	79.17	77.54	81.40	77.91	76.75	74.94	77.61	76.30	78.20	82.50	84.87	88.33	88.44	87.78	88.02	95.04	95.60	96.14	95.17	93.89	92.91	86.90	66.00
TiO_2	4.41	5.56	5.26	5.67	6.03	3.65	2.51	1.66	1.72	1.87	1.86	0.65	1.22	1.24	1.35	1.42	1.34	1.11	1.11	0.94	0.31	0.34	0.34	0.52	0.14	0.11	0.09	0.12	0.14	0.17	0.35	0.50
Al_2O_3	13.58	10.78	12.61	11.40	8.88	9.94	9.49	9.51	9.39	9.36	9.50	9.10	9.91	10.36	10.95	10.76	10.59	10.27	8.09	7.06	6.26	6.04	6.38	5.88	2.57	2.32	2.22	2.79	3.29	4.02	6.82	15.20
Fe_2O_3	26.36	39.08	32.41	39.83	41.88	14.84	9.45	4.55	4.09	3.89	4.19	2.37	3.72	4.06	4.48	3.95	4.07	3.14	2.07	2.26	0.98	1.02	1.10	1.44	0.41	0.35	0.25	0.38	0.50	0.58	1.37	4.50
MnO	0.39	0.49	0.46	0.52	0.51	0.23	0.15	0.08	0.06	0.07	0.07	0.04	0.06	0.07	0.08	0.07	0.07	0.05	0.05	0.04	0.02	0.02	0.02	0.02	0.01	0.01	0.01	0.01	0.01	0.01	0.02	0.07
MgO	4.57	3.95	4.67	4.66	3.65	2.47	1.79	1.14	0.98	0.98	1.02	0.77	1.16	1.39	1.56	1.37	1.32	0.93	0.69	0.57	0.28	0.30	0.32	0.39	0.12	0.10	0.09	0.13	0.16	0.20	0.41	2.20
CaO	3.45	2.71	3.17	2.87	2.17	2.24	2.13	1.45	1.94	1.62	1.99	1.82	2.22	2.41	2.69	1.96	2.41	2.12	1.55	1.31	0.95	0.97	1.05	1.04	0.34	0.28	0.24	0.29	0.45	0.52	1.15	4.20
Na_2O	1.33	1.21	1.09	0.86	0.86	1.19	1.34	1.25	1.69	1.45	1.70	1.70	1.69	1.70	1.77	1.44	1.77	1.87	1.47	1.32	1.27	1.25	1.31	1.20	0.59	0.59	0.51	0.57	0.72	0.79	1.35	3.90
K_2O	1.36	1.16	1.07	0.72	0.75	1.29	1.62	1.19	2.04	1.56	2.06	2.10	2.05	1.97	2.11	1.37	2.09	2.27	1.80	1.62	1.58	1.60	1.67	1.46	0.76	0.62	0.45	0.52	0.82	0.78	1.60	3.40
P_2O_5	0.15	0.21	0.17	0.18	0.20	0.08	0.07	0.04	0.06	0.05	0.07	0.04	0.06	0.06	0.06	0.05	0.06	0.05	0.04	0.03	0.02	0.02	0.03	0.03	0.01	0.01	0.01	0.01	0.01	0.01	0.04	0.16
Trace Elements (ppm)																																
Ba	490	489	451	421	398	479	545	527	644	559	632	689	651	641	665	567	672	726	599	528	538	538	554	483	259	233	210	261	301	311	563	550
Ce	504	1201	820	990	1434	480	260	157	109	134	134	42	82	83	86	112	91	87	83	76	27	31	32	60	19	10	19	19	22	24	27	64
Cr	316	329	320	350	324	206	132	82	63	78	65	50	65	82	86	96	79	57	44	38	18	13	17	19	2	nd	-3	10	7	13	24	35
Ga	6	1	4	nd	nd	10	7	7	7	7	6	5	6	6	7	7	6	5	3	3	0	0	0	nd	nd	nd	nd	nd	nd	nd	1	17
Nb	198	262	236	266	246	121	68	39	25	31	25	11	18	19	21	26	20	17	17	15	7	6	7	9	4	4	4	4	5	5	6	25
Ni	20	16	18	17	15	15	11	11	6	9	7	5	9	11	12	13	10	6	4	3	1	1	2	1	nd	0	1	1	1	3	4	20
Pb	5	0	3	nd	nd	4	9	9	12	10	12	13	13	12	13	12	14	15	13	12	11	11	11	11	6	4	4	5	6	11	11	20
Rb	19	4	9	1	nd	26	40	48	58	54	57	62	58	56	57	53	58	63	54	49	52	50	52	46	27	25	22	27	33	36	51	112
Sc	24	20	24	25	18	17	15	12	9	9	11	8	10	13	13	15	13	11	7	6	4	4	4	4	2	3	1	3	5	2	3	11
Sr	112	75	80	50	45	136	181	197	251	230	253	266	257	257	264	235	264	279	222	199	206	189	202	179	84	72	72	86	107	126	196	350
Th	119	281	194	246	368	108	51	31	21	22	27	10	16	18	20	24	20	19	17	15	8	9	9	15	6	3	5	6	7	6	9	11
V	975	1337	1165	1342	1400	645	358	194	126	154	141	59	105	118	128	149	113	93	86	64	22	19	21	33	6	5	-6	9	0	7	33	60
Y	81	86	91	96	97	57	38	28	20	22	20	12	17	19	22	25	19	16	13	11	5	5	5	7	2	3	3	3	4	4	6	22
Zr	4707	9609	7349	8746	10778	3792	1966	1310	792	1060	933	307	550	538	543	843	613	585	602	541	223	228	230	358	139	145	137	160	153	174	200	
As	4	6	5	7	7	4	3	3	4	4	4	4	3	4	3	3	3	3	2	2	3	3	2	3	1	2	0	2	1	2	3	5
Zn	151	162	170	190	164	102	65	61	31	43	38	20	34	38	41	47	34	27	23	18	10	8	8	9	2	3	1	4	3	7	14	71
Cu	4	3	3	4	3	2	2	3	2	2	2	3	3	2	3	1	2	2	1	2	1	3	2	1	1	0	1	3	2	1	2	25
TS	800	853	750	624	606	606	451	791	583	611	605	537	542	551	533	626	587	567	481	451	456	492	489	481	389	426	445	459	433	496	504	
F	35	58	69	nd	nd	nd	163	nd	36	89	101	101	334	128	24	89	127	nd	76	62	302	115	89	145	62	75	116	116	75	102	75	557
Br	5	4	4	3	3	4	5	7	8	7	8	8	7	7	7	7	7	7	6	6	7	8	7	7	6	6	5	6	6	7	8	2
I	nd	nd	nd	nd	nd	nd	nd	4	13	10	14	14	20	13	14	7	15	20	23	24	31	25	22	26	33	32	32	35	28	30	25	1
Cl	5828		5328	4631	4999	4125	1193	7323	3695	3971	4265	4265	2904	3913	2959	5088	3864	3883	1685	1041	1198	1636	1986	1774	265	669	986	1015	877	1557	1776	370
Mean GS (ϕ)	2	2	2	2	4	0	-1	0	-1	0	0	0	1	1	0	-1	1	1	1	1	0	-1	0	-1	-1	0	0	-1	0	1	1	
Sorting	1	1	1	1	3	2	2	2	2	2	2	2	2	2	2	3	2	2	2	2	2	2	2	2	2	3	2	2	2	2	2	
LOI	-1	-1	-1	-1	-2	0	0	0	1	0	1	1	1	1	0	0	1	1	0	0	1	1	1	1	0	0	1	1	1	1	1	
SiO_2/Al_2O_3	3	3	3	3	4	6	8	8	8	8	8	9	8	7	7	7	7	8	10	12	14	15	14	15	37	41	43	34	29	23	13	4

Table. 4.3.7: Individual XRF analyses and texture of core two (C2), three (C3) and four (C4) sediments from Trincomalee Bay, Sri Lanka

	Core Two										Core Three																Core Four															
S-No	**2C1**	**2C2**	**2C3**	**2C4**	**2C5**	**2C6**	**2C7**	**2C8**	**2C9**	**2C10**	**3C1**	**3C2**	**3C3**	**3C4**	**3C5**	**3C6**	**3C7**	**3C8**	**3C9**	**3C10**	**3C11**	**3C12**	**3C13**	**3C14**	**3C15**	**3C16**	**3C17**	**3C18**	**4C1**	**4C2**	**4C3**	**4C4**	**4C5**	**4C6**	**4C7**	**4C8**	**4C9**	**4C10**	**4C11**	**4C12**	**4C13**	**4C14**	**4C15**	**4C16**	**4C17**
Depth (cm)	2	4	6	8	10	12	14	16	18	20	2	4	6	8	10	12	14	16	18	20	22	24	26	28	30	32	34	36	2	4	6	8	10	12	14	16	18	20	22	24	26	28	30	32	34
Major Oxides (wt%)																																													
SiO_2	82.19	82.24	85.48	83.77	82.37	83.80	83.91	84.41	87.33	87.22	77.59	81.29	78.73	74.07	77.02	76.60	75.65	75.85	77.44	76.56	72.83	70.95	75.59	83.79	85.98	87.60	88.44	89.92	81.20	77.96	78.29	79.93	78.32	77.02	77.15	79.24	78.90	75.79	76.56	77.73	77.78	78.30	77.53	79.19	81.29
TiO_2	0.15	0.21	0.09	0.09	0.14	0.14	0.12	0.10	0.10	0.10	1.00	1.52	1.36	1.31	0.87	0.81	0.80	1.23	1.08	1.06	1.05	1.07	0.69	0.23	0.14	0.24	0.33	0.13	0.58	0.77	0.79	0.57	0.68	0.93	0.94	0.85	0.78	1.79	1.19	0.96	1.00	0.91	1.01	0.78	0.76
Al_2O_3	10.86	10.09	9.24	9.26	10.87	9.09	8.97	8.52	6.91	6.96	12.30	8.26	9.74	12.30	11.47	11.76	12.15	11.41	10.99	11.38	13.74	14.22	13.14	8.98	8.59	7.13	5.95	5.42	10.83	11.53	11.37	10.94	11.42	11.76	11.64	11.00	11.00	11.25	11.61	11.19	11.20	11.01	11.17	10.85	10.16
Fe_2O_3	1.09	1.57	0.59	0.71	1.06	0.97	0.85	0.83	0.78	0.75	3.89	4.03	3.87	4.43	3.26	3.19	3.40	3.97	3.75	4.14	5.38	4.84	4.93	2.04	1.22	1.33	1.67	1.00	1.45	2.04	2.02	1.69	2.04	2.52	2.61	2.16	2.25	3.62	2.84	2.52	2.51	2.51	2.75	2.45	1.98
MnO	0.02	0.03	0.01	0.01	0.02	0.02	0.02	0.01	0.01	0.01	0.04	0.05	0.05	0.06	0.05	0.05	0.05	0.06	0.05	0.06	0.08	0.08	0.16	0.10	0.07	0.05	0.04	0.04	0.03	0.04	0.03	0.03	0.03	0.04	0.04	0.03	0.03	0.06	0.05	0.04	0.04	0.04	0.04	0.03	0.03
MgO	0.50	0.79	0.25	0.25	0.52	0.45	0.34	0.31	0.28	0.29	0.74	0.69	0.78	0.97	0.76	0.76	0.93	0.95	0.90	0.89	1.05	1.61	0.94	0.41	0.29	0.29	0.31	0.20	0.47	0.63	0.62	0.53	0.61	0.69	0.70	0.61	0.62	0.82	0.76	0.70	0.70	0.66	0.70	0.63	0.53
CaO	1.56	1.73	1.09	1.44	1.52	1.55	1.53	1.41	1.25	1.24	1.19	1.22	1.68	2.14	1.96	2.03	2.23	2.08	1.83	1.83	1.64	2.02	1.15	1.07	0.93	0.80	0.73	0.66	1.67	2.18	2.09	1.88	2.10	2.16	2.12	1.83	1.93	2.10	2.12	2.19	2.10	2.03	2.09	1.85	1.59
Na_2O	1.79	1.67	1.62	1.90	1.79	1.85	1.86	1.75	1.41	1.48	1.48	1.29	1.59	1.97	1.93	2.05	2.01	1.89	1.75	1.70	1.80	2.70	1.51	1.44	1.30	1.15	1.07	1.14	1.95	2.28	2.27	2.15	2.24	2.26	2.26	2.11	2.15	2.14	2.27	2.19	2.18	2.15	2.21	2.02	1.87
K_2O	1.83	1.65	1.62	2.55	1.70	2.12	2.38	2.31	1.91	1.92	1.71	1.60	2.14	2.68	2.62	2.69	2.71	2.49	2.14	2.32	2.34	2.36	1.79	1.89	1.47	1.38	1.41	1.46	1.80	2.54	2.50	2.26	2.52	2.60	2.51	2.14	2.31	2.40	2.57	2.45	2.46	2.37	2.45	2.17	1.76
P_2O_5	0.02	0.02	0.01	0.02	0.02	0.02	0.02	0.02	0.01	0.01	0.06	0.04	0.05	0.07	0.05	0.05	0.06	0.06	0.05	0.06	0.10	0.13	0.10	0.04	0.02	0.03	0.03	0.02	0.02	0.03	0.03	0.02	0.03	0.03	0.03	0.03	0.03	0.03	0.03	0.03	0.03	0.03	0.03	0.03	0.02
Trace Elements (ppm)																																												
Cr	40	54	23	21	37	29	20	26	20	21	100	66	54	68	51	58	52	72	72	66	115	100	106	51	53	44	32	28	51	36	43	32	39	46	47	51	41	46	46	38	47	45	48	56	44
Nb	2	2	1	0	1	1	1	0	0	1	12	17	14	14	9	8	9	14	12	12	11	8	9	2	1	2	3	1	7	8	8	6	7	9	9	9	8	16	11	9	9	9	10	8	9
Ni	11	12	10	7	12	10	8	10	8	9	35	25	15	18	15	16	15	15	17	20	38	37	44	21	18	16	14	12	11	6	7	16	10	11	12	12	13	9	13	12	11	11	13	13	12
Pb	20	17	20	20	19	19	18	18	15	16	19	15	16	19	20	19	20	18	19	19	20	19	20	18	20	16	14	16	19	19	19	20	19	19	18	18	17	18	18	17	17	17	18	18	17
Sc	4	7	3	1	7	2	2	1	0	1	18	9	8	10	8	7	9	11	10	10	18	17	17	7	6	5	4	1	9	6	8	4	7	9	9	9	7	11	8	9	8	7	6	9	6
Sr	288	252	271	266	272	256	255	242	200	200	213	171	208	258	254	258	261	240	237	216	199	189	175	195	226	184	134	145	307	304	304	300	298	300	291	292	286	277	283	278	274	271	273	273	274
Th	2	1	1	1	0	1	1	1	2	1	8	15	13	8	7	5	5	10	10	7	8	5	5	2	2	3	3	2	6	5	4	2	3	5	7	5	5	17	11	5	9	6	10	8	7
V	16	42	5	5	10	3	5	5	5	5	162	123	95	102	62	61	71	98	109	99	159	160	181	36	31	24	20	5	48	44	40	31	44	60	58	60	50	98	67	60	59	58	55	65	67
Y	13	14	12	12	13	12	12	11	10	10	23	16	17	20	18	17	18	18	18	19	23	25	26	14	14	13	11	9	15	15	15	15	15	16	16	15	15	18	17	15	16	16	16	16	15
Zr	85	86	85	83	81	86	87	92	88	88	225	258	230	193	166	146	141	197	195	188	159	138	142	105	91	117	126	98	139	152	150	130	141	162	173	166	153	281	212	192	178	182	196	178	174
As	4	4	4	4	3	3	3	3	3	3	4	3	2	3	3	3	3	3	3	2	4	5	6	3	3	3	2	2	3	3	3	3	3	4	3	4	4	4	4	4	4	4	3	4	4
Zn	13	17	7	6	11	9	7	5	6	5	58	38	31	41	31	31	31	35	37	40	65	64	79	29	21	18	17	8	18	18	18	17	19	22	22	22	19	29	24	24	25	23	23	28	22
Cu	3	2	3	2	3	1	2	2	1	2	23	7	6	8	6	6	5	6	7	11	29	39	38	14	8	7	5	4	4	2	3	4	4	3	3	5	5	4	5	5	7	5	5	6	5
TS	746	776	795	614	989	701	584	594	532	598	5782	1189	579	613	514	728	638	874	857	1038	5179	17721	5080	2307	1616	1121	860	819	2558	2261	2840	2948	3607	4127	5163	4575	4892	4112	5628	5959	6188	6382	5568	7422	5483
F	210	62	nd	223	35	nd	49	61	49	145	102	8	36	102	22	114	252	129	16	130	102	62	286	143	60	215	168	nd	141	103	35	nd	175	176	8	89	89	61	219	62	49	nd	23	179	200
Br	8	9	11	9	12	11	10	10	9	10	9	6	6	6	6	7	7	7	7	6	12	41	15	9	8	7	8	9	10	9	10	10	10	9	10	11	11	9	11	12	12	12	12	11	11
I	26	21	27	27	25	26	25	28	26	29	10	13	14	13	12	17	15	15	15	14	17	15	12	23	29	31	25	29	25	22	18	22	19	19	19	18	18	7	12	17	17	17	15	19	20
Cl	5467	6966	7204	4128	10291	5356	3311	2976	2099	3398	5530	1723	1398	2083	776	6453	2122	2625	2702	1014	7474	22810	6528	4407	3392	2001	2374	4443	6924	4730	5629	4562	4829	4416	5861	7253	5826	4734	5160	5611	5938	7441	5701	7361	7559
Mean GS (ϕ)	2.41	1.80	1.06	0.83	1.73	1.44	1.12	0.92	0.24	0.57	2.58	0.04	0.82	1.62	1.53	1.61	1.41	1.22	0.56	1.41	1.36	0.21	0.48	0.17	0.56	-0.19	-0.65	0.02	1.84	1.50	1.94	1.66	2.01	1.68	1.87	1.40	1.27	1.89	1.90	1.78	0.99	2.05	0.75	1.77	1.88
Sorting	2.12	1.62	2.01	1.48	1.20	1.58	1.63	1.78	1.96	2.06	2.64	2.41	2.40	2.31	2.39	2.37	2.43	2.15	2.43	2.32	2.44	0.29	2.89	2.25	2.33	2.40	2.48	2.88	2.39	2.76	2.02	2.05	1.92	2.75	2.21	2.48	2.42	2.22	2.63	2.28	2.41	2.44	2.78	2.07	2.23
LOI	0.85	0.75	0.84	0.76	0.97	0.84	0.78	0.73	0.86	0.88	4.66	1.32	1.05	1.28	1.17	1.31	1.29	1.32	1.29	1.90	6.08	20.76	8.09	2.54	1.53	1.36	1.45	1.14	1.11	0.98	1.19	1.33	1.44	1.49	1.79	1.56	1.71	1.39	2.56	2.58	2.84	2.28	2.36	2.33	2.01
SiO_2/Al_2O_3	7.6	8.1	9.3	9.0	7.6	9.2	9.4	9.9	12.6	12.5	6.3	9.8	8.1	6.0	6.7	6.5	6.2	6.6	7.0	6.7	5.3	5.0	5.8	9.3	10.0	12.3	14.9	16.6	7.5	6.8	6.9	7.3	6.9	6.5	6.6	7.2	7.2	6.7	6.6	6.9	6.9	7.1	6.9	7.3	8.0

4. 3.2.2 Major elements

4.3.2.2.1 Core One (1C)

Major element concentrations show some contrast within the C1. SiO_2 concentration increases towards the bottom of the core, ranging within 33.28 – 44.42 (wt%) for 1C1 – 1C5, 64.07 – 82.50 (wt%) for 1C6 – 1C19 and 84.87 – 96.14 (wt%) for 1C20 to 1C31 (Table 4.3.6). TiO_2 concentration decreases towards the bottom of the core as a consequence of SiO_2 dilution. TiO_2 concentrations are very high (4.41 – 6.03 wt%) in 1C1 to 1C5, falling to 0.65 – 3.65 (wt%) in 1C6 – 1C19, and falling below 1 wt% (0.11 - 0.94) in 1C20 to 1C31. Fe_2O_3 concentrations also decrease towards the bottom of the core (Table 4.3.6). Fe_2O_3 concentrations are extremely high (26.36 – 41.88 wt%) in 1C1 to 1C5, but fall rapidly to 2.07 – 14.84 (wt%) in 1C6 – 1C19, and reach more normal levels 0.25 – 2.26 (wt%) in 1C20 to 1C31.

Among the other major elements MnO, MgO and CaO contents show the greatest contrast (Table 4.3.6). MnO concentrations range between 0.01 – 0.52 (wt%), MgO between 0.09 – 4.67 (wt%) and CaO between 0.24 – 3.45 (wt%). In contrast, Na_2O, K_2O and P_2O_5 variation is less along the core (Table 4.3.6). LOI is very low, from negative values (-1.55) to +0.75) in C1. Samples 1C1 – 1C6 have negative LOI values as a result of their very high Fe_2O_3 contents with negative values produced by oxidation of FeO to Fe_2O_3. SiO_2/Al_2O_3 (also known as chemical maturity index, CMI) gradually increases towards the bottom of the core (Table 4.3.6). In the samples 1C24 - 1C30, CMI ranges from 15.0 to 43.3. Consequently, these samples are classified as highly mature sediments.

4.3.2.2.2 Core Two Three and Four (2C, 3C, 4C)

In C2 the major oxides do not show great change or any decrease or increase down the core (Table 4.3.7). Overall, SiO_2 contents range from 82.19 – 87.33 (wt%), Al_2O_3 from 6.91 – 10.87 (wt%), TiO_2 from 0.09 – 0.21 (wt%) and Fe_2O_3 from 0.59 – 1.57 (wt%). Among the other major elements MnO, MgO, CaO Na_2O, K_2O and P_2O_5 variation is even lower (Table 4.3.7). LOI values are very low and uniform, with values ranging from 0.73 – 0.97 in C2. CMI in C2 is less than in C1, within a total range of 7.6 – 12.5 indicating moderate maturity.

Major oxides show slight variation in C3 (Table 4.3.7). In the upper most part above 8cm and at the bottom part below 26cm Al_2O_3 and SiO_2 shows antipathetic variation. The overall range of SiO_2 is 70.95 – 89.92, TiO2 0.13 – 1.52 (wt%), Al_2O_3 5.42 – 14.22 (wt%) and Fe_2O_3 1.00 – 5.38 (wt%). Among the other major elements MnO, MgO, CaO, Na_2O, K_2O and P_2O_5 contents does not show great variation along the core (Table 4.3.7). LOI is comparatively high (20.76) in one location at 24cm. LOI in the other locations ranges from 1.05 – 8.09. The CMI is 5.0 – 16.6 in C3 where the samples 3C14 – 3C18 have high CMI and 3C11 – 3C13 has the lowest CMI.

In C4 the major oxides also does not show great change or any decrease or increase down the core (Table 4.3.7). SiO_2 ranges from 75.79 – 81.29 (wt%), Al_2O_3 from 10.16 – 11.76 (wt%), TiO_2 from 0.57 – 1.79 (wt%) and Fe_2O_3 from 1.45– 3.62 (wt%). As in core 2, among the other major elements MnO, MgO, CaO Na_2O, K_2O and P_2O_5 variation is much less (Table 4.3.7). LOI is very low in C4 and (0.98 – 2.84) and CMI shows no variation along the core, and very low value of 6.6 – 8.0, reflecting geochemical immature and fine grain size.

4. 3.2.3 Trace elements

4. 3.2.3.1 Core One (1C)

Among the trace elements (Table 4.3.6) Zirconium is the most significant, with contents ranging from 137 – 10778 ppm, especially in the upper 20 cm where concentration ranges from 1060 – 10778 ppm. Cerium is very high in samples 1C1 – 1C5 ranging between 504 – 1434 ppm, 1C8 – 1C11 ranges between 109 – 157 ppm, and the rest of the samples range between 10 – 112 ppm. Th, Nb, Y, V, Cr also concentrated in samples 1C1 – 1C5 and values decreases down along the core. The concentration of elements suggests strong heavy mineral concentration in the upper part of the core. Barium ranges from 210 – 726 ppm where twelve samples in the middle part have higher concentrations than UCC. Strontium ranges from 45 – 279 ppm, Rb range from 0 - 63 ppm and Ga range from 0 – 10 ppm in C1. The TS in C1 range from 389 – 853 ppm. The Pb concentration in C1 is very low ranging from 0 – 15 ppm.

4. 3.2.3.2 Core Two, Three and Four (2C, 3C, 4C)

Except, for Pb, concentration of trace elements in C2 are lower than in C1. Lead content in C2 range from 15 – 20 ppm though it is still less than UCC (Table 4.3.7). Strontium range between 199.6 – 287.9 ppm and is close to the values of the middle part of core 1. The values of V, Y, Nb, Zr, Th and Sc are very low in C2 (Table 4.3.7). Zircon contents in C2 range from 80 – 92 ppm which is very much less than Zr content in C1.

As for the major elements, trace elements in C3 also show only slight variation down the core (Table 4.3.7). Cromium, V, Zr and Th show very similar variations along the core. Zirconium ranges from 91.2 – 275. 5 ppm and Th ranges between 1.8 – 14.7 ppm. Chromium ranges between 28.2 – 114.8 ppm and V ranges between 5.0 – 181.2 ppm. However, these values are less than in C1. Other elements including As, Pb, Zn, Cu, Ni, Y and Sc are considerably very low and within UCC and not show great variation along the core. The TS in C 3 is high in 2 - 4 cm and 20 – 28 cm where the values range between 1190 ppm and more than 17, 000 ppm. The TS is high in the part where there is high organic matter and fine grains (Fig 4.3.8).

In C4 all trace elements show low values, except that most show a slight increase at 20cm. TS values show gradual increase from top to bottom of the core, possibly related to gradual increase of organic matter.

4. 3.2.4 Heavy Minerals

The C1 is the most variable core with interesting features of high concentration of elements typically associated with heavy mineral related elements and also highly variable grain size (Fig 3.2.3). The upper most part has a high content of heavy minerals. Heavy mineral separations of > 0.5 mm fractions of samples 1C1 – 8C1 yielded heavy mineral loads of 30 – 92 %. The greatest was found in 1C4, and the lowest in 1C8 with 91.93% and 30.34% respectively. These high heavy mineral percentages correspond very well with the peak trace element concentrations (Fig 3.2.3). A heavy mineral patch extends to some 2 – 4 Km along the beach in Koddiyar bay. The depth of this deposit is up to about 12 – 14 cm and the heavy mineral content decrease with depth. Therefore, the heavy mineral volume is insufficient for

exploitation purposes. This heavy mineral deposit may be regarded as a very small scale placer deposit.

4.3.3 Ostracode analysis

4. 3.3.1 Grain size

We calculated four grain size parameters (median grain size, sorting, skewness, and kurtosis) using the equation of Folk and Ward (1957) (Table 4.3.8). As a result, the median grain size ranged between 0.49 and 4.6φ, and its average was 2.27φ (Fig. 4.3.10). The sorting ranged between 0.39 and 2.34, and its average was 1.34. The skewness ranged between 0.10 and 0.74, and its average was 0.46. The kurtosis ranged between 0.69 and 3.15, and its average was 1.69. Thus, poorly- to well-sorted medium-grained sand, very poorly- to well-sorted fine- to very coarse-grained sand, and very poorly- to poorly-sorted fine- to medium-grained sand are distributed in the Inner Harbor, Tambalagam Bay, and Koddiyar Bay, respectively.

Table 4.3.8 : Sample information and results of grain size and CN analyses

Sample number	Area	Depth (m)	Grain size analysis (Phi scale, and Grain size division by Folk & Ward, 1957)				CN analysis		
			median	sorting	skewness	kurtosis	TN (wt%)	TOC (wt%)	C/N ratio
TR3	IH	6.4	2.76 fine sand	0.41 well	0.27 positive	2.35 very leptokurtic	0.05	0.41	8.86
TR4	IH	5.2	2.93 fine sand	1.87 poorly	0.79 very positive	2.41 very leptokurtic	0.04	0.30	7.68
TR9	IH	13	2.75 fine sand	1.81 poorly	0.49 very positive	2.33 very leptokurtic	0.04	0.24	6.61
TR10	IH	11.5	2.75 fine sand	1.62 poorly	0.38 very positive	2.01 very leptokurtic	0.02	0.22	10.25
TR17	TB	3.9	2.92 fine sand	2.24 very poorly	0.63 very positive	2.31 very leptokurtic	0.03	0.23	8.17
TR20	TB	3.2	1.83 medium sand	0.39 well	0.24 positive	1.34 leptokurtic	0.02	0.14	6.03
TR25	TB	0.5	2.24 fine sand	1.47 poorly	0.66 very positive	3.15 extremely leptokurtic	0.04	0.35	8.45
TR26	TB	0.5	-0.30 very coarse sand	1.39 poorly	0.74 very positive	0.69 platykurtic	0.03	0.32	10.28
TR27	TB	0.5	2.03 fine sand	1.13 poorly	0.57 very positive	2.34 very leptokurtic	0.03	0.37	13.58
TR28	TB	0.5	2.27 fine sand	0.86 moderately	0.45 very positive	0.98 mesokurtic	0.03	0.29	9.40
TR29	TB	0.5	2.22 fine sand	0.72 moderately	0.12 positive	1.24 leptokurtic	0.03	0.23	8.65
TR30	TB	0.8	3.09 very fine sand	1.59 poorly	0.53 very positive	1.42 leptokurtic	0.04	0.34	8.79
TR37	KB	1.5	3.34 very fine sand	1.11 poorly	0.10 positive	1.17 leptokurtic	0.04	0.49	12.59
TR39	KB	2.3	3.99 very fine sand	2.34 very poorly	0.55 very positive	1.86 very leptokurtic	0.04	0.42	10.47
TR40	KB	0.5	2.28 fine sand	1.12 poorly	0.53 very positive	1.38 leptokurtic	0.03	0.26	10.17

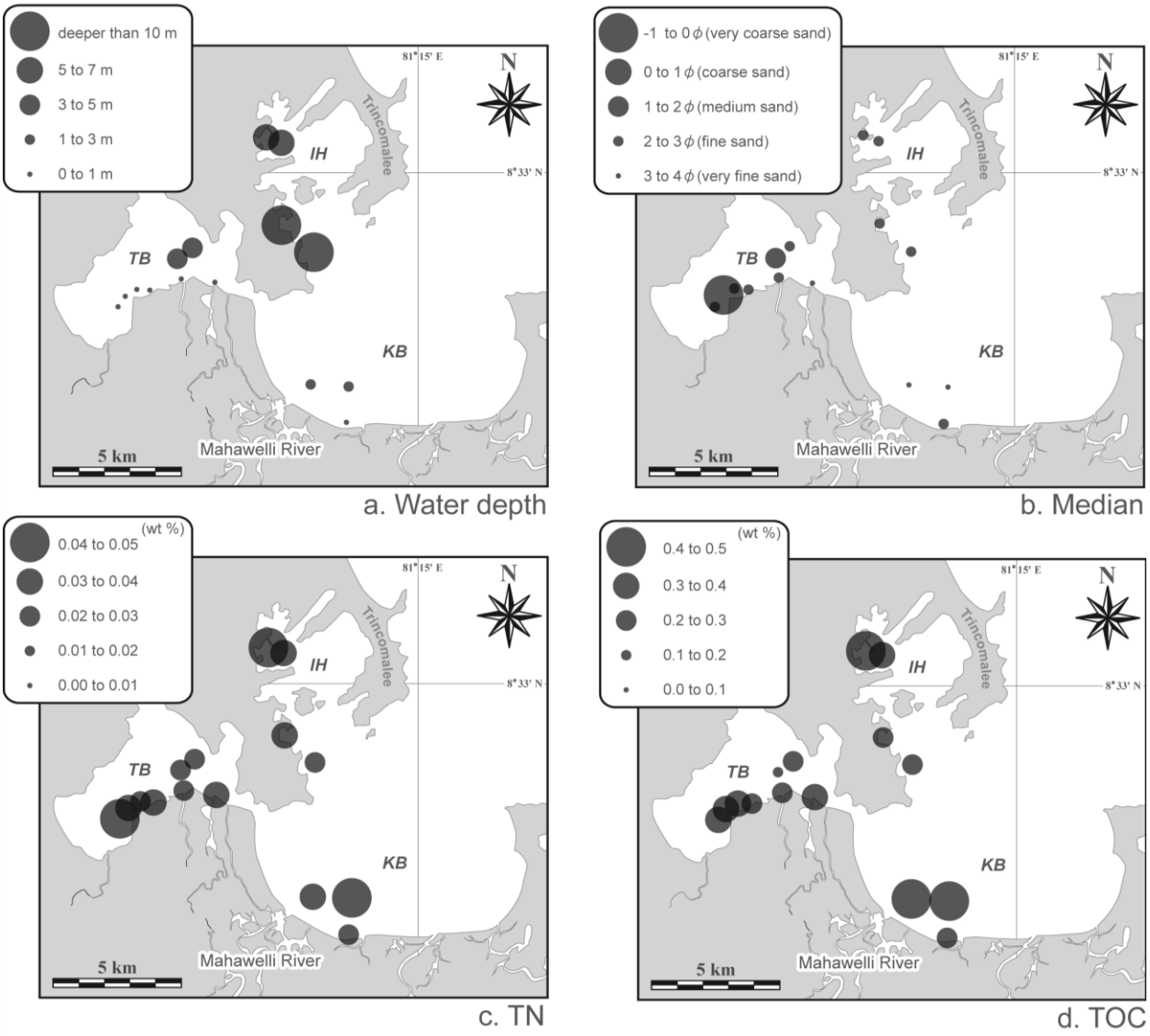

Fig. 4.3.10. Distribution of (a) water depth (b) median grain size, (c) total nitrogen content and (d) total organic carbon content of surface sediments in Trincomalee Bay

4. 3.3.2 TN and TOC contents

The concentration of TN and TOC ranged between 0.02−0.05% and 0.14−0.49%, respectively (Table 4.3.9). TN indicated relatively high values at around the inner part of each Bay with the exception of Koddiyar Bay. TOC is relatively high in the inner part of Inner Harbor and Koddiyar Bay (Fig. 4.3.10). Distributional patterns of TOC are concordant to those of sediment grain size: TOC is high in fine-grained sediments.

Table 4.3.9: List of ostracodes from the Trincomalee Bay. Solid stars show species and samples used for quantitative analyses

Species \ Sample number / Area	IH TR3	IH TR4	IH TR9	IH TR10	TB TR17	TB TR24	TB TR30	KB TR37	KB TR39
★ *Loxoconcha megapora* Benson & Maddocks		5	1	1	2			3	
Loxoconcha paiki Whatley & Zhao			1	1				1	
Loxoconcha aff. *pulchra* Ishizaki									1
★ *Loxoconcha* aff. *tekkaliensis* Varma et al.							40		
Loxoconcha sp.								1	
★ *Macrocypris* cf. *decora* (Brady)	8								
★ *Macrocypris* spp.			2		1			9	
Miocyprideis chaudhuryi (Lyubimova and Guha)					2				
Miocyprideis sp.								1	
★ *Miocyprideis spinulosa* (Brady)		4	2	5		2			
★ *Morkhovenia inconspicua* (Brady)			3	1					
★ *Mutilus pentoekensis* (Kingma)	21	2	13	1				2	2
Mutilus sp. 1			2						
★ *Neocythereromorpha* sp.		1	4						
Neomonoceratina indonesiana Whatley & Zhao									1
★ *Neomonoceratina iniqua* (Brady)					46	96		1	2
★ *Neonesidea* spp.	16							6	2
Neosinocythere cf. *dekrooni* (Kingma)					2				
Paijenborchellina indoarabica Jain									1
★ *Paijenborchellina prona* (Lubimova & Guha)					4			7	10
Paracytheridea aff. *dialata* Gou & Huang	1							1	1
Paracytheridea cf.*tschoppi* van den Bold	2								
★ *Paracytheridea pseudoremanei* Bonaduce et al.			1		3			1	1
Paracytheridea sp. 1					1				
★ *Parakrithe palacida* Mostafawi				3				1	
Phlyctenophora? sp.								1	
★ *Pistocythereis* aff. *bradyformis* (Ishizak)	9	6	14	44				16	11
★ *Pistocythereis* aff. *bradyi* (Ishizak)	18	1	24	4	1			2	
Pontocythere sp. 1					1				
Pontocythere sp. 2					1				
★ *Ruggieria* cf. *darwini* (Brady)			3						2
★ *Semicytherura* sp.									3
Spinoceratina spinosa (Zhao & Whatley)									1
★ *Stigmatocythere bona* Chen	2	63			23	27		19	17
★ *Stigmatocythere* cf. *bona* Chen	2	1	3	2					
★ *Tanella gracilis* Kingama	2	10	4	3			73	10	7
Tanella? sp.	2								
★ *Xestoleberis* spp.	11	3	7	3	1			9	10
Gen et sp. indet		1							
No. of speciemens	170	183	186	176	156	179	113	173	157
No. of species	29	22	33	26	25	7	2	34	30
Sample weight (g)	20	20	20	20	20	20	20	20	20
Total ostracode(/g)	45.33	292.80	198.40	281.60	499.20	71.60	5.65	69.20	125.60
Shannon_H	2.84	2.25	2.88	2.60	2.42	1.39	0.65	2.95	2.77
Evenness_e^H/S	0.59	0.43	0.54	0.52	0.45	0.58	0.96	0.56	0.53

Species \ Sample number / Area	IH TR3	IH TR4	IH TR9	IH TR10	TB TR17	TB TR24	TB TR30	KB TR37	KB TR39
★ *Loxoconcha megapora* Benson & Maddocks		5	1	1	2			3	
Loxoconcha paiki Whatley & Zhao			1	1				1	
Loxoconcha aff. *pulchra* Ishizaki									1
★ *Loxoconcha* aff. *tekkaliensis* Varma et al.							40		
Loxoconcha sp.								1	
★ *Macrocypris* cf. *decora* (Brady)	8								
★ *Macrocypris* spp.			2		1			9	
Miocyprideis chaudhuryi (Lyubimova and Guha)					2				
Miocyprideis sp.								1	
★ *Miocyprideis spinulosa* (Brady)		4	2	5		2			
★ *Morkhovenia inconspicua* (Brady)			3	1					
★ *Mutilus pentoekensis* (Kingma)	21	2	13	1				2	2
Mutilus sp. 1			2						
★ *Neocythereromorpha* sp.		1	4						
Neomonoceratina indonesiana Whatley & Zhao									1
★ *Neomonoceratina iniqua* (Brady)					46	96		1	2
★ *Neonesidea* spp.	16							6	2
Neosinocythere cf. *dekrooni* (Kingma)					2				
Paijenborchellina indoarabica Jain									1
★ *Paijenborchellina prona* (Lubimova & Guha)					4			7	10
Paracytheridea aff. *dialata* Gou & Huang	1							1	1
Paracytheridea cf.*tschoppi* van den Bold	2								
★ *Paracytheridea pseudoremanei* Bonaduce et al.			1		3			1	1
Paracytheridea sp. 1					1				
★ *Parakrithe palacida* Mostafawi				3				1	
Phlyctenophora? sp.								1	
★ *Pistocythereis* aff. *bradyformis* (Ishizak)	9	6	14	44				16	11
★ *Pistocythereis* aff. *bradyi* (Ishizak)	18	1	24	4	1			2	
Pontocythere sp. 1					1				
Pontocythere sp. 2					1				
★ *Ruggieria* cf. *darwini* (Brady)			3						2
★ *Semicytherura* sp.									3
Spinoceratina spinosa (Zhao & Whatley)									1
★ *Stigmatocythere bona* Chen	2	63			23	27		19	17
★ *Stigmatocythere* cf. *bona* Chen	2	1	3	2					
★ *Tanella gracilis* Kingama	2	10	4	3			73	10	7
Tanella? sp.	2								
★ *Xestoleberis* spp.	11	3	7	3	1			9	10
Gen et sp. indet		1							
No. of speciemens	170	183	186	176	156	179	113	173	157
No. of species	29	22	33	26	25	7	2	34	30
Sample weight (g)	20	20	20	20	20	20	20	20	20
Total ostracode(/g)	45.33	292.80	198.40	281.60	499.20	71.60	5.65	69.20	125.60
Shannon_H	2.84	2.25	2.88	2.60	2.42	1.39	0.65	2.95	2.77
Evenness_e^H/S	0.59	0.43	0.54	0.52	0.45	0.58	0.96	0.56	0.53

CHAPTER 5

DISCUSSION

5.1 MAHAWELI RIVER

5.1.1 Provenance Indicators

Elements such as Y, Th, Zr, Nb, Ti and Sc are most suited for provenance and tectonic setting determination (Holland, 1978; Bhatia and Crook, 1986) because of their relatively low mobility during sedimentary processes, and their low residence times in seawater (Holland, 1978; Taylor and McLennan, 1985; Cullers, 1988). These elements are transported quantitatively into clastic sediments during weathering and transport, and hence reflect the signature of the parent material (McLennan et al., 1983a). The incompatible element pairs Th-Y, Th-Zr, and Th-Nb (Fig. 5.1.1a–z) show the effect of heavy mineral concentration and felsic source. Thorium, Y, Zr and Nb abundances in source rocks will increase as their chemistry becomes more evolved. The Th-Y, Th-Zr, and Th-Nb values for the basement rocks show considerable scatter due to the variety of lithotypes analyzed, but most lie within the limits defined by average values in Highland Complex (HC) gneisses (Pohl and Emmermann, 1991). The soils overlap the distribution of the basement rocks, and also lie mainly within the HC gneiss field (Fig. 5.1.1a–c). This overlap suggests that the step from basement rock to the soils does not fractionate these ratios in a systematic manner. Although the stream sediments also partially overlap the basement rocks and soils, the data spread to considerably higher values.

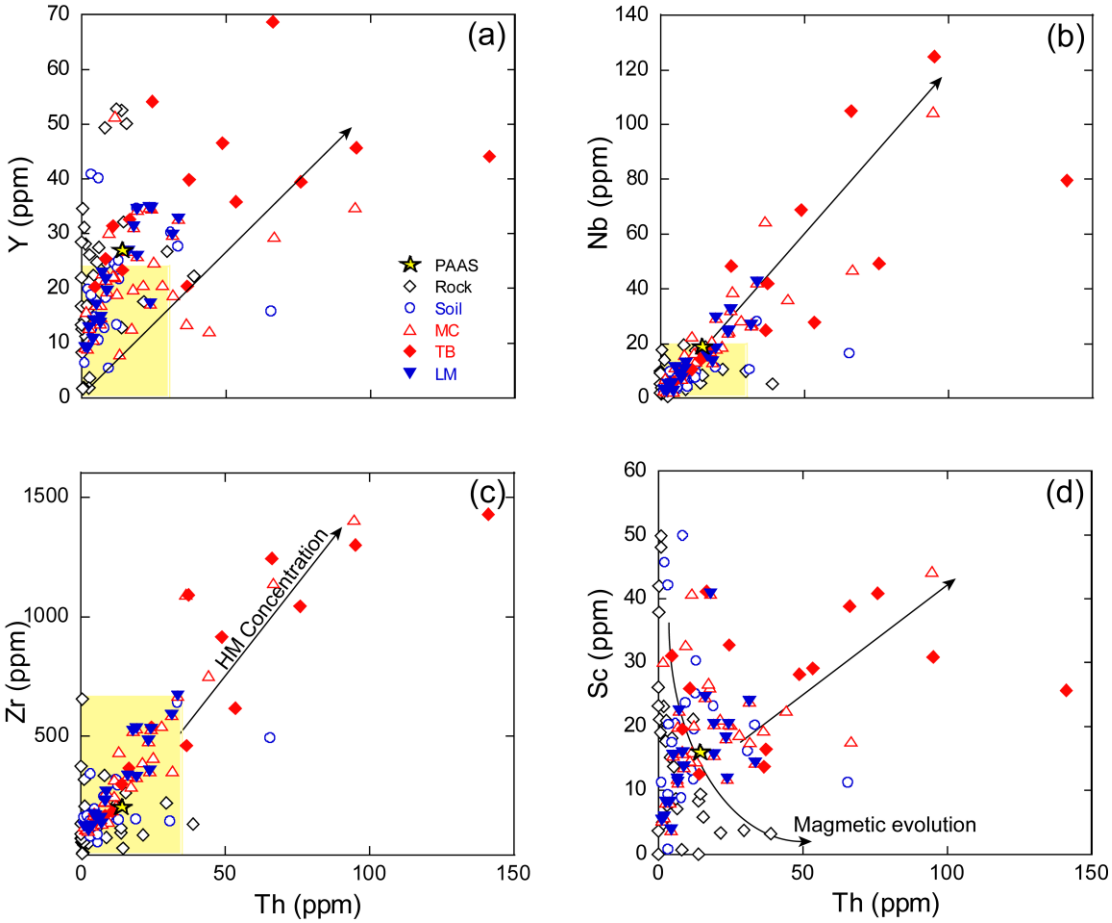

Fig 5.1.1: Plots of (a) Y, (b) Nb, (c) Zr and (d) Sc versus Th for the stream sediments, rocks and soils. Stream sediments are differentiated by location: MC – main channel; TB – tributaries; LM – lower main channel. Yellow areas indicate typical ranges in alkaline rocks in the Highland Complex (data from Pohl and Emmermann, 1991).

The possible role of provenance, sorting or accumulation of heavy minerals such as zircon, monazite, or apatite can be evaluated using Zr/Sc and Th/Sc ratios (McLennan et al., 1993). The Th/Sc ratio is a sensitive index of the bulk composition of the source (Taylor and McLennan, 1985), whereas Zr/Sc ratio serves as a proxy for identifying heavy mineral concentrations, because it is highly sensitive to accumulation of zircon. All elements involved in the ratios are also resistant to weathering processes (Taylor and McLennan, 1985; McLennan et al., 1993). Consequently, plot positions and trends on bivariant Zr/Sc–Th/Sc plots give an

indication of source composition and heavy mineral concentration when compared with compositions of average volcanic and plutonic rocks.

Th/Sc ratios of the bulk river sediments, soils, and basement rocks average 1.16, 1.01, and 1.56 respectively, equal to or slightly greater than the ratio in PAAS (0.97, Taylor and McLennan, 1985). The Th/Sc ratio for post-Archean rocks is typically ~1, and for granitic rocks is higher still; for Archean and basic rocks the ratio is less than 1 (Taylor and McLennan, 1985; Fig. 5.1.2a). The average Zr/Sc ratio of the sediments is 22.80, somewhat greater than PAAS (17.2; Taylor and McLennan, 1985). This suggests that the sediments are slightly enriched in zircon. The Zr/Sc–Th/Sc plot (Fig. 5.1.2a) illustrates that the basement rocks show a range from mafic through to felsic compositions, as do the soils. Scatter among the rocks and soils are considerable owing to the variety of lithotypes analyzed, but most samples fall along a model source evolution line between an average basalt and rhyolite. Basement samples plotting at higher ratios include quartzites and quartzofeldspathic gneisses; higher ratios in these samples may reflect original zircon concentration in their low-grade protoliths. Ratios in the stream sediments show a more restricted range, reflecting homogenization and possibly increased maturity during transport. Zr/Sc and Th/Sc ratios are higher in some samples, suggesting limited zircon concentration. However, these two ratios alone are not adequate to describe provenance, and other combinations of elements must be considered.

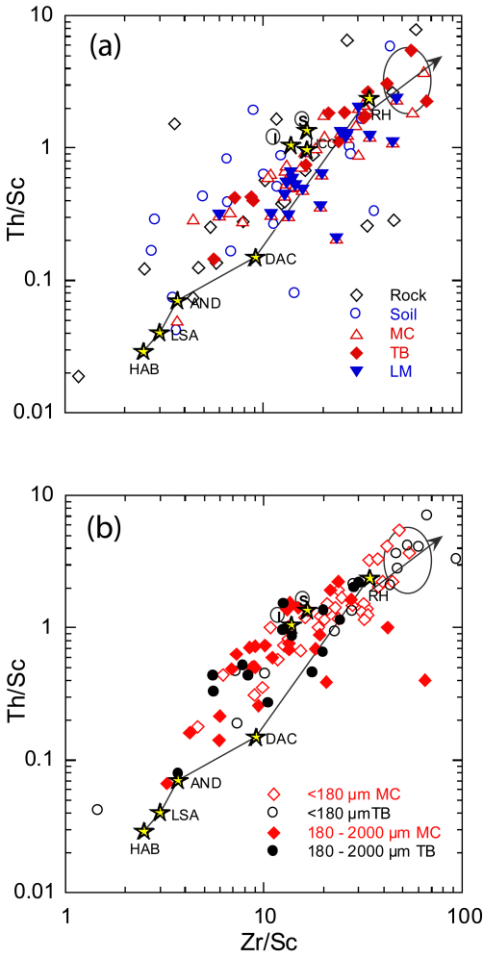

Fig 5.1.2: Zr/Sc–Th/Sc ratio plots (McLennan et al., 1993) for (a) bulk stream sediments, basement rocks and soils from the Mahaweli River, showing zircon concentration (arrow) and typical source rock compositions; (b) <180 µm and 180 - 2000 µm fractions. Stars BAS, AND, DAC, RHY: average basalt, andesite, dacite and rhyolite, as plotted by Roser and Korsch (1999); Stars (I) average I-type granite, (S) average S-type granite (Whalen et al., 1987).

Chromium and Ni are often enriched in sediments due to adsorption on clay minerals. Both elements behave similarly in the Mahaweli stream sediments, with broad decrease downstream through the wet and intermediate zones, and gradual increase in the dry zone, suggesting progressive destruction of Cr- and Ni-bearing detrital phases and increased adsorption on to clay minerals. Garver et al. (1996) showed that shale samples derived from ultramafic rocks had high concentrations of Cr and Ni with Cr/Ni ratio of 1.4, suggesting only minor

geochemical partitioning from their ultramafic source (Cr/Ni 1.6), whereas sandstones had Cr/Ni ratios of >3.0, showing significant sedimentary fractionation due to concentration of detrital chromite in the sands. In the Mahaweli River sediments Ni is depleted relative to PAAS, whereas Cr is highly enriched, but in the rock samples both elements are depleted (Fig. 4.1.2). This may be due to some enrichment process during weathering or sedimentation (McLennan et al., 1983b). The Mahaweli rock samples have average Cr/Ni ratio of 8.9 (including marbles) or 6.1 (excluding marbles), compared to 3.72 for the soils and 5.09 for the river sediments; the PAAS value is 2. The high ratios for the Mahaweli rocks, soils, and sediments thus indicate that Cr has undergone significant fractionation from source rock, to soil, to sediment, and also that no significant ultramafic component is present. Nevertheless, Cr-Ni relations clearly indicate that the Highland Complex samples are post-Archean (2-3 Ga) in nature rather than late or early Archean (Fig. 5.1.3a). This figure shows abundances in the basement rocks are highly variable, whereas the river sediments show less scatter but higher Cr contents, indicating homogenization and enrichment during weathering and transport.

Cr/V-Y/Ni ratios also provide estimates of preferential concentration of chromium over other ferromagnesian elements (Hiscott, 1984; McLennan et al., 1993). The Cr/V ratio measures enrichment of Cr with respect to other ferromagnesian elements, whereas the Y/Ni ratio evaluates the relationship between the ferromagnesian trace elements (represented by Ni) and the HREE, using Y as a proxy (McLennan et al., 1993). Sediments derived from ultrabasic sources typically have high Cr/V ratios (>>1) coupled with low Y/Ni (<1) (Hiscott, 1984), as shown by Ortiz and Roser, (2006b) for sediments from the Hino River in SW Japan. Very high Y/Ni ratios are seen in some basement rock samples (Table 5.1.1), such as Digana-garnet sillimanite gneiss (61.7), Gurudeniya marble (34.3), Kandehandiya quartzo-feldspathic gneiss (22.9), Ginigathhena granitic gneiss (18.5), Victoria hornblende biotite gneiss (11.1) and Girandurukotte - charnockitic gneiss (8.9). Average Cr/V ratios of the rocks, soils and river sediments are all low (0.80, 0.79, 0.84 respectively), whereas Y/Ni ratios (average 0.87, 0.76 and 6.41) are variable. Cr/V ratios in both the soils and river sediments are low, indicating that contribution from ultrabasic sources is negligible (Fig 5.1.3b). Y/Ni ratios generally range across values typical of intermediate to felsic calc-alkaline rocks.

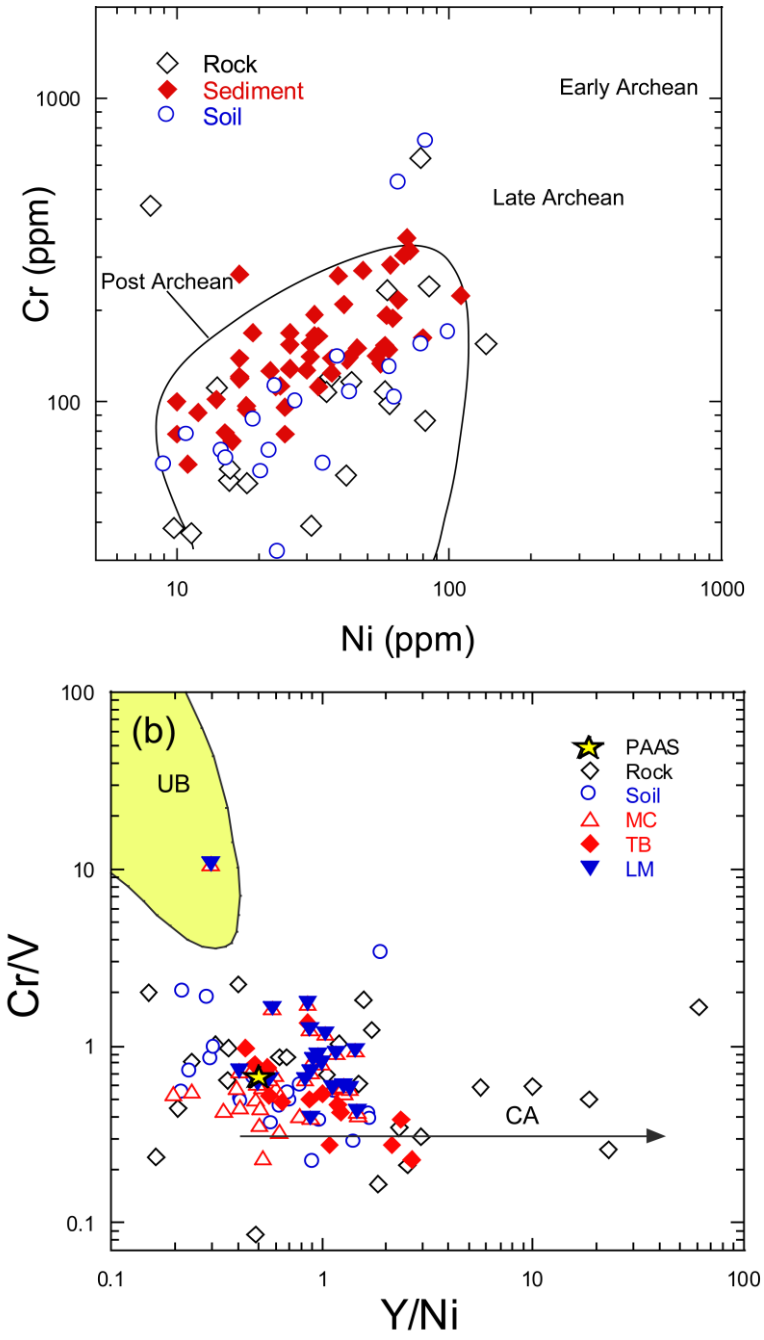

Fig 5.1.3: (a) Cr-Ni plot for the Mahaweli stream sediments, rocks and soils, showing the Post-Archean field (Taylor and McLennan, 1985) and fractionation from source rocks to the sediments. (b) and (c): Cr/V-Y/Ni plots (McLennan et al., 1993) for the stream sediments, rocks and soils (b); and <180 µm and 180 - 2000 µm fractions (c), showing the lack of ultrabasic sources. UB: Ultrabasic; field of sands derived from ultrabasic rocks in the Hino River, South West Japan (Ortiz and Roser, 2006b), CA: typical calc-alkaline trend.

Table 5.1.1: Analyses of basement rocks from the Mahaweli River basin. Major elements as oxide wt%, trace elements ppm. Distance: distance downstream (km) from the uppermost sample point.

S-No	Distance (Km)	Rock type	As	Pb	Zn	Cu	Ni	Cr	V	Sr	Y	Nb	Zr	Th	Sc	TS	TiO_2	Fe_2O_3	MnO	CaO	P_2O_5
Wet Zone																					
1	3	Charnokite	5	38	24	5	3	17	5	175	22	5	132	39	3	306	0.11	1.55	0.01	1.80	0.06
2	4	Leptynite	1	10	3	8	18	54	5	10	4	3	108	3	2	248	0.02	0.05	0.02	0.54	0.03
3	5	Granitic Gneiss	4	30	86	11	3	14	28	203	50	19	263	16	6	748	0.44	5.67	0.06	2.10	0.17
4a	6	Garnetiferrous HBG	3	20	63	4	16	55	44	186	27	10	222	30	4	349	0.57	4.60	0.04	2.82	0.25
4b	6	Garnet Biotite Gneiss	3	34	13	1	4	6	5	135	25	3	78	9	2	248	0.09	1.12	0.01	1.32	0.07
5	6	Marble	0	7	2	0	5	5	5	22	2	2	10	1	22	235	0.02	0.05	0.01	43.37	0.02
6	6	Charnokite	2	11	107	3	5	4	18	24	35	18	657	0	2	367	0.38	6.13	0.14	1.84	0.05
7	14	Charnokitic Gneiss	1	6	108	336	42	57	668	107	20	7	87	1	44	4874	2.06	15.79	0.17	8.21	0.26
8	15	Metabasite	1	11	141	7	78	635	284	73	31	8	48	1	50	404	0.68	11.50	0.15	7.71	0.07
9	17	Hornblende Biotite Gneiss	2	12	95	44	58	108	106	259	18	8	98	5	18	9619	0.56	7.01	0.08	8.70	0.14
10	27	Garnet Biotite Gneiss	1	10	38	8	85	240	119	422	13	6	97	14	8	283	0.62	4.34	0.03	3.20	0.06
11a	46	Quartzofeldspathc Gneiss	4	36	17	1	5	9	5	119	13	5	320	1	2	251	0.14	0.96	0.02	1.09	0.02
11b	46	Migmatitic Gneiss	1	15	39	13	31	39	40	381	11	3	166	1	5	303	0.37	3.36	0.04	3.38	0.07
12	55	Quartzite	0	7	2	3	5	30	5	2	2	1	124	3	2	236	0.06	0.05	0.02	0.55	0.02
13	71	Marble - Calk-gneiss	3	9	2	2	0	30	5	60	10	3	52	3	21	745	0.19	0.69	0.02	27.42	0.09
14	71	Marble -Blue apatite	2	6	0	2	5	4	5	36	2	2	17	1	19	273	0.02	0.05	0.04	37.23	0.99
15	72	Marble -Blue apatite	0	5	2	2	5	5	5	19	2	2	10	0	21	498	0.02	0.05	0.00	40.53	0.03
Wet Zone Avarage			2.0	15.7	43.6	26.2	21.6	77.2	79.6	131.3	16.8	6.1	146.4	7.4	13.6	1175.7	0.37	3.70	0.05	11.28	0.14
Intermediate Zone																					
16a	80	Hornblende Biotite Gneiss	3	28	35	1	5	15	5	44	53	14	117	14	2	228	0.12	0.67	0.01	0.84	0.03
16b	80	Granitic Gneiss	0	9	78	23	82	87	196	408	17	5	74	1	26	1096	0.97	10.92	0.15	8.47	0.34
17	83	Garnet Sillimanite Gneiss	7	36	77	3	1	11	6	179	49	19	337	8	1	353	0.40	4.18	0.04	1.77	0.10
18	84	Garnet Biotite Gneiss	1	8	47	1	60	98	154	59	21	8	127	6	7	245	0.75	6.12	0.08	1.58	0.14
19	85	Charnokitic Gneiss	0	6	65	38	5	33	201	201	8	2	58	0	38	1420	0.53	9.95	0.14	9.73	0.09
20	86	Garnet Biotite Gneiss	0	7	32	1	44	116	134	49	27	7	141	6	9	260	0.75	6.05	0.07	1.45	0.08
21	89	Garnet Sillimanite Gneiss	1	11	63	2	37	121	140	101	25	8	169	5	14	247	0.75	7.38	0.14	1.20	0.06
22	89	Quartzofeldspathc Gneiss	2	25	29	19	1	25	96	778	32	8	33	14	9	244	0.34	3.93	0.04	2.28	0.47
23	90	Hornblende Biotite Gneiss	1	11	149	3	59	233	285	81	14	2	56	1	48	318	1.06	11.79	0.16	9.16	0.15
24	94	Garnet Biotite Gneiss	3	24	54	4	16	60	87	488	16	5	97	3	8	477	0.45	4.06	0.05	3.17	0.22
25	97	Migmatite	2	18	118	75	35	107	175	85	53	17	215	12	21	16002	1.01	10.90	0.14	2.23	0.04
26	100	Charnockite	1	7	81	29	8	442	241	151	13	4	73	0	42	568	0.67	9.90	0.14	9.50	0.13
27	109	Charnockite	2	19	44	11	5	24	41	336	28	14	209	1	5	386	0.32	4.13	0.06	2.42	0.20
28	155	Charnokitic Gneiss	2	12	98	28	14	111	108	1093	17	6	102	2	23	3240	0.52	7.62	0.10	6.24	0.38
Intermediate Zone Avarage			1.7	15.6	69.3	17.1	26.5	105.9	133.4	289.5	26.7	8.6	129.1	5.3	18.0	1792	0.62	6.97	0.09	4.29	0.17
Dey Zone																					
29	157	Charnokitic Gneiss	2	24	15	3	2	14	5	293	13	2	91	1	2	280	0.04	0.58	0.20	1.54	0.05
30	193	Hornblende Biotite Gneiss	2	9	82	129	137	155	654	212	22	4	120	4	15	14421	0.53	3.40	0.02	3.30	0.26
31	223	Charnokitic Gneiss	1	11	91	8	10	38	125	369	28	10	136	1	23	449	0.78	6.54	0.09	5.04	0.22
32	283	Hornblende Biotite Gneiss	1	10	56	21	5	14	14	1878	21	6	102	2	18	254	0.25	3.14	0.05	13.66	0.12
33	284	Biotite Gneiss	3	21	51	9	7	13	62	1754	18	11	88	21	3	291	0.48	3.28	0.03	3.00	0.36
34	286	Charnokitic Gneiss	1	9	66	17	11	37	107	440	26	9	98	3	21	507	0.60	6.97	0.17	5.36	0.24
35	304	Charnokitic Gneiss	2	14	85	3	2	6	10	112	22	9	375	1	4	310	0.28	3.77	0.09	1.76	0.09
Dey Zone Avarage			1.6	13.9	63.8	27.1	24.7	39.5	139.4	722.6	21.6	7.4	144.3	4.8	12.3	2359	0.42	3.95	0.09	4.81	0.19
Overall Average			1.8	15.3	56.7	22.9	24.0	81.3	110.2	294.1	21.4	7.3	139.5	6.1	15.0	1614	0.47	4.97	0.07	7.53	0.16

5.1.2 Sorting

In stream sediments Fe_2O_3 and TiO_2 can be expected to be positively correlated due to sorting effects (Singh, 2009). Linear arrays of data points along lines extending towards the origin in binary Fe_2O_3–TiO_2 plots demonstrate that the elements were immobile, and that they were also hydraulically fractionated in a similar manner. A Fe_2O_3–TiO_2 plot for the Mahaweli data (Fig. 5.1.4a) shows the basement rocks form a linear trend with TiO_2/Fe_2O_3 ratios of ~0.086, similar to the ratio in PAAS (0.099; Taylor and McLennan, 1985). While many of the soils plot within the field of the basement rocks, some also scatter to higher TiO_2/Fe_2O_3. TiO_2 can

accumulate in residual soils due to loss of more mobile constituents (Garcia, 1994; Young and Nesbitt, 1998), and hence may reflect degree of weathering. However, examination of the soil data by climatic zone shows there is no consistent association of higher TiO_2 abundances with the soils in the wet zone, and hence weathering does not seem to control TiO_2 content. Most Mahaweli river sediments have TiO_2/Fe_2O_3 ratios similar to the soils, and trend toward the origin, suggesting hydraulic fractionation and quartz dilution (Singh, 2009). As with the soils, some stream sediments have much higher TiO_2 contents, coupled with high Fe_2O_3, with TiO_2/Fe_2O_3 ratio between 0.13 and 0.31 (Fig. 5.1.4a). This suggests concentration in the sediments of a heavy mineral phase containing both Ti and Fe, such as ilmenite and magnetite.

Sorting effects are also evident when the compositions of the stream sediment size fractions. Fe_2O_3 – TiO_2 ratios for the 180 – 2000 µm fractions in both the main channel (MC) and tributaries (TB) fall between 0.086 and 0.13, whereas ratios in the <180 µm fractions are mainly between 0.13 and 0.31 (Fig. 5.1.4b). However, most of the <180 µm fractions in the tributaries have much higher Fe_2O_3 values than their 180 - 2000 µm fractions. This pattern is also seen in the main channel. The size fraction data thus confirm that hydraulic fractionation of Fe- and Ti-bearing phases has occurred.

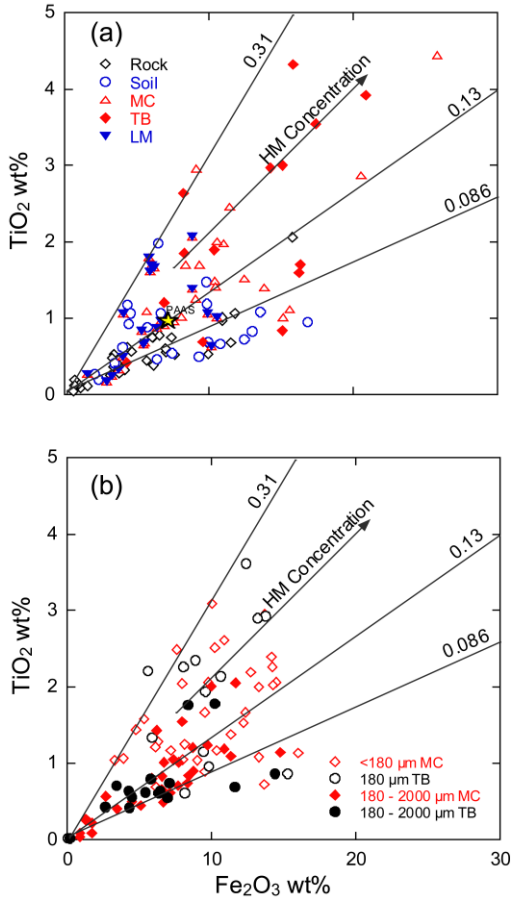

Fig. 5.1.4: Fe_2O_3–TiO_2 plots for (a) bulk stream sediments, rocks and soils, and (b) the <180 µm and 180 - 2000 µm fractions, illustrating hydraulic fractionation and heavy mineral concentration. MC – main channel; TB – tributaries; LM – lower main channel.

A Th/Sc-Zr/Sc plot (Fig. 5.1.2b) for the fractions shows higher values in <180 µm TB samples than in the MC <180 µm equivalents. The MC and TB 180 - 2000 µm fractions exhibit similar Th/Sc-Zr/Sc values to each other. On the other hand, the TB and MC <180 µm fractions both show higher values than their 180 - 2000 µm equivalents (Fig. 5.1.2b). This indicates Zr enrichment in the fine fractions in both the tributaries and the main channel, suggesting transport distance does not greatly affect sorting. Moreover, average Th/Sc (1.01) and Zr/Sc (15.29) ratios in the MC 180 - 2000 µm fractions are low, compared to average values of 3.31 and 25.16 respectively in the <180 µm fraction. These results show that both Th and Zr are enriched in the fine fractions of both the MC and TB samples as a result of sorting.

5.1.3 Heavy mineral indicators

As noted above, elements such as Y, Th, Zr, Nb, Ti and Sc are well suited for provenance and tectonic setting determination (Holland, 1978; Bhatia and Crook, 1986), but they are also good indicators of heavy minerals. Due to high durability, these minerals tend to remain in sediments during transport over long distances. Tourmaline, zircon, and rutile are associated with significant enrichments of Th, Zr and Nb, and suggest a granitic source or recycled detritus. The sediment fractions are useful for detailed description of the heavy minerals related to Th, Zr, Nb and Y.

Niobium and Th contents of the Mahaweli River rock and soil samples are lower than those in the stream sediments, in which the maximum Nb content reaches 125 ppm (Table 5.1.2). There is also no close association between the Nb values of basement rocks and their adjacent sediments. Zirconium shows similar variation to Th, and is strongly enriched in the river sediments relative to the soils and basement rocks (Table 2). The river sediments also show very strong internal correlations between Zr and Nb (+0.91), Zr and Th (+0.91), and Nb and Th (+0.86).

Distributions of these elements in the stream sediments are likely to be controlled by heavy minerals including zircon, monazite, garnet and titanite, with the lesser variability being produced by homogenization of the detrital bedload during transport. For Zr the scatter to higher values is relatively coherent, suggesting zircon concentration is the main cause of the enrichment. The spread to higher values is more scattered for Y and Nb, suggesting that multiple heavy minerals control their abundances. In contrast, Sc abundances in the basement rocks range up to 50 ppm, but decrease with increasing Th, as expected during magmatic evolution (Fig. 5.1.1d). Soils show similar values and considerable scatter, but some stream sediments scatter to higher values of both Sc and Th, suggestive of different heavy mineral concentration in these samples.

The incompatible element pairs Th-Y, Th-Zr, and Th-Nb (Fig. 5.1.5) for the <180 μm and 180 - 2000 μm fractions of the sediments show higher abundances of Y, Nb and Zr are present in the <180 μm fractions. The tributaries also show high values in the <180 μm fraction, suggesting that preferential concentration of heavy minerals in the fine fraction is not a function of transport distance.

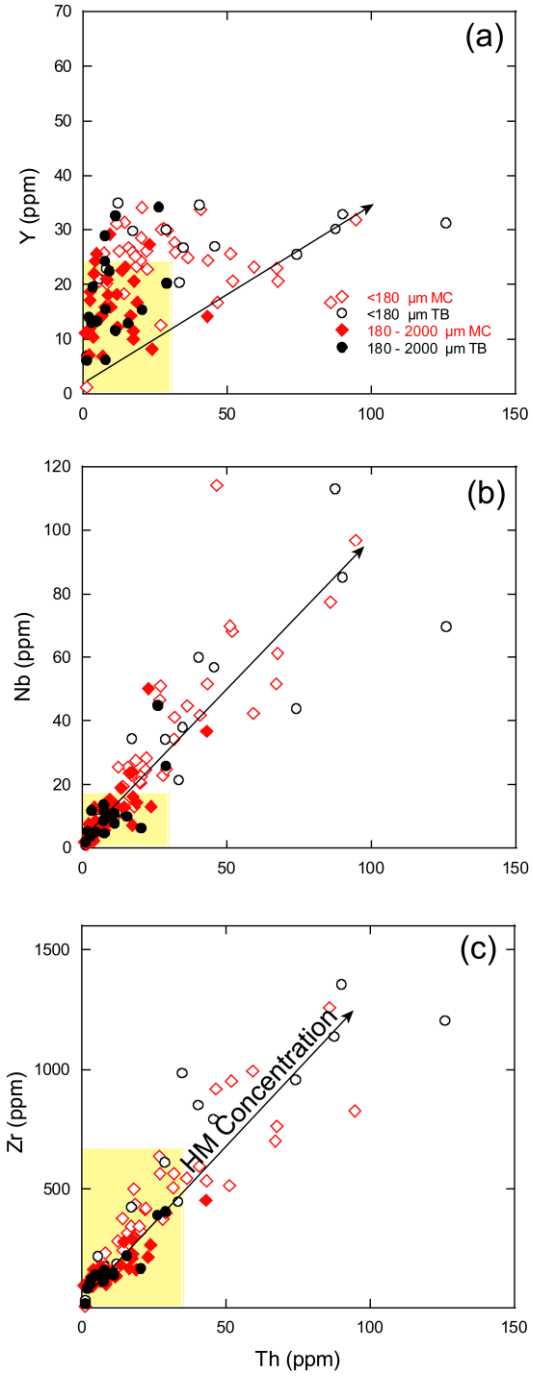

Fig. 5.1.5: Plots of (a) Y, (b) Nb, and (c) Zr versus Th for the <180 µm and 180 - 2000 µm fractions. MC – main channel; TB – tributaries. Yellow areas indicate typical ranges in alkaline rocks in the Highland Complex (data from Pohl and Emmermann, 1991).

Table 5.1.2: Average, minimum and maximum values for the bulk stream sediments, basement rocks, soils and tributaries of the Mahaweli River basin compared to the PAAS values of Taylor and McLennan (1985). Major elements as oxide wt%, trace elements ppm.

	Sediment			Rock			Soil			Tributaries			PAAS
	Avg	Min	Max	Avg	Min	Max	Avg	Min	Max	Avg	Min	Max	
Fe_2O_3	9.83	1.56	25.80	4.95	0.05	15.79	7.77	2.06	16.85	**20.88**	4.29	12.76	7.18
TiO_2	1.57	0.17	4.44	0.47	0.02	2.06	0.84	0.20	1.98	**4.32**	0.42	2.18	0.99
MnO	0.12	0.02	0.28	0.07	0.00	0.20	0.10	0.01	0.25	0.28	0.08	0.17	0.11
CaO	4.63	0.84	53.72	7.51	0.54	43.37	2.40	0.53	18.27	**49.44**	1.23	7.25	1.29
P_2O_5	0.21	0.07	0.50	0.16	0.02	0.99	0.13	0.05	0.40	0.50	0.12	0.28	0.16
As	5	1	10	2	0	7	4	1	10	8	3	6	5
Pb	25	10	43	15	5	38	23	8	75	43	15	31	20
Zn	114	18	1114	57	0	149	58	22	118	183	55	122	85
Cu	31	4	98	23	0	336	34	6	97	59	11	33	50
Ni	37	10	110	24	0	137	38	9	100	68	17	41	55
Cr	156	62	346	81	4	635	138	25	720	**304**	112	194	110
V	304	25	1158	110	5	668	189	8	353	**1158**	84	442	150
Sr	341	31	2713	299	2	1878	159	2	447	**2713**	91	564	200
Y	26	8	69	21	2	53	21	5	41	**69**	20	38	27
Nb	28	3	125	7	1	19	9	3	28	**125**	6	45	19
Zr	466	109	1426	140	10	657	215	59	643	**1426**	170	702	210
Th	26	1	141	6	0	39	13	1	66	**141**	5	45	15
Sc	22	4	44	15	1	50	20	1	50	41	13	28	16
TS	1298	236	16404	1621	228	16002	588	244	2472	**4178**	318	983	621

5.1.4 Climatic zone variation and weathering

Weathering can be determined using various methods. However, most of the commonly used weathering indices such as CIA (Nesbitt and Young, 1982), PIA (Fedo et al., 1995), CIW (Harnois 1988), and WIP (Ohta and Arai, 2007) include CaO in the calculations. The carbonate rocks in the Mahaweli River catchment naturally have high Ca contents, and LOI values of the soils and sediments range between 0.61 - 12.86 and 0.31 – 16.18 wt%, respectively. Due to the very high carbonate contents, the CIA, PIA, CIW, and WIP indexes cannot be used for weathering interpretations in the Mahaweli River. However, the ratios of immobile to mobile elements can be adopted as a measure of the degree of weathering and mobility (Nesbitt and Young, 1982; Gallet et al., 1996). In this study K_2O/Na_2O and $Al_2O_3/(K_2O+Na_2O)$ ratios (Fig. 5.1.6a, b) of the bulk stream sediments have been used to describe the weathering and elemental mobility along the course of the river across the three climatic zones. The $Al_2O_3/(K_2O+Na_2O)$ ratios (Fig. 5.1.6a) of the sediments show a clear change across the climatic zones. The wet zone

sediments are Al-rich indicating the presence of a considerable amount of clay derived from feldspars, and intense weathering in the elevated parts of the upper catchment, with decreasing intensity downstream. The lack of fine-grained material in the stream sediments suggests that mechanical weathering has also occurred. However, the presence of a considerable amount of Na (2.14 wt%) in the wet zone stream sediments indicates that the weathering process is not complete. $Al_2O_3/(K_2O+Na_2O)$ ratios decline across the intermediate zone, and level out in the dry zone, despite the quartzose and well-sorted nature of the sediments in the lower reaches of the river.

K_2O/Na_2O ratios can be strongly modified by both diagenesis and weathering. However, K_2O/Na_2O ratios show no clear trend with the climatic zones along the Mahaweli River (Fig. 5.1.6b). High K_2O/Na_2O ratios at some elevated sites with granites and metabasites in the wet zone indicate intense weathering (Fig. 5.1.6b). However, moderately high contents of K_2O at some of the wet zone stream sediment locations suggest that it is incorporated mainly in felsic fragments, because contents of potassium-rich minerals like K-feldspars, muscovite and illite are generally low in the sand fractions. The cause of the variable Na_2O concentrations between climatic zones is not yet clear; the variability may be related to both source weathering and plagioclase (albite) contributions from tributaries.

The extent and type of vegetation has a complex effect on chemical weathering rates (Stallard 1992). The upper reaches of the Mahaweli catchment area are heavily vegetated. This may affect weathering rates in a complex manner, by decreasing the exposure of fresh bedrock, while increasing moisture retention in the upper catchment. However, the type and extent of vegetation varies with precipitation and temperature, and any effect from vegetation may be incorporated in the overall weathering regime in each climatic zone.

Soils are the main products of weathering. LOI (Loss On Ignition) values for the soils in the Mahaweli River catchment (Fig. 5.1.6c) can be used as a rough measure of the weathering conditions at each site. High CaO contents of the soils (Table 5.1.1b) indicate the presence of carbonates, because gypsum cannot have formed, based on the low TS contents. Organic matter is another factor that could be associated with high LOI. The LOI values of the soils (Fig. 5.1.6c) correlate well with the $Al_2O_3/(K_2O+Na_2O)$ weathering profile (Fig. 5.1.6a), and show the same trend down the river. The high LOI values in the wet zone soils may partially controlled by the organic matter produced by vegetation in that area. The upper part of the Mahaweli catchment is

covered by dense forest, and tea and vegetable cultivation, combined with very high rainfall. The forest almost disappears towards the dry zone, where the vegetation is mainly paddy. The dense vegetation cover in the wet zone and chemical weathering has thus combined to increase the LOI in the soils.

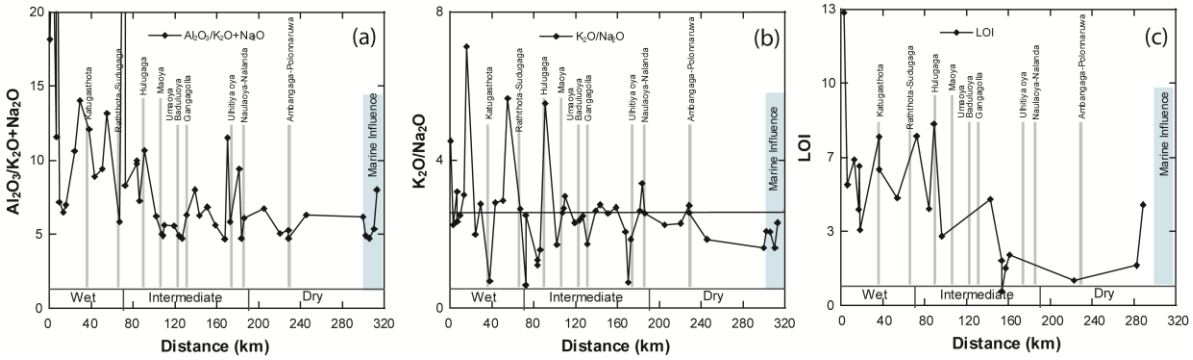

Fig 5.1.6: (a) Al_2O_3/K_2O+Na_2O (b) K_2O/Na_2O ratios in bulk sediments down the Mahaweli River showing the weathering trend with the climatic zones. (c) Loss On Ignition of soils down the Mahaweli River.

The alkaline earth elements Sr and Ca can also be used as weathering indicators. Strontium is depleted in sediments during weathering of feldspar and with increasing sediment maturity (Bhatia and Crook, 1986). The Mahaweli River sediments show strong Sr depletion in the wet zone, where intense weathering of feldspar can be anticipated (Fig. 5.1.7). Abundances in the stream sediments increase sharply in the intermediate zone with the entry of four major tributaries (Katugasthota, Raththota-Sudugaga, Huluganga, Maoya) which contain marbles in their catchments. Values are higher in the Katugasthota and Raththota-Sudugaga than in the Huluganga and Maoya, after which the values drop. The Katugasthota and Rattota-Sudugaga catchments have higher elevations and receive more rainfall than the Huluganga and Maoya catchments. The Katugasthota and Raththota -Sudugaga are thus much larger rivers and carry more water and sediment to the main river. Intense mechanical weathering due to high rainfall and erosion are thus likely to be responsible for the spikes in the Katugasthota and Raththota-Sudugaga catchments. Strontium contents then decrease steadily through the intermediate zone, suggesting progressive weathering of calcareous detritus during transport. Abundances increase

slightly downstream in the dry zone, probably due to contribution of detritus from local calc-silicate rocks, before increasing abruptly in the lower reaches and Trincomalee Bay due to marine influence. A similar pattern is observed for CaO (Fig. 5.1.7). Strontium and CaO contents of soils in the wet zone also tend to be less than those in the intermediate and dry zones (Table 5.1.1). Ranasinghe et al. (2008) observed positive correlation of CaO and Sr in river sediments in the upper Mahaweli, and these elements are also very highly correlated (+0.97) in the sediments in our study. The Sr and CaO contents in the Mahaweli River sediments are thus controlled by both weathering and source rock composition, with major contributions of CaO and Sr from tributaries containing marbles.

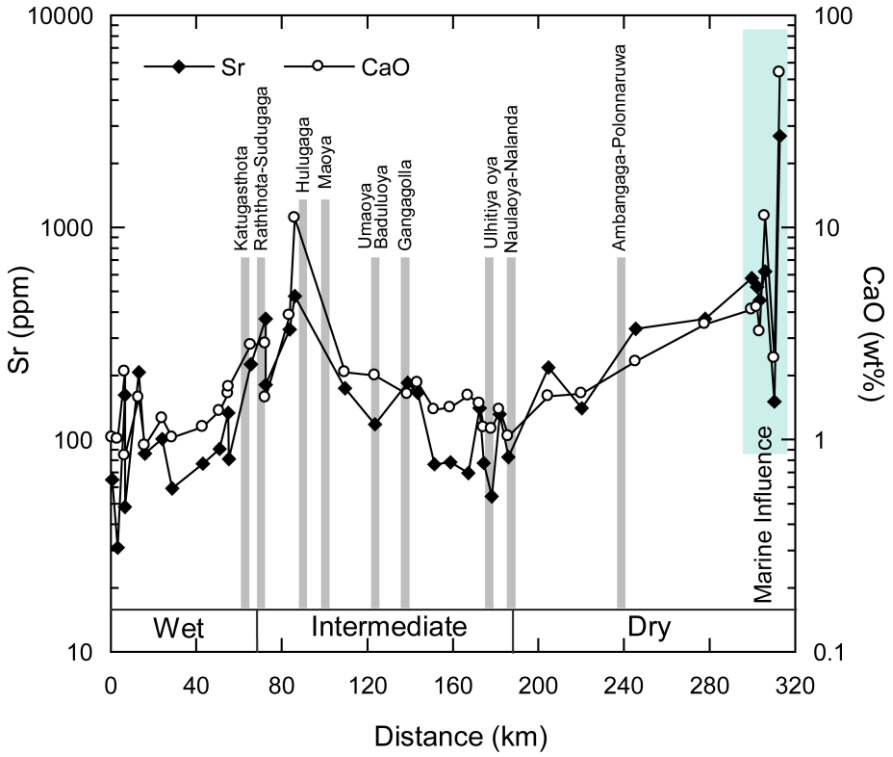

Fig. 5.1.7: Variation in CaO and Sr abundances in bulk stream sediments down the Mahaweli River, also showing tributary entries and the climatic zones.

A plot of Cr/V ratios in <180 µm and 180 – 2000 µm fractions along the main channel (Fig. 5.1.8a) shows that Cr/V is consistently greater in the 180 – 2000 µm fraction. Spikes are seen at the tributary confluences. Contrast between the fractions is slightly higher in the wet zone than in the intermediate zone, but is greatest in the dry zone. A plot of the relative enrichment

between the fractions (Cr/V_{EF}) downstream (Fig. 5.1.8b) clearly shows that Cr is progressively lost from the 180 – 2000 µm fractions in the wet zone, possibly by oxidation of reactive Cr-bearing phases such as chrome spinel (Dissanayake, 1982), chromite (Dissanayake et al., 2000) and hercynite and spinel (Ranasinghe et al., 2008) hence transferring Cr to the fine fraction. The Cr/V_{EF} then steadily increases through the intermediate and dry zones, apart from a large spike where the Ulhitiya Oya and the Naula Oya-Nalanda tributaries enter the main channel (Fig. 5.1.8b), and a large drop with the marine influence in Trincomalee Bay. This suggests that the intermediate zone tributaries supply relatively fresh coarse-grained Cr-bearing detritus to the main channel, which remains in the 180 – 2000 µm fraction down to the sea. This pattern contrasts with the findings of Ortiz and Roser (2006a), who observed a steady decline in Cr/V ratio downstream in the Hino River of SW Japan. This was attributed to progressive oxidation of ultramafic detritus and Cr-bearing heavy minerals, moving Cr from the 180 – 2000 µm fraction to clays in the <180 µm fraction. In the Mahaweli River this trend is only observed in the wet zone (Fig. 5.1.8b).

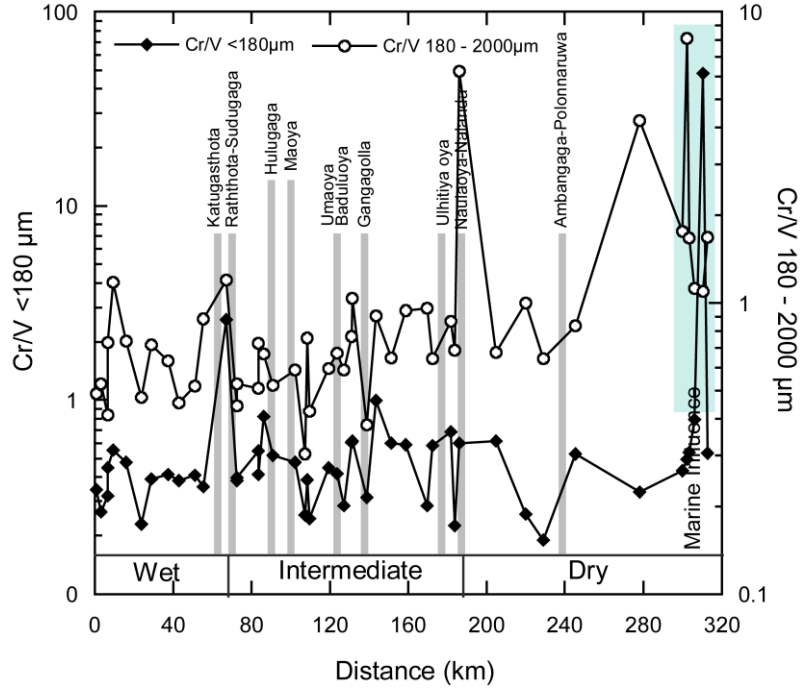

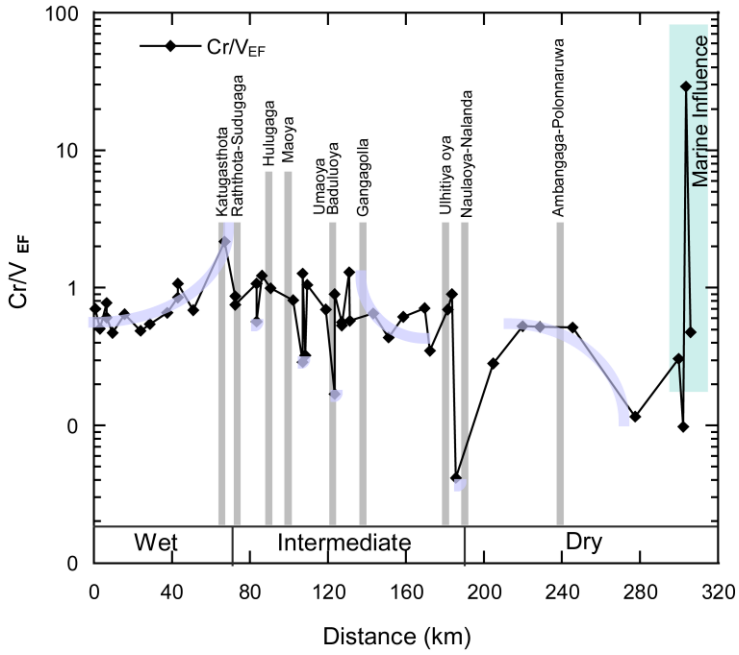

Fig 5.1.8: (a) Variation in Cr/V ratios in <180µm and Cr 180 - 2000 µm fractions in sediments down the Mahaweli River, also showing tributary entries and the climatic zones. (b) Cr/V Enrichment Factor (Cr/V_{EF}) downstream, derived by normalizing Cr/V in the 180 - 2000 µm fraction against Cr/V in the <180µm fraction.

5.1.5 Tributary effect

Stream sediments in most of the tributaries have high elemental concentrations compared to the soils and rocks (Table 1a, highlighted rows represent tributaries; Table 5.1.2). Most of the tributaries rise in elevated areas of the Mahaweli catchment, mainly in the wet and intermediate zones. The source rocks should thus have been subjected to intense weathering. The tributaries display the highest concentrations of Y, Th, Zr, Nb, Ti Sc and Fe (Figs. 5.1.2b, 5.1.4b and 5.1.5a–c)suggesting that the source rocks within them are mainly of mafic composition, and can contribute considerable amounts of heavy minerals. The high values are probably related to the local lithology in the catchment of each tributary. The main lithologies present are garnet–biotite gneiss, hornblende–biotite gneiss, granitic gneiss, charnockite and metabasite. The Umaoya and Baduluoya are the longest of the tributaries, but they do not display high concentrations of the above elements. The Umaoya and Baduluoya thus do not contribute greatly to the load of these

elements in the main river channel. In the main channel, most of these elements tend to accumulate downstream (Table 4.1.1a). The tributaries contribute to these accumulations mainly at the confluences. However, each tributary contains rocks of differing composition, and their contributions to the elemental loadings in the main river channel also differ as a result (Table 4.1.1a). More detailed studies of individual tributaries are required to evaluate local lithological controls, and the contribution of each tributary to the Mahaweli sediment load.

5.1.6 Environmental effects

The enrichment factor (EF) is a good tool to evaluate potential environmental contamination, as it can be used to differentiate between lithogenic and naturally occurring metal sources (Zhang et al., 2009; Olubunmi and Olorunsola, 2010; Naji, 2011) and to assess the degree of anthropogenic influence. EF has here been calculated using Fe as a normalizer, because iron is the fourth most abundant major element in the Earth's crust, and is usually of no contamination concern. The EF for Fe-normalized data is defined by Sutherland (2000) as:

$$EF_{metal} = \underline{(M_x/Fe_x)_{sample}} \,/\, (M_c/Fe_c)_{PAAS}$$

where M_x and Fe_x are the concentrations of the metal and Fe in the sample, respectively, and M_c and Fe_c are the concentrations of the metal and Fe in PAAS, used as an index of upper continental crust composition.

Evaluation of the EF varies a little between authors. Zhang and Liu (2002) state that EF values between 0.5 and 1.5 indicate the metal is derived entirely from crustal materials or natural processes. EF values > 1.5 suggest anthropogenic sources. Sutherland (2000) indicated EF values of <1 indicate background concentrations; values of 1-2 depletion to minimal enrichment suggestive of no or minimal pollution; 2-5 moderate enrichment; 5-20 significant enrichment; 20-40 very high enrichment; and >40 extremely high enrichment.

Plots of the EF for As, Pb, Zn, Cu, Ni and Cr along the main channel of the Mahaweli River are shown in Fig. 5.1.9. With the exception of Cr throughout the river and Pb at a few sites in the dry zone, all other elements are strongly depleted, with EF<1. According to the criteria of both Sutherland (2000) and Zhang and Liu (2002), As, Zn, Cu and Ni abundances in the

Mahaweli sediments thus represent background values, and there is no threat of anthropogenic contamination. The slight Cr and Pb enrichments are related to the local lithology, since there are no industrial point sources of contamination within the area. Spikes at the entries of tributaries are likely to be caused by heavy minerals, and there is no significant change seen with climatic zone. Furthermore, most individual Cr and Pb EFs are <1.5, within the limit for natural sources proposed by Zhang and Liu (2002).

The single Trincomalee harbor sample analyzed has been removed from these plots, since it has high EFs for all elements. The EFs for As, Pb, Zn, Cu, Ni and Cr in this sample are 2.0, 5.1, 28.9, 10.1, 3.26 and 12.5, respectively. It is thus moderately enriched in Pb and Ni, significantly enriched in Cu and Cr, and very highly enriched in Zn, using the criteria of Sutherland (2000). Consequently, there is potential for significant anthropogenic contamination in Trincomalee harbor. This will be examined in future work.

The only similar study carried out in the Mahaweli River was a detailed survey by Ranasinghe et al. (2008), but this was confined to the upper reaches. Some of the results of our study compare well with Ranasinghe et al. (2008), but others do not. Chromium contents in the stream sediments in our study are lower. Lead and Y abundances are almost the same in both studies, and the areas where anomalous Pb values occur correspond. Nickel, V and Sr show much higher values in our current study. Ranasinghe et al. (2008) also observed low Sr values in the wet zone. Copper and Zn values are lower in our current study. The contrasts seen between these two datasets are likely to be a product of the greater variability and regional extent of our sample collection.

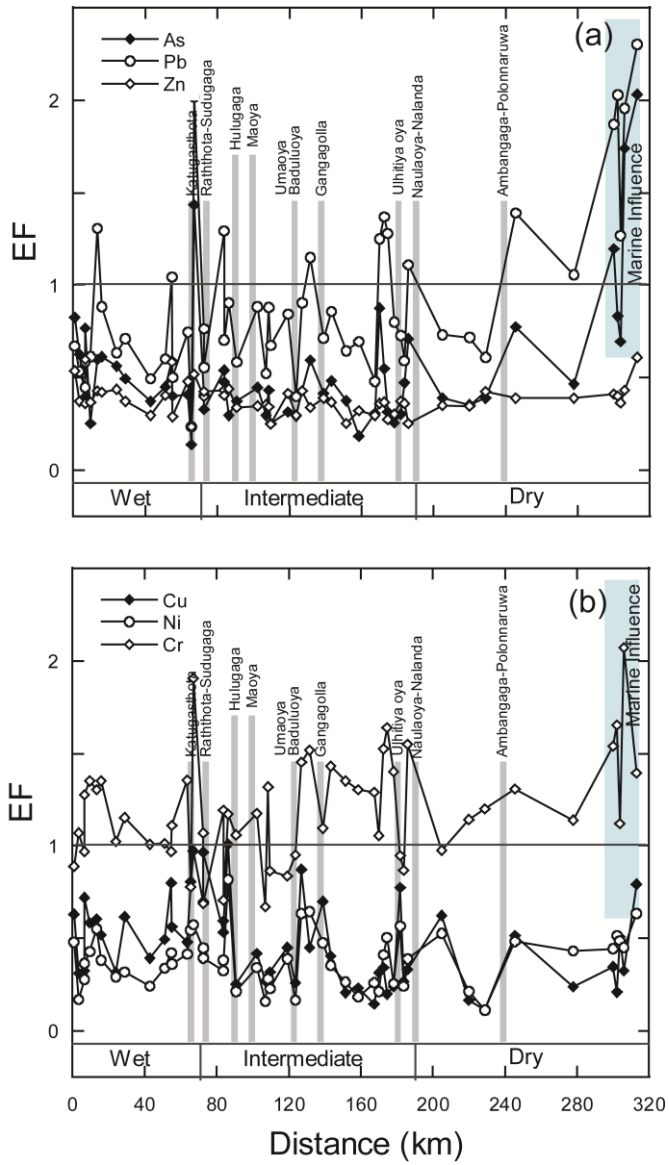

Fig. 5.1.9: Fe-normalized enrichment factors for (a) As, Pb, and Zn, and (b) Cu, Ni, and Cr down the Mahaweli River, also showing tributary entries and the climatic zones.

5.1.7 Heavy Minerals

5.1.7.1 Fractional variations of heavy minerals

The grain size and heavy mineral assemblages of river sediments and their alteration products are indicators of provenance, maturity, and the processes operating during source weathering and transport (Stow, 1929; Yang et al., 2009; Guedes, et al., 2011). It is important to

mention that the local variation of wave and current effects and the conditions under which collection is made will greatly influence the percentages of the minerals found (Stow, 1929). Studies such as those carried out by Stow, 1929; Morton and Hallsworth, 1999; Yang et al., 2009; Joshua and Oyebanjo 2009, 2010 are examples of the significance of heavy mineral assemblages in sediments.

In this study the content of magnetite in both fractions (Fig 5.1.10a,b) is highest in the upstream samples, and gradually decreases downstream. This suggests comminution or destruction of magnetite with downstream transport (Fig 5.1.10b,c). Most of the magnetite, hornblende, ilmenite and hematite in the 0.2-0.3 amp fraction decreases downstream thus, may be transformed into ferrous (oxy) hydroxides (Hounslow and Morton 2004), and thus accumulate in the clay fraction. A small proportion of the more resistant heavy minerals are carried further downstream, and are deposited in Tricomalee Bay. This is evident by the broad downstream decrease in heavy mineral content in the 63-180 μm fraction (Fig. 4.1.3). This suggests that the sediments in the Mahaweli River have been matured during transport, especially by destruction of Fe-bearing heavy minerals.

The 0.3-0.4amp portion had the highest weights of heavy minerals in both fractions, and also the highest contents along the stream, whereas abundances in other fractions decline (Fig. 5.1.10). The 0.3-0.4amp portion consisted mainly of ilmenite, tourmaline, biotite, rutile and garnet. Thus, the resistant heavy minerals are concentrated in the 0.3-0.4 amp portion, and are transported downstream. The variation in the resistant heavy minerals is due to local lithological input from tributaries. Consequently, tributary sediment load affects the heavy mineral proportions in the main channel sediments. The heavy mineral assemblage of magnetite, ilmenite, biotite, tourmaline, rutile, sillimanite, hornblende and garnet indicates derivation from mixed sources of both igneous and high-grade metamorphic rocks. Though the chemical data show that Zr concentration is high in the tributary samples, no zircon grains were found in the heavy mineral separates. Therefore, zircons may be concentrated in the fraction finer than <63 μm. In both fractions (63-180μm and 180-300μm), it is clear that heavy minerals are accumulating in the downstream reaches, and Trincomalee Bay shows high contents of heavy minerals. The detrital heavy minerals carried along the Mahaweli River are thus deposited and concentrated in southwest Tricomalee Bay, as shown by elemental distributions with the bay.

The Minipe Ela tributary (TR109) has high heavy mineral compositions in the 63-180µm fraction, and the Hatton (MC3) and Thalawakele (MC24) tributaries in the upper reached of the Mahaweli River have high magnetite (24, 29%) in both fractions. Mafic rocks are thus likely to significant in the sources in these areas.

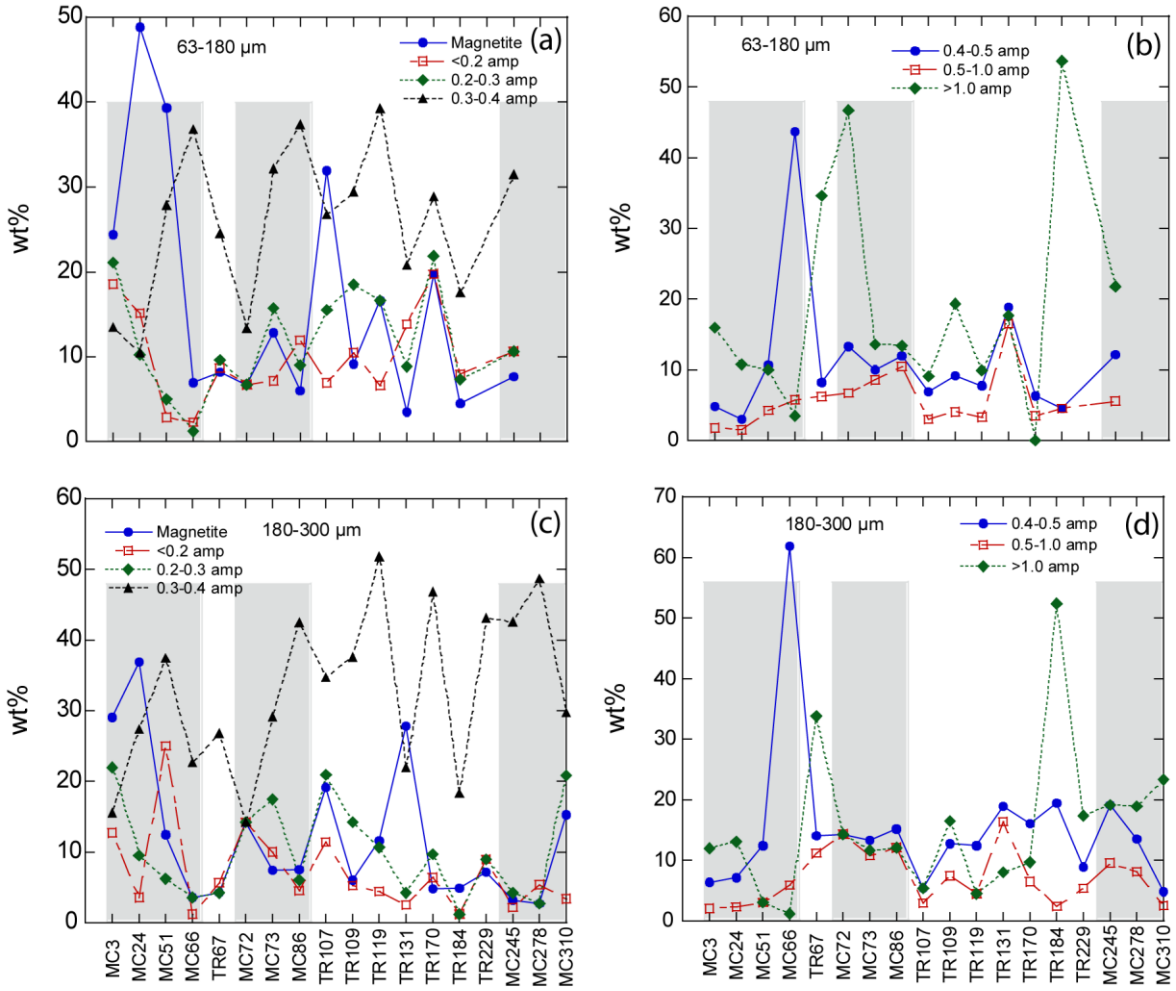

Fig 5.1.10: Variation of magnetite content and Frantzed amp separates (wt%) along the Mahaweli River (a, b): 63-180 µm fraction, (c, d): 180-300µm fraction. MC-main channel; TR—tributary; following number indicates distance (km) from uppermost sample.

5.1.7.2 Downstream chemical variation

Although the combined effects of chemical, biological and physical weathering processes transform bedrocks into soils and ultimately into sediments, original geochemical signatures of the source of sediments remain may still be retained (Formoso 2006). The geochemical compositions of stream sediments also reflect the average composition of an entire drainage basin (Reimann and Melezhik 2001). Although chemical weathering processes strongly modify original sediment compositions (Vital and Stattegger 2000), abundances of trace elements such as Sc, Th, Zr, Cr, Ni and Co are good indicators of the composition of the source (Taylor and McLennan 1985).

5.1.7.1.1 –Variation of Zr, Th, Nb

Zirconium, Th and Nb are very closely related to resistant heavy minerals (zircon, rutile, monazite, thorianite; Dissanayake et al. 2000; Vital and Stattegger 2000). All three elements are clearly enriched in the fine fraction of the sediments relative to the 180-2000 μm fraction along the main channel, except for Th and Nb at a few locations (Fig 5.1.11). The dry zone clearly shows a downstream enrichment in the <63 μm fraction, even though there are very few tributaries in this part of the river. Thus, a strong downstream accumulation of all three elements occurs in the fine fraction, as illustrated by the dotted line in Fig 5.1.11. However, the fine fractions in the Rattota-Suduganga (TR67) tributary, Muttur and Trincomalee Harbor are strongly depleted of Zr, Th and Nb (Table 5.1.3). Zirconium concentration in the coarser fraction of the tributaries is much lower (avg 177) than UCC (Upper Continental Crust, 190 ppm Taylor and McLennan 1985), whereas the fine fraction of the tributaries are enriched relative to UCC (avg 670). Though not prominent as zirconium, Th and Nb concentration are also higher (Th avg 43; Nb avg 42) in the fine fraction when compared to UCC (Th 10.7 ppm; Nb 25 ppm, Taylor and McLennan 1985). Thus, in the tributaries all three elements are strongly enriched in the fine fraction.

Table 5.1.3: Calculated EF values for fine and coarse fraction of the Mahaweli River and its tributaries

S-No	Distance(Km)	Zr	Th	Nb	Ti	Fe_2O_3	Sc	Y	V	Ni	Cr	Ca	P_2O_5	Sr	As	Pb	Zn	Cu	
MC1	1	4.2	3.9	2.9	1.7	1.3	1.4	1.6	1.7	1.3	1.2	1.2	1.2	1.7	1.2	1.4	1.5	1.5	
MC3	3	4.7	3.6	6.0	2.8	1.9	1.9	2.1	3.6	1.5	1.8	1.3	0.2	1.8	1.2	1.3	1.9	1.6	
MC7	7	2.1	1.2	1.9	1.2	1.2	1.3	1.5	1.3	1.9	1.0	1.1	1.5	2.2	1.8	1.6	1.5	2.0	
MC7	7	3.6	4.0	3.8	2.2	1.9	2.0	1.8	2.5	1.6	1.6	1.1	1.8	1.5	1.7	1.5	1.9	2.2	
TR10	**10**	**1.5**	**0.5**	**1.2**	**1.5**	**1.5**	**2.5**	**1.8**	**1.7**	**1.1**	**0.8**	**3.6**	**2.5**	**4.1**	**0.8**	**1.1**	**2.2**	**2.2**	
MC16	16	4.3	3.6	3.6	2.5	1.5	1.7	1.4	2.7	1.2	1.7	1.2	0.2	0.8	1.8	1.2	1.9	1.5	
MC24	24	3.2	2.7	4.8	2.2	1.6	2.0	1.7	2.9	1.1	1.4	1.1	1.4	1.3	1.5	1.2	1.8	1.5	
MC29	29	3.8	3.7	4.0	2.4	1.7	1.4	2.0	2.4	1.4	1.3	1.2	1.5	1.4	1.6	1.4	1.8	1.8	
TR38	**38**	**11.2**	**41.2**	**8.1**	**3.1**	**1.1**	**0.8**	**1.8**	**2.2**	**0.9**	**1.4**	**0.5**	**1.3**	**0.4**	**2.4**	**1.6**	**1.6**	0.7	
MC43	43	3.5	2.5	1.8	1.3	1.7	2.1	2.4	1.7	2.1	1.5	1.4	1.9	3.0	2.0	1.7	2.1	2.6	
MC51	51	1.7	1.2	0.5	0.7	1.1	1.4	1.1	1.0	3.1	1.1	0.9	2.1	1.6	3.3	1.9	2.1	5.7	
MC55	55	7.5	5.1	3.1	1.9	1.6	0.1	1.3	2.6	2.3	1.8	1.0	1.7	1.5	2.2	1.5	1.7	2.5	
TR67	**67**	**0.3**	**0.2**	**0.2**	**0.0**	**0.0**	**3.4**	**0.5**	**0.1**	**0.2**	**0.1**	**33.8**	**1.9**	**20.0**	**1.3**	**0.4**	**0.0**	**0.5**	
MC72	72	1.3	2.5	1.2	1.0	1.1	0.9	1.1	1.0	1.3	0.9	0.6	1.1	0.6	1.4	1.1	1.0	1.5	
MC73	73	2.2	1.8	2.1	1.3	1.3	1.3	1.3	1.5	1.2	1.1	1.1	1.2	1.2	1.1	0.9	1.3	1.3	
MC84	84	2.5	2.3	1.6	1.0	0.8	1.2	0.9	0.9	0.6	0.9	1.6	0.1	1.0	0.9	0.9	0.7	0.5	
MC84	84	3.4	7.1	5.0	2.4	1.9	1.7	1.6	2.6	1.3	1.5	1.0	1.9	0.7	1.3	1.0	1.6	1.5	
MC86	86	1.5	1.6	1.0	1.0	0.8	0.9	1.0	0.9	0.7	1.0	1.2	1.4	1.6	1.6	1.2	0.9	0.8	
TR91	**91**	**1.3**	**1.1**	**1.0**	**1.0**	**1.1**	**1.0**	**1.1**	**1.1**	**1.0**	**1.1**	**1.0**	**1.0**	**1.3**	**1.2**	**1.0**	**1.0**	**1.1**	
MC102	102	2.0	3.1	2.0	1.6	1.1	1.2	1.1	1.4	1.1	1.1	1.3	1.5	1.2	1.0	1.1	1.3	1.2	
TR107	**107**	**5.8**	**5.3**	**13.1**	**3.5**	**1.7**	**1.1**	**5.6**	**3.0**	**0.8**	**0.9**	**3.7**	**1.8**	**17.8**	**2.1**	**1.8**	**3.1**	**1.0**	
TR109	**109**	**11.0**	**29.0**	**7.2**	**4.7**	**2.5**	**1.9**	**1.7**	**6.1**	**0.9**	**2.0**	**1.3**	**0.2**	**0.7**	**2.1**	**1.0**	**3.1**	**1.9**	
TR110	**110**	**1.0**	**0.6**	**1.3**	**0.7**	**1.1**	**1.4**	**1.5**	**0.8**	**2.4**	**0.9**	**1.6**	**2.8**	**3.3**	**1.3**	**1.5**	**1.3**	**1.8**	
TR119	**119**	**5.4**	**3.9**	**2.5**	**3.5**	**1.4**	**1.5**	**1.2**	**2.7**	**0.7**	**1.9**	**1.5**	**0.1**	**0.8**	**1.3**	**0.9**	**1.0**	**1.0**	
TR124	**124**	**25.6**	**27.0**	**25.5**	**83.5**	**59.6**	**0.7**	**4.9**	**58.5**	**2.3**	**9.9**	**0.1**	**0.1**	**0.1**	**1.3**	**2.5**	**42.3**	**2.1**	
MC127	127	5.2	11.1	7.9	4.3	1.5	1.2	1.8	3.8	1.6	2.0	1.3	1.5	1.7	4.0	1.3	2.2	1.6	
MC131	131	1.3	1.0	1.0	0.9	1.2	1.1	1.1	1.1	1.4	1.4	1.2	0.1	1.5	1.2	1.0	1.2	1.4	
TR131	**131**	**2.4**	**1.4**	**3.9**	**2.1**	**2.3**	**1.4**	**1.9**	**2.6**	**1.7**	**1.5**	**0.6**	**2.7**	**0.8**	**2.4**	**1.6**	**2.7**	**3.0**	
MC139	139	5.2	11.1	7.9	4.3	1.5	1.2	1.8	3.8	1.6	2.0	1.3	1.5	1.7	4.0	1.3	2.2	1.6	
TR143	**143**	**2.5**	**2.7**	**2.4**	**1.5**	**0.7**	**0.7**	**1.0**	**0.8**	**0.5**	**0.5**	**1.2**	**0.9**	**1.1**	**0.9**	**0.9**	**0.6**	**0.4**	
MC151	151	5.4	2.6	2.0	2.2	0.7	0.6	1.2	1.4	0.2	0.6	1.5	1.0	2.1	1.9	0.8	0.7	0.4	
MC159	159	2.2	2.2	2.7	2.0	1.9	2.3	2.2	2.4	2.8	1.5	1.5	1.8	3.4	3.1	1.8	2.3	3.8	
TR170	**170**	**1.6**	**4.3**	**2.6**	**1.7**	**5.2**	**4.4**	**2.4**	**5.5**	**7.7**	**3.9**	**0.7**	**0.3**	**0.4**	**2.3**	**1.8**	**5.2**	**9.1**	
MC173	173	7.5	13.7	6.5	3.9	1.6	1.0	1.1	3.8	0.6	1.3	1.1	1.2	0.7	1.4	0.9	1.6	0.6	
MC182	182	2.5	2.7	4.0	2.2	2.0	1.6	2.1	2.2	1.8	1.5	1.3	1.5	1.7	1.9	1.5	2.0	2.1	
TR184	**184**	**3.4**	**4.4**	**6.1**	**3.9**	**2.4**	**2.6**	**1.6**	**6.5**	**2.9**	**5.8**	**2.0**	**2.8**	**3.9**	**1.6**	**1.5**	**3.7**	**3.4**	
MC186	186	5.1	24.4	43.7	27.7	4.4	24.6	3.6	111.9	1.1	4.6	2.9	3.3	4.0	2.6	1.9	5.9	1.6	
MC205	205	4.0	6.1	8.8	4.0	1.4	1.2	1.3	5.0	0.1	1.4	1.5	0.9	0.9	1.1	0.6	1.8	0.2	
MC220	220	2.6	2.8	3.7	3.0	1.8	2.1	1.8	3.9	1.9	2.0	1.9	3.2	3.1	2.1	1.9	1.9	4.2	
TR229	**229**	**3.5**	**4.3**	**3.5**	**2.9**	**2.3**	**2.2**	**1.7**	**3.7**	**2.3**	**1.9**	**1.6**	**7.5**	**1.6**	**1.8**	**1.1**	**2.1**	**1.8**	
MC245	245	4.1	2.7	3.7	2.9	1.1	1.3	1.1	2.1	0.6	1.1	1.2	0.6	1.2	1.5	0.8	1.1	0.6	
MC278	278	4.2	12.3	22.9	52.7	6.0	14.1	3.4	47.6	1.4	5.5	3.3	2.8	3.5	4.3	2.0	9.0	1.5	
MC300	300	3.1	9.4	5.2	4.7	5.6	3.2	2.1	8.0	2.7	2.4	1.3	4.5	1.4	1.8	1.4	5.2	5.9	
MC302	302	3.9	23.5	10.2	11.6	3.7	7.5	1.6	40.1	1.1	3.9	2.6	2.8	1.6	2.6	1.2	4.6	1.9	
MC304	304	0.1	0.3	0.6	0.1	0.2	0.9	0.1	0.2	2.9	7.1	0.5	0.3	0.0	0.5	0.5	78.3	19.0	
MC306	306	2.4	1.0	1.8	1.9	1.5	1.2	2.2	1.9	2.4	0.9	0.5	2.0	1.0	1.0	1.6	2.3	2.0	
MC310	310	0.1	0.3	0.8	0.1	0.2	0.3	0.1	0.2	3.7	8.8	0.3	0.3	0.0	0.4	0.4	64.5	19.0	
MC313	313	22.7	18.0	6.5	53.0	24.3	0.6	4.1	25.9	1.9	8.2	0.1	1.1	0.1	1.5	2.7	34.9	1.5	

Zirconium enrichment is almost ten times in Katugasthota (TR38) and Maoya (TR91) and eight times in Uma Oya (TR119) and more than eight times depleted in Rattota-Suduganga (TR67). In the remainder of the samples, enrichment of Zr is from one to ten times. Thus, the tributaries have considerably higher Zr while Katugasthota (TR38), Maoya (TR91), Uma Oya (TR119), Badulu Oya (TR127) and Ulhitiya Oya (TR170) are the main contributors. Thorium

enrichment is forty times in Katugasthota (TR38), almost thirty times in the Maoya (TR91), Badulu Oya (TR127) and Naulaoya Nalanda (TR184) whereas it is fifteen times in Ulhitiya Oya (TR170) and depleted nine times in Rattota-Suduganga (TR67). Thus, the highest contribution towards Th is from Katugasthota (TR38), Maoya (TR91), Badulu Oya (TR127) and Naulaoya Nalanda (TR184) tributaries. The highest Nb enrichment of fifty times is in Naulaoya Nalanda (TR184) while Maoya (TR91) is fifteen times and Katugasthota (TR38) is eight times while Rattota-Suduganga (TR67) is depleted by nine times. Therefore, in the case of Nb only few tributaries contribute. Granites are rich in Zr, Th, Nb (Pohl and Emmermann, 1991; Agnol et al. 1994; Fraser et al., 1997), and may be the main source of these elements in the tributaries.

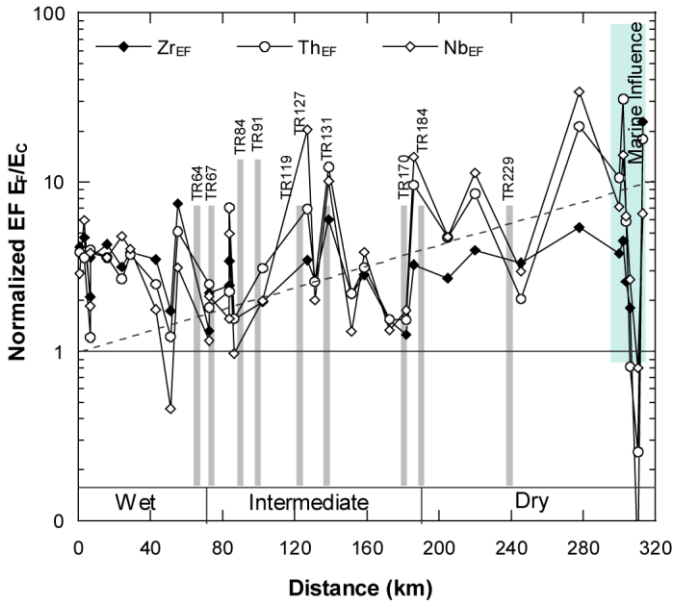

Fig 5.1.11: EF of the <180 µm (E_F – For fine fraction) and 180 – 2000 µm (E_C - For coarse fraction) sediment fractions for Zr, Th and Nb.

5.1.7.1.2 Variation of Ferromagnesian elements - TiO_2, Fe_2O_3, Sc, V, Ni and Cr ,Y

Heavy metals may be of geologic origin entering into the river system due to weathering and erosion or anthropogenic processes (Kaushik et al. 2009; Vital and Stattegger 2000).

Yttrium, TiO_2, Fe_2O_3 and Sc have similar < 180 μm EF trends downstream (Fig 5.1.12, Table 5.1.3). Although Y is a large highly charged cation, it was grouped in this category since its downstream trend is similar to those TiO_2, Fe_2O_3 and Sc. UCC values (Taylor and McLennan 1985) are TiO_2 0.5wt%, Fe_2O_3 5.04 wt%, Y 22 ppm, and Sc 11 ppm but is higher for the Mahaweli fractions in the main stream (Figs 4.1.3a and 4.1.3b).

All four elements show only moderate enrichment (EF 2-4) in the < 180 μm frctaions in the upper 70 km of the Mahaweli, within the wet zone (Table 5.1.3). Enrichments then increase variably with the entry of tributaries in the intermediate zone, and then tend to increase progressively in the lower reaches in the dry zone (Fig. 5.1.12), before becoming relatively depleted in Tricomalle Bay. They thus show changes with climatic zones and positions in the river, suggesting that climate, weathering and transport at least partially control these enrichments in the < 180 μm fraction.

The sample from the Rattota-Suduganga (TR67) tributary differs from the other locations, by showing strong depletion of these elements. In TR67 EFs are 0.6, 0.5 and 0.1 for Y, TiO_2, and Fe_2O_3, and only Sc is enriched, with an EF of 3 (Fig. 5.1.12). This shows that Ti, Fe and Y are more abundant in the 180-2000 μm fraction in this sample. Intensive weathering and high erosion rate in this tributary may cause this depletion and the source may be quartzites.

In this group of elements, the tributaries do not seem to play a key role in the < 180 μm enrichments except for the Naulaoya Nalanda (TR184) and the Badulu Oya (TR127). In the Naulaoya Nalanda (TR184), the EFs for TiO_2 and Sc are >30; and for Y and Fe_2O_3 ~4 (Fig. 5.1.12); for the Badulu Oya (TR127) the EF for TiO_2 is ninety times, and that for Fe_2O_3 sixty times, although those for Sc and Y are less than two. In all the other tributaries, the enrichments are less than five times. The Naulaoya Nalanda (TR184) and Badulu Oya (TR127) may thus influence the downstream accumulation of ferromagnesian elements, indicating contribution from mafic sources. The dry zone shows a gradual increase for all elements, and hence the downstream enrichment in the main channel may be produced accumulation of weathering products the finer sediments.

Overall enrichment in the < 180 μm fraction downstream is indicated by the dotted line in Figure 5.1.12. Yttrium RFs gradually increase from the intermediate to the dry zone. However, in the dry zone the enrichment is much less than for Ti, Fe and Sc. Apatite is a potential carrier of yttrium, but source of yttrium is not clear, since P_2O_5 variation is not coherent with that of Y.

Clays may therefore be the main host of yttrium in the < 180 µm fraction. The heavy mineral assemblage ilmenite > titanite > rutile is abundant in the Mahaweli River sediments, and this likely influences the high Ti and Fe contents in the finer sediments (Dissanayake et al. 2000). According to Dissanayake and Rupasinghe 1986, the charnockite–granite association and related pegmatites of the Highland Complex are the source of Nb and Y. The enrichment factors for all four elements are elevated in the dry zone compared to the wet and intermediate zones. Climatic conditions in the wet, intermediate and dry zones may thus have influenced weathering of the source rocks. The weathering products are transported downstream and accumulate in the finer sediments within the dry zone. Since there are no tributaries entering the dry zone, contribution of fresher material does not occur. Finally, EFs fall in the marine environment of Trincomalee Bay, due to concentration of coarser size grades and heavy minerals around the shore of the harbor and in the Mahaweli delta, and outwash of the finer size grades to the sea.

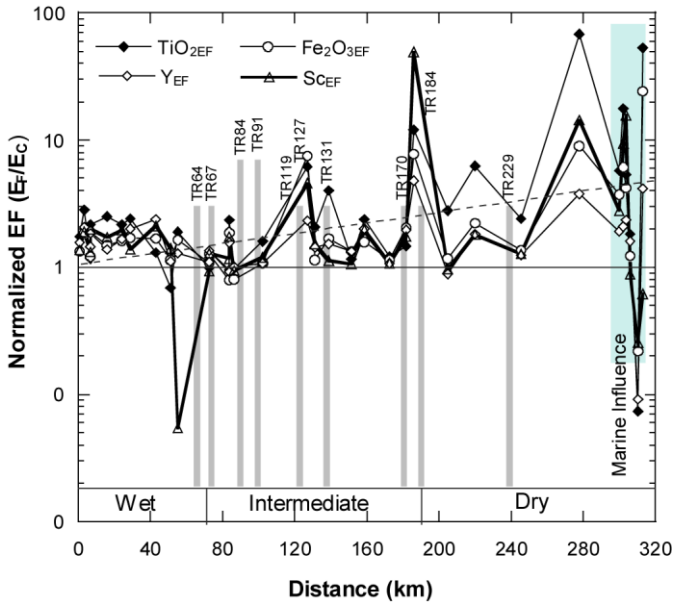

Fig. 5.1.12: EF of the <180 µm (E_F – For fine fraction) and 180 - 2000 µm (E_F – For coarse fraction) sediment fractions for ferromagnesian elements (Ti, Fe, Sc, Ni) and Y.

Vanadium, Ni and Cr are commonly associated with ferromagnesian minerals (McBirney 1998) and are also bound with Fe-oxides (Yu et al. 2001). These elements behave more or less

similarly in the wet, intermediate and dry zones, but upon entering the dry zone the dispersion becomes greater, particularly for Ni (Fig 5.1.13). However, the EFs of all elements in the wet zone are generally 1-3, and in the intermediate zone within 0.2 – 8 and 0.2 – 10 times in the dry zone with a few exceptions. The Maoya (TR91), Badulu Oya (TR127), Ulhitiya Oya (TR170) and Naulaoya Nalanda (TR184) (Fig 5.1.13) are the tributaries that contribute the highest levels of these elements in the < 180 μm fraction. The enrichment for V in Naulaoya Nalanda (TR184) is higher than hundred times (Fig 5.1.13), Badulu Oya (TR127) is sixty times and six times in Maoya (TR91). However, Ni EF is only 8 in the Ulhitiya Oya (TR170). Chromium EFs are <6 in all tributaries. Vanadium shows 0.2 – 0.3 times depletion in one sample from Trincomalee Bay, while enrichments of 40 to 100 times are observed in the dry zone samples.

The results show downstream accumulation of Cr and V in the < 180 μm fraction, but this is not observed for Ni, although it is enriched in some tributaries. This indicates that Ni is contained coarser detritus in the 180-2000 μm fraction in the main channel, whereas in the tributaries it is contained in the fine fraction. The overall accumulation of Cr and V in the finer sediments along the river, as shown by the dotted line (Fig 5.1.13) suggests destruction of Cr and V-bearing heavy minerals and lithic fragments with transport, as has been demonstrated to occur for ultramafic material along the Hino River in SW Japan (Ortiz and Roser, 2006a). The influence of mafic components of V, Ni and Cr is more pronounced in the dry zone than the intermediate and wet zones (Fig 5.1.13). The influence of tributaries is seen in Maoya (TR91), Badulu Oya (TR127), Ulhitiya Oya (TR170) and Naulaoya Nalanda (TR184), especially for V. Chromium is found in garnet, chromite, and gem minerals such as emerald, jade, ruby, spinel and alexandrite, all of which have been reported from the Mahaweli River (Cooray 1984). The heavy mineral separations showed that the fine sand in the lower reaches of the Mahaweli are rich in heavy minerals. Thus, these may accumulate in the fine sediment fraction in the dry zone as gradient decreases. Magnetite is also a main carrier of V (Moskalyk and Alfantazi 2003). Magnetite was observed in considerable quantity during the heavy mineral separation of the Mahaweli River sediments (Fig 5.1.10ac). Comminution and oxidation of magnetite and production of Fe-oxyhydroxides during transport could thus be responsible for transfer of V from the coarser fraction of the bedload to the finer fraction.

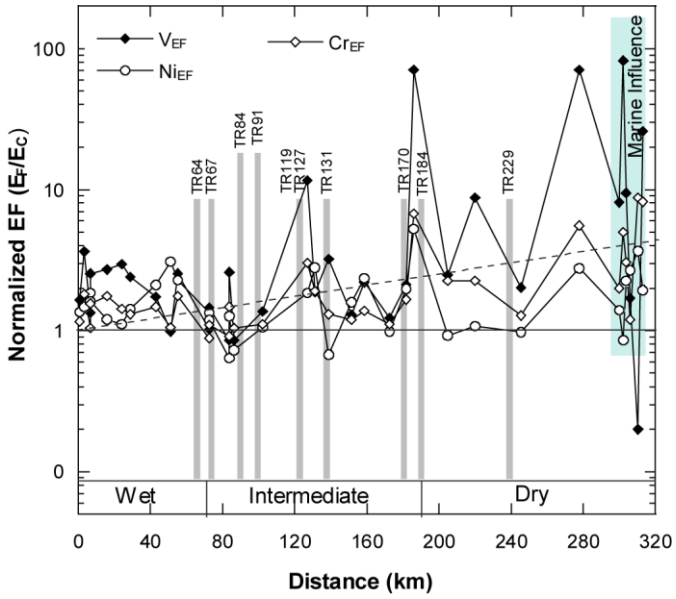

Fig. 5.1.13: EF of the <180 µm (E_F – For fine fraction) and 180 - 2000 µm (E_F – For coarse fraction) sediment fractions for ferromagnesian elements (V , Ni) and Cr.

5.1.7.1.3 Large ion lithophile elements - CaO, P_2O_5, Sr

Calcium and Sr are mainly associated with calcite and aragonite, whereas phosphorous is associated with apatite and Ca-P and Al-P phases (Lookman et al. 1996). Calcium and Sr EFs follow similar trends along the main channel, whereas P is mainly concentrated in the larger fractions, showing depletions in some tributaries in the intermediate zone (Fig 5.1.14). However, P does not show much downstream accumulation. Some P may have been lost from the sediments due to dissolution of soluble phases, so its behavior is likely to be complex.

Calcium and Sr both show general downstream accumulation in the fine fraction. However, considerable enrichment of Ca and Sr (around thirty times) is seen in the Rattota-Suduganga (TR67) tributary, and slight enrichment in the Maoya (TR91; EF 4; Fig 5.1.14, Table 5.1.3). On the other hand, CaO (0.05) and Sr (0.01) show depletion in the Badulu Oya (TR127), (Table 5.1.3). In contrast to the tributaries, depletion is seen in the Trincomalee Bay samples for all three elements. These depletions are probably due to relative concentration of bioclastic $CaCO_3$ in the 180-2000 µm fractions in higher energy environments within the bay.

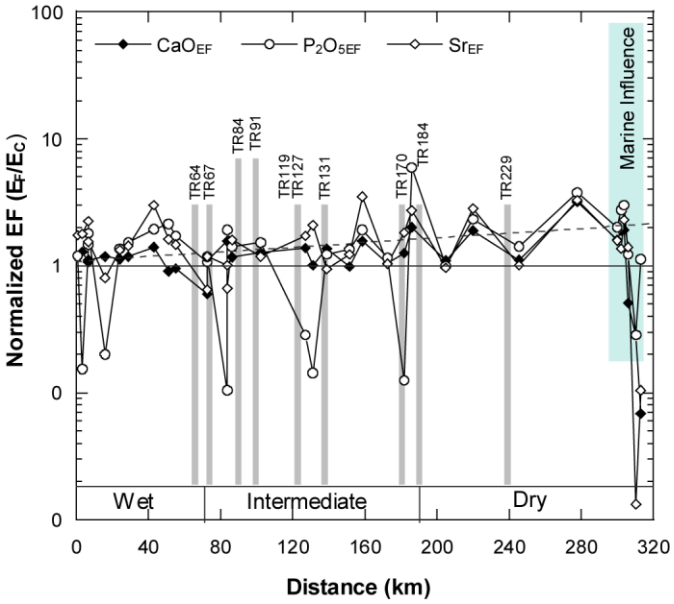

Fig. 5.1.14: EF of the <180 µm (E_F – For fine fraction) and 180 - 2000 µm (E_F – For coarse fraction) sediment fractions for large ion lithophile elements (Ca, P, Sr).

5.1.7.1.4 Chalcophile elements - As, Pb, Zn, Cu

The elements As, Pb, Zn, Cu are often elevated due to contamination (Zdenek 1996; Giusti 2011) and thus sediment quality guide lines have been developed for these elements (Byrne et al. 2010). Arsenic, Pb, Zn and Cu are mainly related to anthropogenic or natural activities if present in amounts significantly greater than UCC. Very high abundance may be related to mining sites (Byrne et al. 2010). Enrichment trends for As, Pd, Zn and Cu in the Mahaweli River show very similar patterns along the main channel (Fig 5.1.15). For all the four elements dispersion is least in the intermediate zone, and greatest in the dry zone. Anomlous enrichments from the tributaries are also limited. Zinc in the Badulu Oya (TR127) is enriched by fifty times and in the Rattota-Suduganga (TR67) this element is depleted by 0.2 times. All four elements generally show EF values of ~1-3 along the river, indicating only moderate concentration in the fine fraction. Most samples in Trincomalee Bay are enriched are < 180 µm fraction with the change to a marine environment. This indicates the possibility of some anthropogenic contamination in the Trincomalee Harbour area, where Cu and Zn enrichments are the most prominent. Except for arsenic, the other three elements are depleted in the Rattota-

Suduganga (TR67). The climatic zones also show no difference in the dispersion of the four elements. This indicates that climatic conditions have little or no influence on the downstream transport of elements along the stream. Nevertheless, a slight downstream accumulation in the fine fraction is evident for all four elements, as shown by the dashed line in Figure 5.1.15.

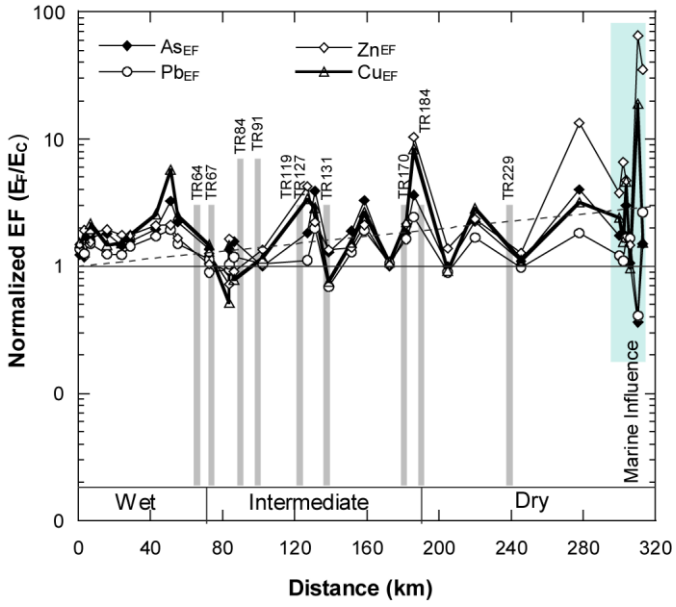

Fig. 5.1.15 : EF of the <180 µm (E_F – For fine fraction) and 180 - 2000 µm (E_F – For coarse fraction) sediment fractions for Chalcophile elements (As, Pb, Zn, Cu).

5.1.7.3 Proportionate tributary contributions

In general, concentrations of heavy metals and heavy minerals tend to increase as grain size decreases (Zdenek 1996; Singh et al. 1999; Yang et al. 2009). As a result of abrasion and sorting, rivers with gravel beds show strong downstream fining (Ferguson et al. 1996). This process takes place by grain size decreasing exponentially with distance, provided there are no lateral inputs of coarse sediment from tributaries and valley sides (Surian 2002; Radoane et al. 2008). Thus, if the sediments undergo fining due to mechanical or hydraulic weathering along the stream, then the heavy minerals and associated metals will wind up in the fine fraction. Consequently, high elemental concentrations in the fine fractions suggest that intense weathering

and hydraulic and mechanical sorting has taken place along the stream. This discussion shows that tributary inputs in the Mahaweli River disturb the downstream sediment composition.

Entries of the tributaries into the Mahaweli River play a major role in the elemental variations along the main channel (Fig 4.1.3, Table 4.1.4a, 4.1.4b). Sediments from the Rattota-Suduganga (TR67) have a very different composition compared to all other tributaries. EFs in this tributary are depleted, except for Ca, P and Sr, which show enrichment (Figs 5.1.10 - 5.1.15). The underlying basement within the Rattota-Suduganga (TR67) catchment is mainly composed of hornblende, marble and carbonate rocks. As a result, bulk sediments (calculated from two fractions) from the Rattota-Suduganga have high Sr (2713 ppm) and Ca 49.44 wt%, and very low Fe_2O_3 (4.29 wt%) contents. This indicates that the EF depletion observed for many elements is due to the unusual compositions of the hornblende, marble and carbonate source rocks. On the other hand, the flow rate of Rattota-Suduganga (TR67) is high, and the rate of erosion and mass transport is large.

Sediments from tributaries may have very different elemental compositions (Caitcheon 1998), and this is seen clearly in the Mahaweli River tributaries. The Ulhitiya Oya (TR170), Naulaoya Nalanda (TR184), Rattota-Suduganga (TR67), Badulu Oya (TR127), Maoya (TR91), Katugasthota (TR38) and Ambangaga-Polonnaruwa (TR229) all contribute significant sediment loads to the main channel. The sediments transported downstream undergo sorting and fining, and hence the high elemental concentrations in sediments in the tributaries are transported to the main river, and consequently alter the main channel sediment composition. The Uma Oya (TR119) is the longest tributary that enters the Mahaweli River, but it does not show very high EF enrichments or depletions. Furthermore, the second longest tributary Badulu Oya (TR127) does not carry large quantities of heavy minerals. The basement rocks in the Badulu Oya are mainly quartzites, and erosion rates are high. These are contributing factors for low heavy mineral load from that source. Ferromagnesian elements are mainly enriched in the Naulaoya Nalanda (TR184), where they are contributed by mafic rocks.

Zircon, Th and Nb are mainly brought into the main river through tributaries, especially in the intermediate zone. Consequently, these tributaries make a major contribution to the high Zr, Th and Nb contents in the main river, by supply of zircon, rutile, monazite and thorianite. Most of the main tributary confluences lie in the wet and intermediate zones. Weathering products from the upper reaches of the wet and intermediate zone are brought to the mainstream

through tributaries, and these would include resistant heavy minerals such as zircon, rutile and monazite. However, the main channel samples in the wet and intermediate zones do not show any notable variation, suggesting the impact of the material entering from the tributaries is rapidly diluted by the larger sediment load in the main channel. However, climatic zones do seem to have a slight influence on the abundances of Zr, Th and Nb, based on the enrichments of these elements in downstream areas in the dry zone, where the resistant heavy minerals can accumulate due to lower gradient. The tributaries also disturb the downstream fining, especially in the intermediate zone.

5.1.8 Major Elements and its geochemical assessment for sediments rock and soil

The geochemistry of clastic sediments is controlled by at least four factors: source rock composition, weathering of the source rocks, sorting of the weathered detritus and post-depositional alteration during diagenesis and metamorphism (Sawyer, 1986). Therefore, consideration of the major element composition is more important.

The Basicity index (BI) is calculated by BI = (TFeO*+MgO)/(SiO_2+K_2O+Na_2O). The difference in basicity index for the <180µm, 180- 2000µm sediment fractions may be due to the relative variations in Na, K and Mg (Fig: 5.1.16).

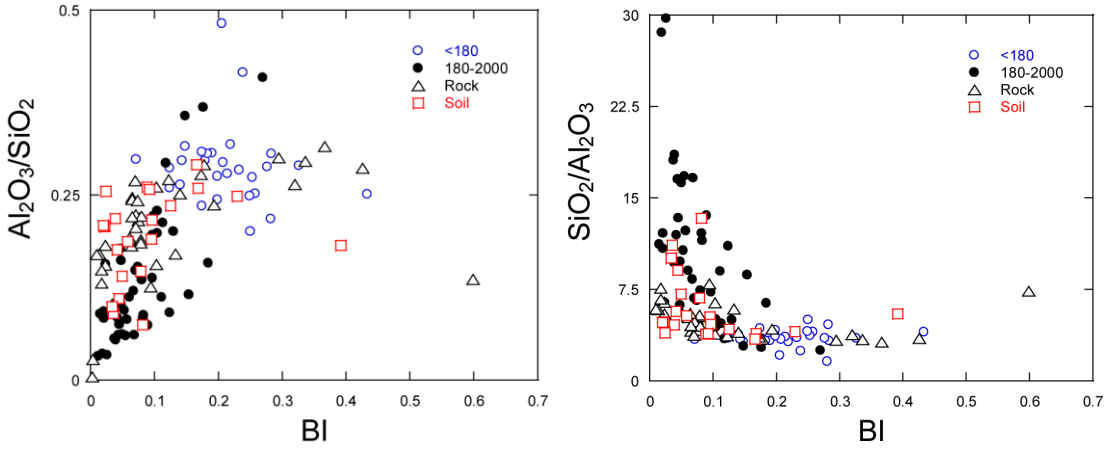

Fig 5.1.16 : Al_2O_3/SiO_2 – Basicity index SiO_2/Al_2O_3 – Basisity index plots for the <180µm, 180-2000µm sediment fractions, rocks and soils of the Mahaweli river basin.

The SiO_2/Al_2O_3 plot show that the <180µm fraction has a low BI and 180- 2000µm sediment fraction has a higher BI. Thus, the detrital trend is from the <180µm to the 180-2000µm fractions while the soils and the rocks are intermediate. The <180µm consists of mainly clays and the <180-2000µm fraction consists mainly of quartzes.

The A-CN-K ternary diagram is very useful for examining provenance and weathering histories (and K-metasomatism) because predictable, systematic trends are associated with the weathering of fresh bedrock (Nesbitt and Young 1984 ; Fedo et al., 1995).

Nesbitt and Young (1982) introduced the simple Chemical Index of Alteration (CIA) which monitors the progressive alteration of plagioclase and potassium feldspars to clay minerals. The wide applicability was from the fact that feldspars are the dominant minerals of the upper crust (Nesbitt and Young, 1984). The CIA equation is:

$$CIA = [Al_2O_3/(Al_2O_3+CaO^* + Na_2O + K_2O)] * 100$$

In A-CN-K diagrams, intensely weathered samples plot in positions commensurate with high CIA's (80 - 100), whereas incipiently weathered samples plot near the feldspar join (CIA = 50-70).

The CIA for the Rock, Soils and sediment fractions (<180µm and 180 - 2000 µm) are within 40 – 100 (Fig 5.1.17a, b, c). The soils show a trend towards Muscovite while the sediments are well within a trend line starting from felsic rock composition. The source rocks are mainly felsic (Fig 5.1.17a).

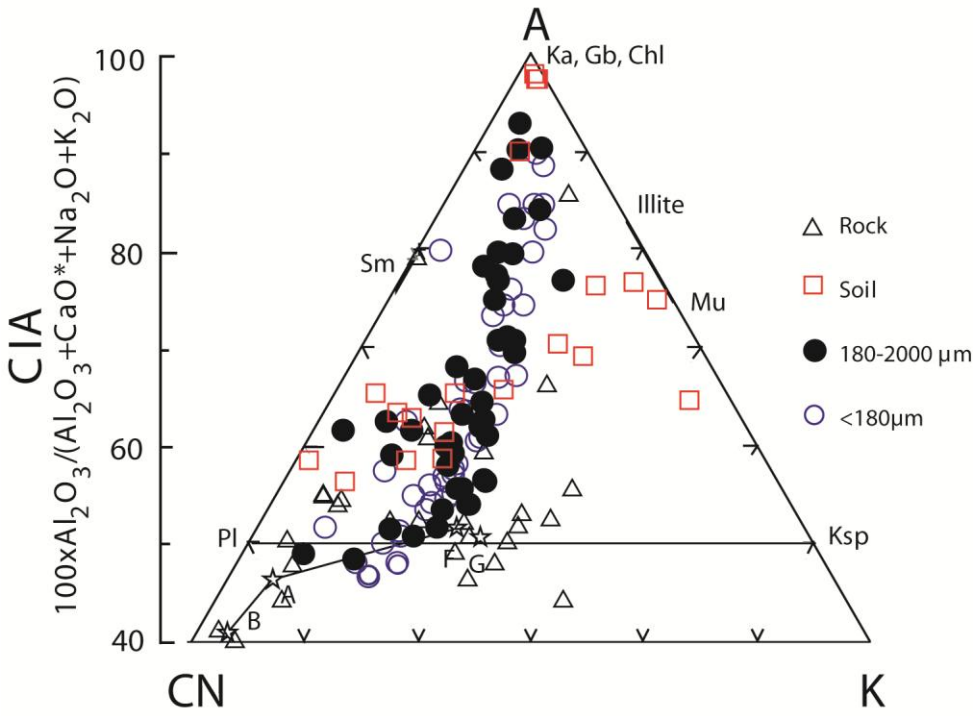

Fig 5.1.17a : A–CN–K plot (Nesbitt & Young 1984) for the Rock Soils and sediment fractions of the Mahaweli River. A = Al_2O_3, CN= CaO* + Na_2O, K = K_2O. Ka, kaolinite; Gb, gibbsite; Chl, chlorite; Mu, muscovite; Pl, plagioclase; Ksp, K-feldspar. Stars, B, A, F, average Late basalt, andesite, and felsic volcanic rock, respectively (Condie 1993).

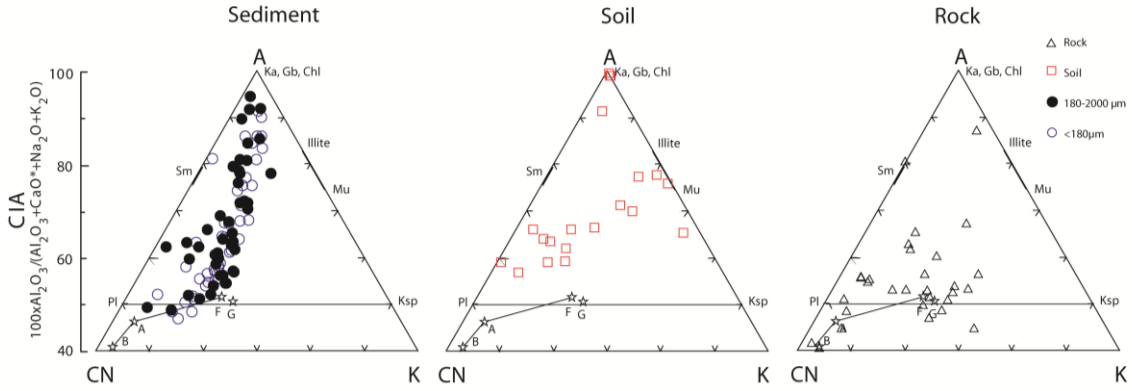

Fig 5.1.17b : A–CN–K plot (Nesbitt & Young 1984) for the (a) sediment fractions (b) soils and rocks of the Mahaweli River.

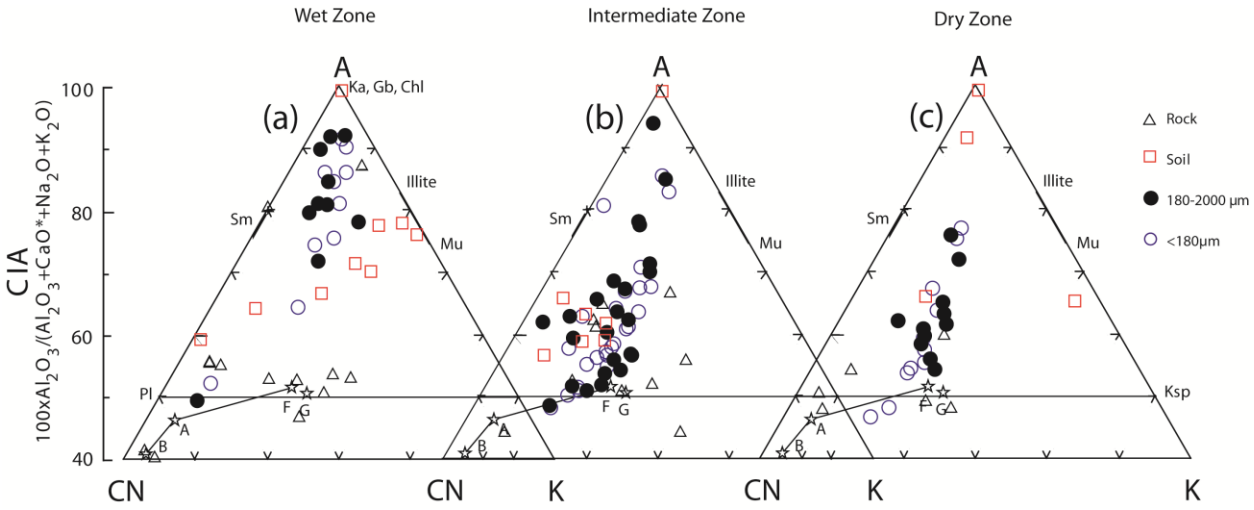

Fig 5.1.17c: A–CN–K plot (Nesbitt & Young 1984) for the Rock Soils and sediment fractions of the Mahaweli River for the three climatic zones.

In the three climatic zones it is clear that the wet zone has the highest weathered sediments and soils (Fig 5.1.17c) with CIA between 65 – 100. The Intermediate and the Dry zones do not show much of a difference with CIA and ranges within 50 – 70. Thus the uppermost weathering is seen in the wet zone while the intermediate and the dry zones are not subject to much weathering and only transport is been taken place.

In modern weathering profiles, kaolinite is the dominant mineral formed from the weathering of plagioclase (Nesbitt and Young, 1989). Plagioclase is destroyed much more rapidly than K-feldspar (Nesbitt and Young, 1984), so that kaolinite is the dominant clay formed during weathering of a plagioclase-rich source rock. The Plagioclase index of alteration (PIA; Fedo et al., 1995) can be used where plagioclase weathering alone needs to be monitored by the following equation:

$$PIA = 100*(Al_2O_3 – K_2O)/(Al_2O_3 + CaO* + Na_2O –K_2O)$$

The PIA values of the sediment fractions are within 50 – 100 and the soils are within 60 – 100 (Fig 5.1.18a and 5.1.18b) indicating the presence of small amounts of plagioclase feldspars in sediments and soils. Both the fractions spared throughout 50 – 100. Susceptibility to weathering in the feldspars is in the order;

Ca-rich plagioclase > Na-rich plagioclase > K-feldspar

Thus, all these three components may be present in the sediments and the soils of the Mahaweli River and basin due to the wide range of PIA.

The PIA of the rocks are within 50 – 80 (Fig 5.1.18b) comparatively low and may be due to presence of various kinds of rocks and mainly of less weathered rocks. The rocks have a scatter and take a different trend than the soils and the sediments. Climatic difference shows clearly that the wet zone sediments and soils are plotting at the A-K apex (Fig 5.1.18c) and PIA is within 80 - 100. Thus, the plagioclase is much altered in the wet zone indicating much less plagioclase feldspars. The intermediate zone sediments have a wide range of PIA of 50 – 100 thus considerable amounts of plagioclase feldspars are present in the sediments. Thus fresh material has been brought in by the tributaries. Dry zone sediments mainly have a PIA of 50 – 70 and thus may consist of small amounts of plagioclase feldspars and only transport the sediments and do not make a difference. Therefore, the wet zone is much weathered compared to the intermediate and dry zones.

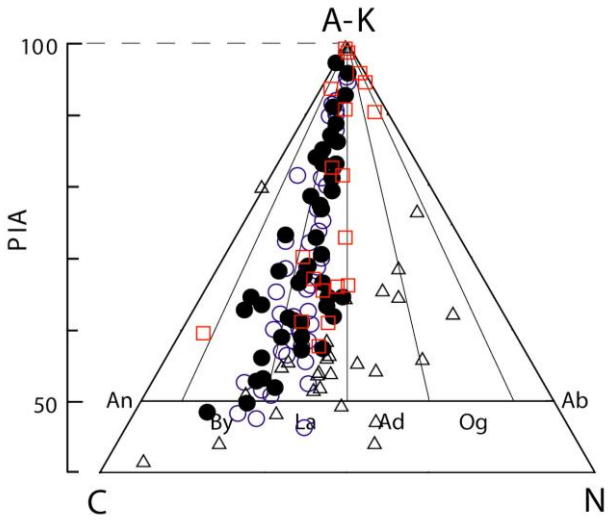

Fig 5.1.18a: (A–K)–C–N plot (Fedo et al. 1997) for the Rock Soils and sediment fractions of the Mahaweli River for the three climatic zones. An, anorthite; By, bytownite; La, labradorite; Ad, andesine; Og, oligoclase; Ab, albite.

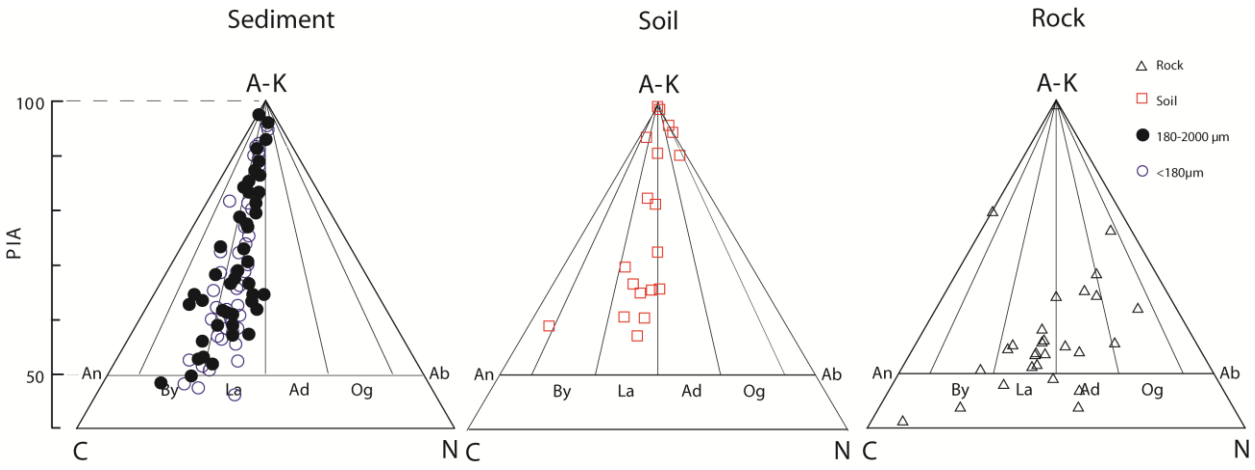

Fig 5.1.18b: (A–K)–C–N plot (Fedo et al. 1997) for the (a) sediment fractions (b) soils and (c) rocks of the Mahaweli River. An, anorthite; By, bytownite; La, labradorite; Ad, andesine; Og, oligoclase; Ab, albite.

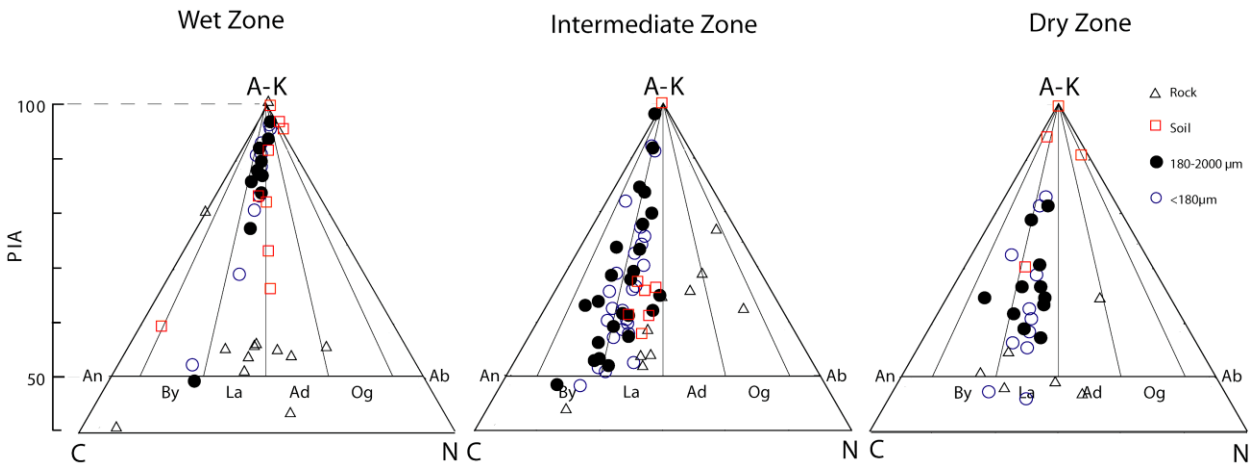

Fig 5.1.18c: (A–K)–C–N plot (Fedo et al. 1997) for the Rock Soils and sediment fractions of the Mahaweli River for the three climatic zones. An, anorthite; By, bytownite; La, labradorite; Ad, andesine; Og, oligoclase; Ab, albite.

To illustrate the approximate mineralogical composition of sediments and sedimentary rocks, major element data of all the samples have been plotted in the mafics triangle (Nesbitt and Young 1984; Nesbitt and Wilson 1992). The sediment and soils plot close to the source rocks of

granites (Fig 5.1.19a). The rocks are a bit scatted indicating many rock types within the Mahaweli river basin. Therefore, the sediments show a scatter within the source rocks. The wet zone soils are much closer to the A apex indicating much weathers clays (Fig 5.1.19b) and the sediments are much closer to the A-FM line with more felsic composition. The intermediate and wet zone sediments are drawing towards the FM apex indicating felsic source.

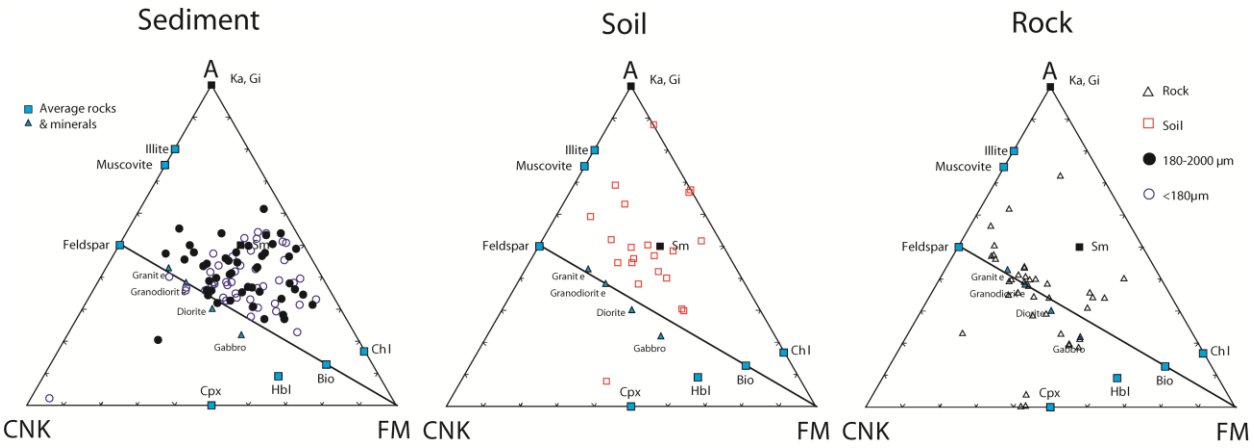

Fig 5.1.19a: Mafics ternary plot of A-CN-K (Nesbitt and Young 1984) and A-CNK-FM (Nesbitt and Young 1989) for the sediment factions, soils and rocks of Mahaweli River and its catchment. A is molar proportions of Al_2O_3, CNK represents $CaO* + Na_2O + K_2O$ and FM identifies FeO_T +MgO. The typical mineral compositions (Nesbitt and Young 1984, 1989) and average igneous rocks (Cox et al., 1979). Mineral and rock abbreviations: Ka – kaolinite, Gb – gibbsite, Chl – chlorite; Musc – muscovite; Plag – plagioclase; Ksp- K-fldspar; Bio-biotite; Hbl-hornblende; Cpx- clinopyroxene; BA – basalt; AN – andesite; GD – granodiorite; GR- granite.

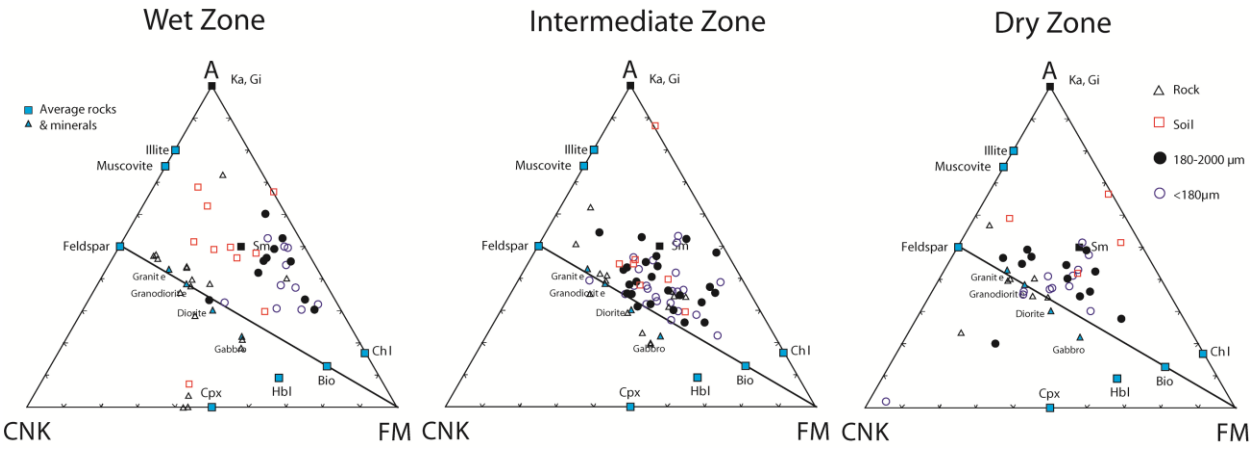

Fig 5.1.19b: Mafics A-CNK-FM ternary plot of Nesbitt and Young (1984). A is molar proportions of Al_2O_3, CNK represents $CaO* + Na_2O + K_2O$ and FM identifies $FeO_T + MgO$ for the sediment factions, soils and rocks of Mahaweli River and its catchment based on the three climatic zones.

The Mahaweli river sediment fractions, soils and rocks have been plotted in silica-alkali-mafic (SAM) diagrams (Kroonenberg, 1994) to show the variability due to lithology, sorting and weathering in each of it (Fig 5.1.20a). acid plutonics produce mainly individual quartz and feldspar grains, their relative proportions depending upon the degree of chemical weathering in the source area. Thus the SAM diagram can plot chemical composition in such a way that;

(1) The geochemical differentiation of magmatic source rocks becomes evident,
(2) The effect of sorting and
(3) The maturity of the sediments as a result of pre- or post-depossitional chemical weathering or recycling of sediment (Kroonenberg, 1994) is seen.

The <180µm sediment fraction plot very close to the M apex indicating mafic composition and the 180 - 2000 µm fraction is away from the M apex and is much scattered towards the S apex indicating much quartz (Fig 5.1.20a). The soils are also much scatted and close to the M apex. Most of the rocks plot well on the source rock line while a few are away and consisting of mafic components.

In all three climatic zones the <180µm and 180 - 2000 µm sediment fractions are well apart from each other. Thus, they show well sorted effect where in the dry zone the 180 - 2000 µm sediment fraction scatter and plotting towards the S apex is due to quartz (Fig 5.1.20b).

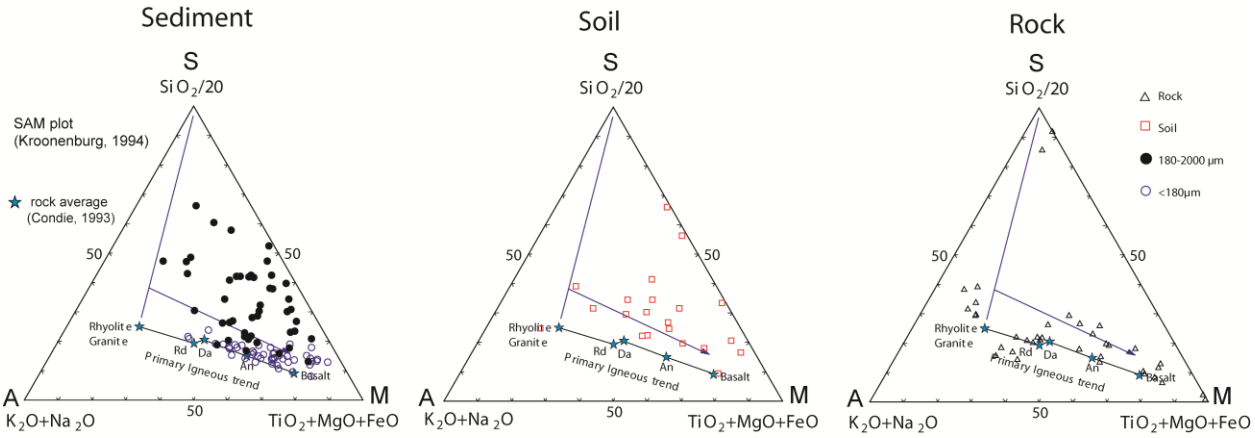

Fig 5.1.20a : SAM-plot (after Kroonenburg, 1994) for the sediment factions, soils and rocks of the Mahaweli River and its catchment. S = $SiO_2/20$; A = K_2O+Na_2O; M = $TiO_2+MgO+FeO_T$ (wt%).

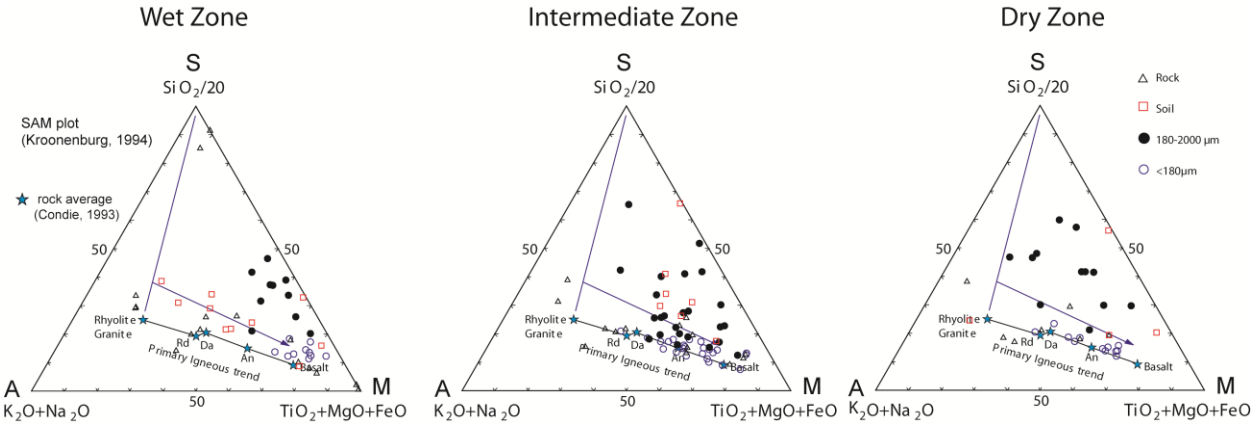

Fig 5.1.20b : SAM-plot (after Kroonenburg, 1994) for the sediment factions, soils and rocks of the Mahaweli River and its catchment based on climatic zones. S = $SiO_2/20$; A = K_2O+Na_2O; M = $TiO_2+MgO+FeO_T$ (wt%).

The MFW (Ohta and Arai, 2007) diagram shows the trend between mafic, felsic sources and weathering trends (Fig 5.1.21a). The M and F vertices characterize mafic and felsic rock source respectively, while the W vertex identifies the degree of weathering of these sources, independent of the chemistry of the unweathered parent rock (Ohta and Arai, 2007). The rocks of the Mahaweli River catchment area plot well on the rock averages trend line (Fig 5.1.21a, 5.1.21b). The <180µm and 180 - 2000 µm sediment fractions show a large scatter within the M-W apexes. The soils are plotting towards the W apex indicating weathering conditions (Fig 5.1.21b).

In the climatic zones the wet zone show sediments plotting close to the W apex indicating strong weathering (Fig 5.1.21c). The intermediate zone is highly scatted and is much close to the M apex thus, indicating less weathering than the wet zone and input of fresh material from the tributaries and the scatter also may be due to heavy minerals (Fig 5.1.21c). In the dry zone the <180µm fraction is drifting towards the M apex while the 180 - 2000 µm fraction is drifting towards the F apex (Fig 5.1.21c). Thus, the <180µm fraction is composed mainly of mafic components while the 180 - 2000 µm fraction is composed of felsic components.

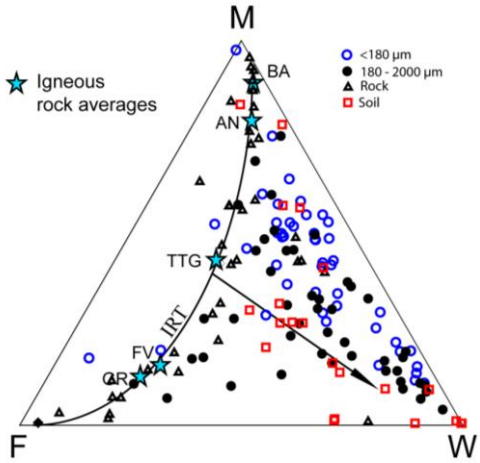

Fig 5.1.21a : MFW ternary plot (Ohta and Arai, 2007) for the sediment factions, soils and rocks of Mahaweli River and its catchment. M=mafic source, F=felsic source and W=weathered material. Calculation procedure for the vertices is given in Ohta and Arai (2007). Curved line (IRT) is the igneous rock trend. Stars are average values for Phanerozoic basalt (BA), andesite

(AN), tonalite-trondhhjemite-granodiorite (TTG), felsic volcanic rock (FV), and granite (GR) from Condie (1993). Arrow indicates weathering trend from a bulk source composition between TTG and FV.

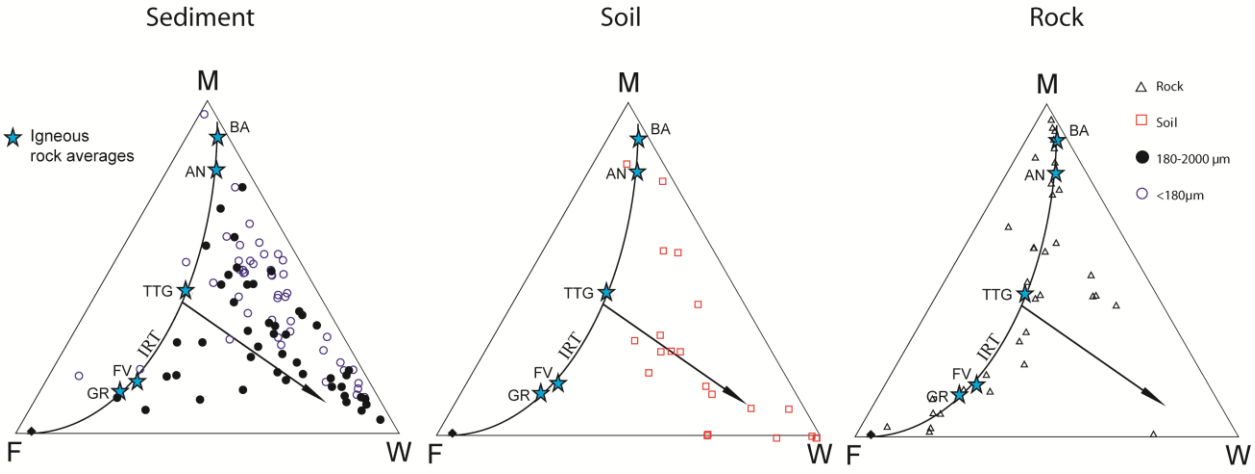

Fig 5.1.21b : MFW ternary plot (Ohta and Arai, 2007) for the sediment factions, soils and rocks of Mahaweli River and its catchment conceded separately. M=mafic source, F=felsic source and W=weathered material. Calculation procedure for the vertices is given in Ohta and Arai (2007). Curved line (IRT) is the igneous rock trend. Stars are average values for Phanerozoic basalt (BA), andesite (AN), tonalite-trondhhjemite-granodiorite (TTG), felsic volcanic rock (FV), and granite (GR) from Condie (1993). Arrow indicates weathering trend from a bulk source composition between TTG and FV.

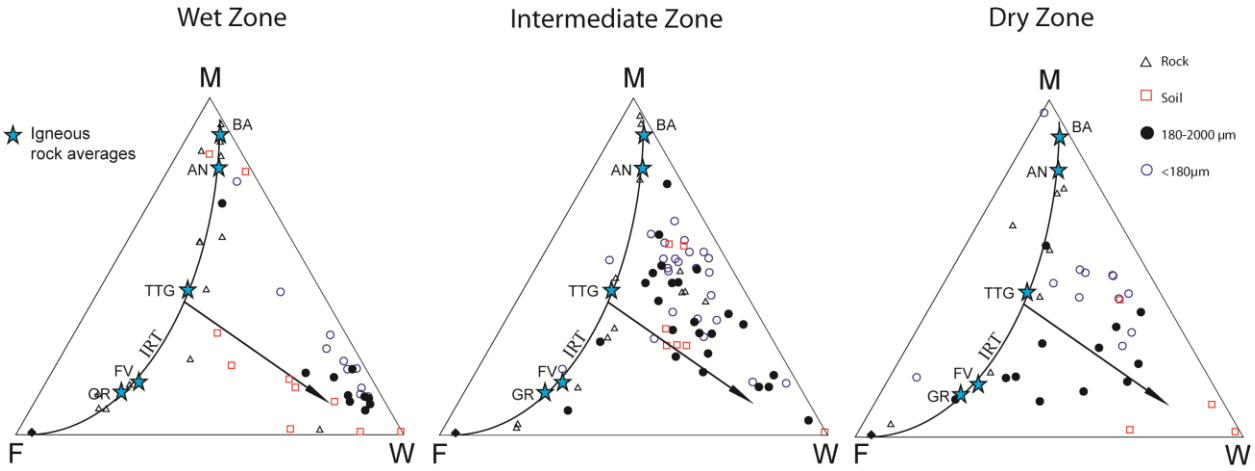

Fig 5.1.21c : MFW ternary plot (Ohta and Arai, 2007) for the sediment factions, soils and rocks of Mahaweli River and its catchment based on climatic zones. M=mafic source, F=felsic source and W=weathered material. Calculation procedure for the vertices is given in Ohta and Arai (2007). Curved line (IRT) is the igneous rock trend. Stars are average values for Phanerozoic basalt (BA), andesite (AN), tonalite-trondhhjemite-granodiorite (TTG), felsic volcanic rock (FV), and granite (GR) from Condie (1993). Arrow indicates weathering trend from a bulk source composition between TTG and FV.

5.2 POLGOLLA DAM

5.2.1 Surface processes

The surface process shows that there are no significant changes in all sediments for each element except a few locations in the surface sediments. The Table 5.2.1 shows the calculated GAI values for all the sediments. The GAI was calculated using the equation; where, Cn = measured concentration of heavy metal in the sediments, Bn = Geological background value in average shale (Turekian and Wedepohl, 1961) of element n, 1.5 is the background matrix correction in factor due to lithogenic effects. Igeo = $Log_2(Cn/1.5Bn)$. There are a number of indexes to account pollution levels. However, the Muller, 1979 GAI is the most used and appropriate for this study. Thus, this GAI has been used to assess environmental activities in this study. The GAI for phosphorus indicates that the sediments are very highly polluted (Table 5.2.2). The phosphorus concentrations in the sediments are more than two times higher than Upper Continental Crust (UCC, Taylor and McLennan 1985). Thus, these sediments are mainly of biogenic and is evident by high organic matter. Thus, the elements that indicate high pollution such as Zn, Cu, Ni, Cr is associated with the organic matter and is hindered. Thus high accumulations are seen in the reservoir sediments which also point out a threat of high pollution. However, the As levels are low showing no pollution threat. Since, the sediments are under high oxic conditions, the very high Fe_2O_3 leads to removal of As and display low values. On the other hand, upon heavy rains the suspended solid levels increase. Thus, the heavy metals associate suspended solids and accumulate but cause no adverse effect.

Table. 5.2.1: Geoaccumulation index for the upper catchment of Mahaweli River and Polgolla reservoir.

S-No	As	Pb	Zn	Cu	Fe_2O_3	P	Ni	Cr
Upstream of Polgolla								
2	2	3	4	3	2	6	3	4
6	2	2	4	3	2	6	3	4
3	2	3	4	3	2	6	3	4
5	2	2	4	3	1	6	3	4
10	2	3	4	3	2	6	3	4
1	2	3	4	3	1	6	3	4
7	2	2	4	3	1	5	3	4
4	2	2	4	3	1	6	3	4
11	2	2	4	3	2	6	3	4
13	2	2	4	3	2	6	3	4
9	2	2	4	3	1	6	3	4
14	2	3	4	3	2	6	3	4
8	2	3	4	3	2	6	3	4
12	2	3	4	3	2	6	3	4
16	1	2	4	3	2	5	3	4
Polgolla core								
PC1	2	3	4	3	2	6	3	4
PC2	2	3	4	4	2	6	3	4
PC3	2	3	4	4	2	6	3	4
PC4	2	3	4	4	2	6	3	4
PC5	2	3	4	4	2	6	3	4
PC6	2	3	4	4	2	6	3	4
PC7	2	3	4	4	2	6	3	4
PC8	2	3	4	4	2	6	3	4
PC9	2	3	4	4	2	6	3	4
PC10	2	3	4	3	2	6	3	4
PC11	2	3	4	4	2	6	3	4
PC12	2	3	4	3	2	6	3	4
PC13	2	3	4	3	2	6	3	4
PC14	2	3	4	4	2	6	3	4

S-No	As	Pb	Zn	Cu	Fe_2O_3	P	Ni	Cr
Polgolla reservoir								
PG1	1	2	4	3	2	6	3	4
PG2	2	3	4	3	2	6	3	4
PG3	2	2	4	3	2	6	3	4
PG4	2	3	4	3	2	6	3	4
PG5	2	2	4	3	1	6	3	4
PG6	2	2	4	4	2	6	3	4
Downstream of Polgolla								
15	2	3	4	3	1	6	3	4
17	1	2	4	3	1	6	3	4
18	2	3	4	3	2	6	3	4
20	1	2	4	3	1	6	4	4
19	2	3	4	3	2	6	3	4
21	2	3	4	3	2	6	3	4
22	1	2	4	3	1	5	3	4
23	1	2	4	3	1	6	3	4
24	2	3	4	3	2	6	3	4
25	2	3	4	3	2	6	3	4
26	1	2	4	3	1	6	3	4
27	2	3	4	3	2	6	3	4
28	1	2	4	3	2	6	3	4
29	2	3	4	3	1	6	3	4
30	2	3	4	3	2	6	3	4

Table. 5.2.2: Geoaccumulation index (Muller, 1979) of heavy metal concentration in sediments. Source Praveena, et al. 2007.

Geoaccumulation index	Class	Pollution Intensity
0	0	Background concentration
0-1	1	Unpolluted
1-2	2	Moderately to Unpolluted
2-3	3	Moderately polluted
3-4	4	Moderately to highly polluted
4-5	5	Highly polluted
>5	6	Very highly polluted

5.2.2 The upper catchments of Mahaweli River

The Total Sulphur (TS) values and phosphorus are high. However, the plots (Fig 5.2.1) indicate that the surface sediments do not show any much difference from each other. Zn shows a good correlation with Fe_2O_3 though As, Pb, Cu is highly scatted. On the other hand, this clearly

shows that the core sediments of the Polgolla dam are enriched by all the elements. Nonetheless, there is no special variation in the upper catchments of the Mahaweli River. This indicates that there is no significant geochemical process taking place within this area.

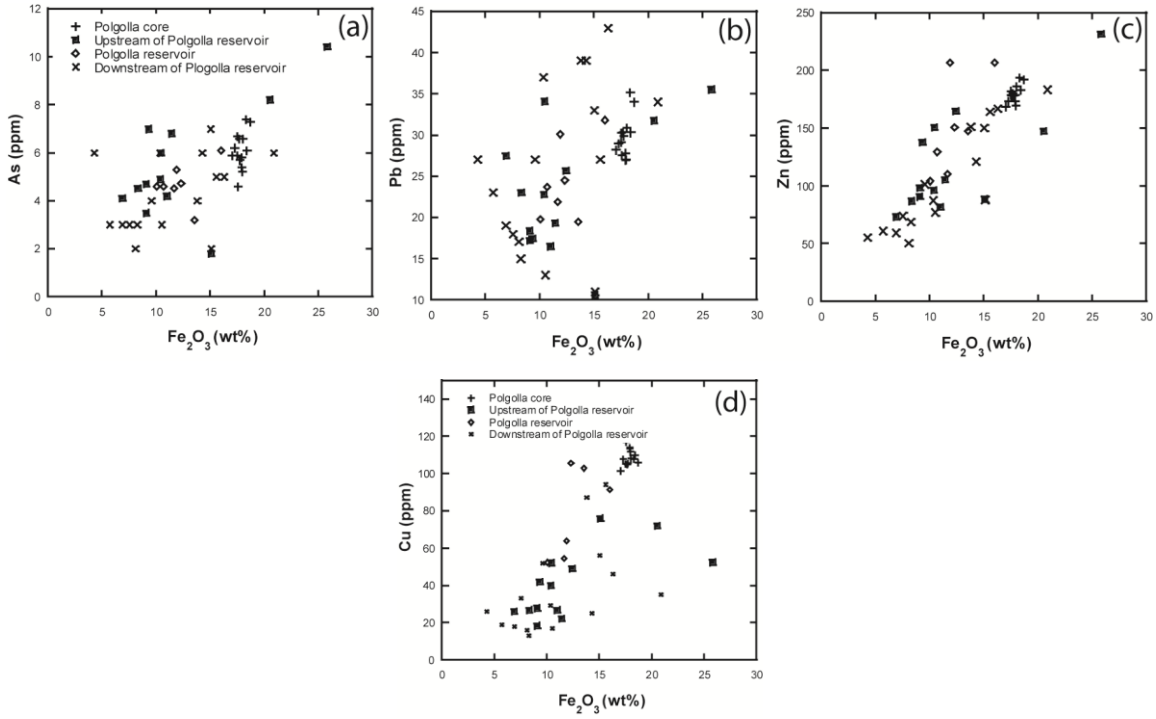

Fig. 5.2.1: Graphs of Fe_2O_3 and As, Pb, Zn and Cu for the upper catchment of Mahaweli River and Polgolla reservoir.

5.2.3 The Polgolla reservoir core sediments

The Polgolla core sediment GIA shows that the sediments are very highly polluted due to phosphorus, highly polluted due to Cr, Ni, Pb, Zn and Cu and moderately polluted for As (Table 5.2.1). However, vertically there is no significant change in the core samples (Fig 5.2.2). This shows that there is no considerable pollution due to anthropogenic activities affecting the reservoir even though there are significant agricultural activities taking place in the upper catchment of Polgolla area and rapid urban developments. Nevertheless, the Zn, Cu, Ni and Cr are very much higher than UCC (Taylor and McLennan 1985) values which is more than two times higher. The CaO, Sr and P_2O_5 show that the increases of these elements are biogenic. Thus, the basement rock weathering could be the main source and process of these elements.

Unfortunately, there is no age data for the core sediments yet. Since the area is subjected to heavy rains the sediment deposition rate increases and the core itself would represent a short term, presumably less than twenty years. The sediments are composed of mud and high organic matter. Thus, the accumulation of heavy metals could also be associated with organic matter and the very fine mud particles. However, though the accumulation is high there is no considerable threat to the health of the population around the area due to the association of sulfur and iron.

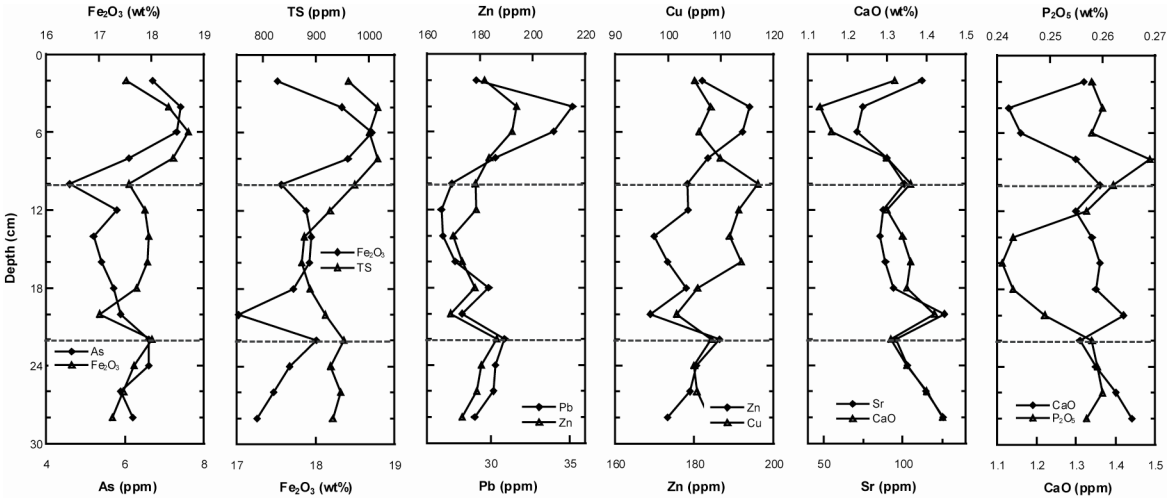

Fig. 5.2.2: Vertical distribution of As, Fe_2O_3, Zn, Total sulfur (TS), Pb, Cu, Sr CaO and P_2O_5 of the Polgolla reservoir.

5.3 TRINCOMALEE BAY

5.3.1 Surface Sediments

5.3.1.1 UCC-normalized geochemical characteristics

Normalization of average compositions of sediments in the three sectors of Trincomalee Bay and the lower reaches of the Mahaweli River against UCC (Taylor and McLennan 1985) highlights contrasts between the four datasets (Fig. 5.3.1). The normalized pattern (UCC_N) for the Mahaweli River sediments is the most regular, although departures from UCC composition are considerable. SiO_2, and TiO_2 are enriched relative to UCC in the Mahaweli River, whilst the more mobile elements (MgO, CaO, Na_2O and K_2O) are strongly depleted. This reflects derivation from a relatively evolved felsic source, and significant modification of original

composition by maturation (relative quartz concentration) and source weathering (Young et al. 2012), by destruction of feldspars and other labile phases. Trace elements in the segment Ba-Th are generally similar to UCC, while Zr and four ferromagnesian trace elements (Cr, V, Sc, Ni) are significantly enriched (Fig. 5.3.1). This suggests some zircon concentration in the lower Mahaweli River, and also the presence of a significant mafic component in its source.

The UCC_N patterns for the three sectors of Trincomalee Bay show considerably more variability, suggesting modification in the marine environment. The pattern for Koddiyar Bay, the most proximal to the Mahaweli delta, shows the same shape for all major elements, although most are enriched relative to the river sediments, except for SiO_2, which is depleted, and K_2O and P_2O_5, which exhibit similar levels. The largest contrasts are for CaO, MgO, and Na_2O (Fig. 5.3.1), all of which could be contributed from marine sources. Trace element abundances in Koddiyar Bay are generally similar to those in the lower Mahaweli, although Y, Th, Zr and Nb are quite strongly enriched. This grouping of elements, and also relative enrichment of TiO_2 and Fe_2O_3, is suggestive of heavy mineral concentration in Koddiyar Bay as current velocity decreases where the delta meets the sea. The Koddiyar sediments thus carry a strong imprint from the Mahaweli River, as to be expected from their proximal position, along with modification from marine sources (CaO, MgO, and Na_2O) and potential heavy mineral concentration (TiO_2, Fe_2O_3, Y, Th, Zr and Nb), as indicated by the PCA analysis.

The Thambalagam Bay UCC_N pattern is a similar shape to that for Koddiyar Bay, with enrichment for TiO_2, Ba, Ce, Th, Zr, Cr and V relative to UCC, and depletion for all other elements (Fig. 5.3.1). This suggests that the Mahaweli River is also the main source of sediment in Thambalagam Bay, despite its semi-enclosed nature. However, average abundances of TiO_2, Fe_2O_3, Ce, Y, Th, Zr, Nb, Cr, and V are all lower than in Koddiyar Bay. This suggests influence of the Mahaweli River is diminished, and heavy mineral concentration is less of a factor in this more distal setting. In contrast, the UCC_N pattern for the Inner Harbour is quite distinctive. Although the pattern for the major elements in the segment SiO_2–MnO is identical to the other three datasets, MgO, CaO, P_2O_5 and Sr are strongly enriched (Fig. 5.3.1). Enrichment of Ca and Sr in sediments is often due to the occurrence of carbonates (Dellwig et al. 2000), and MgO and P_2O_5 are also likely to be associated with bioclastic carbonate or apatite. The Inner Harbour thus shows the greatest marine influence, in keeping with its distal position in relation to the Mahaweli delta, and proximity to the open ocean.

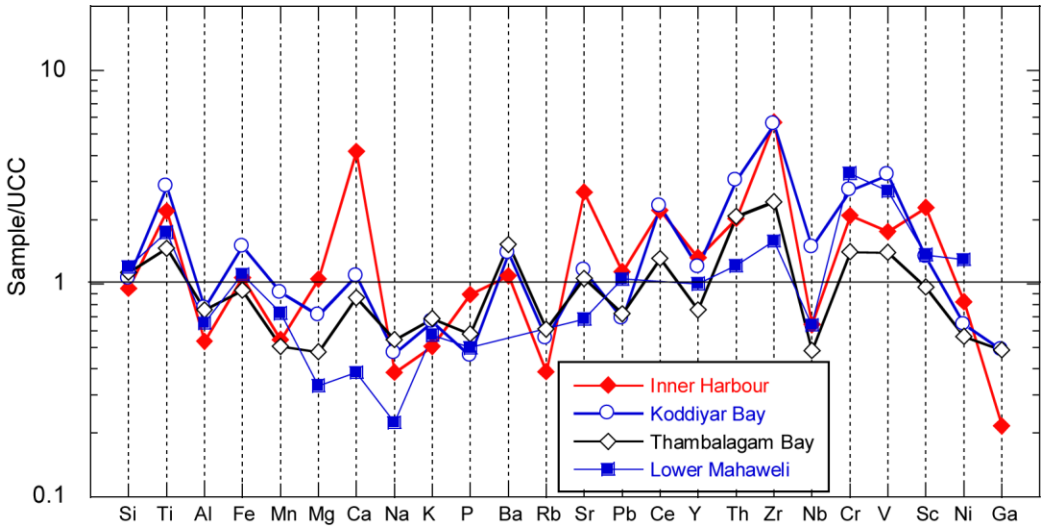

Fig. 5.3.1: UCC-normalized averages for the Trincomalee bay sediments, compared to average lower Mahaweli River sediment (data from Young et al. 2012). UCC values from Taylor and McLennan (1985), except for As (from Rudnick and Gao, 2005). Major elements are normalized as oxides, trace elements as ppm.

5. 3.1.2 Source rock signatures

The significant modification of the Mahaweli River and Trincomalee Bay sediments from UCC compositions (Fig. 5.3.1) suggests that provenance identification in the three sectors using major element compositions is unlikely to be successful. Elements such as Th, Zr, Ti and Sc are most suited for provenance determination due to their low mobility during sedimentary processes, and low residence times in water (Taylor and McLennan, 1985; Cullers, 1988). Immobile element ratios (e.g. Th/Sc, Zr/Sc; McLennan et al. 1993) have been successfully applied to identify source rock composition. Ratios are inherited directly from source, despite weathering or dilution from quartz or carbonate. Combinations such as Zr/Sc can also be used to identify heavy mineral concentration (McLennan et al. 1993).

A Zr/Sc-Th/Sc ratio plot shows that sediments from the three sectors of Trincomalee Bay all lie on a single trend cutting a model source evolution line near UCC, and within the field of lower Mahaweli River sediments (Fig. 5.3.2a). This indicates that the bulk of the clastic sediment in Trincomalee Bay is derived from the Mahaweli River, rather than from local or marine

sources. A companion Zr/Ti–Th/Ti plot shows an identical pattern (Fig. 5.3.2b). The trend across the model source evolution line on both plots reflects zircon concentration, with higher Zr/Sc and Zr/Ti ratios in Koddiyar Bay near the Mahaweli delta, and lowest values in the most distal setting of the Inner Harbour. These features suggest that heavy minerals have played an important role in elemental distributions within Trincomalee Bay.

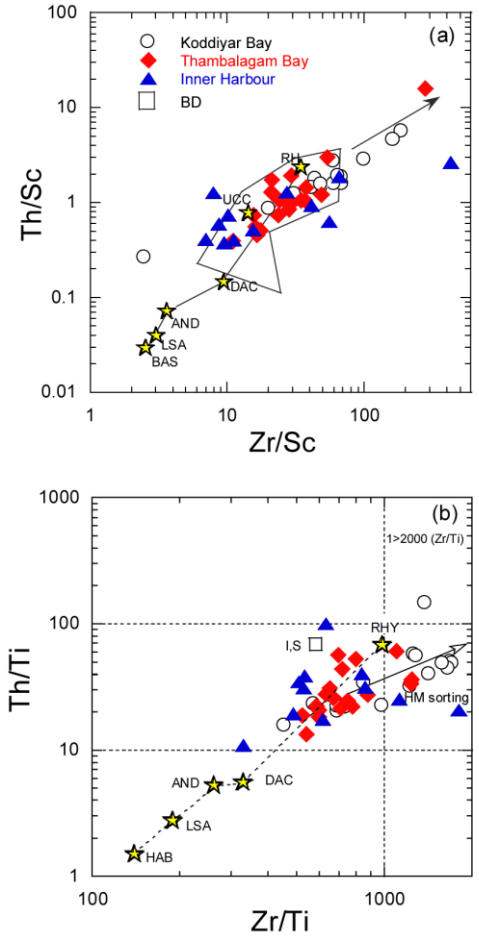

Fig. 5.3.2: (a) Zr/Sc–Th/Sc (McLennan et al. 1993) and (b) Zr/Ti-Th/Ti (Roser et al. 2000) plots for the Trincomalee Bay sediments. Stars BAS, LSA, AND, DAC, RHY: average basalt, low-silica andesite, andesite, dacite and rhyolite, as plotted by Roser and Korsch (1999), representing a model source evolution trend. UCC: Upper Continental Crust (Taylor and McLennan 1985); square [I,S] spans the average compositions of I- and S-type granite (Whalen et al. 1987). Arrow: trend of zircon concentration. Five samples (three Koddiyar, and one each from the Inner Harbour and Thambalagam Bay) plot off scale on (a) at Zr/Sc ratios of 101–430.

5. 3.1.3 Hydraulic sorting and heavy minerals

In sediments Fe_2O_3 and TiO_2 are usually well correlated due to hydraulic sorting effects (Singh 2009), partly due to concentration of heavy mineral phases containing Ti and Fe, such as ilmenite and magnetite, both of which occur in the Trincomalee Bay sediments. As noted above, the Trincomalee Bay sediments are generally very well-sorted (Table 4.3.1, Fig. 4.3.5). Average Ti/Fe ratios in the Koddiyar Bay, Thambalagam Bay, and Inner Harbour sediments (0.23, 0.21 and 0.26, respectively) span the values given by Garcia et al. (2004) for both minerals. On cross-plots of Ti and Fe, linear arrays of data points extending towards the origin indicate that heavy minerals in the sediments have been hydraulically fractionated in a similar manner (Singh 2009). Correlation between Fe_2O_3 and TiO_2 is strongest in the Koddiyar samples (R=0.92; Online Resource Two), with some Thambalagam Bay samples (R=0.57) spreading to higher Fe_2O_3 at ~1 wt% TiO_2 (Fig. 5.3.3a). However, the broadly similar Ti/Fe ratios in all three sectors suggest that Fe- and Ti-bearing heavy minerals in the sediments were hydraulically fractionated in a similar manner, with elevated contents being produced by winnowing and loss of fines.

Heavy mineral enrichments are often associated with particle sorting effects due to wave action and high current velocities (Dellwing et al. 2000). Since Zr is commonly associated with zircon, enrichments of this element also suggest heavy mineral concentrations in higher depositional energy environment related to modern bar building. Ti and Zr are used as indicators of depositional energy because both elements are concentrated by particle sorting effects (Dellwing et al. 2000). Average Zr/Ti ratios of the lower Mahaweli sediments are 0.058, whereas those for Inner Harbour, Thambalagam Bay and Koddiyar Bay sediments are greater (0.105-0.167) (Table 4.3.1). A cross-plot of TiO_2 and Zr (Fig. 5.3.3b) shows the spread of Koddiyar Bay samples is broadly similar to that of the Mahaweli sediments, suggesting deposition of both zircons and Ti-bearing heavy minerals in the proximal delta system as current velocity falls. Shift to higher Zr/Ti ratios in Thambalagam Bay may reflect loss of Ti-bearing phases relative to zircons during transport away from the delta, and hence some decoupling of the heavy mineral assemblages with within the bay. However, this could not be confirmed quantitatively by heavy mineral analysis or microscope observation. Nevertheless, these higher ratios and high abundances of elements often linked with heavy minerals (e.g. Zr, Ce, Ti) suggest grain-size

fractionation, hydraulic sorting and winnowing, circulation, and concentration of heavy minerals in high-energy areas within Trincomalee Bay.

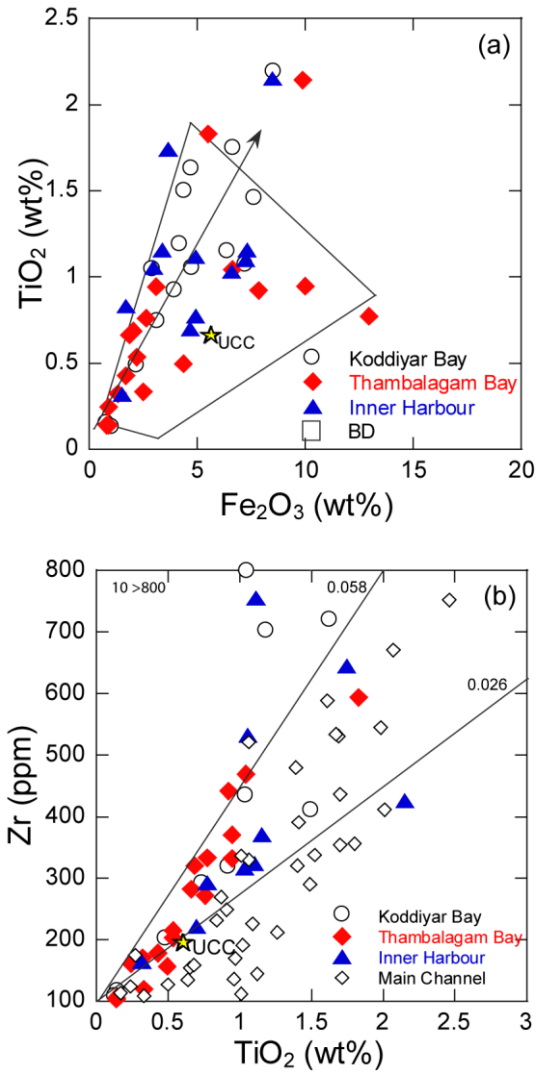

Fig. 5.3.3: (a) Fe_2O_3–TiO_2 and (b) TiO_2–Zr plots for the Trincomalee Bay data, illustrating hydraulic fractionation and heavy mineral concentration. UCC: Upper Continental Crust (Taylor and McLennan 1985)

5. 3.1.4 Spatial geochemical variations

Geographical Information System (GIS) contour maps were made to examine the spatial variation of elements within Trincomalee Bay. The major elements Al_2O_3 and K_2O were selected to represent the distribution of clay and feldspar components. Both elements show peak values in Koddiyar Bay at the main mouth of the Mahaweli, and in the most westerly part of Thambalagam Bay (Fig. 5.3.4a, b), where grain size is generally finest. The Koddiyar Bay high reflects construction of the Mahaweli delta, whereas the high in Thambalagam Bay is likely due to accumulation of fines in the shallower and calmer waters in that semi-enclosed site.

Four chemically immobile high field strength elements (Th, Nb, Y, Sc) were plotted as representative of provenance-related elements which are unlikely to be contributed from anthropogenic sources (Garcia et al. 1994, Dellwing et al. 2000). Of these, Th, Nb and Y show almost the same spatial distribution, with weak highs in the northwestern part of Koddiyar Bay, and lows in Thambalagam Bay and eastern Koddiyar (Fig. 5.3.4c, d, e). The relatively uniform distributions of these elements suggest they are mainly associated with clays or very fine-grained heavy minerals. Scandium shows isolated highs in the Inner Harbour and eastern Koddiyar, although these are defined only by a handful of samples (Fig. 5.3.4f).

Six elements which can be associated with both clays and heavy minerals show quite different distributions. Chromium (Fig. 10a) and V (Fig. 5.3.5b) GIS maps show almost the same distribution, with highest concentrations in northwest Koddiyar Bay, and lows in Thambalagam Bay. Nickel, Ce, Zr and TiO_2 also show peaks in the same area (Fig. 5.3.5c–f), that correspond to the weaker highs shown by Th, Nb, and Y (Fig. 5.3.4c–e). Isolated highs occur for Zr and Ce (defined by a single sample) and Ni in the Inner Harbour; these may be related to an isolated heavy mineral concentration in the former, and contamination from port activity in the latter. Minor highs for all six elements in this group also occur in an arm (China Bay) of eastern Thambalagam Bay (Fig. 5.3.5).

The association of elements enriched in northwest Koddiyar Bay (Cr, V, Th, Sc, Y, Nb, TiO2, Zr, and Ce strongly suggests association with heavy minerals such as Fe-Ti oxides, zircon, monazite, apatite, garnet, titanite, tourmaline and rutile) all of which occur in the sediments. In coastal depositional systems bottom current activity can cause winnowing (Schnetger et al. 2000),

and thus concentration of heavy minerals. The concentration of elements in northwest Koddiyar Bay corresponds to the area in which strongest current activity was observed during sampling.

The spatial variation maps thus suggest that these heavy minerals were carried along the Mahaweli River and deposited as lags in this high-energy environment in Koddiyar Bay. Some heavy minerals are also being transported through the narrow mouth of Thambalagam Bay and deposited in the China Bay area. Except for Ce, Y, Sc and Zr, most other elements are less abundant in the Inner Harbour. The distribution patterns suggest Mahaweli River sediment entering Koddiyar Bay moves towards the northwest, and heavy mineral-rich sands are deposited in a high-energy zone. Fine sand and clay particles are moved away from Koddiyar Bay by currents into Thambalagam Bay, the Inner Harbour, and out to sea.

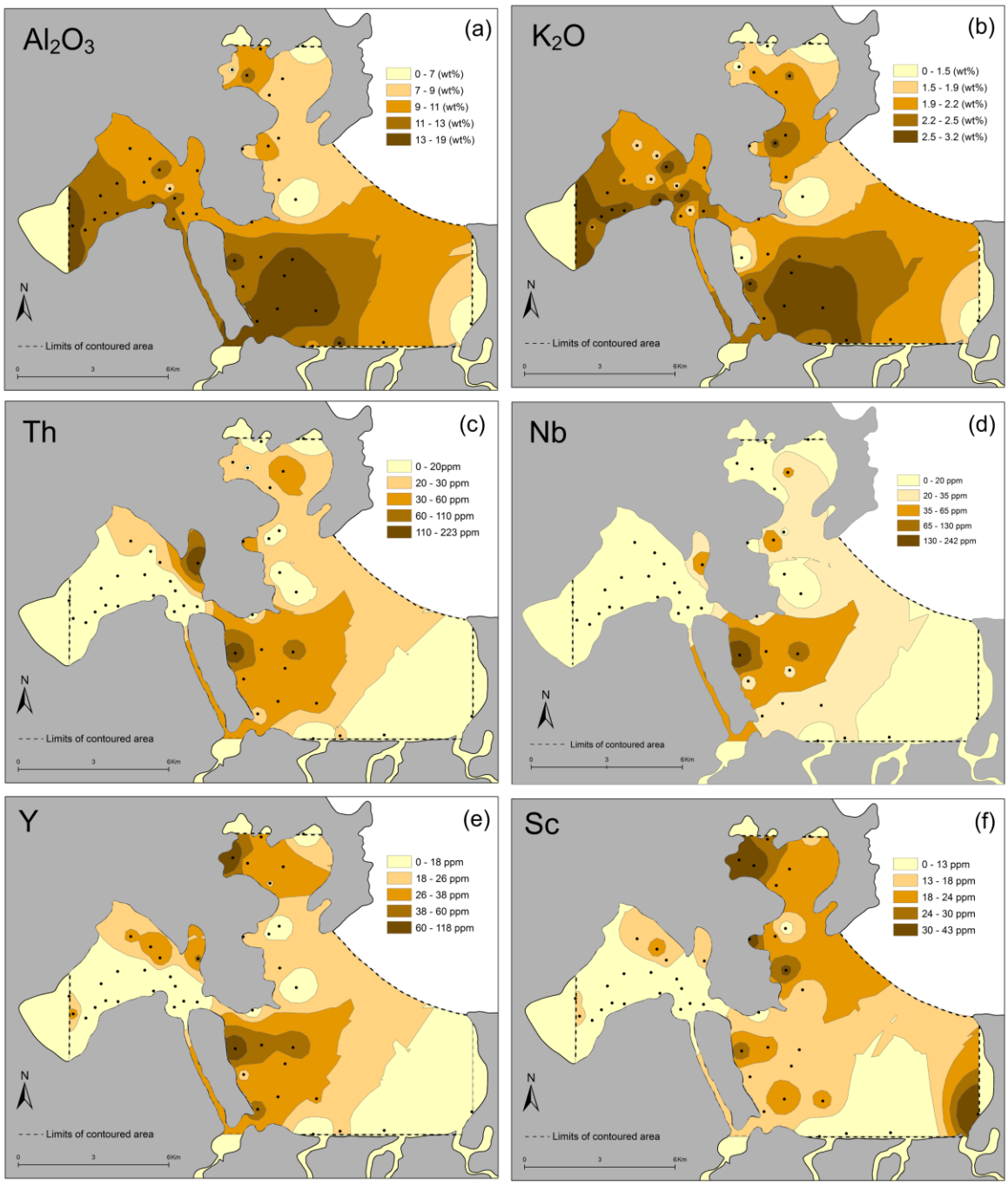

Fig. 5.3.4: GIS contour maps for (a) Al_2O_3, (b) K_2O, (c) Th, (d) Nb, (e) Y and (f) Sc showing spatial elemental distribution within Trincomalee Bay.

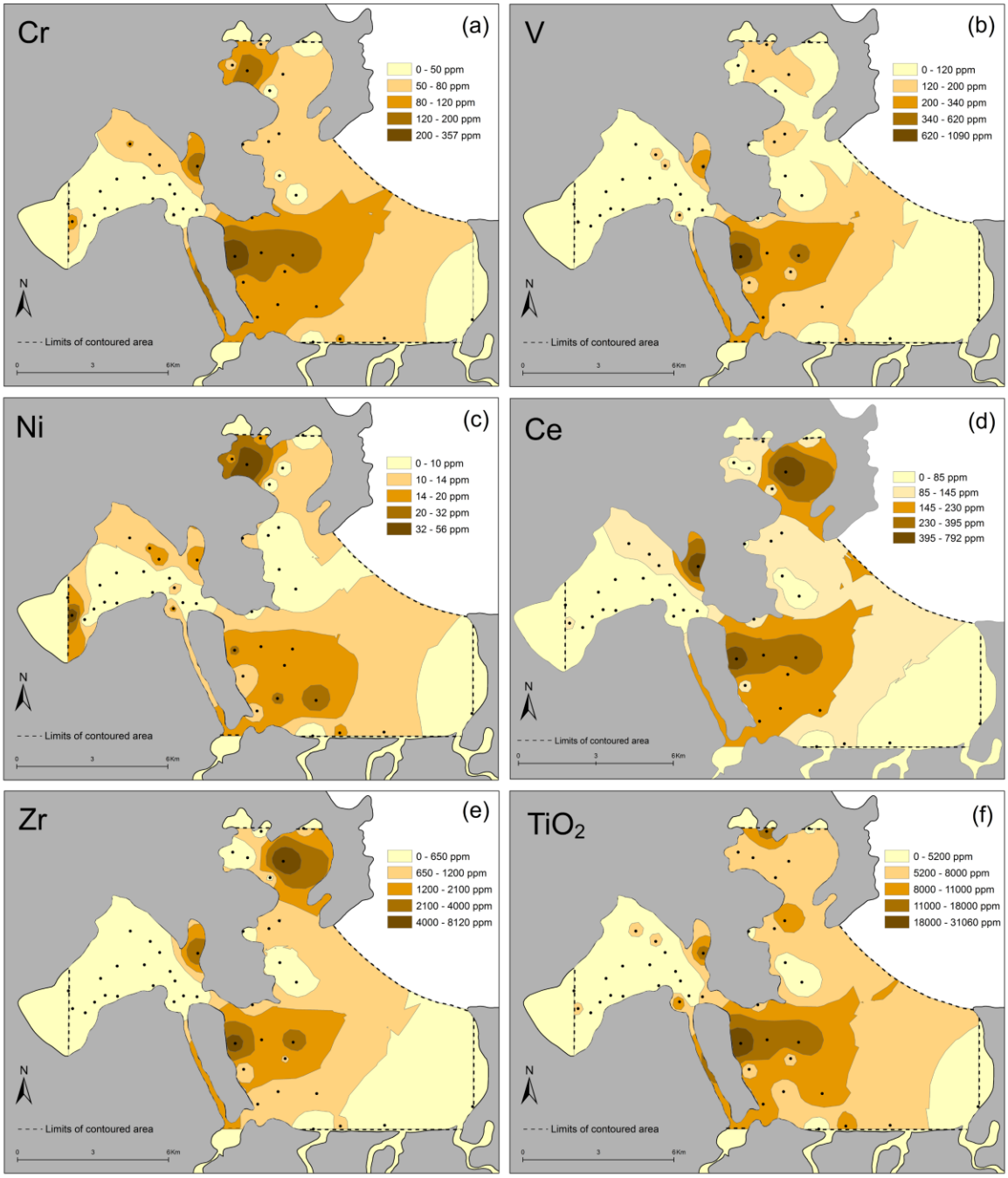

Fig. 5.3.5: GIS contour maps for (a) Cr, (b) V, (c) Ni, (d) Ce, (e) Zr and (f) TiO_2 showing spatial elemental distribution within Trincomalee Bay

5. 3.1.5 Present environmental status

Trace metal concentrations (As, Pb, Zn, Cu, Ni, and Cr) in the Trincomalee Bay sediments were compared with four established international standards to evaluate present pollution status for the elements analyzed (Table 4.3.3). Comparing the data to a single guideline could be misleading. The guidelines used were COSED (Coastal Ocean Sediment Database), the NYSDEC (New York State Department of Environmental Conservation) values of lower effect level (LEL) and severe effect level (SEL), ISQG (Interim Sediment Quality Guidelines) and probable effect level (PEL). The NYSDEC metals criteria are derived from Ministry of Ontario guidelines and NOAA data that make use of the screening level approach. The LEL for each metal is thus the lowest of either the Persaud et al. (1992) LEL or the Long and Morgan (1990) Effect Range-Low. Similarly, the SEL for each metal is the lowest of either the Persaud et al. (1992) SEL or the Long and Morgan (1990) Effect Range-Moderate. Sediments are considered contaminated if either criterion is exceeded. If both criteria are exceeded, the sediment is considered to be severely impacted. If both the LEL and SEL criteria are exceeded, the metal may severely impact on the health of biota. If only the LEL criterion is exceeded, the metal may moderately impact on biotic health (NYSDEC 1999; Graney and Eriksen 2004). The COSED of chemical concentrations in sediments has been compiled from various electronic sources, and contains data for nearly 13500 US coastal sediment samples (Daskalakis and Connor 1995). COSED values are indicative of metal contamination, and are used to quantify the degradation of sediment quality in estuarine and marine ecosystems (Ruiz-Fernández et al. 2003). The Canadian Council of Ministers of the Environment also developed national Interim Sediment Quality Guidelines (ISQG) based on co-occurrence of chemical and biological data from the assessment of Great Lakes contaminated sediments (SAIC 2002). Using guideline values derived from large well-assessed data sets such as those above should result in reasonable results, even though threshold levels may differ between them.

Comparison with the COSED guidelines for As, Pb, Zn, Cu, Ni and Cr show that the Trincomalee Bay sediments are not seriously contaminated. However, average arsenic contents in Thambalagam Bay and the Inner Harbour exceed the LEL (lowest effect level), as does Cr in all three sectors (Table 4.3.3). However, both elements are below the SEL (severe effect level) levels. Both As and Cr also exceed the ISQG values and the level in UCC, but fall below the

probable effect level (PEL) of SAIC (2002). The data thus imply that the sediments in Trincomalee Bay are slightly contaminated by both As and Cr. However, comparison with pollution guidelines can be misleading, if local background values are not taken into account. Consequently, we also examined the data using metal Enrichment Factors (EF) and GIS maps to identify the spatial distribution of potential contamination.

Metal enrichment factor (EF) values of 0.5 – 1.5 suggest that the trace metals concerned may be derived entirely from crustal materials or natural weathering processes (Zhang and Liu 2002). Values greater than 1.5 suggest that a significant portion of the trace metal has been delivered from non-natural (anthropogenic) sources (Zhang et al. 2007). EF values were calculated using the formula given in Zhang et al. (2007):

$$EF = \frac{(Me/Al)Sample}{(Me/Al)Background}$$

Normalization of element contents against an immobile element is a common practice to accommodate grain-size effects and dilution by phases such as quartz and carbonates. Currently, Al is the most frequently used geochemical normalizer in estuarine and coastal sediments, based on the assumption that Al is held exclusively in terrigenous aluminosilicates (Chen and Kandasamy 2007; Karageorgis et al. 2009; Ho et al. 2010). Therefore, in this study we used Al_2O_3 as the normalizer, and the average composition of lower Mahaweli River sediment (Table 4.3.1) for the background values.

The average EF values confirm that Pb, Cu, Ni and Cu are present only at natural levels, with EFs ranging from 0.3–1.4 (Table 4.3.3). However, GIS contour maps of EF values of individual samples show the highest EFs do occur within the Inner Harbour (Fig 5.3.6). Although all except one sample fall within acceptable limits, there may have been slight contamination of these elements in the port area. The GIS plot for As shows that EFs higher than guideline occur in both Thambalagam Bay and the Inner Harbour, and thus some contamination of this element could also have occurred. However, the highs for arsenic also correspond to the highest CaO and Sr contents and clustering in the PCA analysis (Table 4.3.7), suggesting association with biogenic carbonate in the form of shell fragments. This possibility needs to be evaluated by future analysis. Finally, using the lower Mahaweli River sediments as the

normalizer, the apparent enrichment in Cr disappears, with average EF in the three sectors ranging only from 0.4–0.7 (Table 4.3.3), and hence lower than in the Mahaweli River. The GIS map for Cr (Fig 5.3.6) shows a relatively uniform EF distribution across the bay, with weak isolated highs in western Koddiyar Bay and Thambalagam Bay corresponding with areas of heavy mineral enrichment, and a single sample within the port district of the Inner Harbour. The results thus show that Trincomalee Bay is essentially unpolluted for the elements analyzed here when local background levels are taken into account, in contrast to the indication given by the broad-based sediment guidelines. This illustrates the importance of establishing local background values in studies of this type, by determining elemental compositions of fluvial systems entering estuarine or bay environments. These can then be used in conjunction with the sediment guidelines to identify spurious enrichments.

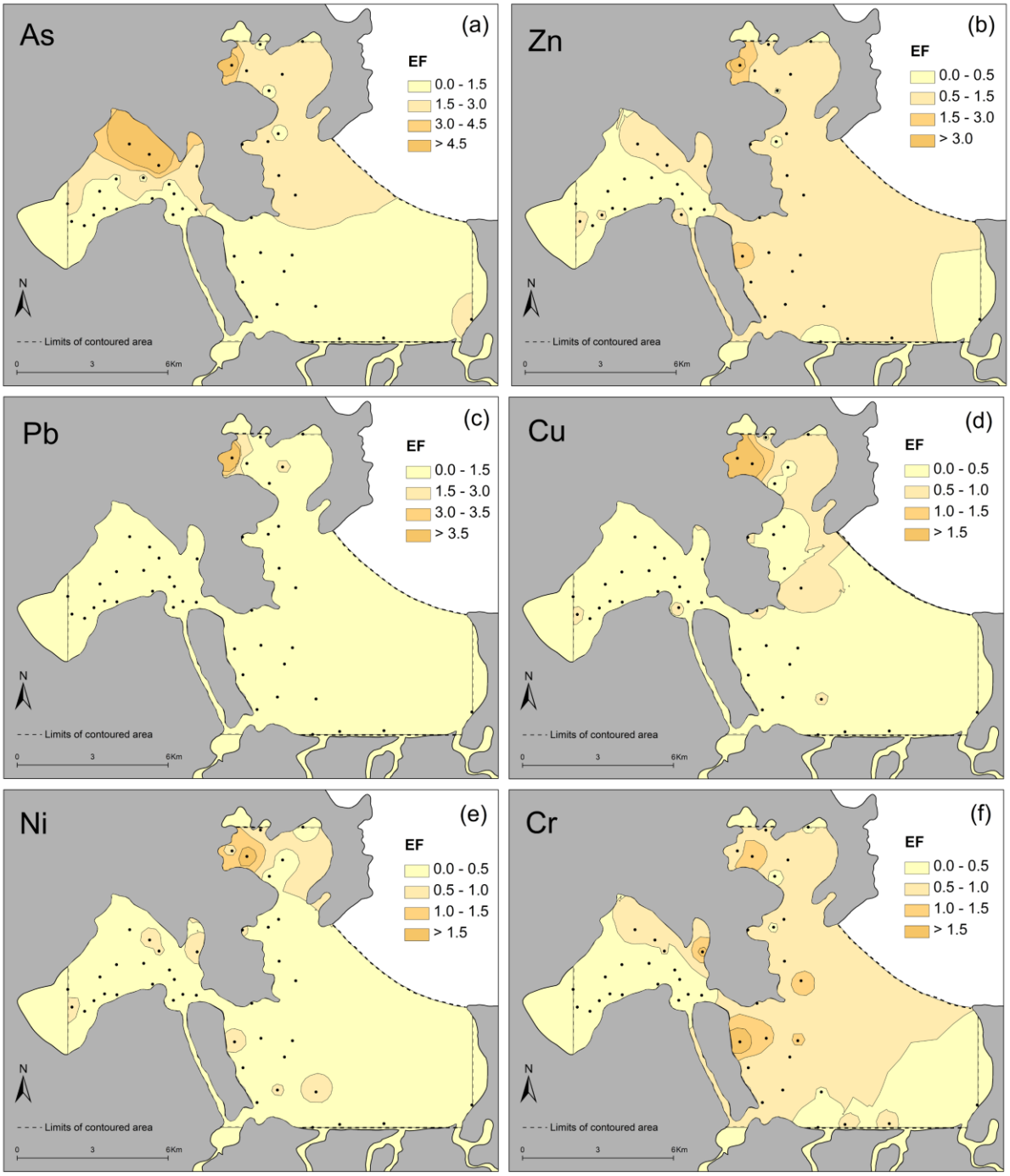

Fig 5.3.6: GIS contour maps for Enrichment Factor (EF) for (a) As, (b) Zn, (c) Pb, (d) Cu, (e) Ni, and (f) Cr showing spatial distribution within Trincomalee Bay.

5.3.2 Core sediments

5. 3.2.1Variation of elements in four cores and its environments

The textural and TS variation of all four cores are showed in Fig. 3.2.2 and the chemical variation of C1 is shown in Fig 4.3.8, and C2 – C4 in Fig 4.3.9. In C1 (Fig 3a) the top 10cm show high SiO_2 and low Al_2O_3. Below 36cm Al_2O_3 decreases sharply and then gradually increases downwards this corresponds to change in sedimentological facies with the interval from 36 – 62 cm consisting of fine to medium sediments (-1. 18 – 1.08 Φ), where the section below 36cm consists of coarse sands rich in quartz, increments of SiO_2. In C1 (Fig 4.3.8) the top 10cm contain very higher concentrations of elements related to heavy minerals (Ti, Fe, Zr, Th, Y, V, N, and Cr Fig. 4.3.8b-e). The heavy mineral separation showed that the heavy minerals present are mainly zircon, monazite, magnetite, apatite, titanate, tourmaline and rutile. The very high values for these elements are thus due to the high heavy mineral content at the top of the C1. Zinc contents increase in the top 16cm and may be reflect slight contamination due to anthropogenic activities (Fig. 4.3.8f). However, Pb concentrations decrease at the top 10cm Fig. 4.3.8f. Therefore, the increase of Zn and the decrease of Pb in this interval are more likely to be due to background variations caused by natural environmental changes, rather than pollution.

C2 is only 20cm long, and thus would not give detailed information compaired to the other three cores. However, the chemical compositions of almost all elements along the core show no great change (Fig 4.3.9). C3 has some difference in chemical composition at 20-25cm for Al_2O_3, SiO_2, TiO_2, Fe_2O_3, Y, Cr, V, Zn and TS (Fig. 3.2.2 and 4.3.9). These are mainly ferromagnesian elements, and some are also related to high organic matter contents and may therefore indicate anoxic conditions (Bastviken et al., 2001). These elements also may be scavenged onto organic matter (Dauby et al., 1993) and thus show high values. C4 shows some increases at 20cm for TiO_2, Fe_2O_3, Zr, Th, Nb and V. However, this cannot be explained clearly but may relate to mafic components or Fe-bearing heavy minerals from the river sediments.

The four cores are chemically and texturally very different from each other (Fig 3.2.2, Fig 4.3.8, Fig 4.3.9). The depositional mechanisms and environments also clearly differ from each other. The main geochemical processes involved could be sorting and heavy mineral concentrations with variations in grain size. The dashed lines in Fig 3.2.2, 4.3.8 and 4.3.9 show breaks in elemental concentrations at different horizons in each core. In C1, the changes are seen

at 10, 22, 40 and 54cm, and C2 shows changes at 6 and 12 cm. In C3 the changes occur at 8, 20 and 26cm, and in C4 the breaks are at 6, 14, and 20 cm. These changes may be due to the differences in tide, northeast monsoons, wave and current activities and flood events. This bay is subject to large waves, and strong long shore currents moving clockwise.

Core two and three are located near the Mahaweli river mouth. The offshore currents, wave dominance, circulation and high energy in this area combine to remove finer detritus from the sediments. The cores one, two and four were deposited in such environments, where finer particles are removed by winnowing and sand particles are deposited as lags.

C1 has high content of fine grained heavy minerals at its top, indicating a high energy area. Larger sand grains at the bottom of the core also indicating high wave and current activity. Large waves deposit larger grains and wash out finer particles (Kasper-Zubillaga and Carranza-Edwards, 2005). Therefore, the lower part of C1 was deposited in an environment dominated by wave action. Gradual sand bar formation away from the river mouth causes smaller currents to enter the core one area. Therefore, with time the top part is composed of finer grains and winnowing and the high energy prevailing in the location causes heavy minerals to be deposit as lags.

The C2 and C4 show great difference in grain size and almost homogeneous chemical composition. Therefore, C2 and C4 were deposited as sand bar formations in a more stable environment not subjected to waves and currents. C2 is an open system in Trincomalee Bay whereas C1 lies in the closed system of Thambalagam Bay. Thus, the C2 consists of larger and well sorted sand grains, whereas the C4 has similar MGS, but is not as well sorted due to a larger mud component deposited in the closed system.

C3 contain of organic matter in the middle part of the core, and slightly higher TS at the top (Fig. 3.2.2). This suggests the location of C3 is somewhat calmer than the other core locations. The C3 receive of fluvial supply because it lies at a river mouth. The organic matter may have undergone degradation and been buried under sand (Burdige, 2005). Therefore, this organic matter could be buried flood material. The overall result in the study suggests that sediment texture is the major controlling factor of the distribution of elements. The dashed lines show a difference in the pattern of elemental concentration and may relate to monsoonal changes or floods. However, we lack age data and hence the data is difficult to interpret.

5. 3.2.2 Heavy mineral concentration in core one

According to Cheepurupalli et al., 2012 concentration of heavy minerals depends on hydrodynamic conditions including sediment flux from the hinterland; wave energy and velocity; long shore current and wind speed which control littoral transport; and sorting and deposition of placer minerals in suitable locations. The heavy minerals at the top of C1 occur as a pocket in the beach on the west side of Koddiyar Bay. The top 8cm of sediment is moderately well sorted and consists of fine sand (MGS 2Φ). As suggested in section 4.1 the heavy minerals are deposited in an environment with low velocity small waves with weaker long shore currents.

Magnetite content is highest in the top most 2cm and decreases downwards. Zircon, monazite, hematite, apatite, titanite, tourmaline and rutile also decrease downwards of C1 and are almost negligible in content below 16cm. The assemblage of ilmenite, magnetite, zircon, allanite, hornblende, garnet and tourmaline indicates derivation from mixed sources of gneissic/granitic, basic and high-grade metamorphic rocks (Hegde et al., 2006). These sediments show the same assemblage and are therefore derived from a mixed source of gneissic/granitic, basic and high-grade metamorphic rocks of the Highland Complex.

LOI value in the top five samples (0 -10cm) in C1 are negative. This is due to oxidation of Fe^{2+} to Fe^{3+} during ignition (Chen, 1998; Mozammel, 2012). In the oxidation process, the FeO present in the ilmenite reacts with oxygen in air and forms hematite or pseudobrookite (Taylor and McLennan, 1985, McLennan; et al., 1993; Tathavadkar et al., 2006). The iron minerals are oxidized, yielding a negative LOI.

5. 3.2.3 Provenance indicators and maturity

ThSc-ZrSc and CrV-YNi ratio are commonly used to determine the provenance of the sediments (McLennan et al., 1993). The Th/Sc ratio is a sensitive index of the bulk composition of the source (Taylor and McLennan, 1985), whereas Zr/Sc ratio serves as a proxy for identifying heavy mineral concentrations, because it is highly sensitive to accumulation of zircon.

ThSc-ZrSc plot for C1 shows that there is high heavy mineral specially related to Zr and falls above rhyolite (Fig 5.3.7). C1 is divided into three parts (top, middle and bottom) based on the SiO_2 and Fe_2O_3 elemental concentrations. The upper part contains high heavy minerals, and

the lower and middle parts have ratios of the Mahaweli River upstream sediments (Young et al., 2012) while the whole core consists of the Trincomalee surface sediment ratios (Young et al., unpublished data, Fig 5.3.7). The three cores C2, C3 and C4 falls within andersite to rhyolite in composition and on the line. The core two is scattered but falls along the line. The core three and core four shows a less scatter and are within the Mahaweli downstream sediment composition (Fig 5.3.7). Only the Mahaweli River supply sediments to the Trincomalee bay. Thus, the source of the four cores is mainly from sediments of the Mahaweli River.

Cr/V ratio measures enrichment of Cr with respect to other ferromagnesian elements, whereas the Y/Ni ratio evaluates the relationship between the ferromagnesian trace elements (represented by Ni) and the HREE, using Y as a proxy (Taylor and McLennan, 1985). In this study the CrV-YNi of the four cores are also used to further determine provenance. The CrV-YNi plot (Fig 5.3.8) for C1 shows a negative correlation for the two ratios indicating less ferromagmesium content. CrV-YNi for C2 and C3 not show large scatter, and plot within the field of Mahaweli River upstream sediments. Cr/V ratio in C2 is high, indicating enrichment of Cr with respect to other ferromagnesian elements. Trace element contents of ilmenite (e.g. Cr, V and Ni) suggest gneissic to basic provenance (Hegde et al., 2006) and the higher Cr/V ratios in C2 may be a product of concentrations of ilmenite from mafic sources.

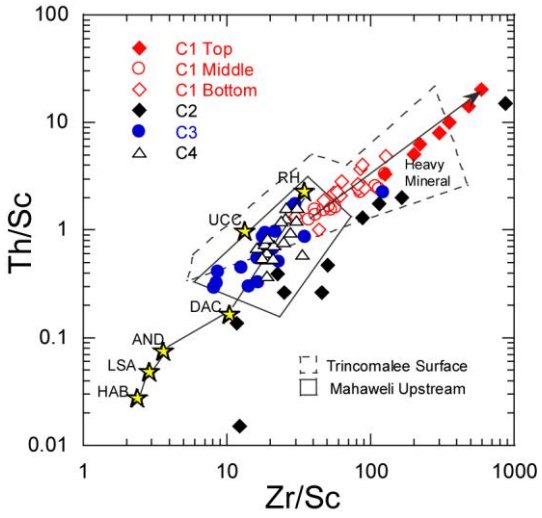

Fig. 5.3.7: Zr/Sc–Th/Sc ratio plots (McLennan et al., 1993) for the four cores from Trincomalee bay, showing zircon concentration (arrow) and typical source rock compositions. Stars BAS,

AND, DAC, RHY: average basalt, andesite, dacite and rhyolite, as plotted by Roser and Korsch (1999).

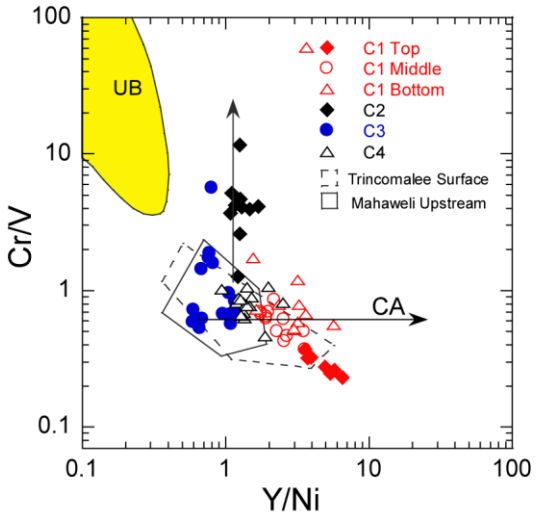

Fig. 5.3.8: Cr/V-Y/Ni plots (McLennan et al., 1993) for the four cores from Trincomalee Bay, showing the lack of ultrabasic sources. UB: Ultrabasic; field of sands derived from ultrabasic rocks in the Hino River, South West Japan (Ortiz and Roser, 2006b), CA: typical calc-alkaline trend.

The MFW (Ohta and Arai, 2007) diagram shows the trend between mafic, felsic sources and weathering trends (Fig 5.3.9). The lower part of C1 and low part of C3 on the primary source line near the F apex, indicating a felsic source. The upper most part of the C1 plot close to the mafic apex due to high heavy mineral content, especially magnetite. C4 plots in the middle of the plot and in a cluster. C3 plots little towards mafic composition in the middle of the plot.

It is established that in terms of chemical maturity the bulk chemical composition of sandstone and siltstone facies are an indication of paleo climate (Fakolade and Obasi, 2012). Cchemical maturity is expressed in terms of the SiO_2 contents and the chemical maturity index (CMI). CIM is expressed as a ratio of SiO_2/Al_2O_3, by Peters (1978). High SiO_2/Al_2O_3 ratio and high silica content (> 80%) of sediments indicate that they are derived from a deeply weathered source, and now have silica contents comparable to quartz arenites (Suttner and Dutta, 1986, Fakolade and Obasi, 2012). These are lightly to have been enhanced by winnowing of clay in the beach depositional environment.

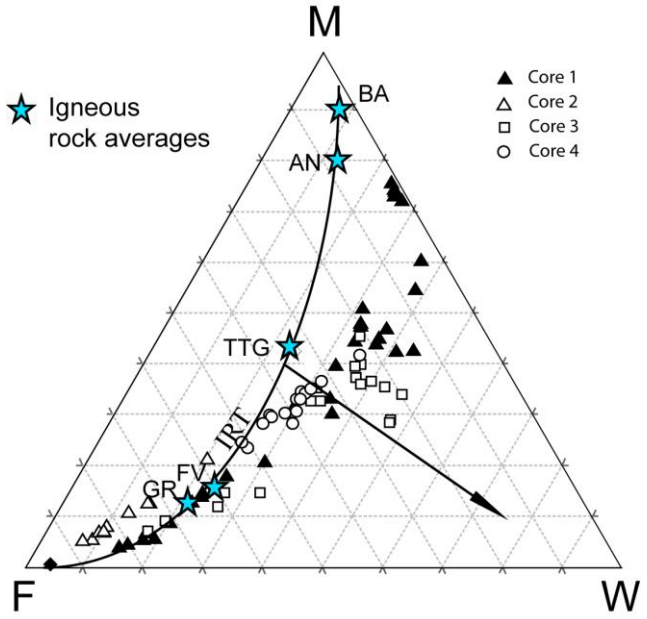

Fig. 5.3.9: MFW ternary plot (Ohta and Arai, 2007) for the four cores of Trincomalee Bay. M=mafic source, F=felsic source and W=weathered material. Calculation procedure for the vertices is given in Ohta and Arai (2007). Curved line (IRT) is the igneous rock trend. Stars are average values for Phanerozoic basalt (BA), andesite (AN), tonalite-trondhhjemite-granodiorite (TTG), felsic volcanic rock (FV), and granite (GR) from Condie (1993). Arrow indicates weathering trend from a bulk source composition between TTG and FV.

The SiO_2 content are higher than 80% in the bottom most part of C1 (38 – 62 cm) and all of core of C2 at depths of 26 cm to 36 cm of C3 and all of C4 except at depths of 2 cm and 34 cm. Fifty five percent of the upstream Mahaweli River sediments >80% SiO_2, and the rest range from 61.85 – 78.95 content. Thus, the Mahaweli River sediments themselves have high maturity. Therefore, the Mahawli River derived Trincomalee bay sediments inherit this high maturity index.

5.3.4 Ostracode assemblages in Trincomalee Bay

At least 89 ostracode taxa were identified from 13 of the 15 samples selected in the study site, and two samples did not contain ostracodes (Table 4.3.7). Many of them are extant and

typical tropical marine species that have been reported from inner bays and shallow marine areas around coasts of the Indo-Pacific region (*e.g.*, Jain, 1981; Hussain, 1998; Hussain and Mohan, 2000; Sridhar *et al.*, 2002; Hussain *et al*., 2006; Gopalakrishna *et al*., 2008; Hussain *et al*., 2010).

(1) Indices of species diversity, equitability and density: To reconstruct the bottom-water environment of the study site, nine samples, each of which contains more than 100 specimens, were selected and evaluated by quantitative analyses. Four samples with less than 100 individuals were omitted. To reconstruct the structure of ostracode assemblages in the study site, the following three indices were used: species diversity {*H(S)*}, equitability (*Eq.*), and density. The species diversity index was determined by the following Shannon-Wiener function: $H(S) = -\Sigma\, pi \ln pi$, where *pi* is the proportion of *i*-th species in a sample. The equitability index was calculated using the equation of Buzas and Gibson (1969): $Eq. = e^{H(S)}/S$, where *S* is the number of species. In this study, ostracode density was expressed by the number of ostracodes per 1 gram of dried sediment. As a result, the species diversity ranged between 0.64 and 2.94. In the Tambalagam Bay, diversity is clearly low in comparison with that in the Inner Harbor and Koddiyar Bay. The equitability ranged between 0.43 and 0.95, and is high at the mouth of Tambalagam Bay (TR-30). The density of ostracodes ranged between 5.65 and 499, indicating its wide ranges. In the Inner Harbor and Koddiyar Bay, it is relatively stable between 100 and 200. On the other hand, in Thambalagam Bay, the density shows different values in each locality.

(2) Biofacies in Trincomalee Bay : To find ostracode biofacies, we performed Q-mode cluster analysis using the same samples of aforesaid analysis and relative abundance data for 41 taxa containing more than three specimens in any of the sample. We used Horn's overlap index as a similarity (Horn, 1966) and UPGMA (unweighted pair group method with arithmetic average) as a clustering method. As a result, four ostracode biofacies (I, II, III, and IV) were discriminated (Fig 5.3.10).

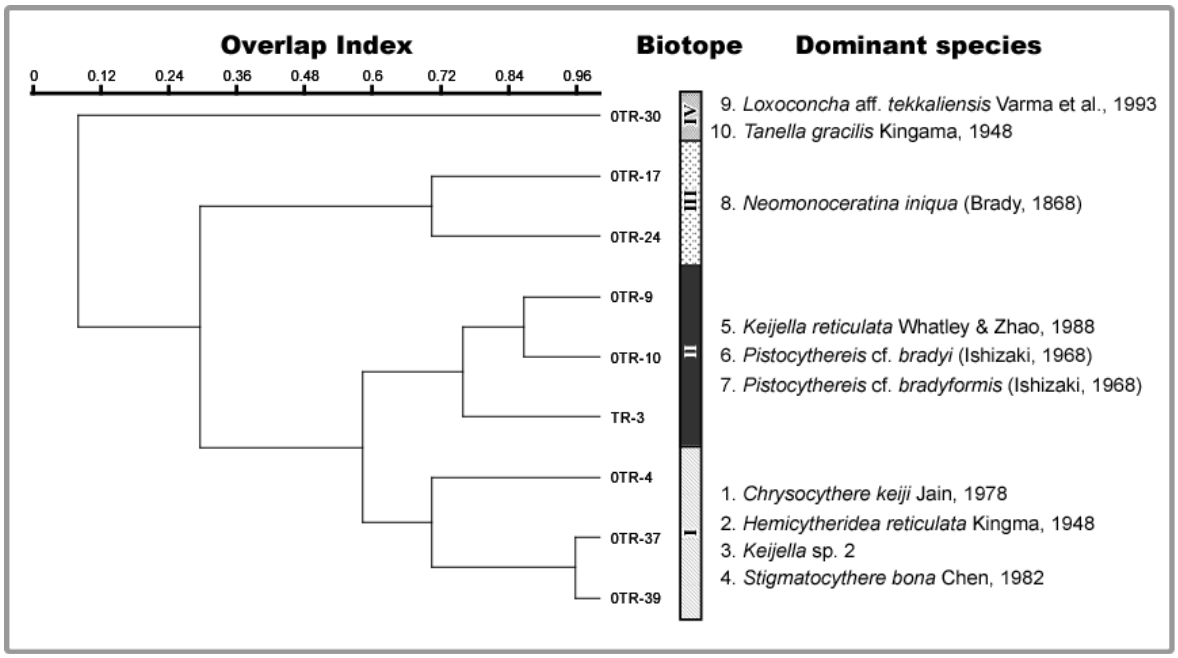

Fig. 5.3.10: Dendrogram showing the result of Q-mode cluster analysis.

Biofacies I comprises three samples (TR-4, 37, and 39) collected from relatively fine-grained sediments in Thambalagam Bay and Inner Harbor (Fig. 5.3.11, 5.3.12). It is characterized by the dominance of *Chrysocythere keiji*, *Hemicytheridea reticulata*, *Keijella* sp. 2, and *Stigmatocythere bona*. *C. keiji* was first described from beach sands of Mandvi, west coast of India by Jain (1978). According to Hussain (1998), this species occurs in Indian coast areas. *H. reticulata* was first described from the Plio-Pleistocene marls in the Atjeh (North Sumatra) and Southern Kendeng area (East Java) by Kingma (1948). According to Sridhar *et al.* (2002), this species is found both in brackish and shallow marine environments. Fauzielly *et al*. (2013) reported that *H. reticulata* lives in oxic environment in Jakarta Bay, Indonesia. *Keijella* sp. 2 has not yet been described. *S. bona* occurs rarely in the Malacca Strait (Whatley and Zhao, 1988).

Biofacies II comprises three samples (TR-3, 9, and 10) collected from relatively deep water areas in the Inner Harbor (Fig. 5.3.11, 5.3.12). This biofacies is dominated by *Keijella reticulata*, *Pistocythereis* aff. *bradyformis*, and *Pistocythereis* aff. *bradyi*. According to Dewi (1997), *K. reticulata* is mainly distributed in the Malacca Strait. The genus *Pistocythereis* lives in fine sand or muddy bottoms in the inner bay areas (Hanai *et al.*, 1977).

Biofacies III is composed of TR-17 and 26 collected from Thambalagam Bay (Fig. 5.3.11, 5.3.12). This biofacies is characterized by the dominance of *Neomonoceratina iniqua*. This species occurs abundantly in Jason Bay of the Southeast Malay Peninsula at water depths of 0–20 m (Zhao and Whatley, 1988). According to Sridhar *et al.* (2002), this species can thrive in brackish as well as shallow marine habitat with silty-sand and sandy bottoms. Lower values of diversity in biofacies III reflect the dominance of this species.

Biofacies IV is composed of only one sample, TR-30, which was collected from the estuary of branch of the Wahawelli River in Thambalagam Bay (Fig. 5.3.11, 5.3.12). It is characterized by the dominance of *Loxoconcha* aff. *tekkaliensis* and *Tanella gracilis*. The former species has not yet been described. According to Sridhar *et al.* (2002), *T. gracilis* is able to tolerate wide ranges of salinity and temperature. Lower values of diversity in biofacies IV reflect the dominance of these species.

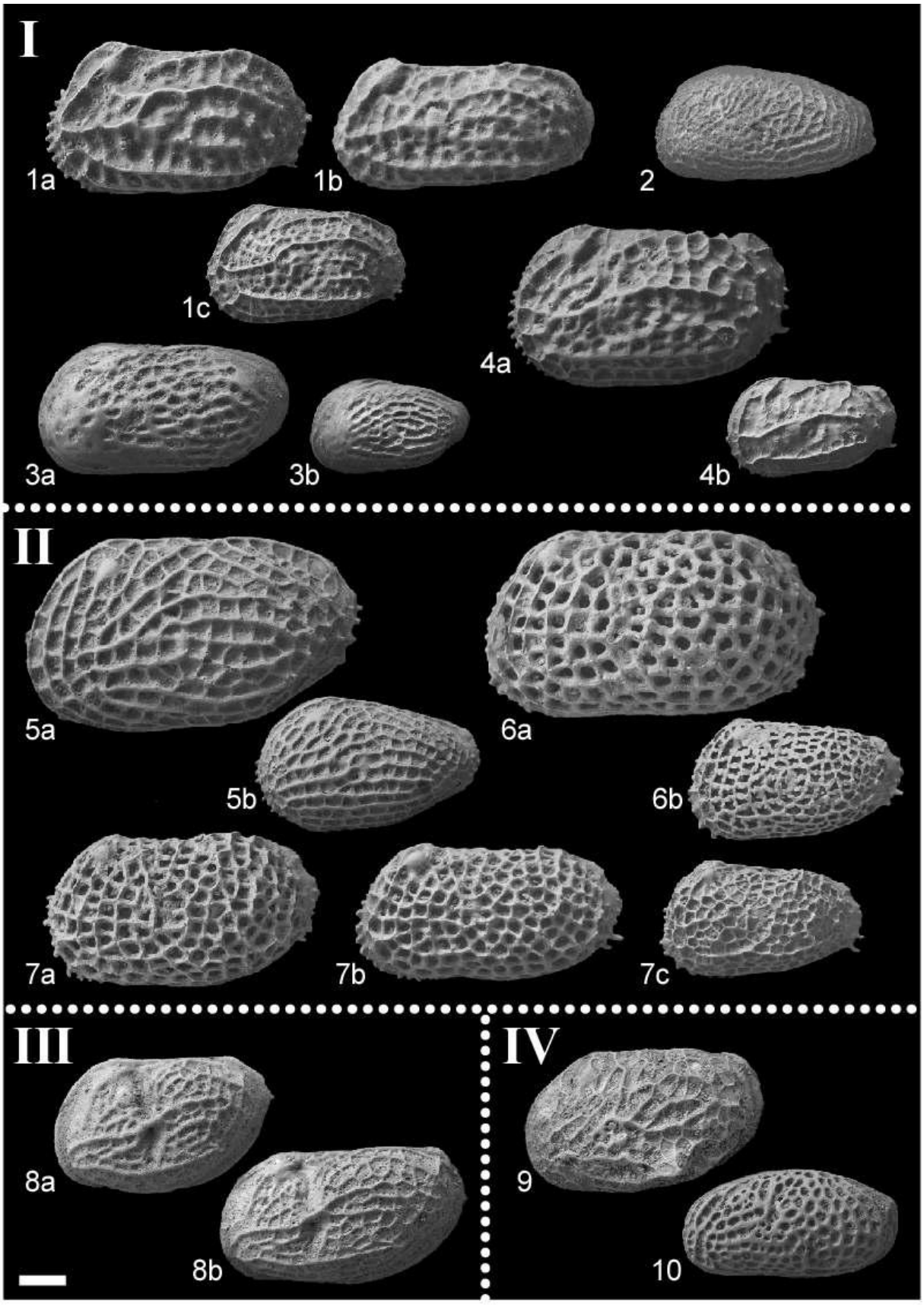
I
1a
1b
2
1c
4a
3a
3b
4b
II
5a
6a
5b
6b
7a
7b
7c
III
8a
8b
IV
9
10

Fig. 5.3.11: Scanning electron micrographs of ostracodes from Trincomalee Bay used for the Q-mode cluster analysis. All are left valves. Scale bar is 0.1 mm. 1a–c. Chrysocythere keiji Jain. 1a: female, sample TR-10; 1b: male, sample TR-4; 1c: juvenile, sample TR-17. 2. Hemicytheridea reticulata Kingma, adult, sample TR-37. 3a, b. Keijella sp. 2. 3a: adult, sample TR-37; 3b: juvenile, sample TR-37. 4a, b. Stigmatocythere bona Chen. 4a: female, sample TR-17; 4b: juvenile, sample TR-4. 5a, b. Keijella reticulata Whatley & Zhao. 5a: female, sample TR-4; 5b: juvenile, sample TR-10. 6a, b. Pistocythereis aff. bradyi (Ishizaki). 6a: female, sample TR-3; 6b: juvenile, sample TR-9. 7a-c. Pistocythereis aff. bradyformis (Ishizaki). 7a: female, sample TR-10; 7b: male, sample TR-10; 7c: juvenile, sample TR-37. 8a, b. Neomonoceratina iniqua (Brady). 8a: female, sample TR-17; 8b: male, sample TR-24. 9. Loxoconcha aff. tekkaliensis Varma et al., adult, sample TR-30. 10. Tanella gracilis Kingama, adult, sample TR-4.

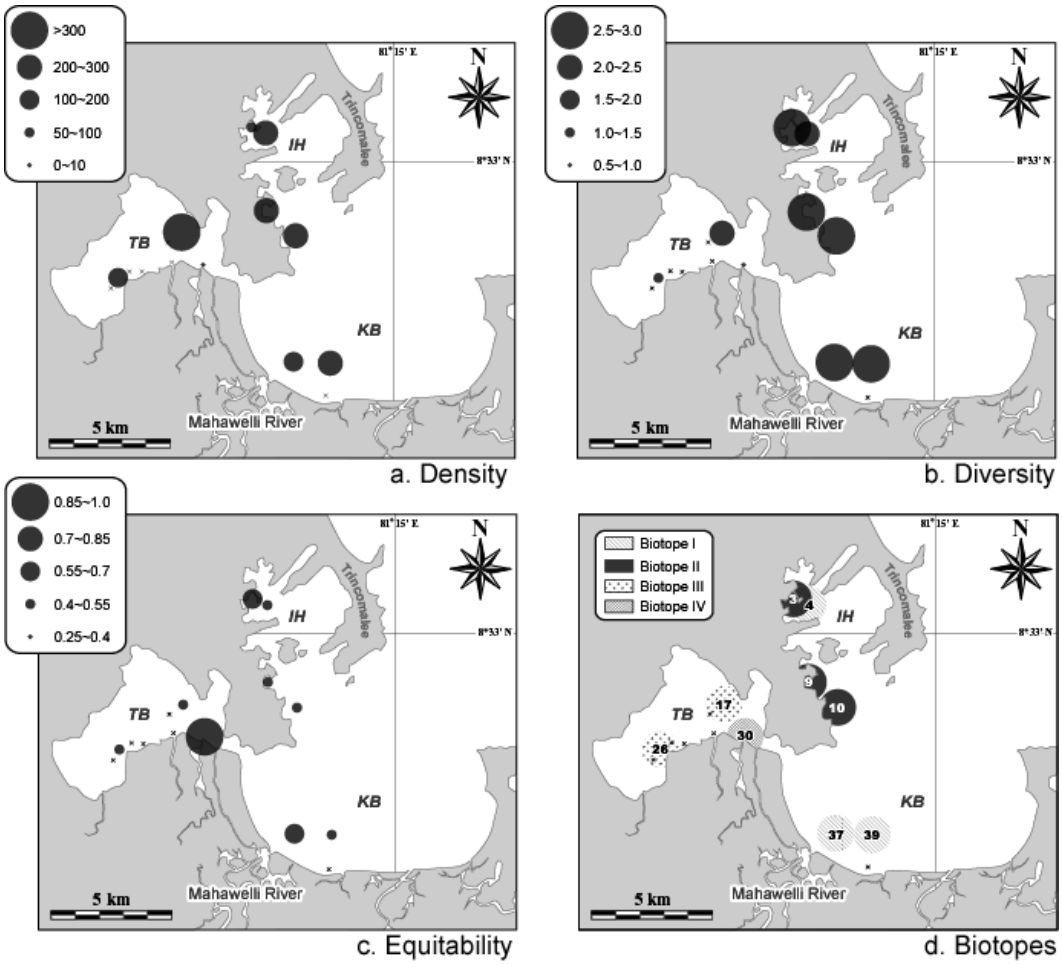

Fig. 5.3.12: Distribution of ostracode density (a), diversity (b), equitability (c), and biofacies (d) in Trincomalee Bay.

Ostracod biofacies are clearly difference each sea area (Fig. 5.3.12). These ostracode distribution patterns may account for differences of marine environmental conditions.

The results of cluster analyses combined with grain size analyses showed that biofacies I corresponds to fine sandy bottoms. Biofacies II corresponds to relatively deep water depth (> 5m) medium sand bottoms. Biofacies III and IV represent relatively shallow coarse bottoms. According to (Table 4.3.6) the Mahawelli River sediment entering the Trincomalee Bay is mainly deposited in the Koddiyar Bay while a small quantity is transported to the Thambalagam Bay and the rest of the Thambalagam Bay sediment is composed of marine sediment. The Inner Harbor is mainly of marine sediment and has negligible amount of Mahawelli River sediment. Therefore, it is possible that biofacies I represents under the strongly influence of fresh water. Biofacies II corresponds to under the sea water. Biofacies III and IV represent a benthic environment with a mixture of sea water and fresh water.

According to Irizuki et al. (2011), ostracode abundance is related with Cu and/or Zn concentrations. (Table 4.3.6) studied heavy metals distributions of surface sediments in Trincomalee Bay. They clarified that Inner Harbor is polluted by Cu and Zn. However, ostracode fauna in our results seems to be unrelated to these heavy metals distributions. In the considerably heavy metal pollution area such as Osaka Bay in the southwest Japan, its concentrations have great effects on ostracod fauna (Yasuhara and Yamazaki, 2005). In the case of Osaka Bay, ostracode abundance decreased coinciding with a rapid increase in concentration of heavy metals (Yasuhara and Yamazaki, 2005, Fig 5.3.11). Compared with these areas, Trincomalee Bay has low human activities and not so seriously heavy metal pollution. (Table 4.3.6) compared heavy metal concentrations in Trincomalee Bay with several sediment quality guidelines. As a result, Cu and Zn concentrations are lower than the standard values on the Coastal Ocean Sediment Database (Table 4.3.6) In Trincomalee Bay, heavy metal pollution seems to be not as heavy as have an impact on ostracod fauna. These ostracods information on the low contamination environment such as the study area is very important as the basic information on environmental change predicted in the future.

CHAPTER 6

CONCLUSIONS OF MAHAWELI RIVER AND TRINCOMALEE BAY SYSTEM

6.1 Mahaweli River

Elemental abundances in Mahaweli River sediments suggest some loss of mobile components from the source rocks and soils during weathering in the three climatic zones, and homogenization of the stream sediments during transport. The lack of fine-grained material in the stream sediments suggests that mechanical weathering has also occurred. The presence of considerable Na_2O in the wet zone stream sediments indicates that the weathering process is not complete. The upper reaches of the Mahaweli catchment area are heavily vegetated, and this affects weathering rates in a complex manner. Most of the stream sediments reflect a felsic source overall, whereas the basement rocks show a range of composition from mafic through intermediate to felsic compositions with a variety of lithotypes, as do the soils. Ti and Fe concentrations in the sediments partly reflect hydraulic fractionation and also concentration of heavy mineral phases containing both Ti and Fe, such as ilmenite and magnetite. High concentrations of Y, Th, Zr, Nb, Ti and Sc indicate significant concentration of heavy minerals (zircon, monazite, garnet, titanite, rutile and tourmaline), especially in the <180 μm fractions. Cr/V ratios and Sr and CaO show some variation with climatic zone, illustrating the link between climate and weathering intensity. The tributaries contribute considerably to elemental loads in the main river channel, but more detailed studies of individual tributaries are required to evaluate local lithological controls, and the contribution of each tributary to the Mahaweli sediment load. There is little evidence for contamination in the Mahaweli, with EF values for As, Zn, Cu and Ni all <1, and slightly higher values for Cr and Pb still within background limits. The results overall suggest that the composition of active sediments in the Mahaweli River is mainly influenced by source lithology, climate, weathering, hydraulic sorting and transport.

6.2 Mahaweli river fractions and heavy minerals

6.2.1 Climate, weathering, downstream accumulation, sorting and transport

The Mahaweli River is not very long compared to long rivers in the world, but geochemical processes influence elemental compositions of its bedload sediments. The bedload is mainly medium-fine sand, indicating relative maturity. Elevated highlands in the source lie within the wet zone, and the river then flows across intermediate and the dry climatic zones. The wet zone receives heavy rainfall, and hence source weathering is intense. Entry of numerous tributaries in the intermediate zone supplies fresher detritus and significant heavy mineral load, which accumulates in the dry zone downstream reaches where gradient is lower and tributaries are fewer. Rapid transport of sediments from the wet zone influences downstream fining. Sorting processes of grains also has taken place along the river.

6.2.2 Heavy minerals and chemical fractionation

Heavy minerals accumulate in the downstream reaches, and mineralogical fractionation is observed between size grades. High EF in <180 μm fractions in the tributaries suggests intense weathering in the wet zone and high heavy mineral contents, and of weathering products of these minerals. The Maoya, Ulhitiya Oya and Naulaoya Nalanda tributaries in the intermediate zone contribute major influxes of heavy minerals to the main channel. The heavy minerals are mainly magnetite, ilmenite, zircon, tourmaline and garnet, while rutile, biotite, sillimanite and hornblende are less abundant. The heavy mineral assemblage of magnetite, ilmenite, biotite, zircon, tourmaline, rutile, sillimanite, hornblende and garnet indicates derivation from mixed sources of plutonic/meta-igneous and high grade metamorphic rocks. Geology of the catchments of individual tributaries influence the heavy mineral contents of the river sediment, as shown by the lower contributions from tributaries contining marbles and quartzites. The heavy minerals present in the Mahaweli River and Trincomalee Bay are similar, indicating that the Mahaweli is the main supplier of sediments to the bay system. Decrease of iron-bearing minerals (especially magnetite) along the main channel suggest that these reactive phases are converted to ferrous (oxy) hydroxides, which are then transferred to the <180 μm fractions, leading to higher EFs for associated elements in the lower reaches. Existence of more than 50% of heavy minerals such as

garnet, ilmenite, and tourmaline in downstream fractions and in Trincomalee Bay indicate that only the most resistant heavy minerals are transported to the sea. Marked geochemical fractionation between the <180 μm and 180-2000 μm fractions is observed, especially in the dry zone. The EF enrichments/depletions for the two fractions and heavy mineral populations aid the understanding of the specific geochemical and physical processes operating in the Mahaweli River. The controls on the composition of the Mahaweli stream sediments include downstream fining, sorting, transport, variable tributary inputs and heavy mineral concentration, as reflected by the high heavy mineral contents in the main channel sediments and in the <180μm fractions.

6.3 Polgolla Dam

The high GAI's for phosphorus in the sediments is due to biogenic sources with reducing conditions. The strong oxic conditions results in deficiency of As values and enrichments of Zn, Cu, Ni, Cr. High organic matter, sulfur, iron and intense weathering processes of the area thus may be the result for higher accumulation of Zn, Cu, Ni, Cr. There is no significant change vertically in the core samples. This implies us that the anthropogenic input is not considerable. However, the natural processes in the area contribute for the accumulation of measured heavy metals. High suspended particles and the organic matter may hinder the heavy metals of the sediments, and therefore, there is a indication of pollution of the heavy metals. However, these are not polluted. Ultimately, it can be suggested that there is no threat on the environment from the human activities.

6.4 Trincomalee Bay surface sediments

Sediments within three sectors of Trincomalee Bay are mostly well-sorted fine- to medium-grained sands, but differ in geochemical composition. Sediments in Koddiyar Bay, closest to the Mahaweli River delta, have geochemical compositions similar those supplied by the river. Sediments in the semi-enclosed and more distal Thambalagam Bay are also mainly derived from the Mahaweli River, but are modified by additions of Ca, Mg, and Sr from marine biogenic carbonate sources. This marine component is even greater in the Inner Harbour. Very high concentrations of elements including Ti, Zr, Ce, Nb and Y in Koddiyar Bay are consistent

with heavy mineral concentration by winnowing in a high-energy zone, creating heavy mineral lags. Although hydraulic sorting effects among Fe-Ti oxides are similar throughout the three sectors, some fraction of heavy mineral assemblages may occur within the bay.

Evaluation of present-day environmental status using established pollution guidelines (COSED LEL, SEL, and PEL) indicates that Zn, Pb, Cu, and Ni are present only at natural background levels. However, As contents exceed LEL in the Inner Harbour and Thambalagam Bay, and Cr exceeds LEL in all three sectors, implying that some contamination of these two elements may have occurred. However, closer evaluation of the data using Al-normalized metal enrichment factors (EFs) and lower Mahaweli River sediments as background indicators reveals that these apparent enrichments are in fact spurious, and As and Cr are present only at locally higher background levels. This emphasizes the importance of establishing local background levels, to be used in conjunction with more global environmental guidelines.

6.5 Trincomalee Bay core sediments

The concentrations of Ti, Fe, Zr, Th, Y, V, N, and Cr in the C1 are very high, due to concentration of heavy minerals. The heavy minerals that were determined were magnetite, hornblende, ilmenite, hematite, sillimanite, tourmaline, biotite, rutile and garnet. However, the age is unknown and thus cannot predict the exact deposition events.

The high CMI ratios indicate that the core one sediments from 1C24 – 1C30 are mature. Three other cores also show high maturity, but not to the extreme values seen in C1. Most of the sediments have SiO_2 > 80% may have silica contents comparable to quartz arenites. Negative LOI indicates gain of weight due to iron bearing minerals. The main mechanism involved in these sediments may be the sorting of grains. Circulation of water currents, the wave and wind direction are controlling factors for the deposition of heavy minerals in C1. The sediments are mainly supplied by the Mahaweli River but may also be partially composed of marine sediments. Coarser lower C1 sediments (40 - 60 cm) may have been deposited by large waves and currents, as evidenced by the presence of large angular grains and only thin mud inter-beds. Sand bar formation in Koddiyar Bay near the river mouth, reduces wave and current activity. The upper part of C1 thus consists of finer grains and abundant heavy minerals. C2 is composed only of Mahaweli River sediment deposited in sand bars. In C3 the interval from 20 – 28 cm may

represent a buried flood deposit. Core 4 is also mainly composed of Mahaweli River sediments, but was deposited in a calmer, semi-enclosed bay, leading to higher content of finer grained detritus bar with smaller quantities of finer clay included.

6.6 Ostracode of Trincomalee Bay

At least 89 ostracode taxa were identified samples selected in the study site except two samples. Based on the sediment of Trincomalee bay environments it is possible that biofacies I represents under the strongly influence of fresh water. Biofacies II corresponds to under the sea water. Biofacies III and IV represent a benthic environment with a mixture of sea water and fresh water. The ostracode fauna in our results seems to be unrelated to Cu and Zn heavy metal distributions.

CHAPTER 7

KUMA RIVER AND YATSUSHIRO BAY SYSTEM-JAPAN

INTRODUCTION TO THE KUMA RIVER AND YATSUSHIRO BAY SYSTEM

7.1.1 Introduction to Kuma River

While the building of dams can be both environmentally and geochemically important, dam destruction will also have a large impact on the environment and on fluvial sediments (Katopodis and Aadland 2006; Hu et al. 2009; Bednarek 2001). The first dam removal in Japan occurred when the control gate was removed from the Arase dam in Kumamoto Prefecture in April 2010. The dam is located ~ 19.9 km from the mouth of the 115 km long Kuma River (Fig. 7.1.1). When a river is dammed, sediments are deposited on the upstream side of the dam, and the dam's sustainability can be threatened by rapid sedimentation (Haregeweyn et al. 2012; Bednarek 2001). This can cause a number of environmental problems in the river channel, such as water stagnation and an increase of minor element concentrations in the river waters due to increasing anoxic conditions below the thermocline (Bellanger 2004). These and other factors have been discussed in numerous dam sediment assessments (Jiongxin 1996; Ghrefat and Yusuf 2006; Cevik et al. 2009), and mitigation strategies based on sediment properties and sedimentation impacts (Haregeweyn et al. 2012; Trabelsi et al. 2012).

Metals are a group of contaminants with high ecological significance. They tend to accumulate in suspended particulates and in sediments. Metals are not removed from the water column by self-purification. Metals tend to enter the food web via lower-level consumption and bio-accumulation, moving to the higher consumers (Ghrefat and Yusuf 2006; Khaled et al. 2006). Areas of mud deposits increase the amount of fine suspended matter in bottom waters. Anoxic conditions are also common, affecting bottom waters and sediments due to temperature changes and stratification, especially through seasonal cycles. This in turn affects river flow, water quality, and river sediments. In addition, grain size variation is a critically important factor in river sediment (Surian 2002; Owens et al. 2005). The rate of change in bed material size has important implications for river ecology (Petts et al. 2000). Thus, dam construction affects many geological features of the river, its water quality and the channel's sedimentary environment.

Consequently dam removal will also have a major impact on river water quality, geology, and ecology.

River sediments are ultimately deposited in estuaries. Estuarine geoenvironmental processes are very complex. The turbulent mixing of fresh water and seawater can generate rapid changes in many trace element concentrations (Feely et al. 1981). In addition to physical mixing of two very different water bodies, biological processes have a large impact on the aqueous environment, modifying many other variables. It is therefore difficult to describe the origins, pathways, and fates of dissolved and particulate materials in coastal marine systems, and especially in estuaries. The Yatsushiro Bay environment is subject to this array of variables and is very complex.

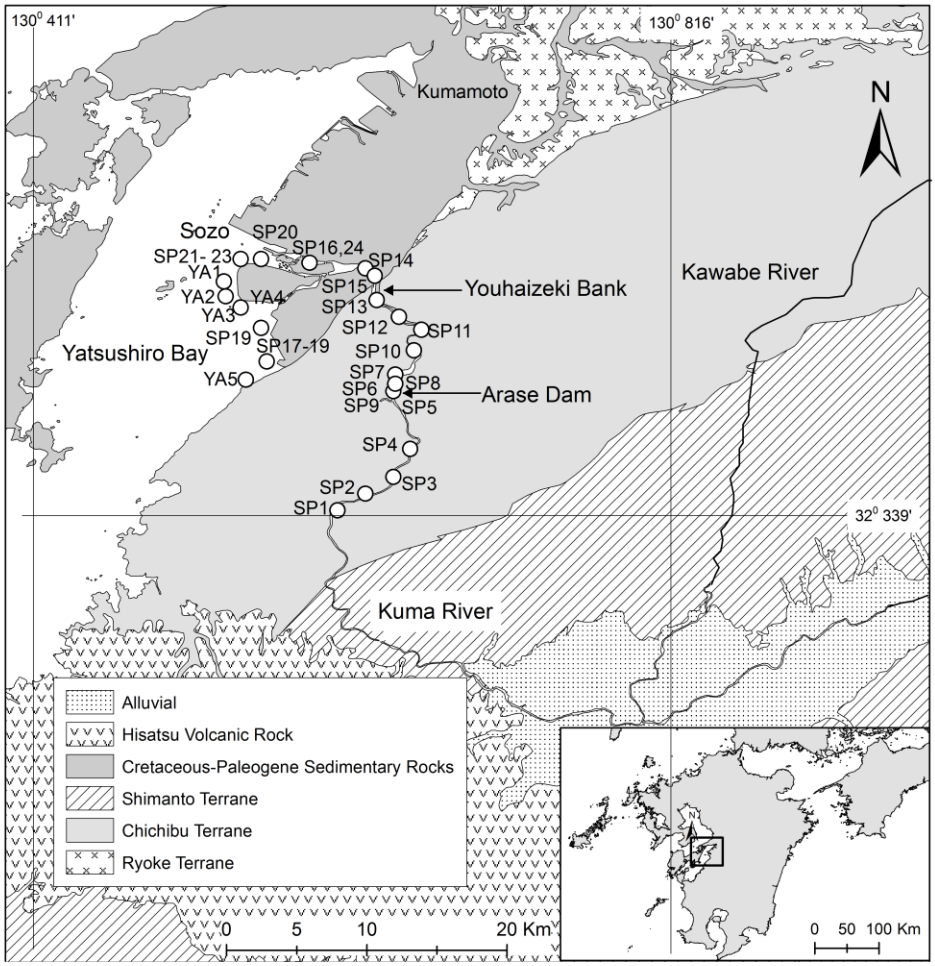

Fig 7.1.1: Geology of the Kuma River and sampling locations in Kumamoto prefecture, Kyushu Island, Japan

7.1.2 Introduction to Yatsushiro Bay

Tidal flats constitute an important interface between land and sea and between marine and fresh water systems (Cardoso et al. 2008). They are enriched in nutrients by oceanic and continental inputs and are among the most productive aquatic ecosystems (Nixon 1988; Cardoso et al. 2008). Coastal lagoons, one typical estuarine environment, receive the by-products of inland human and natural activities. Human activity in coastal lagoons has increased considerably in recent years, and its impact on these productive and economically important environments has become a major concern (Cardoso et al. 2008; Morrison et al. 2001). Therefore tidal flat sediments are among the most important indicators of changes in sediment accumulations and aquatic system geochemistry. Although lake sediments may be better indicators of nutrient and metal accumulation, marine bays and estuaries also record input changes, although they may be less effective in retaining nutrients (Nixon 1988).

Marine sediments serve as the ultimate sink for heavy metals discharged into the aquatic environment (Luoma and Bryan 1981). The fate and flux of heavy metals discharged from continent to ocean is controlled by biogeochemical and sedimentological processes taking place in estuaries (Monbet 2006). Metals accumulate in bottom sediments through several types of reactions: flocculation, coagulation, formation of particulate Fe and Mn oxyhydroxides and absorption on suspended matter (Sholkovitz 1976; Zwolsman et al. 1997).

Sediments reflect the geochemical history of a given region including the local anthropogenic impact. Hence, sediments act as useful indicators of long- and medium-term metal flux. Higher concentrations of heavy metals in sediments may not necessarily indicate anthropogenic contamination, due to different background levels in parent materials and sediment properties. The natural occurrence and chemical speciation of metals can also complicate the evaluation of potentially polluted aquatic sediments (Schiff and Weisberg 1999).

Nutrients and suspended sediment concentration are higher in the inner areas of the coastal lagoon than in the tidal channel (Schwindt et al. 2004). Diatoms (Bacillariophyceae) are also an important and often dominant component of benthic microalgal assemblages in estuarine and shallow coastal environments (Sullivan 1999). Different environmental factors may influence the diatom distributions observed in each zone of the lagoon. Therefore, SEM images

of diatoms in suspended solids can be very useful for understanding the prevailing estuarine environment.

7.2 BACKGROUND

The Kuma River and the Yatsushiro bay is situated in south west Japan. The Kuma River is dammed at Arase dam and can affect the sediments of the Kuma River and the Yatsushiro bay. The Arase dam was decided to be removed starting by April 2010. The dam removal will take about seven years to complete. Therefore, the opening of the dam flushes the sediments and forms point bars in some places beside the Kuma River banks. These changes based on geochemical aspect were decided to be monitored. Previously only one study has been carried out based on geochemical aspect by Dozen and Ishiga 2002. Therefore, it is important to continue further geochemical investigations to understand the changes within the system.

7.3 SCOPE OF THE RESEARCH

- Study the major and trace element distribution patterns of Kuma River and Yatsushiro Bay sediments.
- Human influence on the chemical nature of sediments can be understood.
- The Arase dam removal and its effect on the Kuma River and the Yatsushiro Bay desiments, suspended soilds and water quality is assessed.

7.4 OBJECTIVE OF THE STUDY

7.4.1 Kuma River and Arase Dam

This study is the first attempt to look into the environmental changes in the Kuma River and Arase dam sediments. Arase dam was removed based on a number of environmental issues. It is therefore important to look into the geo-environmental changes that have occurred after the removal of the dam. To do this, elemental concentrations of twenty three major and trace elements (As, Pb, Zn, Cu, Ni, Cr, V, Sr, Y, Nb, Zr, Th, Sc, F, Br, I, Cl, Fe_2O_3, TiO_2, MnO, CaO, P_2O_5 and total sulfur) in the sediments of the Kuma River, Yatsushiro Bay, and the former lake above the Arase dam were examined. The objective was to document the environmental and

geochemical changes that took place in the Kuma River and Yatsushiro bay because of the removal of Arase dam.

7.4.2 Yatsushiro Bay

The aim of this study is to identify the effect of Kuma River sediments on Yatsushiro Bay after the opening of the Arase dam gates and also document the geoenvironmental conditions of Yatsushiro Bay and the Kuma River.

7.5 EXPECTED OUTCOME

- Investigation of possible geochemical and environmental changes and mobilization of major and trace elements along the Kuma River sediments.
- Investigation of causative factors affecting human health.
- Find out effect due to removal of the Arase dam and the changes occurred in the Kuma River and Yatsushiro Bay sediments.

7.6 GEOLOGY OF KYUSHU

Kyushu is the third largest Japanese island with an area of nearly 36,000 square kilometers. Most of the basement of Kyushu is composed of four geologic terranes, from north to south: Sangun, Ryoke, Chichibu, and Shimanto belts. The descriptions of these terranes are found in Kimura et al., 1991; Taira 2001 and has not been discussed in detail in this chapter because the geology of Kyushu Japan is very complex.

Cretaceous to Tertiary sediments basins in Kyushu recorded diverse tectonic processes at the active margin along the East Asian continent, where various types of sedimentary basins were formed in different tectonic settings; transform, oblique-slip and orthogonal convergent margins since Jurasic time (Sakai et al., 1992). The geology of the studied area has been discussed in detail in section 7.7.4.

7.7 GENERAL INFORMATION OF THE PROJECT AND PROJECT AREA

7.7.1 Location and Accessibility

Kyushu is located in the South west of Japan as an Island. The Kuma Rive and the Yatsushiro bay is located in the central western part of Kyushu. The locations can be easily accessed by any mode of transportation.

7.7.2 Historical Perspective of Water Resource Management of Kuma River area

Kuma River is the only large river flowing into the Shiranui Sea from Yashiro City in Kumamoto Prefecture. The main stream flowing from the west, and Kawabe River coming from the north joins in Hitoyoshi city. Kawabe River is a tributary but its flux is more abundant than the main stream.

7.7.3 Historical activities of the Yatsushiro Bay

In 1956, the government of Kumamoto Prefecture constructed Arase dam in Sakamoto-mura in the middle stretch of Kuma River for the hydropower generation. The government of Kumamoto Prefecture had decided to remove Arase Dam in 2009. The reasons for removal are increasing, such as: decrease in need of hydropower and the cost of maintenance. In 1959 an electric power company constructed Setoishi dam in the upper stretch from Arase dam about 10 km. In 1963 the government of Kumamoto Prefecture constructed Ichihusa dam for water supply in the upper stretch of Kuma River. After that the state of Kuma River had changed completely.

7.7.4 Physiography and Geology

7.7.4.1 Kuma River area

The study area is located in Kumamoto prefecture, Kyushu, Japan. Arase dam is one of the few dams on the Kuma River. The geology of the study area is highly complex. The Kuma River flows through the Chichibu terrane, the Hisatu volcanics, the Cretaceous-Paleogene Sedimentary rocks, the Shimanto terrane, and associated alluvial deposits (Fig. 7.1.1). Yatsushiro

Bay is located in the Chichibu terrane (Fig. 7.1.1). The Yatsushiro area is within the inner and outer zones of the Kyushu Cretaceous system (Sakai et al. 1992). The sedimentary basins/accretionary complexes of Kyushu belong to the Cretaceous and Tertiary periods. The Yatsushiro region and the Kuma River catchment intersect Early Cretaceous shallow-marine and turbidite basins and the Late Cretaceous non-marine, shallow-marine, and turbidite basins in the Ryoke terrane (Sakai et al. 1992). The Kawabe River joins the Kuma River. It flows through the Shimanto terrane and the Chichibu terrane (Fig. 7.1.1). The modern geologic setting may be different from that in the past, however, as Kyushu has active island arc type volcanoes, active faults, and significant crustal movement (Ogawa et al. 1992).

Ms. Yoshiko Shiotani, Governor of Kumamoto Prefecture decided the removal of Arase Dam after several public discussions on the environmental recovery of the Kuma River. The dam was too old and the structure has been decayed. In 2010, April 10 all eight gates of the Arase dam were opened and flushing of water accelerated water flow of the Kuma River. Bed form of this river was changed, such as seven bars known before dam construction have been recovered by transportation and accumulation of sands and developments of point bars along the river were apparent (Tsuru, 2011). At tidal flat of the Yatsushiro Bay, Tsuru described changing ecology. Discoloration of "*Aonori*", green laver has not been observed, recovery of *Mya arenasia* shell, small size crabs, *Upogebia pusilla*, green *Lingula jaspidea*, razor clam *Solen strictus*, Manila clam, common orient clam, *Meretrix lusoria* have been recovered. Typical thing is the recovery of *Zostera marina* on the bars. All these are significant change in the Yatsushiro Bay.

The Arase dam was built in 1954 to generate hydroelectric power with a total storage capacity of 10,140,000 cubic meters and the water flooding is 1,230,000 m^3. The width of the dam is 210.8m and the height is 25m. As for the plan of the Kumamoto Prefectural office, the dam gate opening was started in April 2010 (Fig 7.1.2a). The systematic water level change is done by opening two control gates in the center of the dam (Fig 7.1.2a). The water level decrease to the foot of the dam is expected by 2013 March. The removal of dam gates is done from the right side to the left side of the Arase dam. In 2015 two gates are to be completely removed (Fig 7.1.2b). In 2016 the rest of the gates will be removed (Fig 7.1.2c) and by 2017 the dam will be completely removed (Fig 7.1.2d). A bottom sediment removal plan was also established. As for this planning all the bottom sediment is expected to be taken out by 2012. The bottom sediment removal was started in March 2007 at a capacity of 96, 000 m^3. The removal is calculated to be

finished by 2011. The removal of bottom sediment was estimated at 14, 776 m3, 71, 469 m^3, 5600m^3 and 17, 000m^3 for the years 2008, 2009, 2010, 2011 respectively. The Yatsushiro delta has an area of 2, 947 ha and the Yatsushiro annual tidal change is 4m.

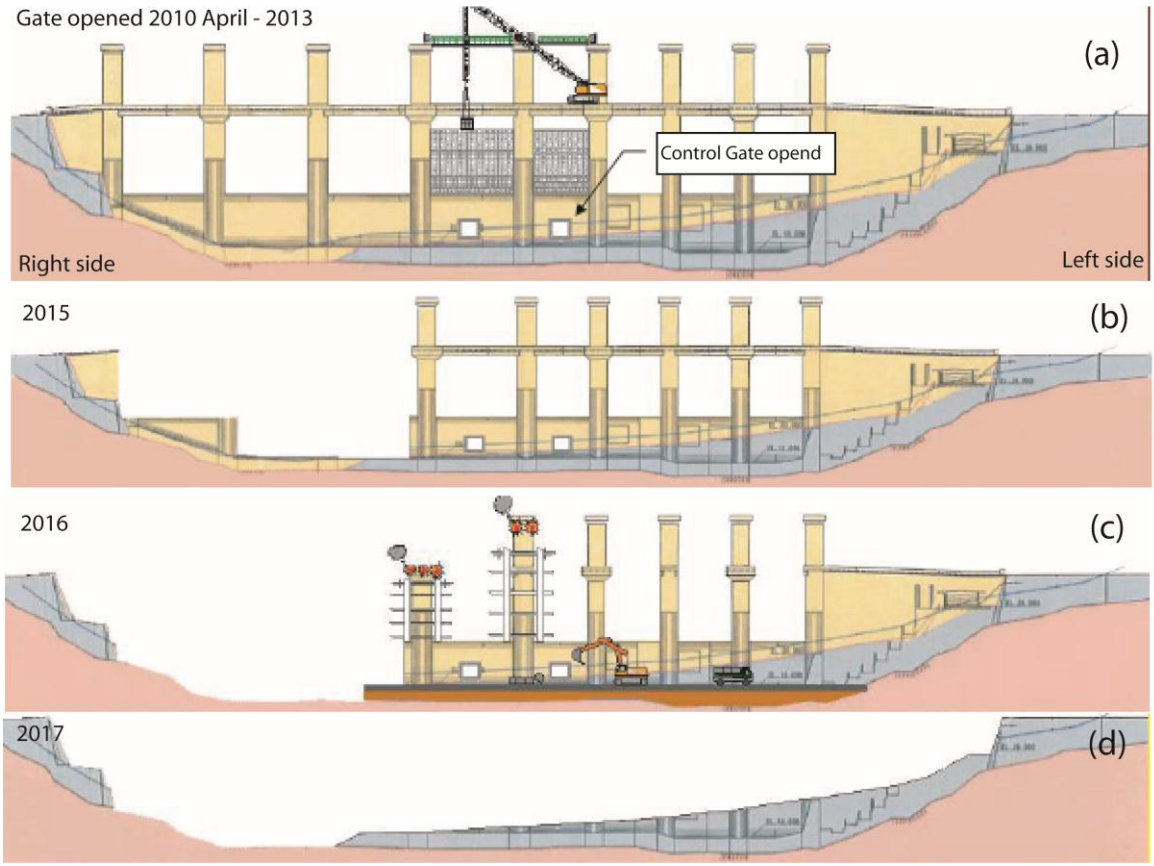

Fig. 7.1.2: Schematic diagram showing Arase dam removal starting from April 2010 to 2017. (a): The control gates were opened to have a systematic water level change by 2013. (b): The removal will be started in 2015 from the right corner of the dam. Initially two gates will be completely removed and the concrete will be removed. (c): The next gates will be removed in 2016. (d) The completion of dam gate removal is expected to in 2017. These are only few figures of the whole process and the figure is sponsored by the Planning and Construction Office of the Kumamotho Prefecture Office, of the government of Japan.

7.7.4.2 Yatsushio Bay area

Arase dam is situated in Kumamoto prefecture, southwest Kyushu, Japan. The Arase dam is on the Kuma River, about 19.9km from the Yatsushiro tidal flat. The process of removing the Arase dam was begun in early 2012. The Arase dam consists of eight gates. Two of these gates were opened in April 2010 to flush the excess water and sediments from above the dam. Gate opening is used to control water levels. When a river is dammed, sediments are deposited on the upstream side of the dam, and the dam's sustainability can be threatened by rapid sedimentation (Haregeweyn et al. 2012). Arase dam is the first dam to be removed in Japan, and removal will take approximately seven years for completion. This action was implemented as a mitigation strategy based on sediment properties and sedimentation impacts (Haregeweyn et al. 2012; Trabelsi et al. 2012).

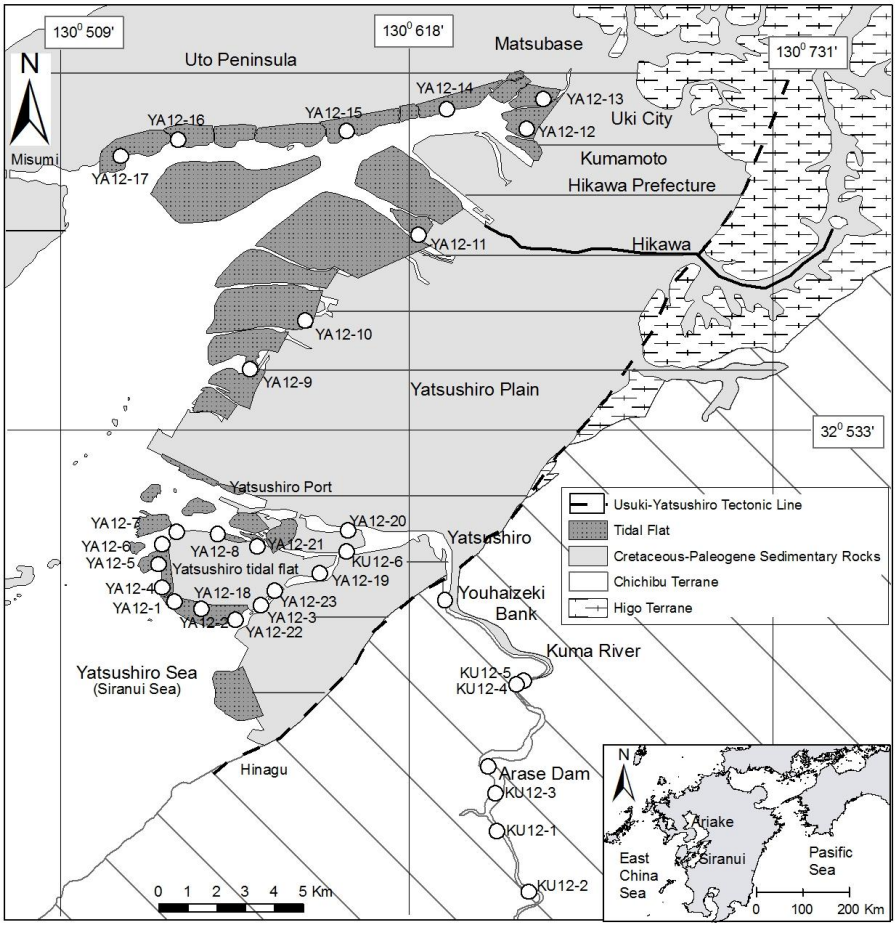

Fig. 7.1.3: Simplified geological map and sediment sampling locations of the Kuma River and the Yatsushiro tidal flat

The Yatsushiro Sea is an inlet of ca. 1,200 km^2, with a tidal range during the spring tide reaching ca. 4m in the innermost part and ca. 3m in the southern part of the inlet. Sandy and muddy tidal flats of ~46 km^2 develop in the northern region of the bay (Subiyanto et al. 1993). Yatsushiro Bay is a semi-closed estuary opening to the East China Sea. The Kuma River flows into Yatsushiro Bay forming a large tidal flat at the river mouth (Fig. 7.1.3). These tidal flats are formed in the southern region of the Uto Peninsula and along the western edge of the Yatsushiro plain (Fig. 7.1.3). The Hikawa River flows along the Hikawa District and is open to the Yatsushiro Sea (Fig. 7.1.3). The drainage area of the Kuma River above the Arase dam is 1880km^2. Typical sea level in the Yatsushiro Sea ranges between +4.67m and -0.16m.

The basement geology of central Kyushu is composed of four geologic terranes. The Yatsushiro Bay basement is composed of the Higo terrane while that underlying the Kuma River is the muddy Jurassic melange of the Chichibu terrane. The Usuki-Yatsushiro tectonic line divides the Higo terrane and the Chichibu terrane (Fig. 7.1.3, Matsumoto and Kanmera 1964; Yamamoto 1992). The Higo terrane consists of three Jurassic metamorphic zones; the Ryuhozan, the Manotani and the Higo metamorphic rocks. The Ryuhozan metamorphics are similar to the Ryoke and consist of granitic gneiss and granites. The Manotani metamorphic rocks consist of pelitic schist and basic schist (Matsumoto and Kanmera 1964; Yamamoto 1992). The Higo metamorphics are psamitec calcarious schist yielding the ultra mafic rocks and limestone of southwest Japan. The geology of the Yatsushiro Bay area is made up of Cretaceous-Paleogene sedimentary rocks, the Chichibu terrane, and the Higo terrane (Matsumoto and Kanmera 1964; Yamamoto 1992). The Kuma River primarily flows in the Chichibu terrain (Fig. 7.1.3). The Higo volcanic rocks (mainly andesite) are widely distributed south of the map area (Fig. 7.1.3, Matsumoto and Kanmera 1964; Yamamoto 1992). Thus, the provenance of Kuma river sediments is from the Chichibu terrane and the Higo volcanics.

Sediment grain size in the southern region of the Uto Peninsula is mostly fine grains. On the Yatsushiro plain and in the Kuma River, sediments are fine to medium grain, and coarse grain respectively (Table 7.1.1).

Table 7.1.1: Elemental concentrations, Loss on Ignition (LOI), Md50 (median grain size) and sorting of surface and bottom sediments, Kuma River and Yatsushiro Bay. NA-Not Analyzed, ND- Not Detected. UCC- Upper continental crust values of Taylor and McLennan 1985. Grain size calculations of Md50 and sorting are as for Folk and Ward (1957).

Sample No	As	Pb	Zn	Cu	Ni	Cr	V	Sr	Y	Nb	Zr	Th	Sc	TS	F	Br	I	Cl	TiO_2	Fe_2O_3	MnO	CaO	P_2O_5	LOI	Md50 Φ	Sorting Φ
Surface																										
SP 2 S	7	16	73	18	25	51	105	107	21	7	98	7	10	273	145	2	9	nd	0.46	5.74	0.10	1.08	0.09	2.83	-0.57	0.61
SP 3 S	9	18	83	27	32	56	115	63	26	10	97	10	11	276	33	2	10	nd	0.57	6.07	0.15	0.84	0.10	3.30	1.13	0.86
SP 4 S	6	14	78	23	39	88	139	129	20	9	97	7	16	275	227	2	6	nd	0.65	7.11	0.12	1.58	0.11	2.62	1.83	1.13
SP 5 S	6	14	65	19	29	52	96	113	19	6	92	7	10	265	nd	1	15	nd	0.44	5.41	0.09	1.21	0.09	18.18	1.07	0.72
SP 6 S	7	15	78	21	29	77	137	125	20	8	99	6	15	273	75	1	13	nd	0.63	6.38	0.10	1.29	0.10	2.52	1.57	1.04
SP 7 S	6	13	73	23	38	87	136	120	21	9	97	7	16	264	47	2	12	nd	0.67	6.61	0.11	1.42	0.11	na	2.30	1.05
SP 8 S	7	13	71	23	34	73	115	119	19	7	101	7	14	283	75	2	14	nd	0.52	6.21	0.10	1.33	0.10	2.57	2.63	1.27
SP 9 S	9	18	105	29	117	141	170	96	23	8	108	7	16	342	8	2	11	nd	0.73	7.79	0.13	1.18	0.11	4.57	0.50	1.02
SP 10 S	7	15	74	23	35	73	129	117	21	9	107	7	12	287	116	2	12	nd	0.59	6.19	0.10	1.30	0.10	2.86	1.90	1.12
SP 11 S	7	15	73	24	36	73	133	121	22	9	103	7	14	290	89	2	13	nd	0.59	6.13	0.11	1.41	0.10	2.99	2.53	1.03
SP 12 S	6	15	76	21	40	106	138	120	20	8	95	7	14	294	61	2	14	nd	0.63	6.50	0.11	1.24	0.11	na	2.07	1.12
SP 14 S	8	16	79	30	36	78	142	132	22	9	124	9	15	371	302	3	8	nd	0.64	6.25	0.11	1.48	0.11	na	2.83	1.05
SP 15 S	6	14	66	20	42	71	93	116	18	6	89	6	9	262	74	1	16	nd	0.43	5.45	0.09	1.23	0.09	2.35	1.10	0.66
SP 16 S	8	18	86	26	38	89	138	125	25	10	137	7	15	998	103	15	19	2939	0.62	6.22	0.10	1.13	0.15	4.86	2.63	1.58
SP 17 S	7	14	70	17	34	82	106	129	21	8	122	7	10	1486	144	13	18	5510	0.55	5.41	0.10	1.17	0.10	na	2.80	1.42
SP 18 S	7	15	73	17	35	79	109	133	22	8	153	8	12	2565	nd	16	15	7098	0.59	5.27	0.08	1.20	0.10	na	2.97	1.38
SP 19 S	9	17	83	22	36	72	114	132	24	10	143	8	13	2332	61	22	14	4584	0.65	5.73	0.11	1.15	0.12	na	3.27	2.19
SP 20 S	8	16	90	18	36	76	113	124	22	8	123	8	14	1391	89	10	16	2449	0.59	5.92	0.08	1.09	0.11	3.76	2.60	1.42
SP 21 S	10	20	90	25	38	66	131	134	27	11	134	9	14	2755	103	36	12	9712	0.64	6.16	0.10	1.30	0.15	8.90	2.40	2.09
SP 24 S	8	13	78	13	34	85	111	121	20	7	110	7	13	659	74	5	18	nd	0.51	5.56	0.09	1.13	0.09	2.66	2.13	1.18
YA 1 S	9	16	80	18	35	65	113	125	22	8	115	8	12	2277	61	19	10	7725	0.57	5.61	0.08	1.22	0.12	4.86	2.37	1.58
YA 2 S	11	20	98	36	42	70	132	131	27	11	130	11	15	2279	89	36	6	12887	0.67	6.48	0.13	1.17	0.17	8.51	2.90	1.67
YA 3 S	7	13	66	21	36	69	99	127	19	7	98	7	10	1425	180	14	16	7728	0.49	5.26	0.10	1.28	0.10	3.41	1.40	1.09
YA 4 S	12	20	103	34	45	72	148	122	29	11	129	12	16	2088	47	41		9928	0.70	6.98	0.15	1.17	0.18	10.19	3.17	2.52
YA 5 S	12	23	120	27	43	69	129	133	27	10	122	11	14	4199	192	41	8	9036	0.66	6.90	0.10	1.60	0.15	8.15	2.90	0.75
Min	6	13	65	13	25	51	93	63	18	6	89	6	9	262	8	1	6	2449	0.43	5.26	0.08	0.84	0.09	2.35	-0.57	0.61
Max	12	23	120	36	117	141	170	134	29	11	153	12	16	4199	302	41	19	12887	0.73	7.79	0.15	1.60	0.18	18.18	3.27	2.52
Bottom																										
SP 2 B	7	14	68	20	31	59	104	111	20	8	95	7	11	274	47	2	15	nd	0.48	5.57	0.09	1.22	0.09	2.76	1.50	1.83
SP 3 B	10	18	83	26	35	59	117	62	26	11	102	11	11	290		2	16	nd	0.56	6.17	0.13	0.83	0.10	3.31	-0.27	0.87
SP 4 B	6	14	70	21	34	66	114	121	20	8	96	7	12	280	261	2	16	nd	0.54	6.03	0.10	1.41	0.10	2.66	0.00	1.00
SP 5 B	7	13	68	23	28	52	108	113	19	6	92	7	10	273	89	1	20	nd	0.46	5.57	0.10	1.18	0.09	2.30	0.93	0.86
SP 6 B	7	14	78	23	32	76	143	120	21	8	101	7	14	300	89	2	11	nd	0.60	6.39	0.10	1.27	0.10	2.77	2.00	1.15
SP 7 B	7	16	77	25	34	63	139	129	22	9	113	8	15	430		2	7	nd	0.62	6.21	0.11	1.46	0.10	na	2.70	1.05
SP 8 B	6	13	67	21	36	81	114	117	19	7	91	7	12	289	62	1	16	nd	0.50	6.17	0.10	1.31	0.10	2.48	-0.93	0.61
SP 9 B	8	16	99	30	121	164	164	91	21	6	96	6	17	281	176	2	9	nd	0.63	8.02	0.11	1.19	0.11	4.04	0.00	0.56
SP 10 B	7	16	76	23	37	73	126	115	21	8	100	7	15	319	170	2	11	nd	0.55	6.13	0.10	1.26	0.10	3.18	2.27	1.12
SP 11 B	7	13	66	19	45	94	104	120	19	6	92	5	11	280	61	1	13	nd	0.43	5.68	0.09	1.22	0.10	2.52	-0.83	0.77
SP 14 B	7	17	76	23	35	90	138	129	22	9	114	8	15	358	49	2	9	nd	0.65	6.18	0.11	1.38	0.11	na	2.83	1.06
SP 15 B	6	12	67	21	46	86	99	114	18	6	90	6	9	270	1	18	nd	nd	0.45	5.57	0.09	1.26	0.09	2.38	1.13	0.60
SP 16 B	8	19	89	28	39	82	138	131	26	11	159	9	13	1122	286	14	16	3631	0.67	6.29	0.10	1.16	0.15	5.75	2.93	1.54
SP 20 B	8	16	83	18	36	76	121	119	21	8	124	7	13	1933	89	16	18	8856	0.57	5.83	0.07	1.12	0.11	3.86	2.27	1.39
SP21 B	9	19	90	25	34	72	113	134	25	9	141	9	15	4068	157	15	20	3967	0.62	5.68	0.08	1.25	0.13	5.69	1.80	1.12
SP24 B	7	13	76	13	36	81	100	117	19	7	104	7	10	731	75	4	21	nd	0.50	5.55	0.08	1.10	0.09	2.76	na	na
YA 1 B	11	18	93	25	39	69	131	126	26	10	125	9	15	2491	178	22	14	6017	0.65	6.40	0.09	1.32	0.14	6.31	1.90	1.37
YA 2 B	10	19	90	28	45	80	135	126	27	10	126	9	16	2109	386	26	13	6613	0.67	6.40	0.12	1.18	0.16	7.51	2.87	2.11
YA 3 B	6	12	63	13	35	68	87	121	18	7	93	6	9	1247	38	13	18	5981	0.46	5.06	0.08	1.22	0.09	3.03	1.33	0.95
YA 4 B	7	16	80	24	42	125	128	124	21	8	100	7	14	2070	23	21	13	11557	0.61	6.13	0.10	1.32	0.13	4.93	1.17	1.18
YA 5 B	12	21	116	26	42	70	130	139	26	10	120	9	15	4786	89	60	10	12061	0.65	6.57	0.09	1.66	0.13	10.65	2.90	1.43
Min	6	12	63	13	28	52	87	62	18	6	90	5	9	270	1	1	7	3631	0.43	5.06	0.07	0.83	0.09	2.30	-0.93	0.56
Max	12	21	116	30	121	164	164	139	27	11	159	11	17	4786	386	60	21	12061	0.67	8.02	0.13	1.66	0.16	10.65	2.93	2.11
UCC	4.8	20	71	25	20	35	60	350	22	25	190	10.7	11		557	1.6	1.4	370	0.5	5	0.1	4.2	0.15			

7.8 DAM CONSTRUCTION AND DESTRUCTION

Man-made dams are structures designed to stop or impede the flow of water in a given body. While dams are most commonly associated with the production of hydroelectric energy, they are used for a variety of purposes such as, freshwater supplies, irrigation, hydroelectric development, industrial activities and flood control. When a river is dammed it creates an artificial body of water. These reservoirs are used to supply the public with drinking water and for regulating the flow of water to surrounding areas.

Dams have left their mark on the landscape and the biota that depend on rivers for their entire life cycle or for a part of it. Aquatic organisms (e.g. fish) are particularly sensitive to changes in habitat connectivity, hydrograph alterations, morphodynamic modifications, as well as hydrogeologic, thermal or chemical deviations from natural levels. The sediment content in a dammed area increases with time and also can cause serious adverse effects to the environment.

Dam destruction with time can reconstruct the natural environment, but also it causes changes in the river bed morphology and aquatic organisms. Therefore, as much as dam construction is important dam destruction is also environmentally very important to be conceded.

7.9 SUSPENDED SOLIDS AND SEM

Suspended particulate matter (SPM) in rivers and estuaries is considered to exert a major influence on the behavior and bioavailability of solutes, especially metals (Stumm 1992; Eisma 1993; Ferrira et al. 1997). Researchers have established that SPM is a significant transport agent for trace metal contaminants in stream environments (e.g. estuary) (Characklis and Wiesner 1997; Neal et al. 1997; Webster et al. 2000). As a result, there is growing interest in the nature of the binding interactions between SPM and trace metal contaminants. Many studies have demonstrated the importance of sorption by SPM in affecting the dissolved concentrations, bioavailability, and residence times of trace metals in waters (Hamilton-Taylor et al. 1997; Grantza et al. 2003; Hatje et al. 2003). The Scanning Electron microscope is a very useful tool to identify the species in the suspended solids and the suspended matter is very useful to understand the environment.

7.10 WATER QUALITY

Water parameters such as pH, temperature, conductivity, ORP, DO and Mn are very useful to identify the water environment. pH is a measure of the hydrogen ion (H+) concentration. Solutions range from very acidic (having a high concentration of H+ ions) to very basic (having a high concentration of OH- ions). The pH scale ranges from 0 to 14 with 7 being the neutral value. The pH of water or wastewater is important to the chemical reactions in both and pH values that are too high or low can inhibit growth of microorganisms. In regards to high and low pH values, high pH values are considered basic and low pH values are considered acidic, natural water varies in pH depending on its source. Pure water has a neutral pH, with an equal number of H^+ and OH^-.

The temperature of groundwater is largely dependent on atmospheric temperature, terrestrial heat, exothermic and endothermic reactions in rocks, infiltration of surface water, insulation, thermal conductivity of rocks, rate of movement of groundwater and interference of man on the groundwater regime.

This is a measure of the capability of a solution such as water in a stream to pass an electric current. This is an indicator of the concentration of dissolved electrolyte ions in the water. It doesn't identify the specific ions in the water. However, significant increases in conductivity may be an indicator that polluting discharges have entered the water. Every creek will have a baseline conductivity depending on the local geology and soils. Higher conductivity will result from the presence of various ions including nitrate, phosphate, and sodium.

The basic unit of measurement for conductivity is micromhos per centimeter (µmhos/cm) or microsiemens per centimeter (µS/cm). Either can be used, they are the same. It is a measure of the inverse of the amount of resistance an electric charge meets in traveling through the water. Distilled water has a conductivity ranging from 0.5 to 3 µS/cm, while most streams range between 50 to 1500 µS/cm. Freshwater streams ideally should have a conductivity between 150 to 500 µS/cm to support diverse aquatic life.

Dissolved oxygen is oxygen gas molecules (O_2) present in the water. Plants and animals cannot directly use the oxygen that is part of the water molecule (H_2O), instead depending on dissolved oxygen for respiration. Oxygen enters streams from the surrounding air and as a

product of photosynthesis from aquatic plants. Consistently high levels of dissolved oxygen are best for a healthy ecosystem.

Levels of dissolved oxygen vary depending on factors including water temperature, time of day, season, depth, altitude, and rate of flow. Water at higher temperatures and altitudes will have less dissolved oxygen. Dissolved oxygen reaches its peak during the day. At night, it decreases as photosynthesis has stopped while oxygen consuming processes such as respiration, oxidation, and respiration continue, until shortly before dawn. Human factors that affect dissolved oxygen in streams include addition of oxygen consuming organic wastes such as sewage, addition of nutrients, changing the flow of water, raising the water temperature, and the addition of chemicals.

Dissolved oxygen is measured in mg/L.

0-2 mg/L: not enough oxygen to support life.
2-4 mg/L: only a few fish and aquatic insects can survive.
4-7 mg/L: good for many aquatic animals, low for cold water fish
7-11 mg/L: very good for most stream fish

Oxidation Reduction Potential or Redox is the activity or strength of oxidizers and reducers in relation to their concentration. Oxidizers accept electrons, reducers lose electrons. Examples of oxidizers are: chlorine, hydrogen peroxide, bromine, ozone, and chlorine dioxide. Examples of reducers are sodium sulfite, sodium bisulfate and hydrogen sulfide. Like acidity and alkalinity, the increase of one is at the expense of the other.

ORP is measured in millivolts (mV), with no correction for solution temperature. Like pH, it is not a measurement of concentration directly, but of activity level. In a solution of only one active component, ORP indicates concentration. As with pH, a very dilute solution will take time to accumulate a measurable charge.

7.11 PREVIOUS WORK AND BACKGROUND

The previous geochemical work of the Kuma River and Yatsushiro Bay has been carried out by Dozen and Ishiga 2002. No other work has been carried out to date. Further discussions of the work of Dozen and Ishiga 2002 are included in the discussion thus not discussed here.

CHAPTER 8

METHOD OF STUDY

8.1 INCEPTION AND BASE DATA COLLECTION

In this phase of the study, mainly the investigation of Google earth images and topographic maps were carried out and morphological conditions of the area were studied before the field investigations.

The Kuma River basin was selected to carry out this study since the Arase dam was decided to be removed and the river has been studied then years before and no more studies have been done. The Kuma River falls into the Yatsushiro Bay and the bay is morphologically tidal flats and thus was selected and investigated.

8.2 FIELD SAMPLING

8.2.1 Kuma River sediment samples

Stream sediment samples were collected along the Kuma River, Arase dam and in the river mouth at Yatsushiro bay using the hand pit method at 1- 6cm depths in November 2011. Sampling has been done taking into account sediment deposition, flow rate, river gradient, erosion and human impact on natural sedimentation. Samples were taken at varying distances based on accessibility (Fig 7.1.1), considering locations of tributaries, geological factors, upstream and downstram of the Arase Dam, and the dam site. Twenty river sediment samples and five bay samples have been collected. Sampling was done during low tide period in the bay area. Samples were collected into plastic bags using a plastic spade and were stored under 4^0C in a cooling bax and transwered to Shimane University and Tokyo University. Samples were taken at locations shown in Fig 7.1.1, matching locations of a previous study (Dozen and Ishiga 2002).

8.2.2 Kuma River Core sediments

Short core samples (8-10cm in length) were collected and divided into “surface“ and “bottom” samples based on color and grain size, representing before and after dam removal (Fig 8.1.1). The surface and bottom boundaries were tentatively determined by a sedimentological and geological specialist in the field. Photographs of each sampling location and the sample have been photographed for clarification. The boundary was confirmed also by the geochemical compositions determined by XRF and LOI values. Twenty-three surface samples and 19 bottom samples were recovered.

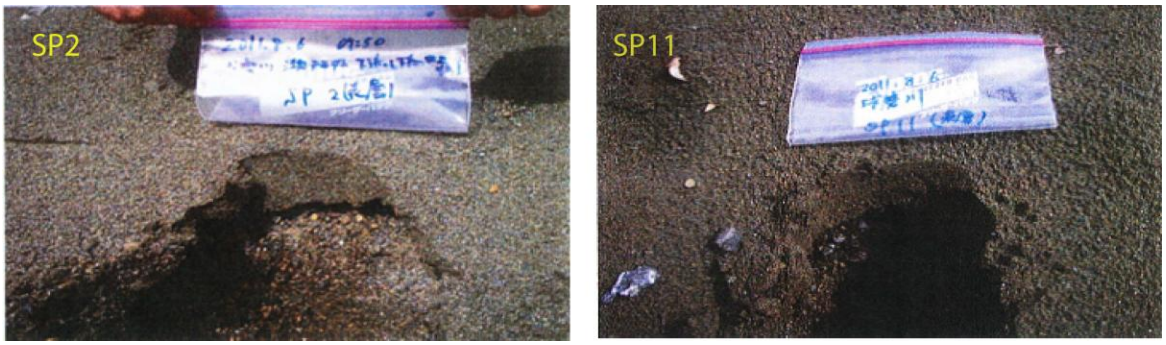

Fig. 8.1.1: Grain size variation of the (a) fine (0.25-0.005mm) and (b) medium (0.25-2mm) fractions of surface and bottom sediments

8.2.3 Yatsushiro Bay sediments

Sediment samples were collected from (a) the Yatsushiro tidal flat at the mouth of the Kuma river, (b) the southern area of the Uto Peninsula and (c) the western margin of the Yatsushiro plain (Fig 7.1.3). These locations cover the northeast region of the Yatsushiro Sea. Twenty two samples of the Yatsushiro Bay have been collected.

8.2.4 Suspended solids and SEM

The water samples were filtered to obtain the suspended solids using Whatman 45µm quartz filter paper. New filter papers were dried at 110^0C for at least two hours and the weight

was recorded prior to filtering. The filtrate was then oven dried at 110^0C for at least two hours and the weight of filtrate was recorded. The filtered suspended solids were then analyzed for 19 major and trace elements by X-ray fluorescence spectrometry using a Rigaku RIX-2000 spectrometer equipped with an Rh-anode tube at Shimane University. The average errors for all elements are less than ±10% relative.

The suspended solids were examined using a scanning electron microscope (SEM) to determine the diatoms in the sediments. SEM images of all the detected species of the Yatsushiro Bay and the Kuma River were recorded.

8.2.5 Water quality analysis

Water samples were collected with the aim of obtaining suspended solids. In addition, water physical parameters, temperature, pH, EC (Electrical Conductivity), DO (Dissolved Oxygen) and ORP (Oxygen Reduction Potential) were determined in the field using a Horiba D-24 pH/Conductivity meter. The Mn content of water samples was determined with an on-site chemical analysis kit for trace components in water using a color development method for the filtrate. Water samples were collected in plastic bottles and stored at 4^0C during transport to Shimane University.

8.3 SAMPLE PREPARATION

8.3.1 Sediment samples

All samples have been oven dried at 110^0C after transport and halved using the cone and quarter method. The fine (0.075 – 0.25mm) and medium (0.25 – 0.85mm) size fractions (n=14) were sieve separated.

8.4 GRAIN SIZE ANALYSIS

The grain size analysis was done using a laser diffraction particle size analyzer SALD-3000 and a settling tube grain size analyzer at Shimane University after treating the oven dried sediments with 30% H_2O_2 for at least twenty four hours to digest the organic matter.

CHAPTER 9

RESULTS

9.1 Kuma River and Arase dam

The river sediment samples were all black in color. The Yatsushiro Bay sediment samples were more gray than black. Almost all the surface and bottom elemental concentrations are within the ranges for UCC (Upper continental crust, Taylor and McLennan 1985) except for Zn, Fe and Ti at a few locations (Table 7.1.1). The geologic terranes in the catchment are highly evolved and thus all elements are very close to UCC. Chloride was detected only in the river locations below SP19 and in Yatsushiro Bay. In these surface and bottom samples chloride ranges are 2449-12887 ppm and 3631-12061 ppm respectively, which is much higher than UCC 370 ppm (Taylor and McLennan 1985). The TS (Total sulphur) content and LOI of the surface and bottom sediments show a considerable difference (Table 7.1.1). The bottom sediments have slightly higher TS and LOI indicating higher organic matter and reduced conditions. There is no clear chemical change between the surface and bottom sediments (Fig. 9.1.1a, b, c, d). The average values of surface and bottom sediments for all elements except TS are almost similar (Table 7.1.1).

The fine and medium size fractions differ from UCC for Ni, Cr and V. They are 1.5 times to just above two times higher than UCC while the other elements are comparable with UCC. LOI is low except for a few samples (Table 7.1.1).

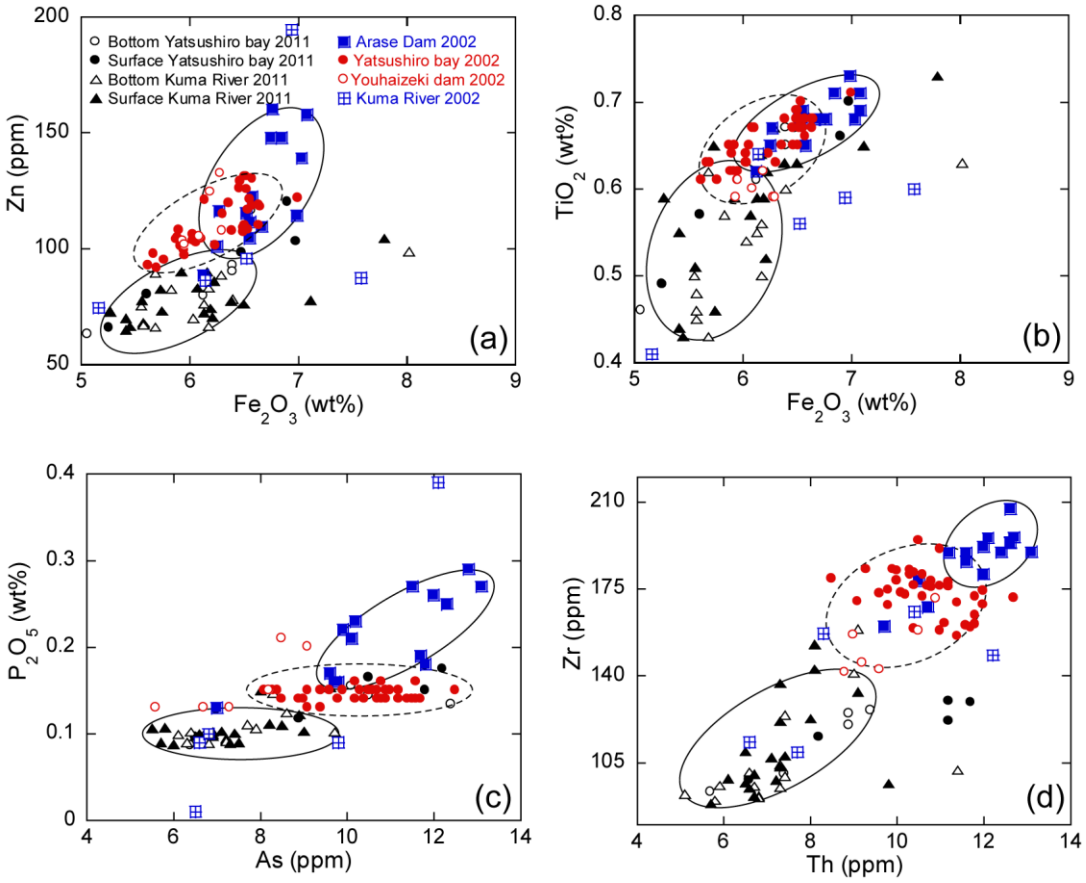

Fig. 9.1.1: (a) Zn-Fe_2O_3 (b) TiO_2-Fe_2O_3 (c) P_2O_5-As (d) Zr-Th plots showing provenance and environmental status for bottom and surface sediments. The data is compared with results from Dozen and Ishiga (2002) from the same locations

The median grain size (Md ϕ) of the surface sediments range between -0.57 and 3.27 ϕ while the bottom sediments are between -0.93 and 2.93 ϕ (Table 7.1.1). It is very clear from the grain size of surface and bottom sediments that the sediments of the Kuma River and the Yatsushiro Bay mainly consist of very coarse sand to very fine sand. Table 9.1.1 gives the chemical data of the fine and medium fractions. Summerized bulk chemical data of Dozen and Ishiga 2002 of Arase dam, Yatsushiro Bay, Youhaizeki and Kuma river is also provided (Table 9.1.1) The elements Sc, Cl, F and MnO were not analyzed in the 2002 study. However, the values of Dozen and Ishiga 2002 are much higher than the 2011 data for almost allelements. The grain size analysis shows that the clay and silt fractions in these sediments (2011) are very less (Table 9.1.2).

In the dam areas (Arase and Youhaizeki bank) the bottom sediment median grain sizes (Φ) are low (-0.93, -0.83) but are high (2.63, 2.53) in the dam surface sediments (Table 7.1.1). This is due to the very low fine fraction in the dam sediments and comparatively higher coarse sand grain percentages at the dams. The median grain size of the river sediments above the Arase dam (upstream) is low in both surface and bottom sediments. The median grain size of surface sediments is higher than that of the bottom sediments. Along the river after the dams (downstream) the median grain size is higher than upstream. The sorting of the grains (Table 7.1.1) along the river and in the bay is moderately to poorly sorted (using the Folk and Ward 1957 classification). The sorting of bottom sediments in the river is low (avg: 1.0), but it is high in the surface sediments (avg: 1.1). Cumulative plots for bottom (Fig. 9.1.2a) and surface (Fig. 9.1.2c) sediments show the grain size variation of the samples. There is no significant change between the surface and bottom cumulative plots.

Table 9.1.1: Elemental concentrations of fine (0.075 – 0.25mm) and medium (0.25-0.85mm) grained sediments of the Kuma River and Yatsushiro Bay

	Trace elements (ppm)																		Major elements (wt%)				
Sample-No	As	Pb	Zn	Cu	Ni	Cr	V	Sr	Y	Nb	Zr	Th	Sc	TS	F	Br	I	Cl	TiO_2	Fe_2O_3	MnO	CaO	P_2O_5
SP2S-fine	6	17	74	25	34	69	115	123	21	8	96	8	12	293	144	2	17	nd	0.54	5.74	0.10	1.31	0.10
SP4S-fine	7	13	74	22	35	96	147	139	20	9	99	7	16	279	115	2	7	nd	0.65	6.82	0.12	1.66	0.11
SP6S-fine	7	14	87	24	34	130	255	121	20	11	116	7	18	274	36	2	nd	nd	1.07	8.62	0.13	1.33	0.11
SP8S-fine	7	16	82	24	35	109	171	134	22	10	106	7	15	298	178	2	1	nd	0.74	7.26	0.13	1.42	0.11
SP8B-fine	10	20	111	32	44	79	153	118	28	11	123	11	16	796		6	5	nd	0.73	7.10	0.14	1.31	0.22
SP11S-fine	6	15	74	25	36	83	127	129	20	9	99	7	16	289	75	2	12	nd	0.60	6.14	0.11	1.48	0.10
SP14S-fine	7	16	80	34	36	95	135	134	21	9	106	6	14	346	103	2	14	nd	0.61	6.14	0.11	1.46	0.11
SP19 fine mix	8	18	83	22	36	77	114	133	23	9	127	8	13	2488	146	20	15	7852	0.63	5.68	0.11	1.15	0.12
Sozou S fine	7	14	77	14	32	89	120	129	20	7	118	7	15	615	324	5	16	nd	0.62	5.64	0.10	1.11	0.09
Sozou B fine	7	14	80	16	34	95	123	131	20	7	111	7	13	697	46	4	18	nd	0.61	5.69	0.09	1.11	0.09
YA-1 fine mix	9	17	88	23	35	77	119	128	23	9	114	7	14	2313	47	19	13	6803	0.61	5.85	0.08	1.25	0.13
YA-4 fine mix	9	19	104	34	53	134	197	127	26	12	137	9	17	2686	215	26		15972	0.84	7.88	0.13	1.37	0.17
SP2S-med	6	14	69	23	31	64	101	112	20	7	93	7	11	265	103	2	19	nd	0.47	5.37	0.09	1.23	0.09
SP4S-med	6	13	79	25	37	82	133	117	20	8	94	6	14	264	61	2	11	nd	0.62	6.95	0.12	1.48	0.10
SP6S-med	6	15	75	21	30	64	108	127	20	7	95	8	14	265		2	9	nd	0.47	5.58	0.09	1.31	0.09
SP8S-med	6	13	74	21	35	74	115	123	19	7	91	7	14	266	192	2	6	nd	0.50	6.06	0.11	1.39	0.10
SP8B-med	9	20	110	34	43	83	144	112	27	10	114	10	15	787	160	6	11	nd	0.67	6.92	0.13	1.33	0.20
SP11S-med	7	15	76	25	36	66	111	109	22	8	98	8	12	286	89	2	11	nd	0.53	5.72	0.10	1.24	0.09
SP14S-med	8	17	82	26	39	70	112	113	23	9	100	8	16	409		3	14	nd	0.53	5.79	0.11	1.35	0.10
SP19 med mix	9	14	79	17	39	76	101	119	20	7	103	7	11	2322		16	18	14599	0.52	5.47	0.10	1.12	0.11
Sozou S med	8	14	80	13	37	61	88	112	18	6	89	6	9	603	103	5	14	nd	0.46	5.51	0.09	1.07	0.09
Sozou B med	8	12	79	15	35	69	94	111	17	6	86	6	10	679	133	4	18	nd	0.43	5.55	0.08	1.07	0.09
YA-1 med mix	10	15	75	18	35	68	96	121	20	7	98	7	13	2666	128	16	18	10856	0.53	5.35	0.07	1.29	0.11
YA-4 med mix	6	14	71	20	39	94	103	123	18	6	89	5	13	1559	227	13	16	9228	0.50	5.60	0.09	1.30	0.11
Dozen and Isiga 2000																							
Arase																							
Min	7	17	89	30	28	60	132	131	22	9	160	10	na	633	na	2	15	na	0.62	6.12	na	1.08	0.13
Max	13	28	160	45	41	76	153	155	30	12	207	13	na	1574	na	22	42	na	0.73	7.08	na	1.52	0.29
Yatsushiro																							
Min	8	18	92	26	29	62	116	147	24	9	156	9	na	3157	na	45	31	na	0.61	5.62	na	1.08	0.13
Max	13	24	131	38	41	87	148	172	29	11	194	13	na	9477	na	87	61	na	0.71	7.00	na	1.99	0.16
Youhaizeki																							
Min	6	17	102	26	31	64	126	145	20	8	141	9	na	763	na	1	24	na	0.59	5.94	na	1.14	0.13
Max	9	24	132	38	39	74	134	156	26	9	171	11	na	1294	na	12	30	na	0.62	6.30	na	1.34	0.21
Kuma River																							
Min	7	13	75	21	20	50	91	84	17	6	109	7	na	368	na	1	25	na	0.41	5.16	na	0.78	0.01
Max	12	29	195	32	28	74	141	184	27	10	166	12	na	2044	na	36	58	na	0.64	7.58	na	1.81	0.39

Table 9.1.2: Grain size analysis data from the Kuma River and Yatsushiro bay.

Bottom Sediments									
Sample Name	Distance (Km)	~2mm	2~0.85mm	0.85~0.25mm	0.25~0.75mm	0.75~0.05mm	<0.05~mm	**0.05-0.25mm**	**0.25-2mm**
Grain size		Gravel	Coarse Sand	Medium Sand	Fine Sand	Silt	Clay	**Fine Grain**	**Large Grain**
SP2	26.28	4.8	7.4	52.7	25.8	6.6	2.7	35.1	65
SP3	26.22	2.9	67.1	28.1	1.8	0.1	0	1.9	98
SP4	23	55.4	1.5	27.6	14.3	1.1	0.1	15.5	85
SP9	23	64.6	15	14.9	5	0.4	0.1	5.6	95
SP5	21	3	16.1	80.4	0.4	0.1	0	0.5	100
SP8	20	49.7	19.7	28	2.4	0.1	0	2.5	97
SP6	19	0	0.5	49.8	48.3	1.3	0.2	49.7	50
SP7	19	0	0.1	22.4	72	4.7	0.7	77.4	23
SP10	20	0	0.3	42.1	54.4	2.5	0.7	57.7	42
SP11	12	47.9	17.7	27.6	5.5	0.9	0.3	6.7	93
SP14	5	0	0.4	11.7	80.4	6.6	0.9	87.9	12
SP15	3	0.1	0.3	99.3	0.2	0	0	0.2	100
SP16	2	0	0	13	69.2	14.3	3.5	87	13
SP20	0	0.7	1.1	40.4	50.6	5.7	1.5	57.8	42
SP21	0	0	0.5	56.2	40.6	2.2	0.4	43.2	57
Ya1	0	0	0.7	52.1	40.9	4.5	1.8	47.2	53
Ya2	0	0	0	25	49.4	19.6	6	75	25
Ya3	0	0	0.6	79.6	17.5	1.7	0.6	19.8	80
Ya4	0	10.6	4	68.1	12.5	3.9	0.9	17.3	83
Ya5	0	0	0	10.9	75.4	9.3	4.3	89.1	11
Surface Sediemnts									0
SP2	26.28	37.5	31.5	26.8	3.9	0.3	0.0	0.3	96
SP3	26.22	0.1	6.7	83.7	9.1	0.2	0.0	0.3	91
SP4	23	1.1	0.4	54.3	42.3	1.4	0.4	1.9	56
SP9	23	22.2	21.7	42.5	10.8	2.0	0.7	2.7	86
SP5	21	0.0	9.9	89.3	0.4	0.3	0.0	0.3	99
SP8	20	9.2	2.5	12.2	71.6	3.4	1.1	4.5	24
SP6	19	0.0	0.2	65.8	33.4	0.6	0.1	0.7	66
SP7	19	0.0	0.0	40.5	59.0	0.5	0.0	0.5	40
SP10	20	0.0	0.3	52.3	46.2	1.1	0.2	1.3	53
SP11	12	0.0	0.3	30.4	66.8	2.3	0.3	2.6	31
SP14	5	0.0	0.5	10.5	81.6	5.5	1.8	7.3	11
SP15	3	2.2	2.0	94.2	1.5	0.1	0.0	0.1	98
SP16	2	0.0	0.9	30.0	55.7	10.8	2.6	13.4	31
SP20	0	0.0	0.2	29.9	60.2	7.7	2.0	9.7	30
SP21	0	0.2	0.6	41.7	31.1	23.3	3.1	26.4	43
Ya1	0	0.0	0.7	39.5	49.9	7.1	2.7	9.9	40
Ya2	0	0.0	0.0	16.6	65.1	14.0	4.3	18.3	17
Ya3	0	0.0	0.3	74.1	21.0	3.5	1.1	4.6	74
Ya4	0	0.0	0.0	30.0	30.3	31.8	7.9	39.7	30
Ya5	0	0.0	0.0	3.6	91.2	3.5	1.7	5.2	4

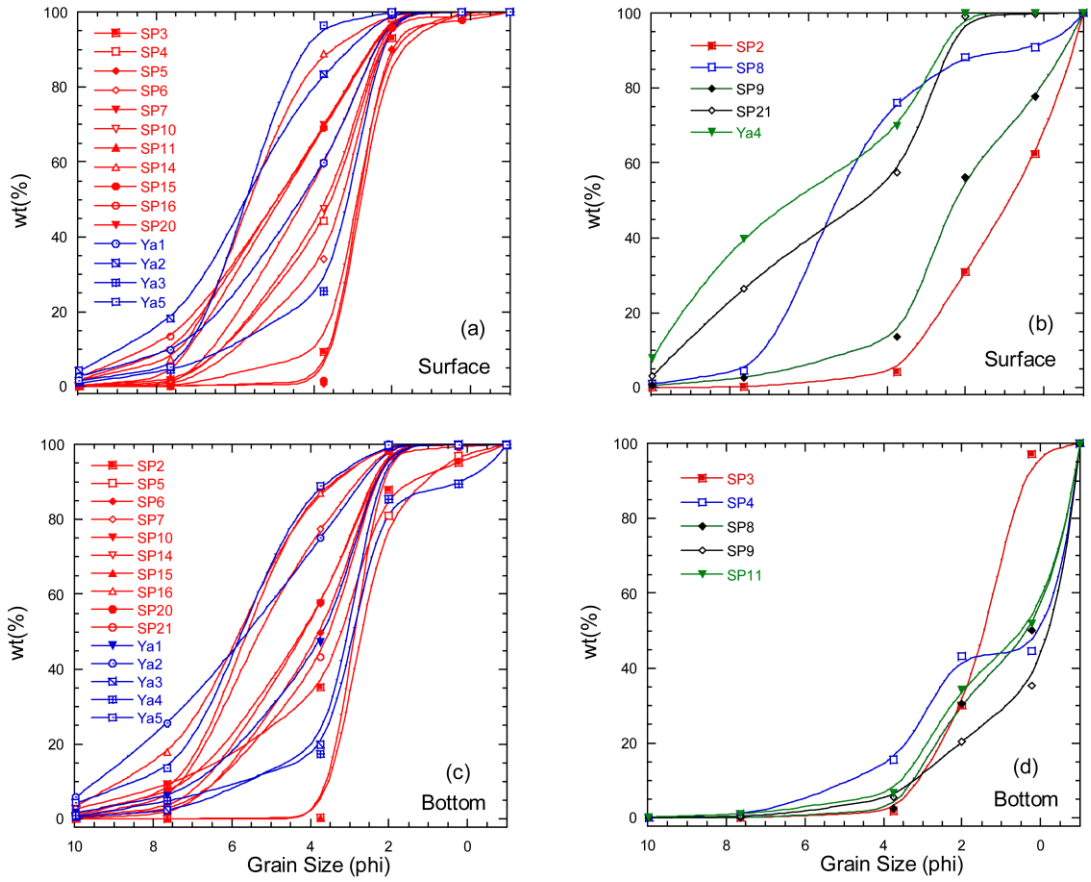

Fig. 9.1.2: (a) Cumulative grain size of surface sediments (b) Locations that do not follow the normal cumulative grain size curve of surface sediments (c) Cumulative grain size of bottom sediments (d) Locations that do not follow the normal cumulative grain size curve of bottom sediments

The fine grain (0.05-0.25mm) sediments are significantly higher in the bottom sediments (Fig. 9.1.3a). In the bottom sediments, fine grain sediments are low in abundance (<20%) above Arase dam, and are very high (50-90%) below the dam (Fig, 9.1.3a). The fines in surface sediments are also low above Arase dam. However, there is an increasing trend in the fines (0.05-0.25mm) of the surface sediments below the dam towards Yatsushiro Bay (Fig. 9.1.3a). The coarser grain-size sediments (0.25-2mm) are high in percentage in both bottom and surface sediments above the Arase dam (Fig. 9.1.3b). These coarser sediments drop in abundance below the dam and gradually decrease along the stream towards Yatsushiro Bay in both surface and

bottom sediments. At the dams themselves, sediments are very low in fines (0.05-0.25mm) in both the bottom and surface sediments. The dams have a much higher coarse sediment proportion in the bottom sediment compared to the surface sediments.

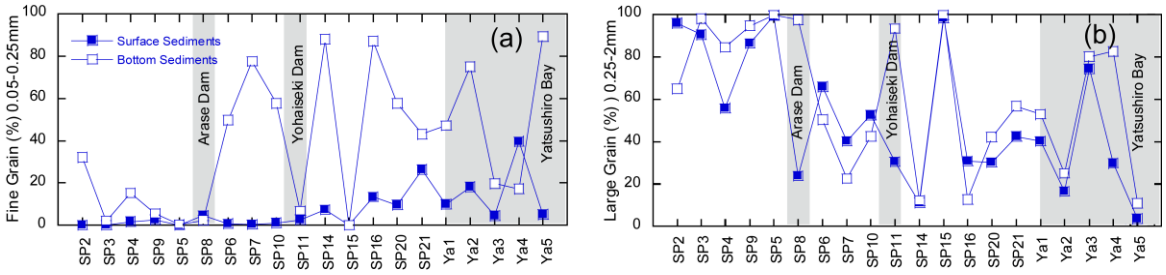

Fig. 9.1.3: Grain size variation of the (a) fine (0.25-0.005mm) and (b) medium (0.25-2mm) fractions of surface and bottom sediments

9.2 Yatsushiro Bay Tidal flat

Most trace and major elemental concentrations are higher in Yatsushiro tidal flat sediments and lower in the Kuma River sediments (Table 9.2.1). Measureable chloride content occurs only in the Yatsushiro tidal flat samples. The Total Sulfur (TS) of the Yatsushiro tidal flat is much higher than in Kuma River sediments. Yatsushiro tidal flat samples YA12-12 to YA12-17 have high elemental values - especially for Fe, Mn, P, Ti, Y, Ni, Cr, Cu, Zn, Pb and As. The Kuma river sediments are relatively uniform in composition, with higher ranges of 72.27–75.35 wt% SiO_2 and 12.09–14.01 wt% Al_2O_3, compared to lower 55.40–77.89 and 11.61–21.44 respectively for Yatsushiro Bay tidal flat sediments. Except for Fe in a few locations, all major oxides are well within UCC (Upper Continental Crust, Table 9.2.1). The LOI shows a clear difference between the Kuma River, the northern bay and the Yatsushiro tidal flat sediments (Table 9.2.1).

9.3 Suspended solids and SEM of Kuma River and Yatsushiro Bay

Table 9.2.2 shows the Yatsushiro bay tidal flat and Kuma River suspended sediment (SS) analysis. Yatsushiro Bay tidal flat SS show higher values for almost all elements than those of

the Kuma River, especially for Fe, Ti and total sulfur (TS). Chloride has been detected only in the Yatsushiro Bay tidal flat samples and not in the Kuma River sediments. Mn is at or below detectable levels in the suspended solids of the Yatsushiro Bay and the Kuma River. The SEM images show that diverse diatom species are found in the Kuma River and Yatsushiro Bay.

9.4 Water Quality of Kuma River and Yatsushiro Bay

Table 9.2.3 shows chemical data of the field measurements, for water and sediment of Yatsushiro bay tidal flat and the Kuma River. The ORP (Oxygen reduction potential), DO (Dissolved Oxygen) and EC (Electrical conductivity) ranges between (-40) – 300 mV, 6.7 – 8.3 mg/L and 0.312 – 6.2 mS/cm respectively.

Table 9.2.1: XRF analyses of Kuma River and Yatsushiro Bay bulk sediments. Major elements as oxide wt% and trace elements are in ppm. MGS-Mean grain size, LOI- Loss on Ignition. MGS and sorting calculated as in Falk and Ward, 1957 (nd-not detected, na-not analyzed)

Sample	SiO_2	TiO_2	Al_2O_3	Fe_2O_3	MnO	MgO	CaO	Na_2O	K_2O	P_2O_5	As	Pb	Zn	Cu	Ni	Cr	V	Sr	Y	Nb	Zr	Th	Sc	TS	F	Br	I	Cl	LOI	MGS	Sorting
Kuma River																															
K12-1	72.27	1.14	12.09	7.53	0.12	2.03	1.35	1.42	1.97	0.09	6	13	48	25	29	116	201	148	19	10	133	8	13	341	472	1	5	nd	2.32	2.01	2.67
K12-2	73.81	0.63	14.01	4.86	0.08	1.51	1.08	1.63	2.28	0.09	6	13	47	26	28	80	142	158	21	10	139	8	13	414	258	2	20	nd	2.99	1.57	2.24
K12-3	74.31	0.64	13.65	4.81	0.09	1.54	1.07	1.57	2.23	0.09	6	14	45	27	28	91	131	147	21	10	144	9	11	382	6608	2	17	nd	2.92	2.56	2.28
K12-4	75.35	0.62	12.43	5.11	0.09	1.71	1.14	1.52	1.95	0.08	6	13	44	25	37	98	135	145	19	9	127	8	10	347	nd	2	14	nd	2.48	-0.05	2.15
K12-5	74.79	0.57	13.30	4.78	0.09	1.75	1.04	1.51	2.10	0.08	6	14	46	25	50	102	134	143	20	9	128	8	10	358	nd	2	16	nd	2.85	1.45	2.77
Average	74.11	0.72	13.09	5.42	0.09	1.71	1.13	1.53	2.11	0.09	6	13	46	26	34	97	149	148	20	9	134	8	11	368	2446	2	14		2.71		
Yatsushiro Bay																															
Y12-1	64.08	0.93	19.22	5.30	0.14	2.51	1.41	3.15	3.01	0.25	13	26	65	47	45	92	169	168	29	12	175	12	11	4778	41	59	24	9029	18.10	0.16	0.16
Y12-2	73.81	0.63	14.01	4.86	0.08	1.51	1.08	1.63	2.28	0.09	8	17	50	23	32	94	126	172	24	10	185	10	10	2745	2261	16	19	3586	5.93	0.50	0.41
Y12-3	73.06	0.67	13.68	4.97	0.10	1.64	1.47	2.18	2.14	0.09	8	17	63	24	30	91	123	177	20	9	197	8	9	1888	nd	9	19	2476	3.65	0.56	0.63
Y12-4	73.75	0.66	13.47	4.49	0.08	1.66	1.36	2.30	2.15	0.08	7	13	44	15	24	108	125	177	20	9	245	8	11	2376	nd	13	23	7076	3.82	0.63	0.61
Y12-5	76.95	0.43	11.96	3.82	0.09	1.41	1.70	1.77	1.81	0.07	7	14	43	12	22	59	96	175	17	7	107	6	10	1138	1325	4	26	nd	2.69	2.87	2.48
Y12-6	75.00	0.56	13.06	4.24	0.08	1.55	1.24	2.14	2.06	0.08	8	13	46	16	28	86	132	169	19	8	147	8	10	2059	2429	13	24	4989	3.63	3.55	2.86
Y12-6a	75.03	0.59	13.17	4.55	0.07	1.60	0.95	1.87	2.09	0.08	7	19	51	33	61	113	159	164	26	12	222	10	11	887	9113	6	12	nd	6.64	0.41	0.37
Y12-7	75.03	0.59	13.17	4.55	0.07	1.60	0.95	1.87	2.09	0.08	7	15	45	18	29	86	115	152	20	9	151	8	7	1166	38	8	18	268	3.22	0.36	0.36
Y12-8	72.63	0.62	14.98	4.37	0.09	1.61	0.99	2.17	2.45	0.08	7	16	45	22	28	88	129	161	23	10	152	9	9	1648	1402	11	23	2195	3.94	1.40	0.35
Y12-9	67.46	0.77	16.98	4.77	0.10	2.22	1.61	3.21	2.71	0.16	8	22	108	31	38	88	145	167	24	11	174	10	11	4854	1845	47	15	12503	8.89	0.17	0.19
Y12-10	66.80	0.78	16.79	5.04	0.09	2.15	2.95	2.62	2.64	0.15	8	20	106	30	40	81	144	185	24	11	167	10	14	4098	37	31	13	8877	8.27	0.13	0.14
Y12-12	60.17	0.97	21.44	7.29	0.26	2.86	1.30	2.54	2.95	0.23	9	24	84	41	57	107	187	152	28	13	162	13	13	2506	111	32	12	7014	10.11	0.08	0.08
Y12-13	60.48	0.97	21.32	7.15	0.30	2.86	1.18	2.65	2.86	0.22	8	24	79	39	57	107	189	153	28	12	164	12	14	2433	nd	33	10	6892	9.90	0.08	0.08
Y12-14	59.79	0.98	21.30	6.72	0.27	3.00	1.30	3.36	3.07	0.22	8	24	79	36	52	97	186	148	28	12	158	12	14	2296	nd	52	18	10473	11.02	0.07	0.07
Y12-15	59.63	1.15	19.40	8.26	0.23	2.65	2.50	3.37	2.64	0.17	7	20	70	26	39	84	205	214	23	10	135	10	15	2070	nd	44	10	10843	9.47	0.07	0.07
Y12-16	55.40	0.96	18.88	9.29	0.20	3.18	7.29	2.64	2.00	0.16	9	19	61	18	20	69	183	403	20	8	97	7	21	2244	nd	24	11	6684	8.99	0.15	0.18
Y12-17	45.61	2.69	14.91	26.57	0.29	3.43	3.26	1.89	1.20	0.15	4	11	74	11		70	696	234	15	9	123	4	18	1329	nd	6	nd	1631	3.28	0.95	2.06
Y12-19a	69.57	0.82	16.52	5.47	0.08	1.74	0.99	1.97	2.68	0.15	8	17	53	31	38	82	162	167	26	12	207	11	11	1466	125	9	15	nd	5.85	0.51	0.47
Y12-20	70.83	0.78	15.68	5.32	0.08	1.71	1.04	1.83	2.59	0.14	7	19	60	32	43	115	157	166	24	11	205	10	13	1071	1437	9	22	nd	5.58	0.73	0.50
Y12-21	71.11	0.73	15.61	4.74	0.09	1.65	1.11	2.27	2.57	0.12	8	16	50	22	29	93	137	168	24	10	194	10	13	1422	nd	12	23	2345	4.26	0.68	0.35
Y12-22	77.89	0.48	11.61	4.17	0.08	1.52	0.83	1.66	1.70	0.07	7	14	45	18	31	114	138	155	20	9	173	8	11	2009	9684	9	26	2038	3.58	1.71	1.44
Y12-22a	74.65	0.67	13.02	4.79	0.08	1.69	1.00	1.93	2.09	0.08	7	12	48	17	34	108	128	146	18	7	131	6	8	694	76	5	27	442	2.53	1.14	1.79
Y12-shell(*Atrina pe*	na	na	na	na	na	na	na	na	na	na	1	5	20	1	nd	nd	nd	724	2	nd	13	nd	71	6532	20	3	nd	1332	na	na	na
Average	68.12	0.81	15.92	6.19	0.13	2.08	1.58	2.32	2.35	0.12	7	16	57	25	36	93	169	193	22	10	155	9	14	1928	2091	16	18	5300	6.52		
UCC	66	0.5	15.2	4.5	0.1	2.2	4.2	3.9	3.4	0.15	1.5	20	71	25	20	35	60	350	22	25	190	10.7	11		557	1.6	1.4	370			

Table 9.2.2: Analyses of Kuma River and Yatsushiro Bay suspended solids. Major elements as oxide wt% and trace elements are in ppm (nd-not detected)

Sample	SS weight (mg/L)	TiO_2	Fe_2O_3	MnO	CaO	P_2O_5	As	Pb	Zn	Cu	Ni	Cr	V	Sr	Y	Nb	Zr	Th	Sc	TS	F	Br	Cl	Mn mg/L
Yatsushiro Bay																								
YA 12-6	153.60	0.94	7.06	0.16	1.02	0.16	8	16	58	40	44	91	184	38	9	4	55	4	14	2603	152	16	3667	0.00
YA 12-9	47.91	0.66	3.65	0.13	1.15	0.19	3	11	59	29	36	64	108	10	4	2	22	1	10	3884	40	13	23199	0/02
YA 12-11	8.91	0.54	2.74	0.10	1.05	0.22	2	11	37	23	33	48	91	6	4	2	24	1	10	3612	300	13	39362	0.00
YA 12-16	388.20	0.72	6.20	0.20	1.62	0.12	8	19	75	30	35	68	137	122	18	7	110	8	15	4025	89	45	14388	<0.02
YA 12-18	1765.00	0.29	1.02	0.03	0.83	0.22	2	10	21	21	24	20	38	1	2	2	19		3	2437	34	5	18851	<0.02
YA 12-19	12.06	0.42	1.31	0.05	0.84	0.19	2	7	362	43	25	60	44	6	4	2	22	1	4	1107	179	3	nd	0.01
Kuma River																								
KU 12-1	10.27	0.22	0.69	0.04	0.87	0.15	1	10	23	16	31	11	24	nd	3	2	18	1	1	637	69	2	nd	0.00
KU 12-6	6.91	0.13	0.38	0.02	0.81	0.13	1	10	21	21	30	7	23	nd	2	2	18	nd	2	595	2	2	nd	0.00

Table 9.2.3: Physical and chemical properties of sediments and water from the Kuma River and Yatsushiro Bay

Sample	Time	pH	EC mS/cm	ORP mV	DO mg/L	T^0C	Type	Mn mg/L
Yatsushiro Bay								
YA 12-6	11.04	na	na	na	na	na	Water	0
YA 12-9	15.50	na	na	na	na	na	Water	0
YA 12-11	12.32	7.32	2.63	177	6.7	12.9	Water	0
YA 12-12	13.10	7.48	na	33	na	na	Sediment	NA
YA 12-16	14.33	na	na	na	na	na	Water	<0.02
YA 12-18	11.00	7.95	1.42	215	7.6	12.6	Water	<0.02
YA 12-19	13.17	7.75	0.31	231	8.3	13.1	Water	0
YA 12-19	13.53	7.66	0.32	215	8.1	14.5	Water	0
YA 12-19	14.17	7.53	0.36	219	8	13.8	Water	0
YA 12-19a	14.32	7.40	na	-40	na	na	Sediment	NA
YA 12-20	15.11	7.51	na	52	na	na	Sediment	NA
Kuma River								
KU 12-1	8.52	na	na	na	na	na	Water	0
KU 12-3	10.24	7.64	6.70	250	7.55	11.80	Sediment	NA
KU 12-6	11.04	7.75	6.60	300	7.73	12.40	Water	0
Min		7.40	0.31	-40	6.7	11.8		0
Max		7.95	6.70	300	8.3	14.5		<0.02

NA- not applicable

na-not analyzed

CHAPTER 10

DISCUSSION

10.1 Kuma River and Arase dam

10.1.1 Surface and bottom sediment chemical variation and grain size

Fine-grained sediment is a natural and essential component of river systems and plays a major role in the hydrological, geomorphological and ecological functioning of rivers (Owens et al. 2005). Surface and bottom sediments were collected to examine the effect that the opening of the Arase dam gate had on the Kuma River and Yatsushiro Bay sediments. Surface sediments represent the recent, post-dam, situation and the bottom sediments represent the composition before the opening of the dam gate. With the opening of the dam gates the dam area has been changed into a fluvial system with dominated current. Since the fine grains have increased downstream, the fine grains have been regularly transported and gradually accumulating downstream on the surface sediments (Fig 9.1.3a). In the bottom sediments, contents of increased fine grains indicated that during flushing, the trapped fine sediments in the dam lake has been transported downstream. When opened the gates the dam area is also converted to a fluvial system and the flow rate in the upstream and downstream became higher. Therefore, most of the bed load sediments were transported downstream and also point bars were formed in the banks of the river. Due to the higher amount of large grains in the upstream the dam also has higher large grains and has gradually decreased downstream (Fig 9.1.3b).

However, SP2, SP8, SP9, SP21 and Ya4 for the surface sediments (Fig. 9.1.2b) and SP3, SP4, SP8, SP9 and SP11 for the bottom sediments (Fig. 9.1.2d) have cumulative curves that are different than the others due to a higher proportion of coarser grains. Thus, the opening of the dam has altered the grain-size distribution in these locations. The slope of the bottom sediment sorting is steeper than that of the surface sediments (Fig 9.1.2c), indicating better sorted grains in the bottom sediments.

Chemical changes between the surface and bottom sediments are not greatly significant when plotted against mean grain size (Fig. 10.1.1a, b, c, d). Cr and Ni are very similar in surface and bottom sediments (Fig. 10.1.1a and b), indicating that grain size has no major effect on Cr

and Ni. Two elements that are notably controlled by grain size here are Zr and Ti. Both show an increase with decreasing grain size, indicating a heavy mineral accumulation involving Zr and Ti (Fig. 10.1.1c and d) in the finer grains. The LOI is low indicating that there is little carbonate dilution taking place (Table 7.1.1). It seems, therefore, that quartz dilution is taking place, involving larger quartz grains, which would not change the chemical composition of the surface or bottom sediments. With the exception of Zr and Ti, the fine and coarse grain size fractions and the median grain size variation coincide with each other in chemical composition. The Kuma river sediments are mainly comprised of sand fractions than clay and silt. Thus, the chemical variation is due to composition of the sand fraction.

Chromium and Ni accumulate in the fine and clay fraction. The results show that, after opening the dam gate, the fine particle fraction has been transported downstream. Therefore, the opening of the dam does not have a great effect on chemical compositions of surface and bottom sediments, it has affected the sediment grain size and the flushing of the fine and large fractions farther downstream towards Yatsushiro Bay. Elevated chloride was detected only below SP19 and in the Yatsushiro Bay samples for both surface and bottom sediments (Table 7.1.1). In this region chloride content is extremely high, indicating the intrusion of marine water and sediments into the river channel during high tides.

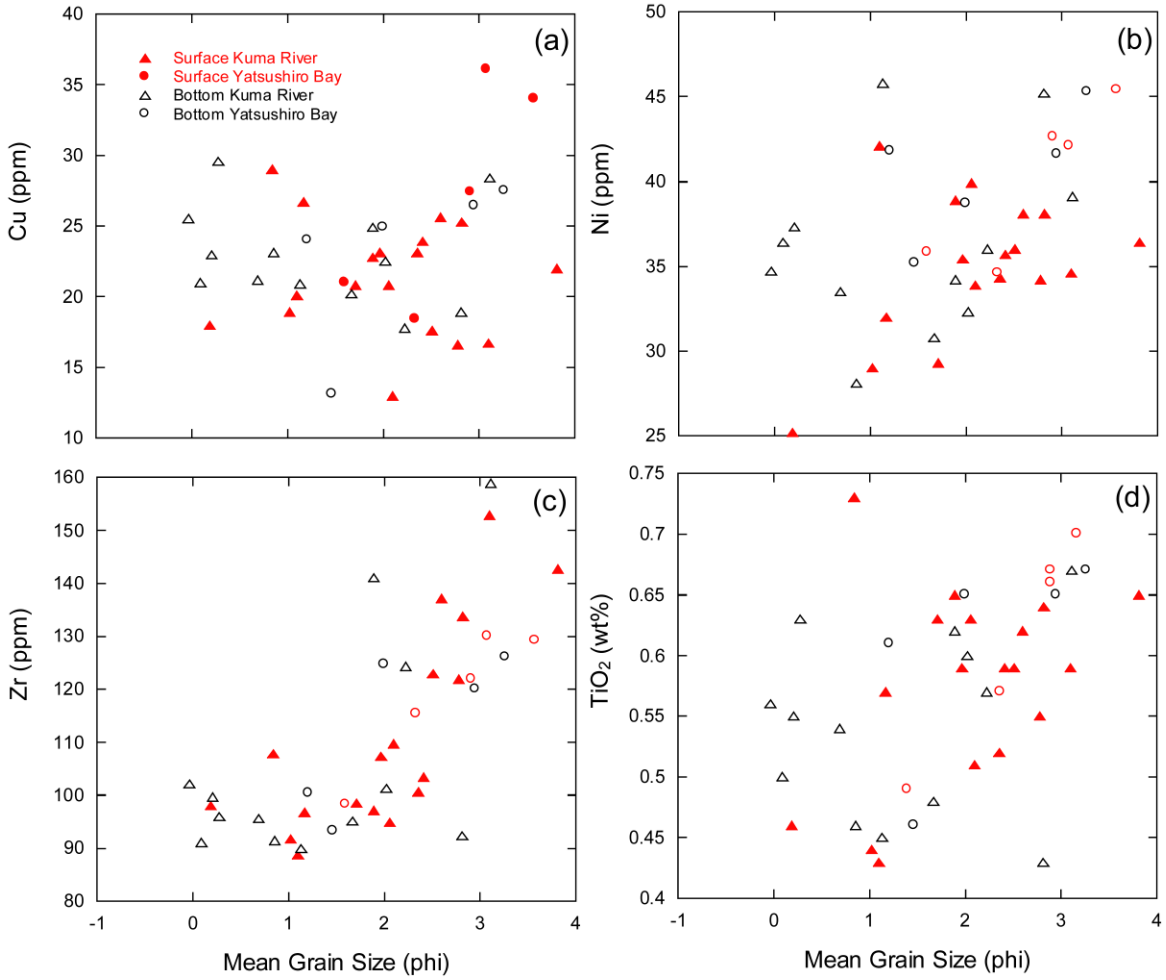

Fig. 10.1.1: (a) Cu-mean grain size (b) Ni- mean grain size (c) Zr- mean grain size (d) TiO_2-mean grain size for the Kuma River and Yatsushiro Bay surface and bottom sediments.

10.1.2 Composition change since 2002

This study shows that the elemental compositions of surface and bottom sediments are variable, but lie within a relatively small range of values. From this we infer that the source of these sediments was very similar throughout the period represented by the short core collections. However, when compared with a previous study (Dozen and Ishiga 2002) it can be seen that prior to 2002 Arase dam sediments had much higher elemental concentrations (Fig. 9.1.1a, b, c, d). It also shows that the Yatsushiro Bay sediments had much higher elemental concentrations

than it does today as seen in Fig 9.1.1 for Zn-Fe, Ti-Fe, P_2O_5-As and Zr-Th. The minimum and maximum values of sediments from Arase dam, Yatsushiro Bay, Youhaizeki and Kuma River is given in Table 9.1.2. The Kuma River sediment samples of Dozen and Ishiga 2002 show highly scattered values (larger range) indicating significant chemical variation along the stream. This may be due to bed sediment heterogeneity. In 2011 Yatsushiro Bay surface samples had high Zn and a good correlation with Fe indicating initiation of recent environmental pollution and partially of higher content of fine fraction (Fig. 9.1.1a). However, the sediments are lower in Fe than that in 2002. The low Fe in 2011 shows more oxygen availability in the sediments than in 2002 indicating more oxic conditions at present. The titanium-iron cross plot of the 2011 samples (Fig. 9.1.1b) does not show a good correlation for either the surface or bottom sediments, implying that little hydraulic sorting is taking place. In contrast, the 2002 data shows a good correlation. This indicates that, in the years prior to 2002, the dams, the Kuma River and the Yatsushiro Bay sediments were well sorted, primarily in the fine and clay fraction.

Arsenic is usually associated with organic rich sediment where pyrite forms under low temperature conditions (Smedley and Kinniburgh 2001). These conditions are common in river or bay environments. The UCC value is 4.8 (Taylor and McLennan 1985). The Yatsushiro Bay sediments have high As (10 – 12 ppm) in both surface and bottom sediments two times higher than UCC. All river sediments are less than 10ppm (Fig. 9.1.1c). Thus, the sediments of the bay environment, containing more organic matter, may be polluted with As in some locations and also may correlate to the background mafic rocks of the area. Organics are associated with anoxia and can lead to pyrite formation. Because, arsenic is highly toxic, accumulation of As is an important issue and must be monitored regularly and in detail for further discussions.

Phosphorus is commonly tied to biogenic processes and therefore the As-P relationship is useful for understanding local biological and environmental conditions. Phosphorus in Yatsushiro Bay sediment is much higher than in the river sediments. However, in comparison with the previous study, the P level for Yatsushiro Bay is lower at present (Fig. 9.1.1c). Zircon and Th are can be used to trace heavy minerals. The Zr-Th relationship (Fig. 9.1.1d) shows a good correlation in both river and bay sediments, with some scatter. The Zr-Th shows how the Arase dam sediments were previously high in Zr and Th, but sediments now contain much lower levels. Yatsushiro Bay sediments were also higher in Zr and Th in the past, but are now lower by a factor of ~2. Thus, as shown in Fig. 9.1.1a, b, c, d and Table 7.1.1 it is evident that the current

sediments have lower concentrations in all the measured elements. Fig. 9.1.1c and d shows a significant difference between the Arase dam sediments of 2002, and the recently sampled river and dam sediments and the surface and bottom sediments. This also indicates that the Arase dam sediments were higher in elemental concentrations in 2002 than both the river sediments of 2002 and the recently collected sediments. In addition, the Youhaizeki bank sediments in 2002 had lower elemental concentration than that of Arase dam in 2002. Arase dam is situated upstream of Youhaizeki bank and has caused more sediment deposition, resulting in higher elemental values. This in turn shows that opening the dam has re-suspended and transported sediments with higher elemental concentrations to and beyond Yatsushiro Bay. Therefore, removal of the dam has caused a decrease in elemental concentrations, not an increase.

Br-Zn in Arase dam sediments were used by Dozen and Ishiga 2002 to trace the accumulation of algae, which was preserved in the sediments under reducing conditions. The present Kuma river bottom sediments have a slight increase in Br in the surface sediments but no change in Zn. A comparison of Dozen and Ishiga 2002 data with that of the present (Fig 9.1.1a, b, c, d and Table 7.1.1 and 9.1.2) indicates that conditions have changed since the dam opening. Although high bromides and Zn were found in 2002, at present both have decreased notably. Therefore, it seems that biogenic processes and redox conditions have changed.

Patterns of similarity in elemental content can be portrayed using cluster analysis of the sediment sample data. The cluster analysis included grain size data to eliminate a grain size effect and to present the controlling elements on the basis of provenance-related elements (Sr, Nb, Y, Zr, Th, Sc, TiO_2, CaO, MnO, F, Br, Cl, I) and elements not tied to provenance (As, Pb, Zn, Cu, Ni, V, Cr, P_2O_5, Fe_2O_3,TS-Total Sulfur). The cluster analysis was done using the complete linkage method, a distance measure of absolute correlation and was partitioned into five clusters for best results.

The five clusters of the non-provenance elements (Fig. 10.1.2a) are cluster one; SP2, SP4 and SP14. Cluster two; SP3, SP5 and SP15. Cluster three has only SP9 which is a tributary. Cluster four; Sp8, SP6, SP7, SP10, SP11, SP12 and SP24. Cluster five has SP16, SP17, Sp18, SP19, SP20, SP21, Ya1, Ya2, Ya3, Ya4 and Ya5. These clusters clearly separate the upstream, downstream and the bay area except for SP14, SP15 and SP24.

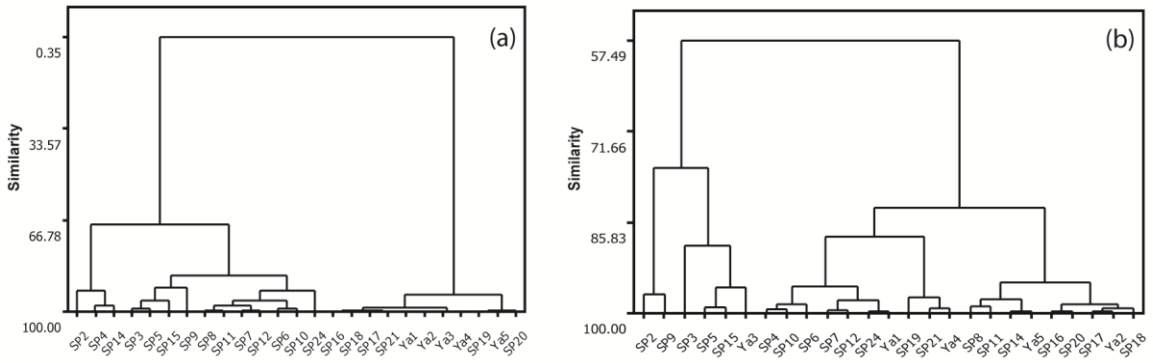

Fig. 10.1.2: (a) Non - Provenance elements cluster analysis plot (b) Provenance elements cluster analysis plot of the Kuma River sediments

The five clusters for the provenance elements (Fig 10.1.2b) are cluster one; SP2 and SP9. Cluster two; SP3, Sp5, SP15, Ya3. Cluster three; SP4, SP6, SP7, SP10, SP12, SP24 and Ya1. Cluster four; SP8, SP11, SP14, SP16, Sp17, SP18, SP20, Ya2 and Ya5. Cluster five has SP19, SP21 and Ya4. The provenance cluster does not show a clear separation of upstream, downstream and bay areas. When the provenance and non-provenance element clusters are compared, the provenance elements clusters are clearly weaker. The cluster analysis (Fig 10.1.2a, b) shows that variation in the elements not related to provenance dominate the sediment composition. Thus, the elements that are related to environmental change: As, Pb, Zn, Cu, Ni, Cr, V, Fe and total sulfur are related to the chemical behavior of the river and bay sediments. However, a more detailed study of Yatsushiro Bay is needed during low tide for a better environmental picture. In order to better understand the variation in the chemistry of the sediments, a chemical analysis of the fine and medium fractions is discussed in the next section.

10.1.3 Fine (0.075-0.25mm) and medium (0.25-0.85mm) fraction

The grain size of river bed sediments is an important property of streams because it is one of the major factors controlling channel morphology and hydraulics. The downstream variation in sediment size, which is characterized by a complex pattern rather than by a simple decreasing

trend, can be portrayed by sediment fraction data (Surian 2002). Since there was no major change in the chemical composition of the surface and bottom sediments of the Kuma River, the chemical composition of two grain size fractions was investigated (Table 9.1.2, Fig 10.1.3 a-l) for only surface sediments. The Kuma River sediments mainly comprise of sand fractions. It is widely agreed that the process of downstream fining of sands depends on some combination of abrasion and sorting, although arguments continue on their relative importance (Ferguson et al. 1998). The high Strontium, Ti, Zr and V in the fine fraction below the Arase dam (Fig. 10.1.3 a-l) indicate downstream fining. The rate of change in bed material grain size has important implications for downstream changes in flow resistance and for sediment transport (Reid et al. 1997). The very high elemental concentrations at Yatsushiro Bay show that river sediments are transported along the stream bed and are deposited in Yatsushiro Bay. However, no obvious dilution or removal due to currents or wave actions can be seen in Yatsushiro Bay because Zn and Cu are elevated at this location. Co-precipitation of iron hydroxide along with the scavenging of other metals has been suggested as the principal mechanism explaining the accumulation of Cu and Zn in estuarine sediments (Balachandran 2006). The present data for Zn and Cu shows much higher values (Fig 10.1.3c, 10.1.3d) than UCC (Zn-71ppm, Cu-25ppm) in the Yatsushiro bay. The River values are much lower except for one location for Cu fine fraction. Therefore, the background values are also lower. Thus, the Yatsushiro Bay may be contaminated by Zn and Cu. At SP8 the bottom sediments have elevated values for Ti, Fe, Zn, P, Ni, Pb, Cu and As (Fig. 10.1.3a-l). At this location the fine fraction sediment has high values of Ti, Fe, Zr and As. All other measured elements in the SP8 sediments have the same concentrations in fine (0.075-0.25 mm) and medium (0.25-0.85 mm) fractions. SP8 is the sampling point for Arase dam, which is at a location where the river is curved. After the dam removal some of the sediments flushed from the river bed are deposited in the river bank forming sand point bars and the rest are transported downstream. The SP8 bottom sediment represents the sediments accumulating while the Arase dam was in place. High Ti, P, Ni, As, Pb, Zn, and Cu in the fractions also indicate that the sediments are still accumulated in the dam lake site. Therefore, these sediments would need more time to be removed from the dam lake site and be converted into the natural conditions of the river sediment.

Although there is no change seen in the bulk surface and bottom sediments, there is an elemental difference in the surface sediments with different grain size fractions. The difference

in fraction composition shows sediments have high concentrations of the heavy minerals. In the fine fractions, Titanium, Fe, Zr and V are high at the Arase dam location (SP8). These may relate to the heavy minerals zircon, magnetite, and ilmenite which may have been deposited before opening of the dam. It is a matter of concern that As content in the dam sediments are high. For As the fine fraction yields more than 10 ppm and the medium size fraction are at 9ppm. As for Rudnick and Gao (2005) Arsenic value is 4.8 and the dam lake values are as much as two times higher. Therefore, this is a matter of some concern for the pre-dam removal sediments. However, after dam removal the As concentration has dropped to 6-7ppm in both fractions. Nevertheless, these values may also relate to natural factors such as background values.

Calcium, Sr, Zn, V, Ti, Zr and Fe are high in the surface sediments of SP4, which is in the farthest upstream area. Ti, Fe and V are much higher in the fine fraction than in the medium size fraction at SP4. Carbonates may be the main source of Ca and Sr while all other elements relate to heavy minerals.

At the Sozo location sediment elemental concentrations for both fractions are decreasing. This may be due to the vicinity of Yatsushiro Bay. Sediment undergoing transport moves through the Sozo region (river mouth) and into the bay, thus showing lower values at Sozo.

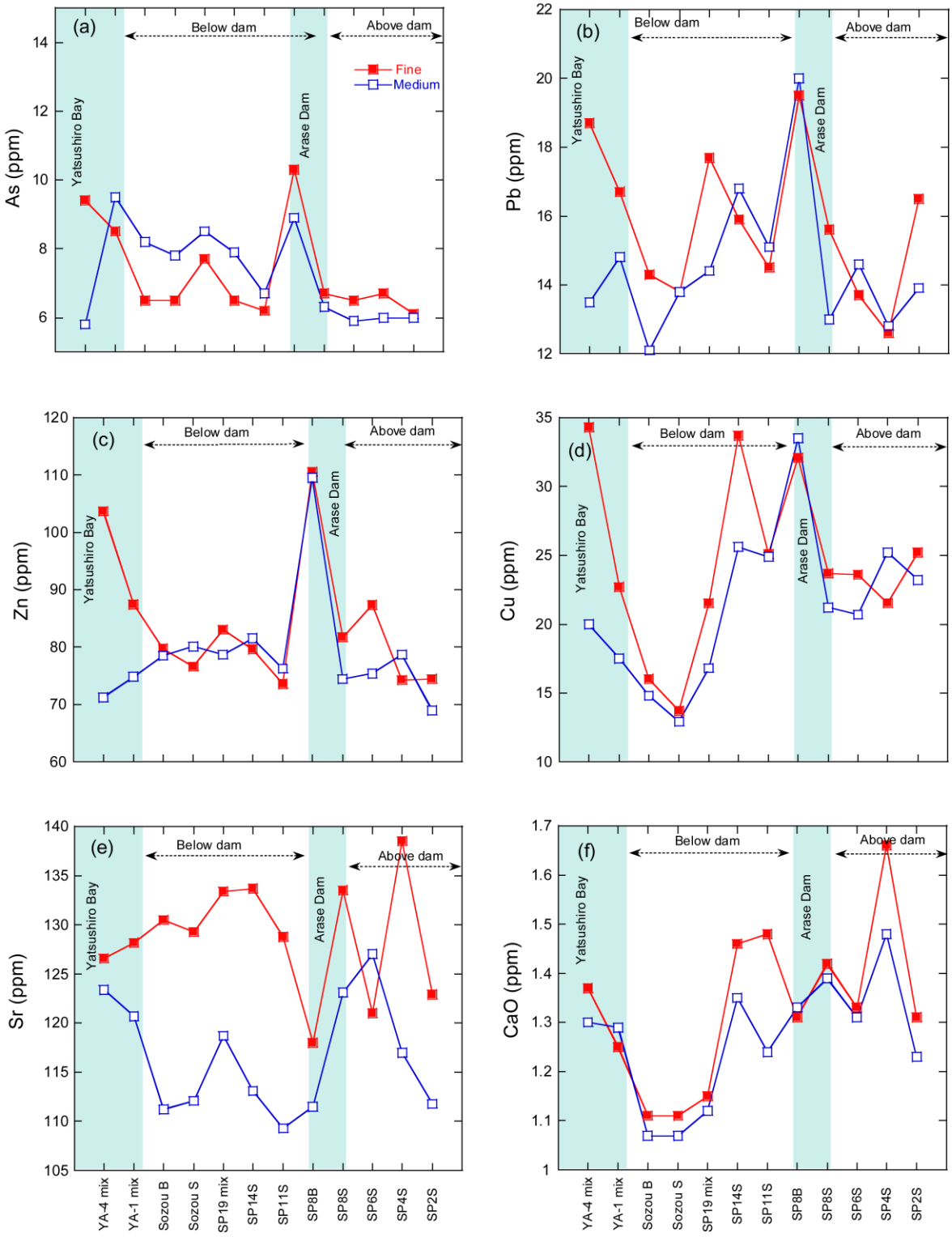
(a)
Below dam
Above dam
Fine
Medium
Yatsushiro Bay
Arase Dam
As (ppm)
(b)
Pb (ppm)
(c)
Zn (ppm)
(d)
Cu (ppm)
(e)
Sr (ppm)
(f)
CaO (ppm)
YA-4 mix
YA-1 mix
Sozou B
Sozou S
SP19 mix
SP14S
SP11S
SP8B
SP8S
SP6S
SP4S
SP2S

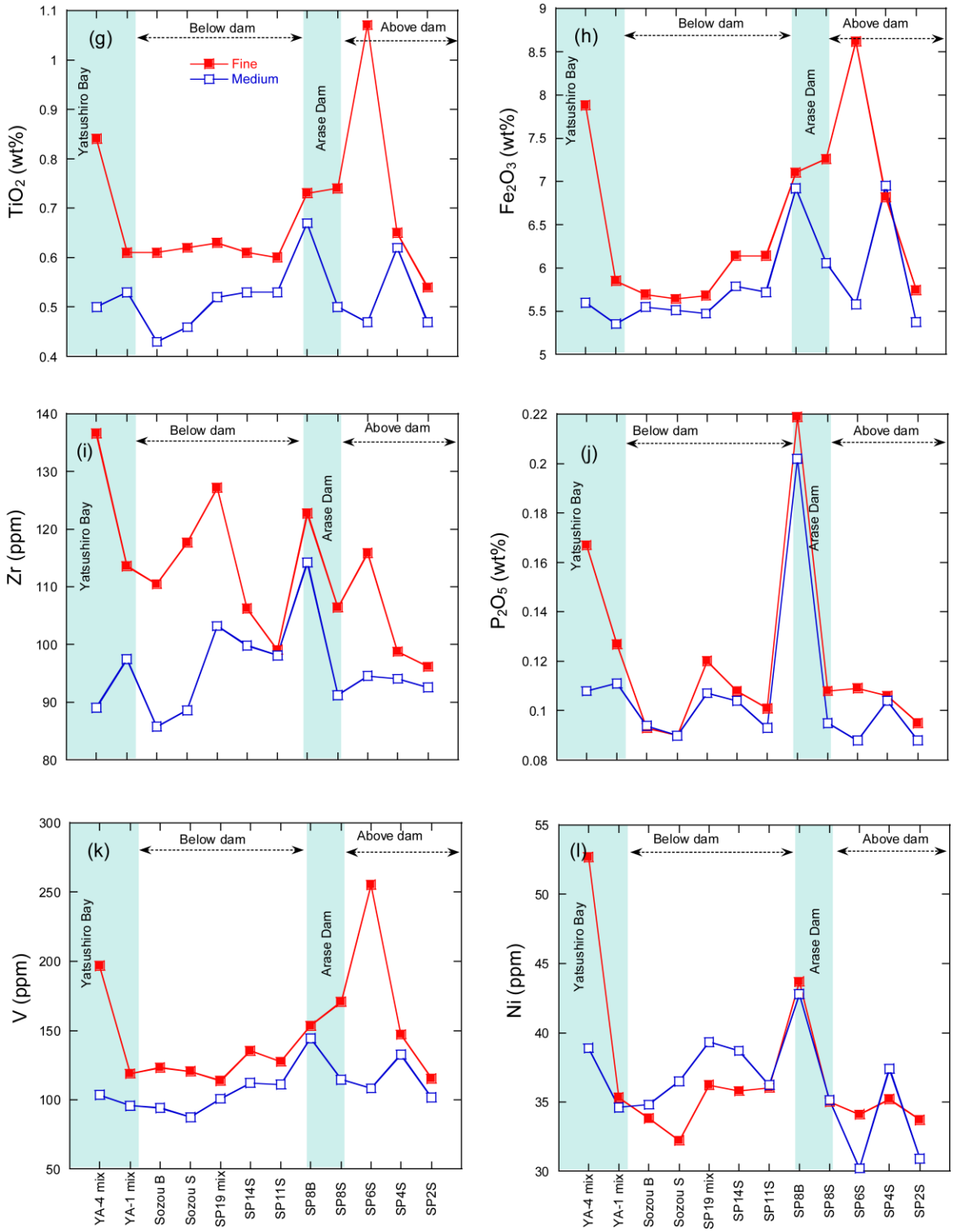

Fig. 10.1.3: (a)-(l) Elemental difference of the fine and medium fraction along the Kuma River and Yatsushiro Bay

10.2 Yatsushiro Bay and Tidal flat

The Yatsushiro tidal flat area shows ripple formations formed by small scale waves, good evidence that sand is deposited in the tidal flat area. In addition, there are large bar formations in the bay organized by higher energy wave activity. There are also many sand bar formations along the Kuma River. This may have resulted from the flushing of sediments after the opening of the dam gates.

Marshes of the Yatsushiro Bay area are comparatively young (Yamamoto 1992) and lack fine material. The tidal flat along the western margin of the Yatsushiro plain may have resulted from sediment accumulation rather than erosion. Large amounts of fine grained material remain suspended in the water column, and may undergo transport to the tidal flats of the southern area of the Uto Peninsula and then to the open sea.

10.2.1 Environmental change between 2002 and the present

Tidal flats are good settings for the study of environmental changes in river sediments and estuaries (Kim et al. 2010; Liu et al. 2009). A large amount of sediment is brought into the Yatsushiro Bay by the Kuma River. The present environment has changed tremendously since the 2002 study of Dozen and Ishiga. Fig. 10.1.4 a, b, and c show the environmental change from 2002 to 2012. Heavy metals are associated with the clay fraction (Robert et al. 2004). Arsenic, Pd and Zn are very sensitive to environmental changes and they are easily absorbed on clay particles. Iron is one of the main elements that is strongly associated with heavy metals and it can exist in several phases (Gurzau et al. 2003; Violante et al. 2010). Thus As, Pd and Zn have been cross plotted with Fe_2O_3 to show the environmental change since 2002. Arsenic, Pb and Zn all have decreased since 2002 (Fig. 10.1.4 a,b,c). The 2002 data reflect the sedimentary environment before the opening of the Arase dam and 2012 data represents the impact of the opening of the Arase dam on sediments. The 2002 data very clearly show an urban trend for As and Zn and a detrital trend for the modern 2012 sediments. Although the northern area sediments show enrichments, they can be plotted on the detrital trend line (Fig. 10.1.4 a,c). Pb content has been lowered since 2002, although it is highly variable (Fig. 10.1.4 b). Variation in Pb content and its relationship with Fe has increased in the 2012 data. In general, after opening the dam As, Pb, and

Zn have decreased in the Kuma River as well as in the Yatsushiro sea area and all values are lower than UCC.

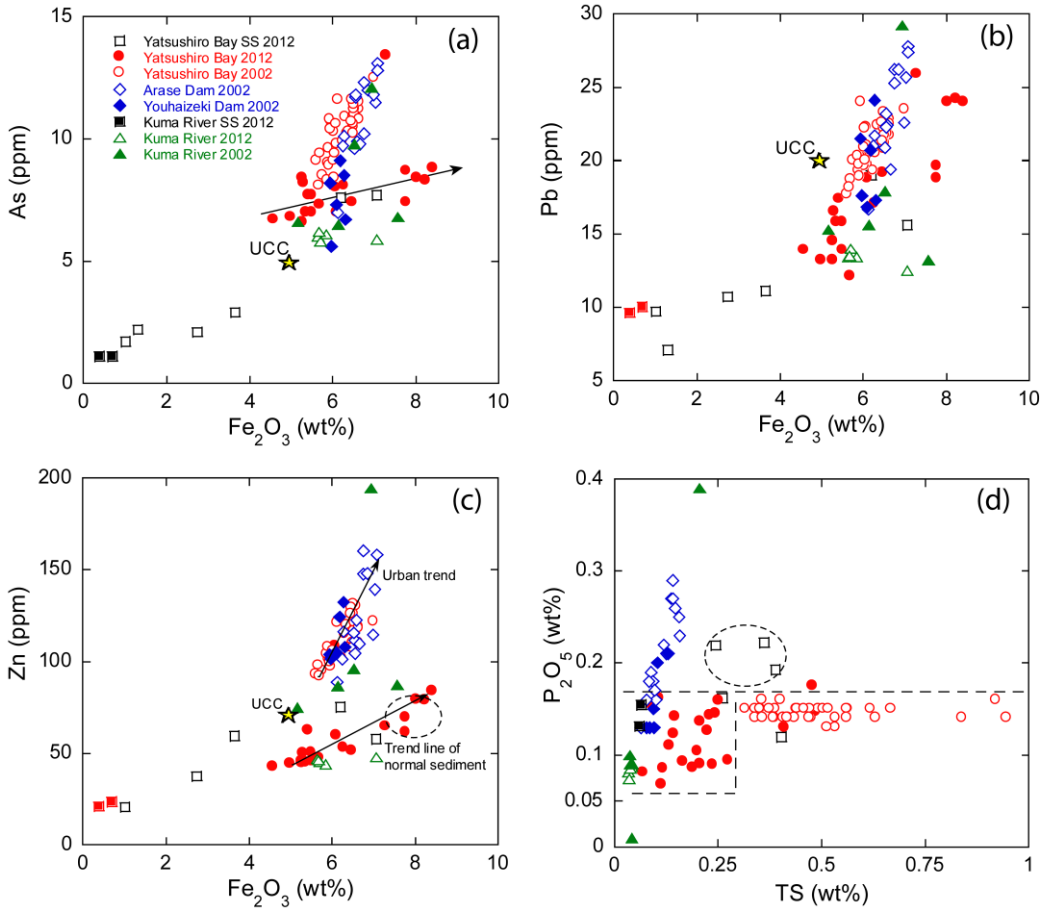

Fig. 10.1.4: Plots of (a) As, (b) Pb, (c) Zn versus Fe_2O_3 and (d) P_2O_5 versus TS for Kuma River and Yatsushiro Bay sediments. Data for 2002 is from Dozen and Ishiga 2002

However, suspended solids show very low elemental concentrations (Fig. 10.1.4 a,b,c). This indicates that the absorption and flocculation of heavy metals onto suspended solids has been reduced in the Kuma River and Yatsushiro Bay; this could be due to strong water circulation in these settings.

Changes in biogenic phases are represented using phosphate and Total Sulfur (TS). In Yatsushiro Bay and the Kuma River sediments P and TS have decreased since 2002 (Fig. 10.1.4 d). The suspended solids of Yatsushiro Bay have higher P and TS than 2002. Yatsushiro Bay has a higher concentration of plankton in the suspended solids than the Kuma River. Therefore, the P

and TS increase in the Yatsushiro Bay is likely due to the presence of a greater amount of plankton.

Nickel and Cr are used to illustrate the mafic components in sediment and adsorption on clay minerals (Taylor and McLennan, 1985). The Ni and Cr contents in Yatsushiro Bay are higher than in the Kuma River (Fig. 10.1.5a). In comparison with 2002, the modern Ni and Cr concentrations are highly scattered and in most locations Ni and Cr have increased. The increase of Ni and Cr content in the Kuma River in 2002 indicates progressive breakdown of Cr- and Ni-bearing detrital phases and higher adsorption onto clay minerals.

The Fe_2O_3 and TiO_2 in sediments can be expected to be positively correlated due to sorting effects (Singh 2009). The linear arrays of data points from the origin of Fe_2O_3–TiO_2 plots show that the elements are immobile, and that they were hydraulically fractionated in a similar manner. The Fe_2O_3–TiO_2 plot for Yatsushiro Bay and the Kuma River shows that the 2012 Yatsushiro sediments sediments are well correlated (Fig. 10.1.5 b). In 2012 Ti and Fe contents are much higher than in 2002. Therefore Yatsushiro Bay sediments are hydraulically fractionated in a similar manner, well sorted in the fine grain fraction. The highest contents are from the southern area of the Uto Peninsula of Yatsushiro Bay. These sediments consist of fine grains (Table 1) and are well sorted compared to the other locations. The suspended solids are much lower in Fe_2O_3–TiO_2 but still plot on a single trend line. This gives a trend line for both the bay and river suspended solids (Fig. 10.1.5 b). Ti and Fe in the Kuma River have changed significantly since 2002: in 2002 Ti was low and Fe was high, while in 2012 Ti is high and Fe is low (Fig 10.1.5 b). Thus, in 2012 the Kuma River sediments are well sorted and have become much more oxic than in 2002.

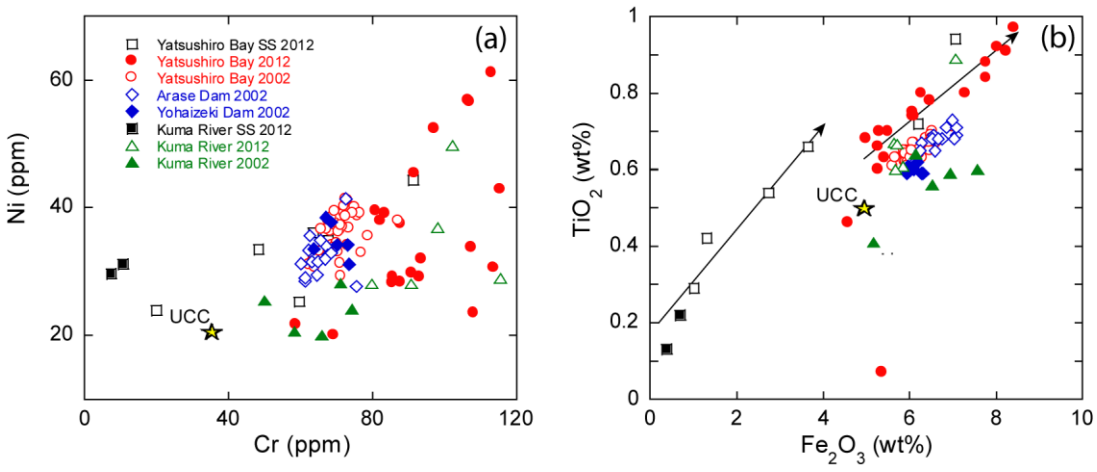

Fig. 10.1.5: (a) Cr-Ni plot and (b) Fe_2O_3–TiO_2 plot showing the mafic contribution and the sorting effect

MnO is a good indicator of oxidized and reduced conditions of sediments (Jung et al. 1996; Lacerda et al. 1999). The relationship between Mn and Fe is well known, and is used for identifying bottom sediment environments and the scavenging of trace elements (Jung et al. 1996; Krupadam et al. 2006; Beck et al. 2008; Feely et al. 1983). Mn scavenging in the water column is coincident with enrichments of Cr, Ni, Cu, Zn and Pb in the suspended matter (Feely et al. 1983). In addition, Mn is scavenged by the newly formed hydrous Mn oxide coatings that exist on the surfaces of particles in estuarine and coastal waters (Feely et al. 1983). The MnO content of the northern part of the Yatsushiro Bay is higher than the other areas (Fig. 10.1.6). The northern area locations plot on a higher trend line for MnO than the other locations in the bay and the Kuma River. The sediment in the southern area of the Uto Peninsula of the Yatsushiro tidal flat consists of fine sediment (Fig. 10.1.7a). These fine particles are easily coated with hydrous Mn oxide and can scavenge trace elements. Therefore, the trace element content of sediments in the southern area of the Uto Peninsula is higher than the southwest and northern parts of the Yatsushiro plain and the tidal flat of the river mouth (Fig. 10.1.4, Fig. 10.1.5).

Manganese enriched bottom water enters the bay with rising tides. At this time anoxic water carrying Mn enters the tidal flat and leads to an anoxic environment. Thus, due to high Mn and Fe in the southern Uto Peninsula tidal flats, this area is more anoxic compared to the other areas of the Yatsushiro tidal flat (Fig, 10.1.6). Yatsushiro Bay is a portion of the larger

embayment known as Siranui, and Siranui locations and Yatsushiro Bay locations chemically resemble each other. The Mn and Fe values of 2006 for Ariake and Siranui (Fig. 7.1.3) have been used for comparison in Fig. 10.1.6. The Mn and Fe concentration in northern and southern Siranui are very similar to the northern Yatsushiro Bay tidal flat. Although Ariake Bay has a wide range for Mn and Fe contents, they fall within the Siranui (2006) and Yatsushiro tidal flat (2012) values. This shows that the bottom sediment redox environment of the Yatsushiro tidal flat has not undergone a large change during the period from 2006 to 2012.

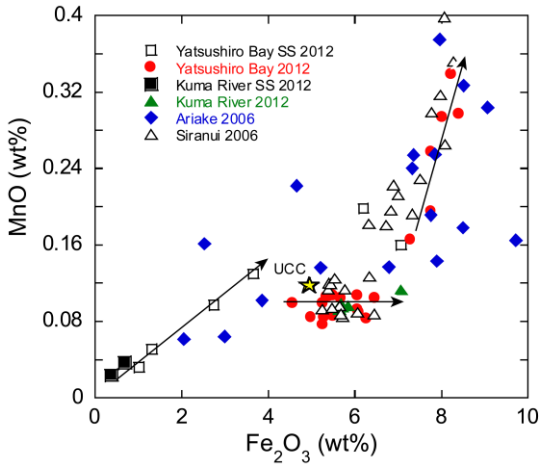

Fig. 10.1.6: MnO and Fe_2O_3 plots showing redox conditions of the Yatsushiro tidal flat, compared with 2006 data for the Ariake and Sirunai area (Unpublished data)

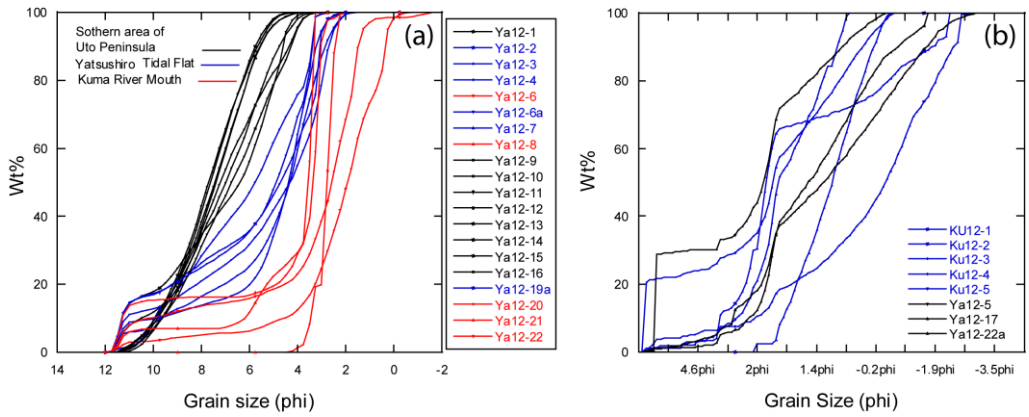

Fig. 10.1.7: Cumulative grain size variation of Kuma River and Yatsushiro Bay sediments

The LOI (Loss on Ignition) values for the Kuma River are low (Table 9.2.1, 2.32-2.99) indicating less carbonates and organic matter (OM) in 2012. The LOI of YA-1 is 18.10 and is very high. This sample contained many shell fragments and this high value is related to the shell carbonates. The southern area of the Uto Peninsula area has a comparatively high LOI (8.27 – 11.02). This is most likely related to high organic matter, since the CaO content is similar in almost all samples.

The pen shell, Atrina pectinata, belongs to the Pinnidae family and is a large (shell length up to 30 cm) suspension-feeding bivalve common along the coasts of Korea, Japan, and China. Atrina pectinata is an infaunal bivalve found in habitats ranging from muddy to sandy sediment and from tidal flats to shallow subtidal environments up to 20 m in depth (An et al. 2012). It is abundant in the tidal flats of the Yatsushiro Sea. It is possible, therefore, that Atrina pectinata shells could absorb trace elements. To test whether these shells are absorbing heavy metals, shells were collected from the bay and analyzed (Table 9.2.1). However, the low elemental values for the shells show that there is no heavy metal absorption taking place on the shell's surface.

10.2.2 Grain size

Grain size variation in Kuma River and Yatsushiro Bay sediments are shown in Fig 10.1.8a and b. Sediments consisting of grains < 3mm have been measured using the SALD-3000S (Fig. 10.1.8a) and grains > 3mm were measured using a settling tube (Fig 10.1.7b). Of the YA12 sediment samples, number 1 to 7 are from the tidal flat, 8 to 16 are from the southern area of the Uto Peninsula, and 19a to 22 are from the river mouth. All the samples of Kuma River, YA12-5, YA12-17 and YA12-22a contain coarse grains compared to other locations (Fig. 10.1.7b). The southern area of the Uto Peninsula, YA12-12 to YA12-16, (Fig. 10.1.7a) shows very fine grains and the other areas have coarse grains. Grain size sorting is calculated as in Folk and Ward 1957 (Table 9.2.1). In Fig. 10.1.7a, samples YA12-6, YA12-8, YA12-20, YA12-21 and YA12-22 are very poorly sorted, while samples YA12-9 to YA12-16 are very well sorted. The other samples are moderately sorted. Samples shown in Fig. 5b are very poorly sorted. Thus, the southern area of the Uto Peninsula in Yatsushiro Bay is very well sorted compared to the other samples. The river brings in coarser material, which is deposited proximal to the river

mouth, while the finer particles are transported and deposited in the distal southern area, the Uto Peninsula of Yatsushiro Bay. This phenomenon occurs because of the anticlockwise water circulation in the Yatsushiro Sea and because of the tidal variation. Grain size variation therefore shows a major control over the chemistry of bay and river sediments.

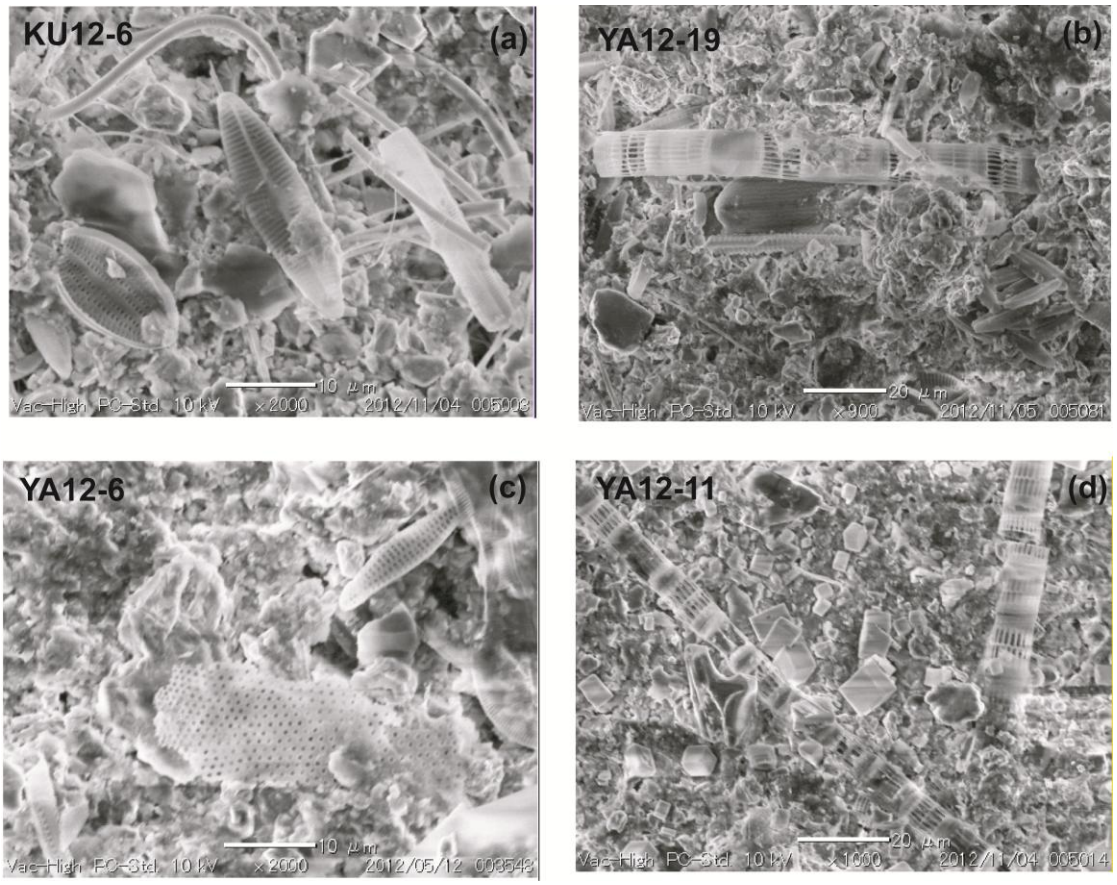

Fig. 10.1.8: SEM images of diatoms (a, b, c) in suspended solids of the Kuma River and Yatsushiro Bay. (d) Salt crystals and diatoms

10.2.3 Water environment

Oxygen reduction potential (ORP), dissolved oxygen (DO), electrical conductivity (EC) and pH were measured at the river mouth across tidal changes to see if there was any change of water quality. However, there was no major change in these parameters within the tidal cycle (Table 9.2.3). ORP ranged between -40 and 300 mV in the water of the Kuma River and the

Yatsushiro Bay. The pH ranged between 7.40 and 7.95, remaining neutral. Redox buffering is used to interpret natural water and sediment environments. Dissolved oxygen ranged from 6.7 to 8.3 mg/L and EC ranges between 0.312 and 6.7 mS/cm in the water and sediments of Kuma River and Yatsoshiro Bay (Table 9.2.3) this indicates oxic and less polluted conditions. ORP and pH is related to the behavior of different elements and they contribute to the behavior of pollutants in the water environment (Chuan et al. 1996). ORP can control the solubility of many species of elements in a solution. In many cases, H^+ ions are also involved in these reactions; hence they are pH sensitive (Bachmann et al. 2001; Takeno 2005; Taylor et al. 2007). However, in Kuma River and Yatsoshiro Bay these parameters remain relatively stable, indicating unpolluted water and sediment conditions.

10.2.4 Scanning electron microscope analysis

Diatoms are distributed worldwide, respond quickly to environmental change, and reflect both physical and chemical characteristics of the overlying water column. Thus, diatoms are helpful to determine the environmental conditions particularly when studying suspended solids. The diatoms of the Kuma River and Yatsushiro Bay were identified and classified using SEM images. Many species of diatoms were found in the Kuma River and Yatsushiro Bay (Fig. 10.1.8a, b, c, d).

The most common species were; *Skeletonema spp, Neodelphineis pelagic, Thalassiosira spp, Nitzschia spp, Gyrosigma, Tryblionella spp, Delphineis spp* and *Achnanthes spp* (Fig. 10.1.8). These species have also been found by Park et al. in 2012 in the Ariake Sea, just north of the Yatsushiro Sea.

Skeletonema is the most abundant species in Yatsushiro Bay and the Kuma River sediments. *Skeletonema* grows primarily in marine and brackish waters in estuaries (Fukuyo et al. 1990). Species within the genus are known to form large blooms in eutrophic and saline inland lakes and large rivers. Specimens of *Skeletonema* may be overlooked in samples due to their very light silicification (Spaulding and Edlund 2009). The habitat of *Neodelphineis pelagic* is marine (Krayesky et al. 2009) and this taxon was very common in Yatsushiro Bay samples.

Nitzschia is a very common genus with a large number of species that are often difficult to identify. Some *Nitzschia* species reach greatest abundance in waters high in organic pollution

(Spaulding and Edlund 2009). *Gyrosigm*a is characteristic of epipelic and endopelic habitats. This genus is widely distributed in fresh waters, with some species found in brackish waters (Spaulding and Edlund, 2009). Although *Tryblionella* was described in 1853, many recent floras include species within the *Nitzschia* genus. Species within the genus *Tryblionella* occur in both freshwater and marine waters (Spaulding 2011) and are common on mud flats (Park 2012). The abundance and taxa of diatoms in the Kuma River and Yatsushiro Bay indicate high nutrient conditions in the bay and river environments.

The SEM images also show the presence of salt crystals and high concentrations of clay particles. Salt crystals were found in Yatsushiro Bay suspended solids, but not in those of the Kuma River (Fig. 10.1.8c). The most abundant salt crystals were found in the sample YA12-11. YA12-19 is from the river mouth and did not contain any salt crystals. This clearly explains the high chloride concentration in the bay samples (Table 9.2.2). The Kuma River (KU12-1) was low in clay content, but at the river mouth (KU12-6) clay content was high, indicating transport of fine particles into the bay. In the bay, the southern area of the Uto Peninsula samples (YA12-16, YA12-18 and YA12-19) showed high clay content. In summary, diatoms are associated with abundant organic matter and show that the bay environment is particularly rich in nutrients. Images of Diatom species in Yatsushiro Bay and the Kuma River can be provided on request.

CHAPTER 11

CONCLUSIONS OF KUMA RIVER AND YATSUSHIRO BAY SYSTEM

11.1 Kuma River

The surface and bottom sediments, representing post-dam removal and dam conditions respectively, do not show significant chemical change. Therefore, opening the dam has not caused a large change in river sediment composition. The grain size difference in the bottom and surface sediments show that opening the dam has flushed most of the fine sediments towards Yatsushiro Bay. However, the two size fractions show clear chemical changes along the stream. Therefore grain size is a main controlling factor for the chemical composition of Kuma River and Yatsushiro Bay sediments. Grain size data shows progressive fining of sediment moving downstream, correlated with increases in Sr, Zr, and Ti. However, sediments are poorly sorted in the river channel. Yatsushiro Bay has high levels of the measured elements in the fine fraction for almost all samples. This indicates that the fine sediments transported by the river are accumulating in the bay. This data shows that Yatsushiro Bay is contaminated with Zn and Cu and has a small contamination due to As in three locations. The non-provenance elements, i.e. the environmentally sensitive elements, are best correlated in the Kuma River and the Yatsushiro Bay. The removal of the Arase dam has caused a decrease in elements of concern and not an increase with no anthropogenic effects.

11.2 Yatsushiro Bay

Sediments at the river mouth show less sorting than those of the Yatsushiro tidal flat, which is moderately sorted. Well sorted fine grain sediments are found in the northern portion of Yatsushiro Bay. Opening the Arase dam has caused impounded Kuma River sediments to be flushed into Yatsushiro Bay. The river deposits coarser material proximal to the river mouth, while the finer particles are transported and deposited in the distal, northern parts of the Yatsushiro Bay because of the anticlockwise circulation of bay waters. Grain size has a major control over the chemistry of bay and river sediments. However, there are also sand bar

formations found along the Kuma River resulting from the opening of the Arase dam. The chemistry of Yatsushiro Bay sediments has changed tremendously between 2002 and 2012. The trace elements are higher in 2002 than 2012. Therefore, the 2002 sediments represent an urban trend while the 2012 sediments represent a trend of more of normal sedimentation. SEM images of the suspended matter are rich in diatoms indicating high nutrient conditions in both the bay and river environments. Water chemistry parameters ORP, DO, EC and pH show that there is no pollution and the environment is oxic. Thus, the environment has become more favorable after the opening of the Arase dam. The southern area of the Uto Peninsula tidal flat is made up of silty sand while the southwest and northern parts of the Yatsushiro plain and the river mouth is sandy tidal flat.

CHAPTER 12

SYNTHESIS

The Mahaweli River is of a continental river and is the longest with a length of 335km and an altitude of 2500m (Fig 12.1.1). The Kuma River is of Japanese Island arc and is the longest river in Kyushu, south west of Japan with a length of 115km and an altitude of 1500m (Fig 12.1.1). Both rivers are dammed and thus were selected to be studied and to find out the mass transfer processes and the geochemical impacts of Mahaweli River and Trincomalee Bay System and the Kuma River and Yatsushiro Bay System.

The Mahaweli River is dammed in four places (Polgolla, Vitoria, Randenigala and Rantambe). The Kuma River is dammed at Arase and banked at Yohaizeki. The Mahaweli River sediments are deposited in four dams and the Kuma River is influenced by dam removal. Therefore, the Mahaweli River sedimentary basin is independent in weathering in the wet, intermediate and dry zones where the sediments are recycled within each climatic zone.

The Mahaweli River is subjected to tropical climate with heavy rain fall. The river flows through the wet, Intermediate and the dry zones. The highest weathering is seen in the wet zone CIA 52- 91 with an average of 83 and a rain fall of 2032-5080mm annually. The intermediate zone shows input of fresh material by the tributaries and high content of heavy minerals with very less weathering with CIA of 50 – 67 with an average of 67 and rain fall of 1750-2500mm annually. The dry zone has the lowest CIA indicating lowest weathering of 46 – 67 with an average of 55 and an annual rain fall of 762-1143mm. The Mahaweli River sediments undergo high erosion activities with high rain fall and severe and drastic climatic conditions. The dry zone thus does not undergo much weathering and mainly transports the sediments. Thus, the climatic zones pay a major role in the chemical composition of the sediments. Thus the Mahaweli River sediments weathering is different in each stage where the river sediments are highly weathered (CIA, 46-97). With increasing quartz composition the sediments are maturing downstream and much matured in Trincomalee Bay where the sand fraction (SiO_2 >80%) is deposited and the finer clays are removed by the waves and currents. The Mahaweli river sediments have high heavy mineral contents, specially input from the tributaries. Thus, the tributaries play a major role in the composition of the Mahaweli main channel sediments. The river is mainly composed of sandy sediments and less clay fractions.

Trincomalee Bay is subject to mainly clock wise wave action and not tidally influenced. The wind speed in the Trincomalee Bay is 7-15 km/h. The Bay is also subjected to cyclone and monsoonal

changes. The strong clockwise wave actions cause the heavy minerals to be deposited in the southwest area of the Koddiyar Bay and the fine clays are washed towards the open sea. Very high concentrations of elements of Ti, Zr, Ce, Nb and Y in Koddiyar Bay are consistent with heavy mineral concentration by winnowing in a high-energy zone, creating heavy mineral lags.

The high CMI ratios indicate that the core one sediments from 1C24 – 1C30 are mature. Three other cores also show high maturity, but not to the extreme values seen in C1. Most of the sediments have SiO2 > 80% may have silica contents comparable to quartz arenites. The main mechanism involved in these sediments may be the sorting of grains. Circulation of water currents, the wave and wind direction are controlling factors for the deposition of heavy minerals in C1. The sediments are mainly supplied by the Mahaweli River but may also be partially composed of marine sediments. Coarser lower C1 sediments (40 - 60 cm) may have been deposited by large waves and currents, as evidenced by the presence of large angular grains and only thin mud inter-beds. Sand bar formation in Koddiyar Bay near the river mouth, reduces wave and current activity. The upper part of C1 thus consists of finer grains and abundant heavy minerals. C2 is composed only of Mahaweli River sediment deposited in sand bars. In C3 the interval from 20 – 28 cm may represent a buried flood deposit. Core 4 is also mainly composed of Mahaweli River sediments, but was deposited in a calmer, semi-enclosed bay, leading to higher content of finer grained detritus bar with smaller quantities of finer clay included.

The Kuma River is dammed at Arase at 19.9km. It was decided to remove the Arase dam gates and was started in 2010 April. The Kima River sediments were thus subject to high flushing due to opening of the Arase dam and consist mainly of sand fractions. Point bars formed in the river banks after opening of the Arase dam. Due to this flushing, the environmental conditions have become favorable in the Kuma River and Yatsushiro Bay sediments. The Kuma River sediments are subject to heavy rain fall of 2300mm/annually and are not much weathered with a CIA of 64 – 67 with an average of 66. The Yatsushiro Bay is subjected to Asian monsoon and typhoons. The wave action is anti clock wise and thus the finer sediments are deposited in the distal end and the coarser sediments are deposited in the distal end of the Yatsushiro Bay. The sediments of the Kuma River are less sorted and the Bay sediments are renewed due to opening of the dam and flushing of the sediments.

The Mahaweli River falls to the Trincomalee Bay a deep natural canyon while the Kuma River forms a large tidal flat at Yatsushiro Bay. The climate in Sri Lanka is tropical and is influenced by very high rainfall in a metamorphic terrane. Therefore, the composition is highly unique. The inflow from tributaries contributes to different compositions along the stream. In the Trincomalee coast recycling occurs and the deposited sand is thus mature. The sorting is very high in the Mahaweli river sediments and the Trincomalee Bay sediments. However, weathering also occurs and is controlled by climatic zones

and such phenomina is not seen in the Kuma River. The rocks in Sri Lanka consist of common concentrations for undurable and durable elements related to heavy minerals much different from the Kyushu geological setting. The soils and the sediments are thus enriched in durable heavy mineral related elements in the Mahaweli catchment area. In the Kuma River the sediment is influenced by transport. The Kuma River forms the Yatsushiro tidal flat and the geological setting is much different to the Mahaweli river and the Trincomalee Bay system. Thus, the process involved in the mass transfer process of the Mahaweli River and Trincomalee Bay system are; fining, accumulation due to transport, influence of tributaries, climatic influence, weathering, grain size, heavy minerals and sorting with high wave action in the Trincomalee Bay. The process involved in the mass transfer process of the Kuma River and Yatsushiro Bay are transport, flushing, grain size and sorting.

Synthesis	
Mahaweli River	**Kuma River**
Continental River	Island arc, Volcanic
Heavy rain fall, 2500-5080mm	Heavy Rain fall 2300mm, Asian Monsoon/Typhoon
Sandy sediments	Sandy sediments
High Weathering, Independent in the wet, intermediate and dry zones	Less weathered
Inflow from tributaries contributes to different composition	No tributary effect
Heavy Mineral Sand	No Heavy Minerals
Many Dams - recycled within each climatic zone	Arase Dam gate open
	Heavy flushing, Point bar's are formed
	Deposit Temporally Renewed
Mahaweli River falls to the Trincomalee Bay a deep natural canyon and sand is deposited, fine fraction is flushed to the open sea	Kuma River forms a large tidal flat at Yatsushiro Bay with mud at distal end and sand at the proximal end
Sediments are fractionated, wet and intermediate zones are mixing in the dry zone due to length and HM deposited in the Koddiyar Bay	No such mixing due to short distance of river
Flooding occur but weakened since river is long, and the sediments are transported to the bay	Flooding causes mud drapes and sand deposits in the Yatsuahiro Bay

Table 12.1.1 The synthesis of the Mahaweli River and Trincomalee Bay System and the Kuma River and Yatsushiro Bay System

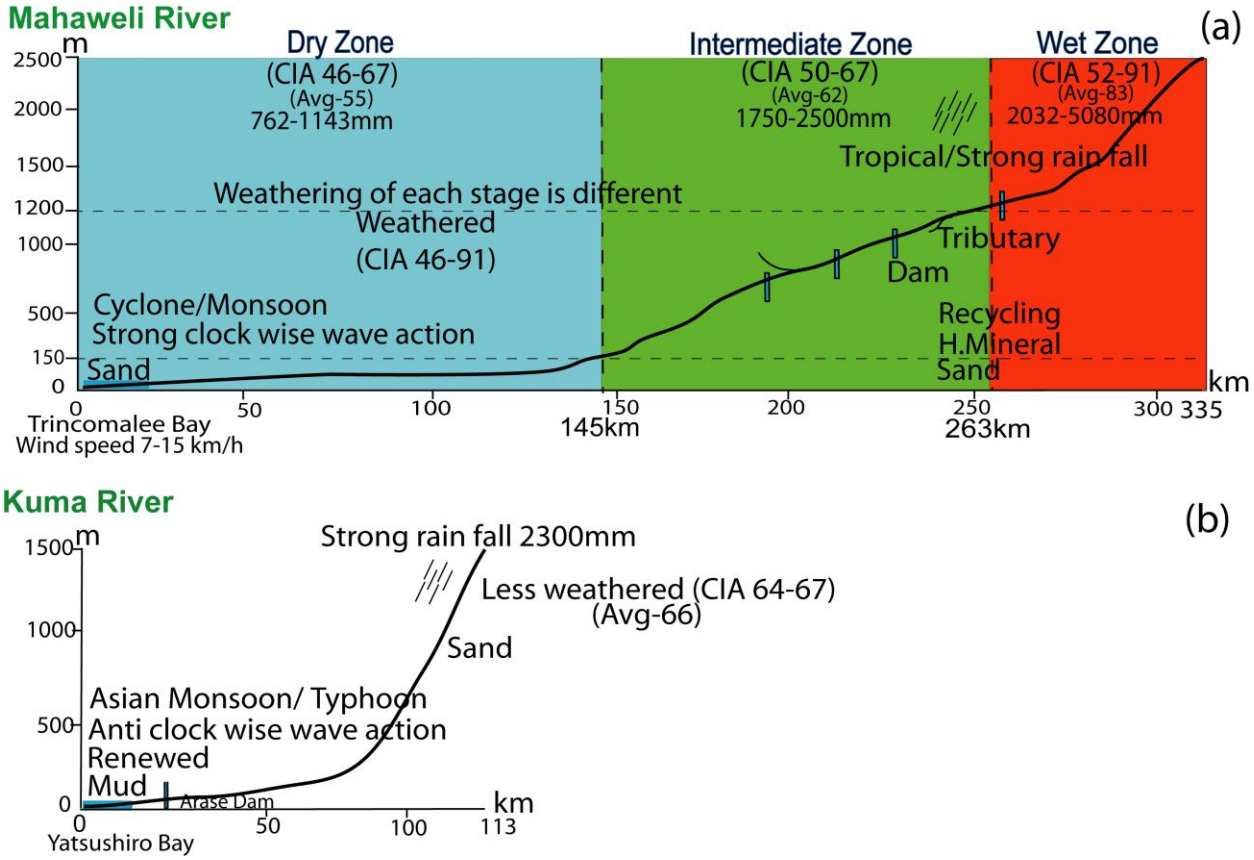

Fig 12.1.1 : Mass transfer processes in the (a) Mahaweli River and Trincomalee Bay system (b) Kuma River and Yatsushiro Bay system

REFERENCES

Ackermann F (1980) A procedure for correcting the grain size effects in heavy metal analyses of estuarine and coastal sediments. Environmental Technology Letters 1: 518–527

Agnol RD, Lafon JM, Macambira MJB (1994) Proterozoic anorogenic magmatism in the Central Amazonian Province, Amazonian craton: Geochronological, petrological and geochemical aspects. Mineralogy and Petrology 50:113-138

Agunbiade FO, Fawale AT (2009) Use of Siam weed biomarker in assessing heavy metal contaminations in traffic and solid waste polluted areas. International Journal of Environmental Science 6. 2: 267-276

Ahmed FM, Bibi H, Seto K, Ishiga H, Fukushima T, Roser BP (2009) Abundances, distribution, and sources of trace metals in Nakaumi–Honjo coastal lagoon sediments, Japan. Environmental Monitoring Assessment 167:473–491

Albering HJ, Rila JP, Moonen EJC, Hoogewerff JA, Kleinjans JCS (1999) Human health risk assessment in relation to environmental pollution of two artificial freshwater lakes in The Netherlands. Environmental Health Perspectives 107.1: 27–35

Alexakis D (2008) Geochemistry of stream sediments as a tool for assessing contamination by Arsenic, Chromium and other toxic elements: East Attica region, Greece. European Water. 21/22: 57-72

Amorosi A, Centineo MC, Dinelli E, Lucchini F, Tateo F (2002) Geochemical and mineralogical variations as indicators of provenance changes in Late Quaternary deposits of SE Po Plain. Sedimentary Geology. 151: 273–92

An HS, Kim BH, Lee JW, Dong CM, Kim SK, Yi Kim C (2011) Comparison between Wild and Hatchery Populations of Korean Pen Shell (Atrina pectinata) Using Microsatellite DNA Markers. International Journal of Molecular Science 12:6024-6039

Anfuso G, Achab M, Coltrane G, Lopez-Aguayo F (1999) Utility of heavy minerals distribution and granulometric analyses in the study of coastal dynamics: application to the littoral between Sanlucar de Barrameda and Rota (Cadiz, southwest Iberian Peninsula), Boletin del Instituto Espanol de Oceanografia 15 (1–4). 243–250

Aprile, FM, Bouvy M (2008) Distribution and enrichment of heavy metals in sediments at the tapacurá river basin, northeastern Brazil. Brazilian Journal of Aquatic Science and Technology 12.1:1-8

Arribas J, Arribas ME (1991) Petrographic evidence of different provenance in two alluvial fan systems (Palaeogene of the northern Tajo Basin, Spain), Geological Society, London, Special Publications. 57: 263-271

Bachmann TM, Friese K, Zachmann DW (2001) Redox and pH conditions in the water column and in the sediments of an acidic mining lake. Journal of Geochemical Exploration 73:75-86

Balachandran KK, Laluraj CM, Martin GD, Srinivas K, Venugopal P (2006) Environmental analysis of heavy metal deposition in a flow-restricted tropical estuary and its adjacent shelf. Environmental Forensics 7(4). 345-351

Bastviken D, Ejlertsson J, Tranvik L (2001) Similar bacterial growth on dissolved organic matter in anoxic and oxic lake water. Aquatic Microbial Ecology 24: 41–49

Basu A and Molinaroli E (1991) Reliability and application of detrital opaque Fe-Ti oxide minerals in provenance determination, Geological Society, London, Special Publications. 57: 55-65 ; DOI: 10.1144/GSL.SP.1991.057.01.06

Basu A, Mckav DS, Gerke T (1988) Petrology and provenance of Apollo 15 drive tube 15007/8. Proceedings of the Eighteenth Lunar and Planetary Science Conference, Cambridge University Press. 283-298

Basu A, Young SW, Suttner LJ, James WC, Mack GH (1975) Re-evaluation of the use of undulatory extinctions and polycrystallinity in detrital quartz for provenance interpretation, Journal of Sedimentary Petrology 45:873-882

Beck M, Dellwig O, Schnetger B, Brumsack HJ (2008) Cycling of trace metals (Mn, Fe, Mo, U, V, Cr) in deep pore waters of intertidal flat sediments. Geochimica Et Cosmochimica Acta 72: 2822–2840

Bednarek AT (2001) Undamming rivers: a review of the ecological impacts of dam removal. Environmental Management 27(6).803–814

Bellanger B, Huon S, Steinmann P, Chabaux F, Velasquez F, Valles V, Arn K, Clauer N, Mariotti A (2004) Oxic–anoxic conditions in the water column of a tropical freshwater reservoir (Pena-Larga dam, NW Venezuela). Applied Geochemistry 19:1295–1314

Bergamaschi L, Rizzio E, Valcuvia MG, Verza G, Profumo A, Gallorini M (2002) Determination of trace elements and evaluation of their enrichment factors in Himalayan lichens. Environmental Pollution 120: 137–144

Berner, K.B and Berner, R.A. (1996) Global Enviromental: water, air and geochemical cycles, New Jersey, USA, Practice Hall, pp 376

Berquist CR, Fishler Jr CT, Calliari LJ, Dydak SM, Ozalpaslan H, Skrabal SA (1990) Heavy-mineral concentrations in sediments of the inner continental shelf. In: C.R. Berquist Jr., Editor, Heavy-Mineral Studies-Virginia Inner Continental Shelf, Virginia Division of Mineral Resource Publication 103: 31–94

Bhatia MR (1983) Plate tectonics and geochemical composition of sandstones, Journal of Geology 91: 611-627

Bhatia MR (1985) Rare earth element geochemistry of Australian Paleozoic greywackes and mudrocks: provenance and tectonic control, Sedimentary Geology 45:97-113

Bhatia MR, Crook KAW (1986) Trace element characteristics of greywackes and tectonic setting discrimination of sedimentary basins, Contributions to Mineralogy and Petrology 92: 181-193

Biksham G, Subramanian V, Griken RV (1991) Heavy metal distribution in the Godavari river basin, Environmental Geology and Water Sciences 17: 117–126

Biswas AB, Roy RN (1976) A study on the depositional processes and heavy mineral assemblage of the quaternary sediments from murshidabad district, west Bengal. Depositional processes and heavy mineral assemblage 42(5). 372-386

Blatt H (1985) Provenance studies and mudrocks. Journal of Sedimentary Petrology, 55, pp 69-75

Bodergat AM, Ikeya N (1988) Distribution of Recent Ostracoda in Ise and Mikawa Bays, Pacific Coast of Central Japan. In: Hanai T, Ikeya N, Ishizaki K, Kodansha (eds), Evolutionary Biology of Ostracoda-Its fundamentals and applications. Tokyo and Elsevier, Amsterdam pp 413−428

Borrego J, Morales JA, De La Torre ML, Grande JA (2002) Geochemical characteristics of heavy metal pollution in surface sediments of the Tinto and Odiel river estuary (southwestern Spain). Environmental Geology 41:785–796

Bradley WC (1970) Effect of weathering on abrasion of granitic gravel, Colorado River (Texas). Bulletin of Geological society of America. 81: 61 – 80

Brady GS (1886) Notes on Entomostraca collected by Mr. A. Haly in Ceylon. Journal of Linnean Society 19: 293-317

Brayshaw AC (1985) Bed microtopography and entrainment thresholds in gravel-bed rivers. Bulletin of Geological society of America. 96: 218 – 223

Burdige DJ (2005) Burial of terrestrial organic matter in marine sediments: A re-assessment. Global biogeochemical cycles. 19. GB4011. doi:10.1029/2004GB002368

Bush SA, Bush PA (1969) Trincomalee and associated canyons. Ceylon Deep-sea Resources 16, 655–660

Buzas MA, Gibson TG (1969) Species diversity: benthonic foraminifera in western North Atlantic. Science 163: 72–75

Byrne P, Reid I, Wood PJ (2010) Sediment geochemistry of streams draining abandoned lead/zinc mines in central Wales: the Afon Twymyn. Journal of Soils and Sediments 10: 683-697

Caitcheon GG (1998) The significance of various sediment magnetic mineral fractions for tracing sediment sources in Killimicat Creek. Catena 32: 131-142

Calvert SE (1976) The mineralogy and geochemistry of near-shore sediments, In: Riley, J.R. & Chester, R. (eds), Chemical Oceanography, Vol. 6 (2nd Ed.), Academic press, pp 187

Cardoso R, Araujo MDF, Freitas MC, Fatela F (2008) Geochemical characterisation of sediments from marginal environments of Lima Estuary (NW Portugal). Rev Electron Cienc. Terra Geosciences On-line Journal 5:1-11

Carranza-Edwards A, Bocanegra-García G, Rosales-Hoz L, De Pablo Galán L (1998) Beach sands from Baja California Peninsula, Mexico: Sedimentary Geology 119: 263-274

Carrol D (1970) Rock weathering. New York, USA, Plenum Press

Cawood PA (1983) Modal compositions and detrital pyroxene geochemistry of lithic sandstones from the New England Fold Belt (east Australia): a Paleozoic forearc terrane, Geological Society of America Bulletin, 94: 1199-1214

Cawood PA (1991) Nature and record of igneous activity in the Tonga arc, SW Pacific, deduced from the phase chemistry of derived detrital grains, Geological Society, London, Special Publications, v. 57, pp 305-321, DOI: 10.1144/GSL.SP.1991.057.01.23

Cevik F, Ziya M, Goksu L, Derici OB, Fındık O (2009) An assessment of metal pollution in surface sediments of Seyhan dam by using enrichment factor, geoaccumulation index and statistical analyses. Environmental Monitoring Assessment 152:309–317

Characklis GW, Wiesner MR (1997) Particles metals and water quality in run off from a large urban watershed. Journal of Environmental Engineering 123:753–762

Cheepurupalli NR, Anu BR, Reddy KSN, Dhanamjayarao EN, Dayal AM (2012) Heavy mineral distribution studies in different micro-envionments of Bhimunipatnam coast, Andhra Pradesh, India. International Journal of Scientific and Research Publications 2(5). 1-10

Chen CT, Kandasamy S (2007) Evaluation of elemental enrichments in surface sediments off southwestern Taiwan. Environmental Geology 54: 1333-1346

Chen Y (1998) Different oxidation reactions of ilmenite induced by high energy ball milling. Journal of Alloys and Compounds 266: 150–154

Chuan MC, Shu GY, Liu CJ (1996) Solubility of heavy metals in a contaminated soil effect of redox potential and pH. Journal of Water, Air and Soil Pollution 90:543-556

Condie KC, Wronkiewicz DJ (1990) The Cr/Th ratio in Precambrian pelites from the Kaapvaal Craton as an index of craton evolution. Earth and Planetary Science Letters 97: 3–4, 256–267

Condie KC (1992) Proterozoic terranes and continental accretion in southwestern North America. In: Condie, K.C. (Ed.), Proterozoic Crustal Evolution. Elsevier Scientific Publishers. Amsterdam 447–480. Chap. 12

Condie KC (1993) Chemical composition and evolution of the upper continental crust: Contrasting results from surface samples and shales. Chemical Geology 104 : 1–37

Cooray PG (1984) The Geology of Sri Lanka (Ceylon). Second (revised) edition, National museums of Sri Lanka publication. pp 340

Cooray PG (1994) The Precambrian of Sri Lanka, a historical overview. Precambrian Resource 66: 3–18

Cox KG, Bell JD, Pankhurst RJ (1979) The interpretation of igneous rocks. George Allen and Unwin, London pp 450

Cronin TM, Vann CD (2003) The sedimentary record of climatic and anthropogenic influence on the Patuxent Estuary and Chesapeake Bay ecosystems. Estuaries 26: 196–209

Crook KAW (1974) Lithogenesis and geotectonics: the significanse of compositional variations in flysch arenites (graywackes). In: DOTT, R. H. & SHAVER, R. H. (eds)Modern and ancient geosynclinals sedimentation, Society of Economic Paleontologists amf Mineralogist Special -Publication, 19:304-310

Cullers RL, Basu A, Suttner LJ (1988) Geochemical signature of provenance in sand-size material in soils and stream sediments near the Tobacco Root Batholith, Montana, U. S. A. Chemical Geology 70:335-348

Cullers R (1988) Mineralogical and chemical changes of soil and stream sediment formed by intense weathering of the Danburg granite, Georgia, U.S.A. Lithos 21 (4) 301-314

Curtis CD (1977) Sedimentary geochemistry: environments and processes dominated by involvement of an aqueous phase. Philosophical Transactions of the Royal society, A286, pp 353

Dai M, Martin J, Cauwet G (1995) The significant role of colloids in the transport and transformation of organic carbon and associated trace metals (Cd, Cu and Ni) in the Rhone delta (France). Marine Chemistry 51: 159 -175

Daskalakis KD, O'Connor TP (1995) Normalization and elemental sediment contamination in the coastal United States. Environmental Science and Technology. 29, 470-77

Daskalakis KD, O'Connor TP (1995) Distribution of chemical concentrations in US coastal and estuarine sediment. Mar Environ Res 40:381–398

Dassanayake H (1984) Shri Lanka. In: Holmgren S (ed) An environmental assessment of the Bay of Bengal region. Nagaraj & Co, Madras, pp 209-218

Dauby P, Baeyens W, Biondo R, Bouqqegneau JM, Chou L, Collette O, Dehairs F, Elskens M, Frankignoulle M, Loijens M, Paucot H, Wollast R (1993) Distribution of particulate trace elements in the Northeastern Atlantic. Progress in Belgain oceanographic research, Brussels. Institute of marine research and air sea interaction. pp 287

Davies DK, Ethridge FG (1975) Sandstone composition and depositional environment, American association of petroleum geologists bulletin 59: 239-264

Dellwig O, Hinrichs J, Hild A, Brumsack HJ (2000) Changing sedimentation in tidal flat sediments of the southern North Sea from the Holocene to the present: a geochemical approach. Journal of Sea Research 44: 195–208

Department of Census and Statistics, Sri Lanka (2012) A2 : Population by ethnic group according to districts

Departrment of Mineralogy Sri Lanka, 1959. Report on the Mitipola Radiometric Survey for the Radio Active Mineral Thorianite, Technical Report, MRH/7

Dewi KT (1997) Ostracoda from the Java Sea, west of Bawean Island, Indonesia. Marine Geological Institute Special Publication 4: pp 79

Dill HG (1998) A review of heavy minerals in clastic sediments with case studies from the alluvial-fan through the nearshore-marine environments. Earth Science Reviews 45, 103–132

Dissanayake CB, Chandrajith R, Tobschall HJ (2000) The geology mineralogy and rare element geochemistry of the gem deposits of Sri Lanka. Bull Geol Soc Finl 72. 1–2: 5–20

Dissanayake CB, Rupasinghe MS (1986) The niobium and yttrium abundances in the sedimentary gem deposits of Sri Lanka. Journal National Science Council Sri Lanka 14. 1: 55-74

Dissanayake CB (1982) The geology and the geochemistry of the Uda Walawe serpentinite, Sri Lanka. Journal of the National Science Council of Sri Lanka. 10 (1) 13-34

Dissanayake CB, Chandrajith R (2003) Gem-bearing stream sediments of Sri Lanka. Publication of the Gem and Jewellery Research and Training Institute and National Gem and Jewellery Authority. Colombo Sri Lanka 121

Dissanayake CB, Chandrajith R, Tobschall HJ (2000) The geology, mineralogy and rare element geochemistry of the gem deposits of Sri Lanka. Bulletin of the Geological Society of Finland. 72: 5–20

Dissanayake CB, Rupasinghe MS (1992) Application of geochemistry to exploration of gem deposits, Sri Lanka. Journal of Gemmology 23 (3) 165–175

Dozen K, Ishiga H (2002) Evaluation of sedimentary environments from compositions of sediments from the Kuma and Kawabe Rivers, Kyushu, Japan. Geoscience report Shimane University 21:17-29

Eisma D (1993) Suspended matter in the aquatic environment. Springer, Berlin

Elliott T (1986) Deltas. In: Reading, H.G. (Ed.), Sedimentary Environments and Facies. Blackwell Scientific Publications, Oxford, pp. 113–154

Evans JA, Stone P, Floyd JD (1991) Isotopic characteristics of Ordovician greywacke provenance in the Southern Uplands of Scotland. In: Morton, A. C., Todd, S. P. and Haughton, P. D. W. (eds.). Developments in Sedimentary Provenance Studies. Geological Society of London, Special Publication, 57: 161-172

Fagbote EO, Olanipekun EO (2010) Evaluation of the status of heavy metal pollution of soil and plant (Chromolaena odorata) of Agbabu bitumen deposit area, Nigeria. American-Eurasian Journal of Scientific Research 5 (4) 241-248

Fakolade OR, Obasi RA (2012) The Geochemical Assessment of Sub Surface Coastal Plain Clastic Deposits of Eastern Dahomey, Basin around Lagos Area, South West, Nigeria. Journal of Science and Technology 1 (6) 300- 307

Fauzielly L, Irizuki T, Sampei Y (2013) Spatial Distribution of Recent Ostracode Assemblages and Depositional Environments in Jakarta Bay, Indonesia, with Relation to Environmental Factors. Paleontological Research 16: 267-281

Fedo CM, Nesbitt HW, Young GM (1995) Unraveling the effects of potassium metasomatism in sedimentary rocks and paleosols, with implications for paleoweathering conditions and provenance. Geology 23 (10)921-924

Feely RA, Massoth GJ, Paulson AJ, Gendron JF (1983) Possible evidence for enrichment of trace elements in the hydrous manganese oxide phases of suspended matter from an urbanized embayment. Estuarine Coastal and Shelf Science 17:693–708

Feely RA, Massoth Gray J, Lamb Marlyn F (1981) The effect of sewage effluents on the flocculation of major and trace elements in stratified estuary. In: Proceedings of NATO Advanced Research Institute on Trace Metals in Sea water, Eltore Majorna International Centre for Scientific Culture. Erice. Sicily. Italy. 227-244

Ferguson R, Hoey T, Wathen S, Werritty A (1996) Field evidence for rapid downstream fining of river gravels through selective transport. Geology 24: 179-182

Ferguson RI, Hoey TB, Wathen SJ, Werritty A, Hardwick RI, Sambrook Smith GH (1998) Downstream fining of river gravels: integrated field, laboratory and modeling study. In: Klingeman PC, Beschta RL, Komar PD, Bradley JB (eds) Gravel-Bed Rivers in the Environment. Water Resources Publications. Highland Ranch. Colorado. 85–114

Fernando GWAR (1995) A scientific approach to locate new gem deposits of high grade metamorphic terrains with special reference to Sri Lanka. M.Phil. Thesis, University of Peradeniya, Peradeniya. Sri Lanka. pp 180

Ferrira JR, Lawlor AJ, Bates JM, Clarke KJ, Tipping E (1997) Chemistry of riverine and estuary suspended particles from the Ouse-Trent system, UK. Colloids Surf A 120:183–198

Ferreira A, Inacio MM, Morgado P, Batista MJ, Ferreira L, Pereira V, Pinto MS (2001) Low-density geochemical mapping in Portugal. Applied Geochemistry 16: 1323–1331

Filipek LH, Owen RM (1979) Geochemical associations and grain size partitioning of heavy metals in lacustrine sediments. Chemical Geology 26 : 105–117

Flores RM, Shideler GL (1978) Factors controlling heavy-mineral variations on the south Texas outer continental shelf, Gulf of Mexico. Journal of Sedimentary Petrology 48 (1) 269-280

Floyd PA, Shail R, Leveridge BE, Franke W (1991) Geochemistry and provenance of Rhenohercynian synorogenic sandstones: implications for tectonic environment discrimination. Developments in Sedimentary Provenance (Morton, A. C., Todd, S. P. and Haughton, P. D. W., eds.), Geological Society of London Special Publication 57: 173–188

Folk RL (1951) Stages of textural maturity in sedimentary rocks. Journal of Sedimentary Research 21 (3) 127-130

Folk RL (1974) Petrology of Sedimentary Rocks: Austin, Texas, Hemphill Publishing Co, pp 182

Folk RL, Ward WC (1957) Brazos river bar: a study of significance of grain size parameters. Journal of Sedimentary Petrology 27: 3–26

Fordyce FM, Green PM, Simpson PR (1993) Simulation of regional geochemical survey maps at variable sample density. Journal of Geochemical Exploration 49: 161-175

Formoso MLL (2006) Some topics on geochemistry of weathering: a review. Anais Da Academia Brasileira De Ciencias 78 (4) 809-820

Forstner U (1990) Contaminated sediments. Lecture Notes in Earth Science. Springer-Verlag, Berlin. 21

Förstner U (1987) In metal speciation, separation and recovery. Lewis, Michigan. pp 3–26

Förstner U, Wittmann GTW (1983) Metal pollution in the aquatic environment. Springer-Verlag, Berlin Heidelberg New York. pp 481

Fraser G, Ellis D, Eggins S (1997) Zirconium abundance in granulite-facies minerals with implications for zircon geochronology in high-grade rocks. Geology 25 (7) 607 – 610

Frihy OE, Dewidar KM (2003) Patterns of erosion/sedimentation, heavy mineral concentration and grain size to interpret boundaries of littoral sub-cells of the Nile Delta, Egypt. Marine Geology 199: 27–43

Frost CD, Winston D (1987) Nd isotope systematics of coarse- and finegrained sediments: Examples from the Middle Proterozoic Belt-Purcell Supergroup: Journal of Geology. 95: 309–327

Fukuyo Y, Takano H, Chihara M, Matsuoka K (1990) Red Tide Organisms in Japan: An Illustrated Taxonomic Guide. 178-179

Gallet S, Jahn BM, Torii M (1996) Geochemical characterization of the Luochuan loess-paleosol sequence, China and paleoclimatic implications. Chemical Geology. 133: 67–88

Gamage SJK, Rupasinghe MS, Dissanayake CB (1992) Application of Rb/Sr ratios in gem exploration in the granulite belt of Sri Lanka. Journal of Geochemical Exploration. 43 (3) 281–292

Garcia D, Fonteilles M, Moutte J (1994) Sedimentary fractionations between Al, Ti and Zr and the genesis of strongly peraluminous granites. Journal of Geology 102: 411–422

Garcia D, Ravenne C, Marechal B, Moutte J (2004) Geochemical variability induced by entrainment sorting: quantified signals for provenance analysis. Sedimentary Geology 171: 113–128

Garrels RM, Christ C (1965) Solutions, minerals and equilibria. San Francisco, Freeman-Cooper. pp 450

Garver JI, Royce PR, Smick TA (1996) Chromium and nickel in shale of the Taconic foreland: A case study for the provenance of fine-grained sediments with an ultramafic source. Journal of Sedimentary Research. Section A. 66 (1)100–106

Garzanti E (1986) Source rock versus sedimentary control on the mineralogy of deltaic volcanic arenites (Upper Triassic, northern Italy): Journal of sedimentary petrology. 56: 267 – 275

Ghrefat H, Yusuf N (2006) Assessing Mn, Fe, Cu, Zn, and Cd pollution in bottom sediments of Wadi Al-Arab Dam, Jordan. Chemosphere 65:2114–2121

Gibbs RJ (1977) Transport phases of transition metals in the Amazon and Yukon Rivers. Geological Society of America Bulletin 88: 829–843

Giusti L (2011) Heavy metals in urban soils of Bristol (UK). Initial screening for contaminated land. Journal of Soils Sediments 11:1385–1398

Goede A (1975) Downstream changes in the pebble morphometry of the Tambo River, Eastern Victoria. Journal of sedimentary petrology 45: 704 – 718

Goldberg ED, Arrhenius GOS (1958) Chemistry of Pacific pelagic sediments, Geochimica Et Cosmochimica Acta 13 : 153-212

Gopalakrishna K, Shabi B, Mahesh BL (2008) Distribution of ostracode assemblages along the nearshore and offshore areas of Malabar Coast, Kerala (west coast of India). Indian Journal of Marine Science 37: 298–306

Gracia D, Fonteilles M, Moutte J (1994) Sedimentary fractionations between Al, Ti and Zr and the genesis of strongly peraluminous granites. Journal of Geology 102: 411–422

Graney JR, Eriksen TM (2004) Metals in pond sediments as archives of anthropogenic activities: A study in response to health concerns. Applied Geochemistry 19: 1177–1188

Grantza DA, Garnerb JHB, Johnson DW (2003) Ecological effects of particulate matter. Environment International 29:213–239

Graybeal AL, Heath GR (1984) Remobilization of transition metals in surfacial pelagic sediments from the eastern Pacific, Geochimica Et Cosmochimica Acta 48: 965-975

Groot AJD, Zchuppe KH, Salomons W (1982) Standardisation of methods of analysis for heavy metals in sediments, Hydrobiologia 92 : 689–695

Grunsky EC, Drew LJ, Sutphin DM (2009) Process recognition in multi-element soil and stream-sediment geochemical data. Applied Geochemistry. 24: 1602–1616

Guedes CCF, Giannini PCF, Nascimento Jr DR, Sawakuchi AO, Tanaka APB, Rossi MG (2011) Controls of heavy minerals and grain size in a holocene regressive barrier (Ilha Comprida, southeastern Brazil). Journal of South American Earth Sciences 31: 110-123

Gurzau ES, Neagu C, Gurzaua AE (2003)Essential metals—case study on iron. Ecotoxicology And Environmental Safety 56:190–200

Hagan GB, Ofosu FG, Hayford EK, Osae EK, Oduro-Afriyie K (2011) Heavy metal contamination and physico-chemical assessment of the Densu River Basin in Ghana. Res J Environmental Earth Science 3 (4) 385-392

Halamic J, Peh Z, Bukovec D, Miko S, Galovic L (2001) A factor model of the relationship between stream sediment geochemistry and adjacent drainage basin lithology, Medvednica Mt., Croatia. Geologia Croatica 54 (1) 37–51

Hamilton-Taylor J, Giusti L, Davison W, Tych W, Hewitt CN (1997) Sorption of trace metals (Cu, Pb, Zn) by suspended lake particles in artificial (0.005 M NaNO3) and natural (Esthwaite Water) freshwaters. Colloids Surf A 120:205–219

Hanai T, Ikeya N, Ishizaki K, Sekiguchi Y, Yajima M (1977) Checklist of Ostracoda from Japan and its Adjacent Seas. Univ. Tokyo Press, Tokyo. pp 119

Haregeweyn N, Melesse B, Tsunekawa A, Tsubo M, Meshesha D, Balana BB (2012) Reservoir sedimentation and its mitigating strategies: a case study of Angereb reservoir (NW Ethiopia). Journal of Soils and Sediments 12:291–305

Harnois L (1988) The CIW index: A new chemical index of weathering. Sedimentary Geology. 55: 319-322

Hatje V, Payne TE, Hill DM, McOrist G, Birch GF, Szymczak R (2003) Kinetics of trace element uptake and release by particles in estuarine waters: effects of pH, salinity, and particle loading. Environment International 29:619–629

Haughton PDW, Todd SP, Morton AC (1991) Sedimentary provenance studies. in: "Morton, A.C., Todd, S.P., Morton, A.C. (Eds), Developments in Sedimentary Provenance Studies". The Geological Society of London. 1-12

Hegde VS, Shalini G, Kanchanagouri DG (2006) Provenance of heavy minerals with special reference to ilmenite of the Honnavar beach, central west coast of India. Current Science 91(5) 644-648

Heier KS (1973) A model for the composition of the deep continental crust. Fortschr. Min., 50, 174; (1978) The distribution and redistribution of heat producing elements in the continents. Phil. Trans. Roy. Soc., A288, 393; (1979) The movement of uranium during higher grade metamorphic processes. Ibid., A293, 413; Tarney, J. & Windley, B.F. (1977) Chemistry, thermal gradients and evolution of the lower continental crust. Journal Geological Society of London 134, 153

Heikoop JM, Risk MJ (1993) Heavy minerals as indicators of longshore drift in beach sediment at Manzanillo, Limon province, Costa Rica. Brenesia. No 39-40, 51-58

Helmke PA, Koons RD, Schmber PJ Iskander IK (1977) Determination of trace element concentration of sediments by multielemental analysis of clay-size fractions. Environmental Science Technology 11 : 984–989

Hirst DM (1962) The geochemistry of modern sediments from the Gulf of Paria, II. The location and distribution of trace elements. Geochimica Et Cosmochimica Acta 26: 1147–1187

Hiscott RN (1984) Ophiolitic source rocks for Taconic-age flysch: trace element evidence. Geological Society of America Bulletin 95:1261-1267

Ho HH, Swennen R, Damme AV (2010) Distribution and contamination status of heavy metals in estuarine sediments near Cua ong harbor, Ha long bay, Vietnam. Geologica Belgica 2: 37–47

Hoffman CW, Grosz AE Nickerson JG (1999) Stratigraphic framework and heavy minerals of the continental shelf of Onslow and Long Bays, North Carolina. Marine Georesources and Geotechnology 17: 173–184

Holdsen GR, Berner RA (1979) Mechanism of feldspar weathering. In: Experimental studies. Geochimica Et Cosmochimica Acta 43: 1161– 1171

Holland HD (1978) The chemistry of the atmosphere and oceans. Wiley. New York, 351 pp. Horn HS (1966) Measurement of “overlap” in comparative ecological studies. American Nature 100: 419–424

Hounslow MW, Morton AC (2004) Evaluation of sediment provenance using magnetic mineral inclusions in clastic silicates: comparison with heavy mineral analysis. Sedimentary Geology 171: 13–36

Hower J, Eslinger EV, Hower ME, Perry EA (1976) The control of illite/smectite stability on the redistribution of potassium during diagenesis and burial metamorphism is a classic example on this regard, Mechanism of burial metamorphism of argillaceous sediment: I Minarological and chemical evidence. GSA Bullatin 87 : 725-737

Hu BQ, Yang ZS, Wang HJ, Sun XX, Bi NS (2009) Sedimentation in the Three Gorges Dam and its impact on the sediment flux from the Changjiang (Yangtze River), China. Hydrol Earth System Science data Discussion 6:5177–5204

Hughes MG, Keene JB, Joseph RG (2000) Hydraulic sorting of heavy-mineral grains by swash on a medium-sand beach. Journal of sedimentary research 70 (5) 994–1004

Humphreys B, Morton AC, Hallsworth CR, Gatliff RW Riding JB (1991) An integrated approach to provenance studies: a case example from the Upper Jurassic of the Central Graben, North Sea, Geological Society, London, Special Publications 57: 1-11 doi:10.1144/GSL.SP.1991.057.01.01

Hussain SM (1998) Recent benthic ostracoda from the Gulf of Mannar, off Tuticorin, southeast coast of India. Journal of Palaeontological Society of India 43: 1–22

Hussain SM, Krishnamurthy R, Suresh GM, Itayaraja K, Ganesan P, Mohan SP (2006) Micropalaeontological investigations on tsunamigenic sediments of Andaman Islands. Current Science 91: 1655–1667

Hussain SM, Mohan SP (2000) Recent Ostracode from Adyar River Estuary, Chennai, Tamil Nadu. Journal of Palaeontological Society of India 45: 25–31

Hussain SM, Mohan SP, Jonathan MP (2010) Ostracoda as an aid in identifying 2004 tsunami sediments: a report from SE coast of India. Natural Hazards 55: 513–522

Ikeya N, Shiozaki M (1993) Characteristics of the inner bay ostracodes around the Japanese islands –The use of ostracodes to reconstruct paleoenvironments–. Mem Geological Society of Japan 39: 15-32

Ip CCM, Li XD, Zhang G, Wai OWH, Li YS (2007) Trace metal distribution in sediments of the Pearl River Estuary and the surrounding coastal area, South China. Environmental Pollution 147: 311–323

Irizuki T, Seto K, Nomura R (2008) The impact of fish farming and bank construction on Ostracoda in Uranouchi Bay on the Pacific coast of southwest Japan - Faunal changes between 1954 and 2002/2005. Paleontological Research 12: 283-302

Irizuki T, Takata H, Ishida K (2006) Recent Ostracoda from Uranouchi Bay, Kamikoshiki-jima Island, Kagoshima Prefecture, Southwestern Japan. Laguna 13: 13-28

Irizuki T, Takimoto A, Sako M, Nomura R, Kakuno K, Wanishi A, Kawano S (2011) The influences of various anthropogenic sources of deterioration on meiobenthos (Ostracoda) over the last 100 years in Suo-Nada in the Seto Inland Sea, southwest Japan. Marine Pollution Bulletin 62: 2030-2041

Ishizaki K (1968) Ostracodes from Uranouchi Bay, Kochi Prefecture, Japan. Sci Rep Tohoku Univ, 2nd Ser (Geol) 40: 1-45

Ishizaki K (1969) Ostracodes from Shinjiko and Nakanoumi, Shimane Prefecture, western Honshu, Japan. Sci Rep Tohoku Univ, 2nd Ser (Geol) 41: 197-224

Ishizaki K. (1971) Ostracodes from Aomori Bay, Aomori Prefecture, northeast Honshu, Japan. Sci Rep Tohoku Univ, 2nd Ser (Geol) 43: 59-97

Jain SP (1978) Recent ostracoda from Mandvi Beach, west coast of India. Bulletin of the Indian Geologists Association 11: 89-139

Jain SP (1981) Checklist of ostracoda from India-1. Cenozoic ostracoda (Marine). Journal of Paleontological Society of India 25: 85–105

James, CS (1993) Entrainment of spheres: and experimental study of relative size and clustering effects. Special publication of the International association of sedimentologists Edited by M.Marzo and C. Puigdefabregas and published by Blackwell scientific publications. 17: 3 – 10

Jayawardena UDS (2005) The stratigraphy and groundwater availability in the delta sediments of river Mahawelli- a study from Sri Lanka. Abstract Volume of the Inter. Conf. on DELTAS (Mekong venue). January 10-16. Ho Chi Minh City. Vietnam. 40

Jiongxin X (1996) Underlying gravel layers in a large sand bed river and their influence on downstream-dam channel adjustment. Geomorphology 17:351-359

Johnsson MJ (1993) The system controlling the composition of clastic sediments. Geological Society of America Special Paper 284: 1–19

Johnsson MJ, Stallard RF, Meade RH (1988) First cycle quartz arenites in the Orinoco River Basin, Venezuela and Colombia. Journal of Geology. 96: 263-277

Johnsson MJ, Stallard RF, Lundberg N (1991) Controls on the composition of fluvial sand s from a tropical weathering environment: sands of the Orinoco River drainage basin, Venezuela and Colombia: Geological society of America bulletin, 103:1622-1647

Joshua EO, Oyebanjo OA (2009) Distribution of heavy minerals in sediments of Osun River Basin Southwestern Nigeria. Research Journal of Environmental and Earth Sciences1.2: 74-80

Joshua EO, Oyebanjo OA (2010) Grain-size and heavy mineral analysis of River Osun Sediments. Australian Journal of Basic and Applied Sciences 4.3: 498-501

Jung HS, Lee CB, Cho YG, Kang JK (1996) A Mechanism for the enrichment of Cu and depletion of Mn in anoxic marine sediments, Banweol Intertidal Flat,Korea. Marine Pollution Bulletin 11:182-787

Juracic M, Bauman I, Pavdic V (1982) Are sediments the ultimate depository of hydrocarbon pollutions? Ves J Etud Pollut Mar Mediterranee CIESM, Cannes. pp 83–87

Juracic M, Bauman I, Pavdic V (1980) Physico-chemical characterisation of recent sediments of the North Adriatic in relation to pollution problems. Ves J Etud Pollut Mar Mediterranee CIESM, Cagliari. pp 977–982

Karageorgis AP, Katsanevakis S, Kaberi H (2009) Use of Enrichment Factors for the Assessment of Heavy Metal Contamination in the Sediments of Koumoundourou Lake, Greece. Water Air Soil Pollution 204:243–258

Kasper-Zubillaga JJ, Carranza Edwards A (2005) Grain size discrimination between sands of desert and coastal dunes from northwest Mexico: Revista Mexicana de Ciencias Geológicas, 22 (3) 383-390

Katopodis C, Aadland LP (2006) Effective dam removal and river channel restoration approaches. International Journal of River Basin Management 4 (3) 153-168

Kaushik A, Kansal A, Santosh, Meena, Kumari S, Kaushik CP (2009) Heavy metal contamination of river Yamuna, Haryana, India: Assessment by metal enrichment factor of the sediments. Journal of Hazardous Materials 164:265–270

Kelley JC, Whetten JT (1969) Quantitative statistical analysis of Colombia River sediment samples, Journal of sedimentary petrology. 39: 1167-1173

Khaled A, El Nemr A, El Sikaily A (2006) An assessment of heavy-metal contamination in surface sediments of the Suez Gulf using geoaccumulation indexes and statistical analysis. Chemistry And Ecology 22 (3) 239–252

Kim KT, Kim ES, Cho SR, Park JK, Ra KT, Lee JM (2010) Distribution of Heavy Metals in the Environmental Samples of the Saemangeum Coastal Area, Korea. Coastal Environmental and Ecosystem Issues of the East China Sea. pp 71–90

Kim JY, Chon HT (2001) Pollution of a water course impacted by acid mine drainage in the Imgok creek of the Gangreung coal field, Korea. Applied Geochemistry 16: 1387– 1396

Kimura T, Hayami I, Yoshida S (1991) Geology of Japan, University of Tokyo Press pp 287

Kimura JI, Yamada Y (1996) Evaluation of major and trace element XRF analyses using a flux to sample ratio of two to one glass beads. Journal of mineralogical and petrological Sciences 91: 62–72

Kingma JT (1948) 'Contributions to the knowledge of the Young-Caenozoic Ostracoda from the Malayan region'. Unpublished doctoral dissertation, Utrecht Univ. pp 119

Klos A, Rajfur M, Wacławek M (2011) Application of Enrichment Factor (EF) to the interpretation of results from the biomonitoring studies. Ecological Chemistry and Engineering S 18 (2) 171-183

Knighton AD (1984) Fluvial forms and processes. Edward Arnold, London. pp 218

Koehnken L (1990) The composition of fine grained weathering products in a large tropical river system, and the transport of metals in fine grained sediments in a temperate estuary [Ph.D. dissertation]: Princeton, New Jersey, Princeton University. pp 246

Komar PD (1976) Beach Processes and Sedimentation: New Jersey, Prentice-Hall pp 429

Koval PV, Burenkov EK, Golovin AA (1995) Introduction to the program 'Multipurpose Geochemical Mapping of Russia'. Journal of Geochemical Exploration. 55: 115–23

Krayesky DM, Meave del Castillo E, Zamudio E, Norris JN, Fredericq S (2009) Diatoms (Bacillariophyta) of the Gulf of Mexico, in Felder, D.L. and D.K. Camp (eds.), Gulf of Mexico–Origins, Waters, and Biota. Biodiversity. Texas A&M 155–186

Krishnaswami S (1976) Authigenic transition elements in Pacific pelagic clays. Geochim. Cosmochim. Acta, 40: 425-435

Kroonenberg SB (1994) Effect of provenance, sorting and weathering on the geochemistry of fluvial sands from different tectonic climatic environments. Proceedings of the 29th International Geological Congress, Part A, 69-81

Krumbein WC (1941) The effect of abrasion on the size, shape and roundness of rock fragments. Journal of Geology 49: 482 – 520

Krumbein WC (1942) Flood deposits of Arroyo Seco, Los angeles County, California, Bulletin of the Geological Society of America. 53: 1355 – 1402

Krupadam RJ, Smita P, Wate SR (2006) Geochemical fractionation of heavy metals in sediments of the Tapi estuary. Geochemical Journal 40:513-522

Lacerda LD, Ribeiro Jr MG, Gueiros BB (1999) Manganese dynamics in a mangrove mud flat tidal creek in SE Brazil. Mangroves and Salt Marshes 3:105–115

Ladipo MK, Ajibola VO, Oniye SJ, Uzairu A, Agbaji EB (2011) Geochemical partitioning of heavy metals in sediments of some locations of the Lagos lagoon. Jenvscs 1 (1) 22–30

Laronne JB, Carson MA (1976) Interrelationships between bed morphology and bed material transport for a small gravel bed channel. Sedimentalogy 23: 67 – 85

Pera LE, Critelli S (1997) Sourceland controls on the composition of beach and fluvial sand of the northern Tyrrhenian coast of Calabria, Italy: implications for actualistic petrofacies: Journal of Sedimentary Research 110 (1-2) 81-97

Persaud D, Jaagumagi R, Hayton A (1992) Guidelines for the Protection and Management of Aquatic Sediment Quality in Ontario. Ontario Ministry of the Environment, Queen's Printer for Ontario

Licht OAB, TarvainenT (1996) Multipurpose geochemical maps produced by integration of geochemical exploration data sets in the Parana Shield, Brasil. Journal of Geochemical Exploration. 56: 167–182

Liu JP, Xue Z, Ross K, Wang HJ, Yang ZS, Li AC, Gao S (2009) Fate of sediments delivered to the sea by Asian large rivers: Long-distance transport and formation of remote alongshore clinothems. The Sedimentary Record 4:4-9

Li Z, Komar PD (1992) Longshore grain sorting and beach placer formation adjacent to the Columbia River, Journal of Sedimentary Petrology 62 (3) 429–441

Li X, Liu L, Wang Y, Luo G, Chen X, Yang X, Gao B, He X (2012) Integrated Assessment of Heavy Metal Contamination in Sediments from a Coastal Industrial Basin, NE China. PLoS ONE 7(6): e39690. doi:10.1371/journal.pone.0039690

Lin C, He M, Zhou Y, Guo W Yang Z (2007) Distribution and contamination assessment of heavy metals in sediment of the Second Songhua River, China. Environ Monit Assess 137(1-3):329-42

Long ER, Morgan LG (1990) The potential for biological effects of sediment-sorbed contaminants tested in the National States and Trends Program. National Oceanic Atmospheric Administration (NOAA) Technical Memorandum No. 5, OMA52, NOAA National Ocean Service, Seattle, Washington.

Lookman R, Geerts H, Grobet P, Merckx R, Vlassak K (1996) Phosphate speciation in excessively fertilized soil: a 31P and 27Al MAS NMR spectroscopy study. European Journal of Soil Science 41: 125- 130

Loska K, Wiechula D (2003) Application of principal component analysis for the estimation of source heavy metal contamination in surface sediments from Rybnik Reservoir. Chemosphere 51: 723–733

Loughnan, F (1969) Chemical weathering of the Silicate Minerals, New York, USA

Luoma SN, Bryan GW (1981) A statistical assessment of the form of trace metals in oxidized estuarine sediments employing chemical extractants. Science of the Total Environment 17:165-196

Ma Y, Lu W, Lin C (2011) Downstream patterns of bed sediment-borne metals, minerals and organic matter in a stream system receiving acidic mine effluent: A preliminary study. Journal of Geochemical Exploration 110 : 98–106

Malmgren BA, Hulugalla R, Hayashi Y, Mikami T (2003) Precipitation trends in Sri Lanka since the 1870s and relationships to el nino-southern Oscillation. International Journal of Climatology 23: 1235 – 1252

Martincic D, Kwokal Z, Branica M (1990) Distribution of zinc, lead, cadmium and copper between different size fractions of sediments I. The Limski kanal (north Adriatic sea). Science of the Total Environment 95: 201–215

Matsumoto T, Kanmera K (1964) Hinagu (Kagoshima-49). Explanatory text of the geological map of Japan. Geological survey of Japan. pp 1-27

McBirney AR (1998) The Skaergaard Layered Series. Part V. Included Trace Elements. Journal of Petrology 30 (2) 255-276

McCann T (1991) Petrological and geochemical determination of provenance in the southern Welsh Basin, Geological Society, London, Special Publications 57: 215-230

McLennan SM (1989) Rare earth elements in sedimentary rocks: Influence of provenance and sedimentary processes. Geochemistry and mineralogy of the rare earth elements. Reviews in Mineralogy and Geochemistry. 21: 169-200

McLennan SM, Hemming S, McDaniel DK, Hanson GN (1993) Geochemical approaches to sedimentation, provenance and tectonics. The Geological Society of America. Special Paper. 284: 21–40

McLennan SM, Taylor SR, Eriksson KA, (1983a) Geochemistry of Archean shales from the Pilbara Supergroup, Western Australia. Geochimica et Cosmochimica Acta. 47 (7) 1211 – 1222

McLennan SM, Taylor SR, Kroner A (1983b) Geochemical evolution of Archean shales from South Africa I. The Swaziland and Pongola Supergroups. Precambrian Research. 22 (1-2) 93–124

McPherson HC (1971) Downstream changes in sediment character in a high energy mountain stream channel. Arctic alpine resource. 3: 65 – 79

Mearns EW (1988) A samarium–neodymium isotopic survey of modern river sediments from northern Britain. Chemical Geology 73: 1–13

Melfi AJ, Cerri CC, Fritsch E, Formoso MLL (1999) Tropical Soils: Genesis, distribution and degradation of lateritic pedological systems. In: Formoso MLL and Cerri CC (Workshop on Tropical Soils), Academia Brasileira de Ciências 7– 30

Meunier A (2003) Argiles. Paris, Contemporary Publishing International – GB Science Publisher. pp 433

Milodowski AE, Zalasiewicz JA (1991) Redistribution of rare earth elements during diagenesis of turbidite/hemipelagite mudrock sequences of Llandovery age from central Wales, Geological Society, London, Special Publications 57: 101-124

Ministry of Environment, Sri Lanka (2011) Sri Lanka's second national communication on climate change. Climate Change Secretariat, Ministry of Environment, Sri Lnaka

Monbet P (2006) Mass balance of lead through a small macrotidal estuary: The Morlaix River estuary (Brittany, France). Marine Chemistry 81:59-80

Moore JN, Brook EJ, Johns C (1989) Grain size partitioning of metals in contaminated, coarse grained river floodplain sediment: Clark Fork river, Montana, USA. Environmental Geology and Water Science 14 : 107–115

Morris AW, Allen JI, Howland RJM, Wood RG (1995) The estuary plume zone: source or sink for land-derived nutrient discharges?. Estuarine Coastal And Shelf Science 40: 387–402

Morris PA (1988) Volcanic arc reconstruction using discriminant function analysis of detrital clinopyroxene and amphibole from the New England Fold Belt, Eastern Australia. Journal of Geology 96: 299-311

Morrison RJ, Narayan SP, Gangaiya P (2001) Trace element studies in Laucala bay Suva, Fiji. Marine Pollution Bulletin 5:39-404

Morton AC (1985) Heavy minerals in provenance studies. In: "Zuff,G.G. (De), Provenance of Arenites". 249-277

Morton AC (1991) Geochemical studies of detrital heavy minerals and their application to provenance research, Geological Society, London, Special Publications. 57: 31-45; DOI: 10.1144/GSL.SP.1991.057.01.04

Morton AC, Hallsworth CR (1999) Processes controlling the composition of heavy mineral assemblages in sandstones. Sedimentary Geology 124 : 3–29

Moskalyk RR, Alfantazi AM (2003) Processing of vanadium: a review. Minerals Engineering 16: 793–805

Mozammel M, Sadrnezhaa, SK, Khoshnevisan A, Youzbashizadeh H (2012) Kinetics and reaction mechanism of isothermal oxidation of Iranian ilmenite concentrate powder. Journal of Thermal Analysis and Calorimetry, DOI 10.1007/s10973-012-2639-1

Nagarajan R, Madhavaraju J, Nagendra R, Armstrong-Altrin JS, Moutte J (2007) Geochemistry of Neoproterozoic shales of the Rabanpalli formation, Bhima basin, northern Karnataka, southern India: implications for provenance and paleoredox conditions. Revista Mexicana de Ciencias Geologicas. 24 (2)150–160

Nahon DD (1991) Introduction to the Petrology of Soils and Chemical Weathering. New York, USA, J Wiley & Sons

Naji A, Ismail A (2011) Assessment of metals contamination in Klang River surface sediments by using different indexes. Environment Asia 4 (1) 30-38

Naseem S, Sheikh SA, Qadeeruddin M, Shirin K (2002) Geochemical stream sediment survey in Winder Valley, Balochistan, Pakistan. Journal of Geochemical Exploration 76: 1 –12

Neal C, Robson AJ, Jeffery HA, Harrow ML, Neal M, Smith CJ (1997) Trace element inter-relationships for the Humber rivers: inferences for hydrological and chemical controls. Sci Total Environ 194/195:321–364

Neale JW (1977) Ostracods from the rice fields of Sri Lanka (Ceylon). In: Loffler H, DC Danielopol (eds) The 6th International Ostracod Symposium, 1976, Saalfeldeen, Austria. pp 271-283

Neale JW, Victor R (1978a) The Lund University Expedition freshwater Ostracoda from Sri Lanka (Ceylon). Canadian Journal of Zoology 56: 1081-1087

Neale JW, Victor R (1978b) On *Indiacypris luxata* (Brady), a freshwater ostracod (Crustacea: Entomostraca) from Sri Lanka. Zoological Journal of Linnean Socciety 64: 71-77

Nelson BK, DePaolo DJ, (1988) Comparison of isotopic and petrographic provenance indicators in sediments from Tertiary continental basins of New Mexico. Journal of Sedimentary Petrology 58:348-357

Nesbitt HW, Young GM (1982) Early Proterozoic climates and plate motions inferred from major element chemistry of lutites. Nature 299: 715–717

Nesbitt HW, Young GM (1984) Predictions of some weathering trends of plutonic and volcanic rocks based on thermodynamic and kinetic conditions. Geochimica Et Cosmochimica Acta 48 : 1523 - 1534

Nesbitt HW, Young GM (1989) Formation and diagenesis of weathering profiles. Journal of Geology 97 : 129 - 147

Nixon SW (1988) Physical energy inputs and the comparative ecology of lake and marine ecosystems. Limnology and Oceanography 33:1005–1025

Nriagu JO (1989) A global assessment of the natural sources of atmosphere trace metals. Nature 338: 47-49

Nwajide CS, Reijers TJA (1996) Chapters on Geology – Sedimentary Geology and sequence stratigraphy in Nigeria. Three case studies and field guide SPDC Special publication, Warri. pp 198

NYSDEC (New York State Department of Environmental Conservation) (1999) Technical guidance for screening contaminated sediments (p. 45). Albany, NY: NYSDEC, Division of Fish, Wildlife and Marine Resources

Ogasawara M (1987) Trace element analysis of rock samples by X-ray fluorescence spectrometry, using Rh anode tube. Bulletin of Geological Survey of Japan 38 (2) 57–68

Ogawa Y, Nishiyama T, Obata M, Nishi T, Miyazaki K, Ikeda T, Yoshimura Y, Nagakawa K (1992) Continental margin tectonics in Kyushu, southwest Japan-Mesozoic paired metamorphic belts and accretionary complexes. Paleozoic and Mesozoic terranes: basement of the Japanese island arcs. 29th IGC field trip guide book Vol.1. Nagoya University. pp 261-315

Ohta T, Arai H (2007) Statistical empirical index of chemical weathering in igneous rocks: A new tool for evaluating the degree of weathering. Chemical Geology 240: 280–297

Olubunmi FE, Olorunsola OE (2010) Evaluation of the Status of Heavy Metal Pollution of Sediment of Agbabu Bitumen Deposit Area, Nigeria. European Journal of Scientific Research. 41 (3) 373-382

Ortiz E, Roser BP (2006a) Geochemistry of stream sediments from the Hino River, SW Japan: source rock signatures, downstream compositional variations, and influence of sorting and weathering. Earth Science (Chikyu Kagaku) 60: 131–146

Ortiz E, Roser BP (2006b) Major and trace element provenance signatures in stream sediments from the Kando River, San'in district, southwest Japan. Island Arc 15: 223- 238

Ottesen RT, Theobald PK (1994) Stream sediments in mineral exploration. In Hale M. & Plant J. A. (eds). Handbook of Exploration Geochemistry, Elsevier, Amsterdam. 6: 147–84

Owens PN, Batalla RJ, Collins AJ, Gomez B, Hicks DM, Horowitz AJ, Kondolf GM, Marden M, Page MJ, Peacock DH, Petticrew EL, Salomons W, Trustrum NA(2005) Fine-grained sediment in river systems: environmental significance and management issues. River Research and Applications 21:693–717

Panda D, Subramanian V, Panigrahy RC (1995) Geochemical fractionation of heavy metals in Chilka lake (east coast of India) – a tropical coastal lagoon. Environmental Geology 26 : 199–210

Pardo R, Barrado E, Perez L, Vega M (1990) Determination and speciation of heavy metals in sediments of Pisuerga river. Water Research 24 : 373–379

Park J, Khim JS, Ohtsuka T, Araki H, Witkowski A, Koh C (2012) Diatom assemblages on Nanaura mudflat, Ariake Sea, Japan: with reference to the biogeography of marine benthic diatoms in Northeast Asia. Botanical Studies 53:105-124

Parker G (1991) Downstream variation of grain size in gravel rivers: Abrasion versus selective sorting. Earth and environmental science, Fluvial Hydraulics of Mountain Regions, Lecture Notes in Earth Science. 37: 345-360. DOI: 10.1007/BFb0011201

Pattan JN, Rao CM, Higgs NC, Colley S, Parthiban G (1995) Distribution of major, trace and rare-earth elements in surface sediments of the Wharton Basin, Indian Ocean. Chemical Geology 121: 201–215

Pedro G (1985) Le sol, composante majeure de la biosphere. Revue du Palais de la Découverte 15(4) 20– 50

Peters SW (1978) Stratigraphic evolution of the Benue Trough and its multiplication for the upper cretaceous paleogeography of West Africa. Journal of Geology 86: 311-322

Pettijhon FJ (1975) Sedimentary Rocks (3rd ed.). Harper & Row. London. pp 628

Petts GE, Gurnell AM, Gerrard AJ, Hannah DM, Hansford B, Morrisey I, Edwards PJ, Kollmann J, Ward JV, Tockner K, Smith BP (2000) Longitudinal variations in exposed riverine sediments: a context for the ecology of the Fiume Tagliamento, Italy. Aquatic Conservation: Marine and Freshwater Ecosystems 10:249– 266

Pirrie D (1991) Controls on the petrographic evolution of an active margin sedimentary sequence: the Larsen Basin, Antarctica, Geological Society, London, Special Publications 57: 231-249 ; DOI: 10.1144/GSL.SP.1991.057.01.18

Pohl JR, Emmermann R, (1991) Chemical composition of the Sri Lankan Precambrian basement, The crystalline crust of Sri Lanka. part I Summary of research of the German-Sri Lankan consortium. Geological Survey Department 94-124

Potter PE, Heling D, Shrimp NF Wie WV (1975) Clay mineralogy of modern alluvial muds of the Mississippi River Basin. Bulletin des centres de Recherches exploration-production Elf Aquitaine, 9: 353-389

Praveena SM, Radojevic M, Abdullah MH (2007) The Assessment of Mangrove Sediment Quality in Mengkabong Lagoon: An Index Analysis Approach. International Journal of Environmental & Science Education 2 (3) 60 – 68

Presley BJ, Koldny Y, Kalpan IR (1972) Early diagenesis in the reducing fjord. Blitish Columbia-II. Trace element distribution in interstitial water and sediment. Geochimica Et Cosmochimica Acta 36 : 1073–1090

Presley BJ, Trefry JH, Shokes RF (1980) Heavy metal inputs to Mississippi Delta sediments. Water Air and Soil Pollution 13 :481– 494

Price NP (1976) Chemical diagenesis in sediments. In: Riley, J.P & Chester, R. (eds), Chemical Oceanography. 6: 2nd ed, Academic Press. 1

Purushothaman P, Chakrapani GJ (2007) Heavy metals fractionation in Ganga River sediments, India. Environmental Monitoring Assessment 132:475–489

Radoane M, Radoane N, Dumitriu D, Miclau C (2008) Downstream variation in bed sediment size along the East Carpathian rivers: evidence of the role of sediment sources. Earth Surf Proc Land DOI: 10.1002/esp.1568

Rajasuriya A, Perera N, Fernando M. (2005) Status of Coral Reefs in Trincomalee, Sri Lanka. In: Souter D, Lindén O (eds) Coral Reef Degradation in the Indian Ocean Status (CORDIO) Report 2005, Stockholm, Sweden. pp 97-192

Rana SA, Simons DB, Mahmood K (1973) analysis of sediment sorting in alluvial chanels. Journal of Hydrology Div. ASCE 99 (HY11). 1967 – 1980

Ranasinghe PN, Fernando GWAR, Dissanayake CB, Rupasinghe MS (2008) Stream sediment geochemistry of the Upper Mahaweli River Basin of Sri Lanka—Geological and environmental significance. Journal of Geochemical Exploration. 99: 1–28

Ranasinghe PN, Fernando GWAR, Dissanayake CB, Rupasinghe MS, Witter DL (2009) Statistical evaluation of stream sediment geochemistry in interpreting the river catchment of high-grade metamorphic terrains. Journal of Geochemical Exploration. 103: 97–114

Rao BK, Murthy PB, Swamy ASR (1990) Sedimentary characteristics of Holocene beach ridges in western delta of Krishna River. In: Rajamanickam, G.V. (Ed.), Sea level Variation and its Impact on Coastal Environments. Tamil University Publication no. 131: 133–143

Rapin F, Tessier A, Campbell PGC, Capigan PR (1986) Potential artifacts in the determination of metal partitioning in sediments by a sequential procedure. Environmental Science & Technology 20: 836–840

Reid I, Bathurst JC, Carling PA, Walling DE, Webb BW (1997) Sediment erosion, transport and deposition. In: Thorne CR, Hey RD, Newson MD (eds) Applied Fluvial Geomorphology for River Engineering and Management. Wiley, Chichester. 95–135

Reid MK, Spencer KL (2009) Use of principal components analysis (PCA) on estuarine sediment datasets: the effect of data pre-treatment. Environmental Pollution 157:2275-2281

Reimann C, Melezhik V (2001) Metallogenic provinces, geochemical provinces and regional geology-what causes large-scale patterns in low density geochemical maps of the C-horizon of podzols in Arctic Europe?. Applied Geochemistry 16: 963–983

Retallack GJ (1990) Soils of the Past. London, Harper-Collins

Rice S (1998) Which tributaries disrupt downstream fining along gravel-bed rivers? Geomorphology 22: 39-56

Ridgway IM, Price NB (1987) Geochemical associations and post depositional mobility of heavy metals in coastal sediments: Loch Estive, Scotland. Marine Chemistry 21 : 229–248

Robert S, Blanc G, Schafer J, Lavaux G, Abril G (2004) Metal mobilization in the Gironde Estuary (France): the role of the soft mud layer in the maximum turbidity zone. Marine Chemistry 87:1–13

Roisenberg C, Formoso MLL, Dani N (2004) Ground water contamination caused by coal processing activities in the Candiota Region, State of Rio Grande do Sul, Brazil. In: Enviromental Geochemistry in Tropical Countries, 4th International Symposium, Búzios, RJ, Brazil. 237– 241

Ronow AB. et al. (1977) Regional metamorphism and sediment composition evolution. Geochemistry International 12: 90

Rosental R, Eagle GA Orren M.J (1986) Trace metal distribution in different chemical fractions of nearshore marine sediments. Estuarine Coastal and Shelf Science 22 : 303–324

Roser BP, Ishiga H, Lee HK (2000) Geochemistry and provenance of Cretaceous sediments from the Euisong block, Gyeongsang basin, Korea. Mem Geological Society of Japan 57: 155–170

Roser BP, Korsch RJ (1988) Provenance signatures of sandstone-mudstone suites determined using discriminant function analysis of major element data. Chemical Geology 67: 119-139

Roser BP, Korsch RJ (1999) Geochemical characterization, evolution and source of a Mesozoic accretionary wedge: the Torlesse terrane. New Zealand. Geological Magazine. 136 (5) 493–512

Ruapasinghe MS (2000) Development of new methods for gem exploration— Application of Rb/Sr ratio. Final Report: Research Grant RG/NR/96/01 National Science Foundation Sri Lanka

Rudnick RL, Gao S (2005) Composition of the continental crust. In: Rudnick RL (ed), The crust. Treatise on Geochemistry, Vol 3, Elsevier-Pergamon, Oxford. pp 1–64

Ruiz F, Abad M, Bodergat AM, Carbonel P, Rodríguez-Lázaro J, Yasuhara M (2005) Marine and brackish-water ostracods as sentinels of anthropogenic impacts. Earth-Science Review 72: 89–111

Ruiz F, Abad M, Olías M, Galán E, González I, Aguilá E, Hamoumi N, Pulido I, Cantano M, (2006) The present environmental scenario of the Nador Lagoon (Morocco). Environmental Research 102: 215–229

Ruiz F, Borrego J, González-Ragalado ML, López Gonzálaz N, Carro B, Abad M (2008) Impact of millennial mining activities on sediments and microfauna of the Tinto River estuary (SW Spain). Marine Pollution Bulletin 56: 1258–1264

Ruiz-Fernandez AC, Hillaire-Marcel C, Paez-Osuna F, Ghaleb B, Soto-Jimenez M (2003) Historical trends of metal pollution recorded in the sediments of the Culiacan River Estuary, Northwestern Mexico. Applied Geochemistry 18: 577–588

Russell RD (1939) Effects of transportation on sedimentary particles. In recent marine sediments (Ed. Trask, P.D.) Ammerican assessment of petrological geology, dover publications, New Yalk. 32 – 47

Russell, MJ, Allison I (1985) Agalmatolite and the maturity of sandstones of the Appin and Argyll groups and Eriboll Sandstone. Scottish Journal of Geology 21: 113-122

SAIC (Science Applications International Corporation, Canada) (2002) Compilation and review of Canadian remediation guidelines, standards and regulations (Final report, B187-413, pp 79). Emergencies Engineering Technologies Office (EETO)–Environment Canada

Saito Y, Yang Z, Hori K (2001) The Huanghe (Yellow River) and Changjiang (Yangtze River) deltas: a review on their characteristics, evolution and sediment discharge during the Holocene. Geomorphology 41: 219–231

Sakai T, Okada H, Aihara A (1992) Cretaceous and Tertiary active margin sedimentation: transect of Kyushu. Paleozoic and Mesozoic terranes: basement of the Japanese island arcs. 29th IGC field trip guide book Vol.1. Nagoya University 317-354

Salomons W Förstner,U (1984) Metals in hydrocycle. Springer-Verlag, New-York Berlin Heidelberg. pp 349

Sanders IS, Morris JH (1978) Evidence for Caledonian subduction from greywacke detritus in the Longford-Down inlier. Journal of Earth Sciences, Royal Dublin Society 1: 53-62

Sawyer EW (1986) The influence of source rock type, chemical weathering and sorting on the geochemistry of clastic sediments from the quetico metasedimentary belt, superior province, Canada. Chemical Geology 55: 77 - 95

Schiff KC, Weisberg SB (1999) Iron as a reference element for determining trace metal enrichment in Southern California coastal shelf sediments. Marine Environmental Research 48:161–176

Schnetger B, Brumsack HJ, Schale H, Hinrichs J, Dittert L (2000) Geochemical characteristics of deep-sea sediments from the Arabian Sea: a high-resolution study. Deep-Sea Research PT II 47: 2735– 2768

Schwindt E, De Francesco C, Iribarne O (2004) Individual and reef growth of the introduced reef-building polychaete Ficopomatus enigmaticus in a south-western Atlantic coastal lagoon. Jounal of Marine Biological Association UK 84:987–993

Scott A (1905) Report on the Ostracoda collected by Herdmann at Ceylon in 1902. Supplementary Rep Ceylon Pearl Oyster Fisheries 22: 365-384

Shaw DM (1954) Trace elements in pelitic rocks. Part I: variations during metamorphism. GSA Bull., 65, 1151; (1954) Trace elements in pelitic rocks. Part II: geochemical relations. GSA Bull., 65, 1167; (1956) Trace elements in pelitic rocks. Part II: Geochemistry of pelitic rocks Part III: major elements and general geochemistry. GSA Bulletin 67. pp 919

Shepard FP (1963) Submarine canyons, In: The Sea. M.N. Hill. ed. Wiley. New York. 480–506

Shepard FP, Dill RF (1966) Submarine canyons and other sea valleys. Rand McNally & Co. Chicago. 203–206

Sholkovitz ER (1976) Flocculation of dissolved organic and inorganic matter during the mixing of river water and seawater. Geochimica Et Cosmochimica Acta 7:831-845

Shriadah MMA (1999) Heavy Metals in Mangrove Sediments of the United Arab Emirates Shoreline (Arabian Gulf). Water, Air and Soil Pollution. 116: 523-534

Sillén LG (1961) The physical chemistry of sea water. In: Oceanography, sears m (Ed), American Association for the Advancement of Science, Washington DC, USA. 549– 581

Silva MGD, Vital H (2000) Provenance of heavy-minerals in the Piranhas-açu River, northeastern brazil. Revista Brasileira de Geociências 30 (3) 453-456

Singh AK, Hasnain SI, Banerjee DK (1999) Grain size and geochemical partitioning of heavy metals in sediments of the Damodar River – a tributary of the lower Ganga, India. Environmental Geology 39 (1) 90-98

Singh M, Sharma M, Tobschall HJ (2005) Weathering of the Ganga alluvial plain, northern India: implications from fluvial geochemistry of the Gomati River. Applied Geochemistry 20: 1–21

Singh P (2009) Major, trace and REE geochemistry of the Ganga River sediments: Influence of provenance and sedimentary processes. Chemical Geology 266: 242–255

Singh P (2010) Geochemistry and provenance of stream sediments of the Ganga River and its major tributaries in the Himalayan region, India. Chemical Geology 269: 220–236

Slingerland R, Smith N.D (1986) Occurrence and formation of water-laid placers: Annual Review of Earth and Planetary Sciences 14: 113–147

Smedley PL, Kinniburgh DG (2001) United Nations Synthesis Report on Arsenic in Drinking-Water. British Geological Survey, Wallingford, Oxon OX10 8BB, UK. pp 1-61

Sneed ED, Folk RL (1958) Pebbles in the lower Colorado River, Texas : a study in particle morpho-genesis. Journal of Geology 66: 114 – 150

Spaulding S (2011) Tryblionella. In Diatoms of the United States. Retrieved November 06, 2012, from http://westerndiatoms.colorado.edu/taxa/genus/tryblionella

Spaulding S, Edlund M (2009) In Diatoms of the United States. Retrieved November 06, 2012, from http://westerndiatoms.colorado.edu/taxa/genus

Sridhar SGD, Hussain SM, Kumar V, Periakali P (2002) Recent benthic ostracoda from Palk Bay, off Rameswaram, southeast coast of India. Journal of Palaeontological Society of India 47: 17–39

Stallard R F (1992) 6 Tectonic processes, continental freeboard, and the rate controlling step for continental denudation. International Geophysics. Global Biogeochemical Cycles. 50: 93-121

Stepanova A, Taldenkova E, Simstich J, Bauch HA (2007) Comparison study of the modern ostracod associations in the Kara and Laptev seas: Ecological aspects. Marine Micropaleontology 63: 111–142

Sternberg, H (1875) Untersuchungen uber Langen- und Querprofil geschiebefuhrender Flusse. Zeitschrift fur Bauwesen 25: 483 – 506

Stewart HB Jr, Shepard FP, Dietl R (1964) Submarine canyons off eastern Ceylon. Abstract Geological Soceity of America Annual Meeting. 197

Stow MH (1929) A Preliminary Investigation of some sediments from James River, Virginia. Journal of mineralogical society of America. 528-533

Stumm W (1992) Chemistry of the solid–water interface. Wiley, New York

Styles MT, Stone P, Floyd JD (1989) Arc detritus in the Southern Uplands: mineralogical characterization of a 'missing' terrane. Journal of the Geological Society, London 146: 397-400

Subiyanto, Hirata I, Senta T (1993) Larval Settlement of the Japanese Flounder on Sandy Beaches of the Yatsushiro Sea, Japan. Nippon Suisan Gakkaishi 7:1121-1128

Sullivan MJ (1999) Applied diatom studies in estuaries and shallow coastal environments. In: Stoermer EF and Smol JP (eds), The Diatoms: Applications for the Environmental and Earth Sciences. Cambridge University Press, London 334–351

Surian N (2002) Downstream variation in grain size along an Alpine river: analysis of controls and processes. Geomorphology 43: 137– 149

Survey Department of Sri Lanka, (1988) National Atlas of Sri Lanka

Sutherland RA (2000) A comparison of geochemical information obtained from two fluvial bed sediment fractions. Environmental Geology 39 (3–4) 330–341

Suttner LJ, Dutta PK (1986) Alluvial sandstone composition and paleoclimate 1. Framework mineralogy. Journal of Sedimentary petrology 56: 329-345

Taira A (2001) Tectonic evolution of the Japanese island arc system: Annual Reviews of Earth and Planetary Sciences 29: 109-134

Takeno N (2005) Atlas of Eh – pH diagrams. Geological Society of Japan Open File Report 419:11-183

Tanabe S, Hori K, Saito Y, Haruyama S, Vu VP, Kitamura A (2003) Song Hong (Red River) delta evolution related to millennium-scale Holocene sea-level changes. Quaternary Science Reviews 22: 2345–2361

Tathavadkar V, Kari C, Rao SM (2006) Oxidation of Indian Ilmenite: Thermodynamics and Kinetics Considerations. Proceedings of the International Seminar on Mineral Processing Technology .Chennai, India. 553 - 558

Taylor KG, Perry CT, Greenaway AM, Machen, PG (2007) Bacterial iron oxide reduction in a terrigenous sediment-impacted tropical shallow marine carbonate system, north Jamaica. Marine Chemistry 107:449-463

Taylor SR, McLennan SM (1985) The continental crust: its composition and evolution. Oxford: Blackwell Scientific. pp 312

Tessier A, Campbell PGC, Bisson M (1982) Particulate trace metal speciation in stream sediments and relationship with grain size: implication for geochemical exploration. Journal of Geochemical Exploration 6: 77–104

Thomson J, Carpenter MSN, Colley S, Willson TRS (1984) Metal accumulation rates in northwest Atlantic pelagic sediments. Geochimica Et Cosmochimica Acta 48: 1935-1948

Thornburg TM Kulm, LD (1987) Sedimentation in the Chile Trench: petrofacies and provenance. Journal of Sedimentary Petrology 57: 55- 74

Tortosa, A., Palomares, M and Arribas, J (1991) Quartz grain types in Holocene deposits from the Spanish Central System: some problems in provenance analysis, Geological Society, London, Special Publications. 57: 47-54; DOI: 10.1144/GSL.SP.1991.057.01.05

Toyoda K, Masuda A (1990) Sedimentary environments and chemical composition of Pacific pelagic sediments. Chemical Geology 88:127-141

Trabelsi Y, Gharbi F, El Ghali A, Oueslati M, Samaali M, Abdelli W, Baccouche S, Tekaya MB, Benmansour M, Mabit L, M'Barek NB, Reguigui N, Abril JM (2012) Recent sedimentation rates in Garaet El Ichkeul Lake, NW Tunisia, as affected by the construction of dams and a regulatory sluice. Journal of Soils abd Sediments 12:784–796

Turekian KK, Wedepohl KH (1961) Distribution of the Elements in some major units of the Earth's crust. Geological Society of America, Bulletin 72: 175-192

Vaithiyanathan P, Ramanathan AL, Subramanian V (1993) Transport and distribution of heavy metals in Cauvery river. Water Air and Soil Pollution 71 : 13–28

Van De Kamp PC, Leake BE (1985) Petrography and geochemistry of feldspathic and mafic sediments of the northeastern Pacific margin. Transactions of the Royal Society of Edinburgh: Earth Sciences. 76: 411-449

Velbel MA, Saad MK (1991) Palaeoweathering or diagenesis as the principal modifier of sandstone framework composition? A case study from some Triassic rift-valley redbeds of eastern North America, Geological Society, London, Special Publications 57: 91-99

Violante A, Cozzolino V, Perelomov L, Caporale AG, Pigna M (2010) Mobility and bioavailability of heavy metals And metalloids in soil environments. Soil Science and Plant Nutrition 3:268–292

Vital H, Stattegger K (2000) Major and trace elements of stream sediments from the lowermost Amazon River. Chemical Geology 168: 151 – 168

Vital H, Stattegger K, Garbe-Schonberg C (1999) Composition and trace element geochemistry of detrital clay and heavy mineral suites of the lowermost Amazon river : A provenance study. Journal of Sediment Research 69 (3) 563 – 575

Webster JG, Brown KL, Webster KS (2000) Source and transport of trace metals in the Hatea River catchment and estuary, Whangarei, New Zealand. New Zealand Journal of Marine and Freshwater Research 34:187–201

Wentworth CK (1922) a field study of the shapes of river pebbles. US geological survey bulletin. 730: 103 – 114

Whalen JB, Currie KL, Chappell BW (1987) A-Type Granites - Geochemical Characteristics, Discrimination and Petrogenesis. Contributions of Mineralogy and Petrology. 95: 407-419

Whatley R, Zhao Q (1988) Recent ostracode of the Malacca Straits, Part 2. Rev Española Micropaleontol 20: 5–37

Whetten JT, Kelley JC, Hanson LG (1969) Characteristics of Colombia river sediment and sediment transport, Journal of sedimentary petrology 39: 1149-1166

Whitney PR (1975) Relationship of manganese-iron oxides and associated heavy metals to grain size in streain sediments. Journal of Geochemical Exploration 4: 251–263

Wignall PB, Ruffell AH (1990) The influence of a sudden climatic change on marine deposition in the Kimmeridgian of northwest Europe. Journal of the Geological Society, London, 147 :365- 371

Wijayananda NP (1985) Geological setting around the heads of the Trincomalee canyon, Sri Lanka. Journal of National Science Council of Sri Lanka 13 (2) 213 – 226

Woods AM, Lloyd JM, Zong Y, Brodie CR (2012) Spatial mapping of Pearl River Estuary surface sediment geochemistry: Influence of data analysis on environmental interpretation. Estuarine, Coastal and Shelf Science 115:218-233

Wraeter JP Graham JR (1989) Ophiolitic detritus in the Ordovician sediments of South Mayo, Ireland. Journal of the Geological Society, London. 146: 213-215

Wronkiewicz DJ, Condie KC (1990) Geochemistry and mineralogy of sediments from the Ventersdorp and Transvaal Supergroups, South Africa: Cratonic evolution during the early Proterozoic: Geochimica et Cosmochimica Acta 54 (2) 343-354

Yamamoto H, (1992) Higo Belt. Regional Geology of Japan, Part 9, Kyushu. p. 22-26. Editorial Committee of Kyushu. Kyoritu Shuppan Co. Ltd., Tokyo. pp 371

Yamane K (1998) Recent ostracode assemblages from Hiuchi-nada Bay, Seto Inland Sea of Japan. Bull Ehime Prefect Sci Mus 3: 19-59 (in Japanese with English Abstract)

Yang S, Wang Z, Guo C, Li C, Cai J (2009) Heavy mineral compositions of the Changjiang (Yangtze River) sediments and their provenance-tracing implication. Journal of Asian Earth Science 35: 56–65

Yasuhara M, Yamazaki H (2005) The impact of 150 years of anthropogenic pollution on the shallow marine ostracode fauna, Osaka Bay, Japan. Marine Micropaleontology 55: 63–74

Yasuhara M, Yamazaki H, Irizuki T, Yoshikawa S (2003) Temporal changes of ostracode assemblages and anthropogenic pollution during the last 100 years, in sediment cores from Hiroshima Bay, Japan. The Holocene 13: 527–536

Yasuhara M, Yamazaki H, Tsujimoto A, Hirose K, (2007) The effect of long-term spatiotemporal variations in urbanization-induced eutrophication on a benthic ecosystem, Osaka Bay, Japan. Limnology and Oceanography 52: 1633–1644

Young SM, Pitawala A, Ishiga H (2011) Assessment of the Geochemical Processes and Environmental Pollution in the Trincomalee Bay, Sri Lanka. 21st Annual V.M. Goldschmidt Conference Abstract, pp 2230

Young SM, Pitawala A, Ishiga H (2012) Geochemical characteristics of stream sediments, sediment fractions, soils, and basement rocks from the Mahaweli River and its catchment, Sri Lanka. Chemie Erde – Geochemistry http://dx.doi.org/10.1016/j.chemer.2012.09.003 Article in press

Young GM, Nesbitt HW (1998) Processes controlling the distribution of Ti and Al in weathering profiles, siliciclastic sediments and sedimentary rocks. Journal of Sedimentary Research. 68: 448–455

Young SM, Ishiga H, Roser BP, Pitawala A. Geochemistry of sediments in three sectors of Trincomalee Bay, Sri Lanka: Provenance, modifying factors, and present environmental status. Submitted to Journal of soils and sediments

Yu KC, Tsai LJ, Chen SH, Ho ST (2001) Correlation analyses on binding behavior of heavy metals with sediment matrices. Water Research 35 (10) 2417–2428

Zdenek B (1996) Trace element levels in sediments of the Czech part of the Elbe River. GeoJournal 40 (3) 299-309

Zhang J, Liu CL (2002) Riverine Composition and Estuarine Geochemistry of Particulate Metals in China—Weathering Features, Anthropogenic Impact and Chemical Fluxes. Estuarine, Coastal and Shelf Science 54: 1051–1070

Zhang L, Ye X, Feng H, Jing Y, Ouyang T, Yu X, Liang R, Gao C, Chen W (2007) Heavy metal contamination in western Xiamen Bay sediments and its vicinity, China. Marine Pollution Bulletin 54: 974–982

Zhang W, Feng H, Chang J, Qu J, Xie H, Yu L (2009) Heavy metal contamination in surface sediments of Yangtze River intertidal zone: An assessment from different indexes. Environmental Pollution. 157: 1533–1543

Zhao Q, Whatley R (1988) The genus Neomonoceratina (Crustacea: Ostracoda) from the Cainozoic of the West Pacific margins. Acta Oceanologica Sinica 7: 562–577

Zuff GG (1991) On the use of turbidite arenites in provenance studies: critical remarks, Geological Society, London, Special Publications 57: 23-29; DOI: 10.1144/GSL.SP.1991.057.01.03

Zwolsman JJG, Van Eck BTM, Van Der Weijden CH (1997) Geochemistry of dissolved trace metals (cadmium, copper, zinc) in the Scheldt estuary, southwestern Netherlands: Impact of seasonal variability. Geochimica Et Cosmochimica Acta 8:1635-1652

APPENDIX

Abbreviations of the Geology maps

pmgrd- granodioritic gneiss
pmgrf-microcline gneiss
pmghb- hornblende biotite gneiss
pmmhb- hornblende biotite migmatite
pmgbh-biotite hornblende gneiss
pmmbh- biotite horn migmatite
pmggb- meta gabbro
pmgh- amphibolite
pmgr-pink granitoid gneiss
pmgrf- very coarse grained to pegmatitic granitoid gneiss
pmgqf- quartzo feldathic gneiss
pmq-quartzite
pmqs-impure quartzite and quartz shist
pmgqf-garnetiferrous quartzo feldspathic gneiss
pmgg- garnet sillimanite biotite gneiss
pmc- marble
pmgb- biotite gneiss
pmgc- calc gneisse and granulite
pmqsy- coarse grain to pegmatitic quartz syenite
pp- pegmatites
pmgk- charnuckitic gneisses
pq- vein quartz
pmgga- Garnet sillimanite biotite gneiss +or - graphite